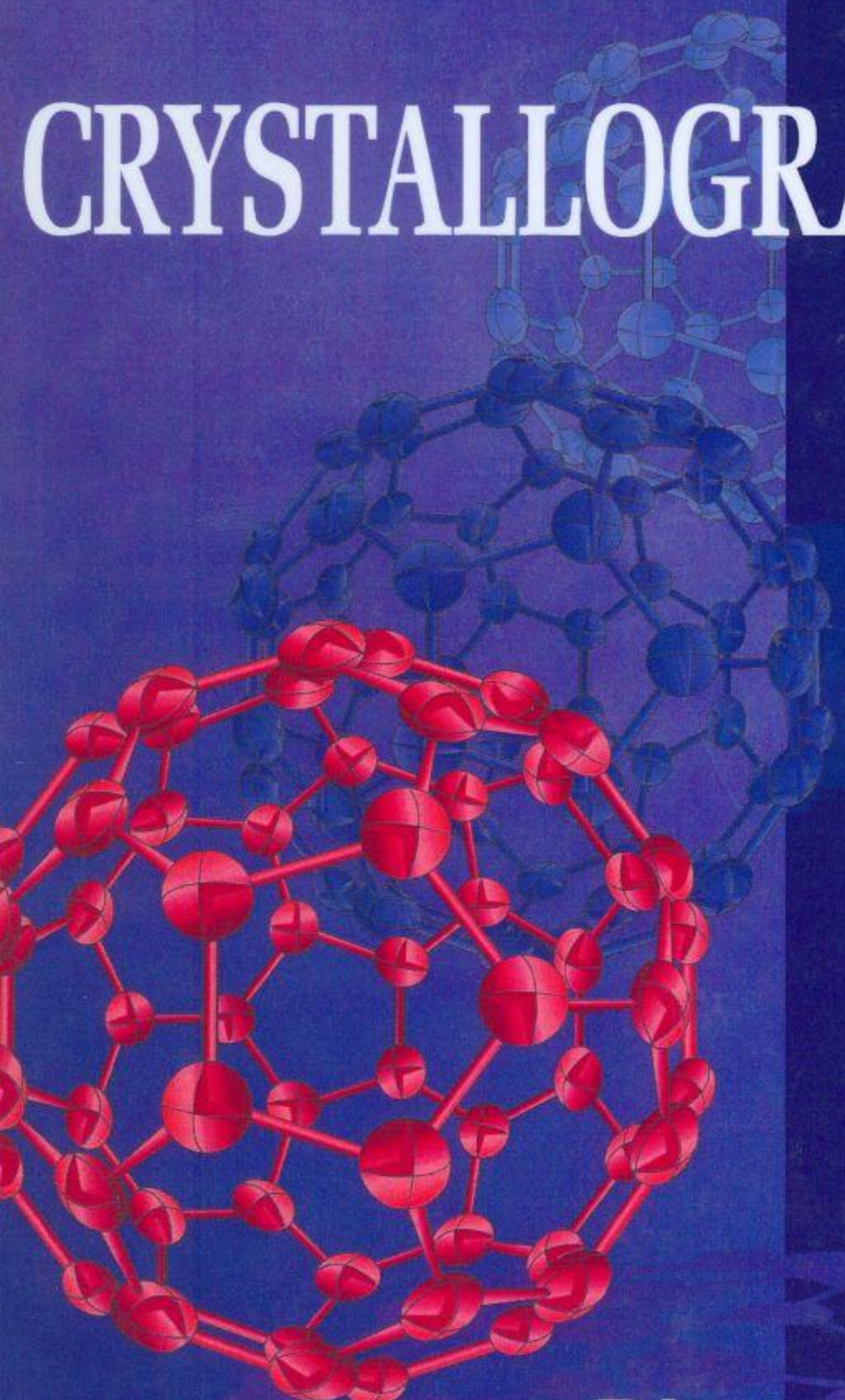




CRYSTALLOGRAPHY



Dieter
Schwarzenbach

Crystallography

Dieter Schwarzenbach

Institute of Crystallography,
University of Lausanne, Switzerland

Translated from the French by A. Alan Pinkerton

University of Toledo, USA

JOHN WILEY & SONS

Chichester · New York · Brisbane · Toronto · Singapore

Copyright © 1996 by John Wiley & Sons Ltd,
Baffins Lane, Chichester,
West Sussex PO19 1UD, England

National 01243 779777
International (+44) 1243 779777

© 1993 Presses Polytechniques et
Universitaires Romandes, 1015 Lausanne, Switzerland

All rights reserved.

No part of this book may be reproduced by any means,
or transmitted, or translated into a machine language
without the written permission of the publisher.

Other Wiley Editorial Offices

John Wiley & Sons, Inc., 605 Third Avenue,
New York, NY 10158-0012, USA

Jacaranda Wiley Ltd, 33 Park Road, Milton,
Queensland 4064, Australia

John Wiley & Sons (Canada) Ltd, 22 Worcester Road,
Rexdale, Ontario M9W 1L1, Canada

John Wiley & Sons (SEA) Pte Ltd, 2 Clementi Loop # 02-01.
Jin Xing Distripark, Singapore 129809

Originally published in French under the title: *Cristallographie*

Library of Congress Cataloging-in-Publication Data

Schwarzenbach, Dieter.

[Crystallographie. English]

Crystallography / Dieter Schwarzenbach ; translated from the
French by A. Alan Pinkerton.

p. cm.

Includes bibliographical references (p. -) and index.

ISBN 0-471-95598-1 (alk. paper)

1. Crystallography. I. Title.

QD905.2.S3813 1996

548'.8 -- dc20

96-11160

CIP

British Library Cataloguing in Publication Data

A catalogue record for this book is available from the British Library

ISBN 0 471 955981

Typeset in 10/12pt Times by Thomson Press (I) Ltd, New Delhi

Printed and bound in Great Britain by Biddles, Guildford, Surrey

This book is printed on acid-free paper responsibly manufactured from sustainable forestation
for which at least two trees are planted for each one used for paper production.

Contents

Foreword	vii
Chapter 1 Geometrical Crystallography	1
1.1 Introduction	1
1.2 Analytical Geometry with Oblique Bases	2
1.3 Polyhedral Crystal Shapes	7
1.4 Periodic Space Tiling and Crystal Structures	11
1.5 What is a Crystal?	18
Chapter 2 Symmetry	23
2.1 Introduction	23
2.2 Symmetry Operations	24
2.3 Symmetry Elements	29
2.4 Symmetry and the Lattice Metric	36
2.5 Crystal Classes and Systems	42
2.6 Classification of Lattices	62
2.7 Symmetry of Periodic Structures	68
2.8 Crystal Structures	84
2.9 Miller–Bravais Indices for Hexagonal Coordinate Systems	86
Chapter 3 Diffraction of X-Rays by Crystals	89
3.1 Introduction	89
3.2 Scattering of X-Rays by an Electron	99
3.3 Scattering of X-Rays by Matter	102
3.4 Diffraction by a Periodic Structure	111
3.5 Experimental Diffraction Methods	120
3.6 Physics of X-Rays	129
3.7 Intensities of Diffracted Beams	137
3.8 Space Group Determination	142
3.9 Comments on the Solution of the Phase Problem	149

Chapter 4	Tensor Properties of Crystals	157
	4.1 Anisotropy and Symmetry	157
	4.2 Tensors	158
	4.3 Stresses and Strains	170
	4.4 Examples of Tensor Properties	176
	4.5 Crystal Optics	200
Chapter 5	Exercises	217
	5.1 Exercises Relating to Chapter 1	217
	5.2 Exercises Relating to Chapter 2	222
	5.3 Exercises Relating to Chapter 3	227
	5.4 Exercises Relating to Chapter 4	232
Index		237

Foreword

A large part of scientific endeavor is dedicated to the elaboration of microscopic models for describing the physical world, in particular in terms of atoms or molecules. These models attempt to link the properties, spatial disposition and dynamic behavior of atoms to macroscopic physical and chemical properties of materials. The diffraction of short wave-length radiation, principally X-rays, by crystals allows us to observe the structure of materials on the atomic scale. The success of this method justifies the current interest in crystallography. The fields of solid state physics, chemistry, mineralogy and materials science use X-ray crystallography as a primary investigative tool, and textbooks in all these disciplines typically include some description of the technique. Is there thus a need for a book dedicated exclusively to crystallography?

The current work has grown out of an introductory course in X-ray crystallography presented to students of physics and materials science at the University of Lausanne and the Swiss Institute of Technology at Lausanne. While presenting this course, I found that despite – or perhaps because of – the interdisciplinary nature of crystallography, there are few available introductory texts concerning the foundations of this discipline. The subject of crystallography has become almost synonymous with structure determination. Even those books entitled *Crystallography* predominantly discuss diffraction methods, structure determination methodology and interpretation of the results in terms of structural chemistry. Thus, these books are concerned with the applications of crystallography rather than with the foundations of the subject. Fundamental ideas such as the Bravais lattices, crystal systems or Bragg's law are frequently presented via some simple diagrams with minimal explanation. These are, however, not trivial concepts and deserve a more profound discussion. Their incomplete definition may lead to imprecise or erroneous interpretation of results obtained from crystallographic techniques.

Today, diffraction equipment is typically available as a self-service facility, at the disposition of any researcher who needs it for material identification or characterization, as well as for aligning single crystals. The present text introduces the basic ideas that the solid state physicist, the materials scientist, the

chemist and the mineralogist will encounter in current experimental methods as well as in crystallographic databases. I am convinced that it is important to distinguish the idea of the crystal lattice from that of the crystal structure; thus we will avoid implying that the structure of brass (CuZn) possesses a centered lattice because its description shows an atom at the center of the unit cell. The symmetry of a structure should be distinguished from the metric parameters of the unit cell; we will thus understand that we cannot determine the crystal symmetry or crystal class from powder diffraction data, but only the metric parameters of the lattice. The frequently employed derivation of Bragg's law which assumes reflection from some poorly defined set of planes is largely meaningless; it is essential to understand that this law is not about atoms, but concerns translational symmetry alone. Even the idea of atoms deserves some clarification; the distribution of electron density in a crystal is approximated by the superposition of free atoms and the structure analysis by diffraction methods is based on this model. Crystallography is derived to a large extent from Euclidean geometry. In order to understand three-dimensional properties, it seems to me that visualization is more important than their algebraic derivation. For this reason, particular attention has been paid to the presentation of figures and diagrams.

This book does not, however, pretend to present the state of the art in crystallographic research. Apart from a few rudimentary ideas, there is no discussion of the fascinating subject of quasi-crystals or aperiodic crystals because these are still quite rare materials. Although synchrotron radiation is the tool of choice for cutting-edge research, the classical sealed X-ray tube is the only source available in most universities and industrial laboratories and will certainly remain so. This book is not an introduction to structure determination, there being a number of modern texts already available in this area.

The publication of this work was made possible by a grant from the Fonds Herbette of the Faculty of Sciences at the University of Lausanne for which I express my gratitude. I also thank my crystallographer friends and colleagues for their comments and suggestions. The students who have patiently attended my courses have contributed much to this book through the questions that they have asked concerning some of the more difficult reasoning. Indeed, we often assume concepts in developing an argument that are not necessarily trivial.

TECHNICAL REMARKS

Most of the figures were produced with the programs MacDraw II (Claris), SHAPE and ATOMS (Eric Dowty, Shape Software). The vectors as well as the tensors in Chapter 4 are represented by bold letters because a tensor of rank 1 is a vector. The norms of vectors are written in italics, $\|\mathbf{a}\| = a$. The scalar product

of two vectors \mathbf{a} and \mathbf{b} is represented by $\mathbf{a} \cdot \mathbf{b}$ and the vector product by $\mathbf{a} \times \mathbf{b}$. The components of a vector \mathbf{a} are written as a column; in other words \mathbf{a} will be left multiplied by a matrix \mathbf{M} , $\mathbf{a}' = \mathbf{M}\mathbf{a}$. The transpose \mathbf{a}^T is a line vector and $\mathbf{a}'^T = \mathbf{a}^T \mathbf{M}^T$. The notation $a:b:c$ represents the ratios of three numbers, i.e. the fractions a/b and b/c .

CHAPTER 1

Geometrical Crystallography

1.1 INTRODUCTION

Crystallography is the branch of the exact sciences that studies the structure of matter on an atomic scale; the determination, classification and interpretation of the geometrical structures of solids and, in particular, those of crystals. A *crystal* is a solid whose microscopic structure is characterized by a *periodic repetition* in three dimensions of a motif composed of atoms. In the case of quartz (rock crystal), for example, the motif is made up of three silicon atoms and six oxygen atoms and occupies a volume of 113 \AA^3 (0.113 nm^3). Thus crystals have ordered structures, and the study of order and disorder is a central preoccupation of the crystallographer. The periodic structure of crystals at the atomic level affects their macroscopic properties; their physical properties (cleavage, hardness, rate of growth, electrical and thermal conductivity, index of refraction, elasticity, piezoelectricity among others) are orientation dependent. Properties that are not direction dependent are termed *isotropic*; those which are directional are termed *anisotropic*. According to an ancient definition, a crystal is a body which is both homogeneous and anisotropic. The polyhedral shapes of crystals follow from an unencumbered growth; they express the regularity of the microscopic structures and provide a striking example of crystalline anisotropy.

Crystallography plays an interdisciplinary role between physics, chemistry, molecular biology, materials science and mineralogy-petrography. The geometrical foundations of solid state physics, the determination of the microscopic structure to atomic resolution of inorganic, organic and macromolecular substances (interatomic distances, bond angles, stereochemistry), the identification of substances and mixtures of substances (rocks and minerals, quality control, for example in cement production, analysis of corrosion products, etc.), texture analysis in rocks and alloys as well as the alignment and orientation control of crystals are all endeavors that call upon crystallography. The principal experimental method used is the diffraction by crystals of X-rays or neutrons with wavelengths of about 1 \AA (100 pm).

The theory of crystal symmetry and of the periodicity of microscopic structures (translational symmetry) was developed during the 18th and 19th centuries from

the exact measurements of polyhedral crystal shapes. This theory was confirmed by the fundamental X-ray diffraction experiments of M. von Laue, W. Friedrich and P. Knipping (1912). Following this work, the theory and techniques for structure determination from diffraction data were developed. One can compare structure analysis to a microscope with atomic resolution, about 0.5 Å (50 pm). Since 1960, X-ray crystallography has blossomed with the development of more and more powerful computers. Today, more than 9000 crystal structures are published each year, along with 2000 new powder diagrams (Chapter 3). Crystallographic data banks and the use of advanced methods of graphical representation aid in the scientific exploitation of these results.

Nineteenth-century crystallography may be considered to be the mathematical branch of mineralogy. It is based on two empirical laws, the *law of constancy of angle* and the *law of rational indices*. These laws will be presented in the following pages after a discussion of some mathematical principles fundamental to crystallography, non-unitary coordinate systems and reciprocal coordinates.

1.2 ANALYTICAL GEOMETRY WITH OBLIQUE BASES

1.2.1 COORDINATE SYSTEMS

The coordinate systems chosen in crystallography are generally defined by three nonorthogonal *base vectors* \mathbf{a} , \mathbf{b} , \mathbf{c} of different lengths (a , b , c). These *non-unitary systems* introduce some complexity into the expressions used in analytical geometry.

CONVENTION. A right-handed coordinate system is chosen; i.e. \mathbf{a} , \mathbf{b} and \mathbf{c} are taken in the order of the thumb, index and middle finger of the right hand; α is the angle between \mathbf{b} and \mathbf{c} , β is the angle between \mathbf{a} and \mathbf{c} , γ is the angle between \mathbf{a} and \mathbf{b} .

A general point P is characterized by the coordinates u , v , w , in other words by the vector $\mathbf{r} = u\mathbf{a} + v\mathbf{b} + w\mathbf{c}$ (Fig. 1.1).

The equation of a plane, as in a unitary system, is $hu + kv + lw = 1$ (Fig. 1.2). For the coordinates $v = w = 0$, we obtain $u = 1/h$; thus, h is the reciprocal value of the segment $O-A$ in units of a , A being the intersection of the plane with the \mathbf{a} axis. If a is given in meters, the length of the segment $O-A$ is a/h meters.

1.2.2 RECIPROCAL COORDINATE SYSTEM

The normal to the plane $hu + kv + lw = 1$ is oriented from the origin towards the plane and may be calculated from the vector product (Fig. 1.2):

$$\mathbf{N} = (\text{sign of } hkl) \left[\left(\frac{\mathbf{a}}{h} - \frac{\mathbf{b}}{k} \right) \times \left(\frac{\mathbf{b}}{k} - \frac{\mathbf{c}}{l} \right) \right] = \frac{1}{|hkl|} \{ h(\mathbf{b} \times \mathbf{c}) + k(\mathbf{c} \times \mathbf{a}) + l(\mathbf{a} \times \mathbf{b}) \}$$

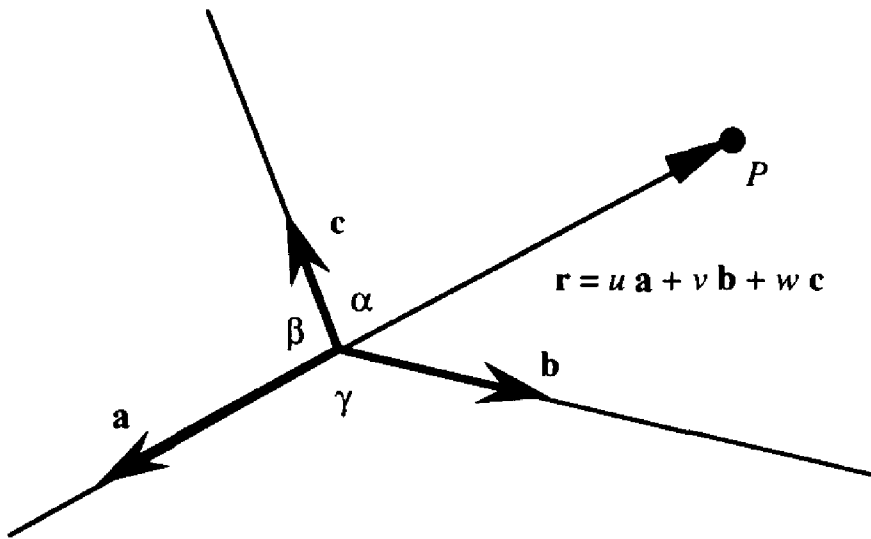


Fig. 1.1. Non-unitary base, coordinates of a point

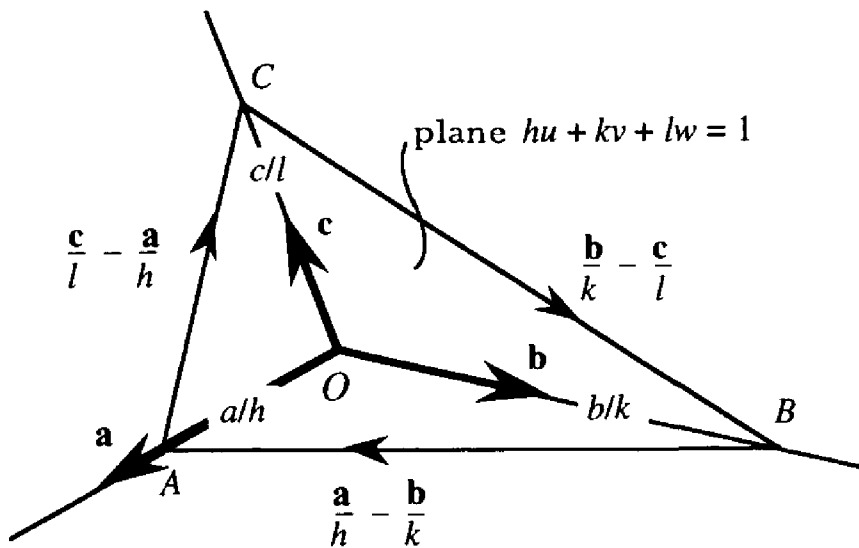


Fig. 1.2. Equation of a plane in a non-unitary base

Consider the pyramid whose vertices are the origin O and the intersections A, B, C of the plane with the axes. Its volume V is equal to one third of the area of the triangle formed by three vertices multiplied by the distance of the triangle from the fourth vertex. Let d be the distance of the plane from the origin. We thus obtain:

$$V = \frac{1}{3} \left\{ \frac{1}{2} \left\| \left(\frac{\mathbf{a}}{h} - \frac{\mathbf{b}}{k} \right) \times \left(\frac{\mathbf{b}}{k} - \frac{\mathbf{c}}{l} \right) \right\| \right\} \{d\} = \frac{1}{6} d \|\mathbf{N}\|$$

Moreover;

$$V = \frac{1}{3} \left| \left[\frac{1}{2} \left(\frac{\mathbf{a}}{h} \times \frac{\mathbf{b}}{k} \right) \right] \frac{\mathbf{c}}{l} \right| = \frac{1}{6|hkl|} (\mathbf{a} \ \mathbf{b} \ \mathbf{c})$$

where $(\mathbf{a} \ \mathbf{b} \ \mathbf{c}) = \mathbf{a} \cdot (\mathbf{b} \times \mathbf{c}) = \mathbf{b} \cdot (\mathbf{c} \times \mathbf{a}) = \dots$ is the volume of the parallelepiped whose edges are \mathbf{a} , \mathbf{b} , \mathbf{c} .

Thus

$$\|\mathbf{N}\| = \frac{1}{d} \frac{(\mathbf{a} \ \mathbf{b} \ \mathbf{c})}{|h \ k \ l|} \quad (1.1)$$

The vector $\mathbf{r}^* = |hkl| \mathbf{N} / (\mathbf{a} \ \mathbf{b} \ \mathbf{c})$ has the following properties (Fig. 1.3):

- $\mathbf{r}^* = h\mathbf{a}^* + k\mathbf{b}^* + l\mathbf{c}^*$;
- $\mathbf{a}^* = (\mathbf{b} \times \mathbf{c}) / (\mathbf{a} \ \mathbf{b} \ \mathbf{c})$, $\mathbf{b}^* = (\mathbf{c} \times \mathbf{a}) / (\mathbf{a} \ \mathbf{b} \ \mathbf{c})$, $\mathbf{c}^* = (\mathbf{a} \times \mathbf{b}) / (\mathbf{a} \ \mathbf{b} \ \mathbf{c})$;
- \mathbf{r}^* is normal to the plane $hu + kv + lw = 1$, oriented from the origin towards the plane;
- the norm of \mathbf{r}^* is $\|\mathbf{r}^*\| = 1/d$.

The coordinate system \mathbf{a}^* , \mathbf{b}^* , \mathbf{c}^* is the *reciprocal* of the system \mathbf{a} , \mathbf{b} , \mathbf{c} . If the lengths a , b , c are given in meters, then the norms a^* , b^* , c^* have the dimensions of (meters)⁻¹. The reciprocal vectors \mathbf{a}^* , \mathbf{b}^* and \mathbf{c}^* are *not* in general parallel to \mathbf{a} , \mathbf{b} and \mathbf{c} , and their norms are *not* equal to $1/a$, $1/b$ and $1/c$. It is easily seen that

$$\mathbf{a}^* \cdot \mathbf{a} = \mathbf{b}^* \cdot \mathbf{b} = \mathbf{c}^* \cdot \mathbf{c} = 1; \quad \mathbf{a}^* \cdot \mathbf{b} = \mathbf{a}^* \cdot \mathbf{c} = \mathbf{b}^* \cdot \mathbf{a} = \mathbf{b}^* \cdot \mathbf{c} = \mathbf{c}^* \cdot \mathbf{a} = \mathbf{c}^* \cdot \mathbf{b} = 0$$

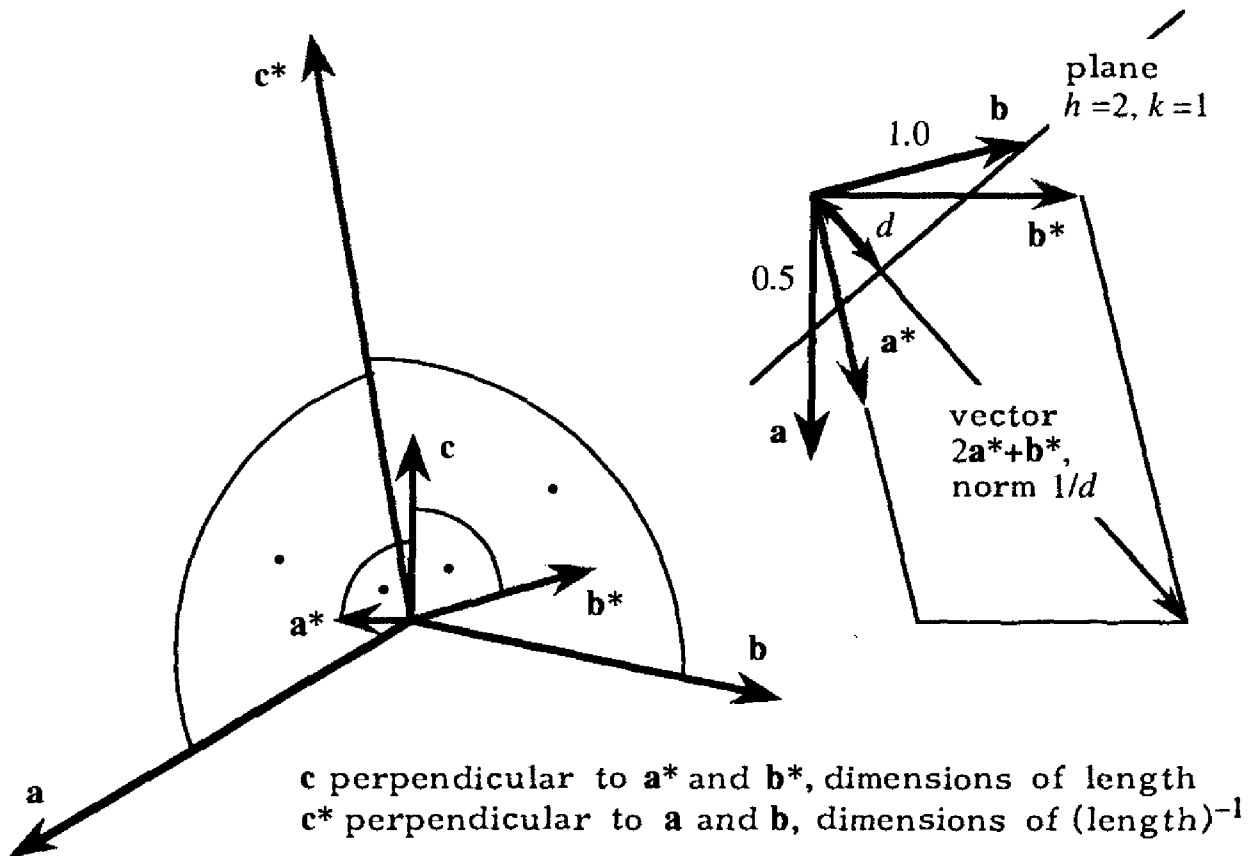


Fig. 1.3. Direct and reciprocal axes. The vector $2\mathbf{a}^* + \mathbf{b}^*$ is normal to the plane $h/k = 2$ which cuts the axes \mathbf{a} and \mathbf{b} at the points $0.5\mathbf{a}$ and $1.0\mathbf{b}$

By labeling the base vectors \mathbf{a}_1 , \mathbf{a}_2 and \mathbf{a}_3 , and the corresponding reciprocal vectors \mathbf{a}_1^* , \mathbf{a}_2^* and \mathbf{a}_3^* , these relationships may be summarized by the following expression which defines the reciprocal vectors in terms of the base vectors and vice versa:

$$\mathbf{a}_i \cdot \mathbf{a}_j^* = \delta_{ij} (= 1 \text{ for } i = j, \text{ and } 0 \text{ for } i \neq j) \quad (1.2)$$

The symmetry of equation (1.2) shows that the reciprocal of the coordinate system \mathbf{a}_1^* , \mathbf{a}_2^* , \mathbf{a}_3^* is the system \mathbf{a}_1 , \mathbf{a}_2 , \mathbf{a}_3 ; $\mathbf{a} = (\mathbf{b}^* \times \mathbf{c}^*) / (\mathbf{a}^* \mathbf{b}^* \mathbf{c}^*)$, etc.

The equation of the plane hkl becomes $hu + kv + lw = \mathbf{r} \cdot \mathbf{r}^* = 1$; the projection of the vector \mathbf{r} on the normal \mathbf{r}^* to the plane is equal to d .

Reciprocal quantities may be calculated using formulae which are derived from multiple scalar and vector products:

$$\begin{aligned} \mathbf{a}^* \cdot \mathbf{b}^* &= (\mathbf{b} \times \mathbf{c}) \cdot (\mathbf{c} \times \mathbf{a}) / (\mathbf{a} \mathbf{b} \mathbf{c})^2 \\ &= [(\mathbf{b} \cdot \mathbf{c})(\mathbf{a} \cdot \mathbf{c}) - c^2(\mathbf{a} \cdot \mathbf{b})] / (\mathbf{a} \mathbf{b} \mathbf{c})^2 \end{aligned} \quad (1.3)$$

$$\mathbf{a}^* \times \mathbf{b}^* = [(\mathbf{b} \times \mathbf{c}) \times (\mathbf{c} \times \mathbf{a})] / (\mathbf{a} \mathbf{b} \mathbf{c})^2 = \mathbf{c} \cdot (\mathbf{b} \mathbf{c} \mathbf{a}) / (\mathbf{a} \mathbf{b} \mathbf{c})^2 \quad (1.4)$$

$$c(\mathbf{a} \mathbf{b} \mathbf{c}) = \|(\mathbf{b} \times \mathbf{c}) \times (\mathbf{c} \times \mathbf{a})\| = abc^2 \sin \alpha \sin \beta \sin \gamma^* \quad (1.5)$$

$$\begin{aligned} (\mathbf{a} \mathbf{b} \mathbf{c})^2 &= a^2 \|\mathbf{b} \times \mathbf{c}\|^2 - \|\mathbf{a} \times (\mathbf{b} \times \mathbf{c})\|^2 \\ &= a^2 b^2 c^2 (1 - \cos^2 \alpha - \cos^2 \beta - \cos^2 \gamma + 2 \cos \alpha \cos \beta \cos \gamma) \end{aligned} \quad (1.6)$$

$$\begin{aligned} (\mathbf{a} \mathbf{b} \mathbf{c}) &= abc \sin \alpha \sin \beta \sin \gamma^* = abc \sin \alpha \sin \beta^* \sin \gamma \\ &= abc \sin \alpha^* \sin \beta \sin \gamma \end{aligned} \quad \begin{array}{l} \text{from (1.5)} \\ \text{from (1.5)} \end{array} \quad (1.7)$$

$$(\mathbf{a}^* \mathbf{b}^* \mathbf{c}^*) = (\mathbf{a} \mathbf{b} \mathbf{c})^{-1} \quad \text{from (1.4)} \quad (1.8)$$

$$a^* : b^* : c^* = bc \sin \alpha : ca \sin \beta : ab \sin \gamma \quad (1.9)$$

$$\cos \gamma^* = (\cos \alpha \cos \beta - \cos \gamma)(\sin \alpha \sin \beta) \quad \text{from (1.3)} \quad (1.10)$$

$$\cos \alpha^* = (\cos \beta \cos \gamma - \cos \alpha)(\sin \beta \sin \gamma) \quad \text{from (1.3)} \quad (1.11)$$

$$\cos \beta^* = (\cos \alpha \cos \gamma - \cos \beta)(\sin \alpha \sin \gamma) \quad \text{from (1.3)} \quad (1.12)$$

$$a^* = (a \sin \beta \sin \gamma^*)^{-1} = (a \sin \beta^* \sin \gamma)^{-1} \quad \text{from (1.7)} \quad (1.13)$$

$$b^* = (b \sin \gamma \sin \alpha^*)^{-1} = (b \sin \gamma^* \sin \alpha)^{-1} \quad \text{from (1.7)} \quad (1.14)$$

$$c^* = (c \sin \alpha \sin \beta^*)^{-1} = (c \sin \alpha^* \sin \beta)^{-1} \quad \text{from (1.7)} \quad (1.15)$$

1.2.3 METRIC TENSOR

The norm of the vector $\mathbf{r} = u\mathbf{a} + v\mathbf{b} + w\mathbf{c}$ is obtained by evaluating term by term $\|\mathbf{r}\|^2 = (u\mathbf{a} + v\mathbf{b} + w\mathbf{c})^2 = ua^2 + vb^2 + wc^2 + 2uv\mathbf{a} \cdot \mathbf{b} + 2uw\mathbf{a} \cdot \mathbf{c} + 2vw\mathbf{b} \cdot \mathbf{c}$. In matrix notation, this equation becomes:

$$\|\mathbf{r}\|^2 = (u \ v \ w) \begin{pmatrix} \mathbf{a}^2 & \mathbf{a} \cdot \mathbf{b} & \mathbf{a} \cdot \mathbf{c} \\ \mathbf{a} \cdot \mathbf{b} & \mathbf{b}^2 & \mathbf{b} \cdot \mathbf{c} \\ \mathbf{a} \cdot \mathbf{c} & \mathbf{b} \cdot \mathbf{c} & \mathbf{c}^2 \end{pmatrix} \begin{pmatrix} u \\ v \\ w \end{pmatrix} = \mathbf{u}^T \mathbf{M} \mathbf{u} \quad (1.16)$$

\mathbf{u}^T represents the line vector $(u \ v \ w)$, the transpose of the column vector \mathbf{u} . \mathbf{M} is called the *metric tensor* whose determinant is:

$$|\mathbf{M}| \doteq (\mathbf{a} \ \mathbf{b} \ \mathbf{c})^2 \quad (1.17)$$

In the same way, the square of the norm of a reciprocal vector is obtained from $\|\mathbf{r}^*\|^2 = (h\mathbf{a}^* + k\mathbf{b}^* + l\mathbf{c}^*)^2 = h^2 a^{*2} + k^2 b^{*2} + l^2 c^{*2} + 2hk\mathbf{a}^* \cdot \mathbf{b}^* + 2hla^* \cdot \mathbf{c}^* + 2kl\mathbf{b}^* \cdot \mathbf{c}^*$, which in matrix notation becomes:

$$\|\mathbf{r}^*\|^2 = (h \ k \ l) \begin{pmatrix} \mathbf{a}^{*2} & \mathbf{a}^* \cdot \mathbf{b}^* & \mathbf{a}^* \cdot \mathbf{c}^* \\ \mathbf{a}^* \cdot \mathbf{b}^* & \mathbf{b}^{*2} & \mathbf{b}^* \cdot \mathbf{c}^* \\ \mathbf{a}^* \cdot \mathbf{c}^* & \mathbf{b}^* \cdot \mathbf{c}^* & \mathbf{c}^{*2} \end{pmatrix} \begin{pmatrix} h \\ k \\ l \end{pmatrix} = \mathbf{h}^T \mathbf{M}^* \mathbf{h} \quad (1.18)$$

\mathbf{h}^T represents the line vector $(h \ k \ l)$, the transpose of the column vector \mathbf{h} . It can be shown that the *reciprocal metric tensor* \mathbf{M}^* is the inverse of \mathbf{M} .

$$\mathbf{M}^* = \mathbf{M}^{-1} \quad (1.19)$$

The metric tensor of a unitary system is represented by a unit matrix $M_{ij} = M_{ij}^* = \delta_{ij}$.

The *scalar product* of two vectors \mathbf{r}_1 and \mathbf{r}_2 is $\mathbf{r}_1 \cdot \mathbf{r}_2 = \mathbf{u}_1^T \mathbf{M} \mathbf{u}_2$, that of two reciprocal vectors \mathbf{r}_1^* and \mathbf{r}_2^* is $\mathbf{r}_1^* \cdot \mathbf{r}_2^* = \mathbf{h}_1^T \mathbf{M}^* \mathbf{h}_2$. The scalar product of \mathbf{r}_1 and \mathbf{r}_2^* is $\mathbf{r}_1 \cdot \mathbf{r}_2^* = \mathbf{u}_1^T \mathbf{h}_2$.

The *vector product* of two vectors \mathbf{r}_1 and \mathbf{r}_2 divided by $(\mathbf{a} \ \mathbf{b} \ \mathbf{c})$ gives:

$$\{\mathbf{r}_1 \times \mathbf{r}_2\} / (\mathbf{a} \ \mathbf{b} \ \mathbf{c}) = (v_1 w_2 - v_2 w_1) \mathbf{a}^* + (w_1 u_2 - w_2 u_1) \mathbf{b}^* + (u_1 v_2 - u_2 v_1) \mathbf{c}^* = \mathbf{r}_{hkl}^*$$

The *vector product* of two vectors \mathbf{r}_1^* and \mathbf{r}_2^* divided by $(\mathbf{a}^* \ \mathbf{b}^* \ \mathbf{c}^*)$ gives:

$$\{\mathbf{r}_1^* \times \mathbf{r}_2^*\} / (\mathbf{a}^* \ \mathbf{b}^* \ \mathbf{c}^*) = (k_1 l_2 - k_2 l_1) \mathbf{a} + (l_1 h_2 - l_2 h_1) \mathbf{b} + (h_1 k_2 - h_2 k_1) \mathbf{c} = \mathbf{r}_{uvw}$$

We describe these relationships by means of the following determinants:

$$\frac{u_1 \begin{vmatrix} v_1 & w_1 \\ v_2 & w_2 \end{vmatrix} \times \frac{w_1}{w_2} \times \frac{u_1}{u_2} \times \frac{v_1}{v_2} \begin{vmatrix} w_1 \\ w_2 \end{vmatrix}}{h \quad k \quad l} \quad \frac{h_1 \begin{vmatrix} k_1 & l_1 \\ k_2 & l_2 \end{vmatrix} \times \frac{l_1}{l_2} \times \frac{h_1}{h_2} \times \frac{k_1}{k_2} \begin{vmatrix} l_1 \\ l_2 \end{vmatrix}}{u \quad v \quad w} \quad (1.20)$$

1.2.4 COVARIANT AND CONTRAVARIANT TRANSFORMATIONS

On changing from coordinate system $\mathbf{a}, \mathbf{b}, \mathbf{c}$ to $\mathbf{a}', \mathbf{b}', \mathbf{c}'$, the reciprocal vectors as well as the coordinates in reciprocal and direct space do not transform in the same way. Let us suppose that the transformations are given by the (3×3) matrices $\mathbf{C}_a, \mathbf{C}_{a^*}, \mathbf{C}_u$ and \mathbf{C}_h :

$$\begin{pmatrix} \mathbf{a}' \\ \mathbf{b}' \\ \mathbf{c}' \end{pmatrix} = \mathbf{C}_a \begin{pmatrix} \mathbf{a} \\ \mathbf{b} \\ \mathbf{c} \end{pmatrix}, \quad \begin{pmatrix} \mathbf{a}^{*'} \\ \mathbf{b}^{*'} \\ \mathbf{c}^{*'} \end{pmatrix} = \mathbf{C}_{a^*} \begin{pmatrix} \mathbf{a}^* \\ \mathbf{b}^* \\ \mathbf{c}^* \end{pmatrix}, \quad \begin{pmatrix} u' \\ v' \\ w' \end{pmatrix} = \mathbf{C}_u \begin{pmatrix} u \\ v \\ w \end{pmatrix}, \quad \begin{pmatrix} h' \\ k' \\ l' \end{pmatrix} = \mathbf{C}_h \begin{pmatrix} h \\ k \\ l \end{pmatrix}$$

The vectors \mathbf{r} and \mathbf{r}^* , as well as their scalar product $\mathbf{r} \cdot \mathbf{r}^*$ are invariant with respect to the transformation:

$$\begin{aligned}\mathbf{r} &= (u \ v \ w) \begin{pmatrix} \mathbf{a} \\ \mathbf{b} \\ \mathbf{c} \end{pmatrix} = (u' \ v' \ w') \begin{pmatrix} \mathbf{a}' \\ \mathbf{b}' \\ \mathbf{c}' \end{pmatrix} = (u \ v \ w) \mathbf{C}_u^T \mathbf{C}_a \begin{pmatrix} \mathbf{a} \\ \mathbf{b} \\ \mathbf{c} \end{pmatrix} \\ \mathbf{r}^* &= (h \ k \ l) \begin{pmatrix} \mathbf{a}^* \\ \mathbf{b}^* \\ \mathbf{c}^* \end{pmatrix} = (h' \ k' \ l') \begin{pmatrix} \mathbf{a}^{*'} \\ \mathbf{b}^{*'} \\ \mathbf{c}^{*' } \end{pmatrix} = (h \ k \ l) \mathbf{C}_h^T \mathbf{C}_{a^*} \begin{pmatrix} \mathbf{a}^* \\ \mathbf{b}^* \\ \mathbf{c}^* \end{pmatrix} \\ \mathbf{r} \cdot \mathbf{r}^* &= (u \ v \ w) \begin{pmatrix} h \\ k \\ l \end{pmatrix} = (u' \ v' \ w') \begin{pmatrix} h' \\ k' \\ l' \end{pmatrix} = (u \ v \ w) \mathbf{C}_u^T \mathbf{C}_h \begin{pmatrix} h \\ k \\ l \end{pmatrix}\end{aligned}$$

It thus follows that:

$$\mathbf{C}_a = \mathbf{C}_h = (\mathbf{C}_{a^*}^T)^{-1}, \quad \mathbf{C}_{a^*} = \mathbf{C}_u = (\mathbf{C}_a^T)^{-1} \quad (1.21)$$

The direct base vectors and the reciprocal coordinates h, k, l transform in a covariant manner. The reciprocal base vectors and the direct coordinates u, v, w transform in a contravariant manner.

1.3 POLYHEDRAL CRYSTAL SHAPES

1.3.1 LAW OF CONSTANT DIHEDRAL ANGLES

This law was proposed by the Dane *Nils Steensen (Nicolaus Steno, 1669)* for crystals of quartz. Generalized by the Italian *Domenico Guglielmini (1688)* and by the Swiss *Moritz Anton Capperler (1723)*, the definitive form was proposed by the Frenchman *Romé de l'Isle (1783)*:

- the angle between two faces does not change during crystal growth; it is thus independent of the distance of the faces from any given point;
- the interfacial angles corresponding to two different samples of the same crystal species are equal (at the same temperature and pressure);
- under well-defined physical conditions, the interfacial angles are thus characteristic of a crystalline species.

(We note that the constant angles observed for different examples of the same species do not imply that crystals of different species are necessarily characterized by different angles.)

From here we arrive at the *Bernhardi principle (1809)*: The number and dimensions of the faces are not characteristic for a crystal; every crystal has its own *habit*. Only the *directions* and *orientations* are important, in other words, the

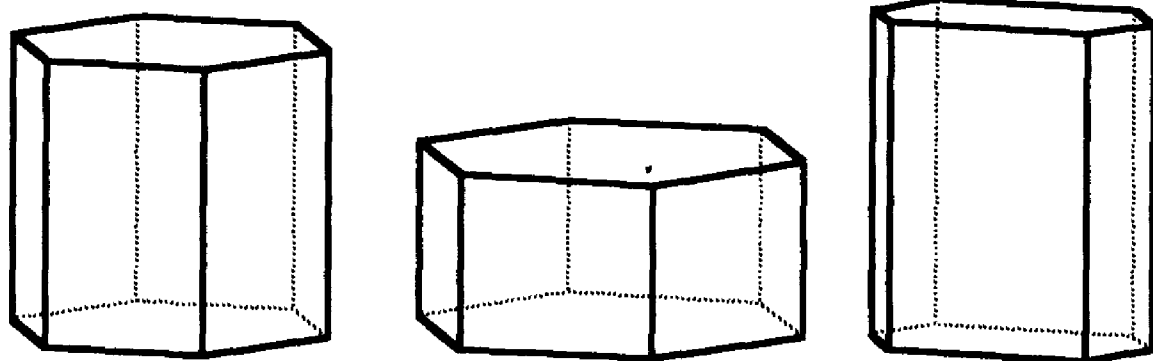


Fig. 1.4. The Bernhardt principle: three polyhedra with the same angles of 60° and 90° between the normals to the faces

directions of the *edges* and the *normals to the faces* (Fig. 1.4). (The orientation of a plane is characterized by the direction of its normal.)

We measure the angle between the normals of the faces of a crystal with an optical goniometer (theodolite) by observing the reflection of a ray of light from the faces. The precision is about 5 seconds of arc.

1.3.2 THE LAW OF RATIONAL INDICES

This law expresses the fact that the faces of a crystal do not form an arbitrary polyhedron. Formulated by the French abbé and mineralogist René Just Haüy (1743–1826), as well as by Ch. S. Weiss, F. Neumann and W.H. Miller (first half of the 19th century), it is equivalent to the laws of stoichiometry in chemistry. We choose a coordinate system adapted to the crystal to describe its shape by analytical geometry. In general it will be a non-unitary system. Three non-coplanar edges are chosen to define the directions of the axes **a**, **b** and **c**. The ratio of the lengths $a:b:c$ can be defined by a fourth edge whose direction is, by definition, $\mathbf{a} + \mathbf{b} + \mathbf{c}$. Note that the individual values of a , b and c are of no interest as the crystal is entirely defined by the *directions* of the edges and the *orientations* of the faces. The equation of a face is thus $hu + kv + lw = \text{some constant}$. We can make the plane pass through the origin; its equation then becomes $hu + kv + lw = 0$; the ratios $h:k:l$ define its orientation. By analogy, the direction of an edge is defined by the ratios $u:v:w$.

In practice, we only measure the orientations of the faces, and not those of the edges. We will thus establish our coordinate system with the aid of this information (Fig. 1.5). We first choose three faces which form a trihedron whose intersections define the directions **a**, **b** and **c**. The choice of a fourth face which cuts these three directions establishes the ratio $a:b:c$. Thus we choose four faces, all other faces being referred to the coordinate system thus defined.

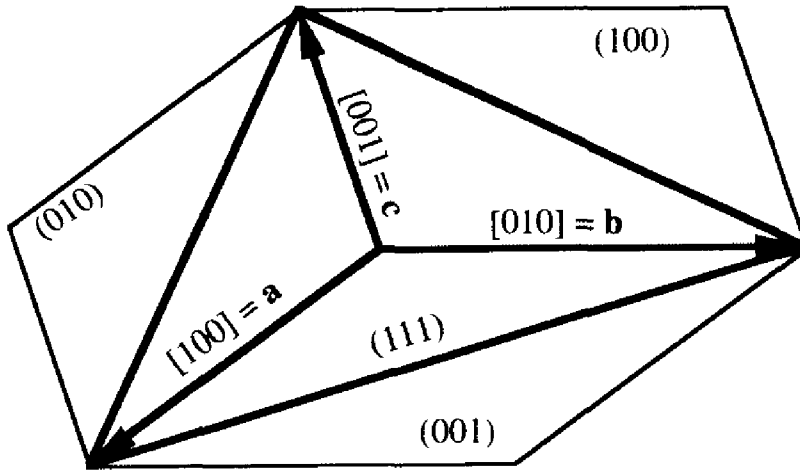


Fig. 1.5. The four faces defining a coordinate system: $[1\ 0\ 0]$, $[0\ 1\ 0]$ and $[0\ 0\ 1]$ represent the axes \mathbf{a} , \mathbf{b} and \mathbf{c} respectively, i.e. $\mathbf{a} = 1\mathbf{a} + 0\mathbf{b} + 0\mathbf{c}$, etc.; $(1\ 0\ 0)$, $(0\ 1\ 0)$ and $(0\ 0\ 1)$ represent the faces parallel to (\mathbf{b}, \mathbf{c}) , (\mathbf{a}, \mathbf{c}) and (\mathbf{a}, \mathbf{b}) respectively. $(1\ 1\ 1)$ is the face whose equation is $u + v + w = \text{constant}$, i.e. $h:k:l = 1:1:1$

Relative to this coordinate system, all the other faces and edges satisfy the *law of rational indices*:

The ratios $h:k:l$ of all the faces, and $u:v:w$ of all the edges are rational.

Note that an irrational ratio between two numbers cannot be observed because a magnitude of finite precision can always be represented by a rational number. The observation of a rational ratio is only meaningful when it concerns a ratio between *small, coprime integers* (i.e. whole numbers with no common factor greater than one).

The coordinates h, k and l for all of the faces as well as the coordinates u, v and w for all the edges of a crystal are small, coprime integers.

These numbers are rarely outside the range ± 10 . We call h, k, l and u, v, w the **Miller indices** of the faces and the edges. For the faces, the indices are written in parentheses, $(h\ k\ l)$, without commas; negative numbers are written $\bar{h}, \bar{k}, \bar{l}$, for example $(1\ 3\ \bar{4})$, $(1\ \bar{1}\ 1)$. The indices $(h\ k\ l)$ and $(\bar{h}\ \bar{k}\ \bar{l})$ represent parallel faces of the polyhedron (or indeed the opposite sides of the same face). Note that all the faces $(h\ k\ 0)$ are parallel to \mathbf{c} , all the faces $(h\ 0\ l)$ are parallel to \mathbf{b} , and all the faces $(0\ k\ l)$ are parallel to \mathbf{a} . The coefficients $(h\ k\ l)$ define the reciprocal vectors $\mathbf{r}^* = h\mathbf{a}^* + k\mathbf{b}^* + l\mathbf{c}^*$. For edges, the indices are written in square brackets, $[u\ v\ w]$, for example $[1\ 3\ \bar{4}]$, $[1\ \bar{1}\ 1]$. The coefficients $[u\ v\ w]$ represent the direct space vectors $\mathbf{r} = u\mathbf{a} + v\mathbf{b} + w\mathbf{c}$.

If we know the indices of two faces $(h_1 \ k_1 \ l_1)$ and $(h_2 \ k_2 \ l_2)$, we can calculate the indices of the edge formed by their intersection $[u \ v \ w]$ by means of equation (1.20). In an analogous manner, we obtain the indices of a face $(h \ k \ l)$ which is parallel to the two edges $[u_1 \ v_1 \ w_1]$ and $[u_2 \ v_2 \ w_2]$. The intersections of $(1 \ 1 \ 1)$ with $(1 \ 0 \ 0)$, $(0 \ 1 \ 0)$ and $(0 \ 0 \ 1)$ are $[0 \ \bar{1} \ 1]$, $[1 \ 0 \ \bar{1}]$ and $[\bar{1} \ 1 \ 0]$ respectively.

1.3.3 ZONE PLANES

First we described a crystal by its faces and its edges. We then replaced the faces by their normals. Analogously we can replace an edge by a plane which contains the normals to the faces parallel to the edge. We say that the faces which are parallel to the same direction belong to the same zone. If the faces intersect, which will depend on the habit of any individual crystal, this direction is parallel to an edge. The word zone, or more precisely zone axis, thus designates an existing edge or an edge that could exist. The normals of the faces form the zone plane.

In geometrical crystallography, the crystal is usually described by means of the normals to the faces and the zone planes. This description is thus made in reciprocal space. The lengths of the segments cut on the \mathbf{a}^* , \mathbf{b}^* and \mathbf{c}^* axes by the zone plane $[u \ v \ w]$ are a^*/u , b^*/v and c^*/w . This description is equivalent to that given by the faces and edges in direct space.

1.3.4 STEREOGRAPHIC PROJECTION

It is useful to have a method of representing the faces of a crystal in two dimensions. To this end we frequently use stereographic projection (Fig. 1.6) and the *Wulff net* (Fig. 1.7).

We imagine that the crystal is placed at the center of a sphere. The points s where the face normals \mathbf{r}^* cut the sphere generate the spherical projection. We then project the points on the sphere onto the equatorial plane in the direction of the opposite pole P . The point p is thus the image of the face \mathbf{r}^* . For the lower part of the sphere, \mathbf{r}'^* and s' , for example, we use the opposite pole P' in order to obtain the projection p' . Stereographic projection conserves the angles; the stereographic projection of a circle is also a circle. A zone plane defined by several face normals \mathbf{r}^* is projected on a great circle (meridian) which contains the projections p of those face normals.

A net of meridians (great circles) and parallels (small circles) allows us to define the coordinates of the points s on the sphere in analogy with terrestrial geography. If we project this net stereographically, we obtain the *Wulff net*. This allows us to easily determine the ratios $a:b:c$ as well as the indices of the faces and zones starting from the angles between the faces of a crystal measured with a goniometer.

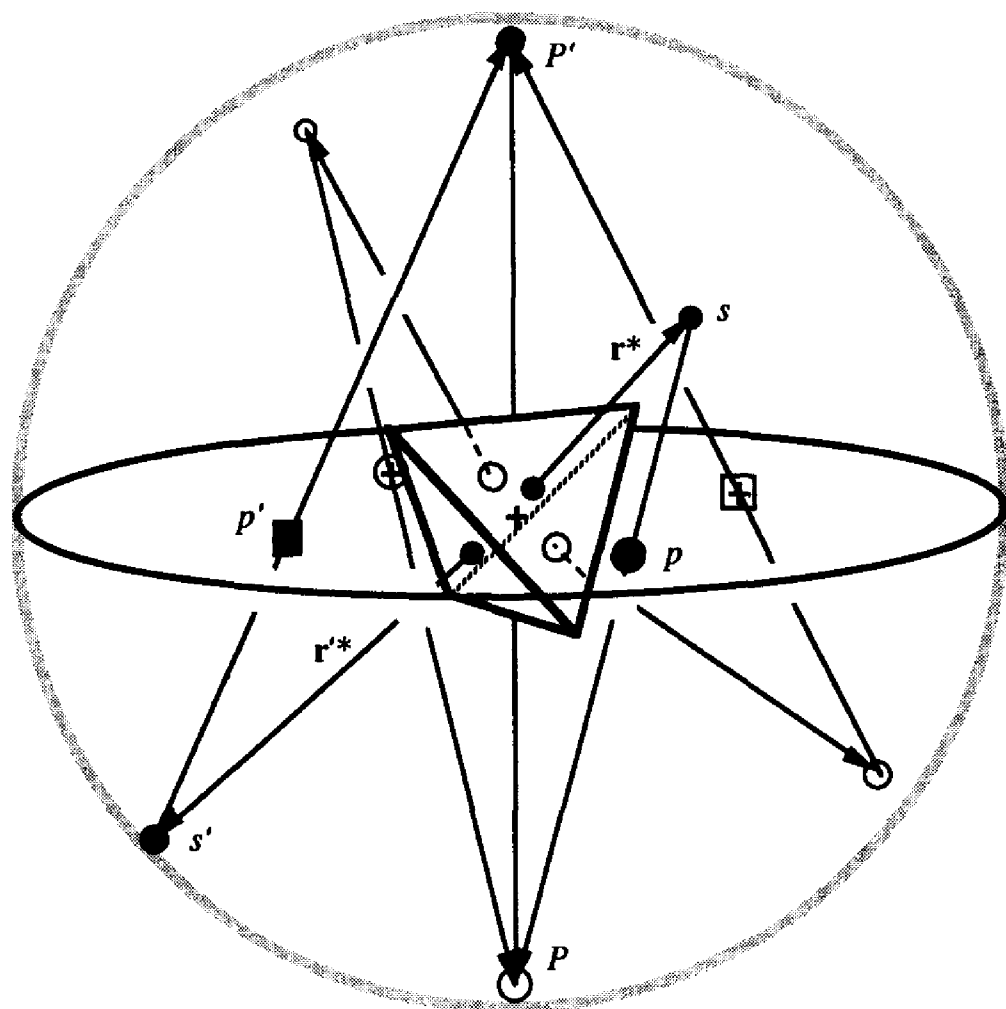


Fig. 1.6. Stereographic projection

1.4 PERIODIC SPACE TILING AND CRYSTAL STRUCTURES

1.4.1 TRANSLATIONAL LATTICE

Cleavage of crystals, in particular of calcite CaCO_3 , and the law of rational indices generated the idea of the periodicity of crystal structures and the theory of translational lattices:

A crystal structure consists of a periodic repeat in three dimensions of some motif.

This theory implies the existence of a microscopic unit of structure (the 'molécule intégrante' of René Just Haüy), which played as fundamental a role in the discovery of atoms as the laws of chemical stoichiometry. The X-ray diffraction experiment (M. von Laue, 1912; Chapter 3) provided brilliant confirmation of its existence.

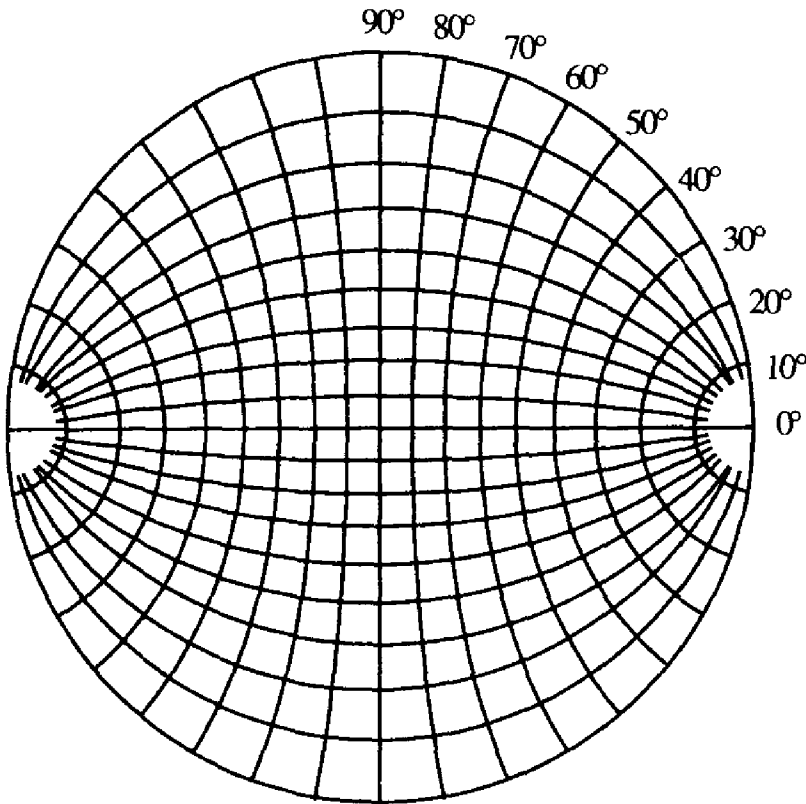


Fig. 1.7. Wulff net with the poles situated in the stereographic plane

We consider that the two-dimensional periodic structure of Fig. 1.8(a) extends to infinity. Let us choose some dot \bullet and all the dots equivalent to this one. We call this set of dots \bullet in Fig. 1.8(a) the *translational lattice*, or simply the *lattice*. The *translation* of the diagram from one dot \bullet to another dot \bullet is an operation which yields an invariance, i.e. this is a *symmetry operation*. We call these dots \bullet *lattice points*. Other examples of two-dimensional periodic structures are given by patterned wallpapers.

The periodically repeating unit is called a *motif*. In Fig. 1.8(a), the contents of one of the parallelograms can be considered to be the motif. It is important to distinguish clearly between the terms lattice, motif and structure:

The periodic structure consists of a motif which is repeated by the lattice translations.

By choosing two non-collinear translations \mathbf{a} and \mathbf{b} in Fig. 1.8(a), we describe the lattice by the translation vectors $\mathbf{r} = u\mathbf{a} + v\mathbf{b}$, u and v being integers. We call this coordinate system the lattice base. The parallelogram (\mathbf{a}, \mathbf{b}) is the *cell* (unit cell). Analogously, the base $\mathbf{a}, \mathbf{b}, \mathbf{c}$ of a three-dimensional lattice is defined by three non-coplanar translations. The cell is hence a parallelepiped. The coordinates x, y, z of a point inside this cell are referred to this non-unitary coordinate system. The set of all the points equivalent by translation to the point x_j, y_j, z_j is given by

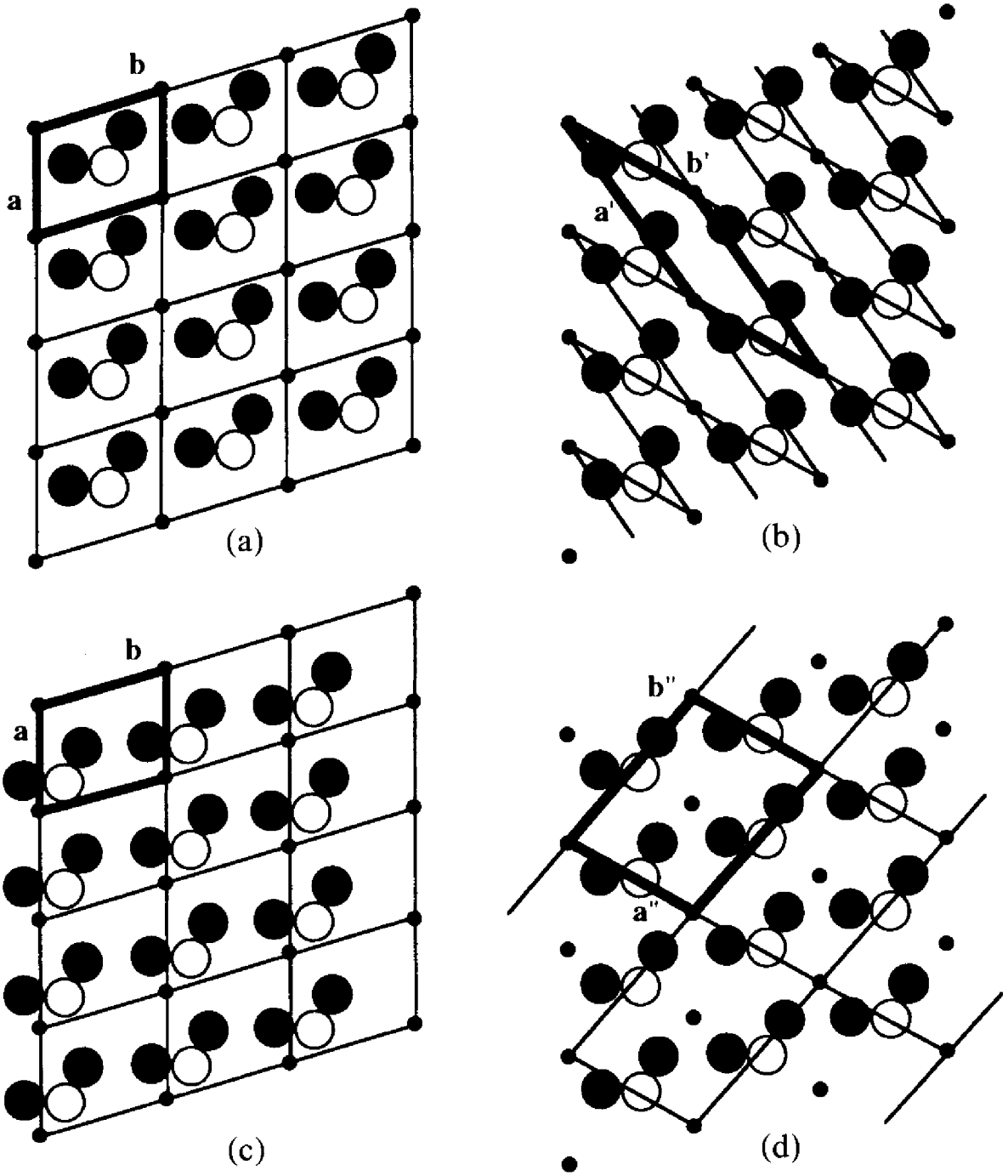


Fig. 1.8. Structure, motif, translational lattice and lattice base

the vectors:

$$\mathbf{R}_{j,uvw} = (x_j + u)\mathbf{a} + (y_j + v)\mathbf{b} + (z_j + w)\mathbf{c} \quad (1.22)$$

where $0 \leq x_j, y_j, z_j < 1$; u, v, w being integers.

The lattice points do not represent atoms or other physical objects. The lattice only describes the periodicity of the structure, i.e. a symmetry property.

Figures 1.8(b), 1.8(c) and 1.8(d) all represent the same structure and the same translational lattice as Fig. 1.8(a). In Fig. 1.8(c) we have chosen another origin for the coordinate system. In Fig. 1.8(b) we have chosen another base $\mathbf{a}' = 2\mathbf{a} + \mathbf{b}$, $\mathbf{b}' = \mathbf{a} + \mathbf{b}$. The area of the cell in Fig. 1.8(b) is the same as in Fig. 1.8(a): $\mathbf{a}' \times \mathbf{b}' = \mathbf{a} \times \mathbf{b}$. If the determinant of the transformation matrix between the systems $(\mathbf{a}', \mathbf{b}')$ and (\mathbf{a}, \mathbf{b}) is equal to ± 1 , the area of the cell remains unchanged. Analogously, if the determinant of the transformation matrix between the systems $(\mathbf{a}', \mathbf{b}', \mathbf{c}')$ and $(\mathbf{a}, \mathbf{b}, \mathbf{c})$ in a three-dimensional structure is equal to ± 1 , the volume of the cell remains unchanged. If the determinant is negative, we pass from a right-handed coordinate system to a left-handed one or vice versa. This determinant is equal to 2 in Fig. 1.8(d) where $\mathbf{a}'' = \mathbf{a} + \mathbf{b}$ and $\mathbf{b}'' = -\mathbf{a} + \mathbf{b}$. The corresponding cell has double the area. The coordinates of the lattice points with respect to $(\mathbf{a}'', \mathbf{b}'')$ are (u, v) and $(u + 1/2; v + 1/2)$ where u and v are integers, i.e. $(\mathbf{a}'' + \mathbf{b}'')/2$ is a translation.

A cell is *primitive* or *simple* if the base is chosen in such a way that the lattice points have integral coordinates. The set of equivalent points is thus given by equation (1.22). A cell is *centered* or *multiple* if there are translations with non-integral coordinates and then the cell contains several lattice points. In this case it is sufficient to give the fractional coordinates of the translations, e.g. we symbolize the set of translations $u + 1/2, v + 1/2, w + 1/2$ with u, v and w being integers by the notation $(1/2, 1/2, 1/2)$. Table 1.1 shows the symbols which represent the set of points equivalent by translation to the point x_j, y_j, z_j for a diverse set of multiple cells.

It is always possible to choose a primitive cell. The discussion of the conditions which lead us, in certain cases to choose a multiple cell will be left until later (Section 2.6.1, Bravais lattices). For the moment, it is sufficient to indicate that, in the presence of rotational or mirror symmetry, we choose the vectors \mathbf{a}, \mathbf{b} and \mathbf{c} to

Table 1.1. Translations and symbols for multiple cells. Alternatively we write $(0\ 0\ 0, 0\ 1/2\ 1/2) +$ for an A centered lattice, or $(0\ 0\ 0, 0\ 1/2\ 1/2, 1/2\ 0\ 1/2, 1/2\ 1/2\ 0) +$ for an F centered lattice, etc.

Translations	Point j	Cell	Symbol
	x_j, y_j, z_j	primitive (or simple) cell	P
$(0, 0, 0) +$	$(0, 1/2, 1/2) +$ x_j, y_j, z_j	cell centered on the (\mathbf{b}, \mathbf{c}) face	A
$(0, 0, 0) +$	$(1/2, 0, 1/2) +$ x_j, y_j, z_j	cell centered on the (\mathbf{a}, \mathbf{c}) face	B
$(0, 0, 0) +$	$(1/2, 1/2, 0) +$ x_j, y_j, z_j	cell centered on the (\mathbf{a}, \mathbf{b}) face	C
$(0, 0, 0) +$	$(0, 1/2, 1/2) +$ $(1/2, 0, 1/2) +$ $(1/2, 1/2, 0) +$ x_j, y_j, z_j	cell centered on all the faces	F
$(0, 0, 0) +$	$(1/2, 1/2, 1/2) +$ x_j, y_j, z_j	body (inner) centered cell	I
$(0, 0, 0) +$	$(2/3, 1/3, 1/3) +$ $(1/3, 2/3, 2/3) +$ x_j, y_j, z_j	rhombohedral cell	R

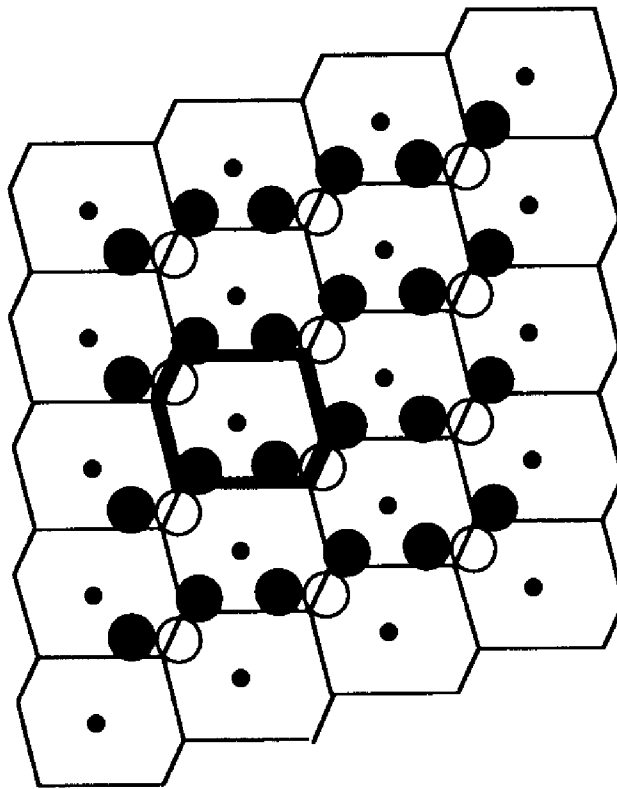


Fig. 1.9. Wigner–Seitz cells, a periodic space tiling

follow the elements of symmetry. The resulting cell thus has its own particular metrical parameters, but it is not necessarily primitive.

Note that it is possible to divide up the structure in a variety of ways into unit volume elements which contain the motif and which allow us to obtain the complete structure by periodic repeats (Fig. 1.9). The only requirement is that these repeating volume elements be a space tiling. However, *the cell of a lattice is always a parallelepiped by definition.*

1.4.2 EDGES, FACES AND LATTICE

A straight line that passes through two, and hence, an infinite number of lattice points is a lattice line. A simple translation vector $\mathbf{T} = U\mathbf{a} + V\mathbf{b} + W\mathbf{c}$ (U, V, W being coprime integers) defines the direction of a set of parallel lattice lines equivalent by translation. It is easy to see that the greater the separation between the lines, the smaller is the norm of the translation $\|\mathbf{T}\|$.

A plane which passes through three lattice points (and hence through an infinite number of *lattice points*) is a ***lattice plane***. Planes equivalent by translation form a family of regularly spaced *lattice planes*. The greater the distance between the planes, the smaller is the area of the primitive two-dimensional cell because all the primitive cells of the lattice have the same volume. Figure 1.10 shows a family of parallel planes numbered consecutively with plane 0 passing

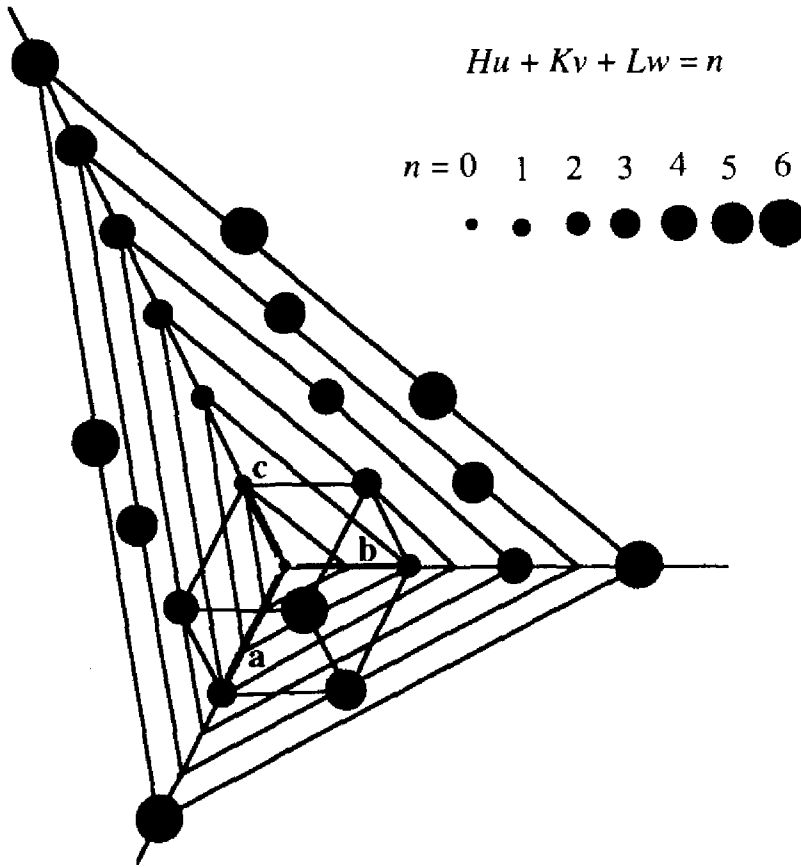


Fig. 1.10. The family of lattice planes $(H \ K \ L) = (3 \ 2 \ 1)$

through the origin. The equation of the first plane is $Hu + Kv + Lw = 1$ where u, v, w are the coordinates of the lattice points in the plane and H, K, L are the reciprocals of the lengths cut by the plane on $\mathbf{a}, \mathbf{b}, \mathbf{c}$ (in units of a, b, c). Because the lengths cut by the n th plane are n times larger than those cut by the first plane, the equation of the n th plane is $Hu + Kv + Lw = n$ (n integer). Each lattice point ($-\infty < u, v, w < +\infty$) is found on one of the planes of the family. It thus follows that H, K and L are whole numbers. If H, K and L have a common factor m , $(H, K, L) = m(H', K', L')$ with H', K', L' and m being integers. The equation of the first plane then becomes $H'u + K'v + L'w = 1/m = \text{integer}$, hence $m = 1$. H, K and L are thus coprime integers.

The analogy between the equations representing the edges and faces of a crystal on the one hand, with lattice lines and lattice planes on the other is the foundation of the theory of the periodic nature of crystal structures. This interpretation of the law of rational indices was formulated by the French abbé Auguste Bravais (1811–1863) as follows:

The faces of a crystal are parallel to lattice planes with a high density of lattice points; the edges are parallel to lattice lines generated by short translations.

1.4.3 RECIPROCAL LATTICE

The reciprocal coordinate system was defined above (1.2). If $\mathbf{a}^*, \mathbf{b}^*, \mathbf{c}^*$ are the reciprocal base vectors of the vectors $\mathbf{a}, \mathbf{b}, \mathbf{c}$, the vector $\mathbf{r}^* = H\mathbf{a}^* + K\mathbf{b}^* + L\mathbf{c}^*$ (H, K, L being coprime integers) represents the normal to the plane $Hu + Kv + Lw = 1$. Its norm is $\|\mathbf{r}^*\| = 1/d_{HKL}$ where d_{HKL} is the distance of the plane from the origin, and hence the distance between consecutive planes in the same family. The *reciprocal lattice* is the set of vectors

$$\mathbf{r}^* = h\mathbf{a}^* + k\mathbf{b}^* + l\mathbf{c}^* \quad (-\infty < h, k, l < +\infty; h, k, l \text{ being integers}) \quad (1.23)$$

The relationships between the direct crystal lattice and the reciprocal lattice are summarized in Table 1.2 and Fig. 1.11.

Table 1.2. Relationships between the direct crystal lattice and the reciprocal lattice

$\mathbf{a} \ \mathbf{b} \ \mathbf{c}$	$\mathbf{a}^* \ \mathbf{b}^* \ \mathbf{c}^*$
family of lattice planes (HKL) with spacing d_{HKL} , (HKL) being coprime integers	lattice line $\mathbf{t}^* = h\mathbf{a}^* + k\mathbf{b}^* + l\mathbf{c}^*$ with $(h \ k \ l) = m(H \ K \ L)$; norm $\ \mathbf{t}^*\ = m/d_{HKL}$
lattice line $\mathbf{t} = u\mathbf{a} + v\mathbf{b} + w\mathbf{c}$ with $(u \ v \ w) = m(U \ V \ W)$; norm $\ \mathbf{t}\ = m/d_{HKL}^*$	family of lattice planes (UVW) with spacing d_{UVW}^* , (UVW) being coprime integers

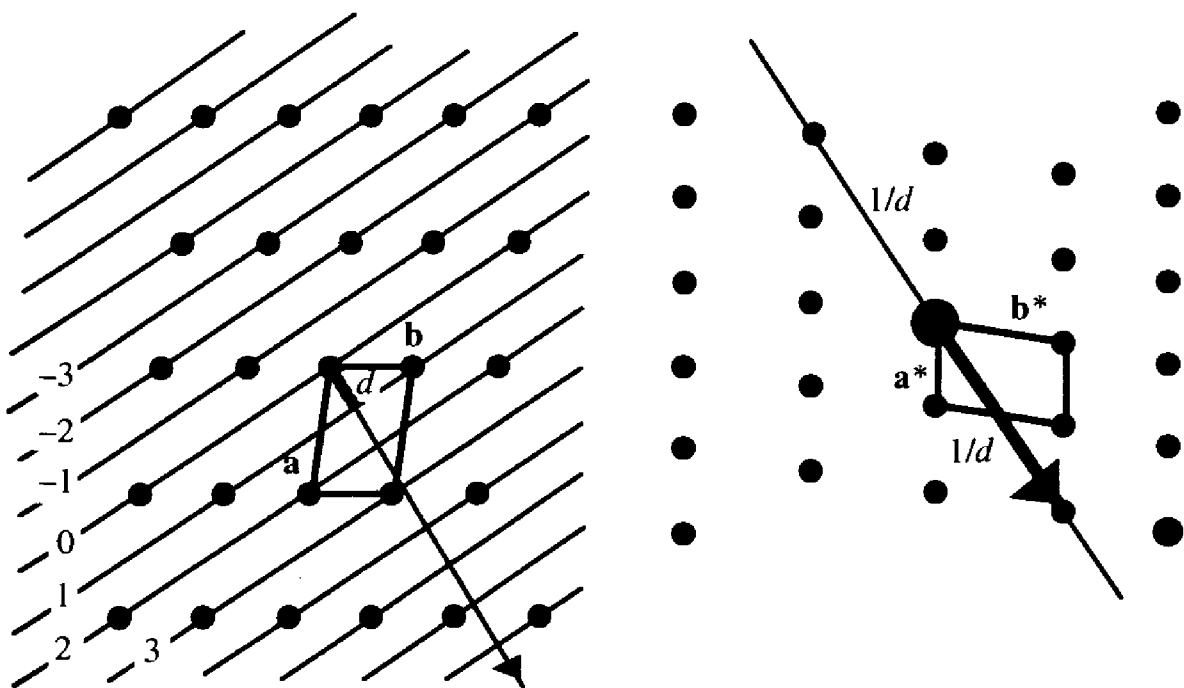


Fig. 1.11. Crystal lattice and reciprocal lattice

1.5 WHAT IS A CRYSTAL?

In the preceding pages, we have defined the idea of a crystal by the three-dimensional periodicity of the atomic distribution; the crystal is thus characterized by long-range order. This classical definition of the crystal is of fundamental importance and, because of this, is the central theme of the present work. However, it does not include all structures which are rigorously ordered, and represents only an idealization of real crystals whose order is never perfect.

1.5.1 QUASI-PERIODIC AND APERIODIC STRUCTURES

These are crystal structures which have perfect long-range order but which are only approximately periodic, *incommensurate crystals* on the one hand, and *quasi-crystals* on the other.

Figure 1.12 shows a simple example of an incommensurate (or modulated) structure. The square grid represents a perfect crystal lattice. However, the atoms do not occupy the corners of the squares. They are displaced relative to the ideal positions according to a plane sinusoidal modulation wave whose wavelength λ is *incommensurate* with the length of the translation b ; λ/b is an irrational number.

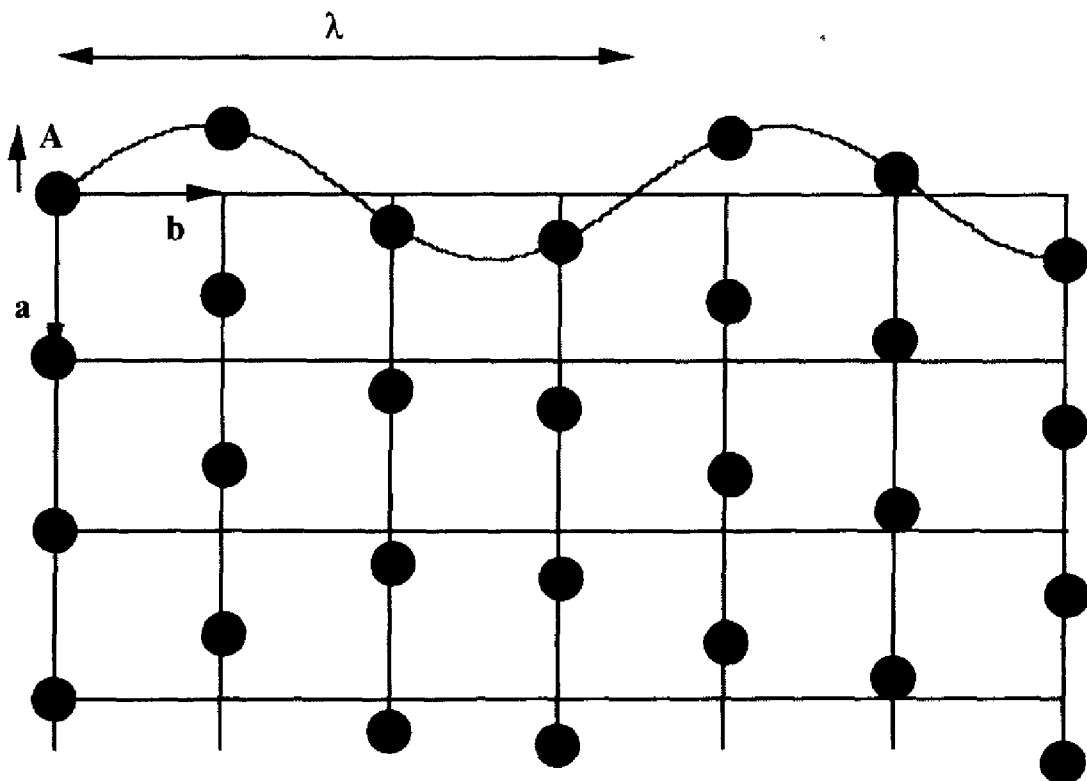


Fig. 1.12. Example of an incommensurate structure. The atoms are displaced from their (a, b) lattice positions by a transverse modulation wave of wavelength λ and amplitude A

The resulting structure is not strictly periodic in the \mathbf{b} direction. The atomic positions of an incommensurate structure made up of several types of atom are

$$\begin{aligned} \mathbf{R}_{j,uvw} &= \mathbf{r}_j + \mathbf{n}_{uvw} + \mathbf{A}_j \sin[\mathbf{q} \cdot (\mathbf{r}_j + \mathbf{n}_{uvw}) + \Phi_j] \\ \mathbf{r}_j + \mathbf{n}_{uvw} &= (x_j + u)\mathbf{a} + (y_j + v)\mathbf{b} + (z_j + w)\mathbf{c} \\ \|\mathbf{q}\| &= 2\pi/\lambda \end{aligned} \tag{1.24}$$

The translations $\mathbf{n}_{uvw} = u\mathbf{a} + v\mathbf{b} + w\mathbf{c}$ are those of the periodic structure whose atomic positions are $\mathbf{r}_j + \mathbf{n}_{uvw}$ following equation (1.22); \mathbf{q} is the wave vector of the modulation and λ the wavelength; \mathbf{A}_j is the amplitude of the modulation of atom j whose polarization may be longitudinal, transverse or oblique with respect to \mathbf{q} ; Φ_j is the phase of the wave with respect to some reference origin. Clearly, the modulation wave can be more complex than a sine wave. We can also imagine several modulation waves in two, or even three, directions in space. Equation (1.24) represents four periodicities, the three of the perfect lattice and that of the modulation wave. We can represent this fact by a *strictly periodic structure in four dimensions*, thus describing the corresponding reciprocal lattice by adding a vector derived from \mathbf{q} to the three-dimensional base $\mathbf{a}^*, \mathbf{b}^*, \mathbf{c}^*$. In the case of several modulations, lattices of five or six dimensions are generated. We obtain the distribution of the atoms from the intersection of the four-dimensional structure with three-dimensional space. The study of incommensurate structures has led to the development of crystallography in dimensions higher than three.

Figure 1.13 shows another type of incommensurate structure called a *composite structure*. It is characterized by the interpenetration of two independent lattices of different atoms whose dimensions are incommensurate. The com-

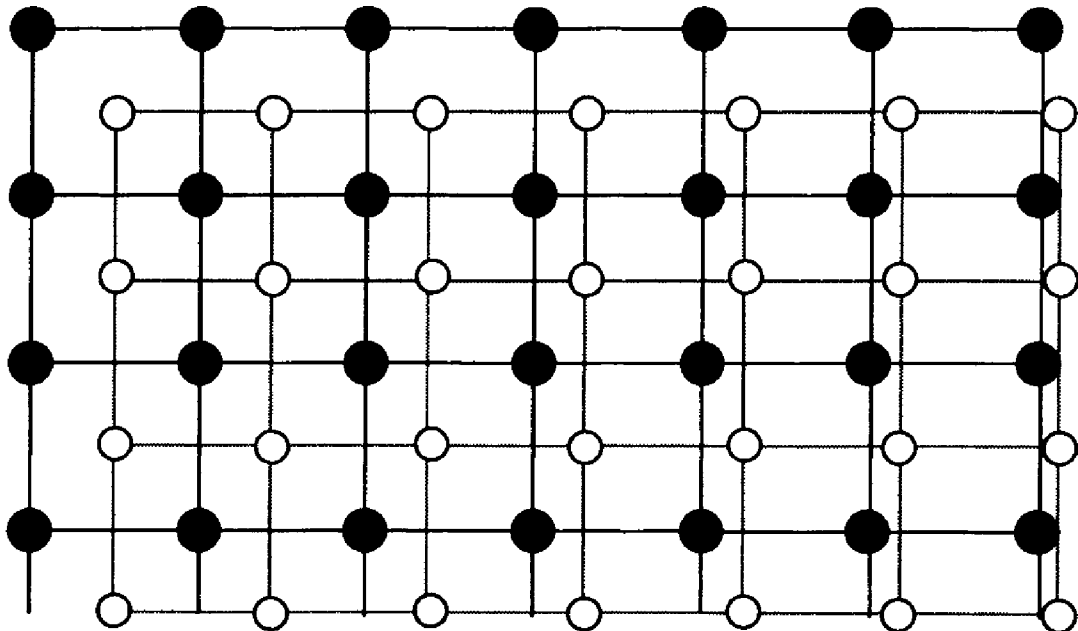


Fig. 1.13. Composite crystal

pound $\text{Hg}_{3-x}\text{AsF}_6$ is a good example of such a structure. The Hg atoms form linear chains whose periodicity is incommensurate with that of the arrangement of the AsF_6 octahedra.

Quasi-crystals have macroscopic symmetries which are incompatible with a crystal lattice (Section 2.4.1). The first example was discovered in 1984; when the alloy AlMn is rapidly quenched, it forms quasi-crystals of icosahedral symmetry (Section 2.5.6). It is generally accepted that the structure of quasi-crystals is derived from aperiodic space filling by several types of unit cell rather than one unique cell. In two-dimensional space, the best-known example is that of Penrose tiling. It is made up of two types of rhombus and has fivefold symmetry. We assume that the icosahedral structure of AlMn is derived from a three-dimensional stacking analogous to Penrose tiling. As is the case for incommensurate crystals, quasi-crystals can be described by perfectly periodic lattices in spaces of dimension higher than three; in the case of AlMn, we require six-dimensional space.

Quasi-crystals are currently of great scientific interest. Nonetheless, the vast majority of all solid bodies are made up of crystals which possess periodic structures. For this reason, the following chapters will deal exclusively with three-dimensional crystallography.

1.5.2 REAL STRUCTURES, ORDER AND DISORDER

Exact, perfect order of a periodic or quasi-periodic crystal is never obtained by a real atomic arrangement. All real crystals are more or less disordered. We describe the disorder by the term *structural defect* with respect to the idealized periodic structure. Many crystal properties (e.g. electrical conductivity and mechanical properties) are strongly dependent on the defect structure.

For certain disorders, we can define an average structure with a perfect translational lattice. The most important ubiquitous disorder is due to the *thermal motion* of the atoms. The atoms vibrate about their average positions which, themselves, form a perfectly periodic arrangement. Translational symmetry is thus obtained only for the time-averaged structure. Another type of defect, observed most frequently in alloys, is *chemical (compositional) disorder*. In this case, the atomic positions form a periodic system, but they may be occupied by different atom types in a more or less random manner. The spatial average of the structure thus has translational symmetry. For example, in the copper–gold alloys AuCu_x , the degree of order is extremely variable according to the composition, x , and the thermal treatment of the material. An incommensurate structure also exists in which the occupation of the atomic sites varies in a periodic manner.

Other types of disorder partially destroy the long-range order and the structure approaches that of a liquid. *Vacancies* and *interstitial atoms* are point defects. *Dislocations* are linear defects of fundamental importance for the mechanical properties of materials. The interface between crystal regions with different

orientations (grain boundaries) constitute two-dimensional defects. Certain structures are only periodic in two dimensions and more or less disordered in the third (e.g. layer stacking in graphite or the micas). Finally, *liquid crystals* are liquids in which the molecules (generally linear organic molecules) are more or less aligned and hence exhibit a certain order.

What is a crystal? The boundary between crystalline and amorphous (or liquid) matter is variable and poorly defined. However, translational symmetry, even if only imperfectly attained, is fundamental to the determination (Chapter 3), the description (Chapter 2) and the theoretical interpretation of solid state structures. It represents the principal characteristic of the majority of solids. For this reason, this is the general theme of the present work.

CHAPTER 2

Symmetry

2.1 INTRODUCTION

Man appears to have an innate appreciation of the principles of symmetry. Every civilization, from ancient Egypt to classical Greece, from the Arabian empires to the American Indians, has produced symmetrical ornaments and friezes, and has intuitively discovered the mathematical principles underlying the construction of periodic patterns. It was not until the 19th and 20th centuries that group theory was rigorously formulated by mathematicians. Today, the fundamental importance of symmetry to the exact sciences is fully appreciated.

Since the original formulation of the *law of symmetry* by R.-J. Haüy (1815), the study of symmetry has become one of the foundations of crystallography. (For an historical overview, see J. J. Burckhardt, *Die Symmetrie der Kristalle*, Birkhäuser, Basel, 1988.) The space groups describing the symmetry of periodic structures were initially tabulated by P. Niggli (*Geometrische Kristallographie des Diskontinuums*, 1919) in order to meet the needs of crystallographers to apply them effectively to the determination of crystal structures by X-ray diffraction (Chapter 3). This work was followed by other compilations which have been continuously improved. The latest edition of the *International Tables for Crystallography* was recently published by the *International Union of Crystallography*:

International Tables for Crystallography, Vol. A, Space Group Symmetry, edited by Theo Hahn, D. Reidel Publishing Company, Dordrecht (Holland)/Boston (USA), 1992.

This chapter serves as an introduction to the contents and use of this reference book which the reader may consult for further details. Note that the previous edition of the *International Tables* is still to be found in many libraries and laboratories:

International Tables for X-Ray Crystallography, Vol. I, Symmetry Groups, edited by Norman F. Henry and Kathleen Lonsdale, The Kynoch Press, Birmingham (England), 1952, 1969.

2.2 SYMMETRY OPERATIONS

2.2.1 AFFINE TRANSFORMATIONS

The invariance of an object or a structure with respect to some operation is called *symmetry*. A *geometrical symmetry operation* is the mapping of space onto itself. It transforms an object into itself without distortion. It is also called an *isometry*.

In a wider sense, the terms symmetry and order are synonymous. Everything which is invariant or structured conveys the presence of symmetry, as, for example, the laws of conservation in physics. Symmetry and the lack of symmetry (asymmetry) play a major role in all artistic expression such as architecture, painting and music.

A geometrical symmetry operation can be *represented* by an *affine transformation* of the type:

$$\begin{pmatrix} x'_1 \\ x'_2 \\ x'_3 \end{pmatrix} = \begin{pmatrix} \Gamma_{11} & \Gamma_{12} & \Gamma_{13} \\ \Gamma_{21} & \Gamma_{22} & \Gamma_{23} \\ \Gamma_{31} & \Gamma_{32} & \Gamma_{33} \end{pmatrix} \begin{pmatrix} x_1 \\ x_2 \\ x_3 \end{pmatrix} + \begin{pmatrix} t_1 \\ t_2 \\ t_3 \end{pmatrix}$$

$$\mathbf{x}' = \mathbf{R} \mathbf{x} + \mathbf{t} \quad (2.1)$$

We designate the operation by the abbreviated symbol (\mathbf{R}, \mathbf{t}) . Figure 2.1 shows a polygon and its image obtained from an affine transformation.

The matrix \mathbf{R} transforming \mathbf{x} into \mathbf{x}' as well as \mathbf{r} into \mathbf{r}' is *independent* of the choice of origin for the coordinate system, however, it clearly depends on the

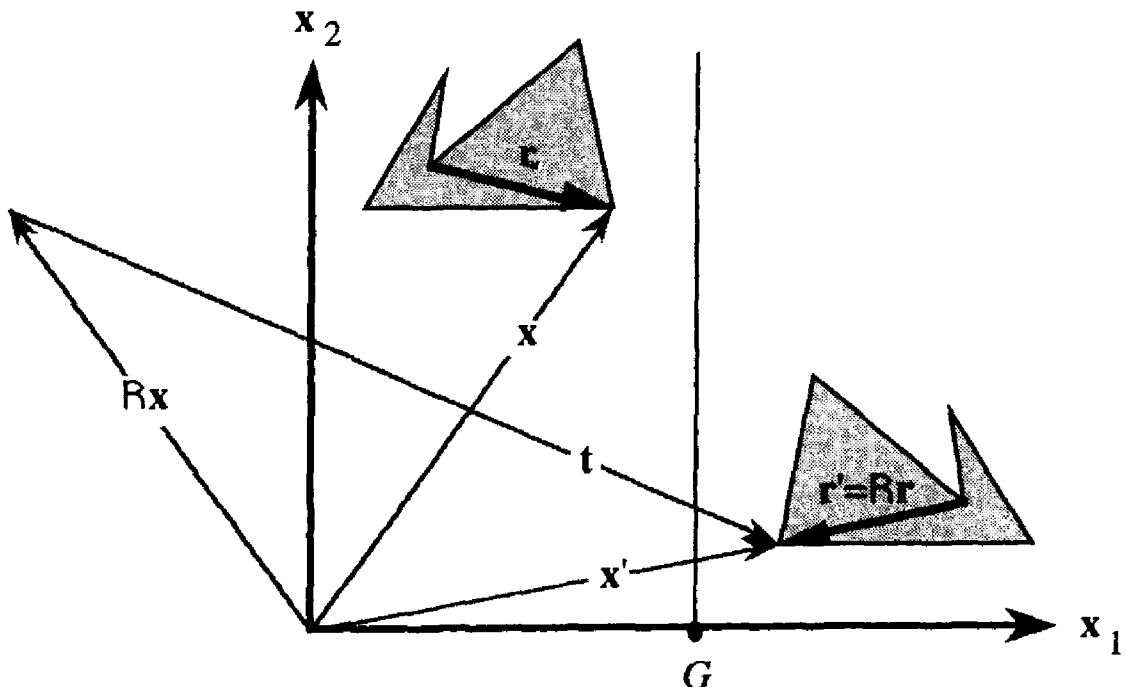


Fig. 2.1. Example of an affine transformation (\mathbf{R}, \mathbf{t}) . The vector \mathbf{r} and its image \mathbf{r}' are associated with equivalent polygons

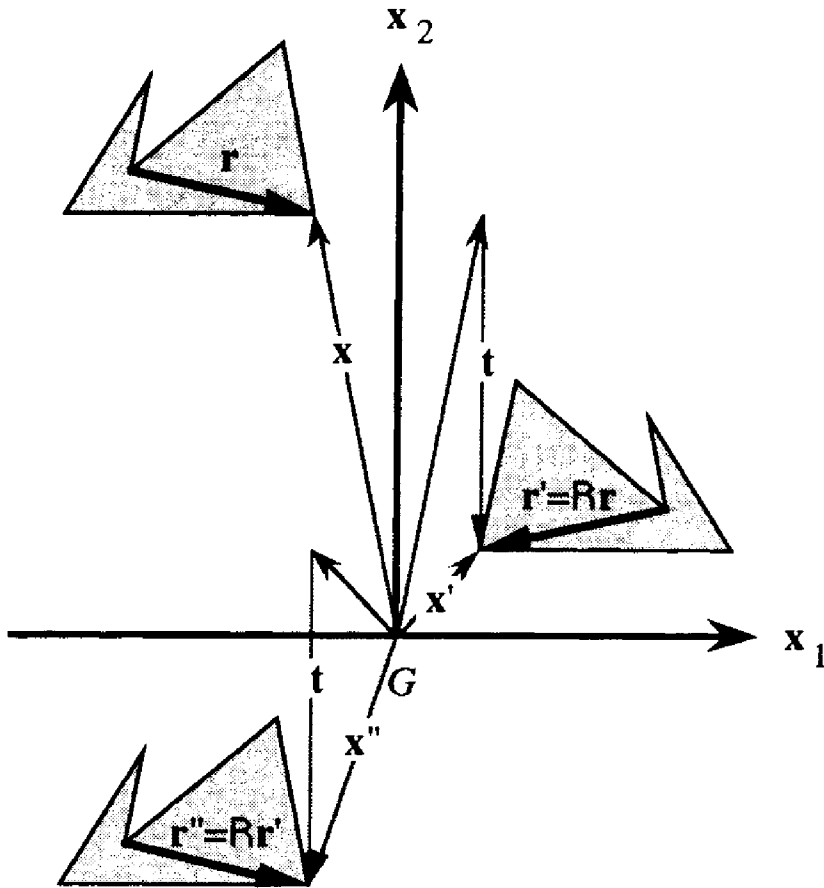


Fig. 2.2. Repeat of the affine transformation in Fig. 2.1

choice of the axes x_1 and x_2 . The vector t is dependent on the choice of the origin. If the point G in Fig. 2.1 is chosen as origin, then the vector t is parallel to x_2 (Fig. 2.2). Successive applications of (R, t) symbolized by $(R, t)^2 = (R^2, Rt + t)$, $(R, t)^3 = (R^3, R^2t + Rt + t), \dots$, generate a symmetrical structure (Fig. 2.2) which is invariant with respect to both (R, t) and its powers $(R, t)^n$.

2.2.2 GROUPS

If a structure is invariant with respect to two symmetry operations (P, t_p) and (Q, t_q) , then it is clearly invariant with respect to the successive application of the two operations. We call this successive application the *product*. If we first apply (P, t_p) and then (Q, t_q) , the vector x is transformed into $x'' = Qx' + t_q = QPx + Qt_p + t_q$. The multiplication of the matrices Q and P is thus carried out *from right to left*. We first apply P and then Q :

$$\begin{aligned} (Q, t_q)(P, t_p) &= (QP, Qt_p + t_q) \\ (P, t_p)(Q, t_q) &= (PQ, Pt_q + t_p) \end{aligned} \tag{2.2}$$

In general, the multiplication is not commutative.

The *identity operation* $(\mathbf{E}, \mathbf{0})$ is a symmetry operation that belongs to all possible objects. \mathbf{E} is the identity represented by a unit matrix and $\mathbf{0}$ is a vector of zero length.

If $(\mathbf{P}, \mathbf{t}_p)$ is a symmetry operation, then the *inverse operation* $(\mathbf{P}, \mathbf{t}_p)^{-1}$ such that $(\mathbf{P}, \mathbf{t}_p)(\mathbf{P}, \mathbf{t}_p)^{-1} = (\mathbf{P}, \mathbf{t}_p)^{-1}(\mathbf{P}, \mathbf{t}_p) = (\mathbf{E}, \mathbf{0})$ is also a symmetry operation. From equation (2.2) we can show that:

$$(\mathbf{P}, \mathbf{t}_p)^{-1} = (\mathbf{P}^{-1}, -\mathbf{P}^{-1}\mathbf{t}_p) \quad (2.3)$$

The product of symmetry operations is *associative*:

$$\begin{aligned} \{(\mathbf{R}, \mathbf{t}_R)(\mathbf{Q}, \mathbf{t}_Q)\}(\mathbf{P}, \mathbf{t}_P) &= (\mathbf{R}, \mathbf{t}_R)\{(\mathbf{Q}, \mathbf{t}_Q)(\mathbf{P}, \mathbf{t}_P)\} \\ &= (\mathbf{RQP}, \mathbf{RQt}_P + \mathbf{Rt}_Q + \mathbf{t}_R) \end{aligned} \quad (2.4)$$

These properties are the axioms defining a group.

The symmetry operations of an object form a group.

The group made up of the operation $(\mathbf{R}, \mathbf{t}_R)$ and its powers $(\mathbf{R}, \mathbf{t}_R)^2, (\mathbf{R}, \mathbf{t}_R)^3, \dots, (\mathbf{R}, \mathbf{t}_R)^n$ is a *cyclic group*. If all the operations of a group commute, $(\mathbf{R}_j, \mathbf{t}_j)(\mathbf{R}_i, \mathbf{t}_i) = (\mathbf{R}_i, \mathbf{t}_i)(\mathbf{R}_j, \mathbf{t}_j)$ for all pairs (i, j) , the group is *Abelian*.

The matrices \mathbf{R} and the vectors \mathbf{t} constitute a *representation of the group* of the symmetry operations linked to the choice of coordinate system and its origin. For a given group, there is an infinite number of representations, each corresponding to a particular coordinate system.

2.2.3 ROTATION, ROTOREFLECTION, ROTOINVERSION

If (\mathbf{R}, \mathbf{t}) is a symmetry operation, the norms of \mathbf{r} and \mathbf{r}' in Figs 2.1 and 2.2 are equal. By choosing a *unitary coordinate system*, we obtain from this condition that $\|\mathbf{r}'\|^2 = \mathbf{r}^T \mathbf{R}^T \mathbf{R} \mathbf{r} = \|\mathbf{r}\|^2$, thus $\mathbf{R}^T \mathbf{R} = \mathbf{E} =$ unit matrix (\mathbf{R}^T is the transpose of the matrix \mathbf{R}). This leads to the result that \mathbf{R} is an *orthogonal matrix*:

$$\mathbf{R}^T = \mathbf{R}^{-1}, |\mathbf{R}| = \pm 1, \text{ unitary coordinate system.} \quad (2.5)$$

The eigenvalues of the orthogonal matrix \mathbf{R} are $e^{i\phi}, e^{-i\phi}, \pm 1$, where ϕ is given by $\cos \phi = [\text{trace}(\mathbf{R}) \mp 1]/2$. We will limit the discussion to $\phi = 2\pi r$, $r = m/n$ being a rational number. \mathbf{R} is related to the matrix \mathbf{U} by a similarity transformation

$$\mathbf{U}(\phi) = \begin{pmatrix} \cos \phi & -\sin \phi & 0 \\ \sin \phi & \cos \phi & 0 \\ 0 & 0 & \pm 1 \end{pmatrix}, \quad \phi = \frac{m}{n} 2\pi; m \text{ and } n \text{ are coprime integers.} \quad (2.6)$$

Thus there must be a matrix \mathbf{X} such that $\mathbf{U}(\phi) = \mathbf{X}^{-1} \mathbf{R} \mathbf{X}$. It is easily shown that $\mathbf{U}^2(\phi) = \mathbf{U}(2\phi)$ and $\mathbf{U}^{-1}(\phi) = \mathbf{U}^T(\phi) = \mathbf{U}(-\phi)$. There must also be an integer $p < n$ such that $pm/n \pmod{1} = 1/n$, hence $\mathbf{U}^p(\phi) = \mathbf{U}(\phi')$, where $\phi' = 2\pi/n$. If $\mathbf{U}(\phi)$

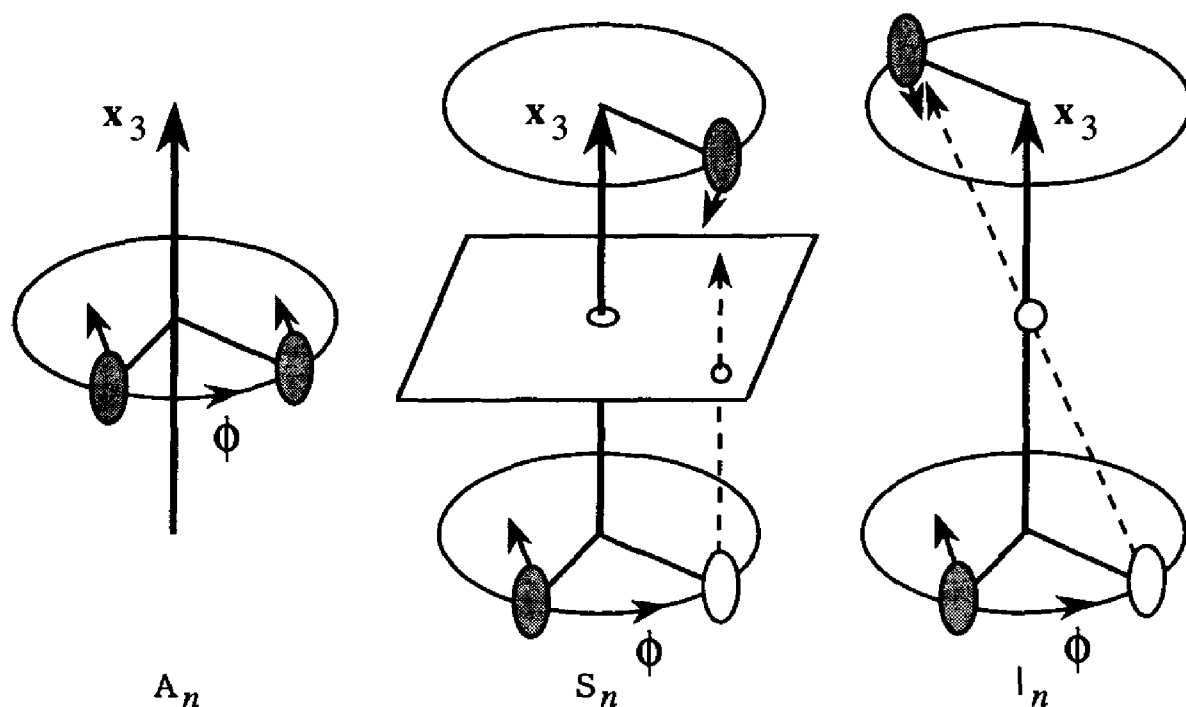


Fig. 2.3. Rotation, rotoreflection and rotoinversion operations

is a symmetry operation, then $U(\phi')$ is also. We distinguish three types of operation as shown in Fig. 2.3. These operations may be represented by the following matrices:

$$\text{rotation } \mathbf{A}_n, \text{ matrix similar to } \begin{pmatrix} \cos \phi & -\sin \phi & 0 \\ \sin \phi & \cos \phi & 0 \\ 0 & 0 & +1 \end{pmatrix}, \quad \phi = \frac{2\pi}{n} \quad (2.7)$$

$$\text{rotoreflection } \mathbf{S}_n, \text{ matrix similar to } \begin{pmatrix} \cos \phi & -\sin \phi & 0 \\ \sin \phi & \cos \phi & 0 \\ 0 & 0 & -1 \end{pmatrix}, \quad \phi = \frac{2\pi}{n} \quad (2.8)$$

$$\text{rotoinversion } \mathbf{I}_n, \text{ matrix similar to } \begin{pmatrix} -\cos \phi & \sin \phi & 0 \\ -\sin \phi & -\cos \phi & 0 \\ 0 & 0 & -1 \end{pmatrix}, \quad \phi = \frac{2\pi}{n} \quad (2.9)$$

A **rotation** \mathbf{A}_n about an axis transforms a left hand into a left hand and a right hand into a right hand. It conserves the *chirality*. It is called an *operation of the first type*. The determinant of any matrix representing an operation of the first type is $|\mathbf{A}_n| = +1$.

A **rotoreflection (improper rotation)** \mathbf{S}_n about an axis is a rotation by the angle ϕ followed by reflection by the plane perpendicular to the axis. This is neither a pure rotation nor a pure reflection, but a combined operation. It transforms a left hand into a right hand and *vice-versa*. This is called an operation of the *second type*. The determinant of any matrix representing an operation of the

Table 2.1. Correspondence between roto-reflections S_n and rotoinversions I_n

$I_1 = S_2 = \text{inversion}$	$S_1 = I_2 = \text{mirror}$
$I_2 = S_1 = \text{mirror}$	$S_2 = I_1 = \text{inversion}$
$I_3 = S_6^{-1} = S_6^5$	$S_3 = I_6^{-1} = I_6^5$
$I_4 = S_4^{-1} = S_4^3$	$S_4 = I_4^{-1} = I_4^3$
$I_5 = S_{10}^{-3} = S_{10}^7$	$S_5 = I_{10}^{-3} = I_{10}^7$
$I_6 = S_3^{-1} = S_3^2$	$S_6 = I_3^{-1} = I_3^2$
$I_7 = S_{14}^{-5} = S_{14}^9$	$S_7 = I_{14}^{-5} = I_{14}^9$
$I_8 = S_8^{-3} = S_8^5$	$S_8 = I_8^{-3} = I_8^5$

second type is $|S_n| = -1$. The roto-reflection S_1 ($\phi = 0$) is identical to the reflection by a symmetry plane, i.e. by a *mirror*. The roto-reflection S_2 ($\phi = \pi$) is an *inversion*, i.e. reflection through a point.

A *rotoinversion* I_n about an axis is a rotation by the angle ϕ followed by an inversion through a point on the axis. This is also a combined operation of the second type which is neither a pure rotation nor a pure inversion. It is easily seen that each rotoinversion is equivalent to a roto-reflection: $I(\phi) = S(\pi + \phi)$, $S(\phi) = I(\pi + \phi)$. Thus, operations of the second type may be represented by either roto-reflections or by rotoinversions. We could limit ourselves to one or other of these two representations. However, the two most commonly used systems of nomenclature applied to geometrical symmetry do not use the same convention. The *Schoenflies* system is based on roto-reflections, whereas the *Hermann–Mauguin* (or *international*) system is based on rotoinversions. In crystallography we prefer to use the Hermann–Mauguin system. The correspondence between I_n and S_n is shown in Table 2.1.

If n is a finite number, $A_n^n = E$ (n even or odd), $S_n^n = I_n^n = E$ (n even), $S_n^{2n} = I_n^{2n} = E$ (n odd), $E = \text{identity}$. The groups formed by the operations A_n and I_n (or S_n) and their powers are *groups of finite order*. If an infinitesimal rotation is a symmetry operation, i.e. $n \rightarrow \infty$, the group is of infinite order (e.g. the symmetry of a cylinder). At least one point in space is invariant with respect to all the A_n and I_n (or S_n) operations.

The groups formed by rotations and rotoinversions (or roto-reflections) are called point groups.

It is important to remember to distinguish between a symmetry operation and its *representation* by a matrix. The latter depends on the coordinate system adopted.

2.2.4 TRANSLATIONS

A simple translation is represented by the operation (E, T_{uvw}) , where E is the identity (represented by a unit matrix), and $T_{uvw} = ua + vb + wc$, a vector of the translation lattice. Translational symmetry allows us to arrange a large number of identical molecules or atoms in such a way that they are all strictly equivalent provided that the crystal is infinitely large (or large compared to the shortest translations). The atoms or molecules on the surface of a crystal are equivalent to each other if they form a two-dimensional translation lattice, i.e. planar faces parallel to specific lattice planes in the three-dimensional lattice (Bravais law, Section 1.4.2).

The group formed by all the translations $T_{uvw} (-\infty \leq u, v, w \leq \infty)$ is of infinite order and Abelian.

The existence of a translation lattice implies long-range order. It is, however, not necessary to assume the existence of forces that act over long distances. For example, a chain under tension has perfect translational symmetry, but each link only interacts with its nearest neighbors (Fig. 2.4). We thus obtain a periodic structure by only specifying the orientation of successive links.

2.3 SYMMETRY ELEMENTS

2.3.1 FIXED POINT, ROTATION AXIS, MIRROR PLANE

Figures 2.1 and 2.2 show that the vector t of a symmetry operation (R, t) depends on the choice of the origin of the coordinate system. Is there a preferred origin?

After a displacement of the origin by a vector v , the affine transformation $x' = Rx + t$ becomes $x' - v = R(x - v) + t_v = (Rx + t) - (Rv + t) + t_v$. The operation (R, t) thus becomes (R, t_v) , the translation being:

$$t_v = (R - E)v + t$$

A point which is transformed into itself by an affine transformation is called a *fixed point*, $x' = Rx + t = x = Ex$; hence $(R - E)x = -t$. We distinguish four cases:

- The matrix $(R - E)$ can be inverted. It has three non-zero eigenvalues and its inverse $(R - E)^{-1}$ exists. By moving the origin of the coordinate system to the



Fig. 2.4. Chain under tension

fixed point, $\mathbf{v} = \mathbf{x} = -(\mathbf{R} - \mathbf{E})^{-1}\mathbf{t}$, the translation vector cancels out, $\mathbf{t}_v = \mathbf{0}$, and the transformation becomes linear $(\mathbf{R}, \mathbf{0})$. This is the case for all the rotoinversions I_n represented by matrices like (2.9), with the exception of the reflection by a mirror characterized by $n = 2$ (or for all the rotoreflections S_n with the exception of $n = 1$). Thus the operation I_1 followed by a translation which transforms the point \mathbf{x} with coordinates (x_1, x_2, x_3) into \mathbf{x}' with the coordinates $(1/2 - x_1, 1/2 - x_2, 1/2 - x_3)$ has a fixed point at $(1/4, 1/4, 1/4)$. We call this point associated with the operation I_1 a *center of inversion* or a *center of symmetry*. Reflection by a plane, $I_2 = S_1$, has no unique fixed point.

- The matrix $(\mathbf{R} - \mathbf{E})$ has one eigenvalue equal to zero and two that are non-zero and, hence, cannot be inverted. This is the case for all the rotations A_n represented by matrices like (2.7) except for the identity \mathbf{E} characterized by $n = 1$. The eigenvector \mathbf{x}_0 corresponding to the zero eigenvalue is the **rotation axis**. It is invariant with respect to \mathbf{R} , $\mathbf{R}\mathbf{x}_0 = \mathbf{x}_0$. A shift of the origin of the coordinate system along the rotation axis does not alter the translation vector \mathbf{t} of the affine transformation, whereas a shift perpendicular to the rotation axis changes the corresponding components of \mathbf{t} . The origin may be chosen to be on the rotation axis. The vector \mathbf{t} can then only have one non-zero component parallel to the axis, e.g. $\mathbf{t} = (0, 0, t_3)$ for a rotation axis parallel to \mathbf{x}_3 . If $\mathbf{t} = \mathbf{0}$, any point on the rotation axis is a fixed point.
- The matrix $(\mathbf{R} - \mathbf{E})$ has two eigenvalues equal to zero and one non-zero eigenvalue. This is the case for a reflection by a plane, $S_1 = I_2$, which is represented by matrices like:

$$I_2 = \begin{pmatrix} 1 & 0 & 0 \\ 0 & 1 & 0 \\ 0 & 0 & -1 \end{pmatrix}, \text{ mirror plane perpendicular to } \mathbf{x}_3.$$

The eigenvector corresponding to the non-zero eigenvalue is normal to the **mirror plane**. The affine transformation (I_2, \mathbf{t}) is invariant with respect to a shift of the origin of the coordinate system in the plane. If we choose an origin in the plane, then the vector \mathbf{t} can have two non-zero components parallel to the plane. Figure 2.2 gives a two-dimensional example: \mathbf{R} represents a reflection line which transforms x_1 into $-x_1$, and \mathbf{t} is parallel to the line. If $\mathbf{t} = \mathbf{0}$, any point on the line is a fixed point.

- The matrix $(\mathbf{R} - \mathbf{E})$ has three eigenvalues equal to zero, thus $\mathbf{R} = \mathbf{E}$. The operation is a pure translation and clearly has no fixed point or preferred origin.

The ensemble of fixed points (points, lines or planes) of a symmetry operation are called **symmetry elements**. To the fixed point of I_n or S_n , we must add the fixed line corresponding to the operation A_n or the plane which is perpendicular to it. Rotation axes correspond to the operations A_n , centers and rotoinversion axes to the operations I_n , and mirror planes and rotoreflection axes to the*

operations S_n . A center of symmetry corresponds to I_1 and a mirror plane to I_2 . Symmetry elements are useful in order to visualize or to represent graphically a symmetry group.

A group is a set of symmetry operations. A symmetry element is a geometrical location. The symbols used to identify symmetry elements are given in Table 2.2. We saw that operations of the second type may be represented either by roto reflections or by rotoinversions (Table 2.1). Table 2.3 shows the equivalence between the corresponding symmetry elements. In terms of elements (and not in terms of operations), the only rotoinversion axes necessary for the representation of groups are $\bar{4}$, $\bar{8}$, etc.. However, all the \bar{n} axes generate cyclic groups; consequently it is preferable to use the symbols $\bar{3}$ and $\bar{6}$ rather than the corresponding combination of rotation axes with a center of symmetry or a mirror plane. Figure 2.5 gives a graphical representation of some of these axes.

Table 2.2. Symbols for the symmetry elements. Note the special symbol m for a mirror plane. $\bar{1}$ represents one unique point

Symmetry element	Symbol
Rotation axis	$1, 2, 3, \dots, x$
Rotoinversion axis	$\bar{1}, \bar{2} = m, \bar{3}, \dots, \bar{x}$
Rotoreflexion axis	$\tilde{1} = m, \tilde{2}, \tilde{3}, \dots, \tilde{x}$

Table 2.3. Equivalence between rotoinversion and roto reflection axes

$\bar{1} = \tilde{2}$	center of symmetry
$\bar{2} = \tilde{1} = m$	mirror plane
$\bar{3} = \tilde{6}$	combination of a threefold axis and a center of symmetry
$\bar{4} = \tilde{4}$	cannot be interpreted as the combination of a rotation axis and either a center of symmetry or a mirror plane
$\bar{6} = \tilde{3}$	combination of a threefold axis and a mirror plane
$\bar{n}, n = 2m + 1$	axis of order n and a center of symmetry, equivalent to a roto reflection axis \tilde{x} , $x = 2n = 4m + 2$
$\bar{n}, n = 4m + 2$	axis of order $1/2n$ and a mirror plane equivalent to a roto reflection axis, \tilde{x} , $x = 1/2n = 2m + 1$
$\bar{n}, n = 4m$	element of symmetry which cannot be decomposed, equivalent to a roto reflection axis \tilde{n}

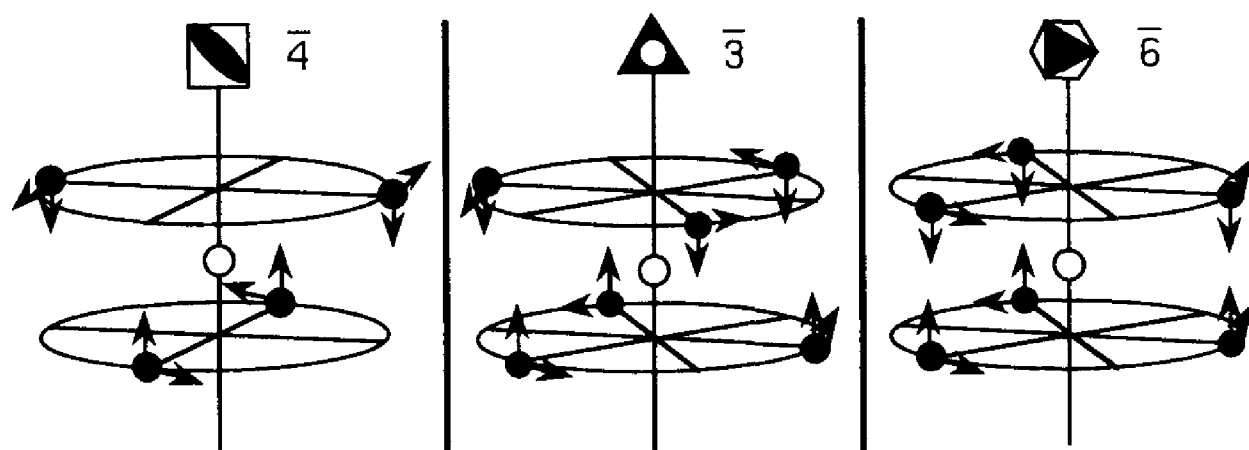


Fig. 2.5. Rotoinversion axes $\bar{4}$, $\bar{3}$ and $\bar{6}$. These axes represent cyclic groups. In contrast, non-cyclic groups are obtained by combining an even-order axis with a center of symmetry or with a perpendicular mirror plane

2.3.2 GLIDE PLANES AND SCREW AXES

Let us suppose that R is of finite order, i.e. $R^n = E$. The successive application of $n(R, t)$ operations then gives us a pure translation T : $(R, t)^n = (E, T)$. Equation (2.2) gives:

$$(R, t)^n = (R^n, [R^{n-1} + R^{n-2} + \dots + R^2 + R + E]t) = \left(R^n, \left[\sum_{x=0}^{n-1} R^x \right] t \right) = (E, T)$$

By pre-multiplying or post-multiplying the sum by R and by $(R - E)$, we obtain:

$$\begin{aligned} R \left[\sum_{x=0}^{n-1} R^x \right] &= \left[\sum_{x=0}^{n-1} R^x \right] R = \left[\sum_{x=1}^n R^x \right] = \left[\sum_{x=0}^{n-1} R^x \right] \\ (R - E) \left[\sum_{x=0}^{n-1} R^x \right] &= \left[\sum_{x=0}^{n-1} R^x \right] (R - E) = 0 \end{aligned} \quad (2.10)$$

0 being a matrix where all the terms are zero. On post-multiplying equation (2.10) by t , we obtain $(R - E)T = 0$ where T is an eigenvector of R , and hence of R^x , with the eigenvalue $+1$. The mean value Ω of the matrices R^x is an idempotent matrix with the properties:

$$\Omega = \frac{1}{n} \left[\sum_{x=0}^{n-1} R^x \right]; \quad \Omega\Omega = \Omega, \quad \Omega t = \frac{1}{n} T$$

The eigenvalues of any idempotent matrix Ω are 0 or $+1$. They correspond to the zero and non-zero eigenvalues of $(R - E)$. We distinguish the same four cases as presented in Section 2.3.1:

- The matrix $(R - E)$ can be inverted, R has a fixed point and $(R - E)^{-1}$ exists, hence, $\Omega = 0$ and $T = 0$. All the eigenvalues of Ω are zero. If the origin of the

coordinate system is located at the fixed point, the operation is a rotoinversion with no translation, I_1, I_3, I_4, \dots , with $t = 0$.

- For the operation A_n corresponding to a rotation axis n where $n \neq 1$, one of the eigenvalues of R and Ω equals 1. The corresponding eigenvector is parallel to the rotation axis. The two other eigenvalues of Ω are zero. If the origin of the

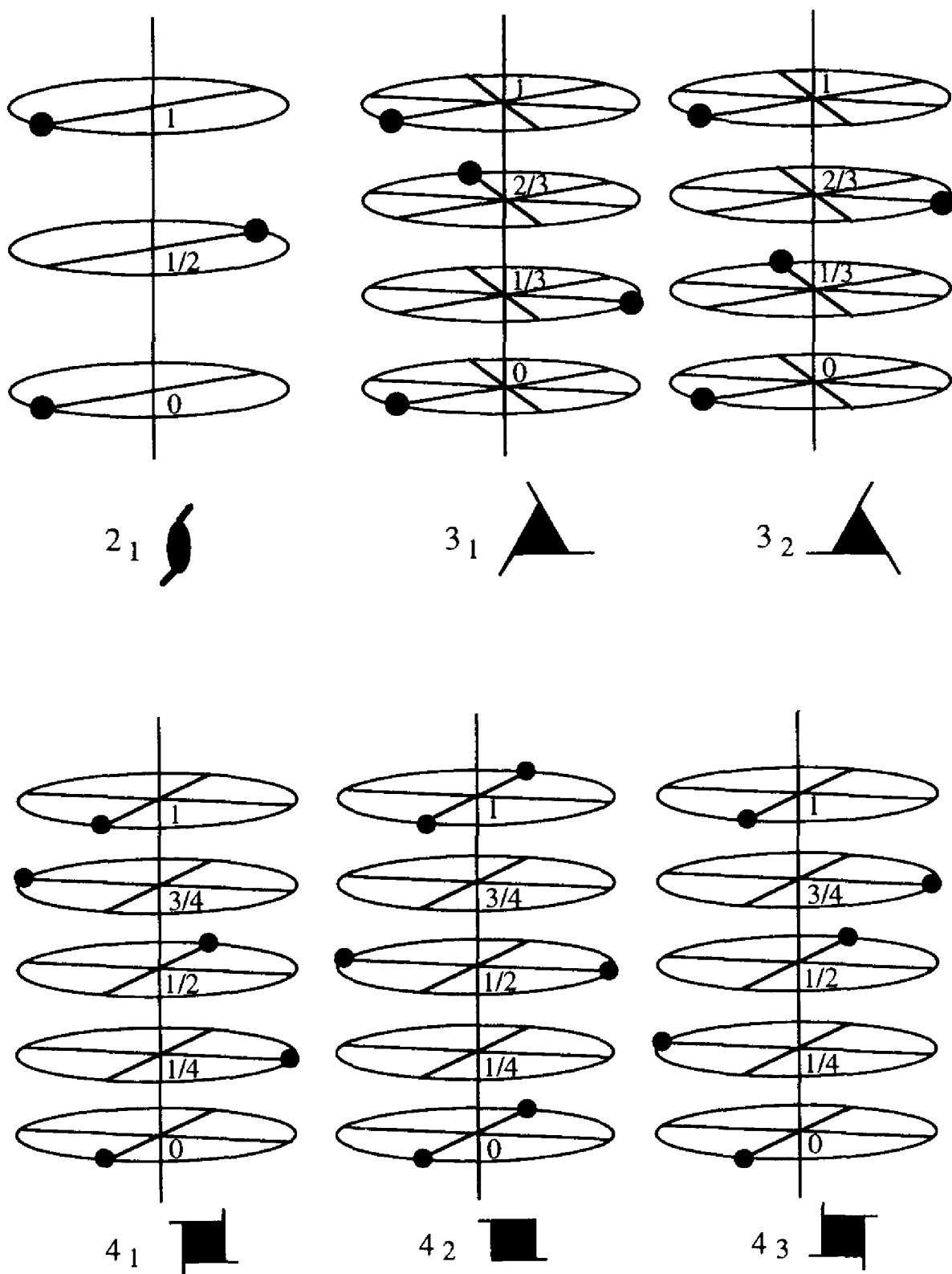


Fig. 2.6. Two-, three- and fourfold screw axes with $t = \frac{1}{2}, \frac{1}{3}, \frac{2}{3}, \frac{1}{4}, \frac{2}{4}$ and $\frac{3}{4}$

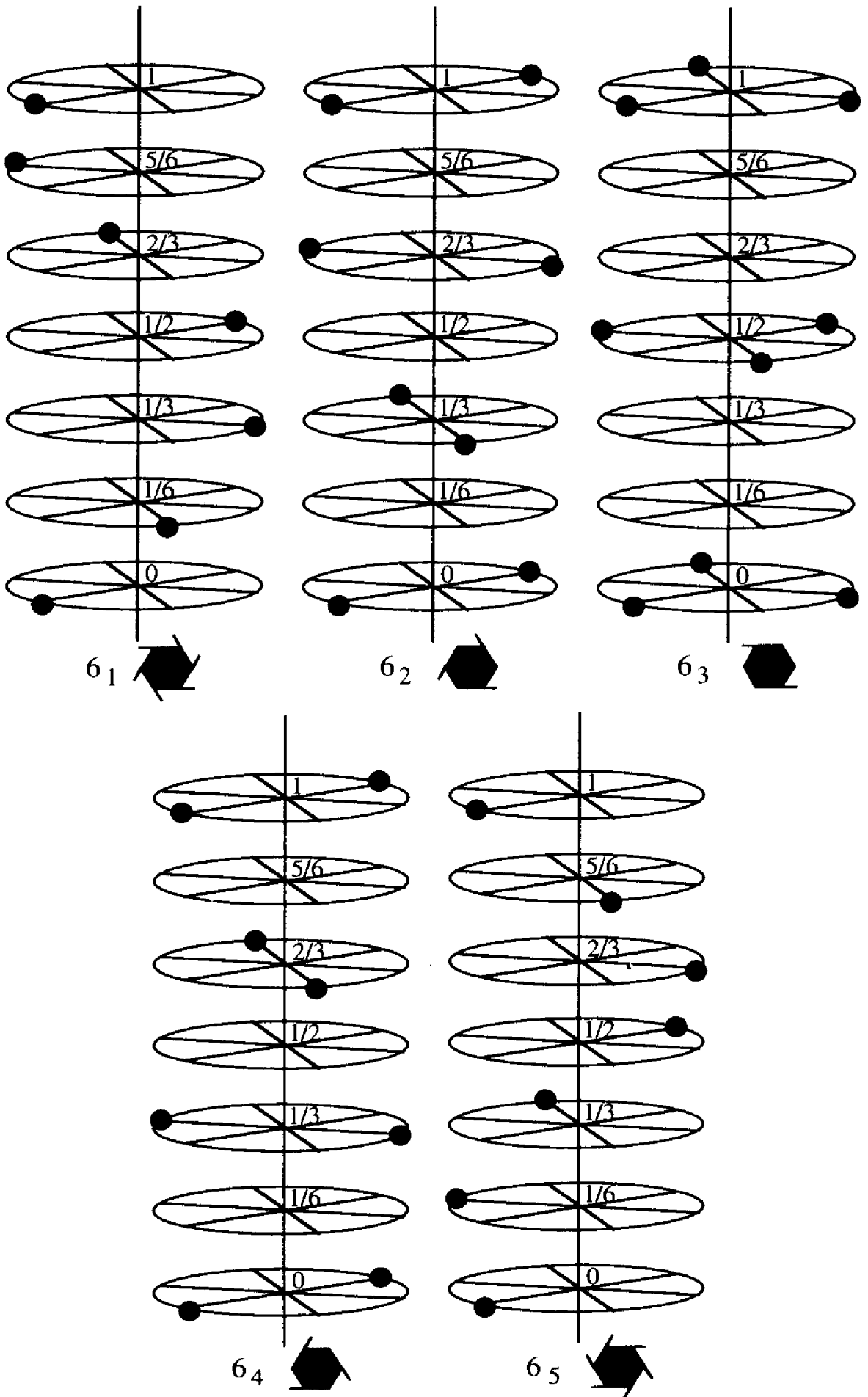


Fig. 2.7. Sixfold screw axes

coordinate system is located on the rotation axis, the vector \mathbf{t} becomes:

$$\mathbf{t} = \frac{m}{n} \mathbf{T}_r, \mathbf{T}_r \text{ being the translation parallel to the rotation axis.} \quad (2.11)$$

The symmetry operation corresponding to the operation (R, \mathbf{t}) is a *screw axis* (the axis is defined by the set of fixed points of A_n). Figures 2.6 and 2.7 show the screw axes corresponding to different values of n and m as well as their numerical (n_m) and graphical symbols.

- For the operation $I_2 = S_1$ (corresponding to a mirror plane m), two of the eigenvalues of R and Ω equal 1. The corresponding eigenvectors are parallel to the mirror plane. If the origin of the coordinate system is located in the plane, the vector \mathbf{t} is reduced to:

$$\mathbf{t} = \frac{1}{2} \mathbf{T}_m, \mathbf{T}_m \text{ being a translation parallel to the mirror plane.} \quad (2.12)$$

This symmetry element is a *glide plane* and is shown in Fig. 2.8 (the plane contains all the fixed points of I_2).

- R is a unit matrix, $R = E = \Omega$, and $\mathbf{t} = \mathbf{T}$ is any translation.

It follows that screw axes and glide planes are the only symmetry elements that are composed of a rotation or a rotoinversion and a translation.

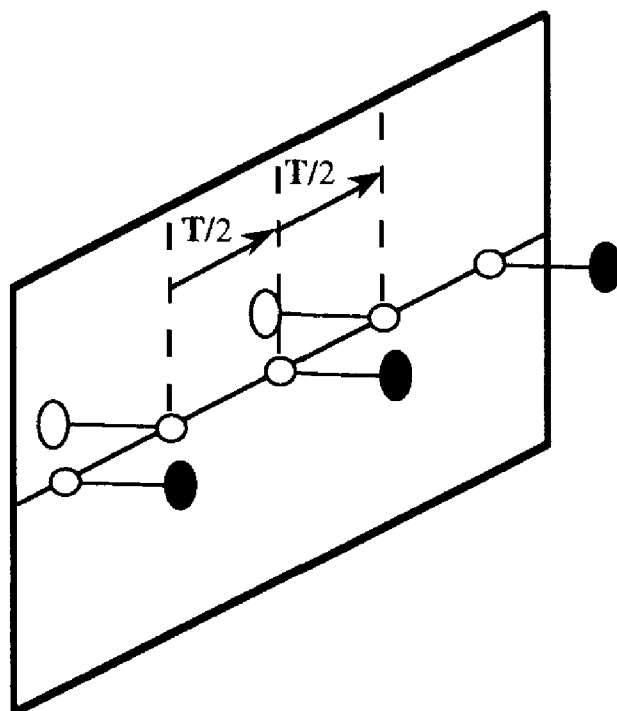






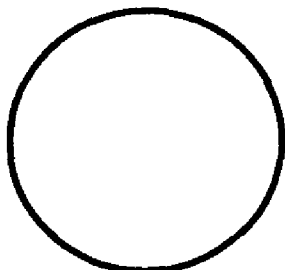







Fig. 2.8. Glide plane

Table 2.4. Symbols for symmetry elements without a translation component

 2-fold rotation axis (operation A_2) symbol 2  2-fold rotation axis parallel to the plane of projection	 3-fold rotation axis (operation A_3) symbol 3
 4-fold rotation axis (operation A_4) symbol 4	 6-fold rotation axis (operation A_6) symbol 6
identity operation A_1 symbol 1	 mirror plane perpendicular to the plane of projection (operation I_2) symbol $m(=2)$  or  mirror plane parallel to the plane of projection
 center of symmetry (operation I_1) symbol $\bar{1}$	
 4-fold rotoinversion axis (operation I_4), symbol $\bar{4}$	
 3-fold rotoinversion axis, equivalent to the combination of a 3-fold rotation axis and a center of symmetry (operation I_3), symbol $\bar{3}$	 6-fold rotoinversion axis, equivalent to the combination of a 3-fold rotation axis and a mirror plane (operation I_6), symbol $\bar{6}$

2.3.3 SYMBOLS USED TO REPRESENT SYMMETRY ELEMENTS

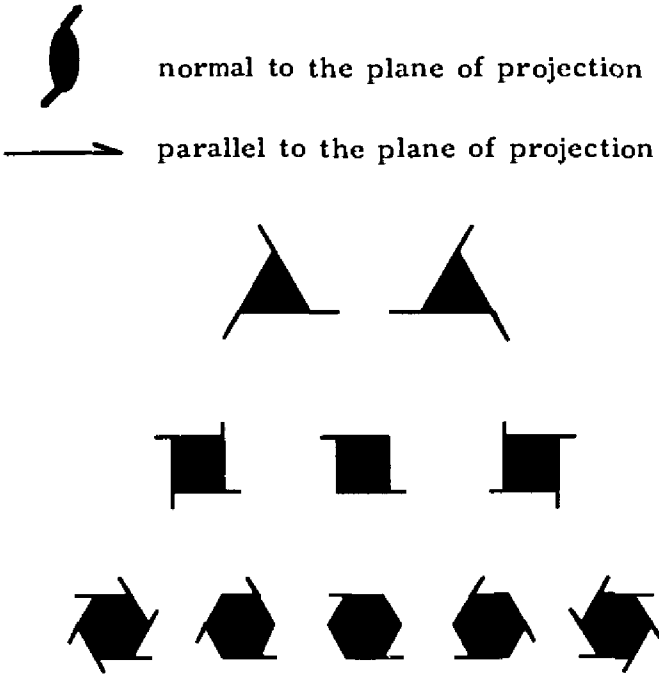

The symbols used to indicate symmetry elements with and without translation components are given in Tables 2.4 and 2.5. Remember that we need to distinguish symmetry operations from symmetry elements, i.e. the operations of rotation (A_n), rotoinversion (I_n) and rotoreflection (S_n) on the one hand, from a rotation axis (n), rotoinversion axis (\bar{n}) or rotoreflection axis (\bar{n}), on the other.

2.4 SYMMETRY AND THE LATTICE METRIC

2.4.1 SYMMETRY ELEMENTS COMPATIBLE WITH TRANSLATIONS

There exist an infinite but enumerable number of point groups formed by the operations A_n and I_n , $1 \leq n < \infty$. They represent the symmetries of macro-

Table 2.5 Symbols for symmetry elements with a translation component

<p>Screw axes</p> <p>2-fold symbol 2_1</p> <p>3-fold symbols $3_1, 3_2$</p> <p>4-fold symbols $4_1, 4_2, 4_3$</p> <p>6-fold symbols $6_1, 6_2, 6_3, 6_4, 6_5$</p>	 <p>normal to the plane of projection</p> <p>parallel to the plane of projection</p>	
<p>Glide planes</p> <p>glide of one half translation a: symbol a</p> <p>glide of one half translation b: symbol b</p> <p>glide of one half translation c: symbol c</p> <p>glide of one half translation a+b, or b+c or a+c: symbol n</p> <p>in F or I centered cells glide of one quarter of the translation a±b, b±c or c±a(F) or a±b±c (I): symbol d</p>	<p>plane perpendicular to the plane of projection</p> <p>— — — — — glide in the plane of projection</p> <p>· · · · · glide normal to the plane of projection</p> <p>, — · · · — glide oblique to the plane of projection</p> <p>: — : > : — : — : < : — glide oblique to the planes d</p>	<p>plane parallel to the plane of projection</p>  <p>the arrow indicates the glide direction</p>

Notes. The d planes may exist in orthorhombic F, tetragonal I, cubic I and cubic F Bravais lattices (Section 2.6.1). In the tetragonal, trigonal, hexagonal and cubic systems (Sections 2.5.8 and 2.5.9) we find mirror planes which are not parallel to the (100), (010) or (001) planes. The glides for the n and d planes corresponding to these orientations are oblique with respect to the a, b, c axes. More detailed information may be found in the *International Tables for Crystallography*.

scopic objects. In contrast, periodic structures do not allow all these symmetry operations, and they are only invariant with respect to a limited number of them.

In a periodic structure we find series of symmetry elements, i.e. series of rotation and rotoinversion axes as shown in Fig. 2.9.

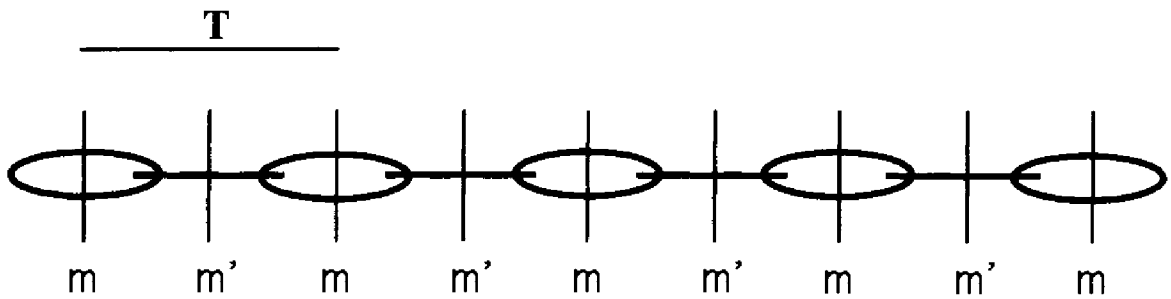


Fig. 2.9. Symmetry of the chain under tension from Fig. 2.4 where \mathbf{T} is the translation. We can distinguish two types (or classes) of mirror, m and m' . In each class the lines are equivalent by translation

If \mathbf{x} is some vector in a periodic structure which has translations $\mathbf{T} = u\mathbf{a} + v\mathbf{b} + w\mathbf{c}$, $-\infty < u, v, w < +\infty$, the extremities of all the vectors $\mathbf{x} + \mathbf{T}$ are points which are equivalent by translation. Let (\mathbf{R}, \mathbf{t}) be a symmetry operation which transforms \mathbf{x} into \mathbf{x}' , $\mathbf{R}\mathbf{x} + \mathbf{t} = \mathbf{x}'$. It also transforms $\mathbf{x} + \mathbf{T}$ into $\mathbf{x}' + \mathbf{RT}$: $\mathbf{R}(\mathbf{x} + \mathbf{T}) + \mathbf{t} = \mathbf{x}' + \mathbf{RT}$. It thus follows that $\mathbf{RT} = \mathbf{T}'$ is also a translation of the lattice.

The lattice must be invariant with respect to the rotations \mathbf{A}_n and to the rotoinversions \mathbf{I}_n .

We have shown that \mathbf{R} is represented by an orthogonal matrix if we choose a unitary coordinate system. The matrices (2.7), (2.8) and (2.9) are examples of orthogonal matrices. Alternatively, we can choose the axes of our coordinate system to be a lattice base $\mathbf{a}, \mathbf{b}, \mathbf{c}$, i.e. three primitive non-coplanar translations. The coordinates of the lattice points u, v, w are then integers and all the terms in the corresponding representation of \mathbf{R} are thus also integers. Let us indicate the orthogonal representation by the matrix \mathbf{U} , and the representation with integers by the matrix \mathbf{N} . The matrices \mathbf{U} and \mathbf{N} are related by a similarity transformation because they represent the same operation. Hence, there must exist a matrix \mathbf{X} such that $\mathbf{N} = \mathbf{X}^{-1}\mathbf{U}\mathbf{X}$. The matrix \mathbf{X} transforms the coordinate system of the lattice to a unitary system. Moreover, \mathbf{U} is similar to one of the matrices (2.7), (2.8) or (2.9). We know that similar matrices have the same trace. It thus follows that:

$$\begin{aligned} \text{trace}(\mathbf{U}) &= \pm(2 \cos \phi \pm 1) = \text{integer, and hence} \\ \cos \phi &= \cos(2\pi/n) = 1/2N, \quad n \text{ and } N \text{ being integers.} \end{aligned}$$

The only allowed values of n are thus $n = 1, 2, 3, 4, 6$. Periodic structures can only be invariant with respect to the rotation axes $\bar{1}, \bar{2}, \bar{3}, \bar{4}, \bar{6}$ and with respect to the rotoinversion axes $\bar{1}, \bar{2} = m, \bar{3}, \bar{4}, \bar{6}$ (or to the corresponding rotoreflection axes).

This important theorem refers to two- and three-dimensional structures. It expresses the fact that tiling of the Euclidean plane by regular polygons can be achieved only with the triangle, the square and the hexagon. A four-dimensional periodic structure can allow other symmetry operations.

2.4.2 METRIC IMPOSED BY THE SYMMETRY

Figure 2.10 shows that the presence of rotation or rotoinversion axes implies a characteristic metric for the lattice. Twofold axes do not impose any special metric; reflection lines are only compatible with a rectangular or diamond lattice; fourfold axes are only compatible with a square (tetragonal) lattice; threefold and sixfold axes are only compatible with a triangular (hexagonal) lattice.

Let T be a translation of the lattice, S_1 a reflection by a mirror plane and T' the translation equivalent to T by the reflection S_1 (Fig. 2.11). The translations $T - T'$ and $T + T'$ are thus respectively perpendicular and parallel to the plane. In a similar manner we can show that

All rotation and rotoinversion (or rotoreflection) axes which are symmetry elements of the lattice are parallel to translations and perpendicular to lattice planes.

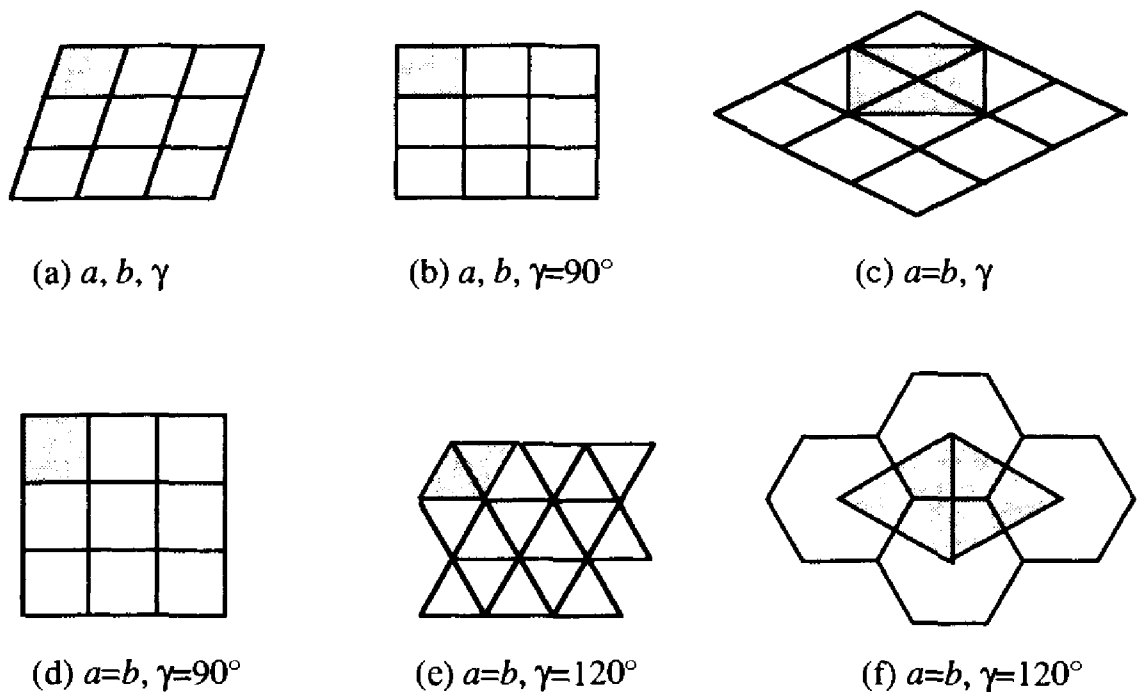


Fig. 2.10. Tiling of two-dimensional Euclidean planes; (a) arbitrary lattice, twofold axes 2; (b) rectangles, reflection lines m ; (c) diamonds, rectangular centered cell, reflection lines m and glide lines g ; (d) squares, fourfold axes 4; (e) triangles, threefold axes 3; (f) hexagons, sixfold axes 6, same type of cell as (e)

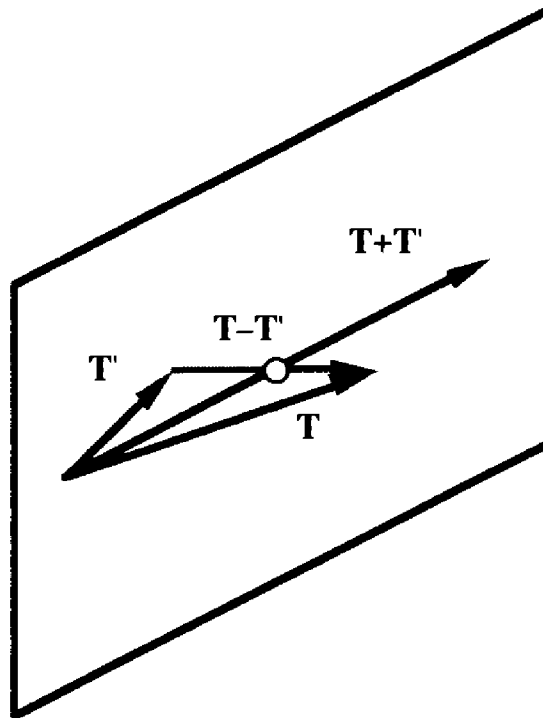


Fig. 2.11. Reflection plane and translation

It thus follows that any symmetry element, except a center of symmetry $\bar{1}$, generates mutually perpendicular translations.

2.4.3 POINT GROUPS AND SPACE GROUPS

The groups formed by rotations and rotoinversions are called point groups (Section 2.2.3):

Point groups describe the symmetry of objects of finite dimensions.

Groups made up entirely or in part by translations are of infinite order; these groups may also contain rotations and reflections with or without a translation component as well as rotoinversions. In the Euclidean plane they are called plane groups and in three-dimensional space, space groups:

Space groups describe the symmetry of periodic structures.

What is the relation between the space group which describes the symmetry of a crystal structure at the atomic level and the point group which describes the symmetry of the corresponding macroscopic crystal? By analogy with the Bernhardt principle (Section 1.3.1), a crystal is characterized by its properties in different *directions*, for example rate of growth, thermal and electrical conductivity, elasticity and piezoelectricity. Let us consider the periodic structure shown in Fig. 2.12. Clearly, the macroscopic properties in the directions of the two large

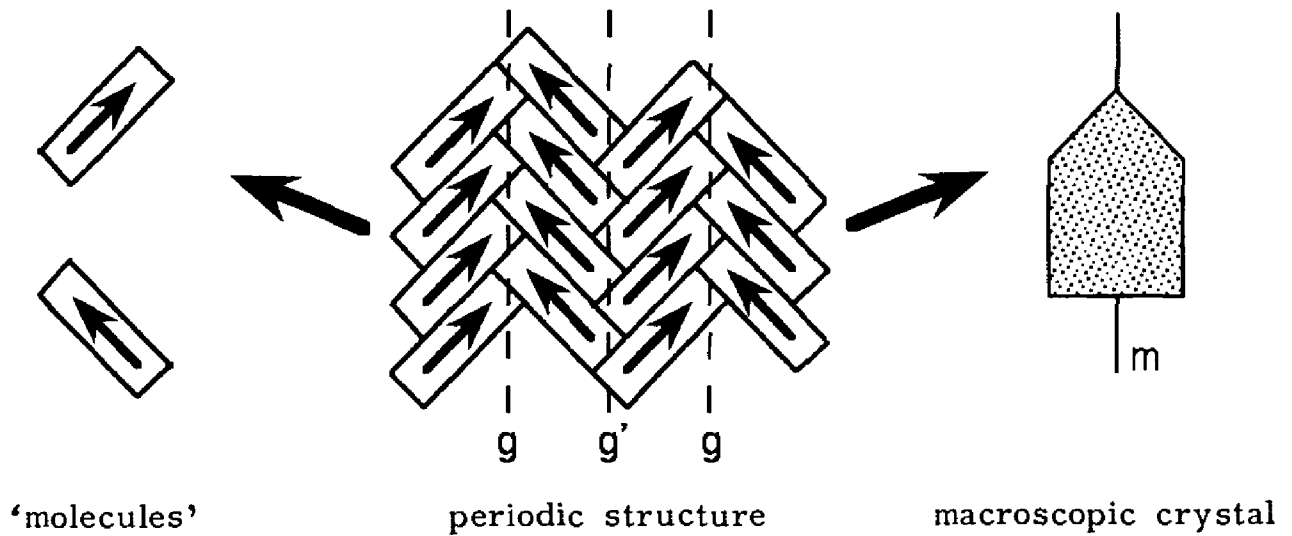


Fig. 2.12. Symmetry of a periodic structure and of the macroscopic crystal

arrows are identical because they make the same angles with the arrows in the bricks. The symmetry of the structure is characterized by the series of glide lines g and g' . In contrast, the macroscopic crystal has a mirror plane m . In all cases, a series of rotation or rotoinversion axes in the periodic structure appear as a single rotation or rotoinversion axis in the macroscopic crystal.

We can express this idea in a more formal manner by using the idea of the *factor group*. Let \mathcal{G} be a group of order m composed of the operations g_k , $1 \leq k \leq m$, and \mathcal{S} a subgroup of order s . The set $g_i \mathcal{S}$ obtained by pre-multiplying all the operations of \mathcal{S} with an operation g_i of \mathcal{G} is a *left coset* of \mathcal{S} ; $g_i \mathcal{S}$ is identical to \mathcal{S} if g_i is included in \mathcal{S} ; $g_i \mathcal{S}$ has no operation in common with \mathcal{S} if g_i is not included in \mathcal{S} . The set $\mathcal{S} g_i$ is a *right coset* of \mathcal{S} . An *invariant subgroup* \mathcal{N} of order n is defined by $g_i^{-1} \mathcal{N} g_i = \mathcal{N}$ for any operation g_i , thus $g_i \mathcal{N} = \mathcal{N} g_i$. \mathcal{N} subdivides \mathcal{G} into m/n cosets, and each operation g_k belongs to a single coset of \mathcal{N} . The cosets of \mathcal{N} form a group of order $q = m/n$ called the *factor group* of \mathcal{G} , $\mathcal{Q} = \mathcal{G}/\mathcal{N}$. \mathcal{N} corresponds to the identity operation of \mathcal{Q} ; q is the index of \mathcal{N} in \mathcal{G} .

The group of translations \mathcal{T} is an invariant Abelian subgroup of the space group \mathcal{E} , the similarity transformation of a translation with any other operation of the group being a translation. Each of the operations of \mathcal{E} belongs to one of the q cosets of \mathcal{T} , q being the index of \mathcal{T} in \mathcal{E} . \mathcal{T} contains all the operations (E, \mathbf{T}) (Section 2.2.4). According to equation (2.2), $(R, \mathbf{t})(E, \mathbf{T}) = (R, R\mathbf{T} + \mathbf{t}) = (R, \mathbf{t}')$ because $R\mathbf{T}$ is a lattice translation. The k th coset of \mathcal{T} thus contains all the operations $(R_k, \mathbf{t}_1), (R_k, \mathbf{t}_2), \dots$, with the same rotation or rotoinversion R_k and different translations. There are as many cosets as there are operations R_k .

The point group \mathcal{P} is isomorphic with the factor group of the group of translations, $\mathcal{P} = \mathcal{E}/\mathcal{T}$. It contains the operations $R_1 = E, R_2, \dots, R_k, \dots, R_p$.

These considerations are illustrated in the structure in Fig. 2.12. The plane group is composed of two cosets: the operations (\mathbf{E}, \mathbf{T}) which generate from any given brick (for example, with an arrow pointing to the right) all the bricks with the same orientation, and the operations $(I_2, \mathbf{t} + \mathbf{T})$ which generate all the bricks with the other orientation (with the arrows pointing to the left; \mathbf{t} is a half translation parallel to \mathbf{g}). The point group contains the operations \mathbf{E} and I_2 , i.e. it is generated by a mirror plane m .

Point groups that are compatible with a crystal lattice are called crystal classes and are thus made up of the operations $A_1, A_2, A_3, A_4, A_6, I_1, I_2, I_3, I_4, I_6$ and their powers.

2.5 CRYSTAL CLASSES AND SYSTEMS

2.5.1 NOTION OF CLASS

The word *class* is used to characterize diverse groupings of objects according to the properties they have in common. An *equivalence class* is made up of like (or conjugate) operations. Let \mathbf{G} be a group of order m made up of the operations $\mathbf{g}_k, 1 \leq k \leq m$. The equivalence class of the operation \mathbf{g}_x contains all the operations $\mathbf{g}_k^{-1} \mathbf{g}_x \mathbf{g}_k, 1 \leq k \leq m$. The cosets of an invariant subgroup introduced above (Section 2.4.3) are an alternative scheme for dividing the operations of \mathbf{G} into classes. Thus the word class is generally used for collections of objects of a certain type: an equivalence class is composed of like operations which perform equivalent transformations; the cosets discussed in Section 2.4.3 collect the bricks of Fig. 2.12 into two different classes; the crystal classes classify crystals according to their macroscopic symmetry; the Laue classes group together certain crystal classes (Sections 2.5.4, 2.5.5 and 2.5.7). Symmetry elements are likewise grouped into classes. For example, in Fig. 2.12, the glide lines \mathbf{g} form one class and the lines \mathbf{g}' form another. Some classes, as, for example, the crystal classes, are also groups.

2.5.2 GROUP GENERATORS

All the crystallographic groups can be generated from a limited number of symmetry operations. A cyclic group, for example, is generated by a single operation. Instead of generating a group from the symmetry operations, it may equally well be generated from the symmetry elements. Figures 2.13 and 2.14 demonstrate the most useful generators.

Two mirror planes whose intersection forms the angle ϕ generate a rotation axis of period 2ϕ . Figure 2.13(a) shows two mirror planes that intersect at an angle of 45° and thus create a 90° rotation. Multiple application of these two reflections yields a fourfold rotation axis and four mirror planes which belong to

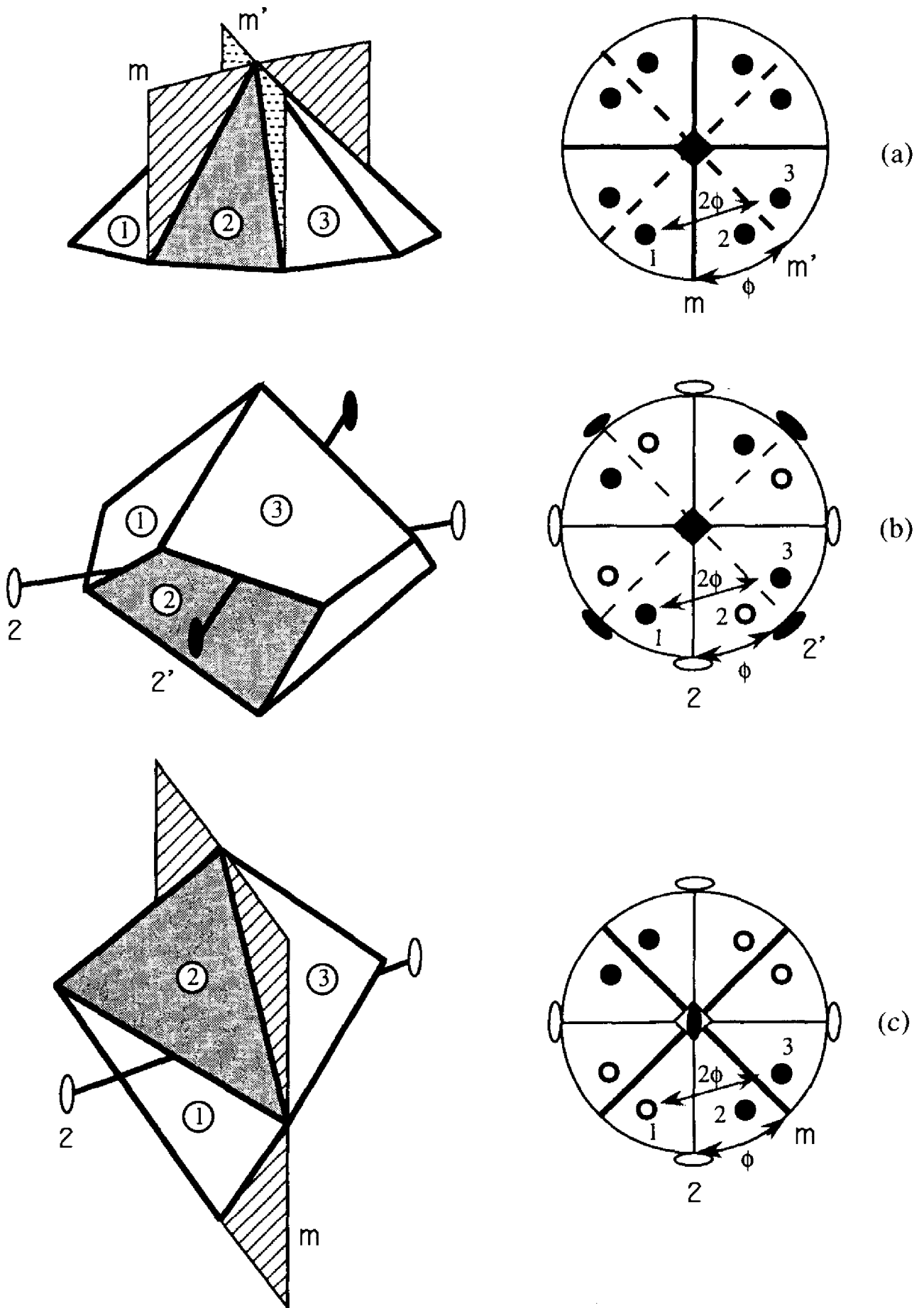


Fig. 2.13. Combination of two mirror planes (a), two twofold axes (b), and a mirror plane with a twofold axis (c). In the stereographic projections, the symbol \bullet represents a face above the plane of projection and \circ a face below the plane

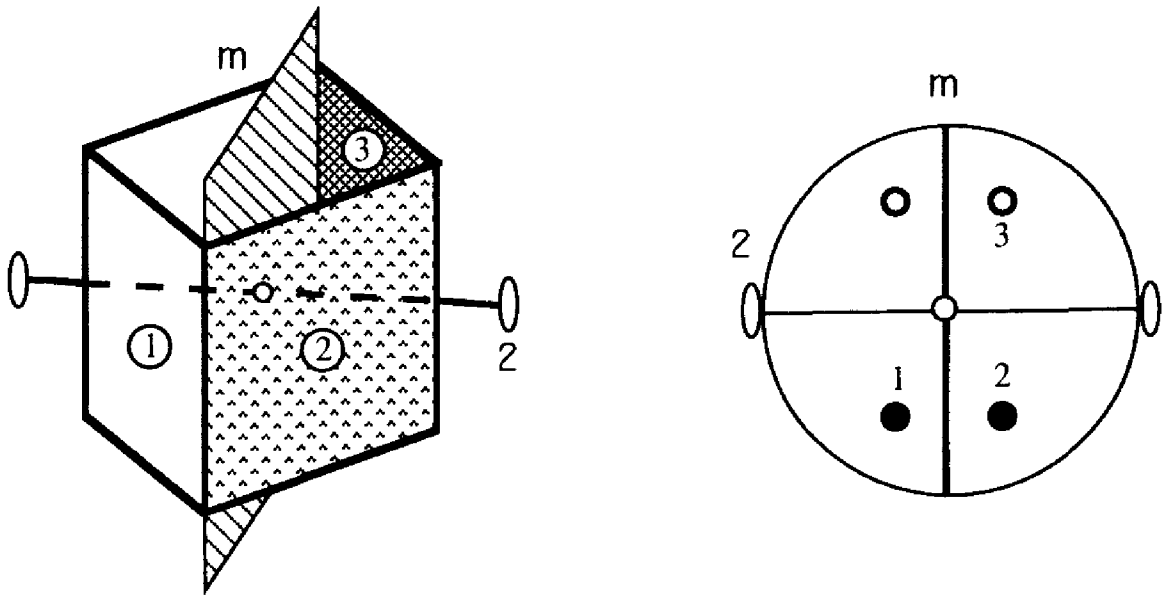


Fig. 2.14. A mirror plane, a twofold axis and a center of symmetry

two different equivalence classes. For any n , two planes forming an angle $\phi = \pi/n$ generate an axis n and a total of n mirror planes which belong to two classes if n is even, and to the same class if n is odd.

Two twofold axes which intersect at an angle ϕ generate an axis of period 2ϕ normal to the plane of the twofold axes. Figure 2.13(b) shows two twofold axes which form an angle of 45° and create a 90° rotation. Multiple application of these two 180° rotations results in a fourfold axis and a total of four twofold axes which belong to two different equivalence classes. For any n , two twofold axes which intersect at an angle $\phi = \pi/n$ generate an axis n and a total of n twofold axes which belong to two classes if n is even, and a single class if n is odd.

A mirror plane and a twofold axis whose intersection forms the angle ϕ generate a rotoreflection of period 2ϕ (or a corresponding rotoinversion). Figure 2.13(c) shows a mirror plane and a twofold rotation axis which make an angle of 45° and which create a 90° rotoreflection axis. Multiple application of these two operations yields a $\bar{4}$ axis, two mirror planes and two twofold axes.

A mirror plane and a twofold (or any even order) axis perpendicular to the plane generates an inversion center (Fig. 2.14 or Fig. 2.13(c) with $\phi = 90^\circ$). Two of these three elements generate the smallest non-cyclic (but Abelian) group: this is a group of order 4 which comprises the operations E , A_2 , I_1 , and I_2 .

2.5.3 GENERATION OF POINT GROUPS

We will first derive the four types of point group that are composed uniquely of rotations (operations of the first type). These groups describe *chiral* objects or *enantiomorphs*. An enantiomorph and its mirror image are not superimposable.

In the same way, a left hand is not superimposable on a right hand, and for any right-handed screw there exists an equivalent left-handed screw.

From the considerations in the preceding pages (Section 2.5.2) we derive two types of rotation groups:

- cyclic groups characterized by an axis p of order p ;
- groups characterized by an axis p of order p perpendicular to p twofold axes such as the example shown in Fig. 2.13(b) (remember that these twofold axes form two equivalence classes if p is even, and a single class if p is odd).

We can derive the other rotation groups in the following manner. Two rotation axes p and q of order p and q which intersect at some angle generate more rotation axes. Around p we obtain p axes of order q : $q, q', q'', \dots, q^{(p-1)}$ which belong to the same equivalence class; around q we obtain q axes of order p : $p, p', p'', \dots, p^{(q-1)}$ which belong to the same equivalence class. In addition we find twofold axes which bisect the angles formed by axes of the same class. Figure 2.15 shows the stereographic projection of the combination of a fourfold ($p = 4$) and a threefold ($p = 3$) axis. The axes thus generated create additional axes for which the poles of the spherical projection (Section 1.3.4) form regular spherical polygons. If the resulting group is of finite order, the sphere is tiled by a finite number of polygons of the same type (squares or triangles in Fig. 2.15). The surface area of a regular polygon of order p may be calculated by spherical

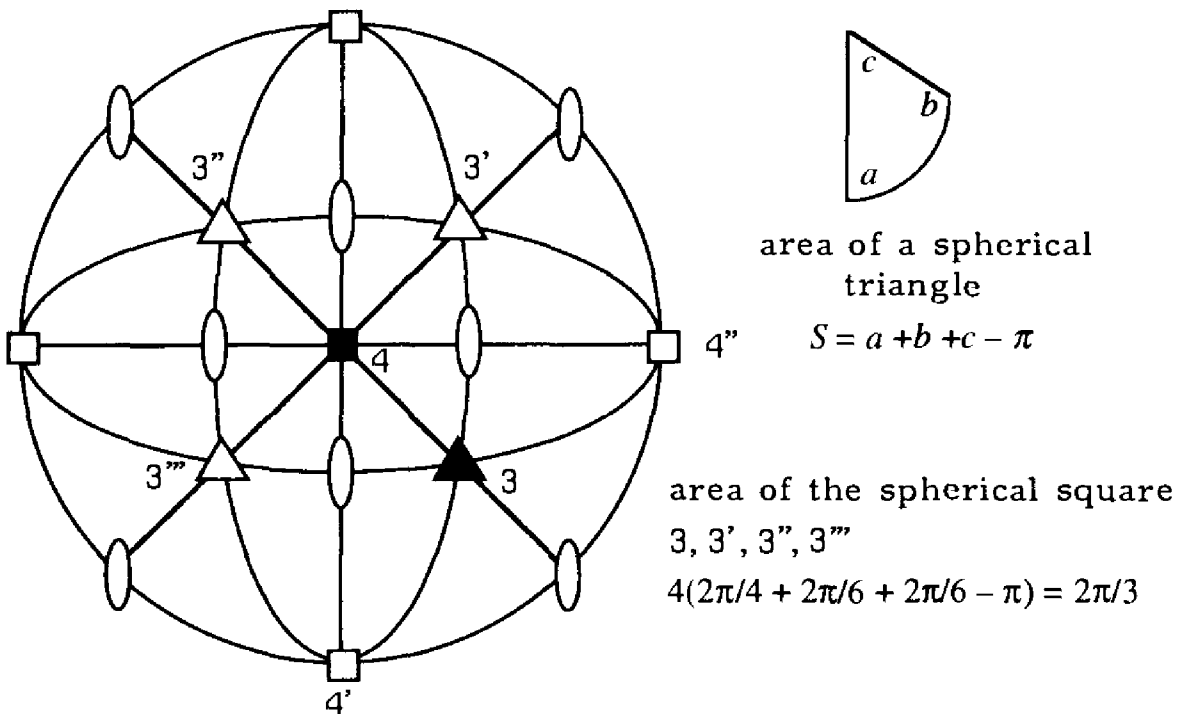


Fig. 2.15. A fourfold axis 4 and a threefold axis 3 generate the axes $3', 3'', 3''', 4', 4''$, etc. They also generate twofold axes

trigonometry:

$$S_{\text{polygon}} = p(2\pi/p + 2\pi/q - \pi); \text{ surface of the sphere } S_{\text{sphere}} = 4\pi$$

Tiling by a finite number of spherical polygons gives $P = S_{\text{sphere}}/S_{\text{polygon}} =$ integer from which we obtain the allowed values for p and q :

$$P = 4q/(2q + 2p - pq) > 0 \text{ and integer, tiling by } p\text{-gons}$$

$$Q = 4p/(2p + 2q - pq) > 0 \text{ and integer, tiling by } q\text{-gons}$$

A twofold axis and another axis of order $p > 2$ which intersect at an angle different from 90° , generate an axis of order $q > 2$. Hence, we need to consider only the solutions to these equations for integers p and $q > 2$ (perpendicular intersections having been discussed above):

$p = 3, q = 3: P = Q = 4$	tetrahedron
$p = 3, q = 4: P = 8, Q = 6$	octahedron and cube
$p = 3, q = 5: P = 20, Q = 12$	icosahedron and dodecahedron

These are the rotations which form the symmetry groups of the *regular* or *Platonic solids*.

Finally, the continuous rotation group of infinite order describes the symmetry of a sphere (in the mathematics literature it is referred to as SO_3).

Starting from the pure rotation groups, we can obtain others by the addition of mirror planes parallel or perpendicular to the rotation axes in such a way as to generate no additional axes. In this manner we can construct all the point groups. In the following we will describe in detail those which are compatible with a translation lattice, i.e. the crystal classes.

The literature contains two different nomenclatures to describe point groups. The older and traditional nomenclature uses the *Schoenflies* notation. Its use is widespread, but it is poorly adapted to express the relation between crystal classes and space groups. This notation uses *rotation axes* and *rotoreflection axes* as symmetry elements. One can hope that it will be progressively abandoned in favor of the *Hermann–Mauguin* (or *international*) notation. This system allows us to characterize both crystal classes and space groups in a coherent manner. It is currently used for all work on crystal structures. This notation uses *rotation axes* and *rotoinversion axes* as symmetry elements. We will present the conventional symbols for both of these notations, but in the discussion we will only use the international symbols. Initially we will only introduce the symbols without any deeper discussion. The complete details (Section 2.5.9) will only be presented after we have introduced the crystal systems. In Fig. 2.17 we find three-dimensional representations of the symmetry elements and examples of polyhedral crystals, and, in Fig. 2.20, the corresponding stereographic projections.

2.5.4 THE 32 CRYSTAL CLASSES: AXIAL GROUPS

Among the symmetry elements of an axial group there is never more than one axis of order greater than two. These groups are listed in Table 2.6 which may be complemented by the following remarks:

- Groups of the type $\frac{x}{m}$ and $\frac{x}{m}m$ are only defined for x even. The symmetry element \bar{x} with $x = 4n + 2$ ($x = 2, 6, 10, \dots$) is equivalent to a rotation axis of order $2n + 1$ normal to a mirror plane m (Table 2.3). Hence $\frac{x}{m}$ with x odd represents a cyclic group within the \bar{x} groups. In the same way, $\frac{x}{m}m$ with x odd is found in the $\bar{x}m$ groups.
- The xm groups contain the operations corresponding to an x axis and x mirror planes m parallel to the axis (Fig. 2.13(a)). These mirror planes are all equivalent (i.e. they all belong to the same equivalence class) if x is odd, and they form two classes if x is even (Fig. 2.16). The international symbols $mm2, 3m, 4mm, 6mm$ list the different classes of symmetry elements. The symbol for the rotation axis x is written first except when $x = 2$ (Section 2.5.9).
- The $x2$ groups have the same structure as the xm groups (Section 2.5.11). They are made up of the operations corresponding to an x axis and x twofold axes perpendicular to this axis (Fig. 2.13(b)). These twofold axes are all equivalent if x is odd but they form two classes if x is even. Because these groups do not contain any mirror operations, they describe chiral objects.
- The $\bar{x}m$ and $\bar{x}2$ groups have the same structure as the xm groups. An example is shown in Fig. 2.13(c). If x is odd, the twofold axes are normal to the mirror planes; if x is even, the twofold axes are oblique with respect to the mirror planes. $\bar{4}m2$ and $\bar{6}2m$ are alternative symbols for $\bar{4}2m$ and $\bar{6}m2$ (Section 2.5.9).

Table 2.6. The seven types of axial crystal classes

Type of group	Group generated by	Order of group	International symbols
x	one unique rotation axis	x	1, 2, 3, 4, 6
\bar{x}	one unique rotoinversion axis	x (x even) $2x$ (x odd)	$\bar{1}, m, \bar{3}, \bar{4}, \bar{6}$
$\frac{x}{m}$	mirror plane m normal to an axis x	$2x$ (x even)	$\frac{2}{m}, \frac{4}{m}, \frac{6}{m}$ ($2/m, 4/m, 6/m$)
xm	mirror plane m parallel to an axis x	$2x$	$mm2, 3m, 4mm, 6mm$
$x2$	twofold axis 2 normal to an axis x	$2x$	$222, 32, 422, 622$
$\bar{x}m$ or $\bar{x}2$	mirror plane m parallel to an axis \bar{x} or twofold axis 2 normal to an axis \bar{x}	$2x$ (x even) $4x$ (x odd)	$\bar{3}_m^2, \bar{4}2m, \bar{6}m2$ ($\bar{3}m, \bar{4}m2, \bar{6}2m$)
$\frac{x}{m}m$	mirror plane m parallel to an axis $\frac{x}{m}$, or twofold axis 2 normal to an axis $\frac{x}{m}$	$4x$ (x even)	$\frac{2}{m} \frac{2}{m} \frac{2}{m}, \frac{4}{m} \frac{2}{m} \frac{2}{m}, \frac{6}{m} \frac{2}{m} \frac{2}{m}$ ($mmm, 4/mmm, 6/mmm$)

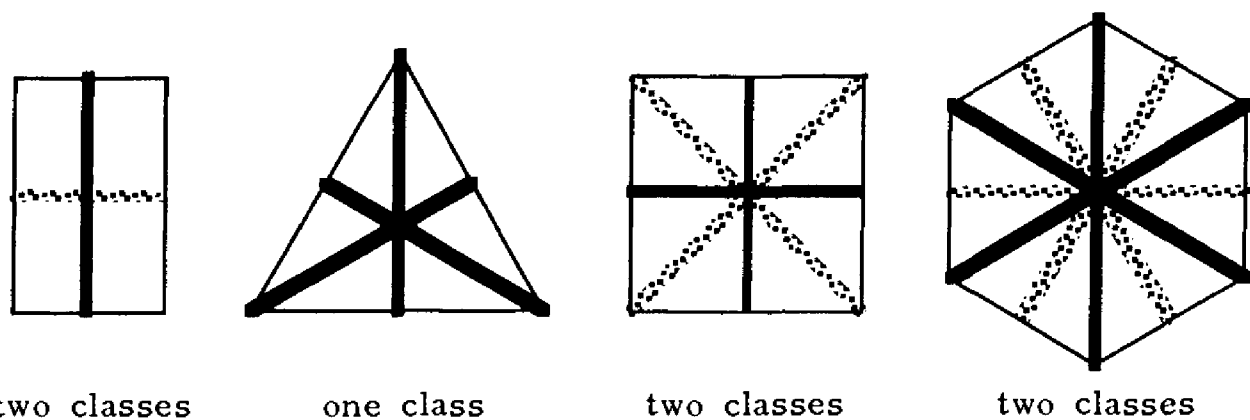


Fig. 2.16. Equivalence classes for the mirror planes in mm_2 , $3m$, $4mm$, $6mm$

- A mirror plane normal to an even order axis generates a center of symmetry (Fig. 2.14). The groups $\frac{2}{m}$, $\frac{4}{m}$, $\frac{6}{m}$, $\frac{2}{m} \frac{2}{m} \frac{2}{m}$, $\frac{4}{m} \frac{2}{m} \frac{2}{m}$, $\frac{6}{m} \frac{2}{m} \frac{2}{m}$ and $\bar{3}\frac{2}{m}$ are thus centrosymmetric. The *abbreviated symbols* for these groups ($2/m$, $4/m$, $6/m$, mmm , $4/mmm$, $6/mmm$ and $\bar{3}m$) are perhaps better adapted for word processing systems.
- The types x , \bar{x} and x/m contain all the groups characterized by *one single* symmetry direction. The other groups contain more than one symmetry direction.

2.5.5 THE 23 CRYSTAL CLASSES: TETRAHEDRAL AND OCTAHEDRAL GROUPS

The five *regular polyhedra* or *platonic solids* (Fig. 2.18) have been known since antiquity and played an important role in Aristotelian and medieval philosophy. Among other things, they were used to symbolize the elements of the alchemists (Table 2.7). The faces of a regular polyhedron are regular polygons. There is only one type of vertex, only one type of edge and only one type of face (semi-regular or Archimedean polyhedra have more than one type of regular face, e.g. triangles and squares).

Table 2.7. Characteristics of regular polyhedra

Polyhedron	Alchemy	Number of faces with (x) edges	Number of vertices with (x) edges	Number of edges
Tetrahedron	Fire	4 (3)	4 (3)	6
Octahedron	Air	8 (3)	6 (4)	12
Cube	Earth	6 (4)	8 (3)	12
Icosahedron	Water	20 (3)	12 (5)	30
Dodecahedron	Ether	12 (5)	20 (3)	30

If we replace the vertices of an octahedron with faces and the faces with vertices, we obtain a cube. Starting from a cube, we can obtain an octahedron in the same way. The technical term for this relationship is *dual*, thus the cube and the octahedron are *dual polyhedra*. In the same way, the dodecahedron and the icosahedron are dual polyhedra, whereas the tetrahedron is its own dual. It thus follows that these five regular polyhedra represent three types of symmetry, tetrahedral, octahedral and icosahedral (Table 2.7). The icosahedral groups contain fivefold axes and are, hence, not crystallographic.

The symmetry elements of the tetrahedral and octahedral groups are oriented with respect to the *characteristic directions for a cube* (Fig. 2.17):

- edges 3 directions
- body diagonals 4 directions
- face diagonals 6 directions

A tetrahedron or an octahedron may, indeed, be easily drawn inside a cube. We derived above (Section 2.5.3) the two chiral groups, one tetrahedral and one octahedral. By adding mirror planes perpendicular or parallel to the rotation axes or in bisecting positions, we generate the non-chiral groups. We thus obtain the five groups shown in Table 2.8.

For the two centrosymmetric groups $\frac{2}{m}\bar{3}$ and $\frac{4}{m}\bar{3}\frac{2}{m}$, we normally use the abbreviated symbols $m\bar{3}$ and $m\bar{3}m$. *We should note that all five groups are characterized by threefold axes which coincide with the body diagonals of the cube.*

2.5.6 NON-CRYSTALLOGRAPHIC POINT GROUPS

The listing of the non-crystallographic point groups is perfectly analogous to that of the crystal classes:

- type x : $5, 7, 8, 9, 10, \dots, \infty$
- type \bar{x} : $\bar{5}, \bar{7}, \bar{8}, \bar{9}, 10, \dots$
- type x/m : $8/m, 10/m, \dots, \infty/m$ (x even)
- type xm : $5m, 7m, 8mm, 9m, 10mm, \dots, \infty m$
- type x^2 : $5^2, 7^2, 8^2, 9^2, 10^2, 22, \dots, \infty^2$
- type \bar{x}^2 : $\bar{5}^2, \bar{7}^2, \bar{8}^2, \bar{9}^2, 10m^2, \dots$
- type $\frac{x}{m}\frac{2}{m}$: $\frac{8}{m}\frac{2}{m}\frac{2}{m}, \frac{10}{m}\frac{2}{m}\frac{2}{m}, \dots, \frac{\infty}{m}\frac{2}{m}\frac{2}{m}$ (x even)
- icosahedral: $235, \frac{2}{m}\bar{3}5$ (Fig. 2.19)
- spherical: $\infty\infty, \frac{\infty}{m}\frac{\infty}{m}$

The spherical groups are better known by the symbols $\infty\infty = SO_3$ (group containing all rotations of three-dimensional Euclidean space, represented by all the orthogonal three-dimensional matrices with determinant +1) and $\frac{\infty}{m}\frac{\infty}{m} = O_3$ (group represented by all the orthogonal three-dimensional matrices).

Table 2.8 The five tetrahedral and octahedral (*cubic*) groups

Symbol	Edges	Body diagonals	Face diagonals	Comments
23	2	3	–	chiral, tetrahedral
$\frac{2}{m}\mathbf{3}$	$\frac{2}{m}$	$\bar{3}$	–	23 plus inversion
$\bar{4}3m$	$\bar{4}$	3	m	symmetry of the tetrahedron
432	4	3	2	chiral, octahedral
$\frac{4}{m}\mathbf{3}\frac{2}{m}$	$\frac{4}{m}$	$\bar{3}$	$\frac{2}{m}$	symmetry of the octahedron

The five groups of infinite order which possess a unique rotation axis may be represented by the following objects (Fig. 2.21):

- ∞ : cone of revolution turning around its axis
- ∞/m : cylinder of revolution turning around its axis, axial vector (e.g. magnetic field)
- ∞m : cone of revolution, polar vector (e.g. electric field)
- $\infty 2$: cylindrical screw of infinite length
- $\frac{\infty}{m} \frac{2}{m}$: cylinder of revolution

2.5.7 THE 11 LAUE CLASSES

Among all the symmetry elements, the center of symmetry plays a special role. All the properties of a centrosymmetric crystal are represented by even functions, which is a significant mathematical advantage. However, the experimental determination of a center of symmetry is not always easy. Many anisotropic properties are centrosymmetric even when the crystal is not (e.g. thermal and electrical conductivity, linear elasticity, Section 4.4.2). In the majority of cases, the diffraction of X-rays produces centrosymmetric diffractograms, independent of the symmetry of the crystal (Friedel's law, Section 3.7.3).

A Laue class comprises all the crystal classes (point groups) that cannot be distinguished by methods that are insensitive to the presence of a center of symmetry. The groups belonging to the same Laue group are hence primarily distinguished by the presence or absence of inversion. Figures 2.17 and 2.20 show this classification by use of separate boxes for different Laue groups. The Laue classes are identified by the symbols of the corresponding centrosymmetric groups:

$$\bar{1}, 2/m, mmm, \bar{3}, \bar{3}m, 4/m, 4/mmm, 6/m, 6/mmm, m\bar{3}, m\bar{3}m$$

The Laue classes represent a classification of the crystal classes. The other significations of the word *class* were discussed in Section 2.5.1.

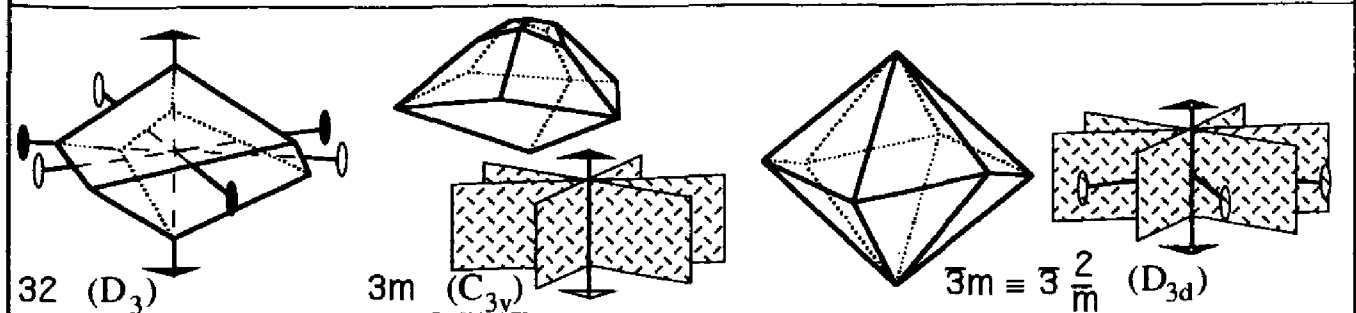
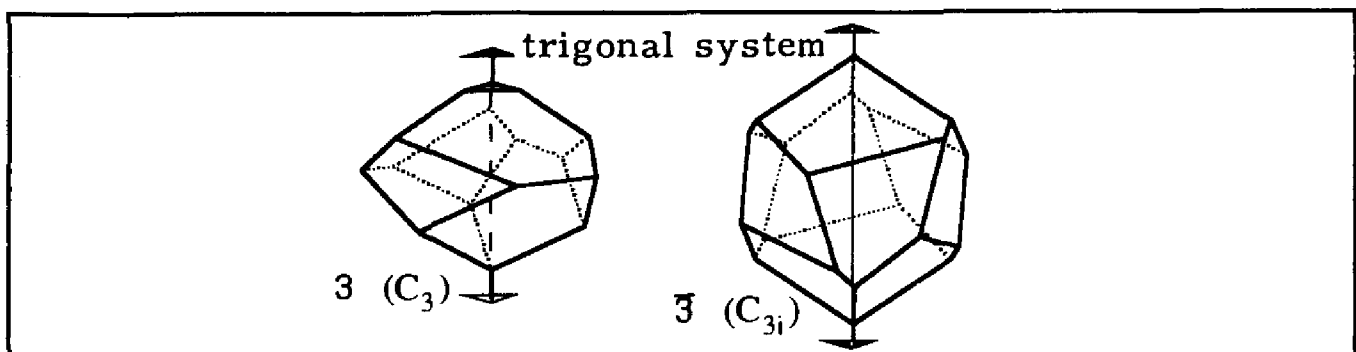
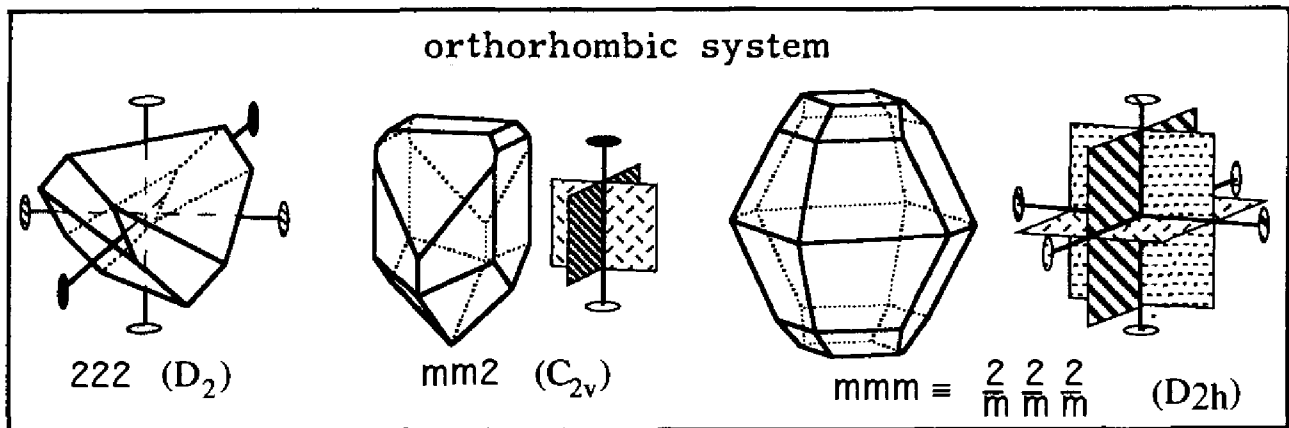
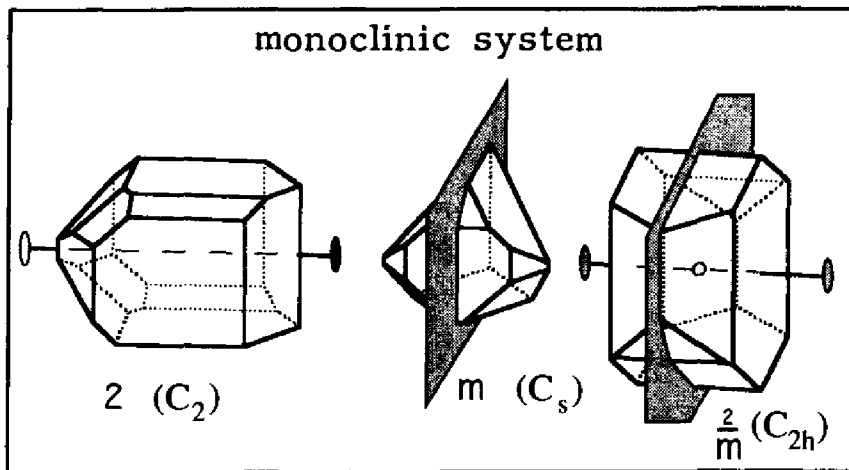
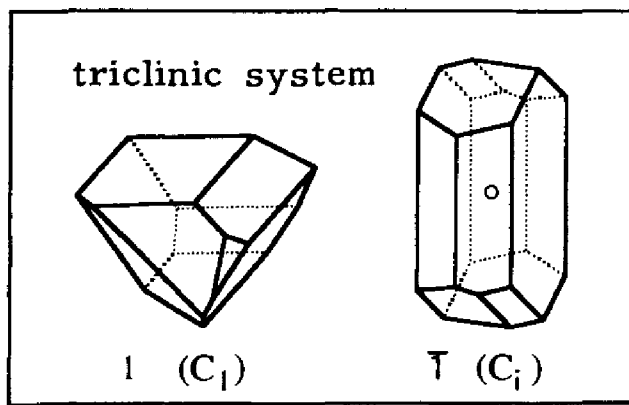
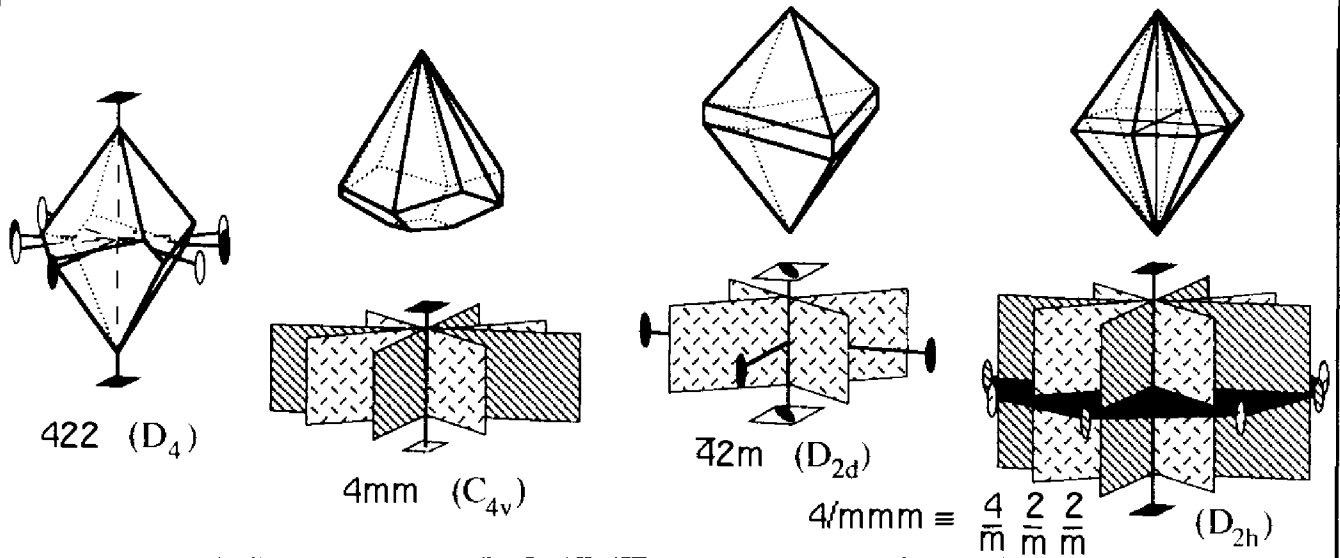
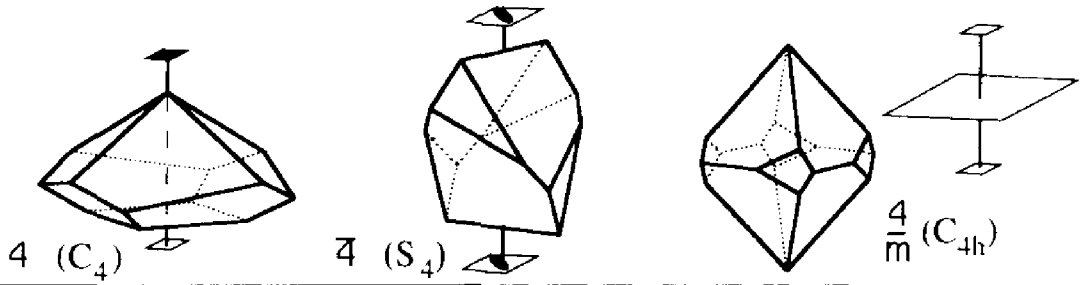


Fig. 2.17. Three-dimensional representations of the 32 crystal classes

tetragonal system



hexagonal system

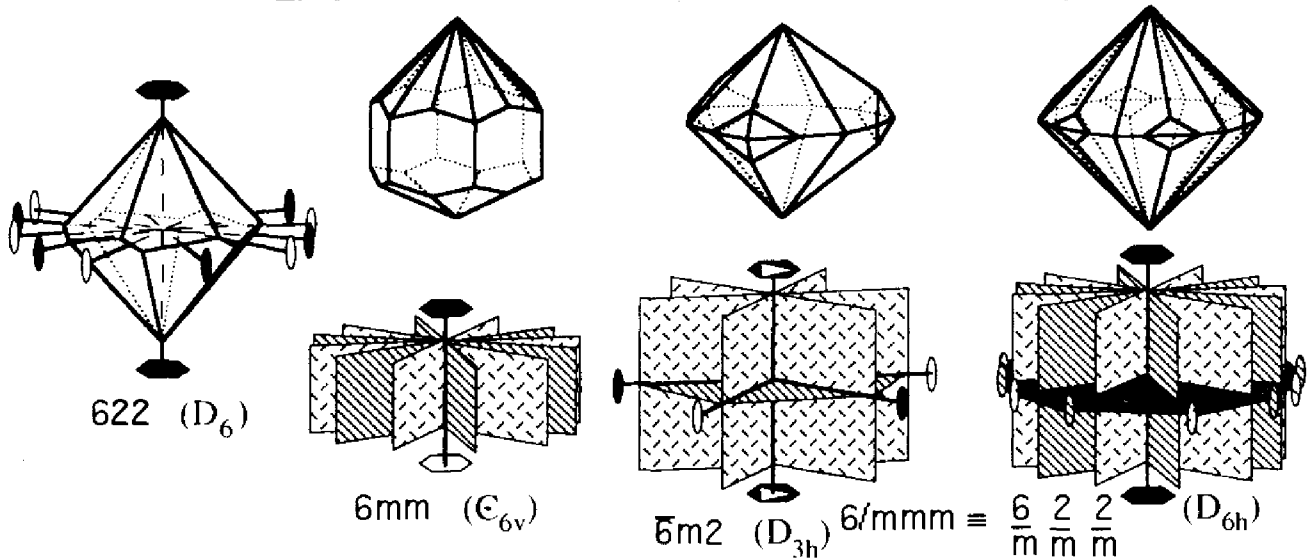
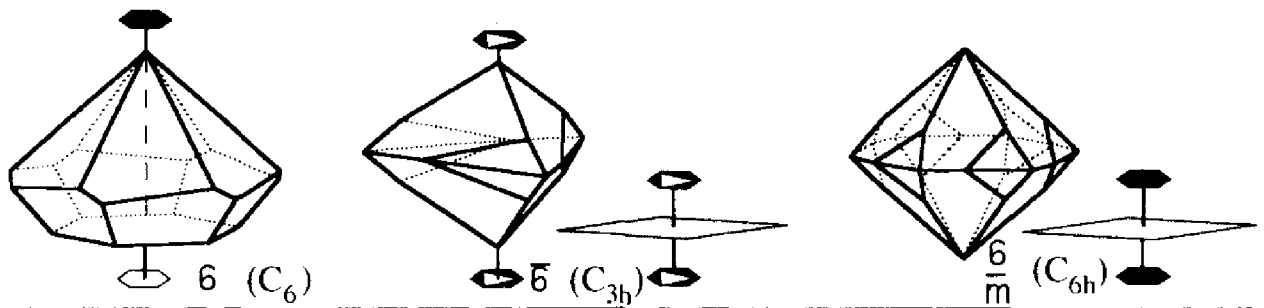


Fig. 2.17. (Contd)

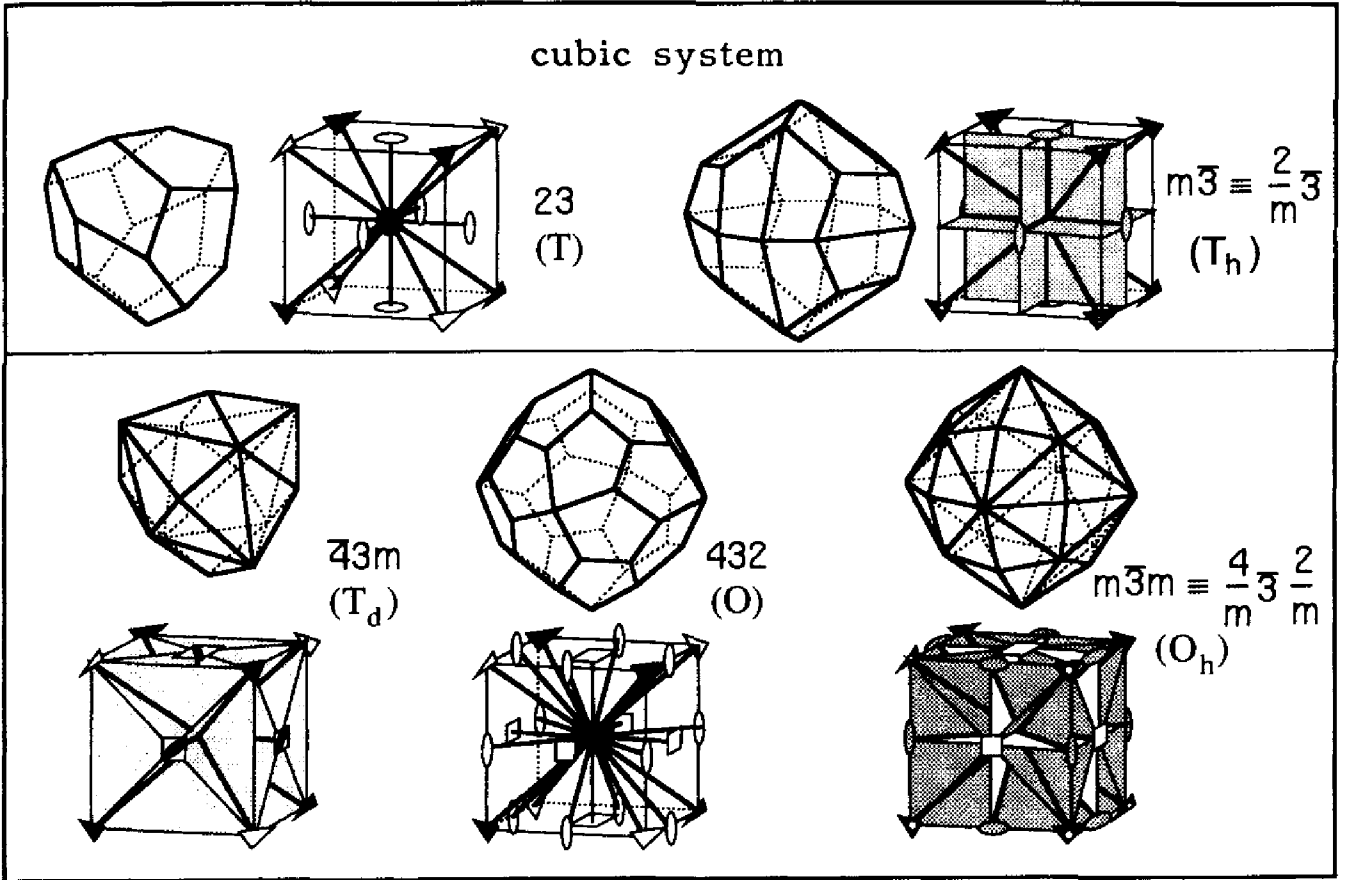


Fig. 2.17. (Contd)

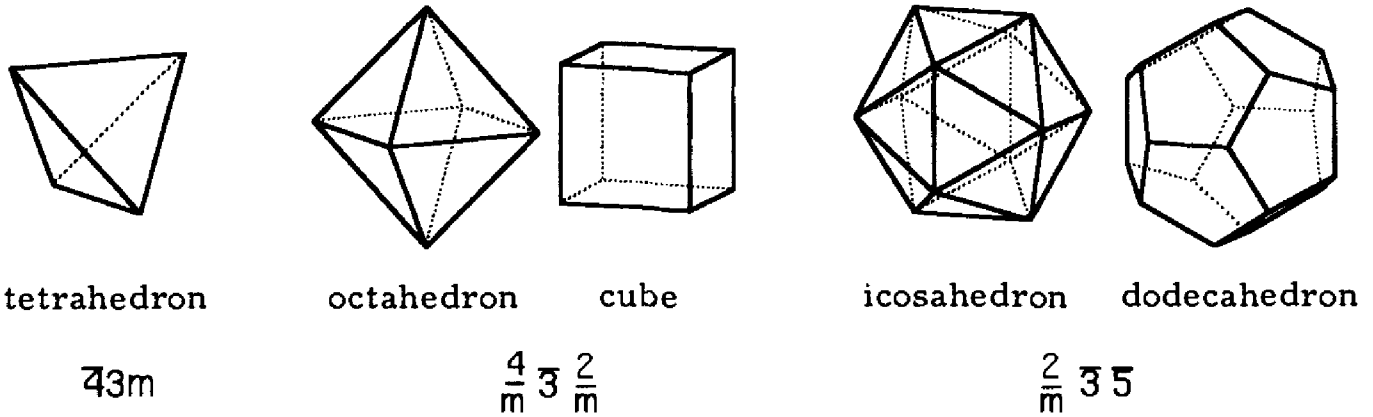


Fig. 2.18. The five Platonic solids

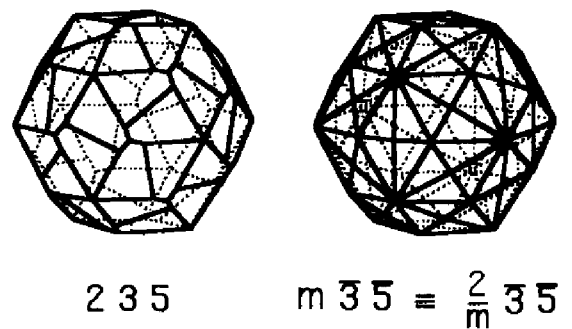


Fig. 2.19. Polyhedra with 60 and 120 faces which have non-crystallographic icosahedral symmetry

- location of the *a, b, c* axes of the coordinate system
- upper part of the sphere
- lower part of the sphere
- ⊙ superposition of two positions above and below the plane

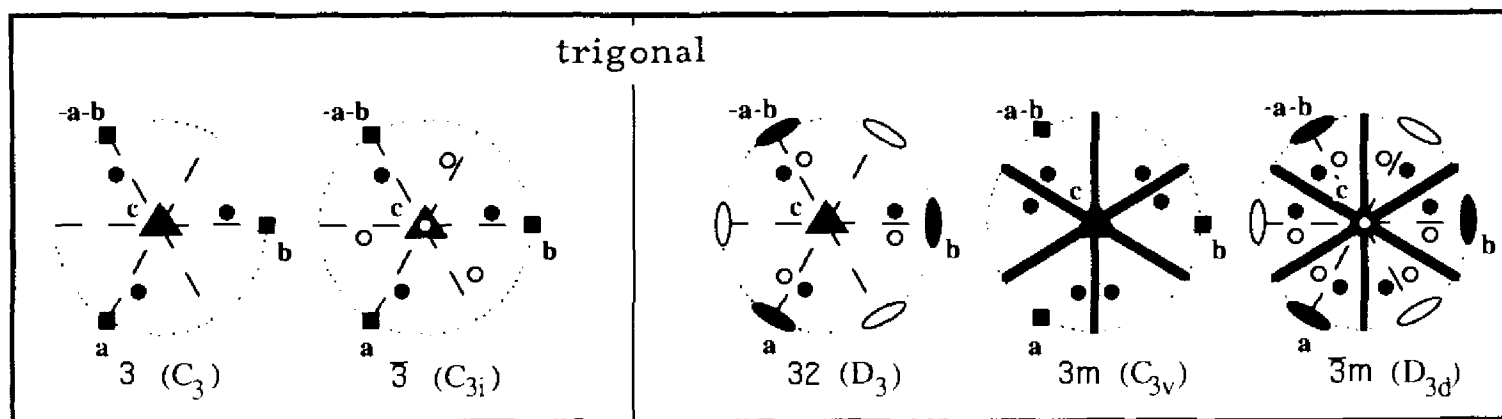
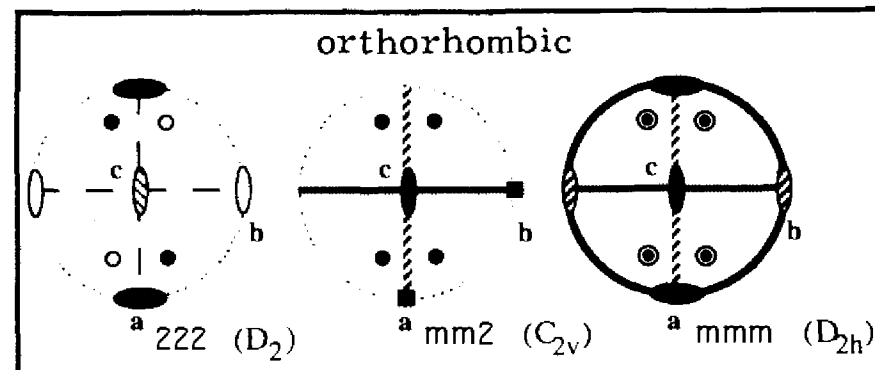
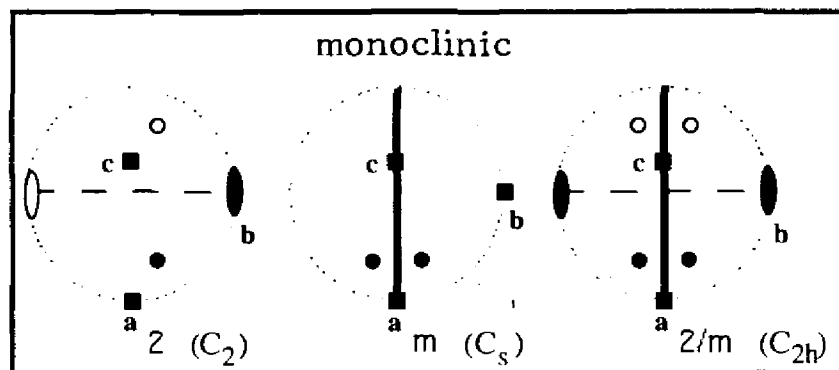
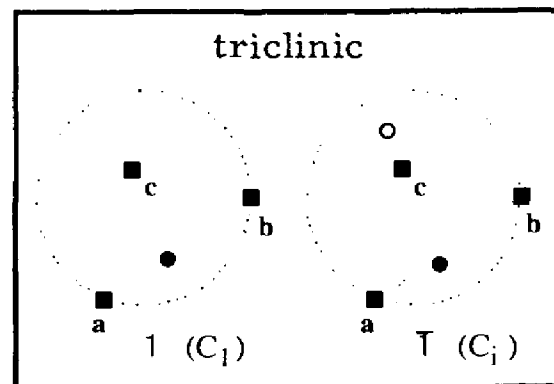
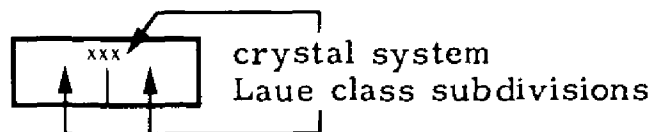


Fig. 2.20. Stereographic projections of the symmetry elements and the equivalent positions for the 32 crystal classes

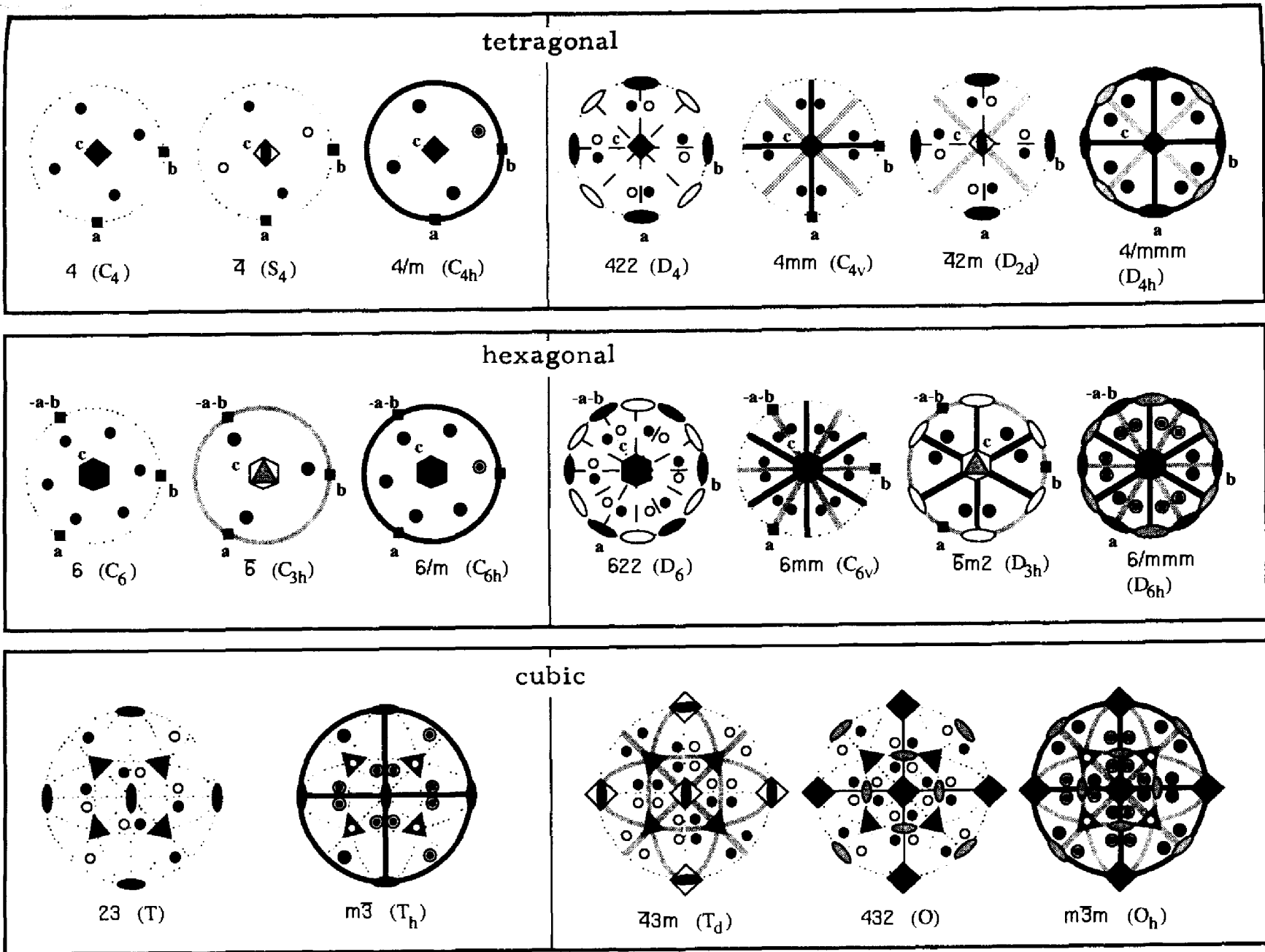


Fig. 2.20. (Contd)

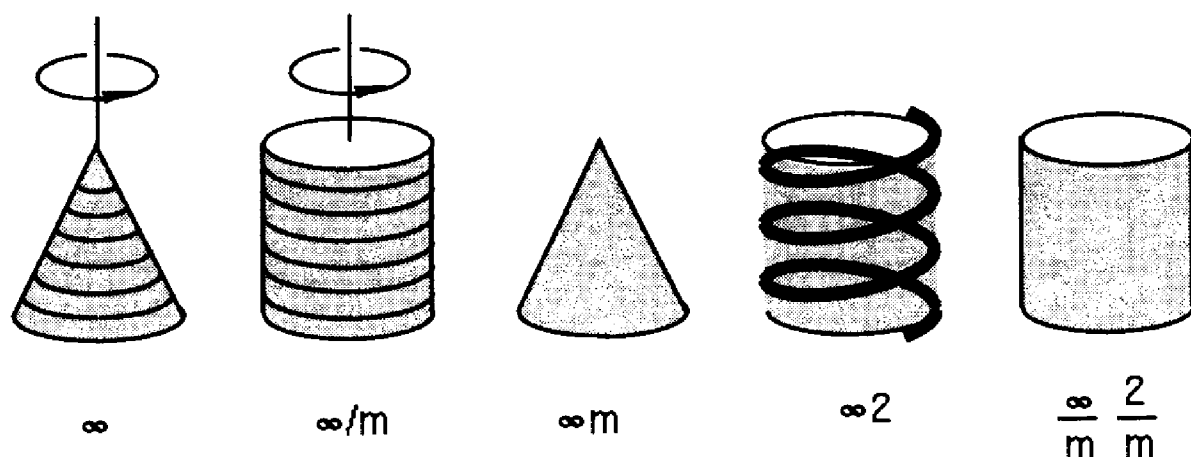


Fig. 2.21. The five groups of infinite order which contain a unique rotation axis

2.5.8 THE SEVEN CRYSTAL SYSTEMS

The crystal systems represent another classification of the crystal classes (Figs. 2.17 and 2.20). In Sections 2.4.1 and 2.4.2 we discussed the relations which exist between the symmetry elements and the translation lattice. In particular we showed that (a) the presence of rotation or rotoinversion axes implies a specific lattice metric, and (b) rotation and rotoinversion axes are parallel to translations and perpendicular to lattice planes. If, for example, a crystal belongs to the crystal class 2, we can choose a lattice base **a**, **b**, **c** with two right angles; by choosing **b** parallel to the twofold axis, and **a** and **c** parallel to two translations belonging to the lattice plane normal to **b**, we obtain $\alpha = \gamma = 90^\circ$. Thus, in general, the class 2 does not allow us to choose a coordinate system with a higher symmetry, hence, this is the base with maximal symmetry. For a crystal of class *m* we can choose an analogous base with **b** perpendicular, and **a** and **c** parallel to the mirror plane. The types of metric with maximal symmetry which follow from the other crystal classes can be easily derived.

A crystal system comprises all the crystal classes which allow the choice of the same type of base with maximal symmetry.

*For each crystal system there is a corresponding characteristic or canonical lattice base (i.e. a coordinate system **a**, **b**, **c**). The unit cell of the crystal structure resulting from such a choice may be primitive or multiple (Section 1.4.1).*

In the above examples, it is the presence of a twofold axis or of a mirror plane which allows the choice of a base with two right angles. However, a crystal with such a metric will not necessarily possess one of these symmetries. Such a metric, due not to the symmetry but to chance, will only exist at a given temperature and pressure, whereas the metric which follows from the symmetry is not a function of

Table 2.9. The seven crystal systems

Name	Definition	Type of metric
Triclinic	classes 1 or $\bar{1}$	$a, b, c, \alpha, \beta, \gamma$ any value
Monoclinic	one unique twofold direction 2 or $\bar{2} \equiv m$	a, b, c, β any value $\alpha = \gamma = 90^\circ$
Orthorhombic	three perpendicular twofold directions	a, b, c any value $\alpha = \beta = \gamma = 90^\circ$
Tetragonal	one unique fourfold direction 4 or $\bar{4}$	$a = b, c$ $\alpha = \beta = \gamma = 90^\circ$
Trigonal	one unique threefold direction 3 or $\bar{3}$	$a = b, c$ $\alpha = \beta = 90^\circ, \gamma = 120^\circ$ (or $a = b = c, \alpha = \beta = \gamma$)
Hexagonal	one unique sixfold direction 6 or $\bar{6}$	$a = b, c$ $\alpha = \beta = 90^\circ, \gamma = 120^\circ$
Cubic	four threefold directions $\bar{3}$ or $\bar{3}$ (cube diagonals)	$a = b = c$ $\alpha = \beta = \gamma = 90^\circ$

the ambient conditions. *It is important to distinguish between a metric imposed by the symmetry and that due to chance:*

The crystal systems are a classification of the symmetry groups. They are not a classification of the different types of metric. The metric is determined by the symmetry but the metric does not determine the symmetry.

Table 2.9 describing the seven crystal systems is complemented by the following remarks:

- $2/m$ ($= \frac{2}{m}$) defines a *unique direction* of twofold symmetry because the normal to the mirror plane (axis $\bar{2}$) coincides with the twofold axis 2 ; $2/m$ allows the same type of metric as m or 2 .
- It is traditional to identify the unique direction of the twofold axis 2 or the normal to m in the *monoclinic system* with b . The angle β can hence take any value, whereas $\alpha = \gamma = 90^\circ$. In the other non-cubic crystal systems, c is *always chosen to be parallel to the unique axis* (threefold, fourfold or sixfold). It would be logical to abandon the tradition for the monoclinic system and also identify the unique direction with c . In this case γ would be the monoclinic angle and $\alpha = \beta = 90^\circ$. Clearly we could also choose a parallel to the unique axis. It is easy to identify the choice of a particular author by whether the angle β or γ or α has been chosen as the monoclinic angle. The traditional choice is found the most frequently in the literature.

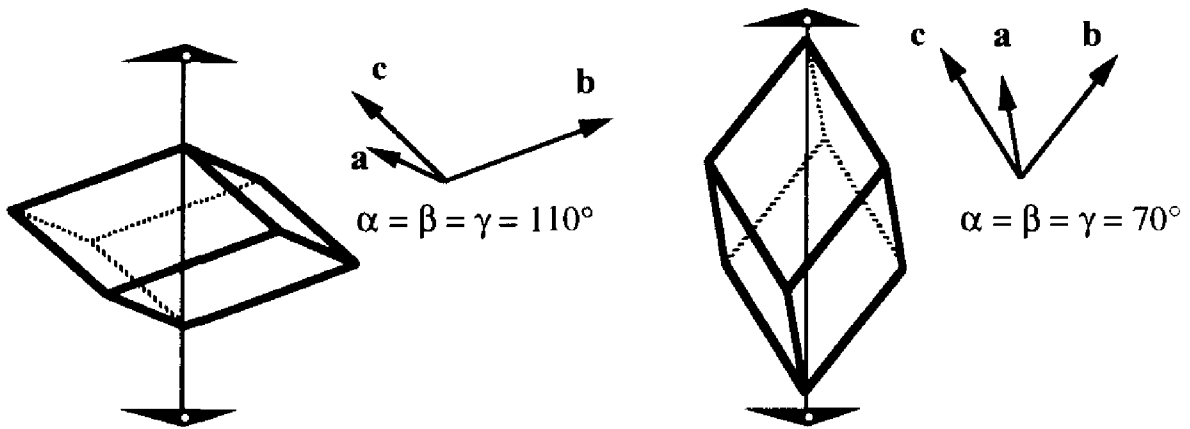


Fig. 2.22. Compressed and stretched rhombohedra

- We use the same type of coordinate system for both the trigonal and hexagonal crystal systems: $a = b, c, \alpha = \beta = 90^\circ, \gamma = 120^\circ$. We choose c to be parallel to the threefold or sixfold axis. However, the trigonal system also allows us to use *rhombohedral axes*, $a = b = c, \alpha = \beta = \gamma$. In this case the axes a, b and c are equivalent due to the threefold axis, but they are neither parallel nor perpendicular to any symmetry element. In the case of the hexagonal system, such a choice would be disadvantageous. The literature contains some confusion concerning the terms *trigonal* and *rhombohedral*. In particular, the trigonal system is often called rhombohedral. The International Union of Crystallography recommends the following terminology:

*The term **trigonal** refers to a crystal system (defined by the presence of a unique 3 or $\bar{3}$ axis); the term **rhombohedral** refers to a choice of coordinate system a, b, c as well as a Bravais lattice (Section 2.6.1).*

The polyhedron that we obtain on stretching or compressing a cube along a body diagonal (Fig. 2.22) is called a *rhombohedron*. The terms *rhombohedral* and *orthorhombic* must not be confused.

- In the *hexagonal system*, the angle γ is, by definition, equal to 120° and not to 60° .
- In the *cubic system*, the vectors a, b, c are parallel to the edges of a cube (symmetry axes $2, \bar{4}$ or 4).

2.5.9 INTERNATIONAL SYMBOLS FOR THE POINT GROUPS

The international symbols list all the unique symmetry elements, i.e. the different classes of symmetry elements. The symmetry elements are indicated by the symbols $1, 2, 3, 4, 6, \bar{1}, m, \bar{3}, \bar{4}, \bar{6}, \frac{2}{m}, \frac{4}{m}$ and $\frac{6}{m}$ (or $2/m, 4/m$ and $6/m$). The center of symmetry is not explicitly indicated because we know that it is implied by the symbols $\bar{1}, \bar{3}, \frac{2}{m}, \frac{4}{m}$ and $\frac{6}{m}$. The symmetry elements are parallel to specific directions in space which are defined relative to the canonical coordinate system a, b, c of the

Table 2.10. Order of the symbols for the symmetry elements which make up the symbol of a point group

System	1st place	2nd place	3rd place
triclinic	1 or $\bar{1}$		
monoclinic	a	b	c
orthorhombic	a	b	c
tetragonal	c	a, b	a + b, a - b
trigonal	c	a, b, a + b	2a + b, a + 2b, -a + b
hexagonal	c	a, b, a + b	2a + b, a + 2b, -a + b
	unique axis	sides of an n-gon	diagonals between sides
cubic	a, b, c	a ± b ± c	a ± b, b ± c, c ± a
	edges of the cube	four body diagonals	six face diagonals

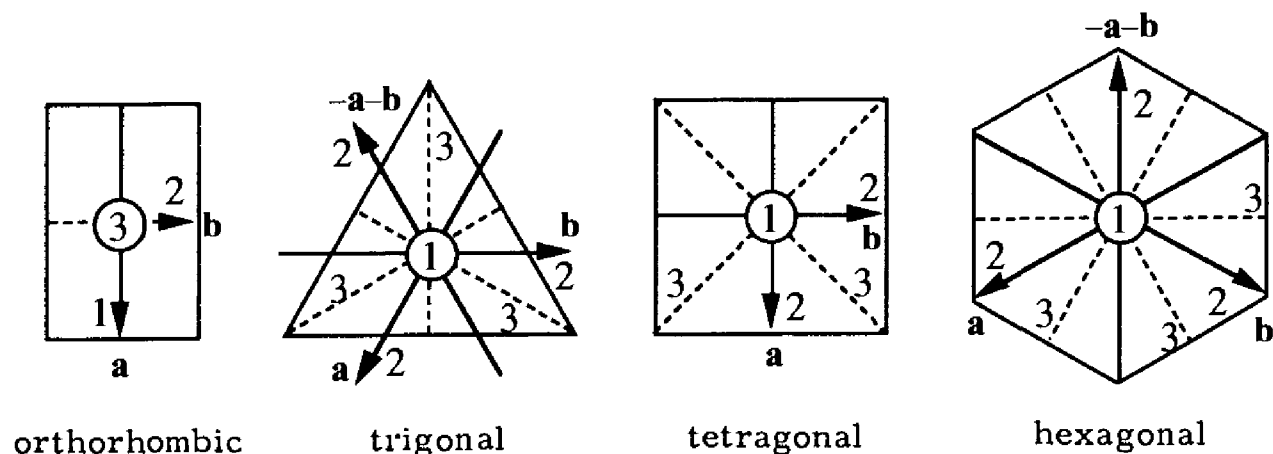


Fig. 2.23. Order of the symbols for the symmetry elements (to be compared with Fig. 2.16)

crystal system to which the group belongs. We consider the orientation of a mirror plane to be determined by the direction of its normal. The international symbol for a point group is made up of one to three symbols which represent the symmetry elements. The symbols for the symmetry elements are arranged in an order which is specific to the crystal system to which the group belongs. This order is defined in Table 2.10 and in Fig. 2.23. Table 2.11 shows the distribution of the crystal classes among the crystal systems.

If necessary, the symbols may be augmented by the addition of axes of order 1 to indicate a specific orientation of the symmetry elements with respect to the coordinate system. Hence the symbol **121** designates the group **2** with the **b** axis parallel to the twofold axis, i.e. the traditional choice of coordinate system for the monoclinic class: there are no symmetry elements parallel to **a** or to **c**. The symbol **112** designates the same group **2** with **c** parallel to the twofold axis. The symbol **m11** designates the group **m** with **a** normal to the mirror plane. The symbol **3m1**

Table 2.11. Distribution of the international symbols among the crystal systems

	triclinic	monoclinic	trigonal	tetragonal	hexagonal
x	1	2	3	4	6
\bar{x}	$\bar{1}$	m	$\bar{3}$	$\bar{4}$	$\bar{6}$
x/m		2/m		4/m	6/m
orthorhombic					
x2		222	32	422	622
xm		mm2	3m	4mm	6mm
$\bar{x}m$			$\bar{3}m$	$\bar{4}2m$	$\bar{6}m2$
x/mmm		mmm		4/mmm	6/mmm
cubic	23	$m\bar{3}$	$\bar{4}3m$	432	$m\bar{3}m$

indicates that the axes **a**, **b** and **a + b** are normal to the mirror planes (as is shown in Fig. 2.20); in contrast, the symbol **31m** indicates that the mirror planes are parallel to these axes. In a similar manner we can make the distinction between **321** and **312**, and between $\bar{3}m1$ and $\bar{3}1m$. Finally, Fig. 2.20 shows the stereographic projections of $\bar{4}2m$ and $\bar{6}m2$; the reader is invited to determine the orientation of the vectors **a**, **b**, **c** for the symbols $\bar{4}m2$ and $\bar{6}2m$.

For the centrosymmetric groups $\frac{2}{m}\frac{2}{m}\frac{2}{m}$, $\frac{4}{m}\frac{2}{m}\frac{2}{m}$, $\frac{6}{m}\frac{2}{m}\frac{2}{m}$, $\frac{3}{m}^2$, $\frac{2}{m}\bar{3}$ and $\frac{4}{m}\bar{3}\frac{2}{m}$ we use the *condensed symbols* **mmm**, **4/mmm**, **6/mmm**, $\bar{3}m$, $m\bar{3}$ and $m\bar{3}m$. In each of these symbols we make no mention of the twofold axes (or the fourfold axes in the case of $m\bar{3}m$) but only indicate the mirror planes which are perpendicular to them. The symmetry elements given in the condensed symbols imply the existence of these twofold (or fourfold) axes.

The international symbol allows us to deduce the crystal system to which the designated group belongs:

- triclinic: 1 or $\bar{1}$
- monoclinic: one single symbol 2 or m, no axis of higher order
- orthorhombic: three symbols 2 or m, no axis of higher order
- trigonal: the symbol begins with 3 or $\bar{3}$
- tetragonal: the symbol begins with 4 or $\bar{4}$
- hexagonal: the symbol begins with 6 or $\bar{6}$
- cubic: the symbol 3 or $\bar{3}$ occupies the second place

2.5.10 SCHOENFLIES SYMBOLS

The non-cubic chiral groups which only contain rotations are identified by the letters C and D. C_x is a *cyclic group* of order *x*, and D_x is a *dihedral group* generated by an axis of order *x* and *x* twofold axes perpendicular to it. The other

Table 2.12. Distribution of the Schoenflies symbols among the crystal systems. This table is organized in the same way as for the international symbols (Table 2.11)

	triclinic	monoclinic	trigonal	tetragonal	hexagonal
$C_x (x)$	C_1	C_2	C_3	C_4	C_6
$S_x (\bar{x})$	C_i	C_s	C_{3i}	S_4	\downarrow
$C_{xh} (x/m)$		C_{2h}		C_{4h}	C_{3h}, C_{6h}
		orthorhombic			
$D_x (x2)$		D_2	D_4	D_4	D_6
$C_{xv} (xm)$		C_{2v}	C_{3v}	C_{4v}	C_{6v}
$D_{xd} (\bar{x}m)$			D_{3d}	D_{2d}	\downarrow
$D_{xh} (x/mmm)$		D_{2h}		D_{4h}	D_{3h}, D_{6h}
cubic	T	T_h	T_d	O	O_h

non-cubic groups are obtained by adding mirror planes to the chiral groups. These planes are indicated in the Schoenflies symbols by the letters *h* (*horizontal*, perpendicular to the principal axis), *v* (*vertical*, parallel to the principal axis) or *d* (*diagonal* between the twofold axes of a dihedral group). If a group contains both a horizontal mirror plane and vertical mirror planes, the symbol *h* is used. In contrast to the international notation, that of Schoenflies uses rotoreflection axes which are, in principle, indicated by S_x . However, most of the rotoreflection axes are equivalent to the combination of a rotation axis and a horizontal mirror plane, or to a rotation axis and a center of symmetry. In these cases we use the symbols C_s (*s* stands for *Spiegel*, mirror in German), C_{3h} (*h* for a horizontal plane), C_i and C_{3i} (*i* for inversion) instead of S_1 ($\bar{1}$), S_3 ($\bar{6}$), S_2 ($\bar{2}$) and S_6 ($\bar{3}$). By analogy with $\bar{6} \equiv C_{3h}$, $\bar{6}m2$ becomes D_{3h} . The chiral cubic groups are designated T (*tetrahedral*) and O (*octahedral*). To indicate the other cubic groups we add the letters *h* and *d*. The Schoenflies symbols for the crystal classes are given in Table 2.12.

2.5.11 ABSTRACT GROUPS

The abstract group of a point group is obtained by setting aside the geometrical significance of the symmetry operations. The *abstract group* is thus *isomorphic* with the point group, i.e. both have the same multiplication table. The abstract cyclic group of order 4, for example, is composed of the objects $R, R^2, R^3, R^4 = E$ (we do not use the term *element* for these objects to avoid any confusion with the *symmetry elements*). It is isomorphic with the groups 4 and $\bar{4}$. Point groups are the *physical realizations* of the abstract groups. The 32 crystal classes are isomorphic with the 18 abstract groups in Table 2.13.

Symmetry operations may be *represented* by matrices. If a three-dimensional coordinate system is chosen, then the relation between the coordinates of equivalent points is given by 3×3 matrices whose determinants are equal to ± 1 .

Table 2.13. The eighteen abstract groups. The parentheses { } contain the isomorphic crystal classes

Order	Cyclic	Abelian non-cyclic	Non-Abelian
1	{1}		
2	{ $\bar{1}$, 2, m}		
3	{3}		
4	{4, $\bar{4}$ }	{2/m, 222, mm2}	
6	{3, 6, 6}		{32, 3m}
8		{4/m}, {mmm}	{422, 4mm, $\bar{4}2m$ }
12		{6/m}	{3m, 622, 6mm, $\bar{6}m2$ }, {23}
16			{4/mmm}
24			{6/mmm}
			{ $m\bar{3}$ }, { $\bar{4}3m$, 432}
48			{ $m\bar{3}m$ }

Each of these matrices is equivalent to an orthogonal matrix (Section 2.2.3). The set of matrices describing the symmetry operations of a point group is a matrix group which is isomorphic with the point group; the matrix group *represents* the point group. Two representations of a group based on two different coordinate systems are *equivalent*. Let R_1, R_2, \dots, R_n be the matrices for the coordinate system $\mathbf{a}, \mathbf{b}, \mathbf{c}$, and R'_1, R'_2, \dots, R'_n the matrices for the system $\mathbf{a}', \mathbf{b}', \mathbf{c}'$; in addition, let T be the matrix which transforms the coordinates of a point (x, y, z) in the system $\mathbf{a}, \mathbf{b}, \mathbf{c}$ into the coordinates (x', y', z') in the system $\mathbf{a}', \mathbf{b}', \mathbf{c}'$. The relation between the matrices R_i and R'_i is thus:

$$R'_i = TR_iT^{-1} \quad (2.14)$$

The crystal classes are those point groups which are compatible with a lattice (Section 2.4.3). For each crystal class, there is a lattice type which is invariant with respect to all the symmetry elements of that class. A three-dimensional crystal class is thus a point group which can be represented by 3×3 matrices whose elements are all integers (Section 2.4.1). The representations of two different crystal classes cannot be changed from one into the other by a change in coordinate system by application of equation (2.14).

2.6 CLASSIFICATION OF LATTICES

2.6.1 THE 14 BRAVAIS LATTICES

The Bravais lattices (or Bravais classes) represent a *classification of the translation lattices according to the symmetry imposed metric*. They were originally derived by

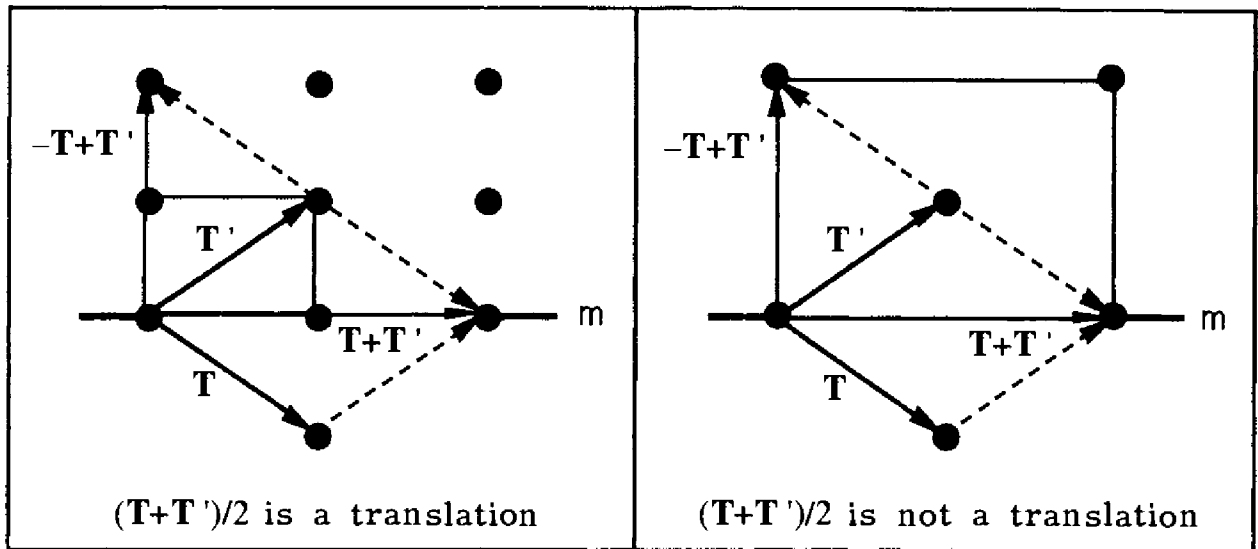


Fig. 2.24. Primitive and centered rectangular lattices

the Abbé M.A. Bravais (*Journal de l'École polytechnique*, Paris, 1850). In Section 2.4.2 we saw that the symmetry imposes a particular metric on the lattice. Figure 2.10 shows the regular tilings that correspond to the Euclidean plane. This observation leads us to choose the usual (or canonical) coordinate system corresponding to the crystal system (Section 2.5.8). However, if we choose such a lattice base, we do not necessarily obtain a primitive cell. We can illustrate this fact by the use of two-dimensional lattices.

In Fig. 2.24, m represents a mirror line. Let \mathbf{T} be a primitive translation and \mathbf{T}' the mirror image of \mathbf{T} . (A translation \mathbf{T} is *primitive* if $1/2\mathbf{T}$ is not a translation.) $\mathbf{T} + \mathbf{T}'$ and $\mathbf{T} - \mathbf{T}'$ are perpendicular and define a rectangular cell. If $\mathbf{T} + \mathbf{T}'$ and $\mathbf{T} - \mathbf{T}'$ are primitive translations, the rectangular cell is centered because there is a lattice point in the middle. We would thus choose the diamond $(\mathbf{T}, \mathbf{T}')$ as the primitive cell. In contrast, if $1/2(\mathbf{T} + \mathbf{T}')$ and $1/2(\mathbf{T} - \mathbf{T}')$ are translations, we then obtain a rectangular primitive cell. These two rectangular planar lattices, primitive, on the one hand and centered or diamond, on the other, are representative of two types of lattice that it is important to differentiate. It is impossible to find a primitive diamond-shaped cell for the first, or a primitive rectangular cell for the second. These considerations lead us to an *operational* definition for the Bravais lattices (or classes). A **Bravais lattice** is characterized by:

- the metric of the cell (see *crystal systems*, Section 2.5.8)
- the type of cell (primitive P, multiple A, B, C, F, I, R as shown in Table 1.1, Section 1.4.1).

The Bravais class of a lattice is given by the metric and the type of the smallest cell that can be obtained by choosing a canonical basis in accord with the crystal system.

It must be noted that the metric is imposed by the symmetry of the crystal. A triclinic lattice at a given temperature and pressure could have a monoclinic metric by coincidence but still not be monoclinic.

Let us remember that there are five two-dimensional Bravais lattices (Fig. 2.10, Section 2.4.2): oblique \mathbf{p} , rectangular \mathbf{p} and \mathbf{c} , square \mathbf{p} and hexagonal \mathbf{p} . In two dimensions we symbolize the cell type by lower-case letters \mathbf{p} (primitive) and \mathbf{c} (centered). In contrast, we use the upper-case letters \mathbf{P} , \mathbf{A} , \mathbf{B} , \mathbf{C} , \mathbf{F} , \mathbf{I} , \mathbf{R} for the fourteen three-dimensional lattices (Fig. 2.25). Figure 2.26 shows that the oblique \mathbf{c} lattice belongs to the same Bravais class as the oblique \mathbf{p} lattice. The two lattices have the same type of metric and a change in coordinate system transforms one into the other. The square \mathbf{c} and \mathbf{p} lattices belong to the same Bravais class for the same reason. In contrast, the rectangular \mathbf{c} lattice cannot be transformed into a rectangular \mathbf{p} lattice (Fig. 2.24).

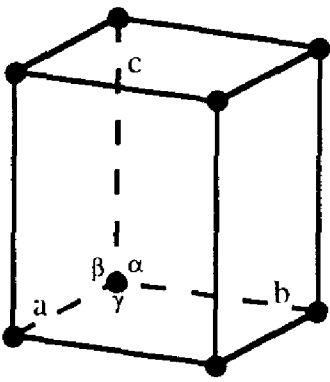
The conventional unit cells for the fourteen three-dimensional Bravais lattices are shown in Fig. 2.25. Each of these cells represents one lattice class. *Some important supplementary information is presented in Section 1.4.1 to which may be added the following comments:*

- *Monoclinic lattices.* Figure 2.25 shows the normal orientation where the unique direction is \mathbf{b} (international symbol $1\ 2/m\ 1$, Section 2.5.8 and 2.5.9). All the $(h\ 0\ l)$ lattice planes are rectangular. In the \mathbf{C} lattice, one of the rectangular planes is centered and, hence, of the *diamond* type. The \mathbf{A} , \mathbf{C} , \mathbf{I} and \mathbf{F} monoclinic lattices all belong to the Bravais class represented by \mathbf{C} because a change of base without changing the type of metric will transform any one into another. The transformation $\mathbf{a}' = -\mathbf{c}$, $\mathbf{c}' = \mathbf{a}$ changes \mathbf{A} into \mathbf{C} ; $\mathbf{a}'' = \mathbf{a} + \mathbf{c}$, $\mathbf{c}'' = \mathbf{c}$ changes \mathbf{I} into \mathbf{C} ; $\mathbf{a}''' = \mathbf{a}$, $\mathbf{c}''' = 1/2(\mathbf{a} + \mathbf{c})$ changes \mathbf{F} into \mathbf{C} . The \mathbf{B} lattice is equivalent to the \mathbf{P} lattice. In the case of the alternative orientation where the unique axis is \mathbf{c} (international symbol $1\ 1\ 2/m$), it is traditional to represent the two monoclinic Bravais classes by \mathbf{P} and \mathbf{B} .
- *Orthorhombic lattices.* The \mathbf{A} and \mathbf{B} lattices are clearly equivalent to the \mathbf{C} lattice.
- *Tetragonal lattices.* \mathbf{C} is equivalent to \mathbf{P} (Fig. 2.26), and \mathbf{F} is equivalent to \mathbf{I} . The existence of \mathbf{A} or \mathbf{B} lattices is forbidden by the fourfold axis.
- *Hexagonal or rhombohedral lattices.* These lattices cannot be unequivocally related to corresponding crystal systems.

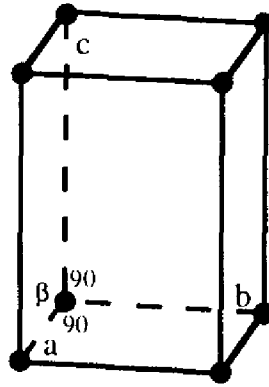
The hexagonal \mathbf{P} lattice is compatible with all the trigonal or hexagonal groups.

Figure 2.25 shows the unit cell for this lattice inscribed in a hexagonal prism. Note that this prism does not represent the unit cell, this latter always being a parallelepiped. We have already noted elsewhere that the hexagonal angle is defined to be 120° and not 60° .

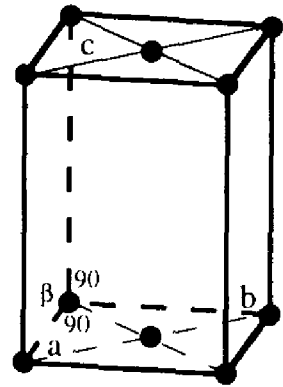
The \mathbf{R} lattice is only compatible with the trigonal groups.



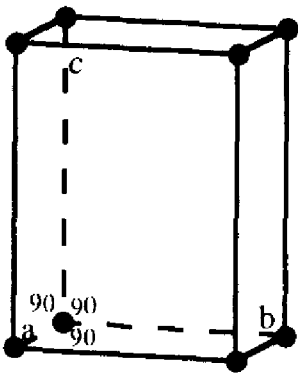
triclinic P



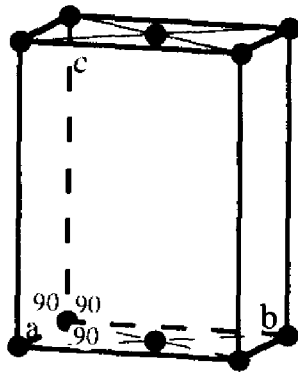
monoclinic P



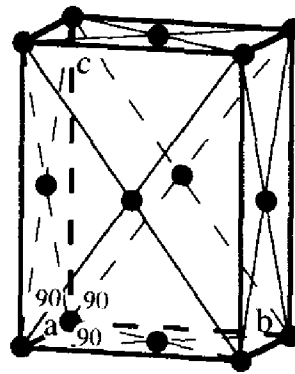
monoclinic C



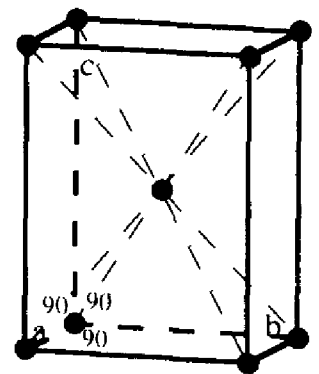
orthorhombic P



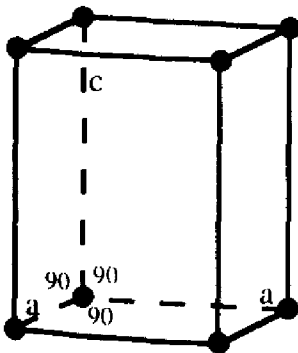
orthorhombic C



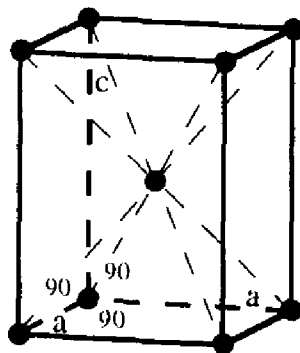
orthorhombic F



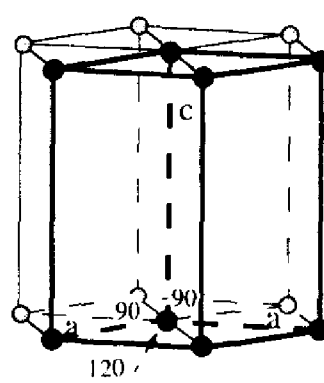
orthorhombic I



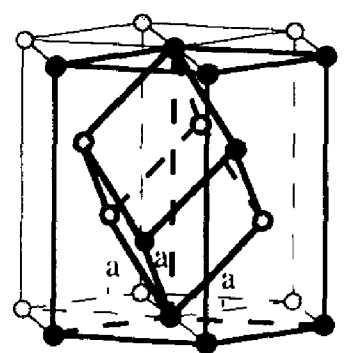
tetragonal P



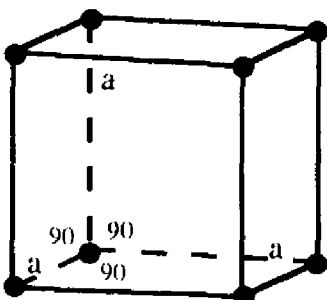
tetragonal I



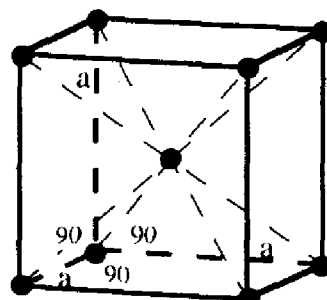
hexagonal P



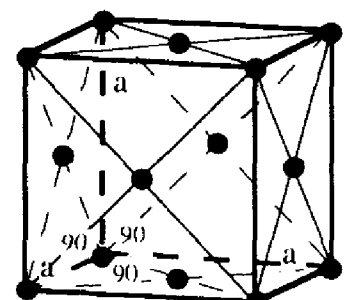
rhombohedral R



cubic P



cubic I



cubic F

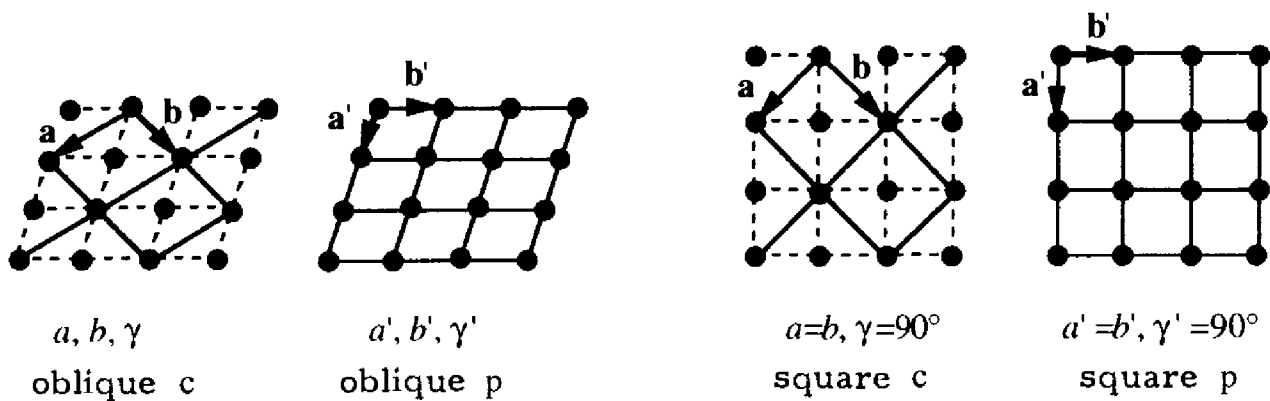


Fig. 2.26. Equivalence of the *c* and *p* oblique lattices and the *c* and *p* square lattices

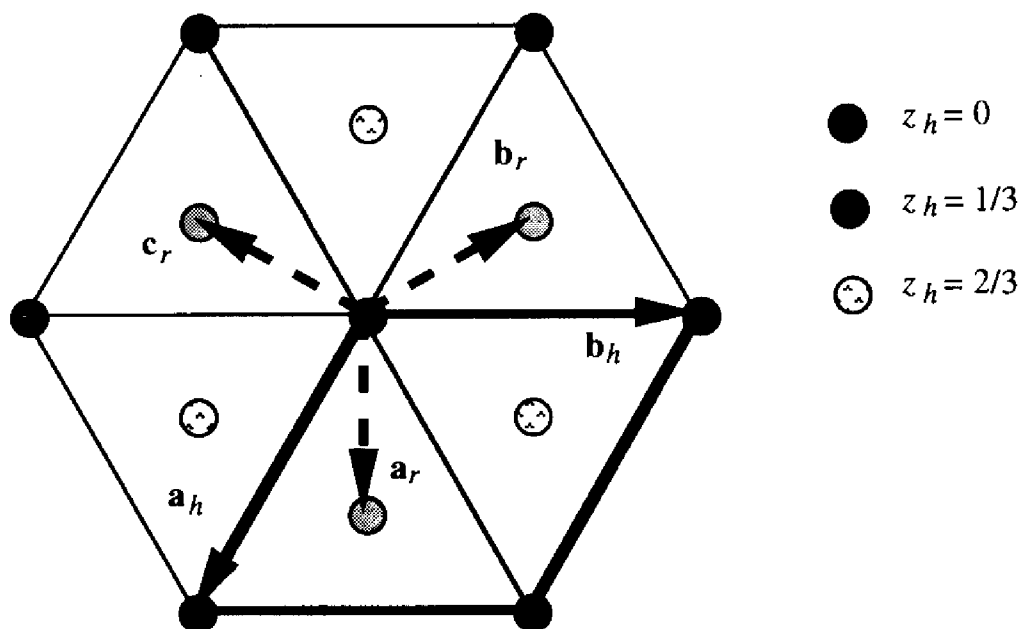


Fig. 2.27. The hexagonal and rhombohedral bases for an R lattice

Figure 2.27 shows a projection down the threefold axis. We can choose a hexagonal cell centered at $(\frac{2}{3}, \frac{1}{3}, \frac{1}{3})$ and $(\frac{1}{3}, \frac{2}{3}, \frac{2}{3})$ with translations $\mathbf{a}_h, \mathbf{b}_h, \mathbf{c}_h$ (\mathbf{c}_h following the threefold axis), or else a primitive rhombohedral cell (Fig. 2.22) with symmetry equivalent translations:

$$\mathbf{a}_r = \frac{1}{3}(2\mathbf{a}_h + \mathbf{b}_h + \mathbf{c}_h), \quad \mathbf{b}_r = \frac{1}{3}(-\mathbf{a}_h + \mathbf{b}_h + \mathbf{c}_h), \quad \mathbf{c}_r = \frac{1}{3}(-\mathbf{a}_h - 2\mathbf{b}_h + \mathbf{c}_h). \quad (2.15)$$

In practice, we often choose the centered hexagonal cell $\mathbf{a}_h, \mathbf{b}_h, \mathbf{c}_h$ because the axes are then oriented with respect to the directions of highest symmetry.

The fact that the hexagonal *P* lattice is compatible with two different crystal systems has been the cause of frequent misunderstandings in the literature. Thus

the trigonal crystal system has been called rhombohedral by certain authors, whereas others have tried to combine the trigonal and hexagonal crystal systems into one single hexagonal system. It is important to follow the usage recommended by the International Union of Crystallography:

- the 32 crystal classes are divided into seven *crystal systems* which are called *triclinic, monoclinic, orthorhombic, tetragonal, trigonal, hexagonal and cubic*;
- the fourteen Bravais lattices (or classes) are divided into seven *Bravais systems* which are called *triclinic, monoclinic, orthorhombic, tetragonal, rhombohedral, hexagonal and cubic*;
- we can define six *crystal families* which unite crystal classes and Bravais lattices: *triclinic, monoclinic, orthorhombic, tetragonal, hexagonal and cubic*.

The term trigonal identifies a set of symmetry groups. The term rhombohedral identifies a type of lattice.

2.6.2 HOLOHEDRY AND MEROHEDRY

Each Bravais system has its corresponding minimum and maximum symmetry. Thus the Bravais lattice *must* be monoclinic (P or C) if the crystal has only one mirror plane or one twofold axis (crystal classes m or 2). However, the monoclinic unit cell will also allow the symmetry $2/m$. Thus the symmetry of the contents of the unit cell (the motif) may be less than that of the empty cell. In this case we speak of *merohedry*. The formation of twins is relatively frequent for merohedral crystals. A *twin* (Fig. 2.28) is an interpenetration or aggregation of several crystals of the same species whose relative orientations follow well-defined laws. These orientations are related by symmetry operations which do not belong to the crystal class of the untwinned crystal, either by a rotation about a translation

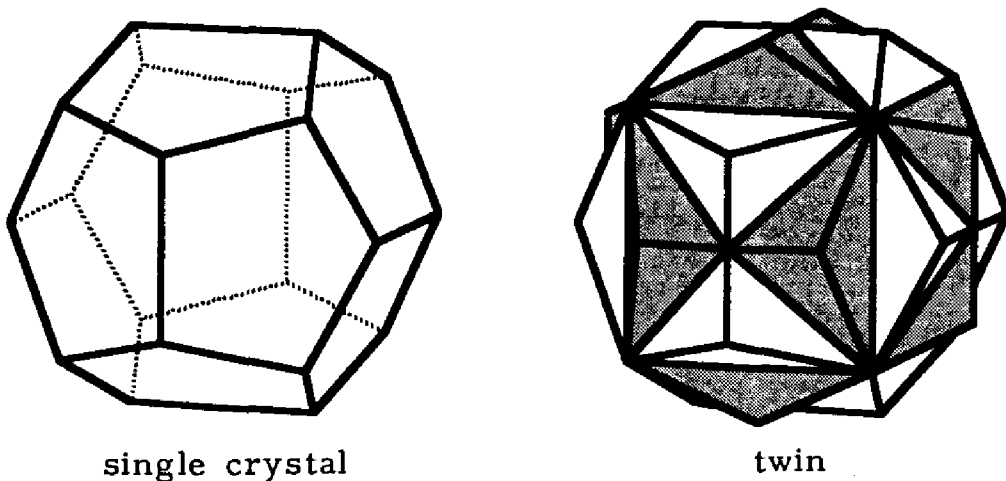


Fig. 2.28. Merohedral interpenetration twin of pyrite, FeS_2 , class $m\bar{3}$

Table 2.14. Holohedral and merohedral classification of the crystal classes

Bravais system	Holohedral groups	Merohedral groups		
		Hemihedral	Tetartohedral	Ogdohedral
triclinic	$\bar{1}$	1		
monoclinic	2/m	2, m		
orthorhombic	mmm	222, mm2		
tetragonal	4/mmm	422, 4mm, $\bar{4}2m$, 4/m	4, $\bar{4}$	
rhombohedral	$\bar{3}m$	32, 3m, $\bar{3}$	3	
hexagonal	6/mmm	622, 6mm, $\bar{6}m2$, 6/m	6, $\bar{6}$	
cubic	$m\bar{3}m$	3m	32, 3m, $\bar{3}$	3
		432, $\bar{4}3m$, $m\bar{3}$	23	

$[u \ v \ w]$ or by reflection by a lattice plane $(h \ k \ l)$. The symmetry of the twin is generally higher than that of the untwinned crystal.

The maximum symmetry of a Bravais system is called *holohedry*. Holohedry is identical to the point group of the empty cell. A merohedral group whose order is one half that of the holohedral group is called *hemihedral*. Likewise, it is called *tetartohedral* if its order is one fourth, or *ogdohedral* if its order is one eighth that of the holohedral group. Table 2.14 gives the holohedral and merohedral classifications of the crystal classes.

The trigonal groups are both holohedral or merohedral rhombohedral groups, and merohedral hexagonal groups. Indeed, the trigonal groups are subgroups of both $m\bar{3}m$ and 6/mmm. The trigonal deformation of a cubic structure (elongation or compression along a body diagonal of the cube) gives an R lattice. The trigonal distortion of a hexagonal structure gives a P hexagonal lattice.

2.7 SYMMETRY OF PERIODIC STRUCTURES

2.7.1 THE 17 PLANE GROUPS

In this section we will describe the two-dimensional space groups, or plane groups, which will serve as an introduction to the 230 space groups. The symmetry elements in the Euclidean plane are:

- the rotation points 1, 2, 3, 4, 6
- the mirror line m
- the translations
- the glide line symbolized with the letter g .

With these symmetry elements we find:

- ten crystal classes: 1, 2, 3, 4, 6, m, 2mm, 3m, 4mm, 6mm. The international symbols are interpreted in the same way as those for the three-dimensional groups (Table 2.10 and Fig. 2.23), except that the first place is always reserved to indicate the order of the rotation point.
- four crystal systems: oblique, rectangular, square, hexagonal
- five Bravais lattices: oblique p , rectangular p and c , square p , hexagonal p
- seventeen plane groups

The two-dimensional Bravais systems are identical to the crystal systems. In two-dimensional space we do not find the *trigonal–hexagonal–rhombohedral* complications described above. Graphical representations of the 17 plane groups are presented in Fig. 2.29. The graphical symbols are explained in Tables 2.4 and 2.5 (Section 2.3.3). The arrows indicate the equivalent positions in the unit cell. We encounter the symmetry of periodic patterns in our daily lives. Those interested are invited to identify the symmetry groups of patterns on wallpapers, wrapping papers, wall tilings, pavings of city streets and squares, bed sheets, tablecloths and window curtains.

Let us remember that in a periodic structure we find *series of symmetry elements* (Section 2.4.1). Thus, a symmetry element is repeated with the periodicity of the lattice. In addition, we obtain several classes of symmetry elements, i.e. inequivalent series of elements. Figure 2.9 showed two equivalence classes of reflection lines m and m' in a periodic one-dimensional pattern. The product of a reflection by a line m and a primitive translation is a reflection by a line m' . In general, we find the following equivalence classes:

- half-way between two twofold points which are equivalent by translation, we find a twofold point belonging to another class. Thus the group $p2$ has four classes of twofold points;
- in the middle of a triangle formed by three threefold points which are equivalent by translation, we find another threefold point of another class. Thus the group $p3$ has three classes of threefold points;
- in the middle of a square formed by four fourfold points which are equivalent by translation, we find another fourfold point of another class. Thus the group $p4$ has two classes of fourfold points. Half-way between two fourfold points which are equivalent by translation, we find a twofold point because a fourfold point is equally a twofold point;
- we only find one class of sixfold points in the group $p6$, but this group also includes a class of threefold points and a class of twofold points;
- half-way between two reflection lines equivalent by translation in a rectangular p lattice we find a reflection line of another class. The group pm thus includes two classes of reflection lines;

- half-way between two glide lines equivalent by translation in a rectangular p lattice we find a glide line of another class. The group pg thus includes two classes of glide lines;
- half-way between two reflection lines equivalent by translation in a rectangular c lattice (*diamond* lattice) we find a glide line. The group cm thus includes a class of reflection lines and a class of glide lines.

We identify the plane groups by the *international symbols* whose interpretation is quite straightforward:

- *first place*
letter p or c to characterize the type of unit cell.
- *second place*
modified international symbol of the corresponding crystal class. The letter m in the symbol is replaced by the letter g if we find a series of glide lines instead of reflection lines in the direction implied by the symbol.

The symbol for the crystal class may be derived from the symbol for a plane group by removing all references to translations (see Section 2.4.3 for the relation between a plane group and the crystal class);

<i>symbol for the plane group</i>	→	<i>symbol for the crystal class</i>
lattice type (p or c)	→	remove the symbol
1, 2, 3, 4, 6	→	1, 2, 3, 4, 6
m	→	m
g	→	m

Note that the symbol for the plane group contains the complete information concerning the crystal system and the Bravais lattice.

By systematically replacing the rotation points and the reflection lines of the ten crystal classes by series of reflection points, by series of reflection lines and by series of glide lines, and taking into account the metric of the Bravais lattices, we can list all the plane groups. From the crystal classes 1, 2, 3, 4 and 6, we obtain the groups $p1$, $p2$, $p3$, $p4$ and $p6$. The groups pm , pg and cm belong to the class m . cg is an alternative (but not employed) symbol for cm because this group contains a succession of glide lines as well as reflection lines. The plane groups which belong to $2mm$ are obtained by replacing zero, one or two m lines by g . The symbol $p2mg$ indicates that the a and b axes are perpendicular to the series of lines m and g respectively. The symbol $p2gm$ designates the same group with a and b interchanged. $c2mg$, $c2gm$ and $c2gg$ are alternative (but unemployed) symbols for $c2mm$. In order to derive the plane groups of $4mm$, it is useful to remember that a *square* is a special case of a *diamond*. We find the same succession of lines m and g parallel to the diagonals of the square as in the group $c2mm$. For this reason, the symbols $p4mg$ and $p4gg$ are alternative symbols for $p4mm$ and $p4gm$ respectively. The unit cell of the hexagonal system is also a special case of a *diamond* and all reflection lines alternate with glide lines. It is necessary to

distinguish between $p3m1$ and $p31m$. In $p3m1$, the reflection lines are perpendicular to the shortest translations of the lattice. In $p31m$, the reflection lines are perpendicular to the long diagonal of the unit cell and its equivalent translations.

2.7.2 EQUIVALENT POSITIONS

A set of points that is equivalent with respect to a symmetry group is called an *orbit*. The polyhedra of Fig. 2.17 represent orbits of point groups. The arrows in Fig. 2.29 represent the orbits of plane groups. For the majority of groups, there are several types of orbit that we refer to as *general positions* and *special positions*. We will illustrate this important point with the aid of the plane group $p2mg$ (Fig. 2.30).

General positions

If an object is placed in the rectangular unit cell, the symmetry operations of the group $p2mg$ generate an infinite number of like objects. In a general position (x, y) we find four of these objects per unit cell with the coordinates $x, y; -x, -y; 1/2 - x, y; 1/2 + x, -y$. We say that the *multiplicity* is 4. *Each of these four coordinates indicates the position of an object as well as those which are equivalent to it by translation.* Each of these four sets of points which are equivalent by translation is generated by the symmetry operations of one of the cosets of the invariant subgroup of the translations T (Section 2.4.3). *Note that the object itself may be asymmetric, point group 1.*

Special positions

If $x = 1/4$, the coordinates x, y and $1/2 - x, y$ are identical. They represent a point on the reflection line. The orbit only includes two objects per unit cell, but these are invariant with respect to reflection. The multiplicity is thus 2, but the *site symmetry* is m . The two periods (.) in the symbol ' $.m$.' mark the positions in the international symbol of the plane group (Section 2.7.1) which refer to the rotation point and the directions a and b ; $.m$. indicates that the reflection line is perpendicular to a .

There are two other special positions located on the twofold points with a multiplicity of 2 and site symmetry $2..$; thus, an object which occupies this position must be invariant with respect to a twofold rotation. Figure 2.30 shows that the point symmetry of the object can be higher but not lower than the site symmetry. The object placed at $(0, 0)$ has the symmetry 2 , whereas the symmetry $2mm$ of the object placed at $(0, 1/2)$ is higher than the site symmetry (mirror planes parallel and perpendicular to the axis of the dumbbell).

The letters a, b, c, d in Fig. 2.30 are called *Wyckoff symbols*. Although they have no special significance, they serve as a rapid reference for the different sites.

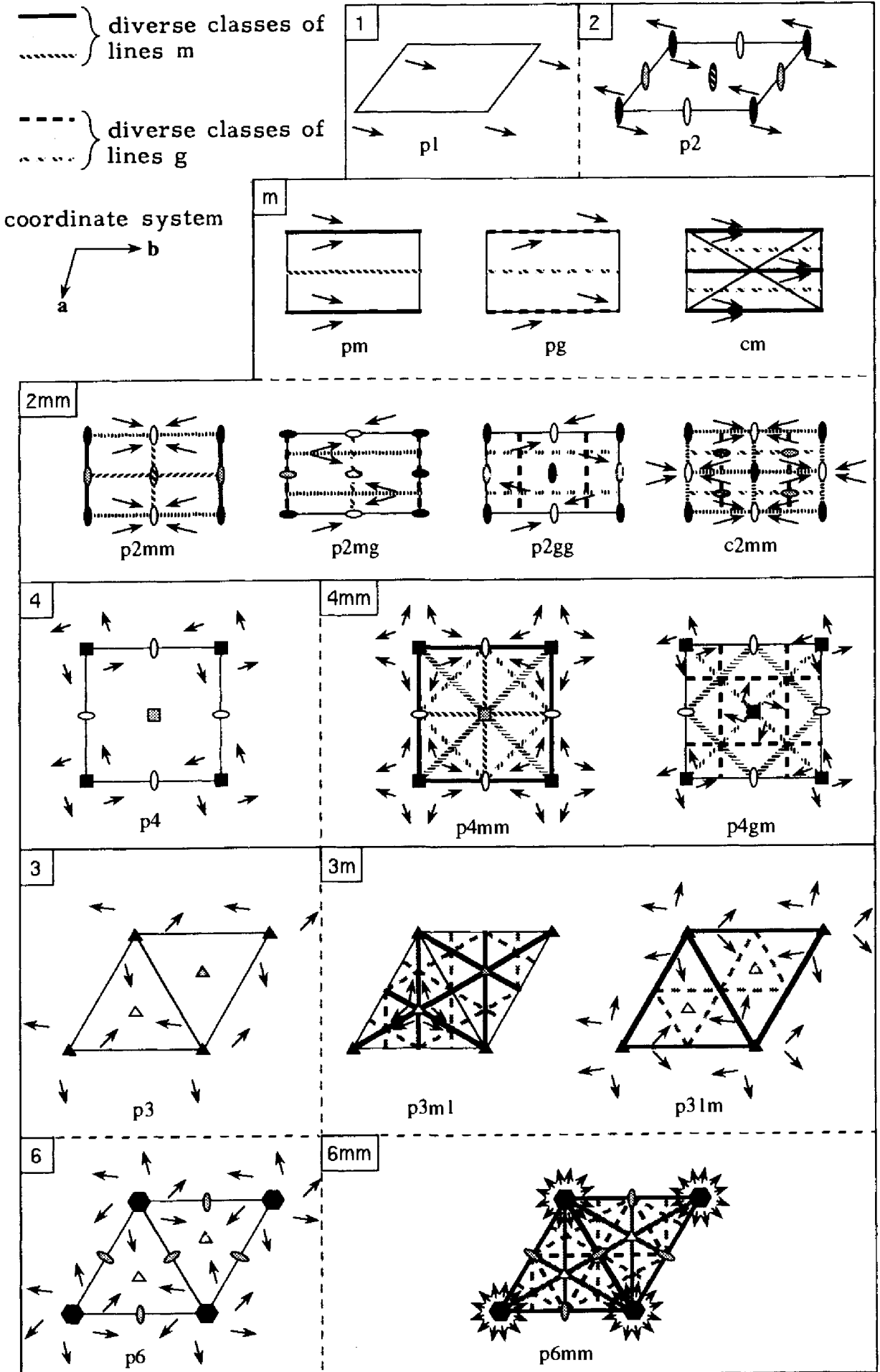


Fig 2 29 The 17 plane groups

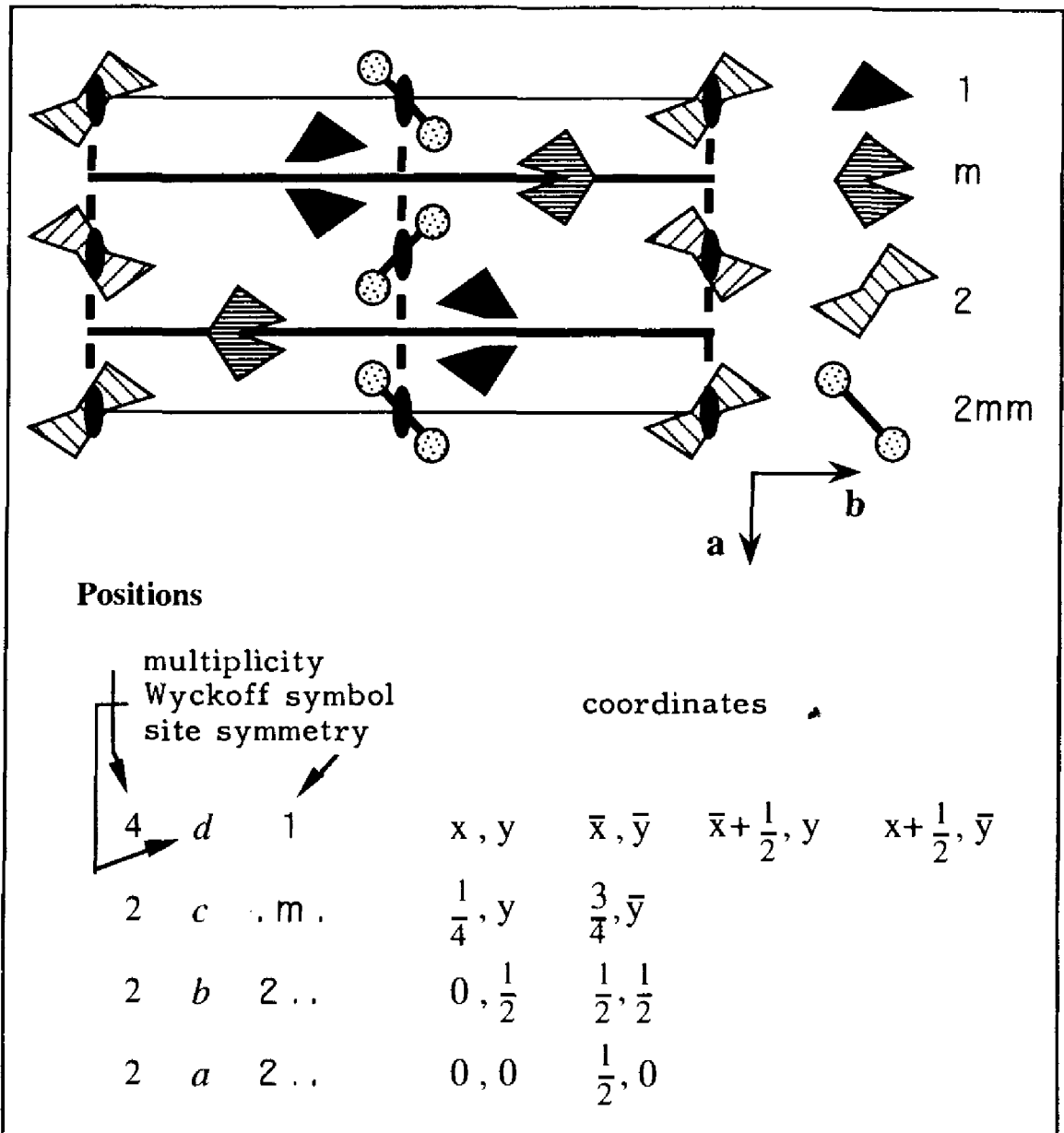


Fig. 2.30. Orbits for p2mg, general and special positions

All the general and special positions for all of the plane groups are listed in the *International Tables for Crystallography*.

2.7.3 THE 230 SPACE GROUPS

The discussion of the plane groups presented in Sections 2.7.1 and 2.7.2 contains all of the ideas necessary to understand space groups. The transition from the Euclidean plane to three-dimensional space requires no new concepts. However, because of the large number of space groups, we will look at only a limited number of examples. The *International Tables for Crystallography* assemble all the information for these groups. It is thus important to know how to use this compilation correctly and efficiently.

We recall that a rotation axis in the crystal class corresponds to a series of rotation axes or screw axes in the space group; a mirror plane in the crystal class corresponds to a series of mirror planes or glide planes in the space group (Section 2.4.3):

<i>crystal class</i>		<i>space group</i>
2	→	2, 2 ₁
3	→	3, 3 ₁ , 3 ₂
4	→	4, 4 ₁ , 4 ₂ , 4 ₃
6	→	6, 6 ₁ , 6 ₂ , 6 ₃ , 6 ₄ , 6 ₅
m	→	m, a, b, c, n, d

A description of these symmetry elements and their symbols may be found in Figs. 2.6–2.8 and in Tables 2.4 and 2.5. This correspondence allows us to characterize space groups with symbols analogous to those used for the plane groups (Section 2.7.1). The *international symbol for a space group* is composed of:

- one of the letters P, A, B, C, F, I or R to indicate the type of unit cell
- the modified international symbol of the crystal class.

As examples, let us list some of the space groups of the crystal class mmm: Pmmm, Pmma, Pbcm, Pbca, Pnm, Ccca, Fmmm, Ibca, etc. By remembering the way in which the international symbol for the crystal class is formed (Section 2.5.9), we can easily interpret the symbols for the corresponding space groups. Because mmm belongs to the orthorhombic system, the first m is a mirror plane normal to **a**, the second m is normal to **b**, and the third m is normal to **c**. For example, the unit cell of the group Pbca is primitive; normal to **a** we find mirror planes with a glide component 1/2**b**; normal to **b** we find mirror planes with a glide component 1/2**c**; normal to **c** we find mirror planes with a glide component 1/2**a**. In fact we can derive all the space groups from mmm by systematically replacing the first m by m, b, c or n, the second m by m, a, c or n, and the third m by m, a, b or n. Clearly we cannot find a plane **a** normal to **a**, nor a plane **b** normal to **b**, nor a plane **c** normal to **c**. (The d glides are always parallel to centered lattice planes and, in the orthorhombic system, we only encounter them for F unit cells. An in-depth knowledge of the geometrical properties of these planes is not essential for the everyday use of the *International Tables*.) We derive the group Ibca from Pbca by adding the translation (1/2, 1/2, 1/2). Note that the different symbols obtained by the above procedure may refer to the same group. For example, Pmmb and Pmma symbolize the same group but with respect to a different coordinate system. The transformation required to pass from Pmmb to Pmma is **a'** = **b**, **b'** = –**a**, **c'** = **c**. The *International Tables* also list these alternative symbols. Some other examples of space groups are P2₁/c, P2₁2₁2₁, P2₁2₁2, I4c2, I42d, P31c, P6₃/mcm, Pn3n, etc.

From these symbols it is easy to derive the *crystal class*, the *Bravais lattice*, and the *crystal system* by removing all reference to translations:

The crystal class is obtained by removing the letter which indicates the type of unit cell and by replacing any screw axes by the corresponding rotation axes as well as the letters a, b, c, n, d by m.

For example, the crystal class for $I\bar{4}c2$ is $\bar{4}m2$, an alternative symbol for $\bar{4}2m$. The crystal system is tetragonal and the Bravais lattice is tetragonal I.

In the majority of cases, the international symbol contains all the information necessary to derive all the properties of the group and, in particular, all the orbits (general and special positions). Let us take the group $Pnma$ as an example. The corresponding pages taken from the *International Tables* are reproduced below. By replacing n and a with m , we obtain the symbol mmm of the crystal class; the crystal system is thus orthorhombic and the unit cell is rectangular and primitive. Let us place a plane n perpendicular to a and passing through $x = 0$ (the reader is invited to complement these explanations by making a sketch). This transforms a general point x, y, z into $\bar{x}, 1/2 + y, 1/2 + z$ (reflection followed by a translation of $1/2b + 1/2c$). Now let us put a plane m perpendicular to b and passing through $y = 0$. This transforms the two points above into x, \bar{y}, z and $\bar{x}, 1/2 - y, 1/2 + z$. Finally, let us put a plane a perpendicular to c and passing through $z = 0$. This last transforms the four points into $1/2 + x, y, \bar{z}; 1/2 - x, 1/2 + y, 1/2 - z; 1/2 + x, \bar{y}, \bar{z}$ and $1/2 - x, 1/2 - y, 1/2 - z$. These eight points and their equivalents by translation constitute a general orbit of multiplicity 8. The complete symbol for the crystal class is $\frac{2}{m} \frac{2}{m} \frac{2}{m}$. The group thus includes twofold axes and centers of symmetry. We can find the corresponding series of centers of symmetry, twofold axes and/or screw axes with the help of a sketch. Finally, we displace the origin to one of the centers of symmetry (there are eight equivalence classes). Thus we find the coordinates as listed in the *International Tables*. We can also obtain this information directly from algebraic operations on the coordinates derived above. Thus, the operation which transforms x, y, z into $1/2 - x, 1/2 - y, 1/2 - z$ is a center of symmetry at the fixed point $1/4, 1/4, 1/4$.

For the group $P\bar{4}2_1c$, the orbits can be generated by placing a twofold screw axis 2_1 parallel to the a axis and a mirror plane m at 45° along the diagonal of the square face of a tetragonal unit cell. By successive application of the corresponding symmetry elements, we can construct an orbit for $P\bar{4}2_1c$ starting from a general point and generate the coordinates given in the *International Tables*, the relevant pages for $P\bar{4}2_1c$ being reproduced below. Note that the orbits of the groups belonging to $\bar{4}2m$ cannot be generated from a $\bar{4}$ axis in combination with a mirror plane or a twofold axis as these symmetry elements do not necessarily intersect, and their positions are not known *a priori*.

Volume A of the *International Tables* contains a complete description of all space groups. A number of examples are given on the following pages. The reader is referred to the explanations given in the *International Tables* for additional information.

2.7.4 EXAMPLES OF SOME PAGES FROM THE INTERNATIONAL TABLES

For the majority of applications, it is sufficient to understand the space group symbol, the crystal class and the crystal system, the corresponding diagrams, the equivalent positions and the conditions for observing reflection of X-rays. Examples are presented in Figs 2.31–2.34.

Comments:

C_s^4 : Schoenflies symbol

Patterson symmetry: Section 3.9.2

b unique: corresponds to $C1c1$

4 projections of the unit cell: down **b**, **a**, **c** (symmetry elements), and down **b** (general orbit)

a_p : projection of **a**

c_p : projection of **c**

○ ⊙ general position

⊙ generated from ○ by an operation of the second type

+, -: coordinate along the projection axis; here +y, -y, 1/2+y, 1/2-y

Origin of the coordinate system

Numbering () of the operations and positions of the planes **c**, **n**

identity, planes **c** at $y = 0, 1/2$

translation, planes **n** at $y = 1/4, 3/4$

Cc	C_s^4	m	Monoclinic
No. 9	$C1c1$	Patterson symmetry $C1\ 2/m\ 1$	
UNIQUE AXIS b , CELL CHOICE 1			
Origin on glide plane c			
Asymmetric unit $0 \leq x \leq 1; 0 \leq y \leq \frac{1}{4}; 0 \leq z \leq 1$			
Symmetry operations			
For $(0, 0, 0)_+$ set			
(1) 1		(2) $C\ x, 0, z$	
For $(\frac{1}{2}, \frac{1}{2}, 0)_+$ set			
(1) $t(\frac{1}{2}, \frac{1}{2}, 0)$		(2) $n(\frac{1}{2}, 0, \frac{1}{2})\ x, \frac{1}{4}, z$	

Fig. 2.31. Group Cc , explanation of the symbols in the *International Tables*

identity, 4 translations,
glide plane

Positions: fig. 2.30
reflection conditions:
systematic absences
(Section 3.8)

(0,0,0)+,(1/2,1/2,0)+:
translations, see Section 1.4.1
4 equivalent points per cell

x,y,z ; $x,-y,z+1/2$;
 $x+1/2,y+1/2,z$;
 $x+1/2,1/2-y,z+1/2$

(see projection of the
cell); (1), (2) identify the
symmetry operations

plane groups and translations
of the projections down
 c , a and b

subgroups of maximal
order: I same translations,
II same crystal class, (a same
base; b, c larger cell);
[] ... () ... = [index of the
subgroup]

full international symbol
and lattice base (conventional
international symbol)

Supergroups of minimal
order: same code as above.
See *International Tables*
for more detailed information
if necessary

CONTINUED		No. 9	Cc
Generators selected			
(1); $t(1,0,0)$; $t(0,1,0)$; $t(0,0,1)$; $t(\frac{1}{2}, \frac{1}{2}, 0)$; (2)			
Positions	Coordinates		Reflection conditions
Multiplicity			
Wyckoff letter			
Site symmetry	(0, 0, 0)+	$(\frac{1}{2}, \frac{1}{2}, 0)+$	General:
4 a 1	(1) x, y, z	(2) $x, \bar{y}, z+\frac{1}{2}$	$hkl: h+k=2n$ $h0l: h, l=2n$ $0kl: k=2n$ $hk0: h+k=2n$ $0k0: k=2n$ $h00: h=2n$ $00l: l=2n$
Symmetry of special projections			
Along [001] $c11m$	Along [100] $p1g1$	Along [010] $p1$	
$a' = a_p, b' = b$	$a' = \frac{1}{2}b, b' = c_p$	$a' = \frac{1}{2}c, b' = \frac{1}{2}a$	
Origin at 0,0,z	Origin at $x,0,0$	Origin at 0,y,0	
Maximal non-isomorphic subgroups			
I	[2]C1(P1)	1+	
IIa	[2]P1c1(Pc)	1; 2	
	[2]P1n1(Pc)	1; $2+(\frac{1}{2}, \frac{1}{2}, 0)$	
IIb	none		
Maximal isomorphic subgroups of lowest index			
IIc	[3]C1c1($b'=3b$)(Cc); [3]C1c1($c'=3c$)(Cc); [3]C1c1($a'=3a$ or $a'=3a, c'=-a+c$ or $a'=3a, c'=a+c$)(Cc)		
Minimal non-isomorphic supergroups			
I	[2]C2/c; [2]Cmc ₂ ; [2]Ccc ₂ ; [2]Ama ₂ ; [2]Aba ₂ ; [2]Fdd ₂ ; [2]Iba ₂ ; [2]Ima ₂ ; [3]P3c1; [3]P31c; [3]R3c		
II	[2]F1m1(Cm); [2]C1m1($2c'=c$)(Cm); [2]P1c1($2a'=a, 2b'=b$)(Pc)		

Fig. 2.31. (Contd)

Pnma

D_{2h}^{16}

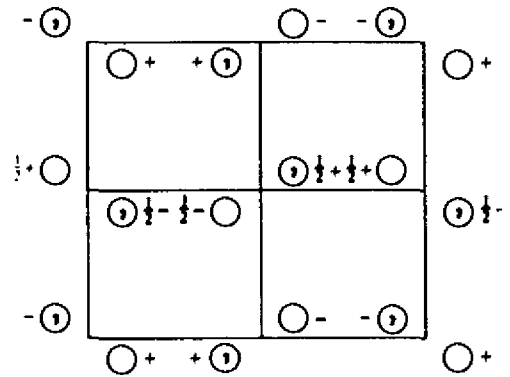
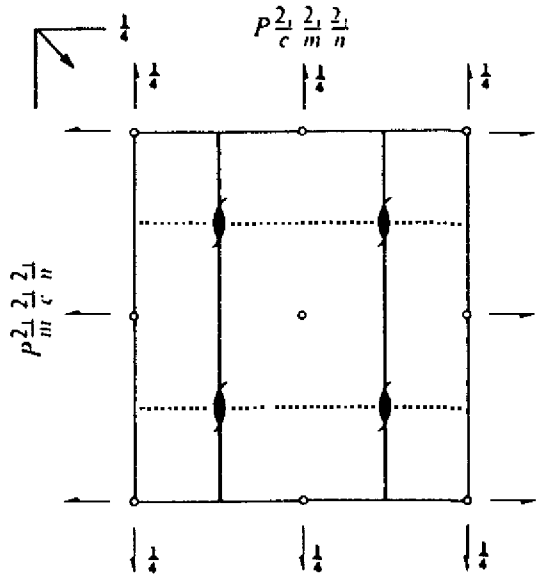
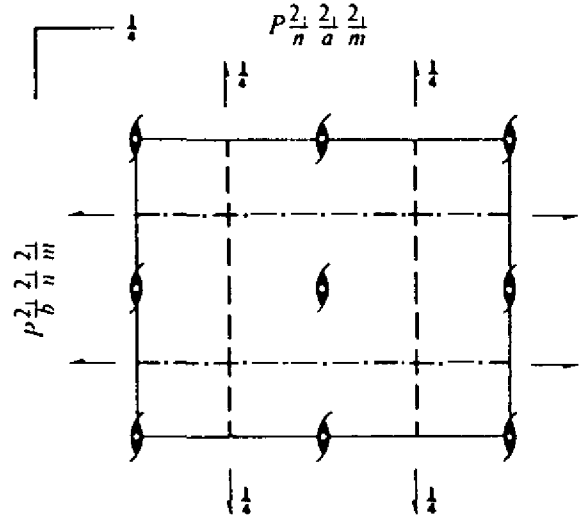
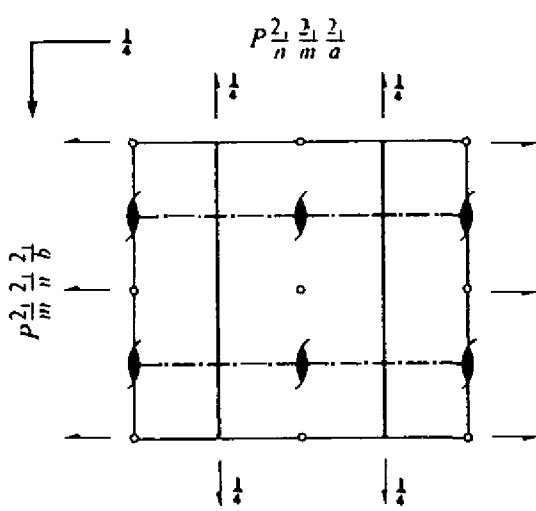
mmm

Orthorhom

No. 62

$P 2_1/n 2_1/m 2_1/a$

Patterson symmetry *Pm*



Origin at $\bar{1}$ on 12_11

Asymmetric unit $0 \leq x \leq \frac{1}{2}; 0 \leq y \leq \frac{1}{2}; 0 \leq z \leq 1$

Symmetry operations

- (1) 1
- (2) $2(0,0,\frac{1}{2}) \frac{1}{2},0,z$
- (3) $2(0,\frac{1}{2},0) 0,y,0$
- (4) $2(\frac{1}{2},0,0) x,\frac{1}{2},\frac{1}{2}$
- (5) $\bar{1} 0,0,0$
- (6) $a x,y,\frac{1}{2}$
- (7) $m x,\frac{1}{2},z$
- (8) $n(0,\frac{1}{2},\frac{1}{2}) \frac{1}{2},y,z$

Fig. 2.32. Space group *Pnma*, copied (with permission) from the *International Tables*

CONTINUED

No. 62

*Pnm*a

Generators selected (1); $t(1,0,0)$; $t(0,1,0)$; $t(0,0,1)$; (2); (3); (5)

Positions

Multiplicity, Wyckoff letter, Site symmetry	Coordinates				Reflection conditions
8 <i>d</i> 1	(1) x, y, z (5) $\bar{x}, \bar{y}, \bar{z}$	(2) $\bar{x} + \frac{1}{2}, \bar{y}, z + \frac{1}{2}$ (6) $x + \frac{1}{2}, y, \bar{z} + \frac{1}{2}$	(3) $\bar{x}, y + \frac{1}{2}, \bar{z}$ (7) $x, \bar{y} + \frac{1}{2}, z$	(4) $x + \frac{1}{2}, \bar{y} + \frac{1}{2}, \bar{z} + \frac{1}{2}$ (8) $\bar{x} + \frac{1}{2}, y + \frac{1}{2}, z + \frac{1}{2}$	General: $0kl: k+l=2n$ $hk0: h=2n$ $h00: h=2n$ $0k0: k=2n$ $00l: l=2n$ Special: as above, plus no extra conditions $hkl: h+l, k=2n$ $hkl: h+l, k=2n$
4 <i>c</i> .m.	$x, \frac{1}{2}, z$	$\bar{x} + \frac{1}{2}, \frac{1}{2}, z + \frac{1}{2}$	$\bar{x}, \frac{1}{2}, \bar{z}$	$x + \frac{1}{2}, \frac{1}{2}, \bar{z} + \frac{1}{2}$	
4 <i>b</i> $\bar{1}$	$0, 0, \frac{1}{2}$	$\frac{1}{2}, 0, 0$	$0, \frac{1}{2}, \frac{1}{2}$	$\frac{1}{2}, \frac{1}{2}, 0$	$hkl: h+l, k=2n$
4 <i>a</i> $\bar{1}$	$0, 0, 0$	$\frac{1}{2}, 0, \frac{1}{2}$	$0, \frac{1}{2}, 0$	$\frac{1}{2}, \frac{1}{2}, \frac{1}{2}$	$hkl: h+l, k=2n$

Symmetry of special projections

Along [001] <i>p</i> 2 <i>g</i> m $a' = \frac{1}{2}a$ $b' = b$ Origin at 0,0,z	Along [100] <i>c</i> 2 <i>m</i> m $a' = b$ $b' = c$ Origin at $x, \frac{1}{2}, \frac{1}{2}$	Along [010] <i>p</i> 2 <i>g</i> g $a' = c$ $b' = a$ Origin at 0,y,0
--	---	---

Maximal non-isomorphic subgroups

- I** [2]*P*2₁2₁2₁ 1; 2; 3; 4
- [2]*P*112₁/a (*P*2₁/c) 1; 2; 5; 6
- [2]*P*12₁/m1 (*P*2₁/m) 1; 3; 5; 7
- [2]*P*2₁/n11 (*P*2₁/c) 1; 4; 5; 8
- [2]*P*nm2₁ (*P*mn2₁) 1; 2; 7; 8
- [2]*P*n2₁a (*P*na2₁) 1; 3; 6; 8
- [2]*P*2₁ma (*P*mc2₁) 1; 4; 6; 7

IIa none

IIb none

Maximal isomorphic subgroups of lowest index

IIc [3]*P*nm*a* ($a' = 3a$); [3]*P*nm*a* ($b' = 3b$); [3]*P*nm*a* ($c' = 3c$)

Minimal non-isomorphic supergroups

I none

II [2]*A*mma (*C*mc*m*); [2]*B*bmm (*C*mc*m*); [2]*C*cmb (*C*mc*a*); [2]*I*mma; [2]*P*nm*m* ($2a' = a$) (*P*mm*n*); [2]*P*cma ($2b' = b$) (*P*bam); [2]*P*bma ($2c' = c$) (*P*bcm)

Fig. 2.32. (Contd)

2.7.5 CLASSIFICATION OF CRYSTALS ACCORDING TO THEIR SYMMETRY

Concepts such as space group, crystal class, Laue class, crystal system, Bravais lattice, Bravais system and crystal family allow us to classify crystals according to a characteristic property that is relatively easy to establish experimentally, namely symmetry. Every crystal has its particular translation lattice with its specific metric at a given temperature and pressure. Thus every crystal has its own symmetry group. When the specific metric of a crystal species is disregarded, its symmetry corresponds to one of the 230 space groups. For this reason, space groups are more accurately referred to as *space group types* (*International Tables*,

$P\bar{4}2_1c$

D_{2d}^4

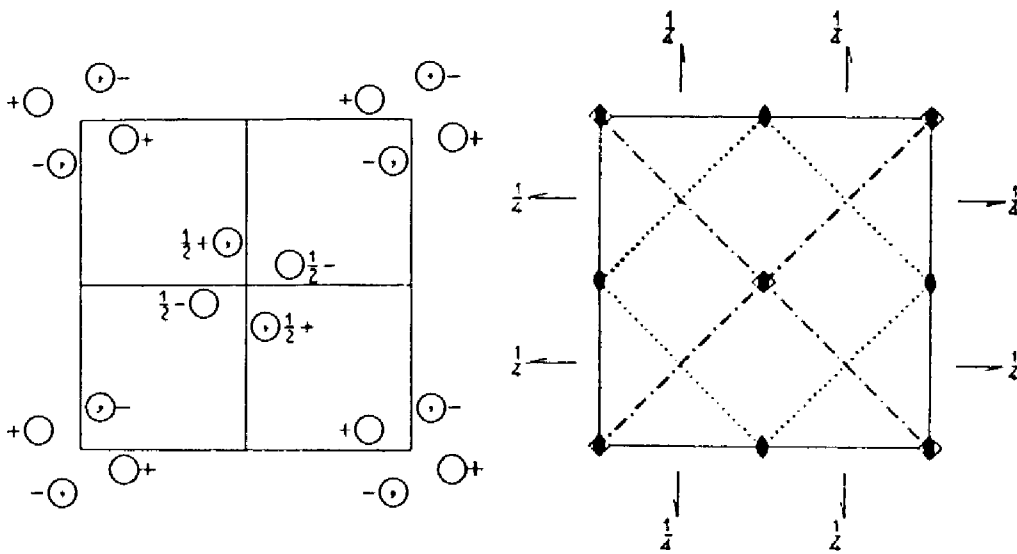
$\bar{4}2m$

Tetragonal

No. 114

$P\bar{4}2_1c$

Patterson symmetry $P4/mmm$



Origin at $\bar{4}1n$

Asymmetric unit $0 \leq x \leq \frac{1}{2}; 0 \leq y \leq \frac{1}{2}; 0 \leq z \leq \frac{1}{2}$

Symmetry operations

- (1) 1
- (2) $2 \ 0,0,z$
- (3) $\bar{4}^+ \ 0,0,z; 0,0,0$
- (4) $\bar{4}^- \ 0,0,z; 0,0,0$
- (5) $2(0,\frac{1}{2},0) \ \frac{1}{2},y,\frac{1}{2}$
- (6) $2(\frac{1}{2},0,0) \ x,\frac{1}{2},\frac{1}{2}$
- (7) $c \ x+\frac{1}{2},\bar{x},z$
- (8) $n(\frac{1}{2},\frac{1}{2},\frac{1}{2}) \ x,x,z$

Fig. 2.33. Space group $P\bar{4}2_1c$, copied (with permission) from the *International Tables*

CONTINUED

No. 114

$P\bar{4}2_1c$

Generators selected (1); $t(1,0,0)$; $t(0,1,0)$; $t(0,0,1)$; (2); (3); (5)

Positions

Multiplicity, Wyckoff letter, Site symmetry	Coordinates	Reflection conditions
8 <i>e</i> 1	(1) x, y, z (2) \bar{x}, \bar{y}, z (3) y, \bar{x}, \bar{z} (4) \bar{y}, x, \bar{z} (5) $\bar{x}+\frac{1}{2}, y+\frac{1}{2}, \bar{z}+\frac{1}{2}$ (6) $x+\frac{1}{2}, \bar{y}+\frac{1}{2}, \bar{z}+\frac{1}{2}$ (7) $\bar{y}+\frac{1}{2}, \bar{x}+\frac{1}{2}, z+\frac{1}{2}$ (8) $y+\frac{1}{2}, x+\frac{1}{2}, z+\frac{1}{2}$	General: $hkl: l = 2n$ $00l: l = 2n$ $h00: h = 2n$
4 <i>d</i> 2..	$0, \frac{1}{2}, z$ $\frac{1}{2}, 0, \bar{z}$ $\frac{1}{2}, 0, \bar{z}+\frac{1}{2}$ $0, \frac{1}{2}, z+\frac{1}{2}$	Special: as above, plus $hkl: l = 2n$ $hk0: h+k = 2n$
4 <i>c</i> 2..	$0, 0, z$ $0, 0, \bar{z}$ $\frac{1}{2}, \frac{1}{2}, \bar{z}+\frac{1}{2}$ $\frac{1}{2}, \frac{1}{2}, z+\frac{1}{2}$	$hkl: h+k+l = 2n$
2 <i>b</i> $\bar{4}$..	$0, 0, \frac{1}{2}$ $\frac{1}{2}, \frac{1}{2}, 0$	$hkl: h+k+l = 2n$
2 <i>a</i> $\bar{4}$..	$0, 0, 0$ $\frac{1}{2}, \frac{1}{2}, \frac{1}{2}$	$hkl: h+k+l = 2n$

Symmetry of special projections

Along [001] $p4gm$ $a' = a$ $b' = b$ Origin at $0, 0, z$	Along [100] $p2mg$ $a' = b$ $b' = c$ Origin at $x, \frac{1}{2}, \frac{1}{2}$	Along [110] $p1m1$ $a' = \frac{1}{2}(-a+b)$ $b' = \frac{1}{2}c$ Origin at $x, x, 0$
--	--	---

Maximal non-isomorphic subgroups

- I [2] $P\bar{4}11(P\bar{4})$ 1; 2; 3; 4
- [2] $P22_11(P2_12_12_1)$ 1; 2; 5; 6
- [2] $P21c(Ccc2)$ 1; 2; 7; 8

IIa none

IIb none

Maximal isomorphic subgroups of lowest index

IIc [3] $P\bar{4}2_1c(c' = 3c)$; [9] $P\bar{4}2_1c(a' = 3a, b' = 3b)$

Minimal non-isomorphic supergroups

- I [2] $P4/mnc$; [2] $P4/ncc$; [2] $P4_2/mbc$; [2] $P4_2/nmc$
- II [2] $I\bar{4}2m$; [2] $C\bar{4}2c(P\bar{4}c2)$; [2] $P\bar{4}2_1m(2c' = c)$

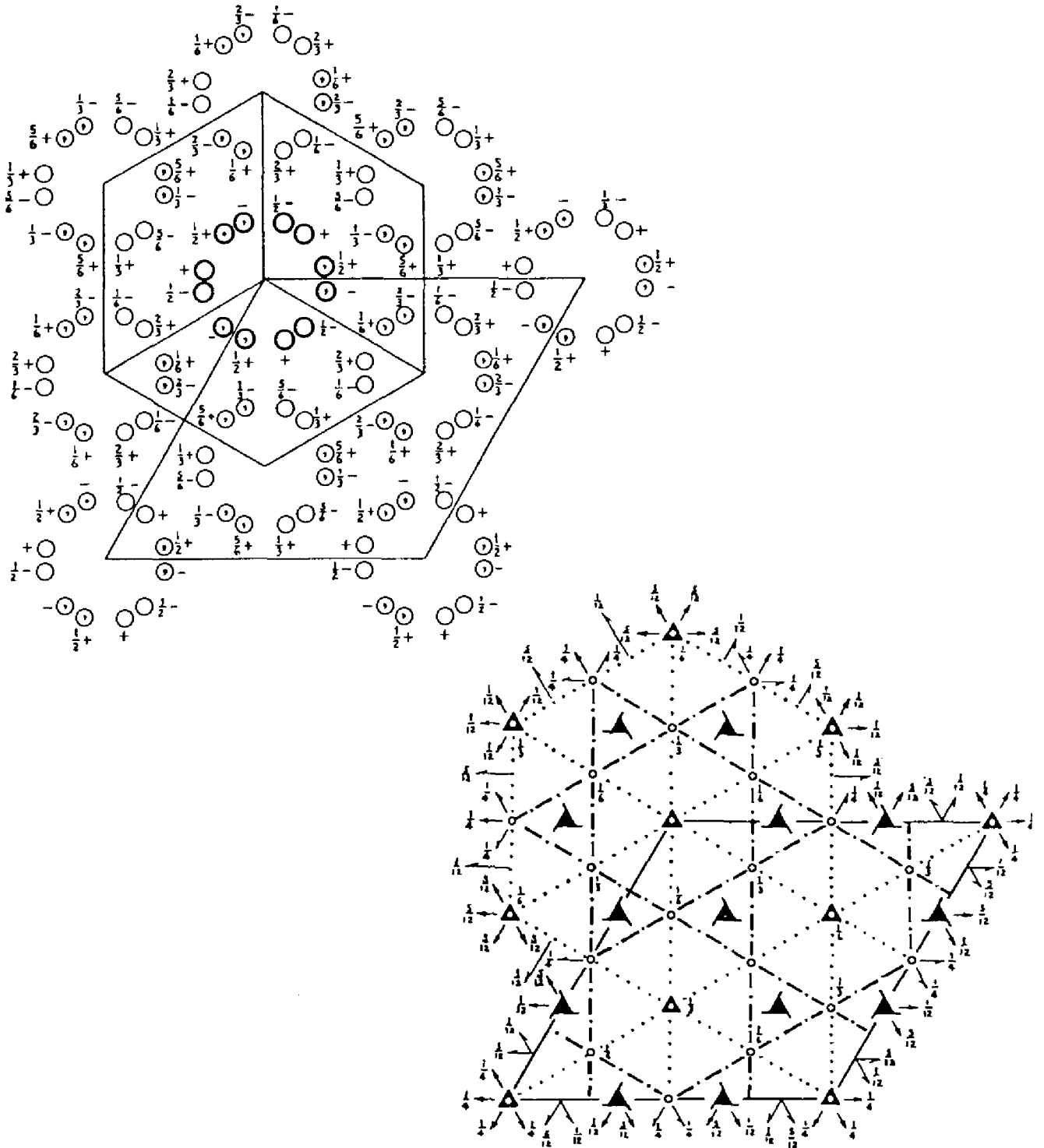
Fig. 2.33. (Contd)

vol. A, p. 718). These space group types are subdivided into crystal classes and crystal systems according to their macroscopic symmetries, on the one hand, and into Bravais lattices (classes) and Bravais systems according to their lattice type, on the other. The crystal families represent the most basic classification. A simplified and traditional (but less satisfactory) classification only uses space groups, Bravais lattices, crystal classes and crystal systems (Fig. 2.35).

$R\bar{3}c$ D_{3d}^6 $\bar{3}m$

Trigona

No. 167

 $R\bar{3}2/c$ Patterson symmetry $R\bar{3}$,Origin at centre ($\bar{3}$) at $\bar{3}c$ Asymmetric unit $0 \leq x \leq \frac{1}{2}$; $0 \leq y \leq \frac{1}{2}$; $0 \leq z \leq \frac{1}{2}$; $x \leq (1+y)/2$; $y \leq \min(1-x, (1+x)/2)$

Vertices	$0,0,0$	$\frac{1}{2},0,0$	$\frac{1}{2},\frac{1}{2},0$	$\frac{1}{2},\frac{1}{2},0$	$0,\frac{1}{2},0$
	$0,0,\frac{1}{2}$	$\frac{1}{2},0,\frac{1}{2}$	$\frac{1}{2},\frac{1}{2},\frac{1}{2}$	$\frac{1}{2},\frac{1}{2},\frac{1}{2}$	$0,\frac{1}{2},\frac{1}{2}$

Fig. 2.34. Space group $R\bar{3}c$, copied (with permission) from the *International Tables*

CONTINUED

No. 167

$R\bar{3}c$

Symmetry operations

For (0,0,0)+ set

- | | | |
|-------------------------|------------------------------|------------------------------|
| (1) 1 | (2) $3^+ 0,0,z$ | (3) $3^- 0,0,z$ |
| (4) $2 x,x,\frac{1}{2}$ | (5) $2 x,0,\frac{1}{2}$ | (6) $2 0,y,\frac{1}{2}$ |
| (7) $\bar{1} 0,0,0$ | (8) $\bar{3}^+ 0,0,z; 0,0,0$ | (9) $\bar{3}^- 0,0,z; 0,0,0$ |
| (10) $c x,\bar{x},z$ | (11) $c x,2x,z$ | (12) $c 2x,x,z$ |

For ($\frac{1}{2},\frac{1}{2},\frac{1}{2}$)+ set

- | | | |
|--|--|--|
| (1) $i(\frac{1}{2},\frac{1}{2},\frac{1}{2})$ | (2) $3^+(0,0,\frac{1}{2}) \frac{1}{2},\frac{1}{2},z$ | (3) $3^-(0,0,\frac{1}{2}) \frac{1}{2},\frac{1}{2},z$ |
| (4) $2(\frac{1}{2},\frac{1}{2},0) x,x-\frac{1}{2},\frac{1}{2}$ | (5) $2(\frac{1}{2},0,0) x,\frac{1}{2},\frac{1}{2}$ | (6) $2 \frac{1}{2},y,\frac{1}{2}$ |
| (7) $\bar{1} \frac{1}{2},\frac{1}{2},\frac{1}{2}$ | (8) $\bar{3}^+ \frac{1}{2},-\frac{1}{2},z; \frac{1}{2},-\frac{1}{2},\frac{1}{2}$ | (9) $\bar{3}^- \frac{1}{2},\frac{1}{2},z; \frac{1}{2},\frac{1}{2},\frac{1}{2}$ |
| (10) $g(\frac{1}{2},-\frac{1}{2},\frac{1}{2}) x+\frac{1}{2},\bar{x},z$ | (11) $g(\frac{1}{2},\frac{1}{2},\frac{1}{2}) x,2x-\frac{1}{2},z$ | (12) $g(\frac{1}{2},\frac{1}{2},\frac{1}{2}) 2x,x,z$ |

For ($\frac{1}{2},\frac{1}{2},\frac{1}{2}$)+ set

- | | | |
|--|--|--|
| (1) $i(\frac{1}{2},\frac{1}{2},\frac{1}{2})$ | (2) $3^-(0,0,\frac{1}{2}) 0,\frac{1}{2},z$ | (3) $3^-(0,0,\frac{1}{2}) \frac{1}{2},\frac{1}{2},z$ |
| (4) $2(\frac{1}{2},\frac{1}{2},0) x,x+\frac{1}{2},\frac{1}{2}$ | (5) $2 x,\frac{1}{2},\frac{1}{2}$ | (6) $2(0,\frac{1}{2},0) \frac{1}{2},y,\frac{1}{2}$ |
| (7) $\bar{1} \frac{1}{2},\frac{1}{2},\frac{1}{2}$ | (8) $\bar{3}^+ \frac{1}{2},\frac{1}{2},z; \frac{1}{2},\frac{1}{2},\frac{1}{2}$ | (9) $\bar{3}^- -\frac{1}{2},\frac{1}{2},z; -\frac{1}{2},\frac{1}{2},\frac{1}{2}$ |
| (10) $g(-\frac{1}{2},\frac{1}{2},\frac{1}{2}) x+\frac{1}{2},\bar{x},z$ | (11) $g(\frac{1}{2},\frac{1}{2},\frac{1}{2}) x,2x,z$ | (12) $g(\frac{1}{2},\frac{1}{2},\frac{1}{2}) 2x-\frac{1}{2},x,z$ |

Generators selected (1); $i(1,0,0)$; $i(0,1,0)$; $i(0,0,1)$; $i(\frac{1}{2},\frac{1}{2},\frac{1}{2})$; (2); (4); (7)

Positions

Multiplicity, Wyckoff letter, Site symmetry	Coordinates			Reflection conditions
	(0,0,0)+	($\frac{1}{2},\frac{1}{2},\frac{1}{2}$)+	($\frac{1}{2},\frac{1}{2},\frac{1}{2}$)+	
36 <i>f</i> 1	(1) x,y,z (4) $y,x,\bar{z}+\frac{1}{2}$ (7) \bar{x},\bar{y},\bar{z} (10) $\bar{y},\bar{x},z+\frac{1}{2}$	(2) $\bar{y},x-y,z$ (5) $x-y,\bar{y},\bar{z}+\frac{1}{2}$ (8) $y,\bar{x}+y,\bar{z}$ (11) $\bar{x}+y,y,z+\frac{1}{2}$	(3) $\bar{x}+y,\bar{x},z$ (6) $\bar{x},\bar{x}+y,\bar{z}+\frac{1}{2}$ (9) $x-y,x,\bar{z}$ (12) $x,x-y,z+\frac{1}{2}$	General: $hkil : -h+k+l = 3n$ $hki0 : -h+k = 3n$ $hh2hl : l = 3n$ $h\bar{h}0l : h+l = 3n, l = 2n$ $000l : l = 6n$ $h\bar{h}00 : h = 3n$
18 <i>e</i> .2	$x,0,\frac{1}{2}$ $0,x,\frac{1}{2}$ $\bar{x},\bar{x},\frac{1}{2}$ $\bar{x},0,\frac{1}{2}$ $0,\bar{x},\frac{1}{2}$ $x,x,\frac{1}{2}$			Special: as above, plus no extra conditions
18 <i>d</i> $\bar{1}$	$\frac{1}{2},0,0$ $0,\frac{1}{2},0$ $\frac{1}{2},\frac{1}{2},0$ $0,\frac{1}{2},\frac{1}{2}$ $\frac{1}{2},0,\frac{1}{2}$ $\frac{1}{2},\frac{1}{2},\frac{1}{2}$			$hkil : l = 2n$
12 <i>c</i> 3.	$0,0,z$ $0,0,\bar{z}+\frac{1}{2}$ $0,0,\bar{z}$ $0,0,z+\frac{1}{2}$			$hkil : l = 2n$
6 <i>b</i> $\bar{3}$.	$0,0,0$ $0,0,\frac{1}{2}$			$hkil : l = 2n$
6 <i>a</i> 32	$0,0,\frac{1}{2}$ $0,0,\frac{1}{2}$			$hkil : l = 2n$

Symmetry of special projections

Along [001] $p6mm$ $a' = \frac{1}{2}(2a+b)$ $b' = \frac{1}{2}(-a+b)$ Origin at 0,0,z	Along [100] $p2$ $a' = \frac{1}{2}(2a+4b+c)$ $b' = \frac{1}{2}(-a-2b+c)$ Origin at $x,0,0$	Along [210] $p2gm$ $a' = \frac{1}{2}b$ $b' = \frac{1}{2}c$ Origin at $x,\frac{1}{2}x,0$
--	--	---

Fig. 2.34. (Contd)

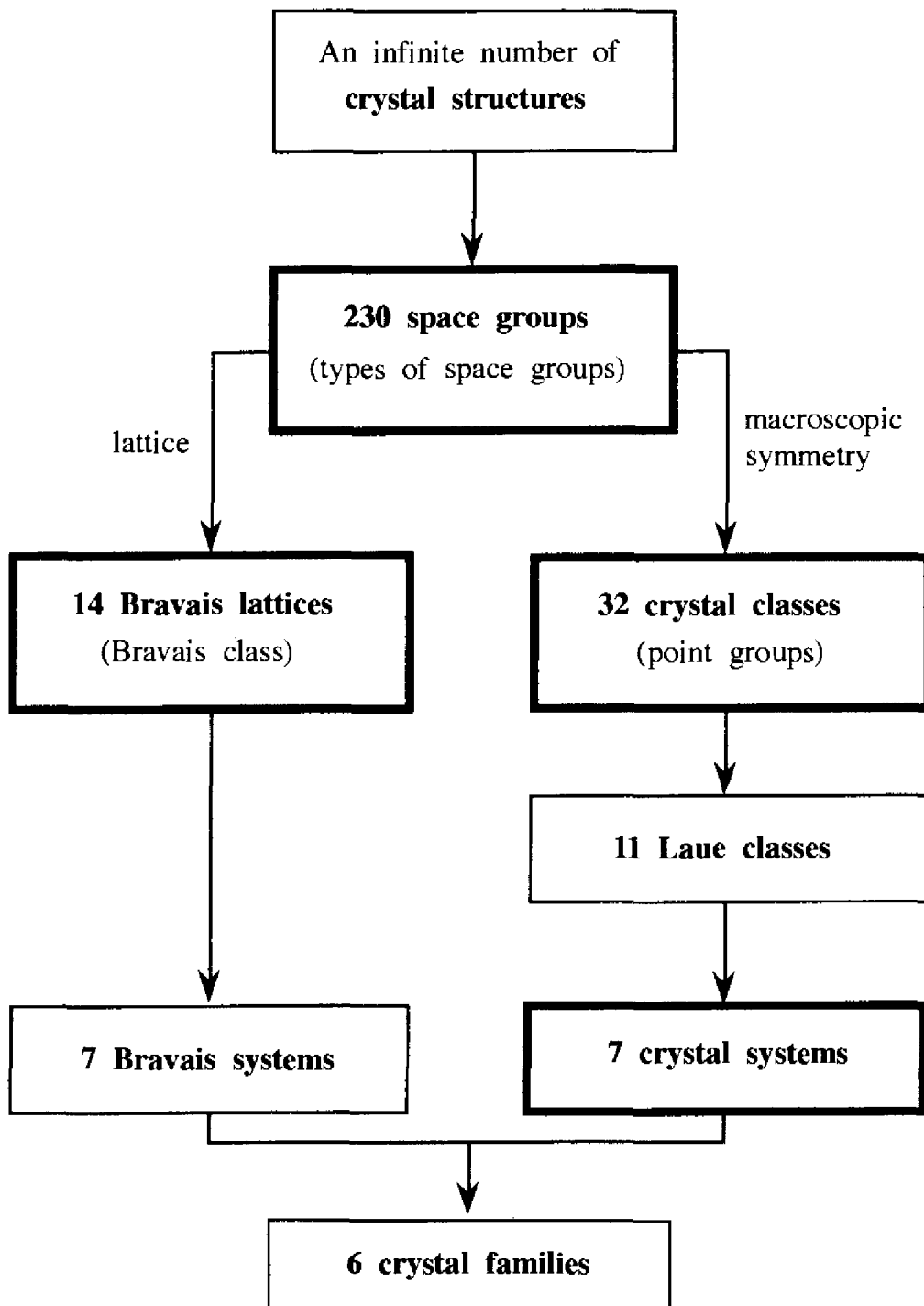


Fig. 2.35. Classification of crystals

2.8 CRYSTAL STRUCTURES

We will see (Chapter 3) that the lattice constants of a crystal $a, b, c, \alpha, \beta, \gamma$ may be determined by X-ray diffraction methods. These methods also allow us to obtain information about the space group of the crystal (Laue class from intensities, systematic absences). If we know the chemical stoichiometry of the material and its density, we can easily calculate the number of atoms per unit cell. Let M be the

molecular (or formula) weight of the substance:

$$M = \sum_{\text{formula unit}} M_A; M_A = \text{atomic weight in grams}$$

With $A = 6.022 \times 10^{23} \text{ mole}^{-1}$ being Avagadro's number, V_{cell} the volume of the unit cell in $\text{cm}^3 = 10^{24} \text{ \AA}^3$, and Z the number of molecules or formula units in the unit cell, we can calculate the density d in g cm^{-3} :

$$d = \frac{ZM}{AV_{\text{cell}}}, \quad Z = \frac{dAV_{\text{cell}}}{M}; \quad Z \text{ being integer} \quad (2.16)$$

In general we find the following information in the literature concerning crystal structures:

- symmetry (space group, possibly crystal class and crystal system)
- lattice constants, number of molecules or formula units in the unit cell
- coordinates of the unique atoms (inequivalent by symmetry).

As an example, let us consider this information for the structure of Fe_3C , an important constituent of steel:

- space group Pnma
- $a = 5.08, b = 6.73, c = 4.51 \text{ \AA}; Z = 4$
- 4 Fe at c : $x = 0.040$ $z = 0.667$
- 8 Fe at d : $x = 0.183$ $y = 0.065$ $z = 0.167$
- 4 C at c : $x = 0.36$ $z = 0.47$

From the symbol Pnma , we deduce that the crystal class is mmm and that the crystal system is orthorhombic. The cell angles are thus $\alpha = \beta = \gamma = 90^\circ$. Because $Z = 4$, the unit cell contains 12 atoms of Fe and 4 of C. From the *International Tables* we learn that the multiplicity of a general position (Wyckoff symbol d) is 8. There are three special positions a, b and c with a multiplicity of 4:

multiplicity

Wyckoff symbol

coordinates

site symmetry

8	d	$\bar{1}$	$x, y, z;$	$\frac{1}{2} + x, \frac{1}{2} - y, \frac{1}{2} - z;$	$\bar{x}, \frac{1}{2} + y, \bar{z};$	$\frac{1}{2} - x, \bar{y}, \frac{1}{2} + z;$
			$\bar{x}, \bar{y}, \bar{z};$	$\frac{1}{2} - x, \frac{1}{2} + y, \frac{1}{2} + z;$	$x, \frac{1}{2} - y, z;$	$\frac{1}{2} + x, y, \frac{1}{2} - z.$
4	c	\bar{m}	$x, \frac{1}{4}, z;$	$\bar{x}, \frac{3}{4}, \bar{z};$	$\frac{1}{2} - x, \frac{3}{4}, \frac{1}{2} + z;$	$\frac{1}{2} + x, \frac{1}{4}, \frac{1}{2} - z.$
4	b	$\bar{1}$	$0, 0, \frac{1}{2};$	$0, \frac{1}{2}, \frac{1}{2};$	$\frac{1}{2}, 0, 0;$	$\frac{1}{2}, \frac{1}{2}, 0.$
4	a	$\bar{1}$	$0, 0, 0;$	$0, \frac{1}{2}, 0;$	$\frac{1}{2}, 0, \frac{1}{2};$	$\frac{1}{2}, \frac{1}{2}, \frac{1}{2}.$

We know *a priori* that the 12 iron atoms must occupy position d and one of the positions c, b or a , or else three positions of multiplicity 4. The four carbon atoms must occupy a or b or c . The data presented above represent the result of a structural analysis. The iron atoms occupy d and c , and the carbon atoms also occupy c , but with different coordinates than for iron. The point symmetry of site

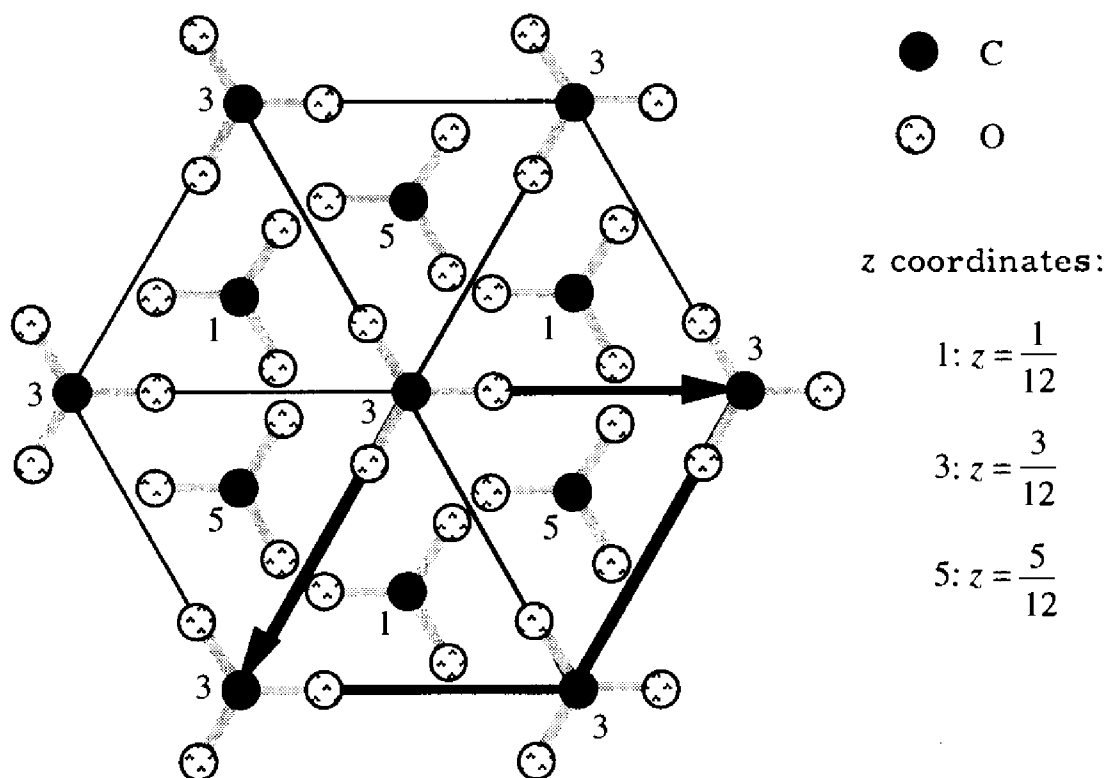


Fig. 2.36. Projection of the carbonate ions CO_3^{2-} of the calcite structure between $z = 0$ and $z = 1/2$ onto the a/b plane

c is m . An equivalent position is represented by the corresponding first coordinates given in the *International Tables*. With the help of the Tables we obtain the coordinates of all the equivalent points of the positions d and c , including the coordinate $y = 1/4$ of the point representing position c . Thus we possess all the necessary information to make a drawing of the structure of Fe_3C and to calculate the interatomic distances and bond angles.

As another example, let us look at the data for the structure of *calcite*, CaCO_3 , the principal constituent of limestone:

- space group $\bar{R}3c$
- $a = 4.990$; $c = 17.002 \text{ \AA}$; $Z = 6$;
- 6 Ca at b
- 6 C at a
- 18 O at e ; $x = 0.257$

Figure 2.36 shows a projection of the structure down c .

2.9 MILLER-BRAVAIS INDICES FOR HEXAGONAL COORDINATE SYSTEMS

The Miller indices of faces equivalent by the symmetry operations of the crystal class are derived by application of equation (1.21) of paragraph 1.2.4. In the

majority of cases we can obtain them by inspection. The following examples may easily be verified with the aid of the stereograms in Fig. 2.20:

class **222**: $(hkl), (h\bar{k}\bar{l}), (\bar{h}\bar{k}l), (\bar{h}kl)$;

class **4**: $(hkl), (\bar{k}hl), (\bar{h}\bar{k}l), (khl)$;

class **23**: $(hkl), (h\bar{k}\bar{l}), (\bar{h}\bar{k}l), (\bar{h}kl), (klh), (k\bar{l}h), (\bar{k}\bar{l}h), (\bar{k}lh), (lkh), (l\bar{h}k), (\bar{l}h\bar{k}), (\bar{l}hk)$; the threefold axis parallel to $[111]$ permutes the indices.

A complication arises from the action of a threefold axis in a hexagonal coordinate system. In this case, the indices of equivalent faces are not obtained simply by permutations and sign changes of (hkl) . To circumvent this problem, we use four indices $(hkil)$ defined with respect to the vectors $\mathbf{a}_1, \mathbf{a}_2, \mathbf{a}_3$ perpendicular to the threefold axis (Fig. 2.37), and \mathbf{c} parallel to the threefold axis. For $h, k > 0$, the length cut by the plane on \mathbf{a}_3 is negative, hence we obtain:

$$i = -(h + k); h + k + i = 0 \tag{2.17}$$

Because the threefold axis permutes the vectors $\mathbf{a}_1, \mathbf{a}_2$ and \mathbf{a}_3 , we obtain the following recipe to obtain the indices of equivalent faces generated by a threefold axis:

- we add a fourth index $i = -(h + k)$ to the usual indices hkl ;
- the equivalent faces $hkil, ihkl, kihl$ are obtained from the cyclic permutation of hki ;
- because the fourth index is clearly redundant, we then eliminate it from all further calculations;
- thus the usual indices for the three faces are $hkl, -(h + k)hl, k - (h + k)l$.

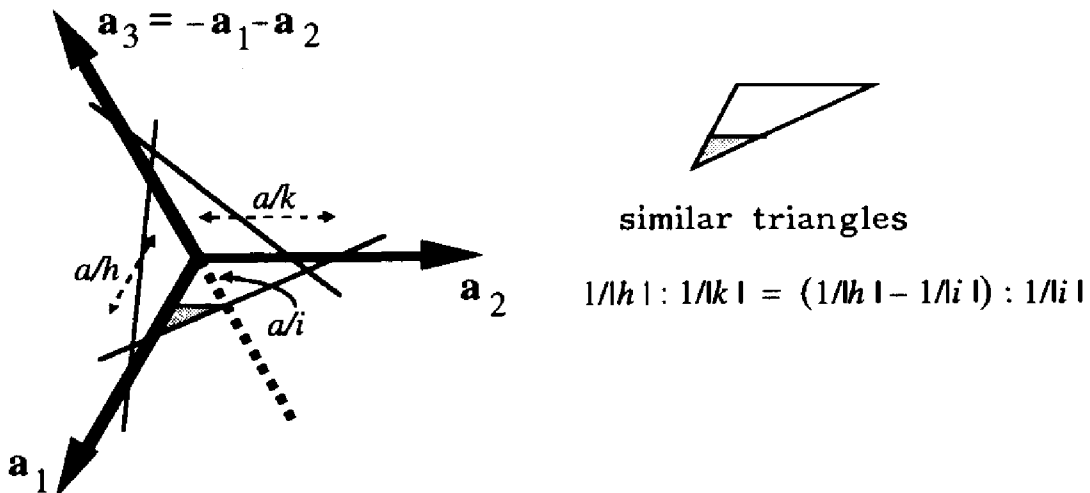


Fig. 2.37. Indices $(hkil)$ with respect to a hexagonal coordinate system: $(32\bar{5}l), (\bar{5}32l), (2\bar{5}3l)$.

The same recipe cannot be applied for the indices $[uvw]$ of translations (zones, edges). A method which defines four indices $[uvw\omega]$ has been published (L. Weber, *Z. Kristallogr.* **57**, 200–203, 1922); however, it is not well known and little used. *We would discourage the use of four indices for translations.* We recall (Section 1.2.4) that (hkl) and $[uvw]$ do not transform in the same way, the first being covariant and the latter contravariant. Accordingly, a threefold axis produces the equivalent indices $[uvw]$, $[\bar{v}(u-v)w]$, $[(v-u)\bar{u}w]$.

CHAPTER 3

Diffraction of X-Rays by Crystals

3.1 INTRODUCTION

3.1.1 X-RAY MICROSCOPE

The study of very small objects and those at a great distance made possible by the development of the microscope and the telescope has played a crucial role in the progress of the exact sciences. The atomistic theories of the 19th century naturally raised the problem of the construction of a microscope which would allow the direct observation of the constituent atoms of matter. We know that the resolving power of an optical system is limited by the wavelength of the radiation used. Two points which are separated by less than approximately 0.36λ cannot be resolved in the image produced by a microscope, λ being the wavelength of the radiation (A.J.C. Wilson, *Acta Crystallogr.* **A35**, 122–130, 1979). By analogy, it is difficult to measure a distance which is much smaller than the smallest division of a ruler.

In a solid, the interatomic distances are of the order of an Ångström ($1 \text{ \AA} = 10^{-10} \text{ m} = 100 \text{ pm}$). For example, the interatomic distance for a C–H bond is 1.08 \AA , for a single C–C bond the distance is 1.54 \AA , and for a metal–oxygen bond it is about 2 \AA . Thus, in order to distinguish two neighboring atoms, a microscope must use radiation with a wavelength of the order of 1 \AA . The image obtained with such a microscope obviously depends on the interaction of radiation with matter.

X-rays are electromagnetic waves just like visible light. They interact with the electrons contained in all matter. Consequently, the image obtained with an ‘X-ray microscope’ reveals the distribution of the electrons, a distribution whose maxima correspond to the atomic positions. In crystallography we use X-rays with wavelengths of the order of 0.5 to 2 \AA .

According to the wave theory of elementary particles, a particle of mass m moving with a velocity v has a wavelength $\lambda = h/mv$, where h is Planck’s constant. ‘Thermal’ (neither ‘hot’ nor ‘cold’) neutrons have a wavelength of about 1 \AA . Neutrons interact with matter in two different ways. On the one hand, they interact with atomic nuclei, thus the image produced by a ‘neutron microscope’

reveals the distribution of the nuclei. On the other hand, neutrons interact with unpaired electrons and permit the determination of the magnetic structure (spin distribution). A beam of electrons interacts with the electrostatic potential of a material, hence with the distribution of both nuclei and electrons. This is the principle of the electron microscope.

According to Abbe, the formation of the image of an object by means of one or more lenses takes place in two steps, diffraction of the radiation by the object followed by recombination of the diffracted radiation by means of a lens (Fig. 3.1). For example, a periodic lattice made up of lines of separation d illuminated by a plane wave with the wave vector perpendicular to the lattice plane will emit diffracted beams concentrated in specific directions given by the equation (Section 3.1.3)

$$d \sin \theta_n = n\lambda \quad (n \text{ being integer}) \quad (3.1)$$

The objective L_1 in Fig. 3.1 transforms the plane waves diffracted by the lattice into spherical waves whose centers are located in the focal plane common to the two lenses. The eyepiece L_2 transforms these spherical waves back into plane

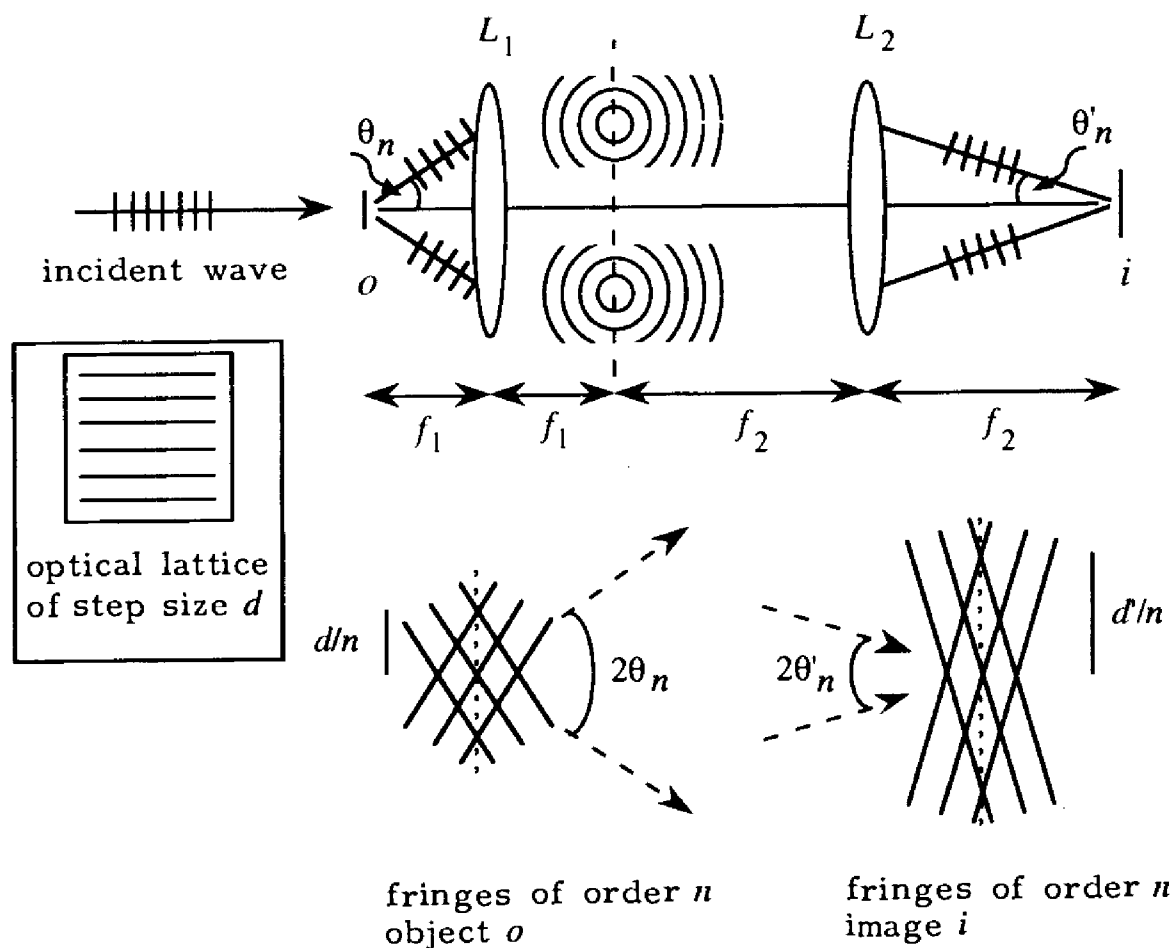


Fig. 3.1. Microscope made up of two lenses. The objective L_1 and the eyepiece L_2 have a focal plane in common. The focal distances are f_1 and f_2 . The object o and its image i are found in the focal planes of the two lenses

waves which interfere with an angle of $2\theta'_n$. The resulting intensity maxima in the plane of the image are separated by the distance $d'/n = \lambda/\sin \theta'_n = ad/n$, $a \approx \sin \theta/\sin \theta' \approx \theta/\theta'$, a ratio commonly referred to as the magnification. In order to reconstruct the exact image of an object, the interference of an infinite number of diffracted beams is necessary. For $n \rightarrow \infty$, hence $\lambda \rightarrow 0$, we obtain a perfect image. However, the lattice is already visible in an image formed by the first order alone, $n = 1$. Thus it is sufficient that $\lambda < d$ for a rudimentary image of the lattice to be formed.

There are no known lenses for neutrons or X-rays. The index of refraction for X-rays in matter is of the order of $1-10^{-5}$, and for neutrons $1-10^{-6}$. Hence a neutron or X-ray microscope analogous to the optical microscope does not exist. In order to reconstruct an image it is necessary to proceed via two steps. In a first step we measure the radiation diffracted by the sample. Due to their *symmetry properties* and in particular to the *periodicity* of their structures, the diffraction patterns produced by crystals are especially simple. In fact, *only crystals allow the detailed study of the structure of matter on the atomic scale*. In a second step we simulate the function of the lenses by numerical calculations with the aid of a computer. Whereas a lens recombines the diffracted *waves*, each wave being characterized by an amplitude and a phase, the diffraction pattern from a crystal only gives us *intensities* proportional to the squares of the amplitudes of the diffracted waves. This loss of information is the origin of the *phase problem*. In other words, the phases of the diffracted waves are unknown. The reconstruction of the image can only be carried out with the aid of models which allow us to recreate the missing information. Thus we define *a priori* the type of image that we wish to obtain. In particular, we suppose that the sample is made up of atoms whose form is known from quantum mechanical calculations. There have been impressive advances in the experimental determination of phases, but this technique is not yet a practical solution to the phase problem.

In this book, we will concentrate mainly on the *diffraction of X-rays by crystals* and the determination of symmetry properties. The solution to the phase problem and structure determination will only be touched upon to illustrate some general principles (there is an abundant literature on this subject already). We will study only *elastic diffraction*, the diffracted waves having the same wavelength as the primary radiation. The interaction of radiation with thermal vibrations produces inelastic scattering. In the determination of crystal structures, this effect is considered as a parasite which limits the precision of the measurements. However, it is very important in neutron scattering and constitutes the principal method which allows the study of thermal vibrations of crystals (phonon waves). Those interested in the electron microscope are referred to the specialized literature in this domain. However, it is worth noting that the basic geometrical theory, in particular Bragg's law (Section 3.4.2) and the Ewald construction (Section 3.4.3), is applicable for all three types of radiation.

3.1.2 INTERFERENCE OF PLANE WAVES

A plane wave (Fig. 3.2) is described by the displacement or electric field ψ at the position \mathbf{r} and at time t

$$\begin{aligned}\psi(\mathbf{r}, t) &= A \cos(\mathbf{k}_0 \cdot \mathbf{r} - \omega t + \phi') \\ &= A \cos 2\pi(\mathbf{s}_0 \cdot \mathbf{r} - vt + \phi)\end{aligned}\quad (3.2)$$

where A is the amplitude, \mathbf{k}_0 the wave vector with $\|\mathbf{k}_0\| = 2\pi/\lambda$, λ the wavelength, $\|\mathbf{s}_0\| = 1/\lambda$, v the frequency, $\omega = 2\pi v$, and ϕ the phase at the origin O ($\mathbf{r} = 0$ and $t = 0$). In books on solid state physics, we generally find the quantities \mathbf{k}_0 and ω . Crystallographers prefer to use \mathbf{s}_0 and v . This convention complicates equation (3.2), on the other hand, it eliminates the factor 2π from the Laue equations (Section 3.4.1). Using the relation $\cos(x + y) = \cos x \cos y - \sin x \sin y$, the superposition of two plane waves with the same wavelength, frequency and direction of propagation gives:

$$\begin{aligned}\psi &= \psi_1 + \psi_2 = A_1 \cos 2\pi(\mathbf{s}_0 \cdot \mathbf{r} - vt + \phi_1) + A_2 \cos 2\pi(\mathbf{s}_0 \cdot \mathbf{r} - vt + \phi_2) \\ &= A \cos 2\pi(\mathbf{s}_0 \cdot \mathbf{r} - vt + \phi),\end{aligned}\quad (3.3)$$

$$A^2 = A_1^2 + A_2^2 + 2A_1A_2 \cos 2\pi(\phi_1 - \phi_2)\quad (3.4)$$

$$\tan 2\pi\phi = \frac{A_1 \sin 2\pi\phi_1 + A_2 \sin 2\pi\phi_2}{A_1 \cos 2\pi\phi_1 + A_2 \cos 2\pi\phi_2}\quad (3.5)$$

These equations represent the sum of two vectors of length A_1 and A_2 , and of phase $2\pi\phi_1$ and $2\pi\phi_2$, $\mathbf{A} = \mathbf{A}_1 + \mathbf{A}_2$ (Fig. 3.3).

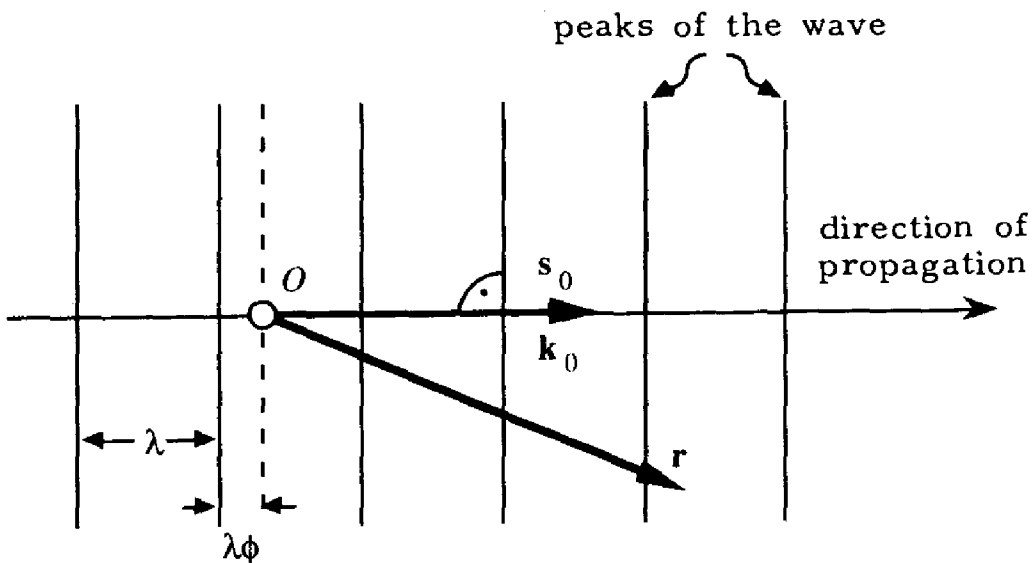


Fig. 3.2. Definition of a plane wave

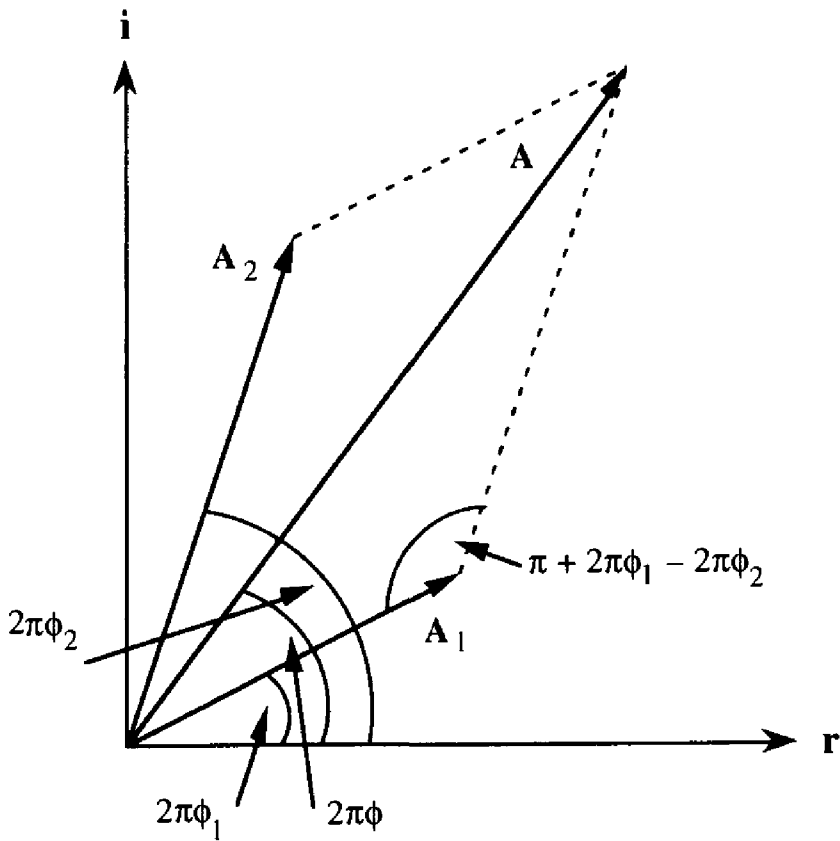


Fig. 3.3. Sum of two vectors in the complex plane

If \mathbf{r} and \mathbf{i} represent the real and imaginary axes of the complex plane, we see that a plane wave is represented more elegantly by the complex function

$$\psi(\mathbf{r}, t) = Ae^{2\pi i(\mathbf{s} \cdot \mathbf{r} - vt + \phi)} \tag{3.6}$$

Thus the vectors in Fig. 3.3 are represented by

$$\xi = Ae^{2\pi i\phi} = A_1e^{2\pi i\phi_1} + A_2e^{2\pi i\phi_2}. \tag{3.7}$$

3.1.3 THE OPTICAL GRATING

Consider a plane wave whose direction of propagation is perpendicular to a wall containing two small holes (Fig. 3.4). According to Huygens' principle, these holes subsequently become sources of spherical waves which then interfere. At a distance which is large with respect to λ and to d , the spherical wave in the direction of observation \mathbf{s} can be treated as a plane wave (Fraunhofer's approximation). The path difference Δ between the two waves ξ_1 and ξ_2 in the direction \mathbf{s} is the projection of \mathbf{d} onto \mathbf{s} :

$$\Delta = d \sin \theta = \lambda \mathbf{d} \cdot \mathbf{s}$$

By setting the phase of ξ_1 equal to zero, it follows from equation (3.7) that the resultant ξ becomes

$$\xi = \xi_1 + \xi_2 = A(e^{2\pi i0} + e^{2\pi i\Delta/\lambda}) = A(1 + e^{2\pi i\mathbf{d} \cdot \mathbf{s}}). \tag{3.8}$$

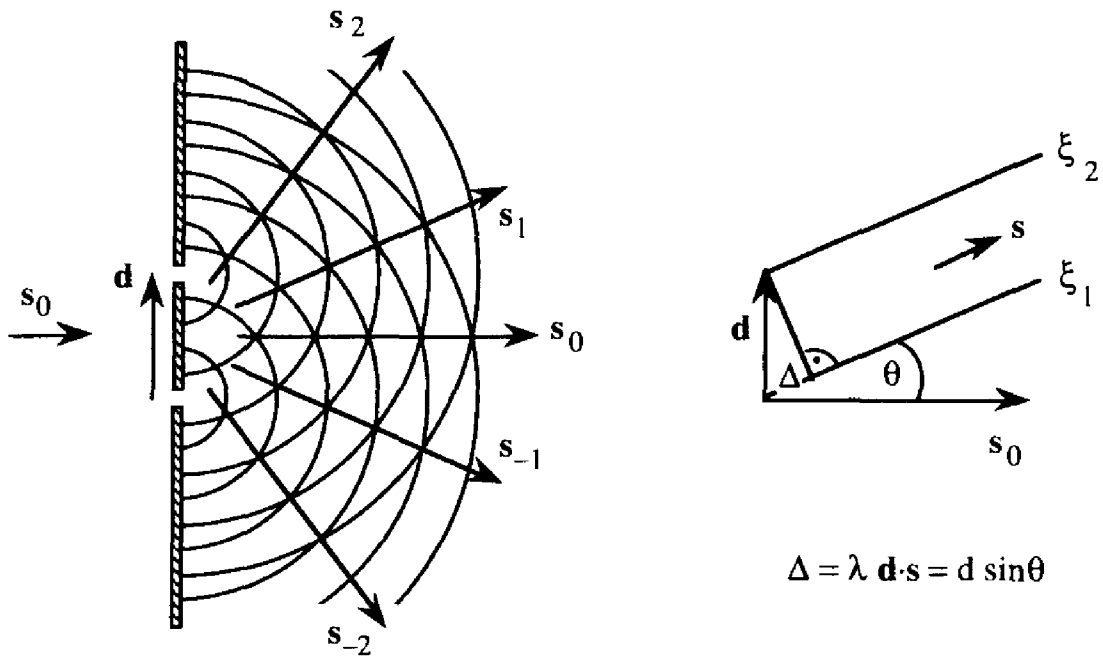


Fig. 3.4. Interference of two waves transmitted by two holes separated by a distance $d = \|\mathbf{d}\|$. \mathbf{s}_0 and \mathbf{s} are the wave vectors of the incident and diffracted waves, $\|\mathbf{s}_0\| = \|\mathbf{s}\| = 1/\lambda$, λ is the wavelength and Δ is the path difference of the waves in the direction \mathbf{s} . The figure is constructed in such a way that $\lambda = 0.4d$; the \mathbf{s}_i are the directions of the diffraction maxima

The intensity I is proportional to the square of the amplitude A ,

$$I = |\xi|^2 = 4A^2 \cos^2(\pi \mathbf{d} \cdot \mathbf{s}) = 4A^2 \cos^2\left(\pi \frac{d}{\lambda} \sin \theta\right). \quad (3.9)$$

The intensity is constant for all directions \mathbf{s} which lie on a cone whose axis is \mathbf{d} . By placing a screen perpendicular to \mathbf{s}_0 , we observe diffuse bands of intensity.

For a wall containing N regularly spaced holes (considered as point sources) located at $0, \mathbf{d}, 2\mathbf{d}, 3\mathbf{d}, \dots, (N-1)\mathbf{d}$, we can calculate the diffraction pattern in an analogous manner. It is necessary to evaluate the sum of N plane waves ξ_n with phase shifts of $\mathbf{s} \cdot \mathbf{d}, 2\mathbf{s} \cdot \mathbf{d}, \dots, (N-1)\mathbf{s} \cdot \mathbf{d}$. By using the formula for the sum of a geometrical progression, the resultant ξ becomes

$$\xi = \sum_{n=1}^N \xi_n = A \sum_{n=0}^{N-1} e^{2\pi i n \mathbf{s} \cdot \mathbf{d}} = A \frac{1 - e^{2\pi i N \mathbf{s} \cdot \mathbf{d}}}{1 - e^{2\pi i \mathbf{s} \cdot \mathbf{d}}} \quad (3.10)$$

$$I \approx |\xi|^2 = \xi \xi^* = A^2 \frac{1 - \cos 2\pi N \mathbf{s} \cdot \mathbf{d}}{1 - \cos 2\pi \mathbf{s} \cdot \mathbf{d}} = A^2 \frac{\sin^2 \pi N \mathbf{s} \cdot \mathbf{d}}{\sin^2 \pi \mathbf{s} \cdot \mathbf{d}} = A^2 J_N^2(\mathbf{s} \cdot \mathbf{d}), \quad (3.11)$$

$$J_N^2(\mathbf{s} \cdot \mathbf{d}) = \frac{\sin^2 \pi N \mathbf{s} \cdot \mathbf{d}}{\sin^2 \pi \mathbf{s} \cdot \mathbf{d}}, \quad \mathbf{s} \cdot \mathbf{d} = \frac{d}{\lambda} \sin \theta. \quad (3.12)$$

J_N^2 is the *interference function* of a one-dimensional crystal with N unit cells, the

lattice repeat being \mathbf{d} . It is a periodic function,

$$J_N^2(\mathbf{s} \cdot \mathbf{d}) = J_N^2(\mathbf{s} \cdot \mathbf{d} + n), \quad n \text{ being integer}$$

$$J_N^2(\sin \theta) = J_N^2(\sin \theta'), \quad \sin \theta' = \sin \theta + n \frac{\lambda}{d} \leq 1 \quad (3.13)$$

With the aid of Hopital's rule, $\lim [\phi(x)/\psi(x)] = \lim [\phi'(x)/\psi'(x)]$ if $\lim[\phi(x)]$ or $\lim[\psi(x)] = 0$ or ∞ , we can show that J_N^2 has principal maxima (3.1) of amplitude

$$\lim_{x \rightarrow 0} \frac{\sin^2 Nx}{\sin^2 x} = N \lim_{x \rightarrow 0} \frac{\sin 2Nx}{\sin 2x} = N^2 \lim_{x \rightarrow 0} \frac{\cos 2Nx}{\cos 2x} = N^2.$$

$$J_N^2 = N^2 \text{ for } \mathbf{s} \cdot \mathbf{d} = n, \quad d \sin \theta = n\lambda, \quad n \text{ integer: principal maxima.} \quad (3.14)$$

We find the minima by setting $J_N^2 = 0$,

$$J_N^2 = 0 \text{ for } \mathbf{s} \cdot \mathbf{d} = m/N, \quad m \neq nN, \quad m \text{ and } n \text{ being integers: minima.} \quad (3.15)$$

There are thus $N - 1$ minima between two principal maxima. This implies $N - 2$ secondary maxima. Figure 3.5 shows J_N^2 for $N = 11$.

J_N^2 is constant for any direction \mathbf{s} situated on a cone of axis \mathbf{d} . Figure 3.6 illustrates that for $N = 6$ we can construct the minima and maxima of J_N^2 in the complex plane (Fig. 3.3) by adding N vectors of equal length representing the waves from N holes. The angle indicates the phase difference of $(360\mathbf{s} \cdot \mathbf{d})^\circ$ between two waves originating from two neighboring holes.

*The scattering of radiation by a periodic structure is called **diffraction**.*

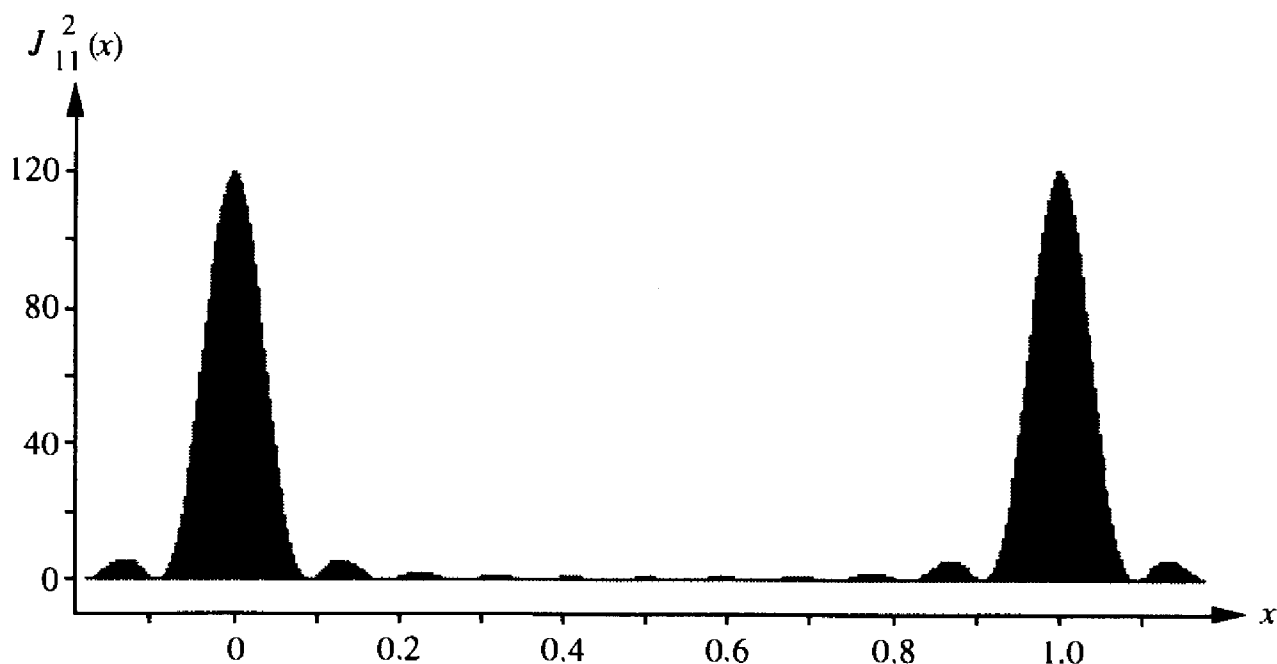
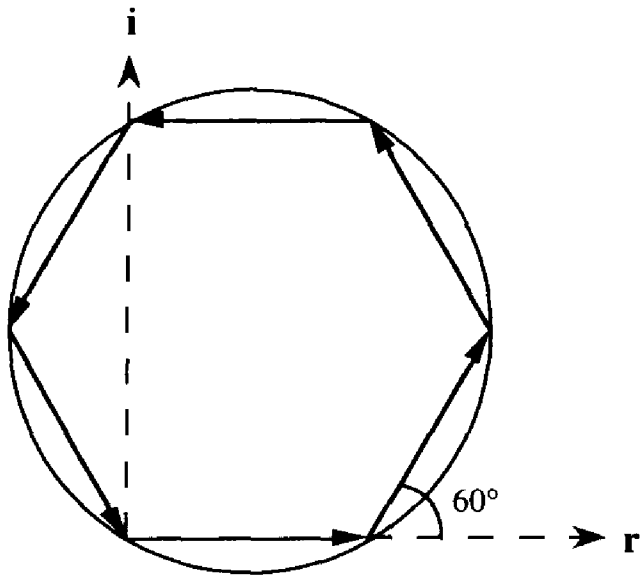
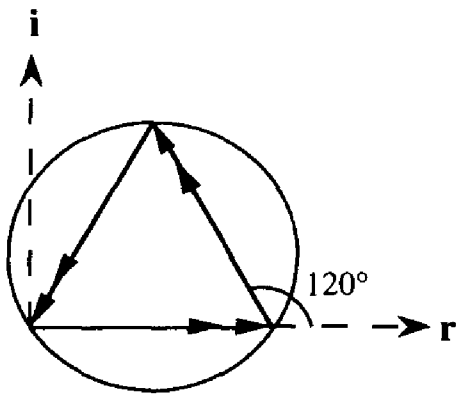
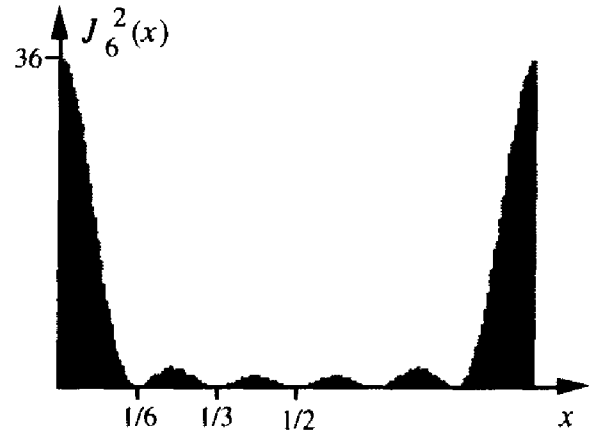


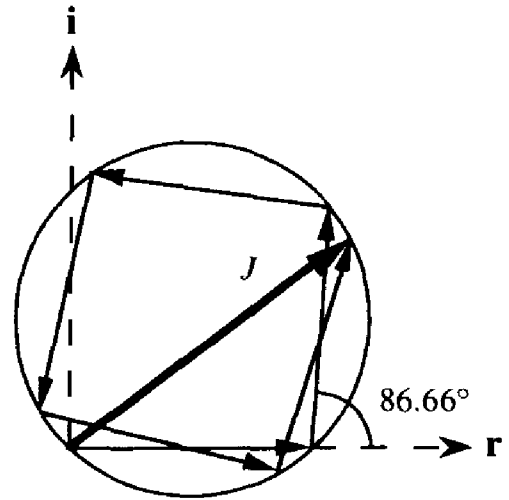
Fig. 3.5. Interference function $J_{11}^2(x)$, $N = \mathbf{s} \cdot \mathbf{d}$



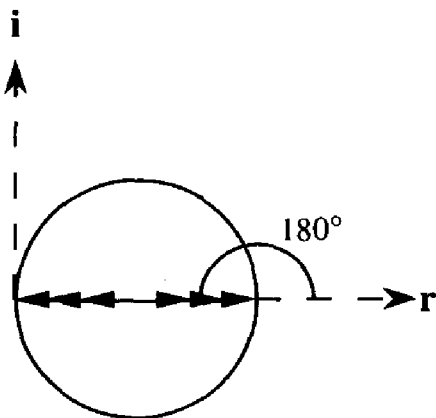
1st minimum, $x = 1/6$, 1 revolution, $J = 0$



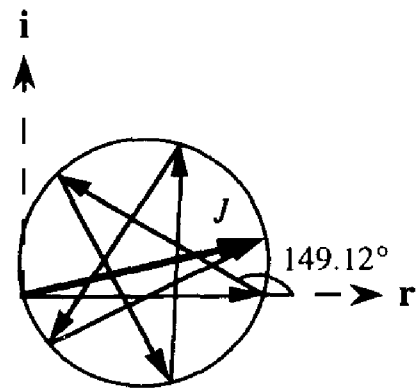
2nd minimum, $x = 1/3$, 2 revolutions, $J = 0$



1st secondary maximum, $x \approx 1/4$, 1.5 revolutions, $J = 1.43507$



3rd minimum, $x = 1/3$, 3 revolutions, $J = 0$



2nd secondary maximum, $x \approx 5/12$, 2.5 revolutions, $J = 1.03634$

Fig. 3.6. Vector diagrams (Fig. 3.3) showing the function $J = \sin \pi 6 x / \sin \pi x$ as the sum of six vectors. The other secondary minima and maxima are obtained by reflection with respect to the axis r

In reality, we observe that the intensities vary with $\sin \theta$. This is due to the fact that holes in the wall have a finite size and are not point sources. We will demonstrate in Section 3.4.1 (equation (3.36) and (3.37)) the following fundamental theorem:

The diffraction pattern of a periodic structure is the product of the diffraction pattern of a single unit cell and the function J_N^2 characteristic of the periodicity.

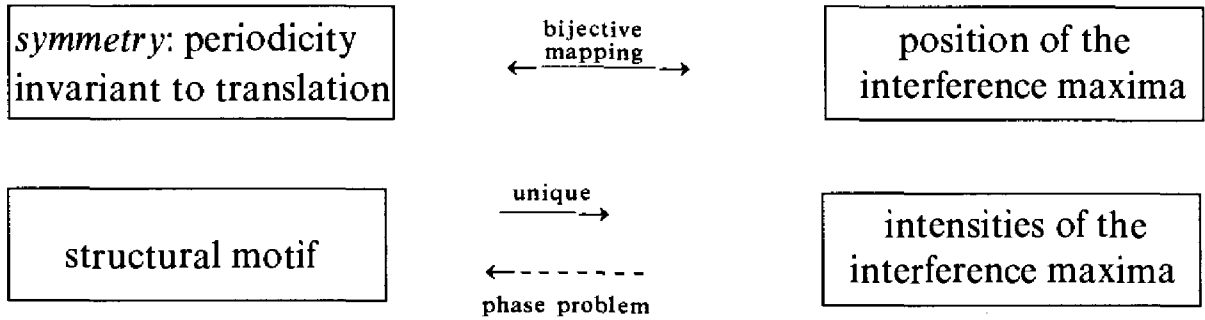


Figure 3.8 illustrates this theorem. Figure 3.7 shows the diffraction patterns produced by two or three circular holes. It is easy to determine the repeat distance d of the lattice by looking for the maxima of J_N^2 . The determination of the size and

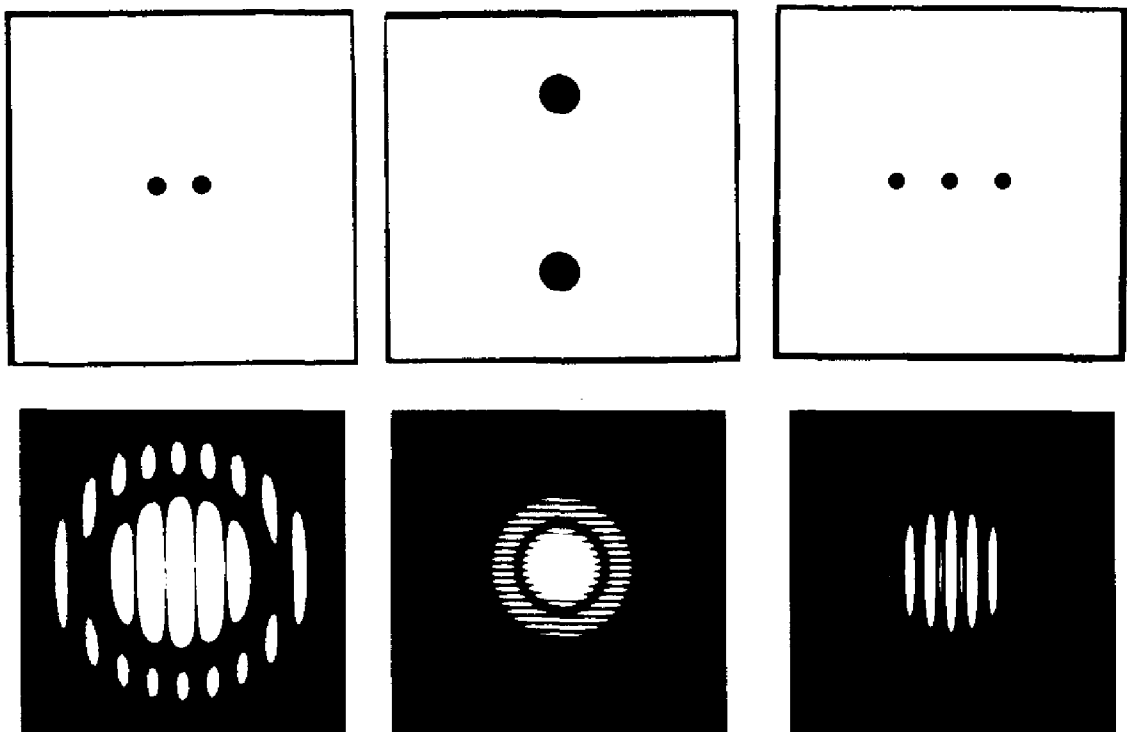


Fig. 3.7. Diffraction patterns obtained from circular holes (G. Harburn, C. A. Taylor & T. R. Welbury, *An Atlas of Optical Transforms*. London: Bell, 1975)

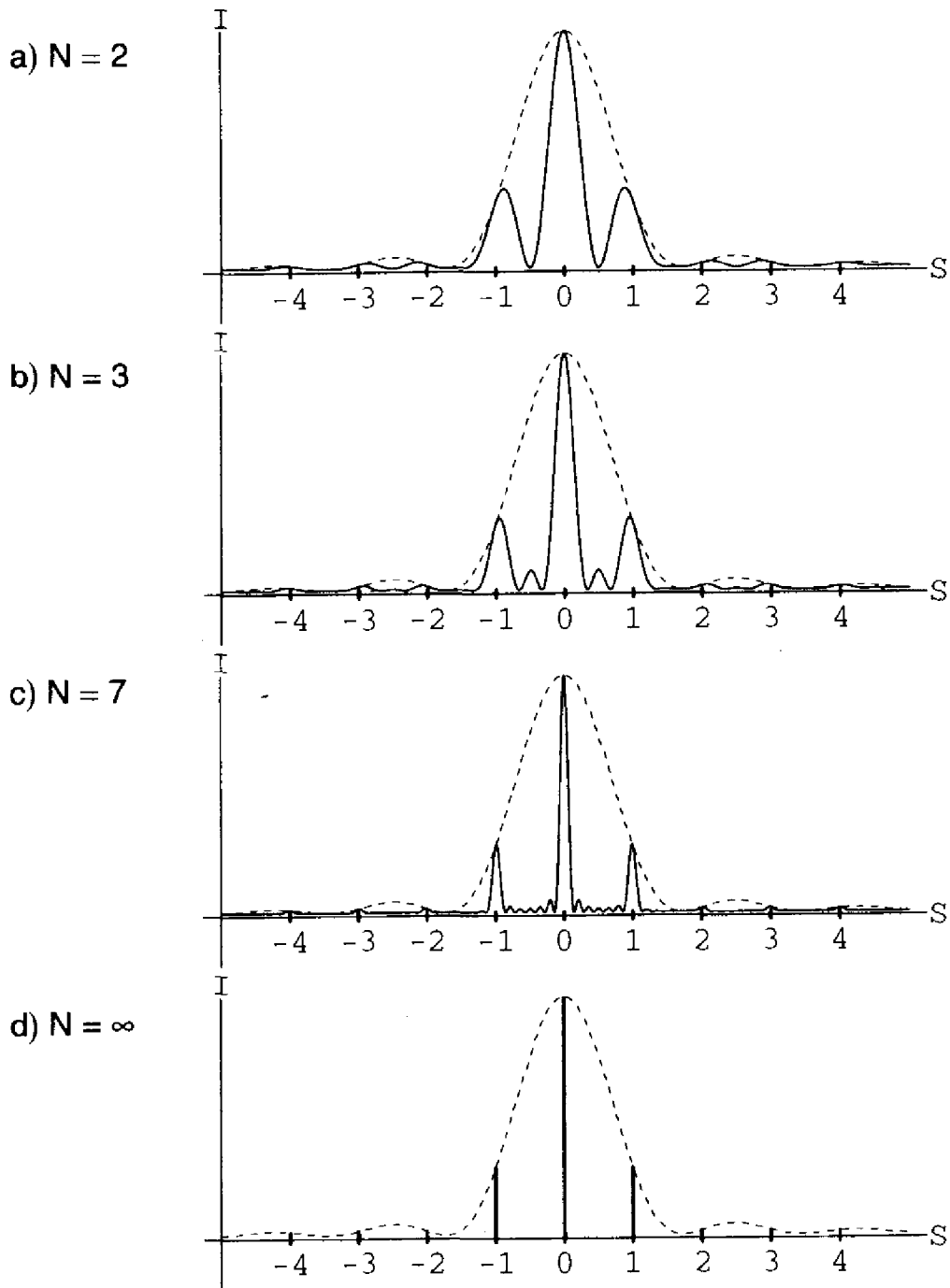


Fig. 3.8. Curves showing the intensity $I(S) = I(\sin \theta/\lambda)$ of the light diffracted by a linear optical grating made up of N identical circular holes. $I(S) = |F(S)|^2 |J_N(S)|^2$. The dotted line shows the intensity $|F(S)|^2$ due to the diffraction by a single hole; the separation of its maxima and minima is a function of the size of the hole. The positions of the maxima of $|J_N(S)|^2$ depend on the repeat distance of the grating

shape of the hole, and hence the complete structure, is more difficult because we are faced with the phase problem.

3.2 SCATTERING OF X-RAYS BY AN ELECTRON

3.2.1 CLASSICAL ELECTRON ACCORDING TO THOMPSON

The interaction of electromagnetic waves, particularly X-rays, with the electrons of matter produces two effects:

- The absorption of radiation which induces changes in the electronic energy levels (Section 3.6).
- The scattering of radiation, i.e. its diffusion in different directions, which has two components, one coherent with the incident radiation (*Thompson* scattering) and the other incoherent with a longer wavelength (*Compton* scattering). The term *coherent* indicates a precise relation between the phases of the incident and scattered wave. The coherent scattering by a periodic structure, hence by a crystal, is called *diffraction*. This may be elastic or inelastic (Section 3.1.1).

The theory of coherent scattering by a *classical free electron* was developed by J. J. Thompson in 1898. The electron is considered to be a classical free particle of charge $-e$ and of mass m accelerated by the oscillating electric field of the

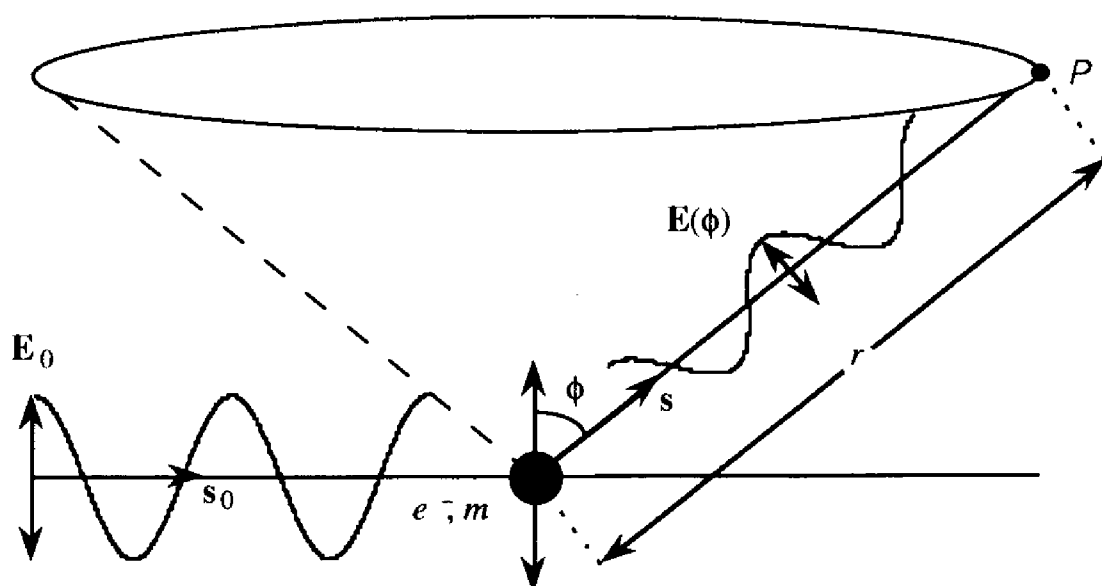


Fig. 3.9. Scattering of a polarized electromagnetic wave of amplitude E_0 and intensity I_0 by a free electron of charge $-e$ and mass m . The accelerated electron emits a secondary wave $E(\Phi)$ of intensity $I(\Phi)$

radiation. Consequently, it emits secondary radiation similar to that of an antenna (Fig. 3.9). The results obtained from the classical theory are essentially the same as those obtained from quantum mechanics.

At the point P , the wave scattered by a free electron is polarized in the plane \mathbf{E}_0/\mathbf{s} . Its amplitude is proportional to the component of the acceleration of the electron perpendicular to \mathbf{s} ,

$$\|\mathbf{E}(\phi)\| = \|\mathbf{E}_0\| \frac{1}{r} \frac{1}{4\pi\epsilon_0} \frac{e^2}{mc^2} \sin \phi, \quad (3.16)$$

c being the speed of light and ϵ_0 , the dielectric constant for a vacuum (SI units). $\|\mathbf{E}(\phi)\|$ is independent of the wavelength. We call the *scattering length* $e^2/4\pi\epsilon_0 mc^2 = d_e = 2.818 \times 10^{-15}$ m the *classical diameter of the electron*. This formula for d_e is obtained by considering that the electron is a conducting sphere of diameter d_e carrying a charge of $-e$ which is uniformly distributed over its surface, and that its electrostatic energy $e^2/4\pi\epsilon_0 d_e$ is equal to the energy mc^2 . The amplitude $\|\mathbf{E}(\phi)\|$ is maximal in any direction of observation \mathbf{s} perpendicular to \mathbf{E}_0 . It is zero in the direction of \mathbf{E}_0 .

3.2.2 POLARIZATION FACTOR

Figure 3.10 shows the case of a primary wave \mathbf{s}_0 with polarization \mathbf{E}_0 which is oblique with respect to the plane $(\mathbf{s}_0, \mathbf{s})$. The amplitude \mathbf{E} of the wave scattered in the direction \mathbf{s} is given by the angle ϕ and by equation (3.16). We then express ϕ in terms of the angles μ and 2θ . The amplitude of the component of \mathbf{E}_0 perpendicular to the plane $(\mathbf{s}_0, \mathbf{s})$ is $\|\mathbf{E}_{0,n}\| = \|\mathbf{E}_0\| \cos \mu$. $\mathbf{E}_{0,n}$ is perpendicular to \mathbf{s} and the

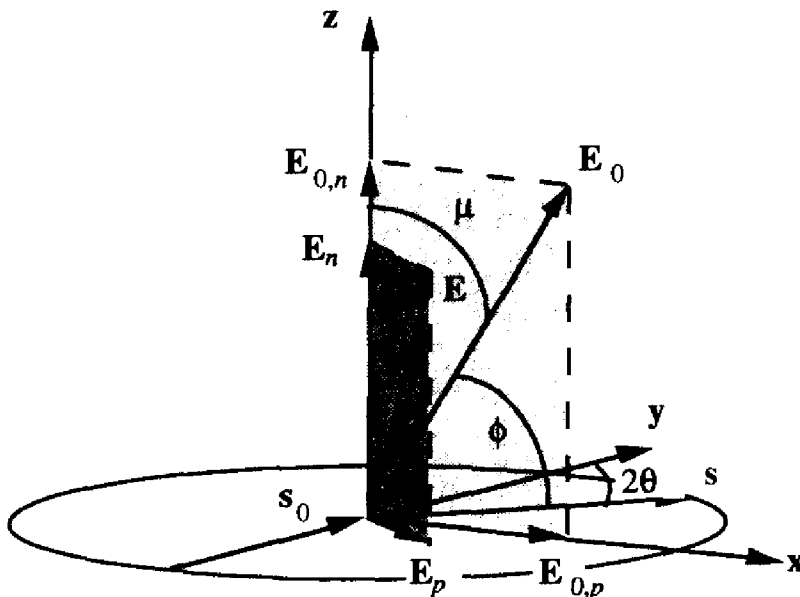


Fig. 3.10. Derivation of the polarization factor. The plane $\mathbf{E}_{0,n}/\mathbf{E}_{0,p}$ is normal to \mathbf{s}_0 ; the plane $\mathbf{E}_p/\mathbf{E}_n$ is normal to \mathbf{E} , \mathbf{E}_0 , \mathbf{s} are coplanar; 2θ is the angle between \mathbf{s} and \mathbf{s}_0 ; μ is the angle of polarization

scattered amplitude $\|\mathbf{E}_n\|$ is thus

$$\|\mathbf{E}_n\| = \|\mathbf{E}_{0,n}\| \frac{1}{r} \frac{1}{4\pi\epsilon_0} \frac{e^2}{mc^2} = \|\mathbf{E}_0\| \frac{1}{r} \frac{1}{4\pi\epsilon_0} \frac{e^2}{mc^2} \cos \mu$$

The component of \mathbf{E}_0 parallel to the plane $(\mathbf{s}_0, \mathbf{s})$, of amplitude $\|\mathbf{E}_{0,p}\| = \|\mathbf{E}_0\| \sin \mu$, makes an angle of $\pi/2 - 2\theta$ with \mathbf{s} , 2θ being the angle between \mathbf{s} and \mathbf{s}_0 . The amplitude $\|\mathbf{E}_p\|$ is thus

$$\|\mathbf{E}_p\| = \|\mathbf{E}_{0,p}\| \frac{1}{r} \frac{1}{4\pi\epsilon_0} \frac{e^2}{mc^2} \cos 2\theta = \|\mathbf{E}_0\| \frac{1}{r} \frac{1}{4\pi\epsilon_0} \frac{e^2}{mc^2} \sin \mu \cos 2\theta.$$

The total scattered amplitude is

$$\|\mathbf{E}(\mu)\| = \|\mathbf{E}_n + \mathbf{E}_p\| = \|\mathbf{E}_0\| \frac{1}{r} \frac{1}{4\pi\epsilon_0} \frac{e^2}{mc^2} \{\cos^2 \mu + \sin^2 \mu \cos^2 2\theta\}^{1/2} \quad (3.17)$$

We can derive equation (3.17) equally well by using spherical trigonometry: $\cos \phi = \sin \mu \sin 2\theta$, hence $\sin^2 \phi = 1 - \sin^2 \mu \sin^2 2\theta = \cos^2 \mu + \sin^2 \mu \cos^2 2\theta$.

The intensity of the radiation is proportional to the square of the amplitude, hence

$$I(\phi) = I_0 \frac{1}{r^2} \left(\frac{1}{4\pi\epsilon_0} \right)^2 \left(\frac{e^2}{mc^2} \right)^2 \sin^2 \phi,$$

and

$$I(\mu, \theta) = I_0 \frac{1}{r^2} \left(\frac{1}{4\pi\epsilon_0} \right)^2 \left(\frac{e^2}{mc^2} \right)^2 \{\cos^2 \mu + \sin^2 \mu \cos^2 2\theta\}. \quad (3.18)$$

A non-polarized beam consists of a series of incoherent waves whose polarization angles μ are uniformly distributed. The sum of a large number of incoherent waves may be obtained by the addition of the squares of their amplitudes, i.e. of their intensities. By introducing the expectation values of $\cos^2 \mu$ and $\sin^2 \mu$, $\langle \cos^2 \mu \rangle = \langle \sin^2 \mu \rangle = 1/2$ into equation (3.18), we obtain the scattering of a nonpolarized beam

$$I_e = I_0 \frac{1}{r^2} \left(\frac{1}{4\pi\epsilon_0} \right)^2 \left(\frac{e^2}{mc^2} \right)^2 \frac{1 + \cos^2 2\theta}{2} = I_0 \left(\frac{d_e}{r} \right)^2 P. \quad (3.19)$$

The expression $P = (1 + \cos^2 2\theta)/2$ is called the **polarization factor**. For a partially polarized primary beam, the expectation values $\langle \cos^2 \mu \rangle$ and $\langle \sin^2 \mu \rangle$ are different from 1/2. 2θ is the angle between \mathbf{s}_0 and \mathbf{s} , i.e. between the direction of the primary beam and that of the scattered beam or the direction of observation. It must be noted that the scattered beams are partially polarized. When the angle $2\theta = 90^\circ$, the polarization is total. This corresponds to *Brewster's Law*: the reflection from a mirror is totally polarized if the refracted and reflected beams are perpendicular. According to Snell's law of refraction, half of the angle between the incident and reflected beams is given by $\cot \theta = n$ where n is the index of refraction. For X-rays, $n = 1$ and hence $2\theta = 90^\circ$. Any reflection of light from

a nonmetallic surface, by snow, a lake, a road, or that part of the sky far from the sun, is partially polarized.

By convention, we express all the intensities scattered by a crystal in units of scattering due to a classical electron, I_e .

In the following discussion, we will suppose that all the experimentally measured intensities have been corrected for the effects of polarization.

It is clear that the electrons in matter are not completely free as they are bound to atoms. Their behavior parallels that of the forced oscillation of a pendulum which depends on the natural frequency and that of the applied force. The majority of electrons, in particular those of the light atoms or the exterior shells of heavy atoms, behave almost like free electrons when they interact with X-rays, their interaction energies with the nuclei, and hence their natural frequencies, being much lower than the frequency of the radiation.

The binding energy of the electrons in the interior shells of the heavy atoms is close to, or superior to, that of the radiation. The amplitude and the phase of the scattered X-ray are thus modified. The scattering power becomes a complex quantity. This phenomenon is called *anomalous dispersion*. It is particularly important if the frequency of the radiation is close to a natural frequency of the electron, i.e. an absorption edge of the atom (Section 3.6.2). We then observe the effects of resonance. By choosing the wavelength, and hence the frequency, of the X-rays to be far from an absorption edge of any atom in the crystal, we can neglect anomalous dispersion to a first approximation.

In the case of visible light, the frequency is less than or close to the natural frequency of the majority of the electrons. The scattering power of the electrons is thus a function of the wavelength, and hence of the color (Rayleigh scattering), whereas, for quasi-free electrons, it is constant.

3.3 SCATTERING OF X-RAYS BY MATTER

3.3.1 FOURIER TRANSFORM, THE PHASE PROBLEM

The distribution of electrons in matter in the crystalline, amorphous, gaseous or liquid states is described by the electron density function $\rho(\mathbf{r})$ whose value is given in units of electrons per unit volume [$e\text{\AA}^{-3}$] or [$e\text{nm}^{-3}$]. The number of electrons contained in a volume element $d^3\mathbf{r}$ is $\rho(\mathbf{r})d^3\mathbf{r}$. This function has pronounced maxima at the centers of atoms and broad minima between them. The function also represents the X-ray scattering power per unit volume, the amplitude of the radiation scattered by the volume $d^3\mathbf{r}$ being proportional to the number of classical electrons that it contains.

As shown in Fig. 3.11, the path difference between the wave A scattered by the volume element at the origin and the wave B scattered by the volume element at

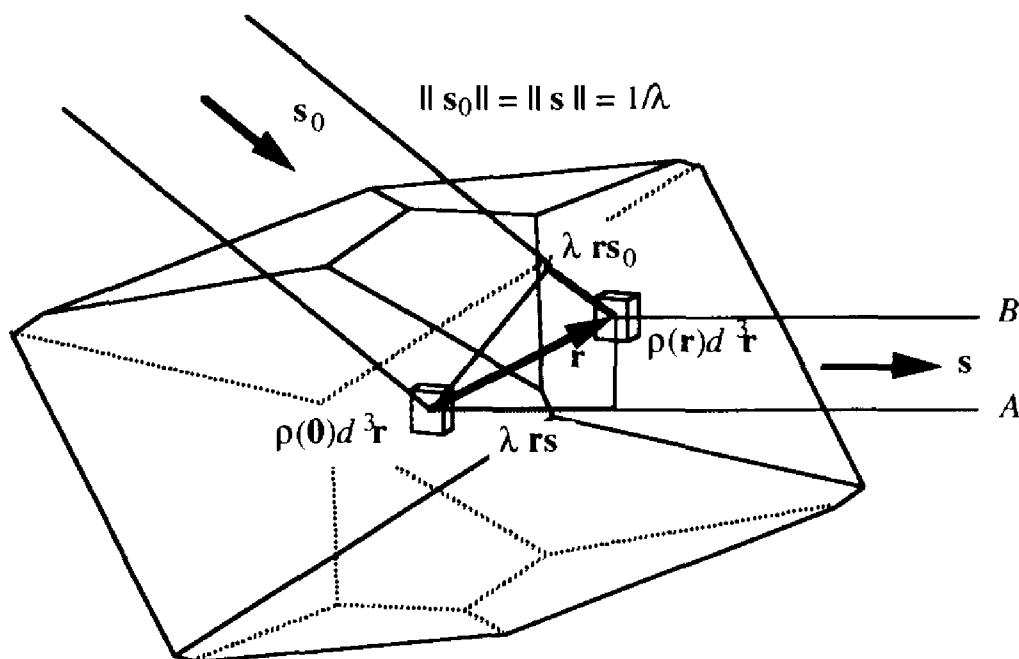


Fig. 3.11. Electron density $\rho(\mathbf{r})$ and scattering of X-rays

the end of the vector \mathbf{r} is $\Delta = \lambda \mathbf{r} \cdot (\mathbf{s} - \mathbf{s}_0)$. The wave B is expressed, according to equation (3.7), as

$$\xi = \rho(\mathbf{r})e^{2\pi i \mathbf{r} \cdot (\mathbf{s} - \mathbf{s}_0)} d^3 \mathbf{r}.$$

The total wave scattered by the sample in the direction \mathbf{s} (Fig. 3.12) is thus given by

$$G(\mathbf{S}) = \int \rho(\mathbf{r})e^{2\pi i \mathbf{r} \cdot \mathbf{S}} d^3 \mathbf{r} = \Phi[\rho(\mathbf{r})], \tag{3.20}$$

$$\mathbf{S} = \mathbf{s} - \mathbf{s}_0, \quad \|\mathbf{S}\| = 2 \sin \theta / \lambda. \tag{3.21}$$

$G(\mathbf{S})$ is the **Fourier transform** of $\rho(\mathbf{r})$. The inverse transformation Φ^{-1} allows us to calculate $\rho(\mathbf{r})$ from $G(\mathbf{S})$:

$$\rho(\mathbf{r}) = \int G(\mathbf{S})e^{-2\pi i \mathbf{r} \cdot \mathbf{S}} d^3 \mathbf{S} = \Phi^{-1}[G(\mathbf{S})]. \tag{3.22}$$

The sum of all the waves given by $G(\mathbf{S})$ rigorously represent the density $\rho(\mathbf{r})$. The limit of resolution of a microscope (Section 3.1.1) is due to the fact that certain vectors \mathbf{S} are experimentally inaccessible because the maximum value of $\|\mathbf{S}\|$ is $2/\lambda$ (3.21) (Fig. 3.12). $G(\mathbf{S})$ is a complex quantity,

$$G(\mathbf{S}) = |G(\mathbf{S})|e^{2\pi i \phi(\mathbf{S})}, \tag{3.23}$$

where $|G(\mathbf{S})|$ is the amplitude and $\phi(\mathbf{S})$ is the phase of the wave. If $\rho(\mathbf{r})$ is a real function, $G(-\mathbf{S})$ is the complex conjugate of $G(\mathbf{S})$, $G(-\mathbf{S}) = G^*(\mathbf{S})$.

The diffracted intensity is proportional to the square of the amplitude:

$$I(\mathbf{S}) \approx |G(\mathbf{S})|^2.$$

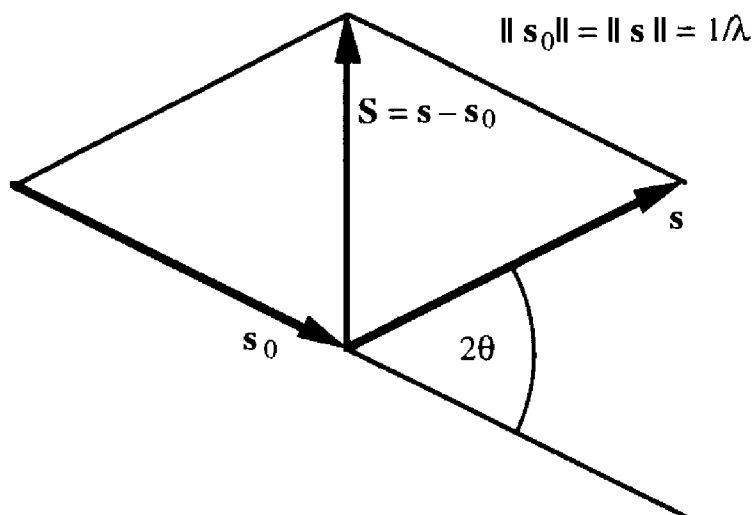


Fig. 3.12. Definition of the vector $\mathbf{S} = \mathbf{s} - \mathbf{s}_0$. $\|\mathbf{s}_0\| = \|\mathbf{s}\| = 1/\lambda$, $\|\mathbf{S}\| = 2 \sin \theta/\lambda$. This figure should be compared with Bragg's law (Section 3.4.2)

This relationship indicates the origin of the *phase problem* (Section 3.1.1) whose solution is one of the important tasks in X-ray crystallography: there exist an infinite number of functions $\rho(\mathbf{r})$ which give rise to the same function $I(\mathbf{S})$. If $\rho(\mathbf{r})$ is given, we can always calculate the corresponding function $|G(\mathbf{S})|$. The passage from $|G(\mathbf{S})|$ to $\rho(\mathbf{r})$, i.e. the solution of the phase problem, is only possible on the basis of models; the most important will be developed in Sections 3.3.3 and 3.4.1.

3.3.2 PRIMARY AND SECONDARY EXTINCTION

The discussion in Section 3.3.1 is based on the following approximations:

- Because of the effects of anomalous dispersion for certain electrons (Section 3.2.2), the scattering power is only approximately given by the electron density function $\rho(\mathbf{r})$. Equation (3.20) is still correct if $\rho(\mathbf{r})$ is replaced by a complex function that describes the distribution of scattering power.
- Part of the primary radiation is not diffracted, but absorbed by the sample (Section 3.6.2). This effect may be taken into account if the exact form of the sample is known.
- The theory presented in Section 3.3.1 is called the *kinematic theory* of scattering. Diffraction by a three-dimensional body is, however, more complex than suggested by Fig. 3.11. On the one hand, the primary radiation is attenuated by diffraction and the secondary beams may be rediffracted. Hence, the different volume elements do not all receive the same primary intensity; for this reason, the kinematic theory does not obey the law of conservation of energy. On the other hand, the interference between the primary wave and the divers diffracted waves has been neglected. All these effects generally lead to diffracted intensities that are weaker than those predicted by the kinematic theory. These

phenomena are referred to as *extinction*. We distinguish *primary extinction* which is composed of the coherent effects due to the interference of the diverse waves, and *secondary extinction* comprised of the incoherent effects described by the addition of intensities. The diffracted intensities are usually weak in comparison to the intensity of the primary beam because the classical diameter of the electron $e^2/4\pi\epsilon_0 mc^2$ is small. The kinematic theory becomes more applicable as $|G(\mathbf{S})|^2$ and the volume of the crystal become smaller. It has had notable success in the majority of the applications of X-ray crystallography. The exact theory was developed for perfect crystals with no defects and with simple shapes. It is known under the name of *dynamic theory*. The diffraction of X-rays by the vast majority of crystals follows neither of these theories exactly, but in general it obeys the kinematic theory better than the dynamic theory. In the case of routine structure determinations, the effects of extinction are often neglected.

- Taking into account the effects of these approximations, the diffracted intensity is given by

$$I(\mathbf{S}) = Kg(\theta)Ay|G(\mathbf{S})|^2, \quad (3.24)$$

where K is a constant which includes the factor $(e^2/4\pi\epsilon_0 mc^2)^2$ and the volume of the crystal, $g(\theta)$ is a function independent of the structure of the material which incorporates the polarization factor (Section 3.2.2 and equation (3.19)), A is the absorption factor ($A \leq 1$), and y is the extinction factor ($y \leq 1$). The theory concerning the evaluation of this latter factor is both laborious and imprecise.

In neutron diffraction, the function which describes the scattering power is given partly by the distribution of the nuclei and partly by the distribution of unpaired electrons. As is the case for X-ray diffraction, the kinematic theory is a useful approximation.

For a beam of electrons, the scattering power of matter is very high. For this reason the kinematic approximation is not very appropriate for electron diffraction.

3.3.3 ATOMISTIC MODEL: THE FORM FACTOR

This model, conceived for the solution of the phase problem, makes the assumption that matter is composed of independent atoms. The electron density distribution of a free atom at rest may be calculated by quantum mechanical methods. For atoms which contain partially filled shells and which are non-spherical, we calculate the spherical average. Hence, in this model, all atoms have spherical symmetry.

We allow that (Fig. 3.13)

$$\rho(\mathbf{r}) = \sum_m^{\text{atoms}} \rho_m(\mathbf{r} - \mathbf{r}_m) \quad (3.25)$$

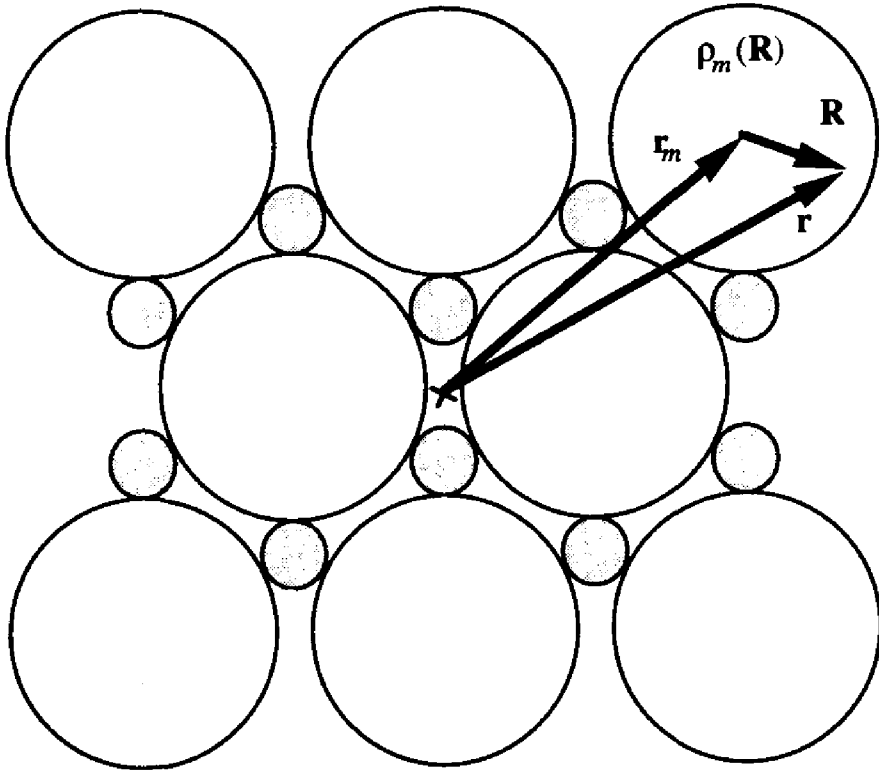


Fig. 3.13. Structure composed of atoms. Each circle represents an atomic electron density $\rho_m(\mathbf{R})$. The vector \mathbf{r}_m represents the coordinates of the m th atom with respect to the origin

i.e. that the distribution $\rho(\mathbf{r})$ is approximately equal to the superposition of the atomic distributions $\rho_m(\mathbf{R})$ centered on the points \mathbf{r}_m . For a spherical atom, $\rho_m(\mathbf{R}) = \rho_m(R)$. $\rho_m(R)$ may be approximately represented by a sum of Gaussians, $\rho_m(R) \approx \sum_g K_{m,g} \exp[-\alpha_{m,g} R^2]$; hence the atomic electron densities overlap.

We neglect the effect of chemical bonding on the electron density distribution. Experience has shown that this is an excellent approximation which allows us to account for the scattered or diffracted intensities to within a few percent. The Fourier transform of a structure composed of atoms is

$$G(\mathbf{S}) = \int \sum_m \rho_m(\mathbf{r} - \mathbf{r}_m) e^{2\pi i \mathbf{r} \cdot \mathbf{S}} d^3 \mathbf{r} = \sum_m f_m e^{2\pi i \mathbf{r}_m \cdot \mathbf{S}}, \quad (3.26)$$

$$f_m(\mathbf{S}) = \int_{\text{atom } m} \rho_m(\mathbf{R}) e^{2\pi i \mathbf{R} \cdot \mathbf{S}} d^3 \mathbf{R} = \Phi[\rho_m] \quad (3.27)$$

As the atom is spherical, we can use spherical coordinates and integrate over the angular coordinates, and obtain for equation (3.27)

$$f_m(\|\mathbf{S}\|) = f_m(S) = \int_0^\infty 4\pi R^2 \rho_m(R) \frac{\sin 2\pi RS}{2\pi RS} dR, \quad (3.28)$$

with $S = \|\mathbf{S}\| = 2 \sin \theta / \lambda$ (3.21). $f_m(\sin \theta / \lambda)$ is the **atomic scattering factor** or **form**

factor. It is the Fourier transform of the atomic electron density distribution. This factor describes the scattering power of an atom. Taking into account anomalous dispersion (Section 3.2.2), the form factor becomes $f_{tot} = f + \Delta f' + i\Delta f''$.

The form factors for all atoms, both neutral and ionic, are tabulated in the *International Tables for Crystallography* (vol. C., pp. 477–503). The corrections $\Delta f'$ and $\Delta f''$ for the most important wavelengths may be found in the same volume (pp. 219–222).

The atomic form factor has the following properties (Fig. 3.14):

- It is a function of $\sin \theta/\lambda$.
- Its value is given in units of classical electrons.
- $f_m(0)$ is equal to the number of electrons belonging to the atom or ion; all three species F^{-1} , Ne and Na^{+1} possess 10 electrons.
- The decrease in $f_m(\sin \theta/\lambda)$ is directly correlated with the diffuseness of the electron density distribution $\rho_m(R)$. The nuclear charge of Na is equal to 11 electrons, that of F is equal to 9 electrons. Because of this fact, the concentration of electrons in the atomic core is higher for the ion Na^{+1} than for the ion F^{-1} ; correspondingly the decrease in f is less rapid for Na^{+1} than for F^{-1} .
- The form factor of a neutral atom only differs from that of its ions at low values of $\sin \theta/\lambda$. This difference is due to the presence or absence of a valence electron which has a diffuse distribution and whose Fourier transform decreases

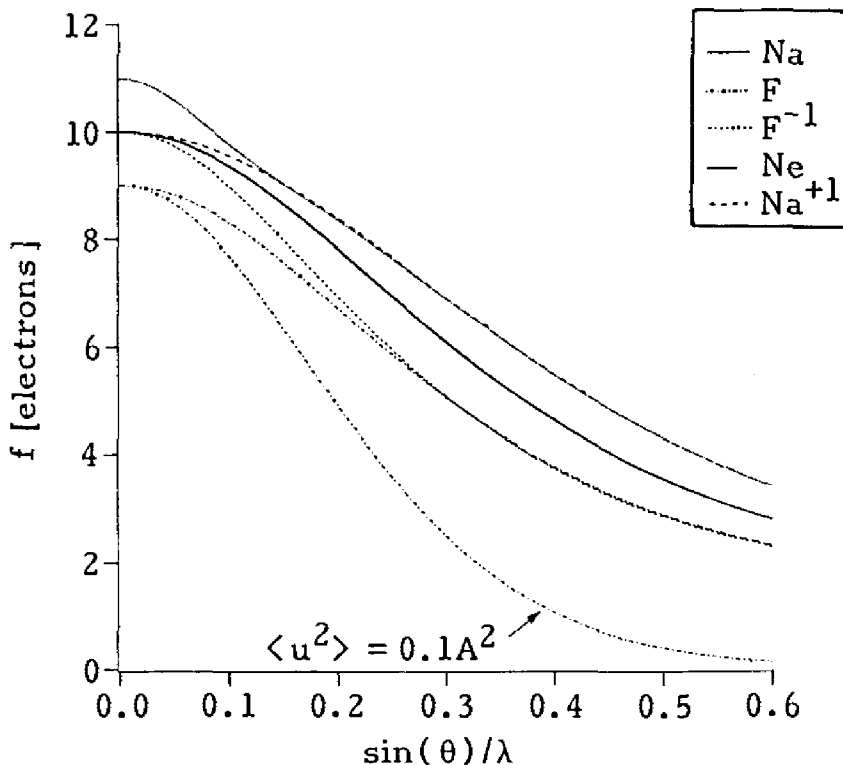


Fig. 3.14. Form factors for the atoms Na, Ne and F, and for the ions Na^{+1} and F^{-1} . For the meaning of $\langle u^2 \rangle = U_{isor}$, see Section 3.3.4, equation (3.34)

rapidly. In general, chemical bonds between atoms are composed of diffuse electron density. For this reason, their contribution to the scattered waves is small (but nonetheless observable in precise measurements).

3.3.4 ATOMISTIC MODEL: THERMAL VIBRATIONS IN A CRYSTAL

The atomic form factor is the Fourier transform of the electron density of an atom *at rest*. However, because of thermal effects, atoms in a crystal oscillate about their mean positions with frequencies of the order of 10^{12} to 10^{14} Hz. The instantaneous structure, during periods of time less than 10^{-14} sec, no longer has translation symmetry. Only the time average of a crystal structure, characterized by the average electron density $\langle \rho \rangle_t$, is periodic and allows the observation of diffraction patterns characteristic of a crystal (Section 3.4). In the following we calculate the Fourier transform of the average electron density of an atom subject to thermal vibrations while neglecting the effect of fluctuations of the electron density about its average.

Let $P(\Delta)d^3\Delta$ be the probability that the center of the atom m , at some given moment, be found in the volume element $d^3\Delta$ at the tip of the vector Δ (Fig. 3.15). The contribution of the displaced atom to the average electron density is

$$P(\Delta)\rho_m(\mathbf{R} - \Delta)d^3\Delta,$$

$\rho_m(\mathbf{R})$ being the electron density of the atom at rest. The average electron density of the atom is obtained by integrating over all the displacements Δ ,

$$\langle \rho_m(\mathbf{R}) \rangle_t = \int P(\Delta)\rho_m(\mathbf{R} - \Delta)d^3\Delta = P_*\rho_m(\mathbf{R}). \quad (3.29)$$

The integral (3.29) is called the *convolution product* of the functions $P(\Delta)$ and $\rho_m(\mathbf{R})$, written as $P_*\rho_m = \rho_m * P$.

The form factor for the average atom $[f_m]_t$ is the Fourier transform of $\langle \rho_m \rangle_t$. It is a fundamental theorem that the Fourier transform of a convolution product is

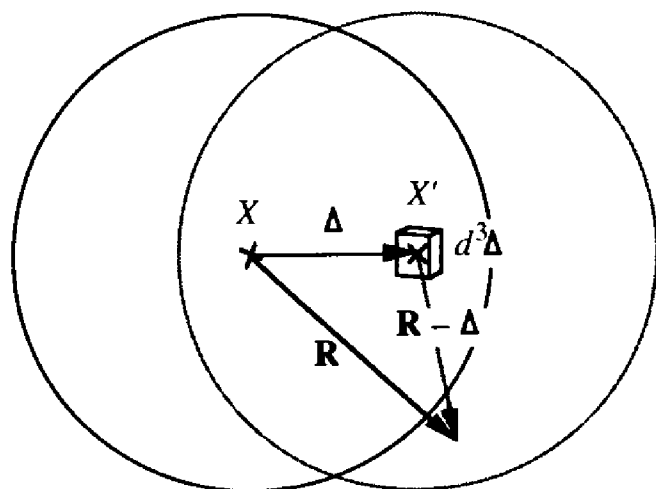


Fig. 3.15. The atom at the average position X is displaced to position X' with the probability $P(\Delta)d^3\Delta$

the product of the Fourier transforms of each of the functions,

$$[f_m]_t = \Phi[\rho_m * P] = \Phi[\rho_m]\Phi[P] = f_m(S)T(S),$$

$$T(S) = \int P(\Delta)e^{2\pi i\Delta \cdot S} d^3\Delta = \Phi[P]. \quad (3.30)$$

The distribution function $P(\Delta)$ may describe not only the dynamic displacements of the atom due to thermal vibrations, but also static displacements. In this latter case a disordered atom can occupy different sites at random which are themselves periodic. The average structure is then a spatial average taken over a large number of unit cells. For this reason $T(S)$ is called the *displacement factor*, thus avoiding the use of the more traditional term of *temperature factor*.

$P(\Delta)$ can in principle be any function that fulfills the conditions for the existence of the Fourier integral. It can be shown that $P(\Delta)$ is a Gaussian distribution if the vibrations of the atoms are harmonic:

$$P(\Delta) = (2\pi)^{-3/2} |\mathbf{V}|^{-1/2} e^{-(\Delta^T \mathbf{V}^{-1} \Delta)/2} \quad (3.31)$$

where \mathbf{V} is the variance-covariance matrix whose terms are the expectation values $V_{ij} = \langle \Delta_i \Delta_j \rangle_t$. By choosing the eigenvectors of \mathbf{V} associated with the eigenvalues V_i as the coordinate system, equation (3.31) becomes

$$P(\Delta) = (2\pi)^{-3/2} (V_1 V_2 V_3)^{-1/2} e^{-(\Delta_1^2/V_1 + \Delta_2^2/V_2 + \Delta_3^2/V_3)/2}.$$

We know that the Fourier transform of a Gaussian is a Gaussian,

$$T(\mathbf{S}) = e^{-2\pi^2 \mathbf{S}^T \mathbf{V} \mathbf{S}} = e^{-2\pi^2 (V_{11} S_1^2 + V_{22} S_2^2 + V_{33} S_3^2 + 2V_{12} S_1 S_2 + 2V_{13} S_1 S_3 + 2V_{23} S_2 S_3)}. \quad (3.32)$$

The expression (3.32) for T is called the *Debye-Waller factor*. The mean square displacement U_s parallel to \mathbf{S} is

$$U_s = \frac{\langle (\mathbf{S} \cdot \Delta)^2 \rangle_t}{\|\mathbf{S}\|^2} = \frac{\mathbf{S}^T \mathbf{V} \mathbf{S}}{\|\mathbf{S}\|^2}$$

With (3.21), expression (3.32) becomes

$$T(\mathbf{S}) = e^{-8\pi^2 U_s (\sin \theta / \lambda)^2}.$$

In the crystal lattice coordinate system (Sections 1.4.1 and 3.4), $\Delta = \Delta_1 \mathbf{a}_1 + \Delta_2 \mathbf{a}_2 + \Delta_3 \mathbf{a}_3$, and $\mathbf{S} = h_1 \mathbf{a}_1^* + h_2 \mathbf{a}_2^* + h_3 \mathbf{a}_3^*$. Hence equation (3.32) may be written as

$$T(h_1 h_2 h_3) = \exp \left\{ - \sum_i^3 \sum_j^3 \beta_{ij} h_i h_j \right\}, \text{ where } \beta_{ij} = 2\pi^2 V_{ij}.$$

The β_{ij} are dimensionless numbers (as is the case for the atomic coordinates x_i). The interpretation of the results of a structure determination is made easier if we choose another coordinate system based on the reciprocal lattice, $\mathbf{e}_i^* = \mathbf{a}_i^* / \|\mathbf{a}_i^*\|$. The \mathbf{e}_i^* are unit vectors but, in general, they are not mutually perpendicular.

Hence equation (3.32) may be written as

$$T(h_1 h_2 h_3) = \exp \left\{ -2\pi^2 \sum_i^3 \sum_j^3 U_{ij} a_i^* a_j^* h_i h_j \right\} \quad (3.33)$$

where the U_{ij} have dimensions of \AA^2 .

Finally, a function P whose amplitude is independent of the direction of Δ is called *isotropic*. In this case $V_{11} = V_{22} = V_{33} = U_{iso}$, $V_{12} = V_{13} = V_{23} = 0$. Thus equation (3.32) becomes

$$T(\sin \theta / \lambda) = e^{-8\pi^2 U_{iso} (\sin \theta / \lambda)^2} \quad (3.34)$$

At ambient temperature, the values for U_{iso} are typically of the order of 0.01 to 0.10\AA^2 . For the carbon atoms in diamond, $U_{iso} \approx 0.002 \text{\AA}^2$ is particularly small. For Na and Cl in the structure of NaCl, we find $U_{iso} \approx 0.02 \text{\AA}^2$. Figure 3.14 shows that the thermal motion reduces the form factor and hence the intensities diffracted at high θ angles. It can be shown that, at a sufficiently high temperature, U_{iso} is a linear function of the temperature if the vibrations are harmonic.

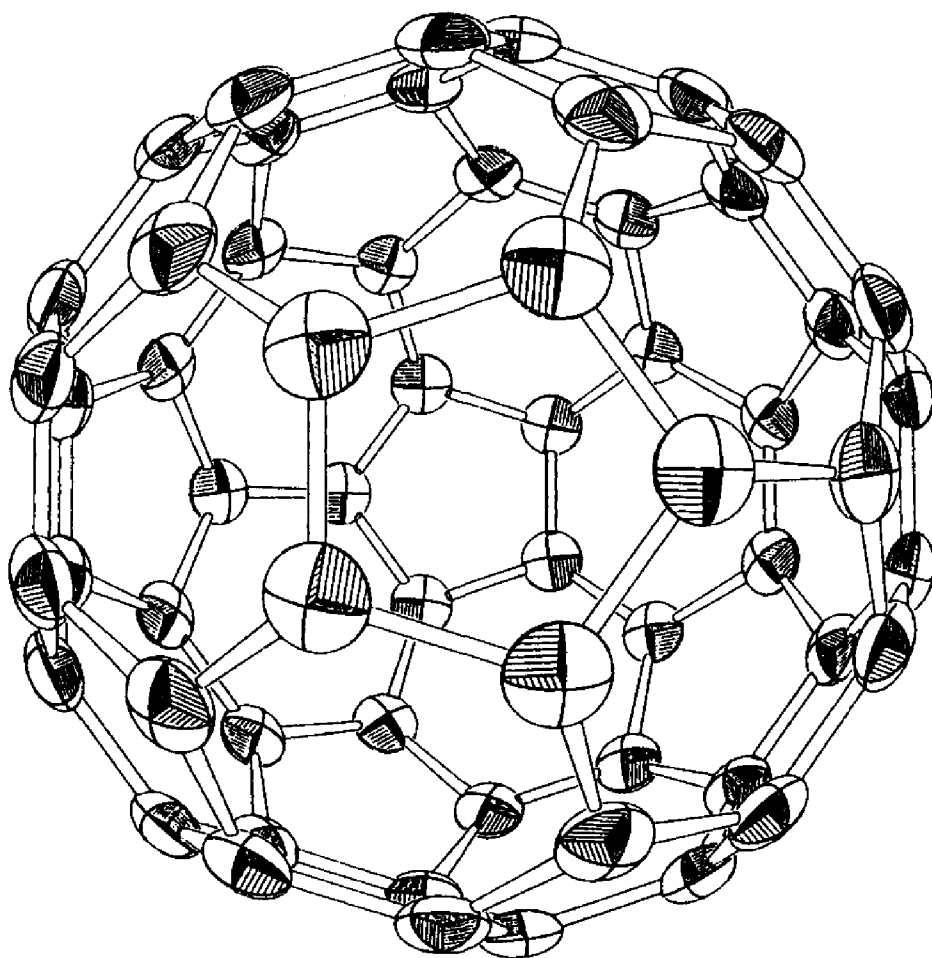


Fig. 3.16. Molecule of C_{60} at a temperature of 200 K. The integral of the Gaussian $P(\Delta)$ (3.31) over the volume of an ellipsoid is equal to 0.5

The tensors \mathbf{V} obtained during a structure determination are represented by ellipsoids (Chapter 4)

$$\mathbf{X}^T \mathbf{V}^{-1} \mathbf{X} = \text{constant.}$$

Figure 3.16 shows an example.

3.4 DIFFRACTION BY A PERIODIC STRUCTURE

3.4.1 LAUE EQUATIONS

In a crystal, the time average of the electron density $\langle \rho(\mathbf{r}) \rangle_t$ is periodic (Section 1.4),

$$\begin{aligned} \langle \rho(\mathbf{r}) \rangle_t &= \rho(\mathbf{r} + u\mathbf{a} + v\mathbf{b} + w\mathbf{c}); \quad u, v, w \text{ being integers} \\ \mathbf{r} &= x\mathbf{a} + y\mathbf{b} + z\mathbf{c}; \quad 0 \leq x, y, z < 1. \end{aligned}$$

The vectors \mathbf{a} , \mathbf{b} , \mathbf{c} form the lattice base. Thus the Fourier transform (3.20) becomes

$$\begin{aligned} G(\mathbf{S}) &= \sum_{\text{cells}} \left\{ \int_{1 \text{ cell}} \langle \rho(\mathbf{r}) \rangle_t e^{2\pi i \mathbf{r} \cdot \mathbf{S}} d^3 \mathbf{r} \right\} e^{2\pi i (u\mathbf{a} + v\mathbf{b} + w\mathbf{c}) \cdot \mathbf{S}} \\ &= F(\mathbf{S}) \sum_u e^{2\pi i u \mathbf{a} \cdot \mathbf{S}} \sum_v e^{2\pi i v \mathbf{b} \cdot \mathbf{S}} \sum_w e^{2\pi i w \mathbf{c} \cdot \mathbf{S}} \end{aligned}$$

Let the crystal have the form of a parallelepiped with M cells in the \mathbf{a} direction, N cells in the \mathbf{b} direction and P cells in the \mathbf{c} direction. We can evaluate the sums of the geometric progressions by using equation (3.10):

$$\sum_{u=0}^{M-1} e^{2\pi i u \mathbf{a} \cdot \mathbf{S}} = \frac{\sin \pi M \mathbf{a} \cdot \mathbf{S}}{\sin \pi \mathbf{a} \cdot \mathbf{S}} e^{\pi i (M-1) \mathbf{a} \cdot \mathbf{S}} = J_M e^{\pi i (M-1) \mathbf{a} \cdot \mathbf{S}}$$

The phase $\frac{1}{2}(M-1)\mathbf{a} \cdot \mathbf{S}$ is dependent on the choice of origin. If we displace the origin to the center of the crystal, for M odd, we obtain

$$\sum_{-(M-1)/2}^{+(M-1)/2} e^{2\pi i u \mathbf{a} \cdot \mathbf{S}} = \sum_{-(M-1)/2}^{+(M-1)/2} \cos 2\pi u \mathbf{a} \cdot \mathbf{S} = \frac{\sin \pi M \mathbf{a} \cdot \mathbf{S}}{\sin \pi \mathbf{a} \cdot \mathbf{S}} = J_M(\mathbf{a} \cdot \mathbf{S}). \quad (3.35)$$

The intensity of the diffracted wave is proportional to $|G(\mathbf{S})|^2$. By using equations (3.26), (3.27) and (3.30), we obtain

$$I \approx |G(\mathbf{S})|^2 = |F(\mathbf{S})|^2 J_M^2(\mathbf{a} \cdot \mathbf{S}) J_N^2(\mathbf{b} \cdot \mathbf{S}) J_P^2(\mathbf{c} \cdot \mathbf{S}), \quad (3.36)$$

$$F(\mathbf{S}) = \int_{1 \text{ cell}} \langle \rho(\mathbf{r}) \rangle_t e^{2\pi i \mathbf{r} \cdot \mathbf{S}} d^3 \mathbf{r} \approx \sum_{\text{atoms}}^{1 \text{ cell}} [f_m]_t e^{2\pi i \mathbf{r}_m \cdot \mathbf{S}}. \quad (3.37)$$

The form factor $[f_m]_t$ contains the effect of thermal vibrations. The Fourier transform of the electron density distribution of one cell $F(\mathbf{S})$ is called the *structure factor*. The functions J^2 of equations (3.12) and (3.36) are characteristic

of the periodicity. Equation (3.37) represents the theorem cited in Section 3.1.2: *the diffraction pattern of a periodic structure is the product of the diffraction pattern of a single cell with the function J^2 characteristic of the periodicity*. The number of cells MNP being very large, the intensity I is zero almost everywhere (Fig. 3.5) except when the three functions J^2 are simultaneously maximal. This is the case for the vectors \mathbf{S} which satisfy the *Laue equations*:

$$\begin{aligned} \mathbf{a} \cdot \mathbf{S} &= h \\ \mathbf{b} \cdot \mathbf{S} &= k \quad h, k, l \text{ being integers.} \\ \mathbf{c} \cdot \mathbf{S} &= l \end{aligned} \quad (3.38)$$

We can find the vector \mathbf{S} satisfying equation (3.38) by remembering the definition of the *reciprocal lattice* (Section 1.4.3):

$$\begin{aligned} \mathbf{r}^* &= h \mathbf{a}^* + k \mathbf{b}^* + l \mathbf{c}^*; \quad h, k, l \text{ being integers} \\ \mathbf{a} \cdot \mathbf{a}^* &= \mathbf{b} \cdot \mathbf{b}^* = \mathbf{c} \cdot \mathbf{c}^* = 1 \\ \mathbf{a} \cdot \mathbf{b}^* &= \mathbf{a} \cdot \mathbf{c}^* = \mathbf{b} \cdot \mathbf{a}^* = \mathbf{b} \cdot \mathbf{c}^* = \mathbf{c} \cdot \mathbf{a}^* = \mathbf{c} \cdot \mathbf{b}^* = 0 \end{aligned}$$

From this we deduce that

$$\mathbf{S} = \mathbf{s} - \mathbf{s}_0 = \mathbf{r}^* \quad (3.39)$$

The Fourier transform of a periodic function is zero except at the reciprocal lattice points where it is proportional to that of a single cell. The scattering of radiation according to equation (3.39), i.e. the scattering by a crystal, is called diffraction.

In solid state physics, one often refers to the wave vector $\mathbf{k} = 2\pi\mathbf{s}$ (Section 3.1.2), hence $\|\mathbf{k}\| = 2\pi/\lambda$; thus equation (3.39) becomes

$$\mathbf{K} = \mathbf{k} - \mathbf{k}_0 = \mathbf{R}^* = 2\pi(h \mathbf{a}^* + k \mathbf{b}^* + l \mathbf{c}^*).$$

The momentum of a photon is given by $\mathbf{p} = (\hbar/2\pi)\mathbf{k}$, $\|\mathbf{p}\| = (\hbar/\lambda)$, \hbar being Planck's constant. The change in momentum during diffraction is thus proportional to a vector of the reciprocal lattice:

$$\Delta \mathbf{p} = (\hbar/2\pi)\mathbf{R}^* = \hbar \mathbf{r}^*.$$

The energy of the photon remains unchanged, i.e. the diffraction is *elastic*. The Fourier transform of a crystal is obtained by introducing equation (3.39) into (3.35). This operation requires a deeper study of the behavior of J_N^2 when N is large, a function which is composed of a set of sharp peaks (Fig. 3.5). The distribution δ is a mathematical representation of an infinitely sharp peak. δ may be considered to be the limit of a Gaussian function

$$\begin{aligned} \delta(x) &= \lim_{\alpha \rightarrow 0} \frac{1}{\sqrt{2\pi\alpha}} e^{-x^2/2\alpha^2}; \quad \int_{-\infty}^{+\infty} \frac{1}{\sqrt{2\pi\alpha}} e^{-x^2/2\alpha^2} dx = 1; \\ \delta(x) &= 0 \text{ for } x \neq 0; \quad \delta(0) = \infty; \quad \int_{-\infty}^{+\infty} \delta(x) dx = 1. \end{aligned}$$

By analogy, the three-dimensional distribution δ_3 may be represented by the limit of a Gaussian function with spherical symmetry:

$$\delta_3(\mathbf{r}) = \delta_3(r) = \lim_{\alpha \rightarrow 0} \frac{1}{(\sqrt{2\pi\alpha})^3} e^{-r^2/2\alpha^2} = \delta(x)\delta(y)\delta(z); \quad r^2 = \|\mathbf{r}\|^2 = x^2 + y^2 + z^2;$$

$$\delta_3(r) = 0 \text{ for } r \neq 0; \delta_3(0) = \infty; \int \delta_3(\mathbf{r}) d^3\mathbf{r} = \int_{-\infty}^{+\infty} 4\pi r^2 \delta_3(r) dr = 1.$$

We will show in the following that each principal maximum in the periodic function J_N converges with increasing N towards a δ distribution. Indeed, the width of the maximum is proportional to $1/N$, whereas the integral of the maximum tends to 1:

$$\int_{-1/2}^{+1/2} J_N(x) dx = \int_{-1/2}^{+1/2} \frac{\sin \pi N x}{\sin \pi x} dx = \int_{-1/2}^{+1/2} \sum_{-(N-1)/2}^{+(N-1)/2} \cos 2\pi n x dx = \int_{-1/2}^{+1/2} dx = 1,$$

by using equation (3.35). Alternatively, by using the approximation for $N \gg 1$

$$\lim_{N \rightarrow \infty} \int_{\max} \frac{\sin \pi N x}{\sin \pi x} dx = \lim_{N \rightarrow \infty} \int_{\max} \frac{\sin \pi N x}{\pi x} dx = \frac{1}{\pi} \int_{-\infty}^{+\infty} \frac{\sin \pi N x}{x} dx = 1$$

we see that $J_N(x)$ tends towards a regularly spaced set of δ distributions:

$$\lim_{N \rightarrow \infty} \frac{\sin \pi N x}{\sin \pi x} = \sum_{-\infty}^{+\infty} \delta(x - n), \quad n \text{ being integer.}$$

In a similar manner we can show that the function $J_M(\mathbf{a} \cdot \mathbf{S}) J_N(\mathbf{b} \cdot \mathbf{S}) J_P(\mathbf{c} \cdot \mathbf{S})$ for a crystal is a sum of three-dimensional distributions δ_3 centered at the reciprocal lattice points $\mathbf{r}^* = h\mathbf{a}^* + k\mathbf{b}^* + l\mathbf{c}^*$. For a position close to a reciprocal lattice point, $\mathbf{S} = \mathbf{r}^* + \varepsilon_1\mathbf{a}^* + \varepsilon_2\mathbf{b}^* + \varepsilon_3\mathbf{c}^*$, we have $\mathbf{a} \cdot \mathbf{S} = h + \varepsilon_1$; $\mathbf{b} \cdot \mathbf{S} = k + \varepsilon_2$; $\mathbf{c} \cdot \mathbf{S} = l + \varepsilon_3$. The volume element of reciprocal space is given by $d^3\mathbf{S} = [d\varepsilon_1\mathbf{a}^* \times d\varepsilon_2\mathbf{b}^*] d\varepsilon_3\mathbf{c}^* = (d\varepsilon_1 d\varepsilon_2 d\varepsilon_3)/V$, $V = [\mathbf{a} \times \mathbf{b}] \cdot \mathbf{c}$ being the volume of the unit cell. If the number of cells MNP is large, the integral over a principal maximum becomes

$$\begin{aligned} \lim_{M,N,P \rightarrow \infty} \int_{\max} J_M J_N J_P d^3\mathbf{S} &= \frac{1}{V} \lim_{M,N,P \rightarrow \infty} \int_{\max} \frac{\sin \pi M \varepsilon_1}{\sin \pi \varepsilon_1} \frac{\sin \pi N \varepsilon_2}{\sin \pi \varepsilon_2} \frac{\sin \pi P \varepsilon_3}{\sin \pi \varepsilon_3} d\varepsilon_1 d\varepsilon_2 d\varepsilon_3 \\ &= \frac{1}{V}. \end{aligned}$$

It follows that the Fourier transform of a periodic structure is

$$\begin{aligned} \lim_{M,N,P \rightarrow \infty} G(\mathbf{S}) &= \frac{1}{V} \sum_{h,k,l} F(\mathbf{S}) \delta(\mathbf{a} \cdot \mathbf{S} - h) \delta(\mathbf{b} \cdot \mathbf{S} - k) \delta(\mathbf{c} \cdot \mathbf{S} - l), \\ G_{\text{crystal}}(\mathbf{S}) &= \frac{1}{V} \sum_{h,k,l} F(\mathbf{S}) \delta_3(\mathbf{S} - \mathbf{r}^*). \end{aligned} \quad (3.40)$$

We will now show that the function J_N^2 also tends towards a sum of δ distributions. The integral over a principal maximum is obtained from equation (3.35):

$$\begin{aligned} \int_{-1/2}^{+1/2} J_N^2(x) dx &= \int_{-1/2}^{+1/2} \frac{\sin^2 \pi N x}{\sin^2 \pi x} dx = \int_{-1/2}^{+1/2} \sum_{m=0}^{N-1} \sum_{n=0}^{N-1} e^{2\pi i(m-n)x} dx \\ &= \int_{-1/2}^{+1/2} \sum_{-(N-1)}^{+(N-1)} (N - |n|) \cos 2\pi n x dx = 1 \end{aligned}$$

Or alternatively, for $N \gg 1$, by the approximation

$$\int_{\max} \frac{\sin^2 \pi N x}{\sin^2 \pi x} dx = \frac{2}{\pi^2} \int_0^\infty \frac{\sin^2 \pi N x}{x^2} dx = N.$$

This result can be accounted for by the fact that the principal maxima of J_N^2 have a value of N^2 and a width of $1/N$. Hence, for N large, J_N^2 converges towards

$$J_N^2(x) \rightarrow N \sum_{n=-\infty}^{+\infty} \delta(x - n), \quad n \text{ being integer.}$$

The integral over a principal maximum of the three-dimensional function $J_M^2(\mathbf{a} \cdot \mathbf{S}) J_N^2(\mathbf{b} \cdot \mathbf{S}) J_P^2(\mathbf{c} \cdot \mathbf{S})$ is

$$\int_{\max} J_M^2 J_N^2 J_P^2 d^3 \mathbf{S} = \frac{1}{V} \int_{\max} J_M^2(\varepsilon_1) J_N^2(\varepsilon_2) J_P^2(\varepsilon_3) d\varepsilon_1 d\varepsilon_2 d\varepsilon_3 = \frac{MNP}{V} = \frac{\Delta}{V^2},$$

$\Delta = MNPV$ being the volume of the crystal. Hence, for the intensity of the beam diffracted by a crystal, we obtain

$$I_{\text{crystal}} \approx |G_{\text{crystal}}(\mathbf{S})|^2 = \frac{\Delta}{V^2} \sum_{h,k,l} |F(\mathbf{S})|^2 \delta_3(\mathbf{S} - \mathbf{r}^*). \quad (3.41)$$

3.4.2 BRAGG'S LAW

The fundamental equation (3.39), $\mathbf{S} = \mathbf{s} - \mathbf{s}_0 = \mathbf{r}^*$, which describes the elastic diffraction by crystals, may be represented by two geometrical constructions. *Bragg's law* is a construction in physical space; the *Ewald construction* is carried out in reciprocal space. These two representations are equivalent and facilitate the visualization of the diverse methods of diffraction.

Let us recall the properties of the reciprocal lattice that are summarized in Table 1.2 of Section 1.4.3. The lattice line of the reciprocal lattice, $\mathbf{r}^* = h\mathbf{a}^* + k\mathbf{b}^* + l\mathbf{c}^*$, with $(h, k, l) = n(H, K, L)$ and H, K, L being coprime integers, is perpendicular to the planes (HKL) of the crystal lattice. The norm of \mathbf{r}^* is $\|\mathbf{r}^*\| = n/d_{HKL}$, where d is the distance between the lattice planes.

Let $d_{hkl} = d_{HKL}/n$ where n is the largest common factor of h, k, l . Figure 3.12 shows that the vector $\mathbf{S} = \mathbf{r}_{hkl}^* = \mathbf{r}_{nH, nK, nL}^*$ is the bisector of the angle between $-\mathbf{s}_0$

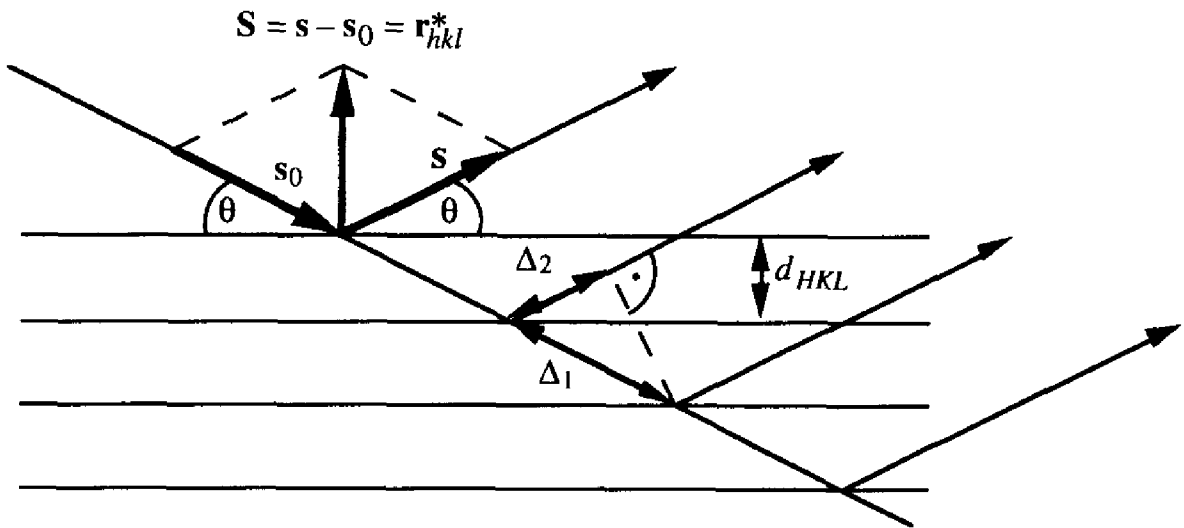


Fig. 3.17. Bragg's law, reflection by lattice planes

and s , and that its norm is $\|S\| = 2 \sin \theta / \lambda$. Hence $2 \sin \theta / \lambda = n / d_{HKL} = 1 / d_{hkl}$ which leads to **Bragg's law**:

Diffraction of order $h, k, l = n(H, K, L)$ may be interpreted as a reflection of the incident radiation from the lattice planes (HKL) .

$$\begin{aligned} 2d_{HKL} \sin \theta &= n\lambda & (H, K, L \text{ being coprime integers}) \\ 2d_{hkl} \sin \theta &= \lambda & (h, k, l = nH, nK, nL) \end{aligned} \quad (3.42)$$

Figure 3.17 shows the conventional interpretation of Bragg's law. The beams reflected by consecutive lattice planes belonging to the series (HKL) , forming an angle θ with them, will reinforce if they are in phase, i.e. if $\Delta_1 - \Delta_2 = n\lambda$, n being integer. By trigonometry we obtain

$$\begin{aligned} \Delta_1 &= d_{HKL} / \sin \theta; & \Delta_2 &= \Delta_1 \cos 2\theta \\ \Delta_1 - \Delta_2 &= 2d_{HKL} \sin \theta = n\lambda \\ 2(d_{HKL}/n) \sin \theta &= 2d_{hkl} \sin \theta = \lambda \end{aligned}$$

As above, the letters H, K, L are coprime integers, and $(h, k, l) = n(H, K, L)$. Hence, the n th-order reflection from the series (HKL) can be interpreted as the first-order reflection from the planes $(nH \ nK \ nL)$, d_{HKL}/n apart. Physically, the series $(nH \ nK \ nL)$ with $n \neq 1$ does not exist as some of its planes do not contain lattice points. Indeed, $(nH \ nK \ nL)$ is the series (HKL) with additional empty planes interleaved. In practice, it is more convenient to refer to the reflection (222) than to the second order of the reflection (111) .

It is very important to realize that Bragg's law refers to the planes of the translation lattice and not to planes formed by the atoms. It follows from the

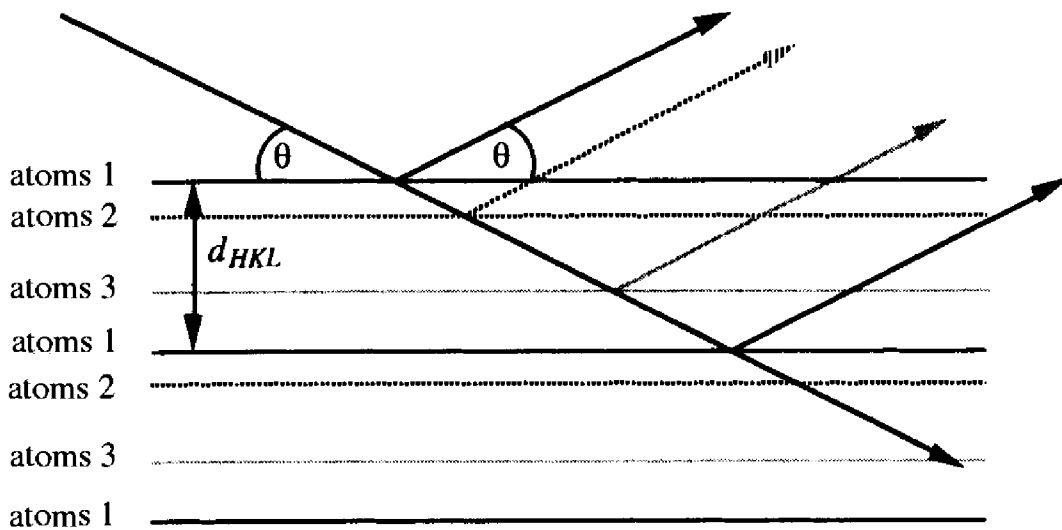


Fig. 3.18. Bragg's law, reflection by planes of atoms

Laue equations and, hence, exclusively from the periodicity of the crystal structure.

Reflection of radiation by planes of atoms furnishes an image which is less abstract than reflection by lattice planes. However, the distribution of the atoms represents both the structural motif as well as the periodicity of the structure. Parallel to the series of lattice planes (HKL), we find planes formed by different atomic species. Figure 3.18 shows the reflection of radiation by such planes. The amplitude is dependent on the atomic species. Beams coming from planes which are equivalent by translation must be in phase, hence Bragg's law. The interference of beams reflected by different types of plane gives rise to the *structure factor* (3.37). The scattering factors $[f_m(S)]_t$ represent the amplitude of the reflected waves, whereas the products $\mathbf{r}_m \cdot \mathbf{S} = \mathbf{r}_m \cdot \mathbf{r}_{hkl}^*$ represent their phases.

3.4.3 EWALD CONSTRUCTION

The *Ewald construction* obtains the direction of a diffracted wave by the intersection of two loci. The first of these loci is the *Ewald sphere*: the relationships $\mathbf{S} = \mathbf{s} - \mathbf{s}_0$, $\|\mathbf{s}\| = \|\mathbf{s}_0\| = 1/\lambda$ (equation (3.21), Fig. 3.12) show that \mathbf{S} is a secant joining two points on the surface of a sphere of radius $1/\lambda$. The second locus is defined by equation (3.39): the vector \mathbf{S} coincides with the vector \mathbf{r}^* of the reciprocal lattice. The construction goes through the following steps (Fig. 3.19):

- sketch the reciprocal lattice;
- draw the vector \mathbf{s}_0 representing the incident beam such that its point coincides with the lattice point (000);
- draw a sphere of radius $1/\lambda$, the Ewald sphere, around the point M which is at the origin of \mathbf{s}_0 and which passes through the point (000);

- any reciprocal lattice point which lies on the surface of the sphere satisfies the Laue equations. The vector \mathbf{s} , representing the reflected beam, joins M and the lattice point lying on the sphere. It is evident that the Laue equations are always satisfied for $h = k = l = 0$, $\mathbf{S} = \mathbf{0}$.

According to Bragg's law, a series of lattice planes (HKL) can only reflect a beam of monochromatic (i.e. single wavelength λ) X-rays for certain angles; $\theta_n = \arcsin(n\lambda/2d_{HKL})$; the reflection is selective. It follows from this that the crystal must be carefully oriented with respect to the primary beam to obtain any desired reflection. This may also be deduced from the Ewald construction. We see that, in general, the lattice point (hkl) is not situated on the Ewald sphere. In order to satisfy this condition, the crystal must either be turned to the desired position or else the wavelength must be changed (and hence the radius of the sphere).

A crystal placed in a random orientation in a beam of monochromatic X-rays will not necessarily produce a diffracted beam.

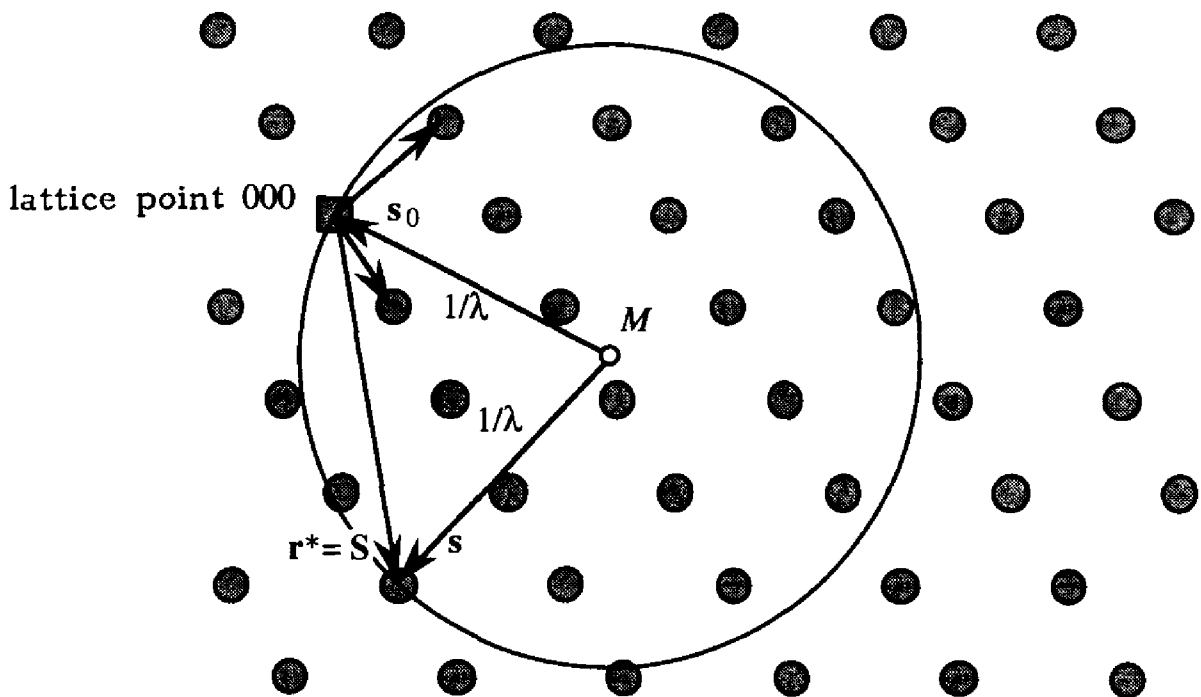


Fig. 3.19. The Ewald construction. The circle represents the intersection of the Ewald sphere and a plane of the *reciprocal lattice* passing through the origin and containing the lattice points (hkl) with $hU + kV + lW = 0$ (U, V, W being coprime integers). The primitive translation of the direct lattice $[UVW]$ is normal to this plane (Section 1.4.3). The reader can imagine other planes of this series which obey the relation $hU + kV + lW = n$, $n \neq 0$, above and below the plane of the figure

3.4.4 ONE- AND TWO-DIMENSIONAL STRUCTURES

In the following we will discuss the Laue equations in a somewhat different manner. This will allow us to compare the diffraction by three-dimensional crystals with that by one- and two-dimensional lattices.

According to the Laue equation $\mathbf{a} \cdot \mathbf{S} = h$, the projection of \mathbf{S} onto \mathbf{a} is equal to h/a . The locus of all the vectors \mathbf{S} which satisfy this equation is a series of planes perpendicular to \mathbf{a} and separated by $1/a$. These planes make up the reciprocal space of a one-dimensional crystal. Their intersections with the *Ewald sphere* of radius $1/\lambda$ (Fig. 3.20) define the directions \mathbf{s} of the diffracted beams. This results in a series of coaxial cones around the \mathbf{a} axis. The angle between the incident wave \mathbf{s}_0 and \mathbf{a} is α_0 . The half-opening angles α of the cones are obtained from the Laue equation,

$$\begin{aligned} \mathbf{a} \cdot \mathbf{s} &= h + \mathbf{a} \cdot \mathbf{s}_0 \\ \cos \alpha &= h\lambda/a + \cos \alpha_0 \end{aligned} \quad (3.43)$$

The diffraction by a two-dimensional crystal is determined by two Laue equations which must be simultaneously satisfied. The locus of all the vectors \mathbf{S} is

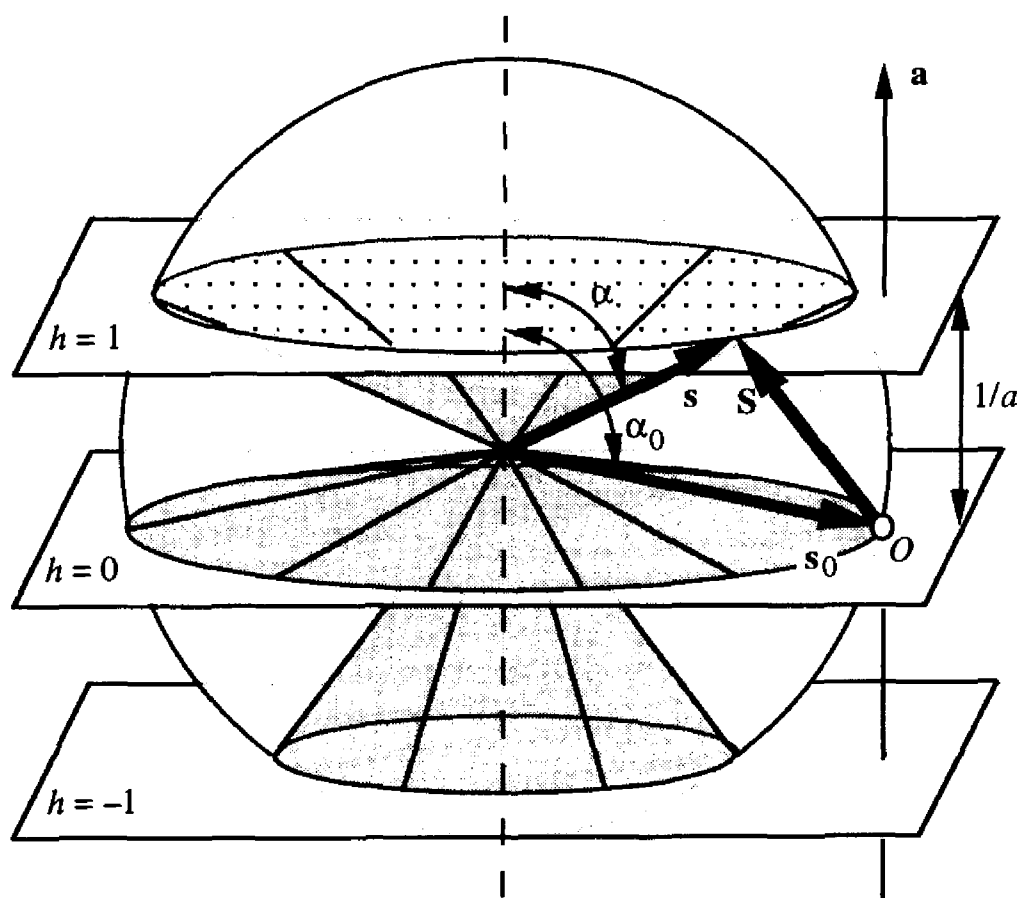


Fig. 3.20. Diffraction by a one-dimensional crystal satisfying a single Laue equation. When recorded on a flat screen parallel to \mathbf{a} , the diffracted beams form a series of hyperbolic lines

given by the lines of intersection of two series of planes, one perpendicular to \mathbf{a} with an interval of $1/a$ and the other perpendicular to \mathbf{b} with an interval of $1/b$ (Fig. 3.21). The directions \mathbf{s} of the diffracted beams are the intersections of two series of coaxial cones around \mathbf{a} and around \mathbf{b} . The cosines of the half-opening angles of these cones are $\cos \alpha = h\lambda/a + \cos \alpha_0$ and $\cos \beta = k\lambda/b + \cos \beta_0$. If we place a planar screen parallel to \mathbf{a} and \mathbf{b} , we observe a lattice of points formed by the intersections of two series of hyperbolic lines (Fig. 3.22).

The locus of all the vectors \mathbf{S} which simultaneously satisfy three Laue equations (the case of a three-dimensional crystal) is a set of points formed by the intersection of three series of planes perpendicular to \mathbf{a} , \mathbf{b} and \mathbf{c} with the intervals $1/a$, $1/b$ and $1/c$ respectively. It is easy to see that this set of points is the *reciprocal lattice* in agreement with equation (3.39). The directions of the vectors \mathbf{s} are the intersections of three series of cones. However, three cones do not in general intersect in a single straight line. It thus follows that the three Laue equations are not generally satisfied at the same time, except for $h = k = l = 0$ corresponding to $\mathbf{s} = \mathbf{s}_0$. Indeed, the direction of a diffracted beam is defined by *two* angles, e.g. by the angles α between \mathbf{a} and \mathbf{s} , and β between \mathbf{b} and \mathbf{s} . In order to determine these angles for a given triplet of integers h, k, l , we have available three Laue equations which have, in general, no solution. A *randomly oriented three-dimensional crystal only diffracts monochromatic X-rays fortuitously*.

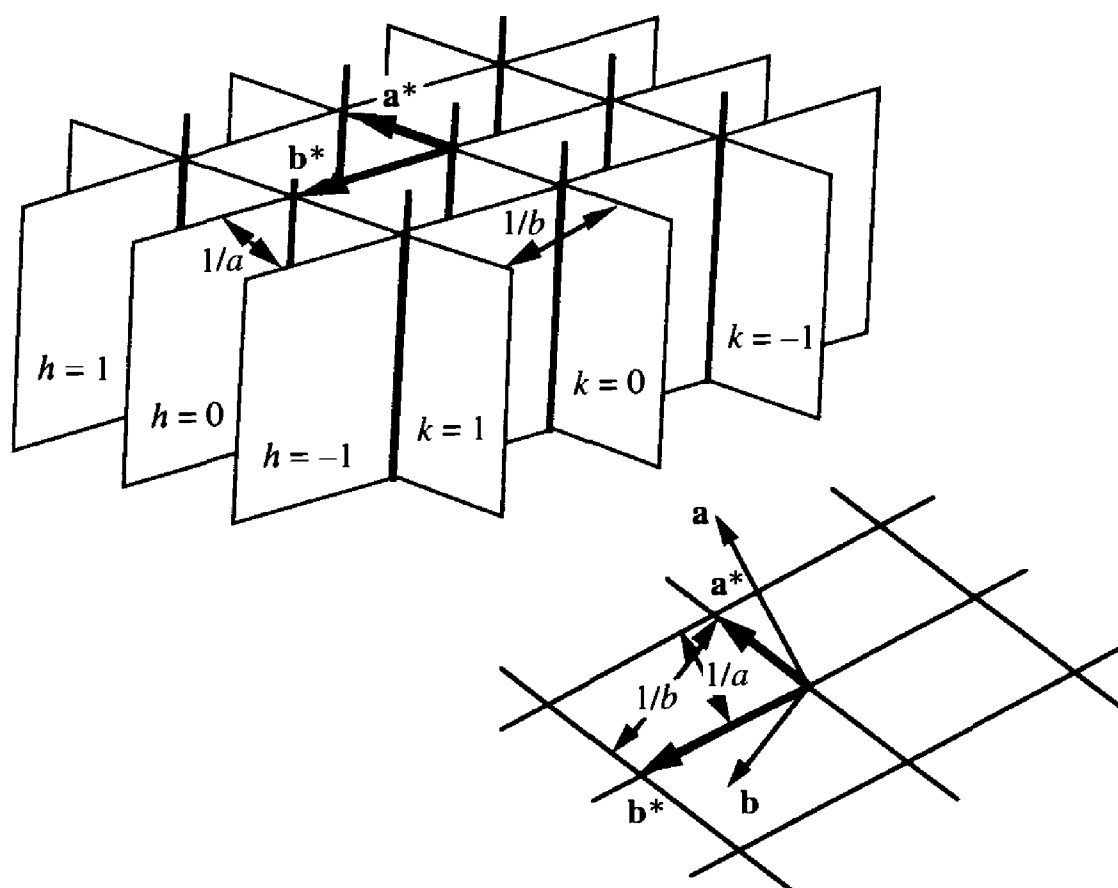


Fig. 3.21. Locus of the vector \mathbf{S} satisfying two Laue equations

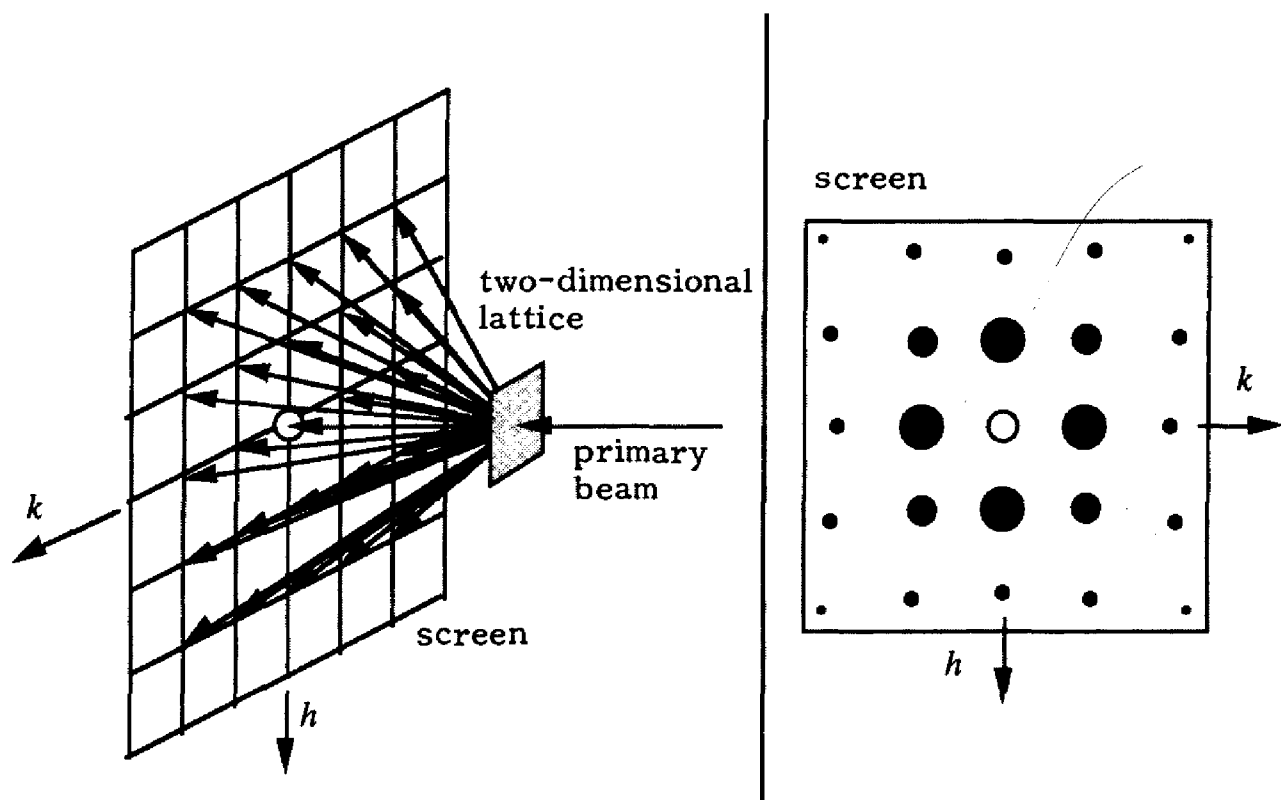


Fig. 3.22. Diffraction by a two-dimensional crystal

3.5 EXPERIMENTAL DIFFRACTION METHODS

In the following we will discuss three methods for satisfying Bragg's law in a systematic manner. For other methods, we refer the reader to the specialized literature.

3.5.1 LAUE METHOD

The name of the Laue method derives from the first X-ray diffraction experiment based on the ideas of M. von Laue and carried out with a crystal of chemical composition $\text{CuSO}_4 \cdot 5\text{H}_2\text{O}$ by W. Friedrich and P. Knipping (Munich, 1912). We use a polychromatic beam possessing a continuous wavelength spectrum, e.g. the radiation emitted by an X-ray tube (Section 3.6). The direction of the incident beam with respect to the crystal remains fixed during the experiment. The angle of incidence θ of the beam at a lattice plane (HKL) depends on the orientation of the crystal. The plane selects the wavelengths that satisfy Bragg's law (3.42), $2d_{HKL} \sin \theta = n\lambda$ (H, K, L being coprime integers). If the first order $n = 1$ diffracts a wave of wavelength λ , the reflected beam may equally contain $\lambda/2, \lambda/3, \dots$ corresponding to the orders $n = 2, 3, \dots$. The intensities of the diffracted beams depend on the structure factors (Section 3.7) of the planes $(hkl) = (nH \ nK \ nL)$ as well as the spectral composition of the incident radiation (Section 3.6).

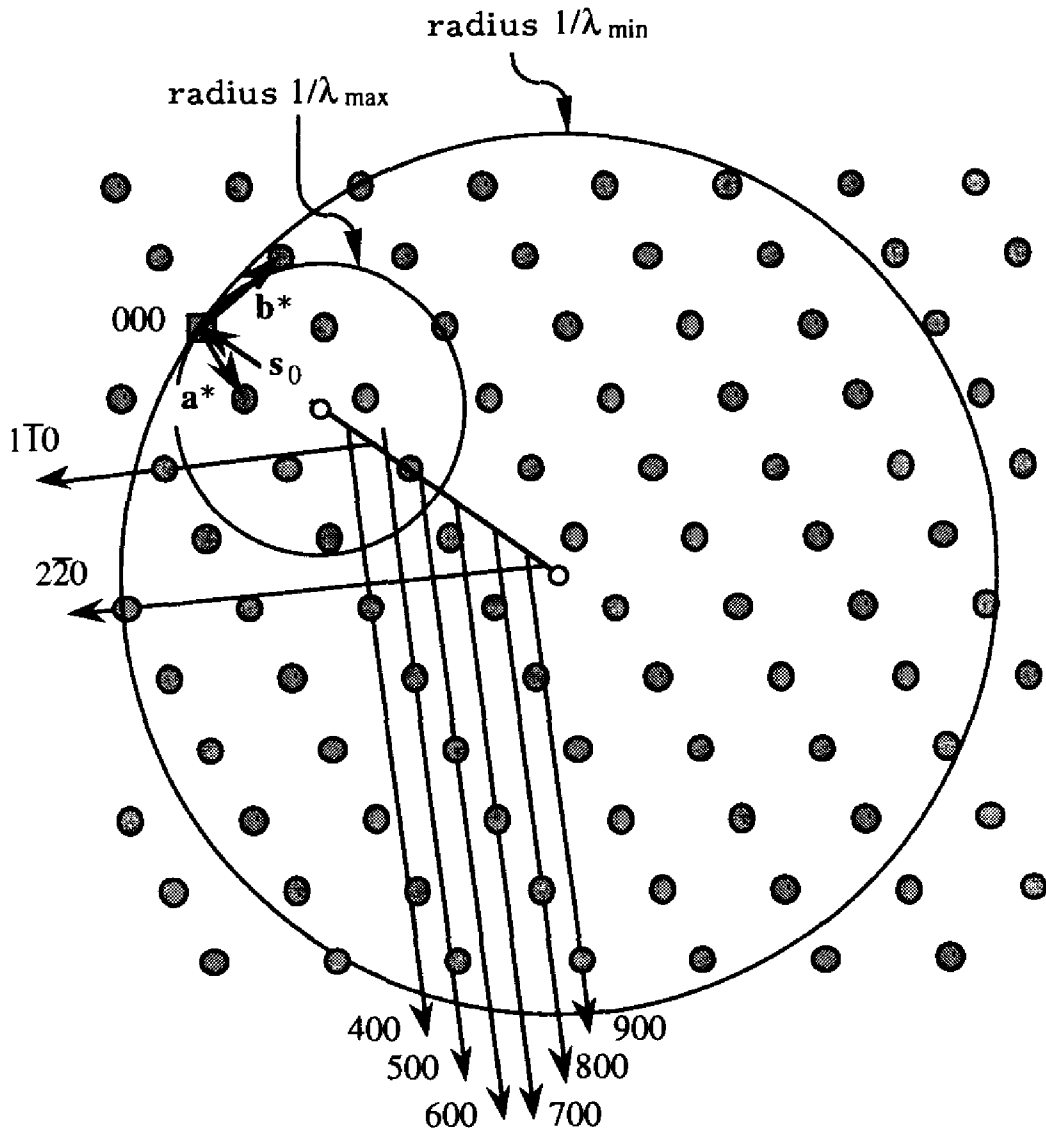


Fig. 3.23. Representation of the Laue method with the aid of the Ewald construction. For each wavelength between λ_{\min} and λ_{\max} , there is an Ewald sphere

Figure 3.23 illustrates the Laue method with the aid of the Ewald construction. All the reciprocal lattice points situated between the spheres of radius $1/\lambda_{\max}$ and $1/\lambda_{\min}$ are in a reflecting position for any intermediate wavelength between λ_{\max} and λ_{\min} . The reflection (100) of Fig. 3.23 contains the orders $n = 4, 5, 6, 7, 8, 9$; the reflection (1 $\bar{1}$ 0) contains only two wavelengths. By turning the crystal by a small amount, the lattice point $2\bar{2}0$ leaves the sphere and (1 $\bar{1}$ 0) becomes monochromatic.

By making a small modification to the Ewald construction, we obtain a more informative representation of the Laue method. By multiplying all the dimensions of the construction by the wavelength λ , we obtain a lattice $\lambda(ha^* + kb^* + lc^*)$ and a sphere of radius 1. Thus, for polychromatic radiation, we obtain a superposition of lattices of variable dimensions intersected by a single

sphere of radius 1. The lattice point (000) is common to all the lattices. In fact, each lattice row passing through the origin becomes a continuous line. We obtain a reflection each time that one of these lines cuts the sphere (Fig. 3.24). This construction clearly shows that the reflections due to points of a lattice line passing through the origin are necessarily superimposed.

The reflections derived from a reciprocal lattice plane passing through the origin (000) form a cone whose axis is normal to the plane (Fig. 3.25). This normal is a translation $[UVW]$ of the crystal lattice (U, V, W being coprime integers). The indices of the lattice points (hkl) of the plane satisfy the equation $hU + kV + lW = 0$. Hence the lattice planes (hkl) belong to the zone $[UVW]$ (Section 1.3.3). The surface of the cone contains the primary beam.

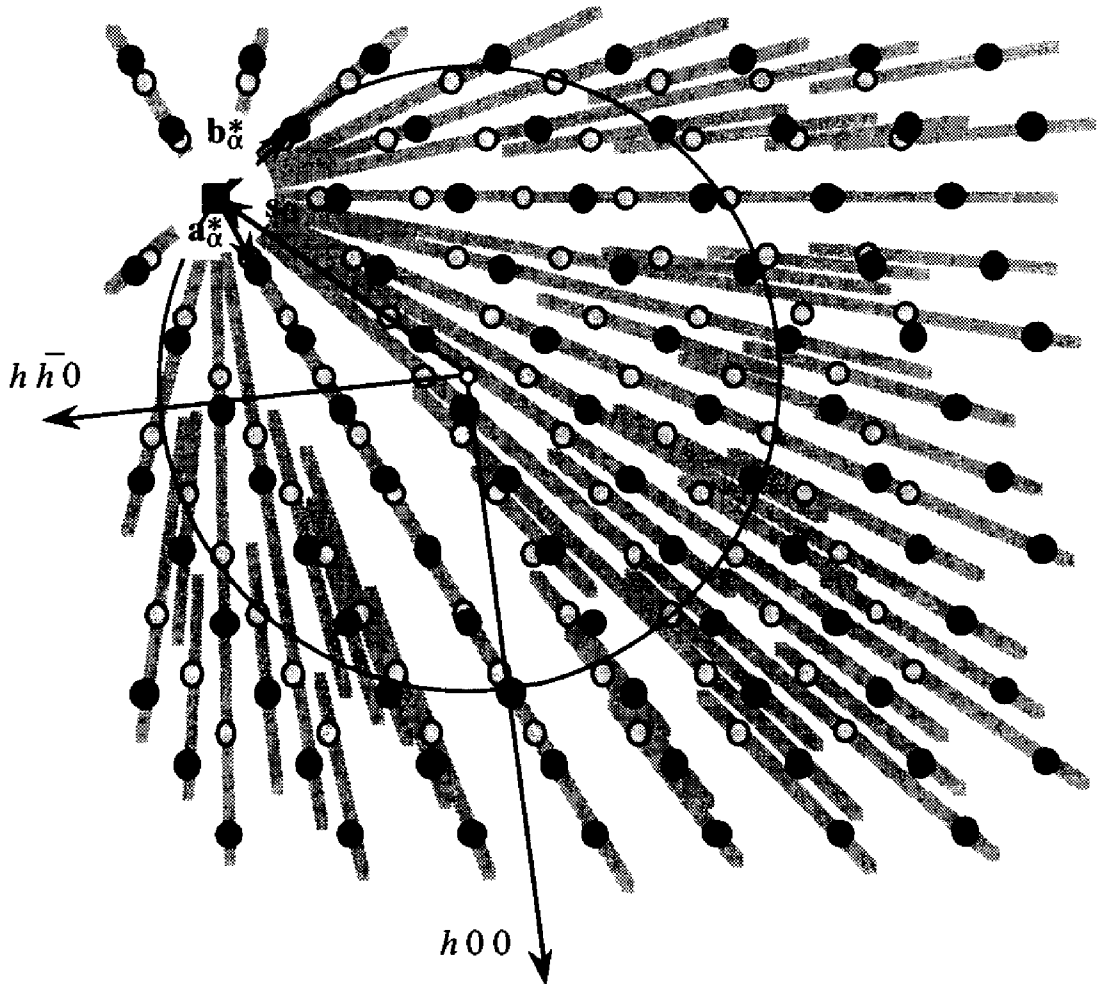


Fig. 3.24. Laue method represented by the intersection of a sphere of radius 1 with a set of lattices $\lambda(ha^* + kb^* + lc^*)$. The orientation and the dimensions of the reciprocal lattice are identical to those of Fig. 3.23. The small circles represent the beams due to $K\alpha$ and $K\beta$ (Section 3.6). If the X-rays are produced using a tungsten (W) tube, we observe essentially only the continuous spectrum represented by the diffuse lines because the $K\alpha$ and $K\beta$ lines are not excited due to their high energies

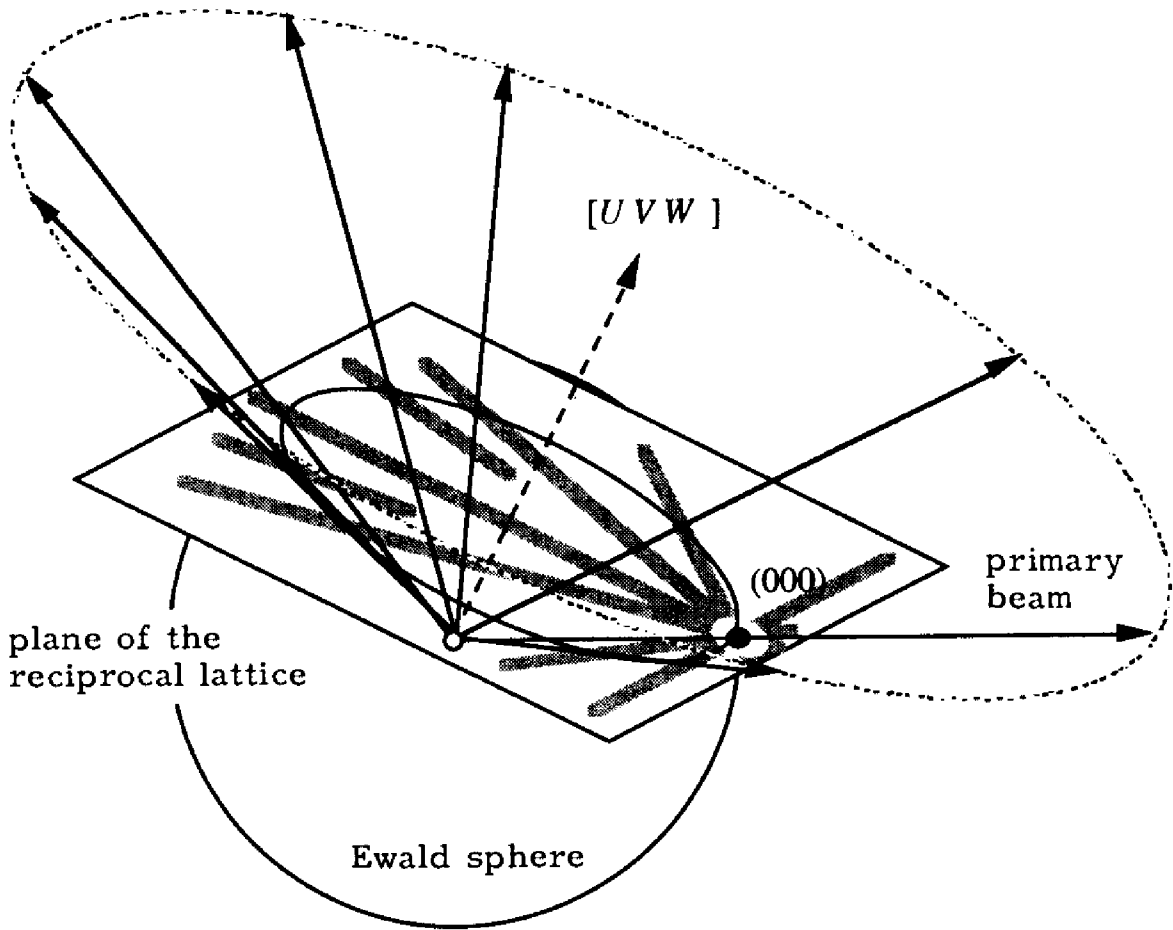


Fig. 3.25. The reflections from a reciprocal lattice plane passing through the origin form a cone whose axis is the translation $[UVW]$ perpendicular to the plane. Remember that the corresponding nets of the direct lattice are all parallel to $[UVW]$

Figure 3.26 shows the origin of the cone by a construction in direct space. The incident and reflected beams make equal angles μ with a straight line contained in the reflecting plane. From this we can deduce that the reflections of a beam of light, produced by a mirror that rotates about an in-plane axis, form a cone.

The Laue method is mainly used for the orientation and alignment of crystals with respect to a chosen direction. In a frequently used experimental arrangement, a flat photographic film is placed perpendicular to the primary beam (Fig. 3.27). The intersection of a plane with a cone is a conic section. Hence, the reflections belonging to a zone are found on ellipses, hyperbolas or parabolas on the film. If the crystal is placed between the X-ray source and the film, the X-rays pass through the crystal and a transmission Laue pattern is obtained. The hyperbolas or ellipses of the zones pass through the image of the primary beam. If the film is placed between the source of X-rays and the crystal, we obtain a pattern by back reflection. All the zones give rise to hyperbolas. This last method is used

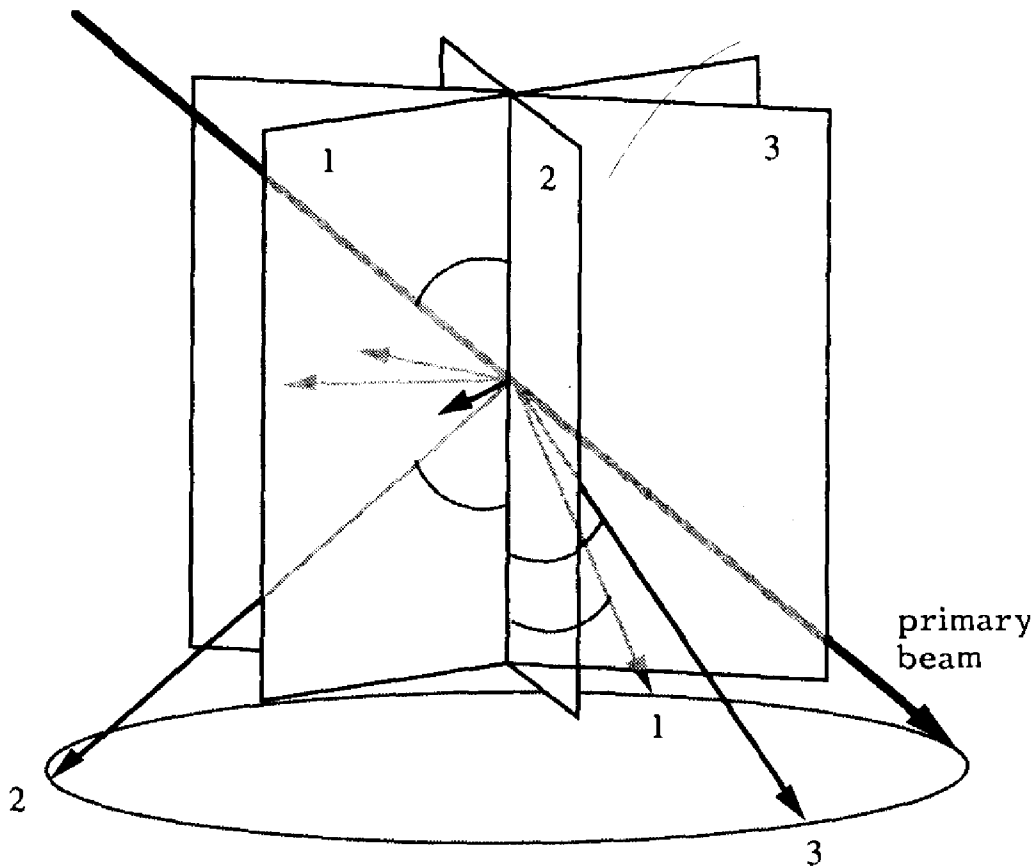


Fig. 3.26. Representation of the cone from Fig. 3.25 in direct space. The beams reflected by the three planes are located on a cone whose axis is the intersection of the planes. The angles formed by the primary and reflected beams with the axis are all equal. In contrast, the angles $90^\circ - \theta$ between the beams and the normals of the faces are not equal

for aligning large crystals. From the Laue patterns, the spatial orientation of the translations $[UVW]$ of the zones as well as the indices of the reflections can be obtained.

The Laue method also allows the determination of the symmetry of the crystal, excepting only the presence or absence of a center of symmetry. According to Friedel's law, the intensities of the reflections (hkl) and $(\bar{h}\bar{k}\bar{l})$ are equal (Section 3.7.3). The symmetry of the diffractogram allows us to distinguish between the 11 *Laue classes* corresponding to the 11 crystallographic point groups which possess a center of symmetry (Section 2.5.7): $(1, \bar{1})$, $(2, m, 2/m)$, $(mm2, 222, mmm)$, $(4, \bar{4}, 4/m)$, $(4mm, 422, \bar{4}2m, 4/mmm)$, $(3, \bar{3})$, $(3m, 32, \bar{3}m)$, $(6, \bar{6}, 6/m)$, $(6mm, 622, \bar{6}m2, 6/mmm)$, $(23, m\bar{3})$, $(\bar{4}3m, 432, m3m)$.

An important new application of the Laue method has been developed since synchrotrons dedicated to the production of high-intensity X-rays have become available (Section 3.6.3). It is used to rapidly obtain diffractograms of macromolecular structures.

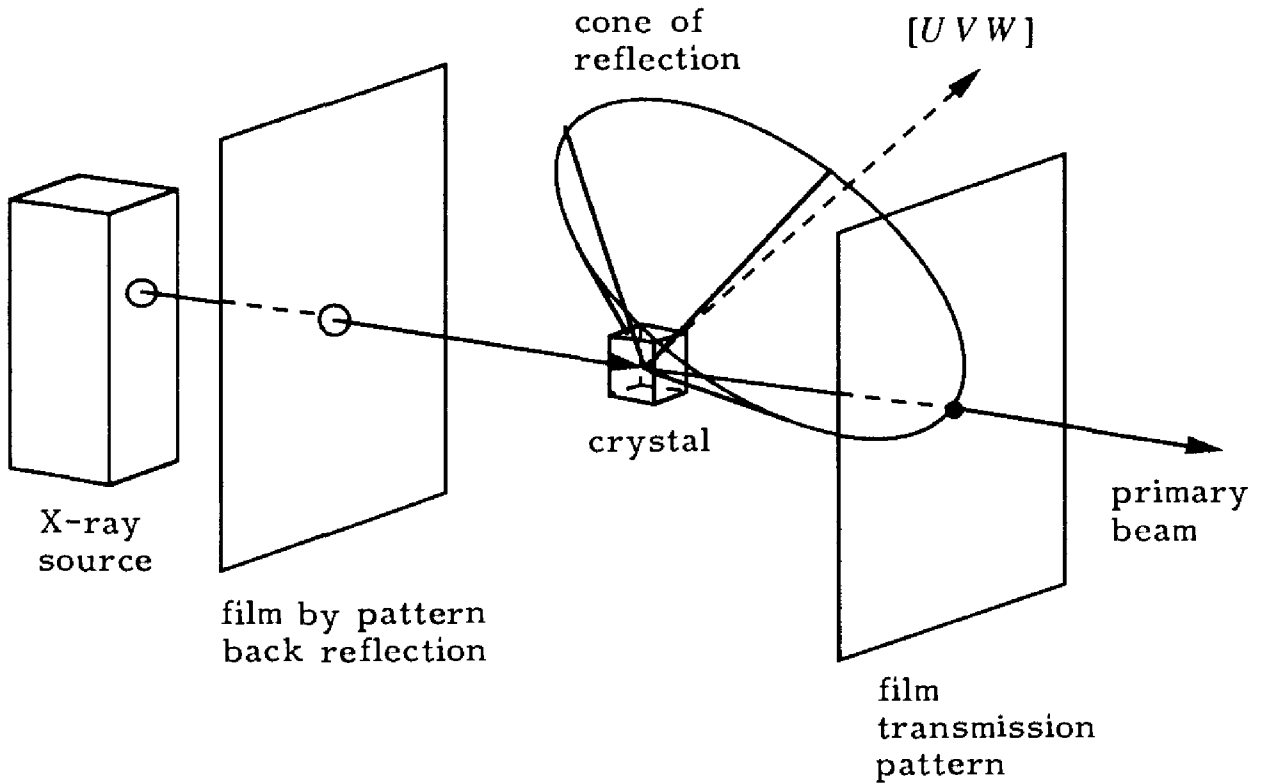


Fig. 3.27. Experimental arrangement with a flat film: transmission and back reflection

3.5.2 ROTATING CRYSTAL METHOD

If we employ a monochromatic beam of X-rays, Bragg's law is obeyed only for certain orientations of the crystal. There exist a number of methods designed to photograph reciprocal space by movements, more or less complicated, of the crystal. In general, the simpler the method, the more complicated is the interpretation of the diffractogram.

In the rotating crystal method, a single crystal is used with dimensions of the order of 0.1 to 0.5 mm (smaller than the diameter of the primary beam). The importance of undesired phenomena such as absorption of the beam and extinction (Section 3.3.2) increases with the size of the crystal. The crystal executes a rotation about a lattice line $[UVW]$ of the translation lattice. Hence, the crystal must be precisely aligned. The planes of the reciprocal lattice whose lattice points hkl satisfy the equation

$$hU + kV + lW = n \text{ (} n \text{ being integer; } U, V, W \text{ being coprime integers)}$$

are perpendicular to the axis $[UVW]$. Hence, for $[UVW] = [001]$, the consecutive planes $hk0, hk1, hk2, \dots$ etc.; $hk\bar{1}, hk\bar{2}, \dots$ etc. are separated by $1/c$. During the rotation of the crystal about $[UVW]$, the lattice points move in their respective planes (Fig. 3.28). The directions of the reflected beams, corresponding to one plane of the reciprocal lattice, form a cone (compare also with Fig. 3.20).

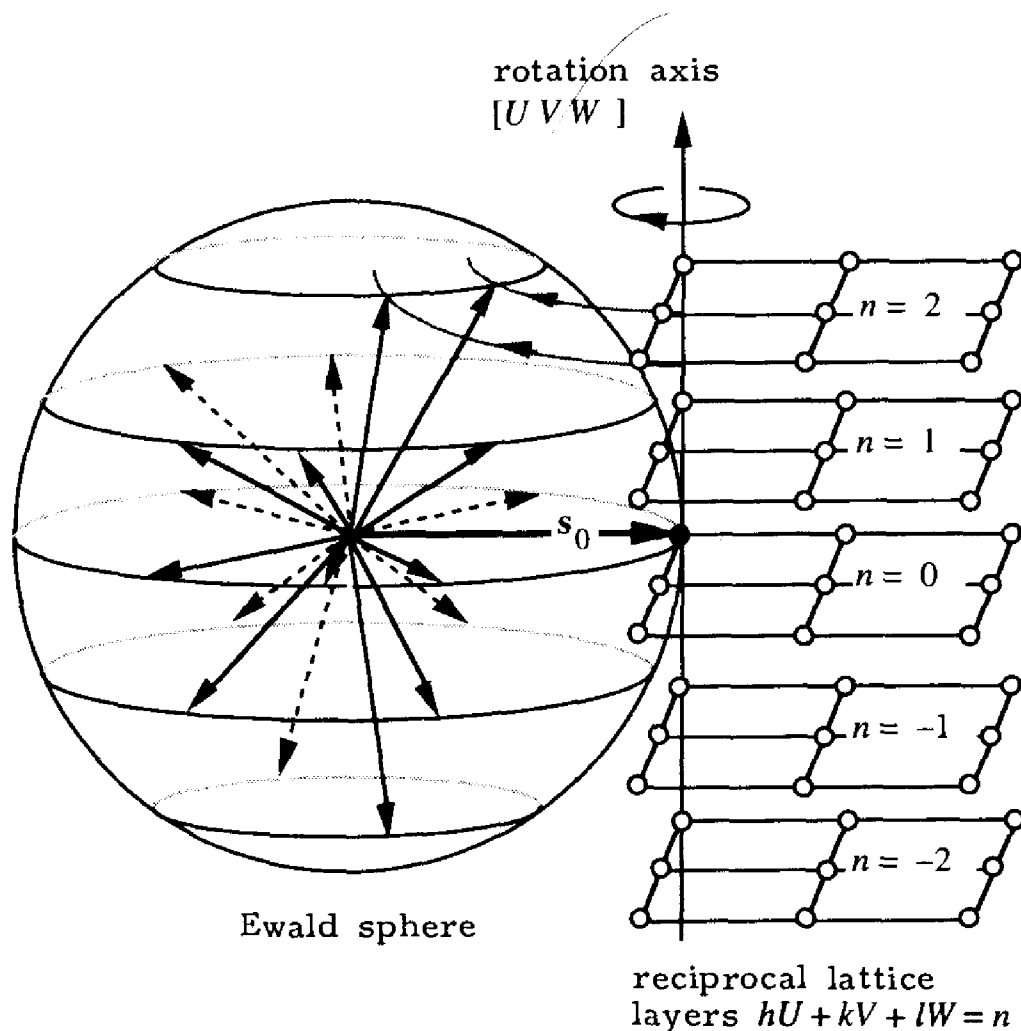


Fig. 3.28. Rotating crystal method, reciprocal space

The primary beam \mathbf{s}_0 is usually chosen to be perpendicular to the rotation axis. Let this be the \mathbf{c} axis, $[001]$. It is easy, with the help of one of the Laue equations (3.38), to calculate the half-opening angles γ_l of the cones, l being the Miller index characterizing the layer (Fig. 3.29):

$$\mathbf{c} \cdot \mathbf{s}_0 = 0, \quad \mathbf{c} \cdot \mathbf{S} = \mathbf{c} \cdot (\mathbf{s} - \mathbf{s}_0) = c \frac{1}{\lambda} \cos \gamma_l = l,$$

$$\cos \gamma_l = \lambda \frac{l}{c} \quad (3.44)$$

We observe the reflections by means of a cylindrical photographic film coaxial with the axis of rotation.

The distance H_1 between the layer line $l = 0$ and the layer line $l = 1$ produced by the intersection of the cones with the cylinder of radius R is

$$H_1 = R \tan(90 - \gamma_1) = R \cot \gamma_1 \quad (3.45)$$

Equations (3.44) and (3.45) allow us to calculate the period c . The other lattice

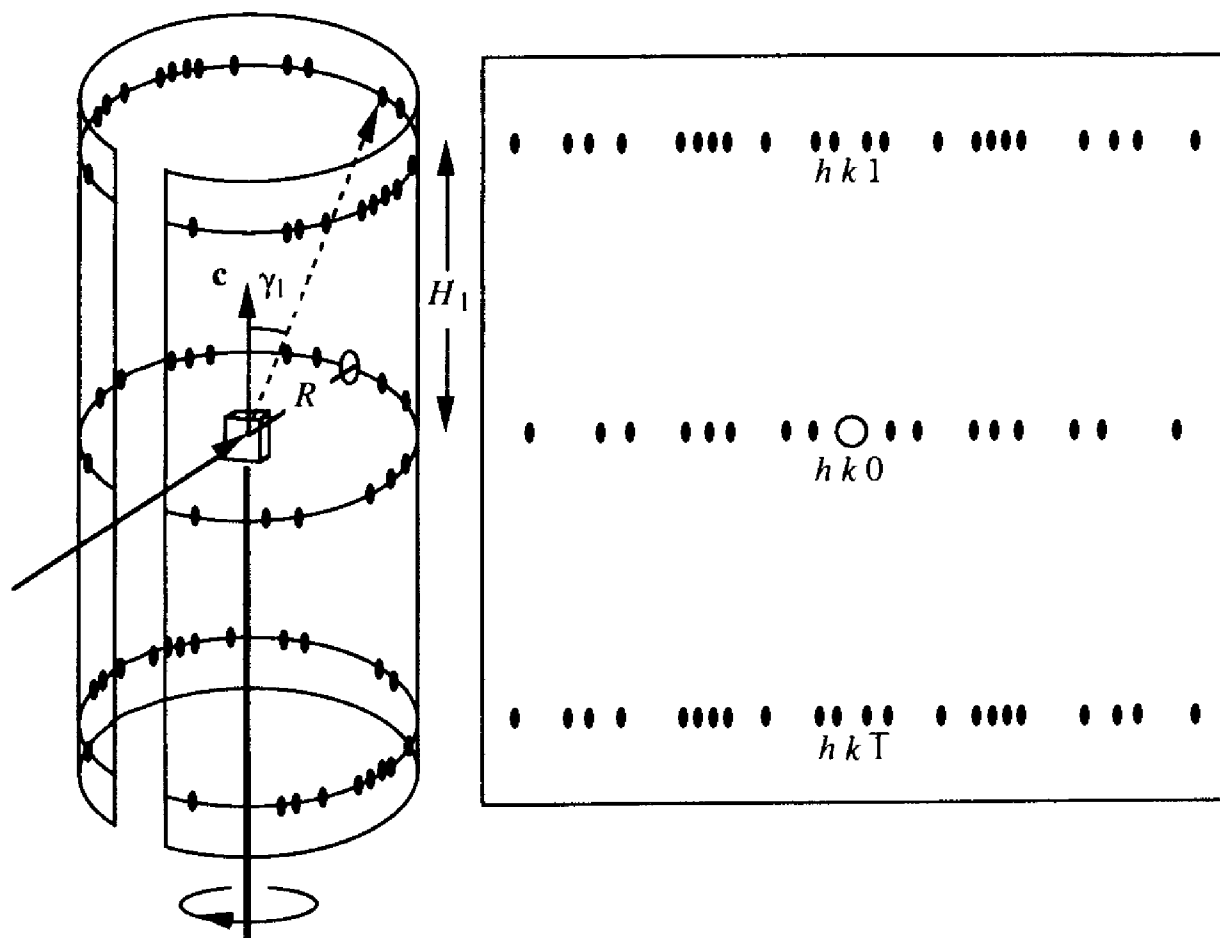


Fig. 3.29. Rotating crystal method, experimental setup

constants, a and b , as well as the indices h and k of the spots forming the layer lines are obtained by a method analogous to that used for the interpretation of powder patterns (Section 3.5.3).

3.5.3 POWDER METHOD

This method (Fig. 3.30) was invented by P. Debye and P. Scherrer, and independently by A. W. Hull. Its importance is derived from its simplicity and from the moderate cost of the equipment, as well as from the difficulties often encountered in the preparation of single crystals.

The radiation used is monochromatic. The sample is composed of a large number of microcrystals of sizes of the order of 0.01 to 0.001 mm. For each lattice plane hkl , the sample contains some microcrystals in a reflecting position. The angle between the reciprocal vector \mathbf{r}_{hkl}^* and \mathbf{s}_0 is $90^\circ - \theta$ (Fig. 3.17). The normals of the hkl planes of all the crystals that are simultaneously in a reflecting position form a cone around \mathbf{s}_0 . The diffracted beams also form a cone of half-opening angle 2θ because the angle between \mathbf{s}_0 and \mathbf{s} is 2θ . Hence, the powder sample emits radiation in the form of coaxial cones. The same result can be obtained from the

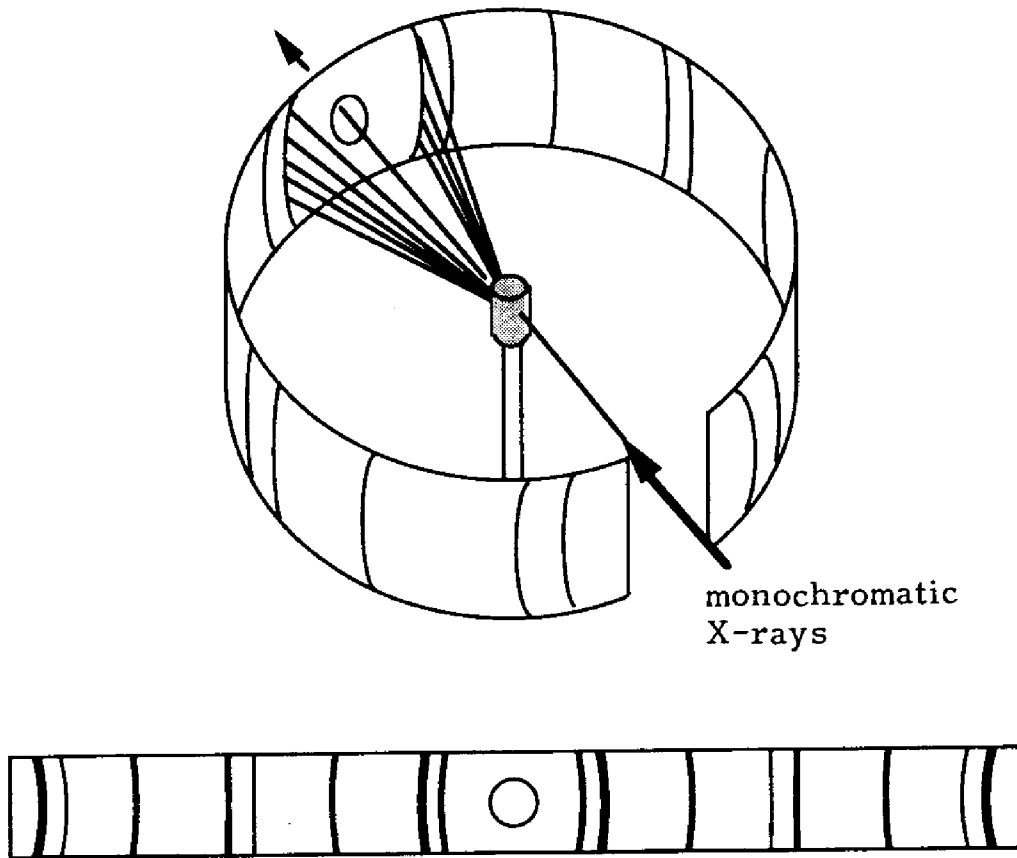


Fig. 3.30. Powder pattern

Ewald construction. The total of the reciprocal lattices of all the single crystals form concentric spheres around the lattice point (000) whose intersections with the Ewald sphere make up the above mentioned cones.

A Debye–Scherrer camera consists of a metal cylinder provided with a photographic film. The primary beam is perpendicular to its axis. The distance between two symmetrical lines, produced by the intersection of a cone with the cylinder, is $4\theta R$, θ being the Bragg angle (in radians) and R the radius of the camera. The interval d_{hkl} is derived from Bragg's law. The powder method gives us only the *norms* of the reciprocal vectors. The set of norms corresponds to the projection of the reciprocal lattice onto a straight line.

The search for a base \mathbf{a} , \mathbf{b} , \mathbf{c} and the indices hkl for each line corresponds to the reconstruction of a three-dimensional lattice from its one-dimensional projection. According to Bragg's law, for each line we obtain an equation of the type

$$\|\mathbf{r}^*\|^2 = \left(\frac{2 \sin \theta}{\lambda}\right)^2 = h^2 a^{*2} + k^2 b^{*2} + l^2 c^{*2} + 2hka^* \cdot \mathbf{b}^* + 2hla^* \cdot \mathbf{c}^* + 2klb^* \cdot \mathbf{c}^*. \quad (3.46)$$

The components of the reciprocal metric tensor are the same in each equation whereas the indices hkl are integers characteristic of individual lines. Theoreti-

cally this system of *diophantine equations* (equations in whole numbers) has a solution. Finding the solution in practice poses some problems due to the limited precision of the experimental values of the θ angles. Several computer programs are now available to find a solution to equation (3.46), even for substances with low symmetry.

Every crystal system corresponds to one type of metric (Section 2.5.8) and consequently to one particular form of equation (3.46). Thus, the solution of the diophantine equations allows us to determine the lattice metric. However, this is not quite enough to establish the crystal system as the symmetry elements are not observed.

For a cubic crystal, equation (3.46) reduces to

$$\sin^2 \theta = \frac{\lambda^2}{4a^2} (h^2 + k^2 + l^2) \quad (3.47)$$

The number $s = h^2 + k^2 + l^2$ is integer and can take all positive values except $s = (7 + 8n)4^m$. The planes which are equivalent by the symmetry $m\bar{3}m$ reflect at the same θ angle. The 48 symmetry operations of this group are represented by all sign combinations and all permutations of the indices hkl . For example, the line with $s = 1$ contains the six reflections $100, 010, 001, \bar{1}00, 0\bar{1}0, 00\bar{1}$; the line with $s = 2$ contains twelve reflections, $110, 101, 011, \bar{1}10, 10\bar{1}, 0\bar{1}1, \bar{1}\bar{1}0, \bar{1}0\bar{1}, 0\bar{1}\bar{1}, \bar{1}\bar{1}0, \bar{1}0\bar{1}, 0\bar{1}\bar{1}$. The number of reflections which superimpose in the same line is called the *multiplicity*.

The solution to the diophantine equations for the cubic system (3.47) is easily found with the aid of a pocket calculator. The equations for tetragonal, hexagonal and rhombohedral lattices can also be solved with quite modest means. The lower the symmetry, the more lines there are in the powder pattern. In the triclinic system, for example, the planes $100, 010, 001$ are not equivalent and they produce three different lines.

The powder method is also used for *identifying substances*. The ICDD (International Center for Diffraction Data) data bank contains all the diffractograms published in the scientific literature and provides the computer software and the bibliographic data to compare them with that of an unknown substance.

3.6 PHYSICS OF X-RAYS

3.6.1 PRODUCTION OF X-RAYS

The classical apparatus used to generate X-rays is made up of a high-voltage generator and an X-ray tube (Fig. 3.31). The X-ray tube comprises an electron gun and a metal block placed in a high-vacuum chamber. The gun is a tungsten filament heated by an electric current, which provides electrons by thermal evaporation. A high voltage of 40 to 60 kV applied between the gun (cathode) and

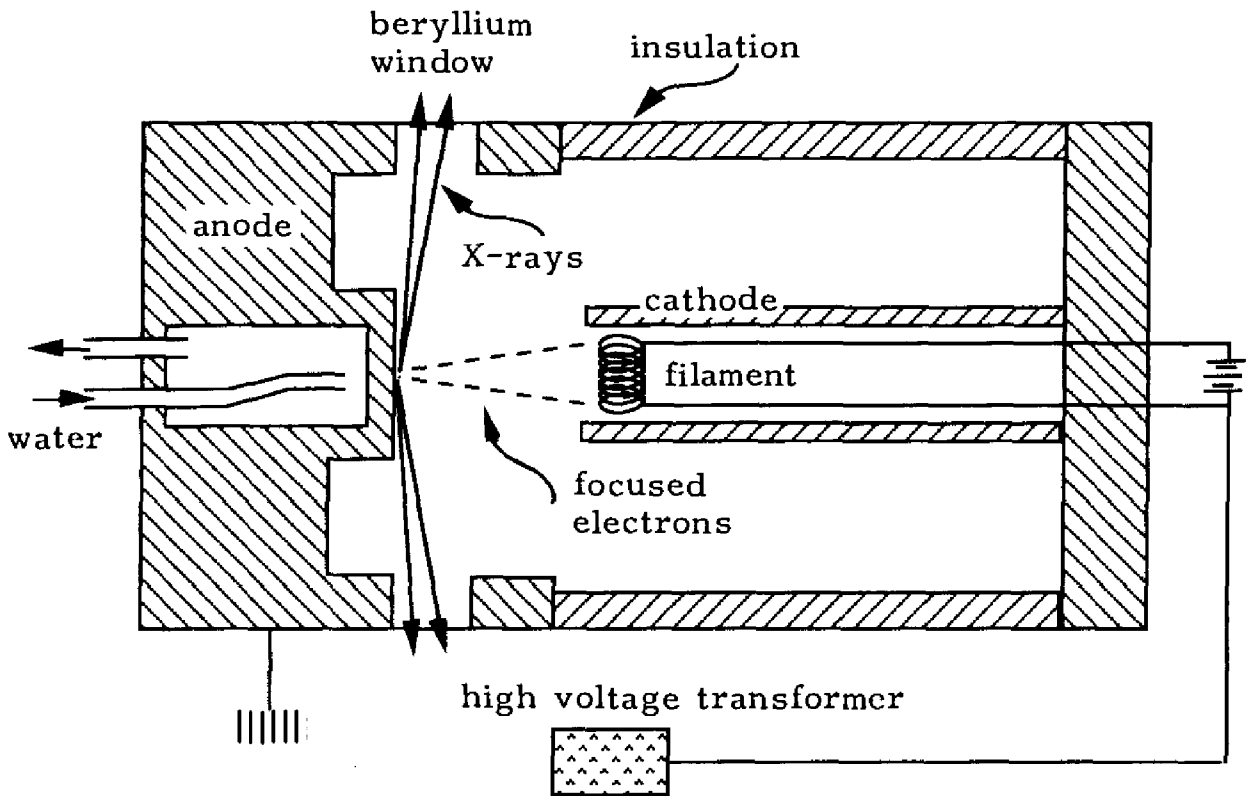


Fig. 3.31. Schematic diagram of an X-ray tube

the metal block (anode) accelerates the electrons. The anode is made from a metal which allows efficient cooling. The X-rays produced by the bombardment of the anode leave the tube through beryllium windows. The emission spectrum is the superposition of a certain number of intense lines characteristic of the anode material, and a continuous background.

The composition of the *continuous spectrum*, or white radiation, is independent of the metal forming the anode. Figure 3.32 shows the intensity I as a function of the wavelength λ for different values of the voltage V . The lower limit of the wavelength λ_{\min} , or the upper limit of the frequency ν_{\max} , corresponds to the transformation of the kinetic energy of an electron of charge $-e$ into a single photon:

$$eV = h\nu_{\max} = \frac{hc}{\lambda_{\min}}$$

$$\lambda_{\min}(\text{\AA}) = 12398 \frac{1}{V(\text{volts})} \quad (3.48)$$

where e is the charge on the electron, h is Plank's constant and c is the speed of light (Duane–Hunt rule). The Laue method discussed above uses the continuous spectrum.

The *characteristic spectrum* depends on the metal forming the anode (Fig. 3.33 for Mo and Cu). It is due to electronic transitions analogous to the atomic spectra

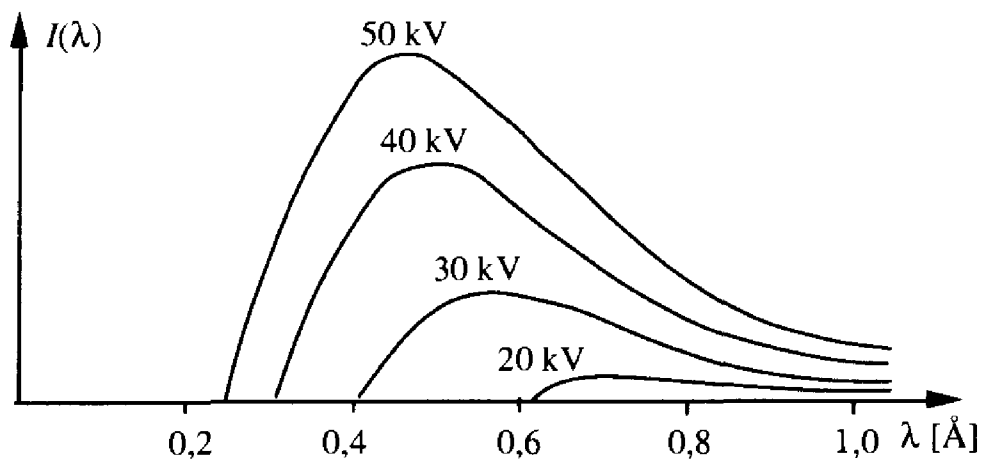


Fig. 3.32. Spectral composition of white radiation according to G. H. Stout and L. H. Jensen, in *X-ray Structure Determination*

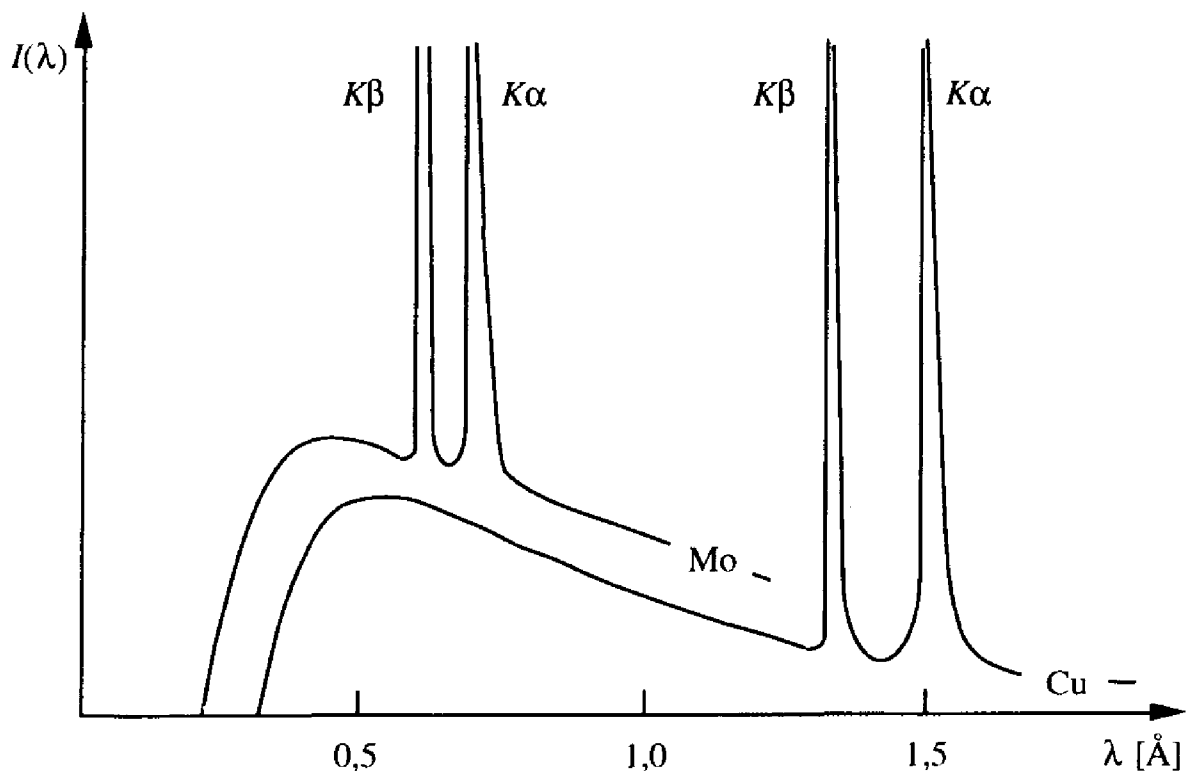


Fig. 3.33. Characteristic spectra according to G. H. Stout and L. H. Jensen, in *X-ray Structure Determination*

of the alkali metals (Na, K). Some atoms of the anode are ionized by the photons of the continuous spectrum which are energetic enough to expel a core electron. In order to study this phenomenon, we will first review the quantum numbers and the spectroscopic symbols which characterize atomic orbitals:

- the principal quantum number $n = 1, 2, 3, \dots$ indicates the electron shell K, L, M, \dots ;

- the orbital angular momentum quantum number l has the values $0, 1, 2, \dots$ corresponding to orbitals of the type s, p, d, \dots respectively; $0 \leq l \leq n - 1$;
- the magnetic quantum number m_l takes the values $-l \leq m_l \leq l$; thus there is one s state, three p states, five d states, etc.;
- the spin of the electron s has the value of $1/2$, and the corresponding magnetic quantum number m_s can take two values, $+1/2$ or $-1/2$;
- the total angular momentum quantum number j for an electron is given by $j = l \pm s$; $j = 1/2$ for an s state, $1/2$ or $3/2$ for a p state, $3/2$ or $5/2$ for a d state, etc.

The core levels of Cu and Mo are all filled and all their electrons are paired. The ionized atom formed by the expulsion of an s electron from a core level is in the $S_{1/2}$ state because it contains an unpaired s electron with $j = 1/2$ ($1S_{1/2}$ or $2S_{1/2}$ for the K or L levels). If it is a p electron that is expelled, we obtain the terms $P_{1/2}$ or $P_{3/2}$; the orbital angular momentum quantum number of the unpaired electron is $l = 1$, that of the total angular momentum is $j = 1/2$ or $3/2$. It is clear that an electron hole created in the K level by ionization will be filled by an electron from a higher level. The transitions $L \rightarrow K$ and $M \rightarrow K$ are designated by $K\alpha$ and $K\beta$ respectively. It is known from atomic physics that the change in quantum numbers during an optical transition (absorption or emission of a photon) obey the selection rules

$$\Delta l = \pm 1; \quad \Delta j = 0 \text{ or } \pm 1. \quad (3.49)$$

The electronic transition that fills the hole in the K level ($l = 0$) creates a hole in a p orbital ($l = 1$) and thus a state $P_{1/2}$ or $P_{3/2}$. Hence all the characteristic K lines are doublets $S_{1/2} \rightarrow P_{1/2}$ or $S_{1/2} \rightarrow P_{3/2}$. The new holes created in the M or L levels will be filled by the transitions $P_{1/2} \rightarrow S_{1/2}$, $P_{1/2} \rightarrow D_{3/2}$, $P_{3/2} \rightarrow S_{1/2}$, $P_{3/2} \rightarrow D_{3/2}$ or $P_{3/2} \rightarrow D_{5/2}$. This cascade of transitions never creates a $2S_{1/2}$ state in the L shell. The occurrence of this state is due to direct ionization by the photons of the white radiation. The $K\alpha$ and $K\beta$ lines in Fig. 3.33 are in fact doublets $K\alpha_1/K\alpha_2$ and $K\beta_1/K\beta_2$. A corresponding splitting of the Bragg reflections is often observed at high θ angles due to the presence of $K\alpha_1$ and $K\alpha_2$. In contrast, the energies of $K\beta_1$ and $K\beta_2$ are very close. The L series contains a number of lines at longer wavelength. The ratio of the intensities $I(K\alpha_1)/I(K\alpha_2)$ is approximately 2:1. Figure 3.34 shows an energy level scheme of all the transitions responsible for the characteristic spectra. The intensity of the $K\alpha$ doublet is given by the equation

$$I(K\alpha) = k(V - V_0)^n, \quad V/V_0 < 4 \quad (3.50)$$

where V is the high voltage applied to the tube, V_0 the minimum voltage to excite $K\alpha$, k a constant and n has a value between 1.5 and 2. V_0 may be calculated by relation (3.48) using the K absorption edge of the atom for λ_{\min} which corresponds to the energy necessary to ionize the K level (Section 3.6.3, Table 3.1).

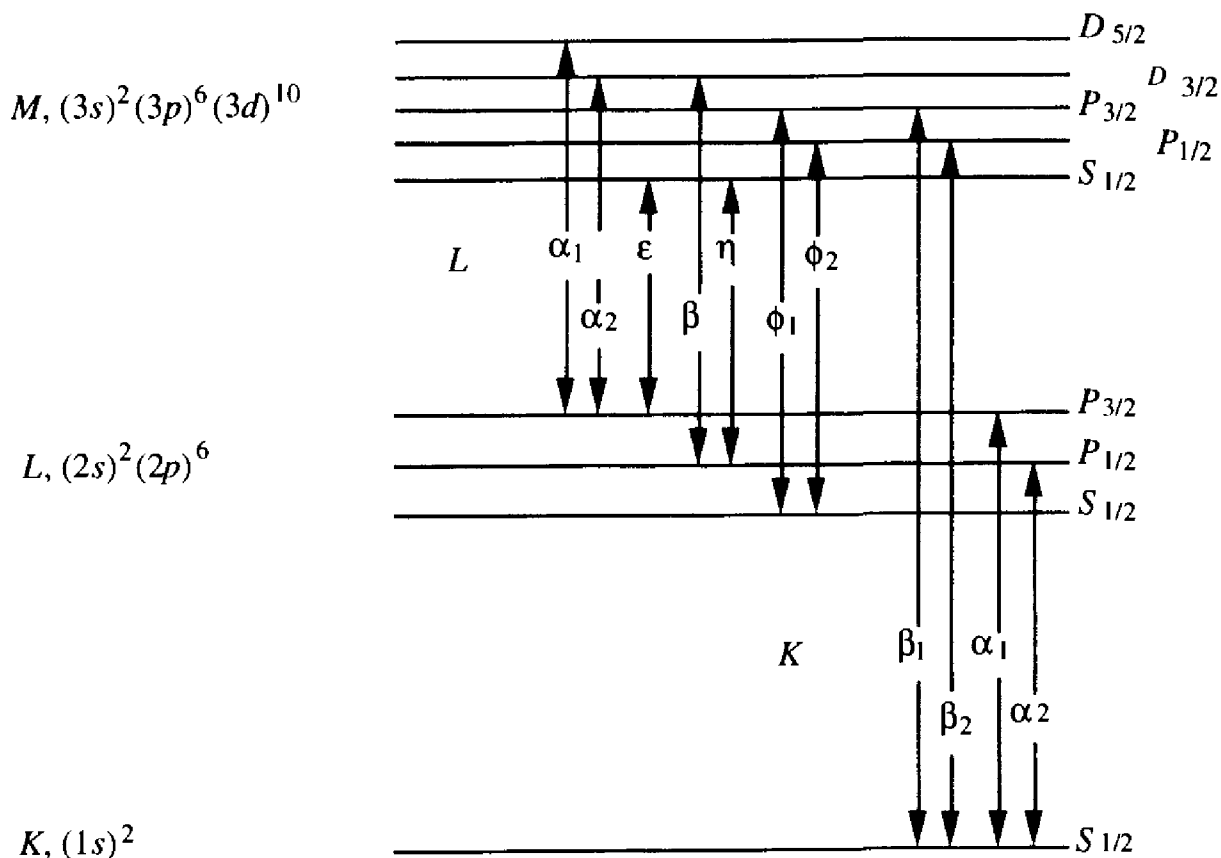


Fig. 3.34. Energy level diagram for transitions that emit X-rays

3.6.2 MONOCHROMATIZATION OF X-RAYS, ABSORPTION

An approximately monochromatic beam may be obtained by isolating the most intense doublet $K\alpha_1/K\alpha_2$. Isolation of the single $K\alpha_1$ line is accompanied by a loss of intensity which is often unacceptable.

There are two methods available to obtain monochromatic X-rays. The simplest method exploits the *absorption rules for X-rays* by matter by using filters. The absorption of radiation by a solid obeys the equation

$$I = I_0 e^{-\mu t}, \tag{3.51}$$

where t is the distance traveled by the radiation in the solid and μ the linear absorption coefficient. This coefficient is characteristic of the chemical element absorbing the radiation. It is a function of the wavelength λ and is composed of continuous zones $\mu \approx k\lambda^3$ separated by abrupt discontinuities. These discontinuities are called *absorption edges*. Figure 3.35 shows the absorption $\mu(\lambda)$ and the emission $I(\lambda)$ curves together for one element. The first discontinuity is the K edge. It corresponds to the energy necessary to ionize the K level by displacing a 1s electron into the energy continuum above the characteristic energy levels of the atom (the ionized atom is in the $1S_{1/2}$ state). We see that the $K\alpha$ and $K\beta$ lines appear to the right of the K edge at longer wavelengths because they correspond

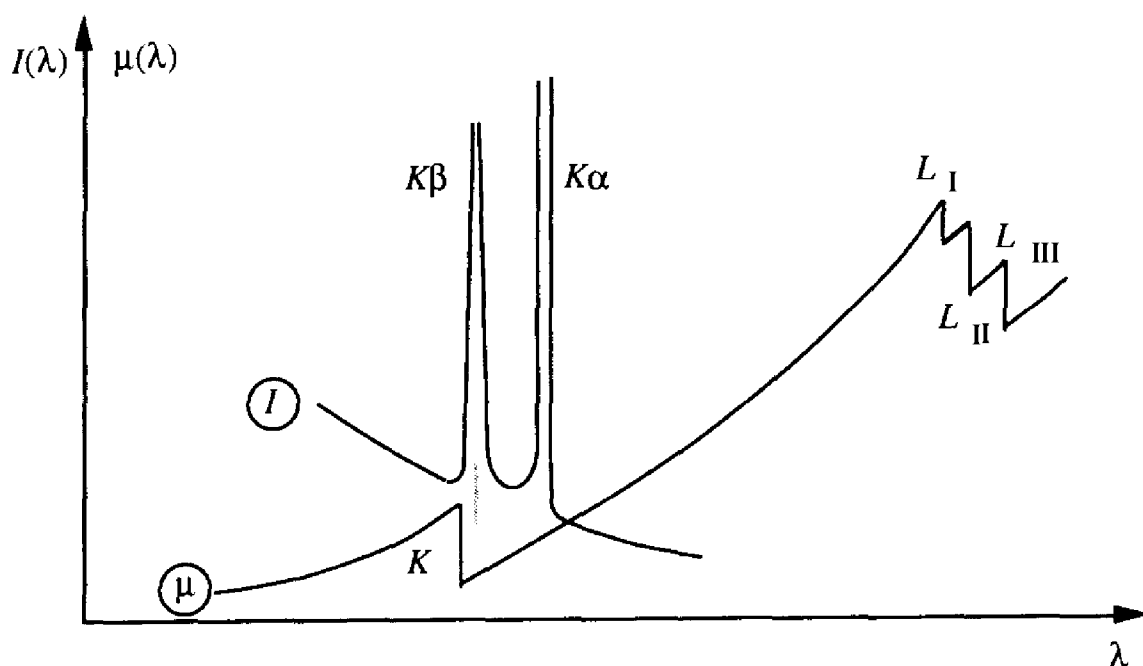


Fig. 3.35. Absorption μ and emission I of X-rays according to G. H. Stout and L. H. Jensen in *X-ray Structure Determination*

to the difference in energy between the L and K , and M and K levels. These levels are occupied in all of the non-excited atoms. It thus follows that

the characteristic emission spectrum of an element is only weakly absorbed by the same element.

The L absorption is made up of three edges corresponding to three states, $2S_{1/2}$, $2P_{1/2}$ and $2P_{3/2}$. Figure 3.36 shows the energy level scheme corresponding to Fig. 3.35.

Monochromatization by a β filter results from the preferential absorption of the $K\beta$ line. For the β filter, we choose an element whose K absorption edge lies between the $K\alpha$ and $K\beta$ lines of the element used for the anode. The element which lies to the left of the latter in the periodic table fulfills this requirement. Figure 3.37 shows the effect of a Nb filter on the radiation from Mo. Table 3.1 lists the most important radiations. In addition, the elements that are two or three places to the left of the emitting element strongly absorb the $K\alpha$ line. Thus, the K edge of Co is found at 1.60811 \AA and that of Fe at 1.74334 \AA . For this reason, it is not a wise choice to use $\text{Cu}K\alpha$ radiation to study alloys of Co and Fe. The radiation is mainly absorbed rather than diffracted. The atoms in the sample responsible for the absorption then emit their own characteristic X-radiation which covers the Bragg reflections with an important background.

A better monochromatization is obtained by using a *crystal monochromator* rather than a filter. This crystal is aligned in such a way that it obeys Bragg's law and efficiently reflects the $K\alpha_1/K\alpha_2$ line. It is important that the structure factor

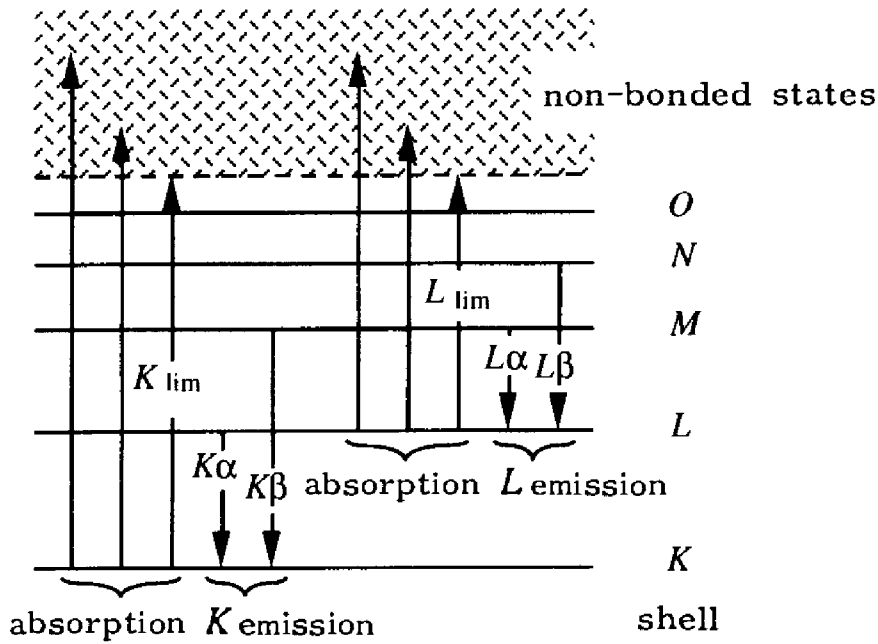


Fig. 3.36. Energy level diagram for emission and absorption. K_{lim} and L_{lim} represent the minimum ionization energies for the K and L levels. For the multiplets of the emission lines, consult Fig. 3.34

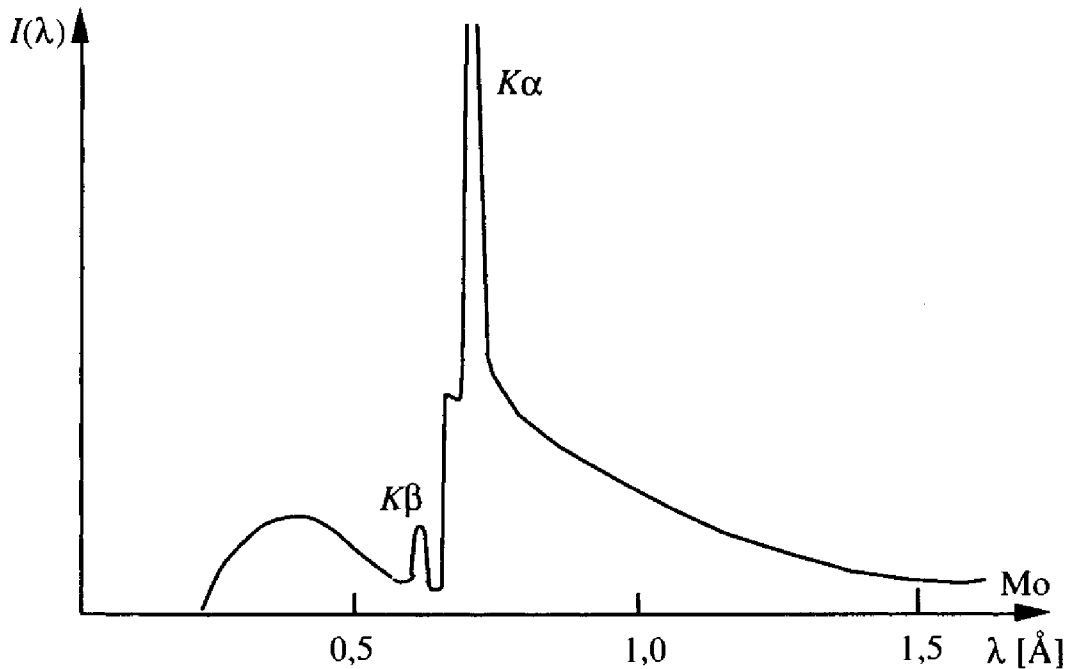


Fig. 3.37. Emission spectrum obtained with the use of a β filter (G. H. Stout and L. H. Jensen, *X-ray Structure Determination*)

(and hence the intensity) of the reflection (Section 3.7) be large. The reflection (002) of graphite is used most commonly for single crystal diffractometers and the (101) reflection of quartz for powder diffractometers. With a good quartz monochromator, the K_{α_1} and K_{α_2} lines may be separated at the price of a loss in intensity. This method has two major inconveniences:

Table 3.1. Wavelengths (\AA) and β filters

anode element	$\lambda(K\alpha_2)$	$\lambda(K\alpha_1)$	$\lambda(K\bar{\alpha})$	$\lambda(K\beta_1)$	λ K edge	filter	λ K edge of filter
Fe	1.93991	1.93597	1.93728	1.75653	1.74334	Mn	1.89636
Cu	1.54433	1.54051	1.54178	1.39217	1.38043	Ni	1.48802
Mo	0.713543	0.70926	0.71069	0.63225	0.61977	{ Nb Zr	0.65291
Ag	0.563775	0.559363	0.56083	0.497069	0.48582	{ Pd Rh	0.50915

Source: *International Tables for Crystallography*, vol. C, pp. 177–179.

Intensities: $I(\alpha_2)$: $I(\alpha_1) \approx 0.5$; $I(\beta)$: $I(\alpha_1) \approx$ between 0.167 (Fe) and 0.290 (Ag).

- The alignment of a crystal monochromator is more difficult than the use of a β filter.
- A crystal which reflects the wavelength λ can also reflect the harmonics $\lambda/2$, $\lambda/3$, etc. (Section 3.5.1). By applying a voltage of 50 kV to the tube, from equation (3.48) we obtain $\lambda_{\min} = 0.248 \text{\AA}$. The wavelengths of the harmonics are thus present in the white radiation (for $\text{Cu}K\alpha$, $\lambda/2, \dots, \lambda/6$). However, their intensities are much lower than those of the $K\alpha$ lines. They can be eliminated with the aid of an electronic discriminator if the intensities are measured with a counter. The reflection (111) of Si or Ge is also used. For these materials, the structure factor $F(222)$ is almost zero, whereas $F(111)$ is large. Hence, the reflection 111 does not contain the harmonic $\lambda/2$.

Crystal monochromators are also used to obtain monochromatic neutrons as well as to analyze the spectrum of electromagnetic radiation or neutron beams of unknown spectral composition.

3.6.3 SYNCHROTRON RADIATION

The X-ray tube is a very widespread source of radiation in university and industrial research laboratories. However, the intensity of its radiation is limited mainly by the ability to remove heat from the anode. For most applications, suitable intensities are obtained only for the characteristic $K\alpha$ and $K\beta$ lines of a few metallic elements with a high thermal conductivity. The choice of wavelengths is thus rather limited. It is possible to produce more intense beams with rotating anodes. However, the purchase and maintenance of such a machine is much more expensive than the utilization of a classical tube with a stationary anode.

The X-rays produced by a synchrotron do not suffer from the above limitations. The electrons or positrons which circulate with relativistic velocities in a storage ring emit very intense radiation which is strongly polarized in the plane

of the ring. With crystal monochromators, it is possible to isolate a desired wavelength from the wide range of energies produced. In particular, a perfect crystal of silicon behaves as a very narrow band-pass filter. The first synchrotrons were built to meet the needs of high-energy physics and the X-rays produced were considered to be a nuisance and a loss of energy. Today, synchrotrons are constructed which are optimized for the production of radiation. In the region of X-rays (useful wavelengths between 0.4 and 5 Å), there are already several installations in service. The most advanced synchrotron in this domain, the European Synchrotron Radiation Facility (ESRF) in Grenoble (France), puts X-rays of an unprecedented intensity at the disposition of researchers. Several beam lines are dedicated to diffraction experiments. These X-rays are of high intensity, finely focused and extremely monochromatic, and allow new cutting edge experiments.

The synchrotrons have initiated a revolution in research in the domain of solid and liquid materials. However, they have not replaced the classical X-ray tube which still remains an essential tool for all the previously existing applications.

3.7 INTENSITIES OF DIFFRACTED BEAMS

3.7.1 STRUCTURE FACTOR

Let us recapitulate the fundamental theorem of diffraction. A crystal structure is characterized by:

- a translation lattice (periodicity),
- a motif (contents of the unit cell).

These properties are expressed in the diffractogram (Section 3.1.3 and 3.4.1) by:

- constructive and discrete interference according to Bragg's law,
- the intensities of the diffracted rays.

According to equations (3.36), (3.37) and (3.41), the intensity of a Bragg reflection is proportional to the square of the absolute value of the structure factor $|F(\mathbf{S})|^2$. The Laue equations (3.38) and (3.39) allow us to replace \mathbf{S} with hkl : $\mathbf{S} = \mathbf{r}^* = h\mathbf{a}^* + k\mathbf{b}^* + l\mathbf{c}^*$, hence $F(\mathbf{S}) = F(hkl)$. The *integrated intensity* is measured by turning the crystal through the reflecting position, for example by varying the Bragg angle from $\theta_{hkl} - \delta\theta$ to $\theta_{hkl} + \delta\theta$, and integrating over the intensity profile of the radiation reflected by the crystal. In a powder pattern, integration is over the intensity profile of the line hkl . According to the theory presented in Section 3.7.2, the integrated intensity of the reflection hkl is given by:

$$I(hkl) = Kg(\theta)A_y|F(hkl)|^2 \quad (3.52)$$

where K is a constant which includes the scattering power of a classical electron $(e^2/4\pi\epsilon_0 mc^2)^2$ (Section 3.2.1) and the intensity of the primary beam; A is the absorption factor; y is the extinction coefficient (Section 3.3.2); $g(\theta) = L(\theta)P(\theta)$ and $P(\theta)$ is the polarization factor according to equation (3.19); if the primary beam is not polarized, $P(\theta) = (1 + \cos^2 2\theta)/2$; the Lorentz factor $L(\theta)$ represents the speed at which the reciprocal lattice point hkl passes through the Ewald sphere (Section 3.7.2); and $|F(hkl)|$ is the *structure amplitude* equal to the absolute value of the structure factor.

As a general rule, the measurements yield *relative intensities*, i.e. integrated intensities with an arbitrary scale K , because it is difficult to know what part of the intensity of the primary beam passes through the crystal. The constant K is thus an unknown. The function $g(\theta)$ is analytic and its values can be easily calculated. The calculation of the absorption factor A is carried out with a computer and, today, poses no major problem. The theory of extinction is still poorly understood, but the factor y is often close to 1. Thus, from the intensity measurements, structure amplitudes $|F(hkl)|$ are obtained on a relative scale, typically with a precision of the order of 1–5%. The values of $|F(hkl)|$ represent the experimental information about the distribution of the atoms in the unit cell. A discussion of this information forms the subject of this section. However, we will discuss neither the theory nor the practice of structure determination by diffraction.

The scalar product of $\mathbf{S} = \mathbf{r}^* = h\mathbf{a}^* + k\mathbf{b}^* + l\mathbf{c}^*$ and $\mathbf{r} = x\mathbf{a} + y\mathbf{b} + z\mathbf{c}$ in relation (3.37) is equal to $\mathbf{r} \cdot \mathbf{S} = hx + ky + lz$; the volume element $d^3\mathbf{r}$ is equal to the product $[dx\mathbf{a} \times dy\mathbf{b}]dz\mathbf{c} = V_{\text{cell}} dx dy dz$. Consequently, relation (3.37) becomes

$$F(\mathbf{S}) = F(hkl) = V_{\text{cell}} \int_0^1 dx \int_0^1 dy \int_0^1 dz \langle \rho(xyz) \rangle_t e^{2\pi i(hx + ky + lz)}, \quad (3.53)$$

$$F(hkl) = \sum_{\text{atoms}}^{1 \text{ cell}} [f_m]_t e^{2\pi i(hx_m + ky_m + lz_m)}; \quad [f_m]_t = f_m(\sin \theta/\lambda) T(hkl). \quad (3.54)$$

Equation (3.53) is valid for all periodic electron density distributions $\langle \rho(xyz) \rangle_t$. Equation (3.54) is valid for the atomistic model (Section 3.3) and can be used to calculate the structure factor if the atomic coordinates and the thermal displacements are known. Remembering that the structure factor represents a wave, it is, in general, a complex number:

$$\begin{aligned} F(hkl) &= \sum_{\text{atoms}}^{1 \text{ cell}} [f_m]_t \cos 2\pi(hx_m + ky_m + lz_m) + i \sum_{\text{atoms}}^{1 \text{ cell}} [f_m]_t \sin 2\pi(hx_m + ky_m + lz_m) \\ &= A + iB. \end{aligned} \quad (3.55)$$

The structure amplitude is given by

$$|F(hkl)|^2 = A^2 + B^2 = \left[\sum_{\text{atoms}}^{1 \text{ cell}} [f_m]_t \cos 2\pi(hx_m + ky_m + lz_m) \right]^2 + \left[\sum_{\text{atoms}}^{1 \text{ cell}} [f_m]_t \sin 2\pi(hx_m + ky_m + lz_m) \right]^2. \tag{3.56}$$

Equation (3.56) expresses the observations $|F(hkl)|^2$ as a function of the atomic coordinates x_m, y_m, z_m . In order to determine an unknown structure, a number of intensities are measured, N_I , which is much greater than the number of symmetrically inequivalent atoms, N_A , $N_I \approx 100 N_A$. The parameters to determine are the three coordinates x_m, y_m, z_m and one or several thermal displacement parameters for each atom according to equations (3.33) and (3.34). The solution to the phase problem in terms of the atomistic model is thus equivalent to the solution of the N_I equations (3.56). A classical method to obtain this goal, the *Patterson function*, will be described in Section 3.9.2. On the other hand, there exist today very powerful algorithms, called *direct methods*, for solving this problem algebraically. In a first approximation, we account for the thermal displacements (Section 3.3.4) with a single global factor U_{iso} according to equation (3.34) that is applied to all the atoms. Once the atomic coordinates are approximately known, all the parameters are adjusted, including the U_{ij} in equation (3.33), by the method of least squares which minimizes the function $\sum_{hkl} w [|F_{\text{observed}}| - |F_{\text{calculated}}|]^2$ or $\sum_{hkl} w [|F_{\text{observed}}|^2 - |F_{\text{calculated}}|^2]^2$ where w is the weight attributed to the observation hkl .

3.7.2 INTEGRATED INTENSITY, LORENTZ FACTOR

We will give here a brief overview of the calculation of the intensity of a Bragg reflection according to kinematic theory. We suppose (Fig. 3.38) that a crystal of volume Δ rotates with an angular velocity ω through the reflecting position. The axis of rotation is contained in the reflecting plane hkl . These conditions are satisfied for all the reflections in the equatorial layer, $n = 0$, in the rotating crystal method (Section 3.5.2). The intensity of the primary beam received by the crystal is I_0 photons per unit time and area. A photon counter or a photographic film placed at a distance r from the crystal receives all of the photons E reflected from the plane during the rotation. If the incident wave is polarized, the amplitude of the wave scattered in the direction of the vector s is:

$$\xi(\mathbf{S}) = \xi_0 \frac{1}{4\pi\epsilon_0} \frac{e^2}{mc^2} \frac{1}{r} G(\mathbf{S}) \sin \phi, \quad \mathbf{S} = \mathbf{s} - \mathbf{s}_0,$$

according to equations (3.16) and (3.20), where ϕ is the angle between the direction of polarization of the incident wave and s . For a non-polarized

incident wave, the scattered intensity in the direction of \mathbf{s} is hence $I(\mathbf{s}) = I_e |G(\mathbf{S})|^2$. I_e is the number of photons scattered by a classical electron and contains the polarization factor P (3.19). We can calculate E by integrating over the angular coordinates Ω of the interference function $J^2(\mathbf{a} \cdot \mathbf{S})J^2(\mathbf{b} \cdot \mathbf{S})J^2(\mathbf{c} \cdot \mathbf{S})$ using equation (3.36):

$$E = \int_{\theta - \delta\theta}^{\theta + \delta\theta} d\theta \int_{1 \text{ refl}} Id(\text{surface}) = r^2 |F(hkl)|^2 \frac{I_e}{v_n} \int_{\text{angles}} J_M^2 J_N^2 J_P^2 d\Omega. \quad (3.57)$$

The term v_n is a function of ω and θ and represents the rate of passage of a reciprocal lattice point through the Ewald sphere (Fig. 3.38). Because the integrations are carried out over the angular coordinates, we calculate v_n with the aid of the modified Ewald construction (Section 3.5.1): the radius of the sphere is equal to 1 and the dimensions of the reciprocal lattice are multiplied by λ .

By turning the crystal with an angular velocity ω , the reciprocal lattice point hkl moves with a speed $v = \lambda r^* \omega$. Its rate of passage through the sphere is equal to the projection of v onto the direction of the diffracted beam \mathbf{s} , $v_n = v \cos \theta$. The norm of λr^* is $2 \sin \theta$, hence, $v_n = 2 \sin \theta \omega \cos \theta = \omega \sin 2\theta$. The larger the value of v_n , the smaller becomes the integrated intensity. The quotient $L(\theta) = \omega/v_n$ is called

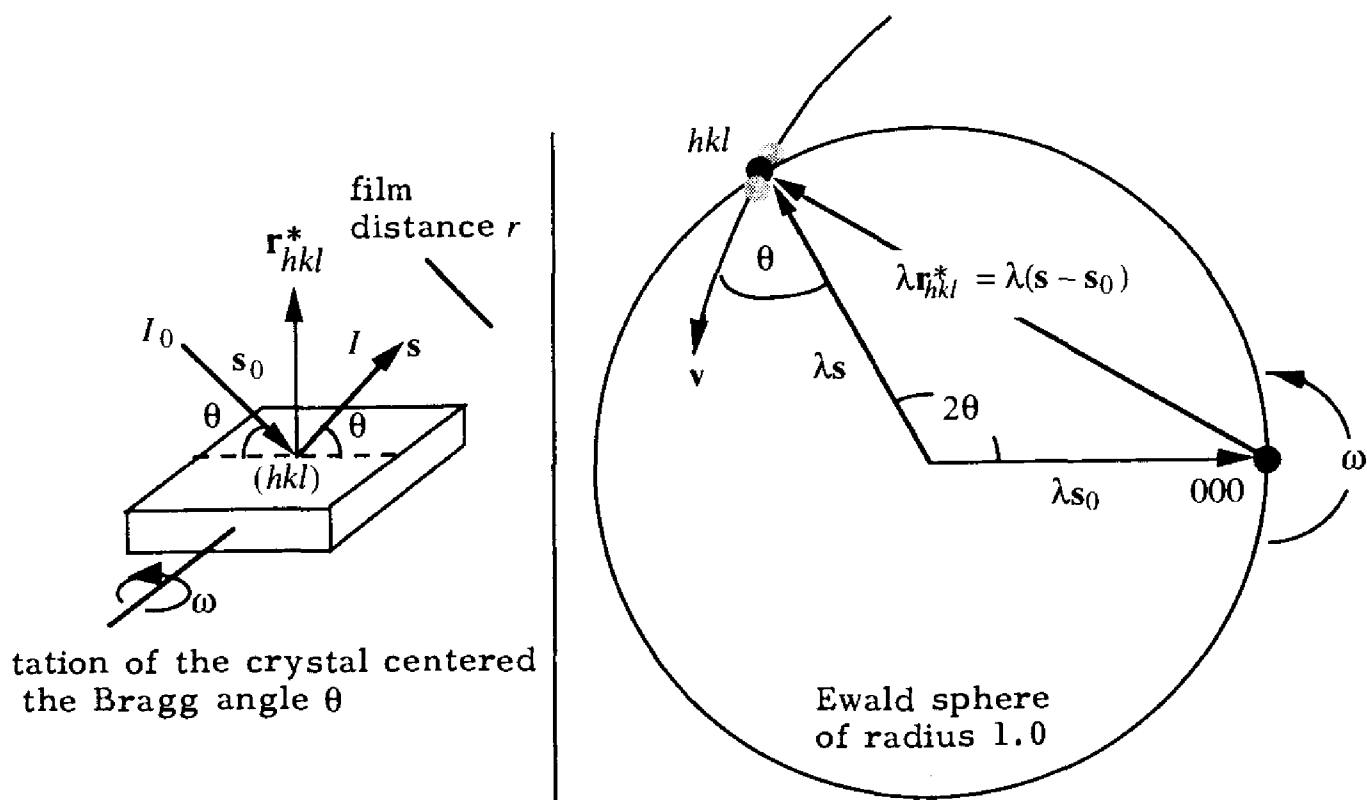


Fig. 3.38. Lorentz factor corresponding to a rotation of the crystal about an axis lying in the reflecting plane and centered at the Bragg angle for the reflection hkl

the *Lorentz factor*. For the experimental arrangement in Fig. 3.38

$$L(\theta) = \frac{1}{\sin 2\theta} \quad (3.58)$$

The Lorentz factor $L(\theta)$ is contained in the term $g(\theta)$ of equation (3.52). The lower the rate of passage of the point through the sphere, the higher is the integrated intensity. The point (000) always lies on the sphere, independent of the position of the crystal. Consequently, $L(0) = \infty$. If the rotation axis does not lie in the reflecting plane, we obtain a speed v which is lower than that in equation (3.58). Hence $L(\theta)$ depends on the experimental technique used. For the rotating crystal method (Section 3.5.2), with the rotation axis parallel to \mathbf{c} and the primary beam perpendicular to \mathbf{c} , the result for the n th layer is:

$$L(\theta) = (\sin^2 2\theta - \zeta^2)^{-1/2}, \quad \zeta = \frac{n\lambda}{c} \quad (3.59)$$

The expression for the powder method (Section 3.5.3) is:

$$L(\theta) = \frac{1}{\sin^2 \theta \cos \theta} \quad (3.60)$$

According to equation (3.41), the integral over a reciprocal lattice point becomes

$$\int_{\text{angles}} J_M^2 J_N^2 J_P^2 d\Omega = \int_{\text{max}} J_M^2 J_N^2 J_P^2 d^3(\lambda\mathbf{S}) = \lambda^3 \int_{\text{max}} J_M^2 J_N^2 J_P^2 d^3(\mathbf{S}) = \frac{\lambda^3 \Delta}{V_{\text{cell}}^2} \quad (3.61)$$

By inserting equations (3.19), (3.58) and (3.61) into (3.57), we obtain

$$\frac{E\omega}{I_0} = \left(\frac{1}{4\pi\epsilon_0} \right)^2 \left(\frac{e^2}{mc^2} \right)^2 \lambda^3 \Delta \frac{1 + \cos^2 2\theta}{2 \sin 2\theta} \left| \frac{F(hkl)}{V_{\text{cell}}} \right|^2 = KL(\theta)P(\theta)|F(hkl)|^2 \quad (3.62)$$

for the kinematic integrated intensity.

As indicated in equation (3.52), we obtain a better agreement with the observations by adding to this expression a correction for the absorption of the primary beam as well as a correction for extinction.

3.7.3 FRIEDEL'S LAW

The structure factor of the reflection $\overline{h\overline{k}\overline{l}}$ is equal to the complex conjugate $F^*(hkl)$ of $F(hkl)$. The structure amplitudes of the reflections hkl and $\overline{h\overline{k}\overline{l}}$ are thus equal:

$$|F(\overline{h\overline{k}\overline{l}})|^2 = |F(hkl)|^2 \quad (3.63)$$

Equation (3.63) represents Friedel's law: the intensities of the reflections hkl and $\overline{h\overline{k}\overline{l}}$ are equal, even if the crystal is non-centrosymmetric. These reflections are produced on opposite sides of the same lattice plane.

It thus follows that X-ray diffraction, and in particular the Laue method (Section 3.5.1), only allows us to classify crystals according to the 11 Laue classes (Section 2.5.7) and not according to the 32 crystal classes.

However, Friedel's law is based on an approximate argument. Consequently it is not strictly valid. When deriving equation (3.63), we assumed the form factors $[f_m]_t$ to be real quantities. This is only approximately so. Anomalous dispersion (Section 3.2.2) introduces an imaginary component into the form factors which is important if the wavelength of the X-ray is close to an absorption edge of certain atoms present in the structure. In this case, the structure factors do not obey Friedel's law. This effect is exploited in macromolecular crystallography. It also serves to determine the absolute configuration of a structure, e.g. to make the distinction between a right-handed and a left-handed helix. However, Friedel's law is, in general, an excellent approximation and it agrees well with the observations made with the methods of Section 3.5.

If the structure is *centrosymmetric*, and if the origin of the coordinate system is placed on a center of symmetry, then the structure factor is a real number. In this case, the electron density is an even function $\langle \rho(\mathbf{r}) \rangle_t = \langle \rho(-\mathbf{r}) \rangle_t$. An atom located at x, y, z is accompanied by an equivalent atom at $\bar{x}, \bar{y}, \bar{z}$ and the imaginary part in equation (3.55) cancels:

$$F_{\text{centro}}(hkl) = \sum_{\text{atoms}}^{\text{1 cell}} [f_m]_t \cos 2\pi(hx_m + ky_m + lz_m) = \pm |F_{\text{centro}}(hkl)|. \quad (3.64)$$

The presence of a center of symmetry is of particular importance in structure determination. The solution to the phase problem, in this case, consists only of the determination of the signs of the structure factors. On the other hand, the phases for a non-centrosymmetric structure can take any of the values between 0 and 2π . However, it is often difficult to detect unambiguously the presence or absence of a center of symmetry.

3.8 SPACE GROUP DETERMINATION

3.8.1 DETERMINATION OF THE CRYSTAL SYSTEM AND OF THE LAUE CLASS

The symmetry of the diffractogram from a single crystal in principle allows us to classify the crystal according to one of the 11 Laue classes (Section 2.5.7 and 3.7.3). For a crystal belonging to the Laue class $4/m$, the reflections $hkl, \bar{h}kl, h\bar{k}l, k\bar{h}l, \bar{h}\bar{k}l, k\bar{h}\bar{l}, h\bar{k}\bar{l}, \bar{h}k\bar{l}$ are equivalent and hence have the same intensity. The Laue class $4/m$ is composed of the crystal classes $4, \bar{4}$ and $4/m$. The symmetry of a Laue photograph taken with the fourfold axis oriented parallel to the incident X-ray beam is tetragonal, plane group 4 .

For a crystal belonging to the Laue class $4/m\bar{m}m$ (crystal classes $4mm$, 422 , $4\bar{2}m$ and $4/m\bar{m}m$), we observe, in addition to the symmetry $4/m$, the equivalence of the reflections hkl and khl . Consequently, in general there are 16 equivalent reflections ($h \neq k$, $h \neq 0$, $k \neq 0$, $l \neq 0$). A Laue photograph oriented in the same way as above has the plane symmetry $4mm$.

In the case of the powder method, all the symmetry equivalent reflections superimpose because they all have the same spacing d_{hkl} (Section 3.5.3). Thus, this method does not allow us to observe the Laue symmetry, only the metric of the unit cell. For the same reason, the rotation method is also poorly adapted for the determination of the symmetry. There are other diffraction methods, which are not described in this work, by which all the reflections may be individually observed without superposition from which it is also possible to determine the Laue class of a crystal and consequently the crystal system. Is it possible to obtain other information about the symmetry and, in particular, the Bravais class and the space group?

In the majority of diffractograms, certain reflections are absent due to structure amplitudes which are weak or zero.

An absence is systematic if the indices of the reflections concerned satisfy certain parity rules. Systematic absences indicate the presence of translations, glide planes and screw axes, i.e. symmetry elements without a fixed point (Section 2.3).

We distinguish three types of systematic absences: integral, zonal and serial. An *integral* absence concerns all the reflections hkl . A *zonal* absence is satisfied only by a reciprocal lattice plane passing through the origin, e.g. the reflections $hk0$. A *serial* absence is satisfied only by a reciprocal lattice line which passes through the origin, e.g. the reflections $h00$.

3.8.2 INTEGRAL ABSENCES, CENTERED CELLS

All the rules for systematic absences may be derived from the expression for the structure factor (3.54). Let us derive the rule for a C centered cell. The vector $(\mathbf{a} + \mathbf{b})/2$ is a lattice translation (Section 1.4.1). An atom of type m in position x, y, z is accompanied by an identical atom in position $\frac{1}{2} + x, \frac{1}{2} + y, z$. The contribution of these two atoms to the structure factor of the reflection hkl is

$$[f_m]_l e^{2\pi i(hx + ky + lz)} \{1 + e^{\pi i(h+k)}\}; \quad 1 + e^{\pi i(h+k)} = \begin{cases} 2 & \text{for } h+k \text{ even} \\ 0 & \text{for } h+k \text{ odd} \end{cases}$$

Thus we conclude that the intensities for all the reflections with $h+k$ odd are zero. In an analogous manner we can derive rules of integral systematic absences characteristic for each of the lattice types I, A, B, C, F, R (Table 3.2). A P lattice generates no systematic absences.

Table 3.2. Integral and zonal systematic absences

Reflections	Conditions for observation	Type of lattice or symmetry element	Translations
hkl	$h + k + l = 2n$	I lattice	$\frac{1}{2}(\mathbf{a} + \mathbf{b} + \mathbf{c})$
	$h + k = 2n$	C lattice	$\frac{1}{2}(\mathbf{a} + \mathbf{b})$
	$h + l = 2n$	B lattice	$\frac{1}{2}(\mathbf{a} + \mathbf{c})$
	$k + l = 2n$	A lattice	$\frac{1}{2}(\mathbf{b} + \mathbf{c})$
	h, k, l all even } or all odd }	F lattice	$\frac{1}{2}(\mathbf{a} + \mathbf{b}), \frac{1}{2}(\mathbf{a} + \mathbf{c}), \frac{1}{2}(\mathbf{b} + \mathbf{c})$
	$-h + k + l = 3n$	R lattice (<i>inverse</i>)	$\frac{1}{3}(2\mathbf{a} + \mathbf{b} + \mathbf{c}), \frac{1}{3}(\mathbf{a} + 2\mathbf{b} + 2\mathbf{c})$
	$h - k + l = 3n$	R lattice (<i>obverse</i>)	$\frac{1}{3}(\mathbf{a} + 2\mathbf{b} + \mathbf{c}), \frac{1}{3}(2\mathbf{a} + \mathbf{b} + 2\mathbf{c})$
$0kl$	$k = 2n$	b glide plane, (100)	$\frac{1}{2}\mathbf{b}$
	$l = 2n$	c glide plane, (100)	$\frac{1}{2}\mathbf{c}$
	$k + l = 2n$	n glide plane, (100)	$\frac{1}{2}(\mathbf{b} + \mathbf{c})$
	$k + l = 4n$	d glide plane, (100)	$\frac{1}{4}(\mathbf{b} + \mathbf{c})$
$h0l$	$h = 2n$	a glide plane, (010)	$\frac{1}{2}\mathbf{a}$
	$l = 2n$	c glide plane, (010)	$\frac{1}{2}\mathbf{c}$
	$h + l = 2n$	n glide plane, (010)	$\frac{1}{2}(\mathbf{a} + \mathbf{c})$
	$h + l = 4n$	d glide plane, (010)	$\frac{1}{4}(\mathbf{a} + \mathbf{c})$
$hk0$	$h = 2n$	a glide plane, (001)	$\frac{1}{2}\mathbf{a}$
	$k = 2n$	b glide plane, (001)	$\frac{1}{2}\mathbf{b}$
	$h + k = 2n$	n glide plane, (001)	$\frac{1}{2}(\mathbf{a} + \mathbf{b})$
	$h + k = 4n$	d glide plane, (001)	$\frac{1}{4}(\mathbf{a} + \mathbf{b})$
hhl	$l = 2n$	c glide plane, (1 $\bar{1}$ 0)	$\frac{1}{2}\mathbf{c}$
	$2h + l = 2n$	n glide plane, (1 $\bar{1}$ 0)	$\frac{1}{2}(\mathbf{a} + \mathbf{b} + \mathbf{c})$
	$2h + l = 4n$	d glide plane, (1 $\bar{1}$ 0)	$\frac{1}{4}(\mathbf{a} + \mathbf{b} + \mathbf{c})$

It is instructive to note that the origin of these rules lies in the choice of coordinate system and that they may be derived without using structure factors. Any centered cell may be transformed into a primitive cell which, in general, does not convey the symmetry of the motif and which may thus be unsatisfactory from this point of view (Sections 1.4.1 and 2.6.1). Thus the transformation $\mathbf{a}' = (\mathbf{a} - \mathbf{b})/2$, $\mathbf{b}' = (\mathbf{a} + \mathbf{b})/2$ transforms a C cell into a diamond-shaped primitive cell. The indices hkl transform in a covariant manner (Section 1.2.4), $h' = (h - k)/2$, $k' = (h + k)/2$. As h' and k' must be integers according to the Laue equations, then $h + k$ must be an even number. The indices with $h + k$ odd do not correspond to a reciprocal lattice vector (Fig. 3.39).

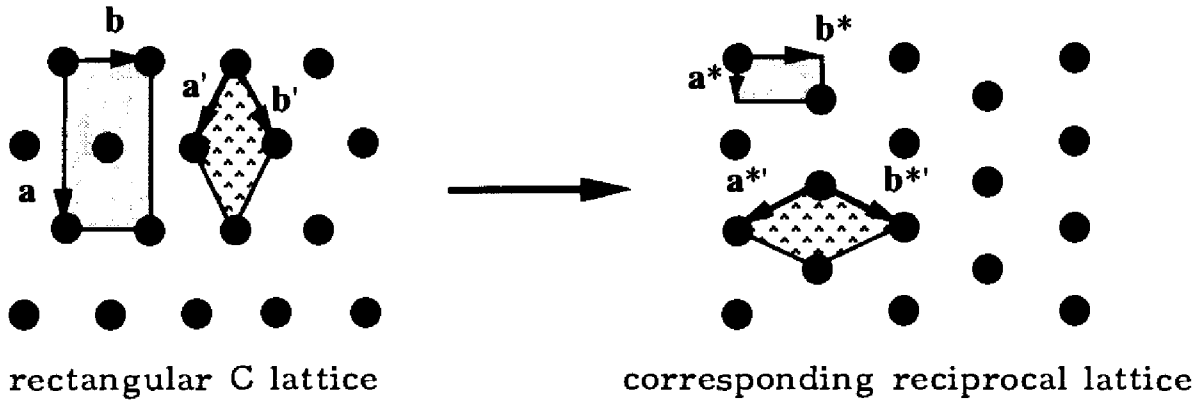


Fig. 3.39. Transformation of a rectangular C lattice into a primitive P lattice

3.8.3 ZONAL ABSENCES, GLIDE PLANES

Let us suppose that there is a glide plane *a* perpendicular to *c* and passing through the origin (Section 2.3.3; Table 2.5). Thus, an atom of type *m* in position *x, y, z* is accompanied by an equivalent atom in position $\frac{1}{2} + x, y, -z$ (or $\frac{1}{2} + x, y, \frac{1}{2} - z$ for a plane *a* located at *c*/4). The contribution of these two atoms to the structure factor is

$$[f_m]_t [e^{2\pi i(hx + ky + lz)} + e^{2\pi i(hx + ky - lz)} e^{\pi i h}].$$

For *l* = 0, we obtain:

$$[f_m]_t e^{2\pi i(hx + ky)} \{1 + e^{\pi i h}\}; \quad 1 + e^{\pi i h} = \begin{cases} 2 & \text{for } h \text{ even} \\ 0 & \text{for } h \text{ odd} \end{cases}$$

We conclude from this result that the intensities of all the reflections *hk0* are zero for *h* odd. For each type and orientation of glide plane, there exist characteristic zonal absences (Table 3.2).

The origin of the zonal absences lies in the periodicity of the projection of the structure onto the glide plane. The Fourier transform of the projection of the electron density down *c* onto the plane (001) is the set of structure factors *F*(*hk0*):

$$\begin{aligned}
 F(hk0) &= V_{\text{cell}} \int_0^1 dx \int_0^1 dy \int_0^1 dz \langle \rho(xyz) \rangle_t e^{2\pi i(hx + ky + 0z)} \\
 &\hspace{20em} \text{according to equation (3.53)} \\
 &= \frac{V_{\text{cell}}}{c} \int_0^1 dx \int_0^1 dy \left[\int_0^1 d(cz) \langle \rho(xyz) \rangle_t \right] e^{2\pi i(hx + ky)}. \\
 F(hk0) &= S_{\text{ab}} \int_0^1 dx \int_0^1 dy \langle \rho'(xy) \rangle_t e^{2\pi i(hx + ky)}. \tag{3.65}
 \end{aligned}$$

*S*_{ab} is the area of the cell [*a* × *b*] and $\langle \rho'(xy) \rangle_t$ is the projection of $\langle \rho(xyz) \rangle_t$. If

(001) is an \mathbf{a} glide plane, this projection is invariant with respect to the translation $\mathbf{a}' = \mathbf{a}/2$: $\langle \rho'(xy) \rangle_t = \langle \rho'(\frac{1}{2} + x, y) \rangle_t$. It thus follows that $h' = h/2$ is an integer for all the reflections $hk0$.

A zonal absence indicates that a projection of the structure onto a plane has a different periodicity from that of the three-dimensional structure. It is in general due to the presence of a glide plane.

3.8.4 SERIAL ABSENCES, SCREW AXES

Let us suppose that a 2_1 screw axis exists parallel to \mathbf{c} and passing through the origin. An atom of type m in position x, y, z is accompanied by an equivalent atom in position $-x, -y, \frac{1}{2} + z$. (An axis which does not pass through the origin generates an equivalent atom at $p - x, q - y, \frac{1}{2} + z$ with $(p, q) = (0, \frac{1}{2})$ or $(\frac{1}{2}, 0)$ or $(\frac{1}{2}, \frac{1}{2})$ according to the position of the axis.) The contribution of these two atoms to the structure factor is:

$$[f_m]_t [e^{2\pi i(hx + ky + lz)} + e^{2\pi i(-hx - ky + lz)} e^{\pi i l}]$$

For $h = k = 0$, we obtain:

$$[f_m]_t e^{2\pi i l z} \{1 + e^{\pi i l}\}; \quad 1 + e^{\pi i l} = \begin{cases} 2 & \text{for } l \text{ even} \\ 0 & \text{for } l \text{ odd} \end{cases}$$

From this we conclude that the intensities of all the $00l$ reflections are zero if l is odd. Each type and each orientation of screw axis has a corresponding characteristic serial absence (Table 3.3).

The origin of the serial absences lies in the projection of the structure onto the screw axis. By analogy with equation (3.65) we find that

$$F(00l) = c \int_0^1 dz \langle \rho''(z) \rangle_t e^{2\pi i l z} \quad (3.66)$$

$\langle \rho''(z) \rangle_t$ being the projection of $\langle \rho(xyz) \rangle_t$ onto the \mathbf{c} axis. If the direction of \mathbf{c} coincides with a 2_1 or a 4_2 or a 6_3 screw axis, the projection is invariant with respect to the translation $\mathbf{c}' = \mathbf{c}/2$. Consequently, $l' = l/2$ is an integer for all the $00l$ reflections.

A serial absence indicates that the period of the projection of the structure onto a line is a fraction of the period of the three-dimensional structure ($1/2, 1/3, 1/4$ or $1/6$). In general, this is due to the presence of a screw axis.

3.8.5 ROTATIONS AND ROTOINVERSIONS

The presence of symmetry elements without a translation component, i.e. rotation axes \mathbf{x} and rotoinversion axes $\bar{\mathbf{x}}$, cannot be detected by systematic absences.

Table 3.3. Serial systematic absences

Reflections	Conditions for observation	Symmetry element; orientation	Translations
$h00$	$h = 2n$	$2_1, 4_2$ screw axes; $[100]$	$\frac{1}{2}\mathbf{a}$
	$h = 4n$	$4_1, 4_3$ screw axes; $[100]$	$\frac{1}{4}\mathbf{a}$
$0k0$	$k = 2n$	$2_1, 4_2$ screw axes; $[010]$	$\frac{1}{2}\mathbf{b}$
	$k = 4n$	$4_1, 4_3$ screw axes; $[010]$	$\frac{1}{4}\mathbf{b}$
$00l$	$l = 2n$	$2_1, 4_2, 6_3$ screw axes; $[001]$	$\frac{1}{2}\mathbf{c}$
	$l = 3n$	$3_1, 3_2, 6_2, 6_4$ screw axes; $[001]$	$\frac{1}{3}\mathbf{c}$
	$l = 4n$	$4_1, 4_3$ screw axes; $[001]$	$\frac{1}{4}\mathbf{c}$
	$l = 6n$	$6_1, 6_5$ screw axes; $[001]$	$\frac{1}{6}\mathbf{c}$
$hh0$	$h = 2n$	2_1 screw axis; $[110]$	$\frac{1}{2}\mathbf{c}$

This is particularly regrettable for a center of symmetry. In principle we can find the Laue class and the crystal system by means of the distribution of intensities in reciprocal space. In certain cases, symmetry elements with a translational component generate a center of symmetry and the corresponding space group is unambiguously indicated by the systematic absences. In other cases, it is not possible to deduce the space group unambiguously using diffraction methods alone (Section 3.8.7).

3.8.6 FORMAL DERIVATION OF THE SYSTEMATIC ABSENCES

Let the space group be composed of the symmetry operations $(\mathbf{A}_s, \mathbf{t}_s)$, where \mathbf{A}_s represents a rotation or rotoinversion, and \mathbf{t}_s a translation vector (Section 2.2.1). It is sufficient to consider the coordinates given in the *International Tables* which have \mathbf{t}_s vectors with components $0 \leq t_{s1}, t_{s2}, t_{s3} < 1$. The set of matrices \mathbf{A}_s ($1 \leq s \leq S$) represent the point group of order S . The atoms of type m occupy the equivalent positions $\mathbf{r}_{ms} = \mathbf{A}_s \mathbf{r}_m + \mathbf{t}_s$ and the structure factor of the reflection $\mathbf{h} = (h_1 h_2 h_3)^T$ is

$$F(\mathbf{h}) = \sum_m^{\text{inequiv. atoms}} [f_m]_t \left[\sum_s^{\text{symmetries}} \exp(2\pi i \mathbf{h}^T \mathbf{r}_{ms}) \right] = \sum_m^{\text{inequiv. atoms}} [f_m]_t C_m(\mathbf{h}),$$

$$C_m(\mathbf{h}) = \sum_{s=1}^S \exp[2\pi i \mathbf{h}^T (\mathbf{A}_s \mathbf{r}_m + \mathbf{t}_s)].$$

The vectors \mathbf{t} , \mathbf{h} and \mathbf{r} are *column vectors*; their transposes \mathbf{t}^T , \mathbf{h}^T , \mathbf{r}^T are *line vectors*. The structure factor for the equivalent plane $\mathbf{h}_j = \mathbf{A}_j^T \mathbf{h}$ (Section 1.2.4) is

calculated as follows:

$$\begin{aligned}
 C_m(\mathbf{h}_j) &= \sum_{s=1}^S \exp[2\pi i \mathbf{h}_j^T \mathbf{r}_{ms}] = \sum_{s=1}^S \exp[2\pi i \mathbf{h}^T \mathbf{A}_j \mathbf{r}_{ms}] \\
 &= \exp[-2\pi i \mathbf{h}^T \mathbf{t}_j] \sum_{s=1}^S \exp[2\pi i \mathbf{h}^T (\mathbf{A}_j \mathbf{r}_{ms} + \mathbf{t}_j)] \\
 &= \exp[-2\pi i \mathbf{h}^T \mathbf{t}_j] \sum_{s=1}^S \exp[2\pi i \mathbf{h}^T \{ \mathbf{A}_j (\mathbf{A}_s \mathbf{r}_m + \mathbf{t}_s) + \mathbf{t}_j \}] \\
 &= \exp[-2\pi i \mathbf{h}^T \mathbf{t}_j] \sum_{s'=1}^S \exp[2\pi i \mathbf{h}^T (\mathbf{A}_{s'} \mathbf{r}_m + \mathbf{t}_{s'})] = \exp[-2\pi i \mathbf{h}^T \mathbf{t}_j] C_m(\mathbf{h}). \\
 F(\mathbf{A}_j^T \mathbf{h}) &= \exp[-2\pi i \mathbf{h}^T \mathbf{t}_j] F(\mathbf{h}) \tag{3.67}
 \end{aligned}$$

Hence, the structure factors for different lattice planes are distinguished by their phases:

$$\begin{aligned}
 &\text{For } \mathbf{h}_j = \mathbf{A}_j^T \mathbf{h} = \mathbf{h}, \text{ we obtain either } \exp[-2\pi i \mathbf{h}^T \mathbf{t}_j] = 1, \text{ or } F(\mathbf{h}) = 0. \\
 &F(\mathbf{h}) \neq 0: \mathbf{h}^T \mathbf{t}_j = N \text{ integer;} \\
 &\mathbf{h}^T \mathbf{t}_j \neq N \text{ integer: } F(\mathbf{h}) = 0. \tag{3.68}
 \end{aligned}$$

A simple program based on equation (3.68) allows the facile identification of the systematic absences.

3.8.7 EXAMPLES

The systematic absences for each space group are given in the *International Tables for Crystallography, Volume A: Space Group Symmetry*. We will discuss here the examples from Section 2.7.3.

Pnma: There are no integral systematic absences. Hence, the lattice is of type P. The condition $0kl: k + l = 2n$ indicates the presence of an n glide plane perpendicular to \mathbf{a} ; the condition $hk0: h = 2n$ indicates the presence of an a glide plane perpendicular to \mathbf{c} . The plane m perpendicular to \mathbf{b} does not produce any systematic absence. The absences concerning $h00, 0k0$ and $00l$, which indicate the presence of screw axes, are special cases of the rules concerning $0kl$ and $hk0$. The group $\text{Pn}2_1\mathbf{a}$ is characterized by the same absences. The space group Pnma is obtained by adding a center of symmetry to the group $\text{Pn}2_1\mathbf{a}$. The group $\text{Pn}2_1\mathbf{a}$ is found in the *International Tables* under the name $\text{Pna}2_1$. This symbol is obtained by the transformation $\mathbf{c}' = \mathbf{b}; \mathbf{b}' = -\mathbf{c}$.

$\bar{\text{P}}4_2\mathbf{c}$: This group is characterized unambiguously by the systematic absences indicating the presence of the symmetry elements which generate 2_1 and \mathbf{c} . The symmetry being tetragonal, the condition $hhl: l = 2n$ implies $h\bar{h}l: l = 2n$ (c); the

condition $h00$; $h = 2n$ implies $0k0$: $k = 2n$ (2_1). The absence $00l$ is a special case of the condition hhl .

$R\bar{3}c$: The R lattice is indicated by the integral absence $-h + k + l = 3n$. The zonal absence $h\bar{h}0l$: $l = 2n$ indicates the presence of one of the three equivalent c glide planes parallel to the threefold axis. The absences due to the other two c glide planes are generated by rotations of $\pm 120^\circ$: $h0\bar{h}l$: $l = 2n$ and $0k\bar{k}l$: $l = 2n$. The other absences cited in the *International Tables* are special cases of the conditions due to the c glide planes. The group $R3c$ is characterized by the same absences. By adding a center of symmetry to the group $R3c$, we obtain $R\bar{3}c$. The Miller–Bravais indices $hkil$ with four numbers are discussed in Section 2.9. The corresponding indices with three numbers are $h\bar{h}l$, $h0l$ and $0kl$.

Cc : The group is characterized by the integral absences hkl : $h + k = 2n$ (C) and $h0l$: $l = 2n$ (c). The other absences are special cases of these. The group $C2/c$ is obtained by adding a center of symmetry to Cc and is characterized by the same systematic absences.

3.9 COMMENTS ON THE SOLUTION OF THE PHASE PROBLEM

3.9.1 FOURIER SERIES

With equations (3.55) and (3.56), the structure factors and structure amplitudes can be calculated if the atomic coordinates are known. With the inverse Fourier transform, the electron density $\langle \rho(xyz) \rangle_t$ is obtained starting from the structure factors. With the help of equations (3.22) and (3.40), we obtain the *Fourier series*

$$\langle \rho(xyz) \rangle_t = \frac{1}{V_{\text{cell}}} \sum_{h=-\infty}^{\infty} \sum_{k=-\infty}^{\infty} \sum_{l=-\infty}^{\infty} F(hkl) e^{-2\pi i(hx + ky + lz)}. \quad (3.69)$$

According to equation (3.55), $F(hkl) = A(hkl) + iB(hkl)$ and $F(\bar{h}\bar{k}\bar{l}) = A(hkl) - iB(hkl)$, hence:

$$\langle \rho(xyz) \rangle_t = \frac{1}{V_{\text{cell}}} \left[F(000) + 2 \sum_h \sum_k \sum_l^{\text{half recip. space}} A(hkl) \cos 2\pi(hx + ky + lz) + 2 \sum_h \sum_k \sum_l^{\text{half recip. space}} B(hkl) \sin 2\pi(hx + ky + lz) \right]. \quad (3.70)$$

For a centrosymmetric crystal, (Section 3.7.3), $B(hkl) = 0$. In principle, one of the sums in equation (3.70) extends from 0 to $+\infty$ and the two others from $-\infty$ to $+\infty$. In practice, all the sums are limited to the number of measured intensities. This limitation of the Fourier series corresponds to the resolution limit of an optical microscope (Section 3.1.1). The structure factor

$F(000) = A(000)$ is equal to the number of electrons in the unit cell; $B(000) = 0$. Alternatively, equation (3.69) may be derived by employing the periodicity of the electron density, $\langle \rho(xyz) \rangle_t = \langle \rho(x + u, y + v, z + w) \rangle_t$, u, v, w being integers. The function $\langle \rho(xyz) \rangle_t$ is continuous. It has continuous derivatives because it represents the thermally averaged electron density and not the static electron density (Section 3.3.4). A continuous and periodic function can be represented by a Fourier series,

$$\langle \rho(xyz) \rangle_t = \sum_{h=-\infty}^{\infty} \sum_{k=-\infty}^{\infty} \sum_{l=-\infty}^{\infty} K(hkl) e^{-2\pi i(hx + ky + lz)}.$$

By introducing this expression into equation (3.53), we obtain equation (3.69):

$$\begin{aligned} V_{\text{cell}} \sum_{h'=-\infty}^{\infty} \sum_{k'=-\infty}^{\infty} \sum_{l'=-\infty}^{\infty} K(h'k'l') \int_0^1 dx \int_0^1 dy \int_0^1 dz e^{-2\pi i[(h-h')x + (k-k')y + (l-l')z]} \\ = V_{\text{cell}} K(hkl) = F(hkl). \end{aligned}$$

The sums (3.70) may be calculated by efficient computer programs if the structure factors $F(hkl)$ are available. But, remember, experimentally we measure only the structure amplitudes $|F(hkl)|$. How much structural information is contained in the structure amplitudes alone?

3.9.2 PATTERSON FUNCTION

According to the standard model which allows the resolution of the phase problem, the structure is composed of independent atoms. We will show in the following that the structure amplitudes give us information about the distances between the atoms. The square of a structure amplitude is given by $|F(hkl)|^2 = F(hkl)F(\bar{h}\bar{k}\bar{l})$,

$$\begin{aligned} |F(hkl)|^2 &= \left[\sum_{\text{atoms}}^{1 \text{ cell}} [f_m]_t e^{2\pi i(hx_m + ky_m + lz_m)} \right] \left[\sum_{\text{atoms}}^{1 \text{ cell}} [f_n]_t e^{-2\pi i(hx_n + ky_n + lz_n)} \right] \\ &= \sum_m \sum_n [f_m]_t [f_n]_t e^{2\pi i[h(x_m - x_n) + k(y_m - y_n) + l(z_m - z_n)]} \\ &= \sum_m [f_m]_t^2 + \sum_m \sum_{n \neq m} [f_m]_t [f_n]_t \cos 2\pi [h(x_m - x_n) + k(y_m - y_n) + l(z_m - z_n)] \end{aligned} \quad (3.71)$$

Equation (3.71) is similar to equation (3.64) which represents the structure factor for a centrosymmetric crystal. Equation (3.71) can be interpreted as the structure factor for a fictive squared structure. The squared structure is centrosymmetric. It is made up of atoms with a scattering power $[f_m]_t [f_n]_t$ at the positions $\mathbf{r}_m - \mathbf{r}_n = (x_m - x_n)\mathbf{a} + (y_m - y_n)\mathbf{b} + (z_m - z_n)\mathbf{c}$. These coordinates represent the interatomic vectors of the real structure. An atom with the scattering power $\sum [f_m]_t^2$ is found at the origin which represents all the zero vectors. If the

real structure contains N atoms in the unit cell, the cell of the squared structure contains $N(N - 1)$ atoms excluding the atom at the origin.

By analogy with equation (3.70), the electron distribution of the squared structure may be calculated by use of a Fourier series whose coefficients are the squares of the structure amplitudes,

$$P(uvw) = \frac{1}{V_{\text{cell}}} \sum_{h=-\infty}^{\infty} \sum_{k=-\infty}^{\infty} \sum_{l=-\infty}^{\infty} |F(hkl)|^2 e^{-2\pi i(hu + kv + lw)}$$

$$= \frac{1}{V_{\text{cell}}} \left[|F(000)|^2 + 2 \sum_{\substack{\text{half} \\ \text{recip.} \\ \text{space}}} \sum_h \sum_k \sum_l |F(hkl)|^2 \cos 2\pi(hu + kv + lw) \right]. \quad (3.72)$$

$P(uvw)$ is called the *Patterson function* (A. L. Patterson, *Phys. Rev.* **46**, (1934) 372–376). The values of the function are expressed in $e^2 \text{\AA}^{-3}$. According to crystallographic usage, coordinates in the squared cell are represented by u, v, w instead of x, y, z (clearly these are fractional numbers, not integers). Alternatively, we may derive equation (3.72) by inserting equation (3.69) into an integral analogous to equation (3.29) to obtain the *autoconvolution product* of $\langle \rho(x, y, z) \rangle_t$:

$$P(uvw) = V_{\text{cell}} \int_0^1 dx \int_0^1 dy \int_0^1 dz \langle \rho(x, y, z) \rangle_t \langle \rho(x + u, y + v, z + w) \rangle_t. \quad (3.73)$$

According to the convolution theorem (Section 3.3.4), the Fourier transform of $P(uvw)$ is the set of the $|F(hkl)|^2$, that of $\langle \rho(x, y, z) \rangle_t$ being the set of the $F(hkl)$. Equation (3.73) represents the interatomic distances in direct space in a similar manner to equation (3.71) in reciprocal space. If u, v, w does not represent an interatomic vector, at least one of the terms $\langle \rho(x, y, z) \rangle_t$ or $\langle \rho(x + u, y + v, z + w) \rangle_t$, as well as their product, is small whatever the value of x, y and z ; hence, the value of $P(uvw)$ is also small. In contrast, the terms are both large if x, y, z and $x + u, y + v, z + w$ are atomic coordinates; hence $P(uvw)$ has a maximum and u, v and w correspond to an interatomic vector. Thus, the Patterson function does indeed represent the squared structure. In other branches of physics, it is called the *correlation* or *autocorrelation function*.

Figure 3.40 shows two cells of a one-dimensional structure containing three well-resolved atoms per cell, as well as the corresponding Patterson function or squared structure. In this example, it is easy to derive the positions of the maxima from $P(u)$ and thus solve the phase problem. It can be shown that this is always possible if all the interatomic vectors of $\langle \rho(r) \rangle_t$ can be observed as maxima in $P(u)$. We observe that the most pronounced maxima in $P(u)$ represent the vectors between heavy atoms. The maxima of $P(u)$ are broader than the atoms in $\langle \rho(r) \rangle_t$, and are larger in number. They often overlap and their resolution is not always possible. In fact, it is impossible to identify the set of 90 interatomic vectors for a three-dimensional structure with 10 atoms in the unit cell; we are able to interpret only $P(uvw)$ in special cases. However, the study of the Patterson function is a very useful tool for structure determination, especially if we make use

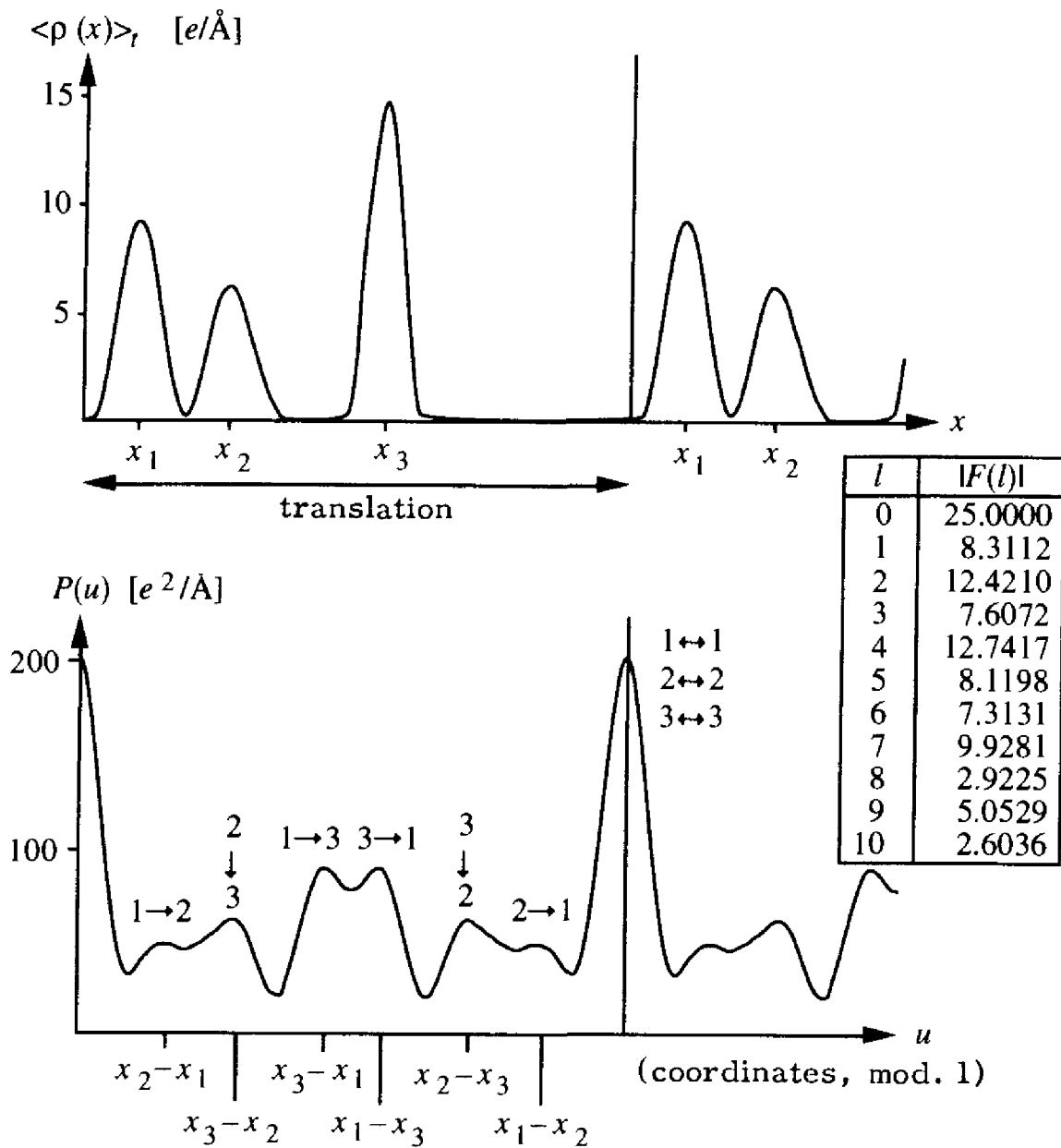


Fig. 3.40. One-dimensional crystal represented by the function $\langle \rho(r) \rangle_t$ and the corresponding Patterson function $P(u)$. (Structural parameters: translation of 10 Å; O atoms at $x_1 = 0.10$; C at $x_2 = 0.27$; Na at $x_3 = 0.55$; vectors $O \leftrightarrow C$ at $u_{12} = \pm 0.17$; $Na \leftrightarrow C$ at $u_{23} = \pm 0.28$; $Na \leftrightarrow O$ at $u_{13} = \pm 0.45$)

of the space group symmetry. The following examples will serve to illustrate this.

(a) KH_2PO_4 (A. L. Patterson, *Z. Kristallogr.*, **90** (1935) 517).

Figure 3.41 shows the projection of the structure of KH_2PO_4 as well as the corresponding Patterson function. The distribution of the (K,P)–(K,P) vectors in (b) is identical to the atomic positions (K,P) in (a). These atoms would in fact be equivalent by translation if the oxygen atoms were absent. The (K,P)–O vectors

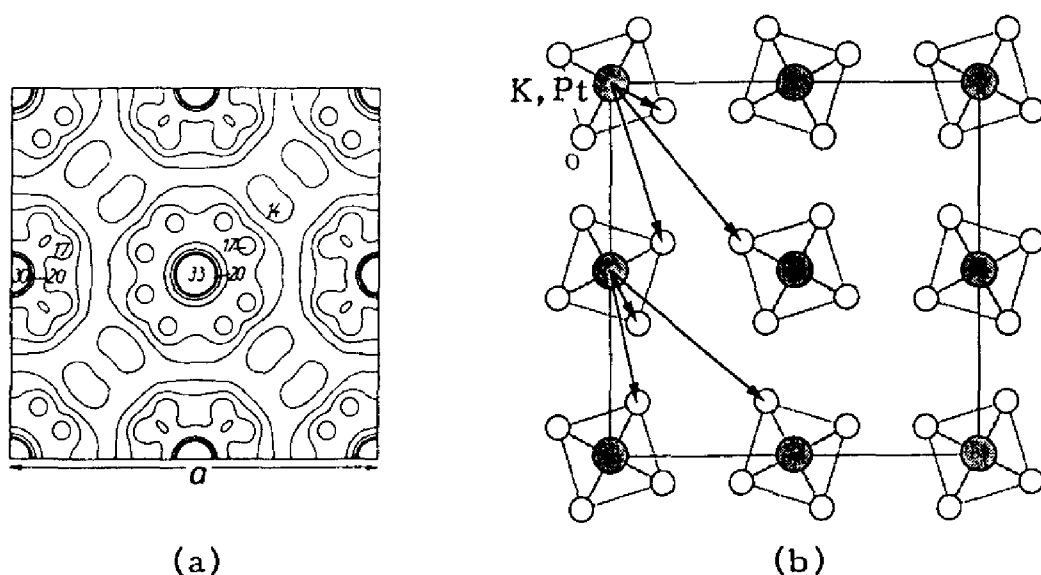


Fig. 3.41. Projections on (001) of the structure (a) and of the Patterson function (b) of KH_2PO_4 . The K and P atoms are superimposed. The H atoms have been omitted because of their low scattering power. The two-dimensional tetragonal unit cells are C centered

are easy to identify. The maxima corresponding to the O–O vectors are weak and of no importance for the solution of the structure. In this example, we see an important property of the Patterson function: it is the superposition of the structure seen from the (K,P) atom at $0, 0$ or $\frac{1}{2}, \frac{1}{2}$, and of the structure seen from the (K, P) atom at $0, \frac{1}{2}$ or $\frac{1}{2}, 0$.

(b) Platinum phthalocyanine, $\text{C}_{32}\text{N}_8\text{H}_{16}\text{Pt}$ (J. M. Robertson & I. Woodward, *J. Chem. Soc.* (1940) 36)

The molecule of phthalocyanine (Fig. 3.42) has an empty space in its center. It is possible to place a metal atom such as Ni or Pt in this space. The structure of Pt-phthalocyanine was the first to be solved by the so-called *heavy atom method*. The unit cell is monoclinic and contains two centrosymmetric molecules. The space group is $\text{P}2_1/\text{a}$. Pt occupies the positions $0, 0, 0$ and $\frac{1}{2}, \frac{1}{2}, 0$ (special position of site symmetry 1). The Patterson function correspondingly shows two large maxima at $u, v, w = 0, 0, 0$ and $\frac{1}{2}, \frac{1}{2}, 0$. Structure factors can then be calculated following equation (3.64) using uniquely the Pt atoms. Because the heavy atoms dominate the scattering, we thus obtain a good estimation of the phases. In the next step, we use these approximate phases along with the measured structure amplitudes to calculate the electron density distribution using equation (3.70). In the case of Pt-phthalocyanine, the molecule is approximately parallel to (010). The unit cell of the projection of the structure down **b** onto the (010) plane is $\mathbf{a}' = \frac{1}{2}\mathbf{a}$, $\mathbf{c}' = \mathbf{c}$ (Section 3.8.3). It contains a single atom of Pt which occupies the center of symmetry at $0, 0$. Because f_{Pt} is very large in comparison to the form

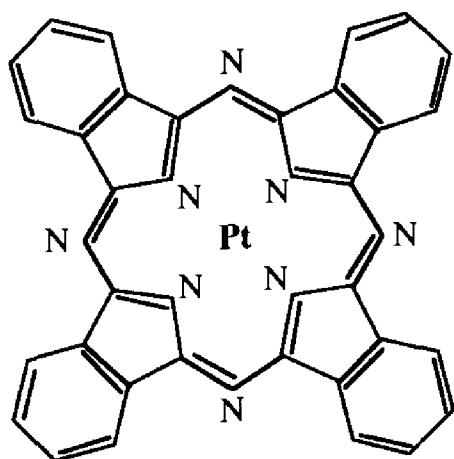


Fig. 3.42. Pt-phthalocyanine. The unlabeled apices represent C or C-H

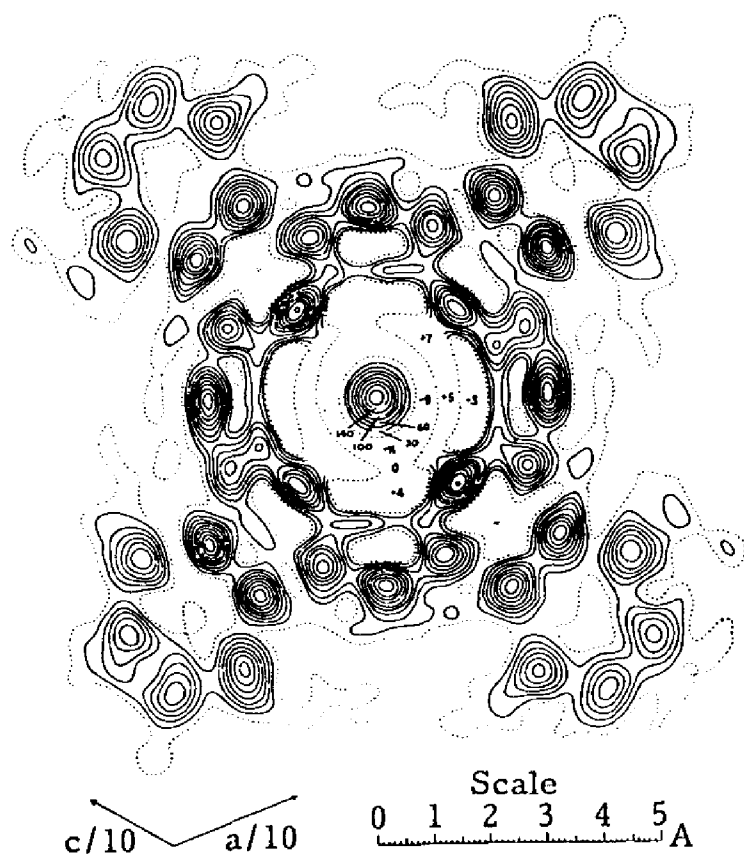


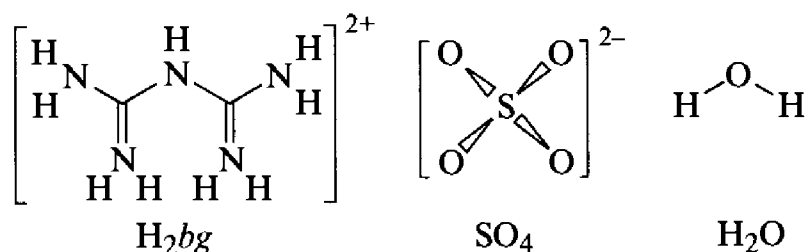
Fig. 3.43. Projection of the electron density of Pt-phthalocyanine. The contour interval is $1 e \text{ \AA}^{-3}$ except for the Pt atom

factors of the other atoms, equation (3.64) indicates that the signs of almost all the structure factors $h0l$ are positive. The projection of the molecule (Fig. 3.43) is revealed by the summation of a two-dimensional Fourier series using the structure factors $F(h0l) = +|F_{\text{observed}}(h0l)|$.

In general, knowledge of the heavy atom positions alone is not sufficient for the determination of all the phases. The Fourier series using these phases will show only a few of the light atoms, in particular those which are located in the neighborhood of the heavy atom. The process is then repeated. The set of known atomic positions will provide a better estimation of the phases and the subsequent Fourier series will reveal additional atomic positions.

(c) Biguanidinium sulfate, $[\text{H}_2\text{bg}][\text{SO}_4]\cdot\text{H}_2\text{O}$

This example illustrates the utilization of the space group symmetry. $[\text{H}_2\text{bg}]$ is an abbreviation for the dication of biguanide,



The cell is orthorhombic, $a = 7.208$, $b = 11.805$, $c = 20.507 \text{ \AA}$. The systematic absences are $0kl: k = 2n$, $h0l: l = 2n$, $hk0: h = 2n$; hence, we deduce that the space group is **Pbca**. The density is 1.65 g cm^{-3} , hence the unit cell contains eight units of formula $\text{C}_2\text{H}_{11}\text{N}_5\text{O}_5\text{S}$ (Section 2.8). First we look for the positions of the sulfur atoms with the help of the space group symmetry, the S–S vectors being the most important in the Patterson function.

According to the *International Tables for Crystallography* (Section 2.7.3), the general position in **Pbca** has a multiplicity of 8; thus eight sulfur atoms may occupy the eight equivalent general positions:

$$\begin{array}{cccc}
 x, y, z; & \frac{1}{2} + x, \frac{1}{2} - y, \bar{z}; & \bar{x}, \frac{1}{2} + y, \frac{1}{2} - z; & \frac{1}{2} - x, \bar{y}, \frac{1}{2} + z; \\
 \bar{x}, \bar{y}, \bar{z}; & \frac{1}{2} - x, \frac{1}{2} + y, z; & x, \frac{1}{2} - y, \frac{1}{2} + z; & \frac{1}{2} + x, y, \frac{1}{2} - z.
 \end{array}$$

We now calculate the 56 vectors between the eight equivalent positions of **Pbca** which should correspond to the highest maxima in the Patterson function. Note that the corresponding space group of the Patterson function is **Pmmm**. The general position of this group also has a multiplicity of 8,

$$\begin{array}{cccc}
 u, v, w; & u, \bar{v}, \bar{w}; & \bar{u}, v, \bar{w}; & \bar{u}, \bar{v}, w; \\
 \bar{u}, \bar{v}, \bar{w}; & \bar{u}, v, w; & u, \bar{v}, w; & u, v, \bar{w}.
 \end{array}$$

The list of the 56 vectors is

	[$\pm 2x,$	$\pm 2y,$	$\pm 2z$]	8 vectors
double	[$\frac{1}{2},$	$\frac{1}{2} \pm 2y,$	$\pm 2z$]	8 vectors
double	[$\pm 2x,$	$\frac{1}{2},$	$\frac{1}{2} \pm 2z$]	8 vectors
double	[$\frac{1}{2} \pm 2x,$	$\pm 2y,$	$\frac{1}{2}$]	8 vectors
quadruple	[$\frac{1}{2} \pm 2x,$	$\frac{1}{2},$	0]	8 vectors
quadruple	[0,	$\frac{1}{2} \pm 2y,$	$\frac{1}{2}$]	8 vectors
quadruple	[$\frac{1}{2},$	0,	$\frac{1}{2} \pm 2z$]	8 vectors

Thus, we should find in one asymmetric region of the cell $0 \leq u, v, w \leq \frac{1}{2}$, one maximum in a general position, three maxima of double the intensity on each of the three mirror planes **m** perpendicular to **a** ($u = \frac{1}{2}$), **b** ($v = \frac{1}{2}$) and **c** ($w = \frac{1}{2}$), and three maxima of quadruple intensity on the twofold axes $[u, \frac{1}{2}, 0]$, $[0, v, \frac{1}{2}]$, $[\frac{1}{2}, 0,$

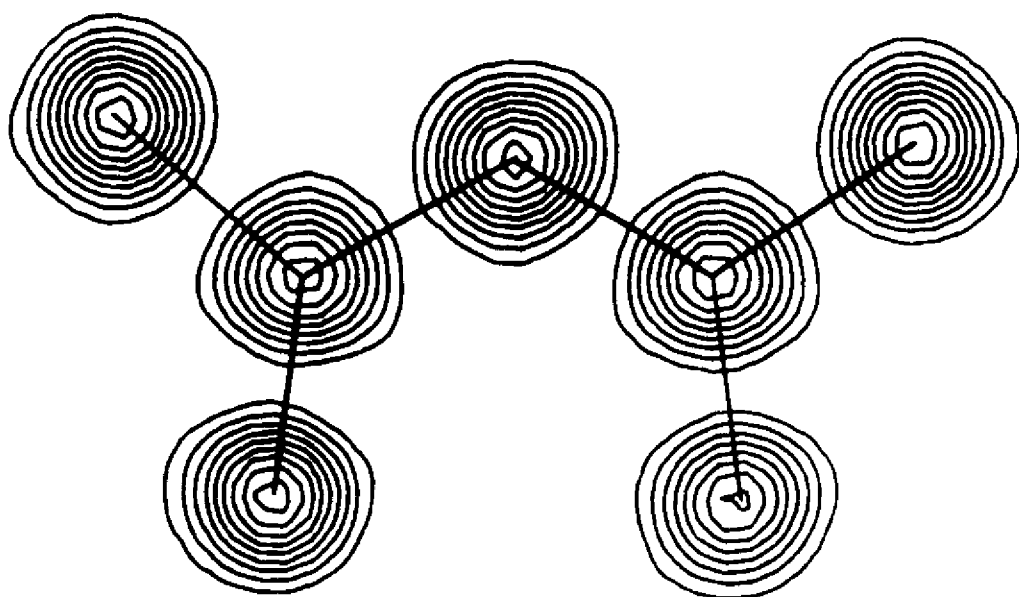


Fig. 3.44. Electron density of $[\text{H}_2\text{bg}]^{+2}$. The contour interval is $1.5 e \text{ \AA}^{-3}$. The hydrogen atoms are not visible

w]. The Patterson function of $[\text{H}_2\text{bg}][\text{SO}_4] \cdot \text{H}_2\text{O}$ contains all these maxima. From this the coordinates of S are deduced: $x = 0.064$; $y = 0.236$; $z = 0.134$. Several cycles of structure factor calculations followed by the summations of the Fourier series reveal all the other atomic sites. The agreement between the $|F_{\text{observed}}|^2$ and the $|F_{\text{calculated}}|^2$ is then optimized by refining the positions and the displacement factors U_{ij} according to equation (3.33) using least squares methods. For $[\text{H}_2\text{bg}][\text{SO}_4] \cdot \text{H}_2\text{O}$, the average difference between the 1547 measured structure amplitudes and those calculated from the final coordinates is

$$R = \frac{\sum \{ |F_{\text{observed}}| - |F_{\text{calculated}}| \}}{\sum |F_{\text{observed}}|} = 0.046$$

Figure 3.44 shows the electron density in the plane of the molecule. By counting the number of contour lines for each atom, it is easy to distinguish C from N. The electron density at the center of N is $14.5 e \text{ \AA}^{-3}$ and at the center of C $12.5 e \text{ \AA}^{-3}$. The electron density of H is too small to be visible in this figure, but these atoms can, in fact, be seen by choosing a finer contour interval.

The heavy atom method may be used to determine structures with more than 100 independent atoms. However, it cannot be used to determine structures composed of similar atoms, as is the case for many organic molecules and for many alloys. In order to determine structures of this type, algebraic (*direct*) methods are available, however, they are beyond the scope of this book. Readers interested in the area of structure determination are referred to the numerous specialized books.

CHAPTER 4

Tensor Properties of Crystals

4.1 ANISOTROPY AND SYMMETRY

Crystalline matter is *anisotropic* (Section 1.1). Hence, a number of its properties are dependent on the direction of observation. Thus, electrical conductivity may depend on the orientation of the electrical potential applied to the crystal; Young's modulus which describes the linear strain of a material resulting from a linear stress is equally a function of direction. In contrast, no property of an isotropic material has directional dependence. Anisotropy is also the source of characteristic properties that are lacking in isotropic materials. As examples, we may consider piezoelectricity (coupling between mechanical force and electric polarization) and birefringence. With the longitudinal effects, additional transverse effects may occur. In a crystal, an electric current does not necessarily flow parallel to the applied electric field. In general, a crystal under a longitudinal stress will undergo not only a longitudinal dimension change but also shear.

The description of anisotropic crystal properties is based on the concept of symmetry. The macroscopic symmetry of a crystal is described by one of the 32 crystallographic point groups (crystal classes, Sections 2.5.4 and 2.5.5). We remember that the symmetry elements generating these groups are the rotation axes x and the rotoinversion axes \bar{x} which link the *directions* which are equivalent with respect to all the properties. Thus the strains of a tetragonal crystal subjected to longitudinal stress parallel to $[uvw]$, or $[\bar{v}uw]$, or $[\bar{u}\bar{v}w]$, or $[v\bar{u}w]$ must be equivalent. Indeed, the symmetry of a crystal is determined by studying the symmetry of its properties. The external shape, for example, expresses the anisotropy of the rate of crystal growth; the phenomenon of diffraction also provides evidence for equivalent directions (Laue method, Section 3.5.1); measurements of conductivity, elasticity or piezoelectricity can all contribute to the determination of the symmetry of a crystal. Isotropy, i.e. the equivalence of all directions in space, implies at least the pure rotation group $\infty\infty$ (Section 2.5.6).

A crystal property may, however, have intrinsic symmetry. Thus, according to Friedel's law of diffraction (Section 3.7.3), the intensities hkl and $\bar{h}\bar{k}\bar{l}$ are approximately equal, even for a non-centrosymmetric crystal. The intrinsic symmetry of

diffraction is thus (approximately) $\bar{1}$. The observation of a single property is generally not sufficient to determine the symmetry. The real symmetry of a crystal may be a sub-group of that deduced from the observations.

The origin of the anisotropic macroscopic properties of a crystal is its ordered microscopic structure, i.e. the crystal lattice which is demonstrated by the diffraction of X-rays. This order which gives rise to these very special effects has been characterized by W. Voigt (*Lehrbuch der Kristallphysik*, 1910) in the following manner:

Imagine several hundred excellent violinists all playing the same piece with perfectly tuned instruments in a large room. However, they start to play the piece from different places, each playing for himself with no consideration for the other violinists. The effect would be hardly delightful; it would be a pitiful mixture of sounds, characteristic, not of the piece being performed, but only of the average of all the notes played. This is the music of molecules in gases and liquids. These are perhaps very talented molecules with a marvelous architecture, but each one disturbs the others in their activity. The crystal corresponds to the same orchestra directed by a capable conductor. The piece performed is now shown to advantage, the melody and the rhythm are now reinforced and not destroyed by the large number of musicians. This image shows us that crystals possess properties that are lacking in other bodies or which are expressed in drab and monotonous ways in gases and liquids. The music of the laws of physics manifests itself in the physics of crystals by the most rich and beautiful chords.

The applications of crystallography in modern technology are many. The development of the technology of high frequencies, semiconductors and lasers are based on crystal properties. In this chapter we will only develop a few fundamental ideas. Non-tensor properties (crystal growth, hardness, cleavage, phase transitions) will not be discussed.

4.2 TENSORS

4.2.1 CAUSE AND EFFECT

In order to avoid the mathematical difficulties associated with the metric (Section 1.2), in crystal physics we use only unitary coordinate systems: three mutually perpendicular axes $\mathbf{e}_1, \mathbf{e}_2, \mathbf{e}_3$ of length $\|\mathbf{e}_i\| = 1$. In this coordinate system, a vector \mathbf{A} is represented by a 3×1 matrix (a *column vector*); the transposed representation \mathbf{A}^T is a *line vector*.

A physical property is the relation between two measurable quantities which, in themselves, represent no property of the material in question. The density is the

mass divided by the volume; the electrical conductivity is the current density divided by the electric field strength. In the second example, the conductivity appears as the relation between two vectors which is represented only by a scalar (number) for the case where the two vectors are parallel.

Let us represent the electric current density by the vector $\mathbf{J} = (J_1, J_2, J_3)$ and the electric field by $\mathbf{E} = (E_1, E_2, E_3)$. The general relation between the two vectors is represented by the functions:

$$\left. \begin{aligned} J_m &= J_m(E_1, E_2, E_3); \quad m = 1 \text{ to } 3 \\ J_m(000) &= 0 \end{aligned} \right\} \tag{4.1}$$

We develop J_m into a Taylor series about the point (0, 0, 0):

$$\begin{aligned} J_m(E_1, E_2, E_3) &= \sum_n \frac{\partial J_m}{\partial E_n} E_n + \frac{1}{2!} \sum_n \sum_p \frac{\partial^2 J_m}{\partial E_n \partial E_p} E_n E_p + \dots \\ J_m(\mathbf{E}) &= \sum_n \sigma_{mn} E_n + \sum_n \sum_p \sigma'_{mnp} E_n E_p + \dots \end{aligned} \tag{4.2}$$

We call σ_{mn} and σ'_{mnp} *tensors*. The number of indices is the *rank* of the tensor.

- rank 0: 1 coefficient, scalar (density, temperature);
- rank 1; 3 coefficients, vector (electric field);
- rank 2; 9 coefficients (linear conductivity);
- rank 3; 27 coefficients (non-linear conductivity, piezoelectricity);
- rank 4; 81 coefficients (linear elasticity);
- etc.

Hence, the physical properties of materials are represented by tensor equations:

$$\begin{matrix} \text{effect} & = & \text{property} * & \text{cause} \\ \mathbf{B} & & \boldsymbol{\sigma} & \mathbf{A} \end{matrix} \tag{4.3}$$

If the cause \mathbf{A} is a tensor of rank M and the effect \mathbf{B} a tensor of rank N , then the linear property $\boldsymbol{\sigma}$ is a tensor of rank $M + N$:

$$\begin{matrix} B_{mnop} & = & \sum_{rstu\dots} & \sigma_{mnop\dots rstu\dots} & A_{rstu\dots} \\ N & & & M + N & M \end{matrix} \tag{4.4}$$

Non-linear properties are of rank $M + N + 1, M + N + 2, \dots$

It is clear that a consequence of the tensor equation for the conductivity (4.2) is that \mathbf{E} and \mathbf{J} are not necessarily parallel, and that the absolute value $\|\mathbf{J}\|$ is a function of the direction of \mathbf{E} . The property is thus anisotropic. Isotropy is characterized by the equation $\sigma_{ij} = \delta_{ij}\sigma$. Figure 4.1 shows an example of a tensor relationship.

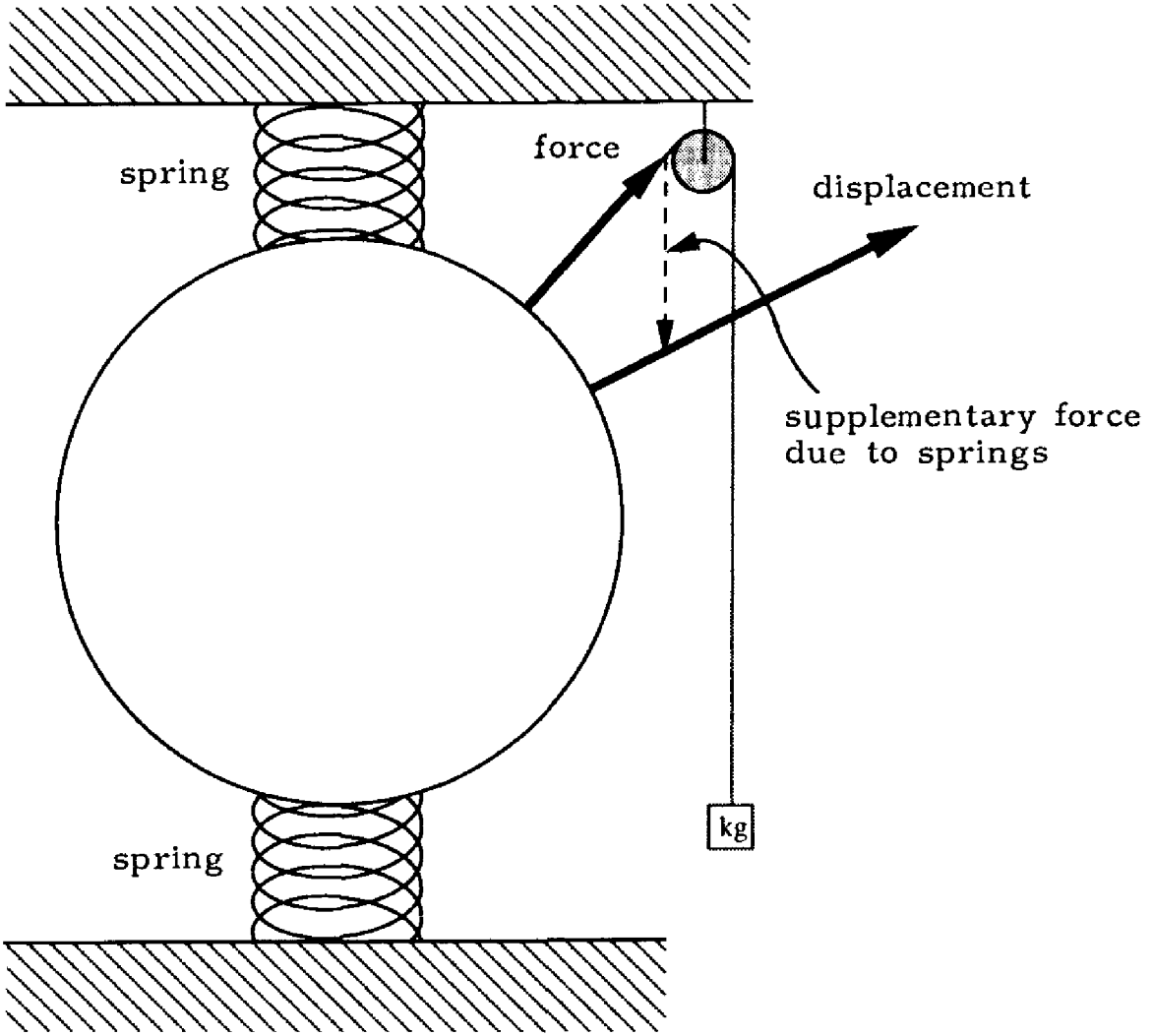


Figure 4.1. The displacement of a ball suspended between two springs is not generally parallel to the applied force

4.2.2 INVARIANCE WITH RESPECT TO THE CHOICE OF COORDINATE SYSTEM

A tensor of rank 2 can be represented by a 3×3 matrix (three-dimensional space \mathbb{R}^3). However, this must not be confused with a matrix which describes a change in coordinate system. A physical magnitude is invariant with respect to a change in coordinates. In particular, the norm of a vector ($\|\mathbf{E}\|^2$, $\|\mathbf{J}\|^2$) and the scalar product of two vectors $(\mathbf{E} \cdot \mathbf{J}) = \mathbf{E}^T \mathbf{J} = \mathbf{J}^T \mathbf{E}$ must be independent of the chosen coordinate system.

A change in coordinate system is represented by an orthogonal transformation matrix \mathbf{U} (unitary coordinate system),

$$\begin{pmatrix} \mathbf{e}'_1 \\ \mathbf{e}'_2 \\ \mathbf{e}'_3 \end{pmatrix} = \begin{pmatrix} u_{11} & u_{12} & u_{13} \\ u_{21} & u_{22} & u_{23} \\ u_{31} & u_{32} & u_{33} \end{pmatrix} \begin{pmatrix} \mathbf{e}_1 \\ \mathbf{e}_2 \\ \mathbf{e}_3 \end{pmatrix} = \mathbf{U} \begin{pmatrix} \mathbf{e}_1 \\ \mathbf{e}_2 \\ \mathbf{e}_3 \end{pmatrix},$$

$|\mathbf{U}| = \pm 1$, $\mathbf{U}^{-1} = \mathbf{U}^T$ (\mathbf{U}^T is the transpose of matrix \mathbf{U} , Section 2.2.3).

The vectors \mathbf{E} and \mathbf{J} transform according to

$$\begin{aligned} \mathbf{E}' &= \mathbf{U}\mathbf{E}, \mathbf{J}' = \mathbf{U}\mathbf{J}, \mathbf{E}'^T \mathbf{J}' = \mathbf{E}^T \mathbf{U}^T \mathbf{U} \mathbf{J} = \mathbf{E}^T \mathbf{J}, \\ E'_m &= \sum_n^3 u_{mn} E_n; J'_m = \sum_n^3 u_{mn} J_n. \end{aligned} \tag{4.5}$$

The conductivity links equally \mathbf{J} and \mathbf{E} , and \mathbf{J}' and \mathbf{E}' :

$$\mathbf{J} = \boldsymbol{\sigma}\mathbf{E}, \mathbf{J}' = \boldsymbol{\sigma}'\mathbf{E}'.$$

The invariance of the product $\mathbf{J} \cdot \mathbf{E} = \mathbf{J}' \cdot \mathbf{E}'$ shows that $\mathbf{E}^T \boldsymbol{\sigma} \mathbf{E}$ must be invariant. By using equation (4.5) we can write

$$\begin{aligned} \mathbf{U}^{-1} \mathbf{J}' &= \boldsymbol{\sigma} \mathbf{U}^{-1} \mathbf{E}', \text{ thus } \mathbf{J}' = \mathbf{U} \boldsymbol{\sigma} \mathbf{U}^T \mathbf{E}', \\ \boldsymbol{\sigma}' &= \mathbf{U} \boldsymbol{\sigma} \mathbf{U}^T, \\ \sigma'_{mn} &= \sum_p^3 \sum_q^3 u_{mp} u_{nq} \sigma_{pq}. \end{aligned} \tag{4.6}$$

For tensors of higher rank (which can no longer be described by matrices), we proceed in an analogous manner. Thus, when expressing equation (4.4) in two different coordinate systems,

$$\mathbf{B}(\text{rank } N) = \boldsymbol{\sigma}(\text{rank } M + N) \mathbf{A}(\text{rank } M),$$

and

$$\mathbf{B}'(\text{rank } N) = \boldsymbol{\sigma}'(\text{rank } M + N) \mathbf{A}'(\text{rank } M),$$

and, by knowing the transformations of the tensors of rank M and N , we can derive the transformation of the tensor of rank $M + N$. For a tensor of rank τ , we obtain:

$$\begin{aligned} \sigma'_{mnop\dots} &= \sum_{rstu\dots}^3 u_{mr} u_{ns} u_{ot} u_{pu} \dots \sigma_{rstu\dots} \\ \tau & \qquad \qquad \tau \text{ factors} \qquad \qquad \tau \end{aligned} \tag{4.7}$$

The idea of a tensor may be characterized by using equation (4.7). A tensor is defined by its transformation properties. In other words, a tensor represents an entity whose description is independent of the choice of coordinate system.

Let $\mathbf{x} = (x_1, x_2, x_3)$ be a vector of coordinates that transform like equation (4.5). Thus the products of τ coordinates transform according to equation (4.7):

$$x'_m = \sum_p^3 u_{mp} x_p; \text{ hence } x'_m x'_n = \sum_p^3 \sum_q^3 u_{mp} u_{nq} x_p x_q, \quad (\tau = 2) \tag{4.8}$$

$$x'_m x'_n x'_o = \sum_{pqr}^3 u_{mp} u_{nq} u_{or} x_p x_q x_r. \quad (\tau = 3) \tag{4.9}$$

The products $x_m x_n$ have the properties of a tensor of rank 2, the products $x_m x_n x_o$ those of a tensor of rank 3, etc. However, here we are concerned with tensors which are totally symmetric with respect to the indices. Because $x_m x_n = x_n x_m$, the term (12) is equal to the term (21); for the case of $\tau = 3$, the terms (123), (231), (312), (213), (132), (321) are all the same. Taking this constraint into account, the products of the coordinates allow us to rapidly obtain the transformation of a tensor.

EXAMPLE $(x'_1, x'_2, x'_3) = (x_1, x_2, -x_3)$

$$x_i'^2 = x_i^2 \quad (i = 1, 2, 3)$$

$$x'_1 x'_2 = x_1 x_2$$

$$x'_1 x'_3 = -x_1 x_3$$

$$x'_2 x'_3 = -x_2 x_3$$

Hence, an inversion of the coordinate e_3 into $-e_3$ transforms the tensor σ into

$$\sigma' = \begin{pmatrix} \sigma_{11} & \sigma_{12} & -\sigma_{13} \\ \sigma_{21} & \sigma_{22} & -\sigma_{23} \\ -\sigma_{31} & -\sigma_{32} & \sigma_{33} \end{pmatrix}.$$

If the transformation matrix U permutes the coordinates x_i , it is generally necessary to apply relation (4.7) which is easy to program for numerical calculations by computer.

4.2.3 NEUMANN PRINCIPLE

We stated above that the physical properties of a crystal correspond to its symmetry. In fact, a symmetry operation represents an invariance with respect to all the properties of a crystal. The symmetry of a property (e.g. the conductivity) can, however, be higher than that of the crystal. This is the origin of the *Neumann principle*:

The symmetry group of any property is a super-group, either trivial or non-trivial, of the point group of the crystal.

It follows that the symmetry of a crystal is a sub-group common to all the symmetry groups of its properties.

As an example, let us describe the case of the tensor, σ_{mn} , of rank 2:

- Center of symmetry $\bar{1}$. A center of symmetry transforms the vector \mathbf{x} into $\mathbf{x}' = -\mathbf{x} = (-x_1, -x_2, -x_3)$. The products of two coordinates are thus invariant, $x'_m x'_n = x_m x_n$, and the transformation $\bar{1}$ does not change the representation of the tensor: $\sigma'_{mn} = \sigma_{mn}$. Thus a tensor of rank 2 has the intrinsic symmetry $\bar{1}$; the corresponding property is centrosymmetric, even if the crystal is not. If

the direction of the electric field is reversed, so is the direction of the current flow. This is not so for non-linear conductivity.

- Reflection m perpendicular to e_3 . The vector x transforms into $x' = (x_1, x_2, -x_3)$. The transformation of σ_{mn} was described above (Section 4.2.2):

$$\sigma'_{mn} = \begin{cases} -\sigma_{mn}, & \text{for } m \neq n; m \text{ or } n = 3 \\ \sigma_{mn} & \text{otherwise} \end{cases}$$

If the crystal has symmetry m (e_3 perpendicular to the mirror plane), the tensor must also have this same symmetry, $\sigma'_{mn} = \sigma_{mn}$, and consequently $\sigma_{13} = \sigma_{23} = \sigma_{31} = \sigma_{32} = 0$. From the tensor's own symmetry of $\bar{1}$, it follows that this condition is equally valid for the groups 2 and $2/m$:

$$\sigma = \begin{pmatrix} \sigma_{11} & \sigma_{12} & 0 \\ \sigma_{21} & \sigma_{22} & 0 \\ 0 & 0 & \sigma_{33} \end{pmatrix} \quad \begin{array}{l} \text{groups } 2, m, 2/m \\ \text{(monoclinic, unique axis } e_3) \end{array} \quad (4.10)$$

- The three orthorhombic groups 222 , $mm2$ and mmm have twofold axes or mirror planes in the three directions e_1 , e_2 and e_3 :

$$\sigma = \begin{pmatrix} \sigma_{11} & 0 & 0 \\ 0 & \sigma_{22} & 0 \\ 0 & 0 & \sigma_{33} \end{pmatrix} \quad \begin{array}{l} \text{groups } 222, mm2, mmm \\ \text{(orthorhombic)} \end{array} \quad (4.11)$$

- Consider the presence of a fourfold axis parallel to e_3 . The vector x transforms into $x' = (-x_2, x_1, x_3)$. Equation (4.6) gives:

$$\sigma' = \begin{pmatrix} \sigma_{22} & -\sigma_{21} & -\sigma_{23} \\ -\sigma_{12} & \sigma_{11} & \sigma_{13} \\ -\sigma_{32} & \sigma_{31} & \sigma_{33} \end{pmatrix}, \text{ and } \sigma' = \sigma \text{ according to Neumann.}$$

We obtain the same result for a threefold, fourfold or sixfold axis. For the Laue classes (Section 2.5.7) $\bar{3}$, $4/m$, $6/m$, we thus obtain:

$$\sigma = \begin{pmatrix} \sigma_{11} & \sigma_{12} & 0 \\ -\sigma_{12} & \sigma_{11} & 0 \\ 0 & 0 & \sigma_{33} \end{pmatrix} \quad \begin{array}{l} \text{groups } \bar{3}, \bar{3} \\ 4, \bar{4}, 4/m \\ 6, \bar{6}, 6/m \end{array} \quad (4.12)$$

- For the classes $4/mmm$, $\bar{3}m$ and $6/mmm$, equation (4.12) combined with the mirror plane perpendicular to e_1 gives:

$$\sigma = \begin{pmatrix} \sigma_{11} & 0 & 0 \\ 0 & \sigma_{11} & 0 \\ 0 & 0 & \sigma_{33} \end{pmatrix} \quad \begin{array}{l} \text{Laue classes} \\ \bar{3}m, 4/mmm, 6/mmm \end{array} \quad (4.13)$$

- A threefold axis down $[111] = e_1 + e_2 + e_3$ transforms x into $x' = (x_2, x_3, x_1)$ from which we derive the conditions $\sigma_{11} = \sigma_{22} = \sigma_{33}$; $\sigma_{12} = \sigma_{23} = \sigma_{31}$; $\sigma_{21} = \sigma_{32} = \sigma_{13}$. For the cubic group 23 , these conditions are added to those

obtained for mmm (4.11). The tensor of rank 2 is thus *isotropic* for the group 23 and equally so for all of the other cubic groups:

$$\sigma = \begin{pmatrix} \sigma & 0 & 0 \\ 0 & \sigma & 0 \\ 0 & 0 & \sigma \end{pmatrix} \quad \begin{array}{l} \text{cubic groups, isotropic with} \\ \text{respect to a tensor of rank 2} \end{array} \quad (4.14)$$

For a *symmetric tensor* of rank 2, $\sigma_{mn} = \sigma_{nm}$. We can distinguish five cases:

<i>triclinic</i>	:	6 terms;	<i>uniaxial</i> 3, 4, 6	:	2 terms;
<i>monoclinic</i>	:	4 terms;	<i>cubic</i>	:	1 term, isotropic;
<i>orthorhombic</i>	:	3 terms.			

4.2.4 POLAR VECTORS AND AXIAL VECTORS

Vectors which transform according to equation (4.5) are called *polar*. The vector product of two polar vectors \mathbf{p} and \mathbf{q} , $\mathbf{r} = \mathbf{p} \times \mathbf{q}$, is equally considered as a vector. The transformation properties of \mathbf{r} , however, differ from those of \mathbf{p} and \mathbf{q} . \mathbf{r} is invariant with respect to a mirror plane perpendicular to the vector and inverted by a mirror plane parallel to the vector. The symmetry of \mathbf{p} and \mathbf{q} is ∞m , that of \mathbf{r} is ∞/m . \mathbf{r} is an *axial vector*. As an example, we cite the magnetic field \mathbf{H} . If the components of \mathbf{p} and \mathbf{q} are p_i and q_i respectively, the components of \mathbf{r} are:

$$\mathbf{r} = (r_1, r_2, r_3) = [(p_2q_3 - p_3q_2), (p_3q_1 - p_1q_3), (p_1q_2 - p_2q_1)]. \quad (4.15)$$

Because it concerns products of coordinates, equation (4.15) transforms like a tensor of rank 2 ((4.6) and (4.8)). Indeed, this is an antisymmetric tensor

$$\mathbf{p} \times \mathbf{q} = \begin{pmatrix} 0 & r_3 & -r_2 \\ -r_3 & 0 & r_1 \\ r_2 & -r_1 & 0 \end{pmatrix}; \quad (\mathbf{p} \times \mathbf{q})_{mn} = p_mq_n - p_nq_m. \quad (4.16)$$

The transformation of $\mathbf{r} \rightarrow \mathbf{r}'$ by the matrix \mathbf{U} is easily obtained by the use of either equation (4.15), or (4.16) and (4.6),

$$r'_1 = (u_{22}u_{33} - u_{23}u_{32})r_1 + (u_{23}u_{31} - u_{21}u_{33})r_2 + (u_{21}u_{32} - u_{22}u_{31})r_3 \quad (4.17)$$

and the analogous expressions for r'_2 and r'_3 . The sub-determinants $u_{mp}u_{nq} - u_{mq}u_{np}$ are proportional to the coefficients v of the inverse matrix \mathbf{U}^{-1} , for example:

$$(u_{23}u_{31} - u_{21}u_{33}) = |\mathbf{U}|v_{21}.$$

For an orthogonal matrix, $|\mathbf{U}| = \pm 1$, $v_{21} = u_{12}$, and equation (4.17) becomes

$$\mathbf{r}' = \pm \mathbf{U}\mathbf{r}, \quad r'_m = \pm \sum_n^3 u_{mn}r_n \quad (4.18)$$

+ for a rotation
- for a rotoinversion

A tensor which connects two axial vectors transforms as one which connects two polar vectors. Thus, the magnetic susceptibility which connects the magnetic field with the magnetization is a polar tensor of rank 2.

In contrast, the electromagnetic susceptibility, i.e. the magnetization of a crystal obtained by the application of an electric field, is described by an axial tensor of rank 2 (also called a pseudo-tensor), which transforms as:

$$\sigma'_{mn} = \pm \sum_p^3 \sum_q^3 u_{mp} u_{nq} \sigma_{pq}, \quad \text{+ for rotation, - for rotoinversion.} \quad (4.19)$$

An axial tensor of rank 2 vanishes in the presence of a center of symmetry $\bar{1}$. For a mirror plane m perpendicular to e_3 , only $\sigma_{13}, \sigma_{23}, \sigma_{31}, \sigma_{32}$ survive, whereas, for a twofold axis, we obtain equation (4.10). In addition, we note that the pseudo-scalar (axial tensor of rank 0) also exists, for example, the rotation power of an optically active solution.

4.2.5 TENSORS OF RANK 2: REFERENCE SURFACE

A general tensor of rank 2 may be considered to be the sum of a symmetric tensor and an antisymmetric tensor:

$$\begin{aligned} \sigma &= \sigma(s) + \sigma(a) \\ \left. \begin{aligned} \sigma(s)_{ij} &= \frac{1}{2}(\sigma_{ij} + \sigma_{ji}); & \sigma(a)_{ij} &= \frac{1}{2}(\sigma_{ij} - \sigma_{ji}) \\ \sigma(s)_{ji} &= \sigma(s)_{ij}; & \sigma(a)_{ji} &= -\sigma(a)_{ij} \end{aligned} \right\} \quad (4.20) \end{aligned}$$

The antisymmetric tensor describes a pure transverse part B_a of the effect $B: B_a = \sigma(a)A, B_a \cdot A = A^T \sigma(a)^T A = 0$ for any vector A . The vector B_a is also perpendicular to the axis of $\sigma(a)$, i.e. the direction of the axial vector $[\sigma(a)_{23}, \sigma(a)_{31}, \sigma(a)_{12}]$. This vector is the real eigenvector of $\sigma(a)$ with an eigenvalue of zero. The vector B_a must not be confused with the transverse part B_T described below.

It turns out that B_a is difficult to measure experimentally. However, the majority of the tensors of rank 2 of physical interest are symmetric with $\sigma(a) = 0$. We will derive this characteristic for equilibrium properties (Sections 4.4.1, 4.4.2 and 4.4.6).

The tensor relation $B = \sigma A$ implies that B and A are not necessarily parallel, even if σ is symmetric. The longitudinal effect is the projection of B onto A , $B_L = B \cdot A / \|A\|$. The longitudinal property is thus $\sigma_L = B \cdot A / \|A\|^2$ as $B_L = \sigma_L A$. The transverse effect is perpendicular to $A: B_T \cdot A = 0; B = B_L + B_T = \sigma_L A + B_T$. If the vector A is represented by its direction cosines $A = (A_1, A_2, A_3) =$

$\|\mathbf{A}\|(l_1, l_2, l_3); l_1^2 + l_2^2 + l_3^2 = 1$, we obtain:

$$\begin{aligned} B_m &= \|\mathbf{A}\| \sum_n^3 \sigma_{mn} l_n, \\ \mathbf{B} \cdot \mathbf{A} &= \sum_m^3 A_m B_m = \|\mathbf{A}\|^2 \sum_m^3 \sum_n^3 \sigma_{mn} l_m l_n, \\ \sigma_L &= \sum_m^3 \sum_n^3 \sigma_{mn} l_m l_n. \end{aligned} \quad (4.21)$$

For the transverse tensor, we find that $(\sigma_T)_{mn} = \sigma_{mn} - \delta_{mn} \sigma_L$, $\mathbf{B}_T = \sigma_T \mathbf{A}$. Note that this is not the antisymmetric tensor described above.

We can equally define a longitudinal effect for each direction $\mathbf{l} = (l_1, l_2, l_3)$ as well as transverse effects (Section 4.4.2) for tensors of rank superior to 2.

In certain directions, the transverse effect \mathbf{B}_T is absent. For tensors of rank 2, it is sufficient to calculate the eigenvectors of the matrix σ . Effectively, $\mathbf{B}_T = \mathbf{0}$ if \mathbf{A}_0 satisfies

$$\mathbf{B} = \sigma \mathbf{A}_0 = \lambda \mathbf{A}_0, \quad (\sigma - \lambda \mathbf{E}) \mathbf{A}_0 = \mathbf{0},$$

\mathbf{E} being the unit matrix, $E_{mn} = \delta_{mn}$. If σ is symmetric, the three vectors \mathbf{A}_0 and eigenvalues λ are real.

The tensor σ may be represented by a second-order surface

$$\sum_{m=1}^3 \sum_{n=1}^3 \sigma_{mn} x_m x_n = 1.$$

This expression represents only the symmetric part because, for $m \neq n$ we obtain the term $(\sigma_{mn} + \sigma_{nm})x_m x_n$. Let us suppose that the *eigenvalues* of σ are *all positive*. The surface is then an ellipsoid:

$$\left. \begin{aligned} \sigma_{11}x_1^2 + \sigma_{22}x_2^2 + \sigma_{33}x_3^2 + 2\sigma_{12}x_1x_2 + 2\sigma_{13}x_1x_3 + 2\sigma_{23}x_2x_3 = 1 \end{aligned} \right\} \quad (4.22)$$

reference ellipsoid

Let \mathbf{r} be the vector directed from the origin to the point $P(x_1, x_2, x_3)$ on the ellipsoid.

$$(x_1, x_2, x_3) = r(l_1, l_2, l_3), \quad l_i = \text{the direction cosine of } \mathbf{r}, \text{ and } r = \|\mathbf{r}\|,$$

$$\sum_m^3 \sum_n^3 \sigma_{mn} x_m x_n = r^2 \sum_m^3 \sum_n^3 \sigma_{mn} l_m l_n = r^2 \sigma_L = 1,$$

$$r = \frac{1}{\sqrt{\sigma_L}} \quad (\text{Fig. 4.2}). \quad (4.23)$$

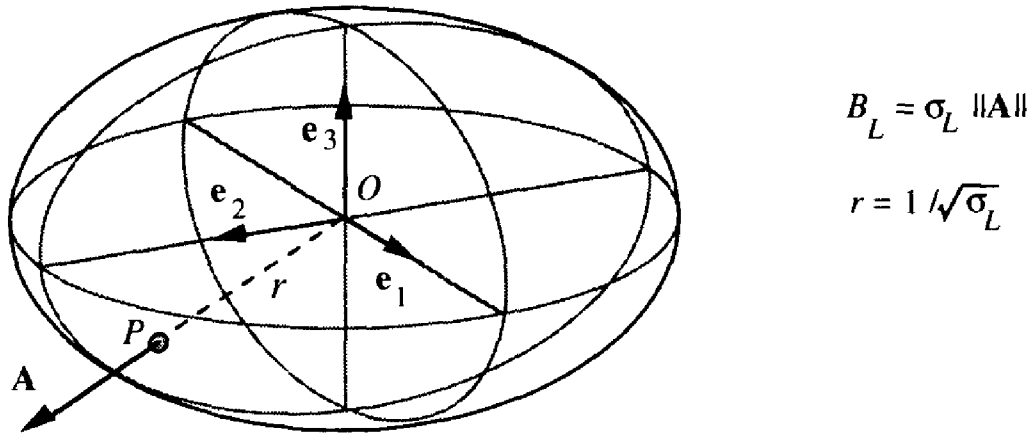


Fig. 4.2. The distance from the origin O to the point $P(x_1, x_2, x_3)$ in the direction of the vector \mathbf{A} (e.g. the electric field) is equal to $r = 1/\sqrt{\sigma_L}$, σ_L being the longitudinal property (e.g. the longitudinal conductivity parallel to the electric field)

The plane tangent to the ellipsoid at the point $P(x_1, x_2, x_3)$ is

$$r \sum_m \left\{ \sum_n \sigma_{mn} l_n \right\} x'_m = p_1 x'_1 + p_2 x'_2 + p_3 x'_3 = \mathbf{p}^T \mathbf{r}' = 1 \tag{4.24}$$

$$\mathbf{p} = \boldsymbol{\sigma} \mathbf{r}, \quad p_m = r \sum_n \sigma_{mn} l_n; \text{ tangent plane}$$

Clearly, the plane $\mathbf{p}^T \mathbf{r}' = \mathbf{r}^T \boldsymbol{\sigma} \mathbf{r}' = 1$ and the ellipsoid $\mathbf{r}^T \boldsymbol{\sigma} \mathbf{r} = \sum_m \sum_n \sigma_{mn} x_m x_n = 1$ have only one point in common: $\mathbf{r}^T \boldsymbol{\sigma} (\mathbf{r} - \mathbf{r}') = 0$ implies that $\mathbf{r} = \mathbf{r}'$ if the eigenvalues of $\boldsymbol{\sigma}$ are all non-zero. The vector \mathbf{p} is normal to the tangent plane. Its direction is the same as that of \mathbf{B} (Fig. 4.3),

$$\mathbf{B} = \boldsymbol{\sigma} \mathbf{A} = (\boldsymbol{\sigma} \mathbf{r}) \frac{\|\mathbf{A}\|}{r} = \frac{\|\mathbf{A}\|}{r} \mathbf{p}. \tag{4.25}$$

By choosing the eigenvectors of $\boldsymbol{\sigma}$ to be the coordinate system, the tensor is reduced to a diagonal matrix whose elements are the eigenvalues $\sigma_I, \sigma_{II}, \sigma_{III}$. The reference ellipsoid becomes $\sigma_I x_1^2 + \sigma_{II} x_2^2 + \sigma_{III} x_3^2 = 1$ and its semi-axes are $1/\sqrt{\sigma_I}, 1/\sqrt{\sigma_{II}}, 1/\sqrt{\sigma_{III}}$. If one or two of the eigenvalues are negative, the reference surface is a hyperboloid. If $\sigma_{III} < 0, \sigma_I$ and $\sigma_{II} > 0$, two surfaces have to be considered:

$$\begin{aligned} \sigma_I x_1^2 + \sigma_{II} x_2^2 - |\sigma_{III}| x_3^2 &= 1, \text{ positive longitudinal effect;} \\ \sigma_I x_1^2 + \sigma_{II} x_2^2 - |\sigma_{III}| x_3^2 &= -1, \text{ negative longitudinal effect.} \end{aligned}$$

Figure 4.4 shows an analogous construction to that of Fig. 4.3.

The point symmetry of an ellipsoid or a hyperboloid is *mmm*. The characteristic symmetry of a symmetric tensor of rank 2 is thus *mmm*. By using the Neumann

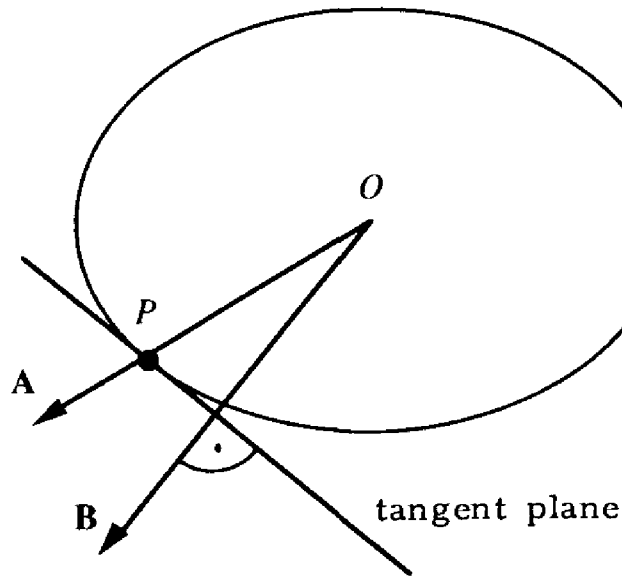


Fig. 4.3. The normal to the tangent plane at the point P of Fig. 4.2 indicates the direction of \mathbf{B} (e.g. \mathbf{A} = electric field, \mathbf{B} = current)

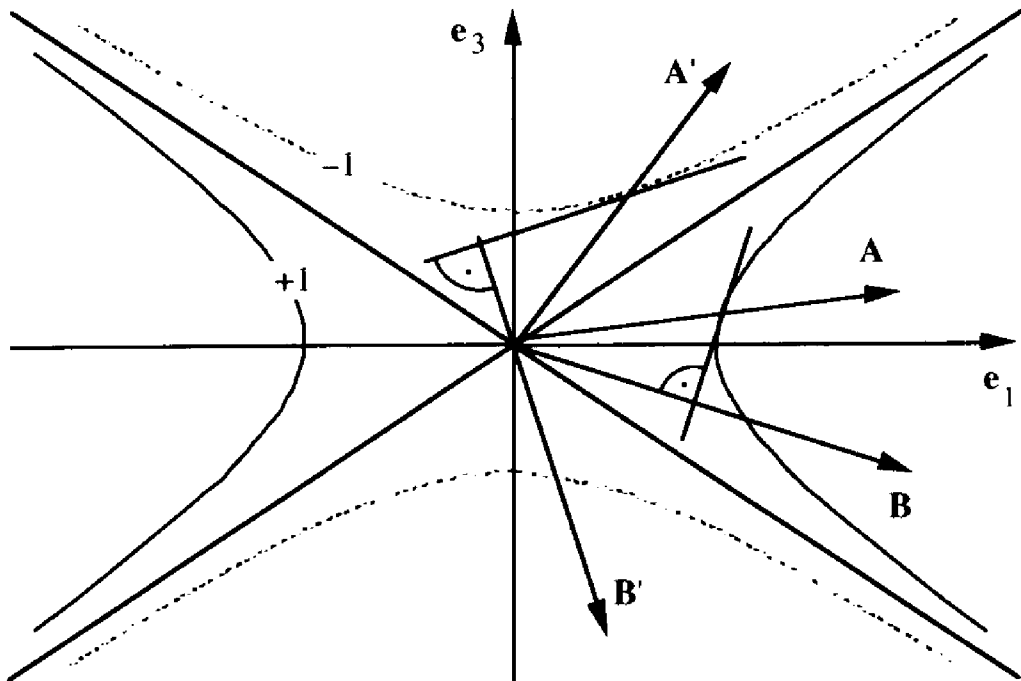


Fig. 4.4. Hyperboloids in the plane $x_2 = 0$. \mathbf{A} , \mathbf{B} : positive longitudinal effect; \mathbf{A}' , \mathbf{B}' : negative longitudinal effect

principle (Section 4.2.3) we can deduce the symmetry of the ellipsoids for the different crystal systems:

- triclinic: the six terms of the tensor correspond to three eigenvalues and to three orientation angles for the ellipsoid; different properties are represented by ellipsoids of different orientations:

- monoclinic: one eigenvector is necessarily parallel to the twofold axis or normal to the mirror plane; the four terms of the tensor (4.10) correspond to three eigenvalues and a single orientation angle;
- orthorhombic: the orientation of the ellipsoid is determined by the symmetry; the three terms of the tensor (4.11) correspond to the three eigenvalues;
- trigonal, tetragonal, hexagonal: the tensor is represented by an ellipsoid of revolution whose principal axis is parallel to the unique axis; the two terms of the tensor (4.13) correspond to the two eigenvalues parallel and perpendicular to the unique axis;
- cubic: the tensor (4.14) is represented by a sphere; all the eigenvalues are identical; the crystal is isotropic with respect to a tensor of rank 2.

An inverse property is represented by the inverse matrix σ^{-1} : $\mathbf{B} = \sigma\mathbf{A}$ hence $\mathbf{A} = \sigma^{-1}\mathbf{B}$. If σ is the conductivity, σ^{-1} is the resistance. The tensor σ^{-1} is represented by the ellipsoid whose principal axes are $\sqrt{\sigma_I}$, $\sqrt{\sigma_{II}}$, $\sqrt{\sigma_{III}}$. For inverse tensors of higher order, no simple analogy with matrices exists.

The norm of \mathbf{B} is given by $\|\mathbf{B}\|^2 = \mathbf{B}^T\mathbf{B} = \mathbf{A}^T\sigma\sigma\mathbf{A}$ (σ symmetric). For the inverse we obtain $\|\mathbf{A}\|^2 = \mathbf{B}^T[\sigma\sigma]^{-1}\mathbf{B}$. If $\mathbf{B} = \|\mathbf{B}\|(b_1, b_2, b_3)$, b_i being the direction cosines of \mathbf{B} , and $[\sigma\sigma]^{-1} = \mathbf{S}$:

$$\|\mathbf{A}\|^2 = \|\mathbf{B}\|^2 \sum_m \sum_n S_{mn} b_m b_n, \text{ and for } \|\mathbf{A}\| = 1:$$

$$\|\mathbf{B}\| = \left(\sum_m \sum_n S_{mn} b_m b_n \right)^{-1/2} \tag{4.26}$$

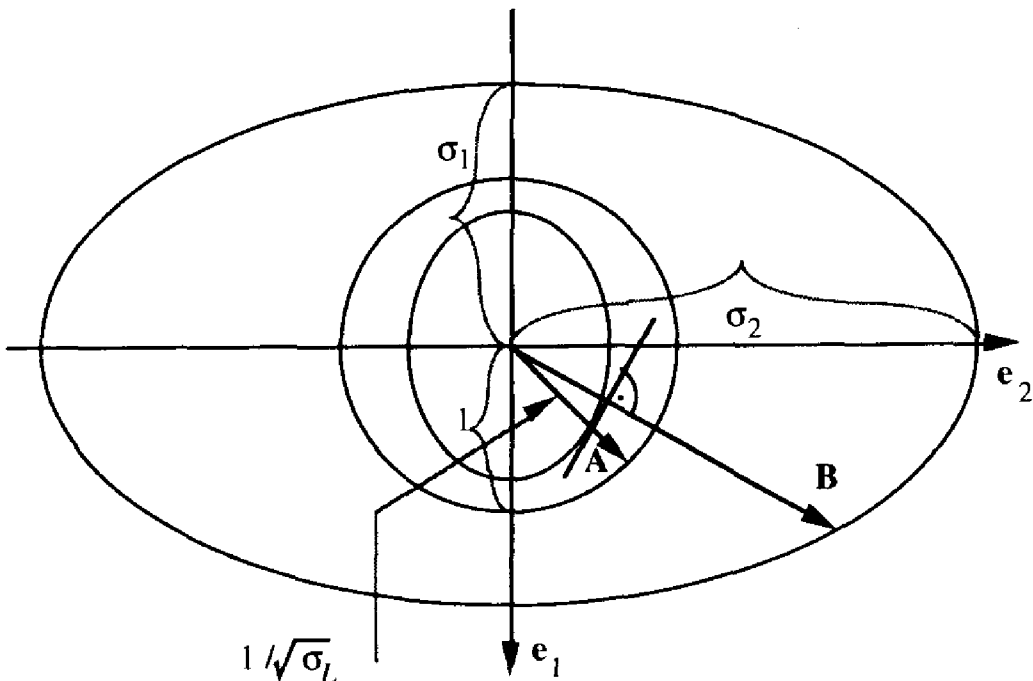


Fig. 4.5. Ellipsoid representing the value of $\|\mathbf{B}\|$ for $\|\mathbf{A}\| = 1$; sphere of radius 1; reference ellipsoid (e.g. \mathbf{A} = electric field, \mathbf{B} = current)

The ellipsoid $\sum\sum S_{mn}x_mx_n = 1$ (Fig. 4.5) represents the value of $\|\mathbf{B}\|$ for $\|\mathbf{A}\| = 1$. Referred to the eigenvectors of σ , its equation becomes:

$$\frac{x_1^2}{\sigma_I^2} + \frac{x_2^2}{\sigma_{II}^2} + \frac{x_3^2}{\sigma_{III}^2} = 1. \quad (4.27)$$

COMMENTS

- It is possible to construct a surface whose radius parallel to \mathbf{A} represents the longitudinal property. However, such a surface would not be second order. The surface

$$r^{-3} \sum_m \sum_n \sigma_{mn} x_m x_n = 1; \quad r = \sqrt{x_1^2 + x_2^2 + x_3^2}$$

has the property that the distance from the origin to the surface in the direction of the vector \mathbf{A} is equal to σ_L .

- In order to determine the tensor σ , the longitudinal effects are measured in different directions (6 for a tensor of rank 2). A possible antisymmetric component would be neglected because it would create only transverse effects.

4.3 STRESSES AND STRAINS

4.3.1 MECHANICAL STRESS TENSOR

Let us consider the forces acting on a volume element of a solid body in the form of a parallelepiped (Fig. 4.6).

A stress is a force per unit area. It acts on two opposite parallel faces (couple). In particular, σ_{mn} is the stress parallel to \mathbf{e}_m acting on the faces perpendicular to \mathbf{e}_n . The stresses σ_{mn} normal to the faces are *positive* in the case of an *extension* of the solid.

The component of the resulting torque in the direction \mathbf{e}_1 is given by:

$$M_1 = \Delta_2 \mathbf{e}_2 \times (\sigma_{32} \Delta_1 \Delta_3) \mathbf{e}_3 + \Delta_3 \mathbf{e}_3 \times (\sigma_{23} \Delta_1 \Delta_2) \mathbf{e}_2 = \delta V (\sigma_{32} - \sigma_{23}) \mathbf{e}_1. \quad (4.28)$$

The torque resulting from all the σ_{mn} is thus:

$$\mathbf{M} = -\delta V [(\sigma_{23} - \sigma_{32}) \mathbf{e}_1 + (\sigma_{31} - \sigma_{13}) \mathbf{e}_2 + (\sigma_{12} - \sigma_{21}) \mathbf{e}_3]. \quad (4.29)$$

This is an axial vector. If the volume element is in equilibrium, $\mathbf{M} = 0$. It thus follows that

$$\sigma_{mn} = \sigma_{nm}. \quad (4.30)$$

The stress tensor is symmetric. For inhomogeneous stresses where σ_{mn} is a function of position, consult J. F. Nye, *Physical Properties of Crystals*.

Let us calculate the forces acting on a plane of orientation $\mathbf{l} = (l_1, l_2, l_3)$; $\|\mathbf{l}\| = 1$. We allow that the tetrahedron in Fig. 4.7 is in equilibrium. The resultant of all of

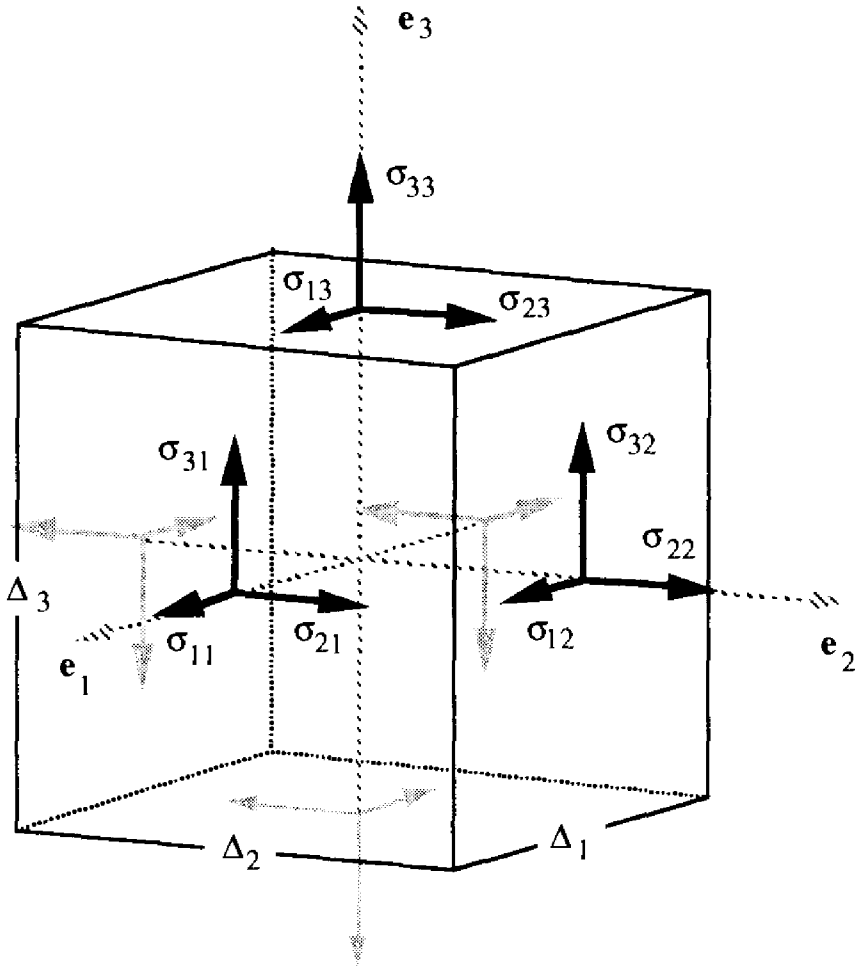


Fig. 4.6. Stresses acting on a parallelepiped in static equilibrium; dimensions $\Delta_1, \Delta_2, \Delta_3$; volume δV

the forces acting on its faces is hence zero. If we represent the area of the triangle OP_iP_j by S_{ij} , for the component f_1 of the force \mathbf{f} , we obtain:

$$f_1 = \sigma_{11}S_{23} + \sigma_{12}S_{13} + \sigma_{13}S_{12}$$

The stress \mathbf{p} is

$$\mathbf{p} = \mathbf{f}/S_{123}, S_{123} \text{ being the area of the triangle } P_1P_2P_3.$$

As the ratio of the areas is $S_{ij}/S_{123} = l_k$ ($i \neq j \neq k \neq i$), it results that

$$p_m = \sum_n^3 \sigma_{mn}l_n; \quad \mathbf{p} = \boldsymbol{\sigma}\mathbf{l}. \tag{4.31}$$

The longitudinal component normal to the plane is equal to

$$p_L = \sum_m^3 \sum_n^3 \sigma_{mn}l_m l_n \tag{4.32}$$

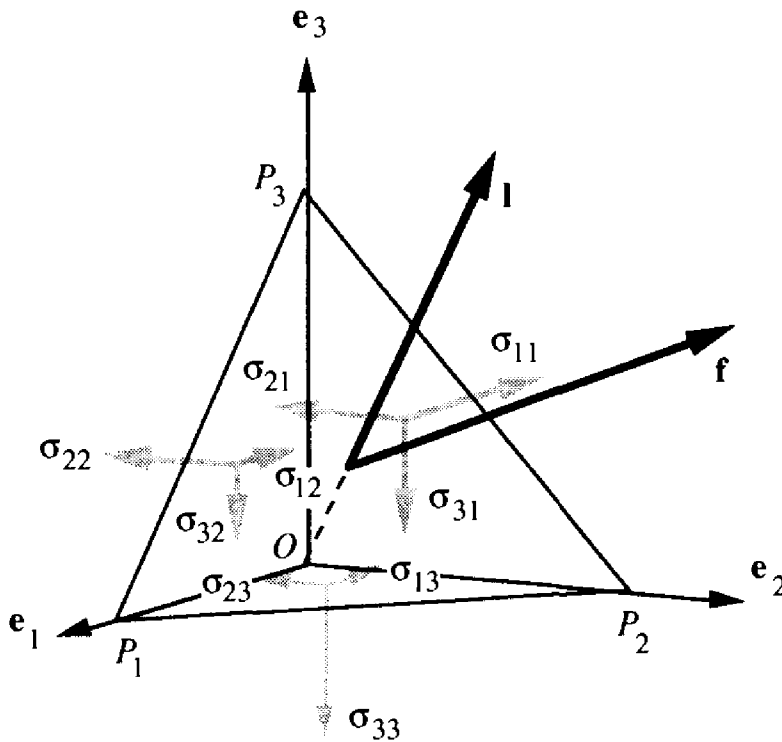


Fig. 4.7. Stresses on the faces of a tetrahedron

The reference ellipsoid $\sum \sum \sigma_{mn} x_m x_n = 1$ represents

- the stress parallel to \mathbf{l} (distance origin-surface = $1/\sqrt{p_L}$);
- the direction of the total stress \mathbf{p} acting on the plane (normal to the tangent plane).

A *uniaxial* stress σ parallel to the direction $\mathbf{l} = (l_1, l_2, l_3)$ is given by the tensor $\sigma_{mn} = \sigma l_m l_n$:

$$\sigma \begin{pmatrix} l_1^2 & l_1 l_2 & l_1 l_3 \\ l_1 l_2 & l_2^2 & l_2 l_3 \\ l_1 l_3 & l_2 l_3 & l_3^2 \end{pmatrix}, \quad \text{uniaxial stress.} \quad (4.33)$$

Indeed, equation (4.31) becomes $p_m = \sigma \sum_n l_m l_n^2 = \sigma l_m$. Any stress can be decomposed into three mutually perpendicular uniaxial stresses (the three eigenvectors and the three eigenvalues of σ). Hydrostatic pressure, for example, is given by

$$-\sigma \begin{pmatrix} 1 & 0 & 0 \\ 0 & 1 & 0 \\ 0 & 0 & 1 \end{pmatrix}.$$

4.3.2 STRAIN TENSOR

The homogeneous longitudinal tensile strain of a solid, of a metal bar, for example (Fig. 4.8), is defined as the expansion per unit length of the undeformed

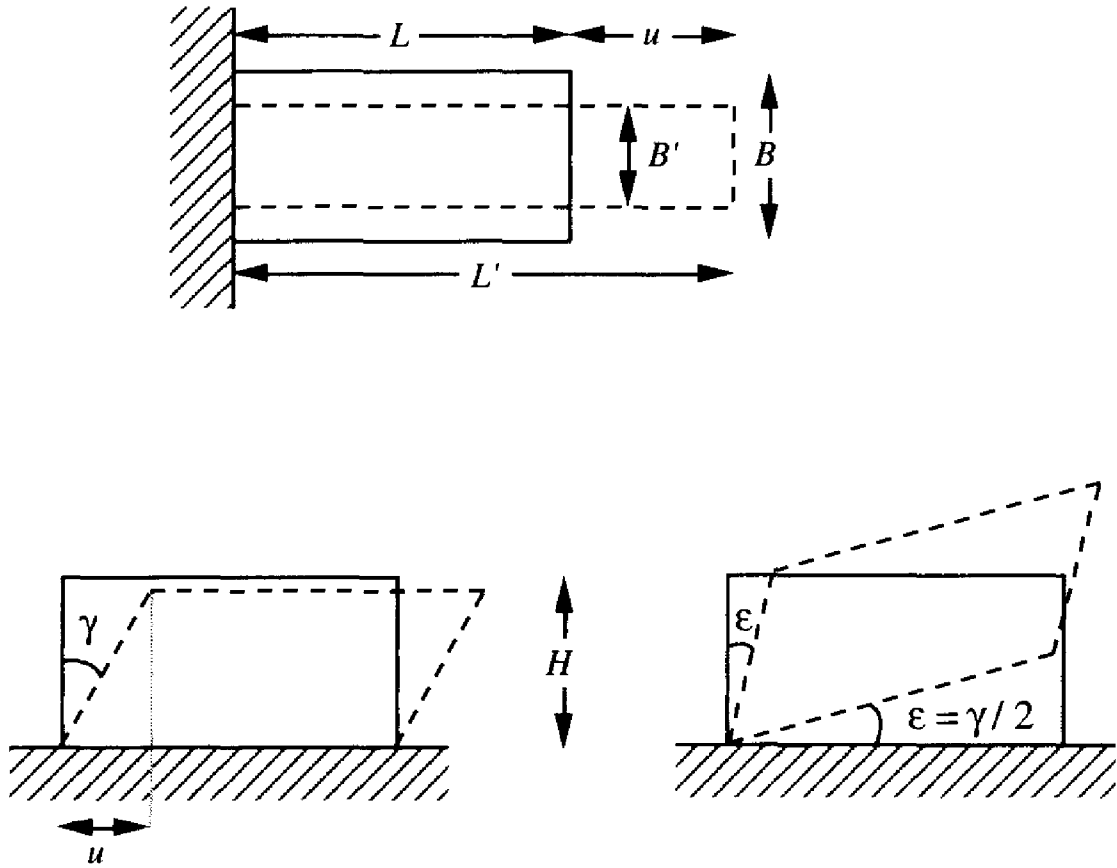


Fig. 4.8. Tensile strain and shear strain

body:

$$\epsilon = \frac{L' - L}{L} = \frac{\mu}{L} \tag{4.34}$$

By analogy, the homogeneous shear strain of a parallelepiped (Fig. 4.8) is the ratio of the displacement caused by the strain to the dimension of the solid perpendicular to the displacement:

$$\gamma = \frac{u}{H} \approx \text{angle of shear} \tag{4.35}$$

A rotation of the deformed body allows us to use the angle $\epsilon = \gamma/2$ as an alternative description.

In general, we measure the homogeneous strain of a solid by the relative displacement of two points P_1 and P_2 separated by the vector \mathbf{r} , keeping the coordinate system invariant (Fig. 4.9). The strain displaces the point $P_1(x_i)$ to the point $P'_1(x_i + \xi_i)$ and the point $P_2(x_i + r_i)$ to $P'_2(x_i + r_i + \xi_i + u_i)$. The vector $\mathbf{r} + \mathbf{u}$ gives the relative position of the two points of the strained solid. By analogy with equation (4.34) and (4.35), the strain tensor $\boldsymbol{\epsilon}$ expresses the displacement \mathbf{u} per unit

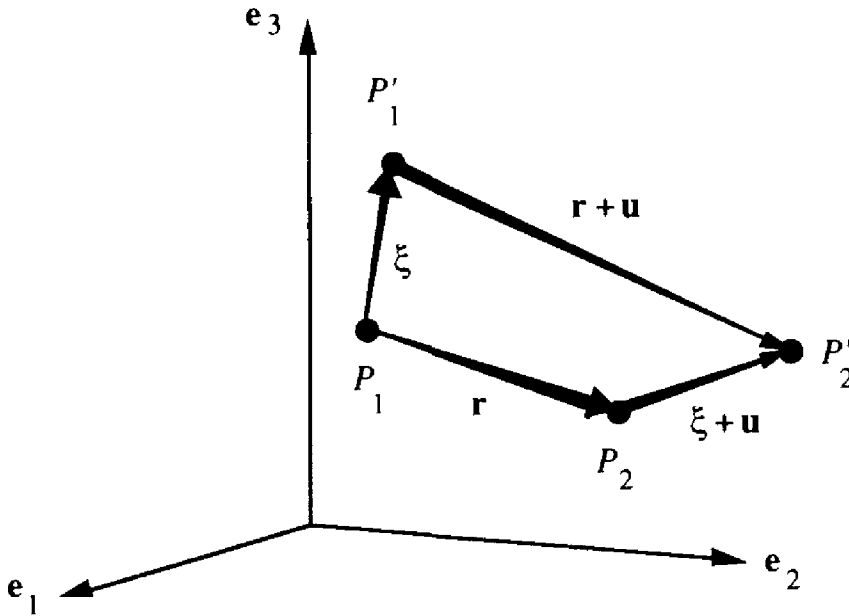


Fig. 4.9. Description of the homogeneous strain of a solid

length of \mathbf{r} . The components of $\mathbf{u}(\mathbf{r})$ may be expanded as a Taylor series,

$$u_m = \sum_n \frac{\partial u_m}{\partial r_n} r_n + \frac{1}{2!} \sum_n \sum_p \frac{\partial^2 u_m}{\partial r_n \partial r_p} r_n r_p + \dots$$

On retaining only the linear terms, we obtain the *strain tensor*,

$$\mathbf{u} = \mathbf{e} \mathbf{r}; \quad e_{mn} = \frac{\partial u_m}{\partial r_n}. \quad (4.36)$$

The e_{mn} are dimensionless numbers.

In the case of inhomogeneous strain, we consider the behavior of two points P_1 and P_2 which are very close together; \mathbf{u} and \mathbf{e} are functions of the position (x_1, x_2, x_3) .

Following equation (4.20), we decompose \mathbf{e} into symmetric and antisymmetric tensors:

$$\varepsilon_{mn} = \frac{1}{2}(\mathbf{e}_{mn} + \mathbf{e}_{nm}); \quad \rho_{mn} = \frac{1}{2}(\mathbf{e}_{mn} - \mathbf{e}_{nm}). \quad (4.37)$$

The antisymmetric part $\boldsymbol{\rho}$ expresses a rotation of the solid around the eigenvector \mathbf{v}_0 of $\boldsymbol{\rho}$ having the eigenvalue 0, $\boldsymbol{\rho} \mathbf{v}_0 = 0$,

$$\mathbf{v}_0 = (\rho_{23}, \rho_{31}, \rho_{12})^T = (\mathbf{e}_{23} - \mathbf{e}_{32}, \mathbf{e}_{31} - \mathbf{e}_{13}, \mathbf{e}_{12} - \mathbf{e}_{21})^T. \quad (4.38)$$

The antisymmetric part of the vector \mathbf{u} , $\mathbf{u}_a = \boldsymbol{\rho} \mathbf{r}$ is perpendicular to \mathbf{r} and to \mathbf{v}_0 : $\mathbf{r}^T \mathbf{u}_a = \mathbf{r}^T \boldsymbol{\rho} \mathbf{r} = 0$, $\mathbf{v}_0^T \mathbf{u}_a = \mathbf{v}_0^T \boldsymbol{\rho} \mathbf{r} = 0$. Consequently \mathbf{u}_a does not contribute to the strain of the solid. The actual strain, obtained after subtraction of the rigid body

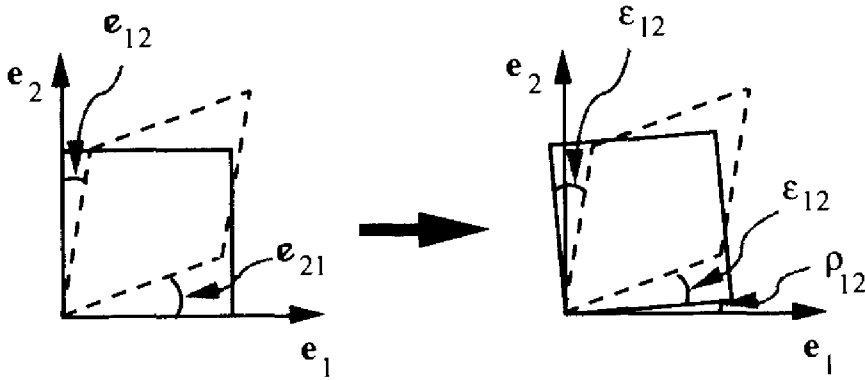


Fig. 4.10. Illustration of the tensors \mathbf{e} , $\boldsymbol{\varepsilon}$ and $\boldsymbol{\rho}$

motion, is expressed by the *symmetric tensor* $\boldsymbol{\varepsilon}$,

$$\mathbf{u} = \boldsymbol{\varepsilon} \mathbf{r}. \tag{4.39}$$

In the case of inhomogeneous strain, local rotations may exist, but they do not contribute to the strain energy. Figure 4.10 illustrates the significance of the tensors \mathbf{e} , $\boldsymbol{\varepsilon}$ and $\boldsymbol{\rho}$. The terms ε_{ii} represent the longitudinal tensile effects (expansions and contractions), whereas the terms ε_{ij} ($i \neq j$) represent shear.

The reference ellipsoid $\sum \varepsilon_{ij} x_i x_j = 1$ represents:

- the tensile strain parallel to \mathbf{l} (distance of origin to surface $1/\sqrt{\varepsilon_L}$);
- the direction of the relative displacement \mathbf{u} of two points separated by the vector \mathbf{l} (normal to the tangent plane).

EXAMPLE. Under the effect of a homogeneous strain $\boldsymbol{\varepsilon}$, a cube of linear dimension D , characterized by the edges $\mathbf{a}_i = D\mathbf{e}_i$ ($i = 1, 2, 3$), is transformed into a parallelepiped. Following equation (4.39), the displacement \mathbf{u}_1 along the edge \mathbf{a}_1 is given by

$$\mathbf{u}_1 = D\{\varepsilon_{11}\mathbf{e}_1 + \varepsilon_{12}\mathbf{e}_2 + \varepsilon_{13}\mathbf{e}_3\} = D\{\varepsilon_{11}, \varepsilon_{12}, \varepsilon_{13}\}.$$

After deformation, the equation of the edge becomes

$$\mathbf{a}'_1 = \mathbf{a}_1 + \mathbf{u}_1 = D\{(1 + \varepsilon_{11}), \varepsilon_{12}, \varepsilon_{13}\}.$$

In an analogous manner, for the other edges, we obtain

$$\begin{aligned} \mathbf{a}'_2 &= D\{\varepsilon_{12}, (1 + \varepsilon_{22}), \varepsilon_{23}\}, \\ \mathbf{a}'_3 &= D\{\varepsilon_{13}, \varepsilon_{23}, (1 + \varepsilon_{33})\}. \end{aligned}$$

By retaining only the linear terms, the strained parallelepiped is characterized by:

$$\begin{aligned} \|\mathbf{a}'_1\| &\approx D(1 + \varepsilon_{11}); & \|\mathbf{a}'_2\| &\approx D(1 + \varepsilon_{22}); & \|\mathbf{a}'_3\| &\approx D(1 + \varepsilon_{33}); \\ \cos \alpha_1 &\approx \frac{2\varepsilon_{23}}{1 + \varepsilon_{22} + \varepsilon_{33}}; & \cos \alpha_2 &\approx \frac{2\varepsilon_{13}}{1 + \varepsilon_{11} + \varepsilon_{33}}; & \cos \alpha_3 &\approx \frac{2\varepsilon_{12}}{1 + \varepsilon_{11} + \varepsilon_{22}}; \\ \alpha_1 &\approx \frac{\pi}{2} - 2\varepsilon_{23}; & \alpha_2 &\approx \frac{\pi}{2} - 2\varepsilon_{13}; & \alpha_3 &\approx \frac{\pi}{2} - 2\varepsilon_{12}. \end{aligned}$$

The volume of the strained cube is approximately:

$$V' = D^3(1 + \varepsilon_{11} + \varepsilon_{22} + \varepsilon_{33}) = V(1 + \varepsilon_{11} + \varepsilon_{22} + \varepsilon_{33}),$$

$$\frac{V' - V}{V} \approx \varepsilon_{11} + \varepsilon_{22} + \varepsilon_{33}. \quad (4.40)$$

Equation (4.40) is a good approximation, independent of the shape of the solid.

4.3.3 VOIGT NOTATION

For some applications it is useful to write the stress and the strain tensors as six-dimensional vectors. The indices are assigned as follows:

tensor:	11	22	33	23	13	12
'vector'	1	2	3	4	5	6

The stress tensor becomes:

$$\begin{pmatrix} \sigma_{11} & \sigma_{12} & \sigma_{13} \\ \sigma_{12} & \sigma_{22} & \sigma_{23} \\ \sigma_{13} & \sigma_{23} & \sigma_{33} \end{pmatrix} \rightarrow \begin{pmatrix} \sigma_1 & \sigma_6 & \sigma_5 \\ \sigma_6 & \sigma_2 & \sigma_4 \\ \sigma_5 & \sigma_4 & \sigma_3 \end{pmatrix} \rightarrow (\sigma_1 \ \sigma_2 \ \sigma_3 \ \sigma_4 \ \sigma_5 \ \sigma_6)^T. \quad (4.41)$$

For the strain we will use the engineers' notation, who prefer to use the angles $2\varepsilon_{ij}$ ($i \neq j$) (Fig. 4.8):

$$\begin{pmatrix} \varepsilon_{11} & \varepsilon_{12} & \varepsilon_{13} \\ \varepsilon_{12} & \varepsilon_{22} & \varepsilon_{23} \\ \varepsilon_{13} & \varepsilon_{23} & \varepsilon_{33} \end{pmatrix} \rightarrow \begin{pmatrix} \varepsilon_1 & \frac{1}{2}\varepsilon_6 & \frac{1}{2}\varepsilon_5 \\ \frac{1}{2}\varepsilon_6 & \varepsilon_2 & \frac{1}{2}\varepsilon_4 \\ \frac{1}{2}\varepsilon_5 & \frac{1}{2}\varepsilon_4 & \varepsilon_3 \end{pmatrix} \rightarrow \varepsilon_k = 2\varepsilon_{ij} \ (i \neq j, \ k = 9 - i - j) \quad (4.42)$$

COMMENT. The 'vectors' only represent a notation! If there is a change in coordinate system, only the rules for the transformation of tensors are applicable.

4.4 EXAMPLES OF TENSOR PROPERTIES

In this section we will present a number of equilibrium properties of crystals such as the electric polarization, elasticity and piezoelectricity. Transport properties will not be covered in this book.

4.4.1 ELECTRIC POLARIZATION: TENSOR OF RANK 2

In a vacuum, the electric displacement \mathbf{D} is proportional to the electric field \mathbf{E} ,

$$\mathbf{D} = \varepsilon_0 \mathbf{E}, \quad (4.43)$$

$$\varepsilon_0 = 8.854188 \times 10^{-12} \text{ C/Vm, permittivity of a vacuum,}$$

$$[D] = \text{Coulomb/m}^2,$$

$$[E] = \text{Volt/m.}$$

$D = \|\mathbf{D}\|$ is the charge density induced into a metal plate, or the charge density necessary to create the field $E = \|\mathbf{E}\|$ in a condenser.

In an isotropic dielectric, the relation between \mathbf{D} and \mathbf{E} is:

$$\mathbf{D} = \epsilon\epsilon_0\mathbf{E}, \tag{4.44}$$

where $\epsilon \geq 1$ is the dielectric constant (relative permittivity) of the material and \mathbf{E} the electric field in the interior of the material. The electric polarization \mathbf{P} is defined by:

$$\begin{aligned} \mathbf{D} &= \epsilon_0\mathbf{E} + \mathbf{P} = \mathbf{D}_0 + \mathbf{P}, \\ \mathbf{P} &= \epsilon_0(\epsilon - 1)\mathbf{E} = \epsilon_0\chi\mathbf{E}, \end{aligned} \tag{4.45}$$

where $\chi \geq 0$ is the electric susceptibility of the material.

\mathbf{P} is the electric dipole moment per unit volume, $P = \|\mathbf{P}\|$ being the polarization charge per unit area normal to the vector \mathbf{P} . $D = \|\mathbf{D}\|$ also expresses the charge density of a condenser required to maintain the field \mathbf{E} at the interior of the dielectric (Fig. 4.11).

COMMENT. The field \mathbf{E} created in the dielectric by a homogeneous field \mathbf{E}_v generally depends on the shape of the dielectric. The dielectric creates a depolarization field \mathbf{E}_d such that $\mathbf{E} = \mathbf{E}_v + \mathbf{E}_d$. Clearly, for the plate represented in Fig. 4.11, these values are given by $\mathbf{E} = \mathbf{E}_v/\epsilon$, hence $\mathbf{E}_d = -(\epsilon - 1)\mathbf{E} = -\chi\mathbf{E}$ and $\mathbf{P} = -\epsilon_0\mathbf{E}_d$. For a long bar of isotropic material whose axis is parallel to \mathbf{E}_v , $\mathbf{E} = \mathbf{E}_v$ and $\mathbf{E}_d = 0$ because the field is continuous across the vacuum/solid interface. In general, \mathbf{E} is not homogeneous, even if \mathbf{E}_v is.

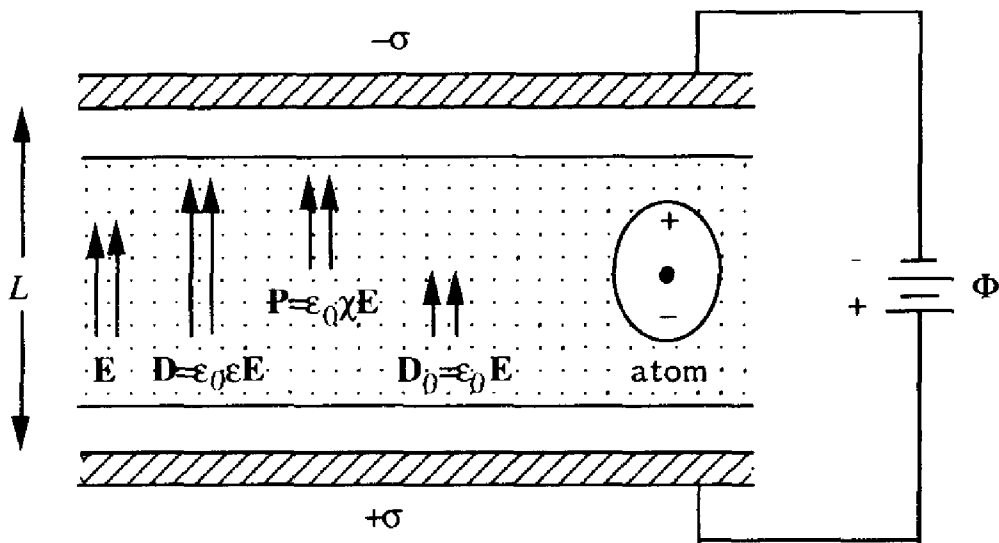


Fig. 4.11. Condenser containing an isotropic dielectric material. The value of the field \mathbf{E} is $E = \Phi/L$ and the charge density is $\sigma = D = \epsilon\epsilon_0E$. In the empty spaces, the field is $E_v = \sigma/\epsilon_0 = \epsilon E > E$. The field \mathbf{E} polarizes the atoms and induces the polarization \mathbf{P}

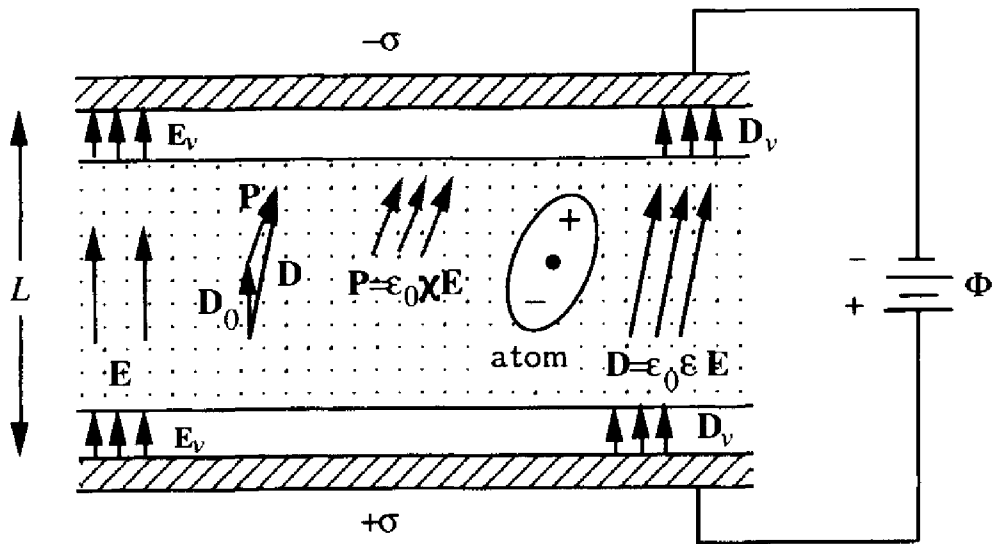


Fig. 4.12. Condenser containing an anisotropic dielectric material. The empty spaces are very narrow compared to the distance L . According to D. F. Nye, *Physical Properties of Crystals*

In an anisotropic dielectric, the relation between \mathbf{D} and \mathbf{E} is characterized by a tensor of rank 2,

$$D_m = \varepsilon_0 \sum_n^3 \varepsilon_{mn} E_n, \quad (4.46)$$

$$P_m = \varepsilon_0 \sum_n^3 \chi_{mn} E_n, \quad \chi_{mn} = \varepsilon_{mn} - \delta_{mn}.$$

\mathbf{E} , \mathbf{D} and \mathbf{P} are generally not parallel. Figure 4.12 shows the relations which link these vectors.

The electrostatic potential is constant over the surface of the condenser plates. Hence, in a vacuum, the field \mathbf{E}_v is perpendicular to the plates. The electric displacement in a vacuum is $\mathbf{D}_v = \varepsilon_0 \mathbf{E}_v$, $\|\mathbf{D}_v\| = \sigma$. The crystal/vacuum interface obeys the following continuity conditions:

- the tangential component of the electric field and the normal component of the electric displacement are continuous across the interface;
- the normal component of the electric field and the tangential component of the electric displacement may be discontinuous across the interface.

The tangential component of \mathbf{E}_v being zero, \mathbf{E} is also perpendicular to the plates. The width of the empty spaces is negligible compared to the thickness of the crystal, hence $\|\mathbf{E}\| = \Phi/L$. The electric displacement may acquire a tangential component at the surface, i.e. \mathbf{D} is not necessarily parallel to \mathbf{D}_v . The normal

component D_L is equal to \mathbf{D}_v ,

$$D_L = \epsilon_0 \epsilon_L \|\mathbf{E}\| = \|\mathbf{D}_v\| = \sigma,$$

$$\epsilon_L = \sum_m^3 \sum_n^3 \epsilon_{mn} l_m l_n \text{ according to equation (4.21).}$$

The direction cosines l_i define the orientation of the crystal lattice with respect to the condenser plates. The longitudinal susceptibility is

$$\chi_L = \sum_m^3 \sum_n^3 \chi_{mn} l_m l_n = \epsilon_L - 1; \quad l_1^2 + l_2^2 + l_3^2 = 1.$$

The field in a vacuum is

$$\|\mathbf{E}_v\| = \frac{1}{\epsilon_0} \|\mathbf{D}_v\| = \epsilon_L \|\mathbf{E}\|.$$

The capacity C of the condenser per unit area is σ/Φ ,

$$C = \epsilon_0 \epsilon_L \|\mathbf{E}\|/\Phi = \epsilon_0 \epsilon_L/L$$

The longitudinal dielectric constant is obtained from the relation:

$$\frac{C \text{ (with anisotropic crystal)}}{C \text{ (with no dielectric)}} = \epsilon_L.$$

Thus the transverse effect is not measured. The symmetric tensor for a triclinic crystal may be obtained from the measurement of ϵ_L in six different directions. Any possible antisymmetric contribution will not be revealed by these measurements (Section 4.2.5).

A condenser with plates of area F to which a potential Φ has been applied contains a total charge of $F\sigma$. Its electrostatic energy is

$$W = \int \Phi d(\sigma F) = F \int L \|\mathbf{E}\| d(\epsilon_0 \epsilon_L \|\mathbf{E}\|) = FL \epsilon_0 \epsilon_L \int \|\mathbf{E}\| d\|\mathbf{E}\|.$$

The energy per unit volume is thus

$$w = \frac{W}{FL} = \frac{1}{2} \epsilon_0 \epsilon_L \|\mathbf{E}\|^2 = \frac{1}{2} \epsilon_0 \|\mathbf{E}\|^2 \sum_m^3 \sum_n^3 \epsilon_{mn} l_m l_n.$$

Setting $\mathbf{E} = \|\mathbf{E}\|(l_1, l_2, l_3)$, we obtain:

$$w = \frac{1}{2} \epsilon_0 \sum_m^3 \sum_n^3 \epsilon_{mn} E_m E_n = \frac{1}{2} \epsilon_0 \mathbf{E}^T \epsilon \mathbf{E} = \frac{1}{2} \mathbf{D} \cdot \mathbf{E}. \tag{4.47}$$

A possible antisymmetric component will not add any contribution to the energy because it would induce a polarization, i.e. a charge separation, in a direction normal to the field. The transverse polarization implied by the symmetric tensor

$\frac{1}{2}(\varepsilon_{mn} + \varepsilon_{nm})$ is linked to the anisotropy of the longitudinal effect ε_L . In contrast, there is no justification for the existence of an antisymmetric tensor component and no possible method for its observation. In a more formal way, we apply the following reasoning. The energy w depends only on the state of the solid and not on its history. Hence, it is a *state function*. It follows that

$$\text{curl grad } w(\mathbf{E}) = \text{curl } \mathbf{D} = 0;$$

$$\frac{\partial^2 w}{\partial E_m \partial E_n} = \frac{\partial^2 w}{\partial E_n \partial E_m},$$

$$\varepsilon_{mn} = \varepsilon_{nm}, \text{ the tensor is symmetric.} \quad (4.48)$$

Note that $\mathbf{D} = \text{grad } w(\mathbf{E})$ is the normal to the plane tangent to the reference ellipsoid (equation (4.25), Fig 4.3).

The tensors compatible with different symmetries have the forms (4.10), (4.11), (4.13) and (4.14). The reference ellipsoids are described in Section 4.2.5. The eigenvalues of ε are all positive. For an alternating electric field, the tensor ε is a function of the frequency.

EXAMPLES: quartz SiO_2 (group 32): $\varepsilon_{11} = \varepsilon_{12} = 4.5; \varepsilon_{33} = 4.6$
 rutile TiO_2 (group 4/mmm): $\varepsilon_{11} = \varepsilon_{22} = 89; \varepsilon_{33} = 173$
 at a frequency of 4×10^8 Hz.

The following properties are characterized by symmetric tensors of rank 2: magnetic susceptibility (negative eigenvalues for diamagnetic materials); electrical and thermal conductivities (these tensors are symmetrical according to the Onsager principle); thermal expansion.

4.4.2 ELASTICITY: TENSOR OF RANK 4

The coefficients of elasticity describe strains caused by stress. The *two moduli* of linear elasticity for *isotropic solids* are well known:

- longitudinal effect (Fig. 4.8), stress σ , strain $\varepsilon = u/L$:

$$\left. \begin{aligned} \varepsilon &= \frac{1}{E} \sigma, & E &= \text{Young's modulus} \\ & & & \text{(Hooke's law)} \end{aligned} \right\} \quad (4.49)$$

- shear (Fig. 4.8 and equation (4.13)), transverse stress τ , $\gamma = \frac{u}{H}$:

$$\gamma = \frac{1}{G} \tau, \quad G = \text{shear modulus.} \quad (4.50)$$

A bar which is subjected to a longitudinal stress (4.49) parallel to its axis undergoes a contraction ε' perpendicular to its expansion (Fig. 4.8):

$$\left. \begin{aligned} \varepsilon' &= \frac{B' - B}{B} = -m\varepsilon = -\frac{m}{E}\sigma \\ \text{where } m &= \text{Poisson's number.} \end{aligned} \right\} \quad (4.51)$$

The volume of the bar after dilation LB'^2 cannot be less than the volume LB^2 before the deformation, from which we obtain that

$$0 \leq m \leq \frac{1}{2}. \quad (4.52)$$

If a cube of edge A is subjected to a transverse stress τ (Fig. 4.13, $\tau = \sigma_{12} = \sigma_{21}$ in the terminology of Section 4.3.1), by using the shear γ defined in equation (4.50), we can calculate the diagonals of the deformed cube:

$$\left. \begin{aligned} \text{long diagonal: } & 2A \cos\left(\frac{\pi}{4} - \frac{\gamma}{2}\right) \approx \sqrt{2}A\left(1 + \frac{\gamma}{2}\right) \\ \text{short diagonal: } & 2A \cos\left(\frac{\pi}{4} + \frac{\gamma}{2}\right) = \sqrt{2}A\left(1 - \frac{\gamma}{2}\right) \end{aligned} \right\} \gamma = \frac{1}{G}\tau.$$

By changing the coordinate system $\mathbf{e}_1\mathbf{e}_2$ into $\mathbf{e}'_1\mathbf{e}'_2$ (Fig. 4.13), according to equation (4.6), the stress tensor transforms as

$$\tau \begin{pmatrix} 0 & 1 & 0 \\ 1 & 0 & 0 \\ 0 & 0 & 0 \end{pmatrix} \rightarrow \tau \begin{pmatrix} 1 & 0 & 0 \\ 0 & -1 & 0 \\ 0 & 0 & 0 \end{pmatrix}.$$

The transverse stress τ is thus equivalent to a dilation stress parallel to \mathbf{e}'_1 plus a compression stress along \mathbf{e}'_2 ; in Fig. 4.13, $\tau = \sigma$. According to equations (4.49) and (4.51), the two diagonals change as follows:

$$\left. \begin{aligned} \text{long diagonal: } & A\sqrt{2}(1 + \varepsilon)(1 + m\varepsilon) \approx A\sqrt{2}[1 + (1 + m)\varepsilon] \\ \text{short diagonal: } & A\sqrt{2}(1 - \varepsilon)(1 - m\varepsilon) \approx A\sqrt{2}[1 - (1 + m)\varepsilon] \end{aligned} \right\} \varepsilon = \frac{1}{E}\sigma$$

From which we obtain the relation between G , E and m :

$$\frac{\gamma}{2} = (1 + m)\varepsilon,$$

$$m = \frac{E}{2G} - 1, \quad (4.53)$$

$$2G \leq E \leq 3G; \quad \frac{E}{3} \leq G \leq \frac{E}{2}. \quad (4.54)$$

The linear elasticity of an *anisotropic solid* is a tensor property of rank 4. It

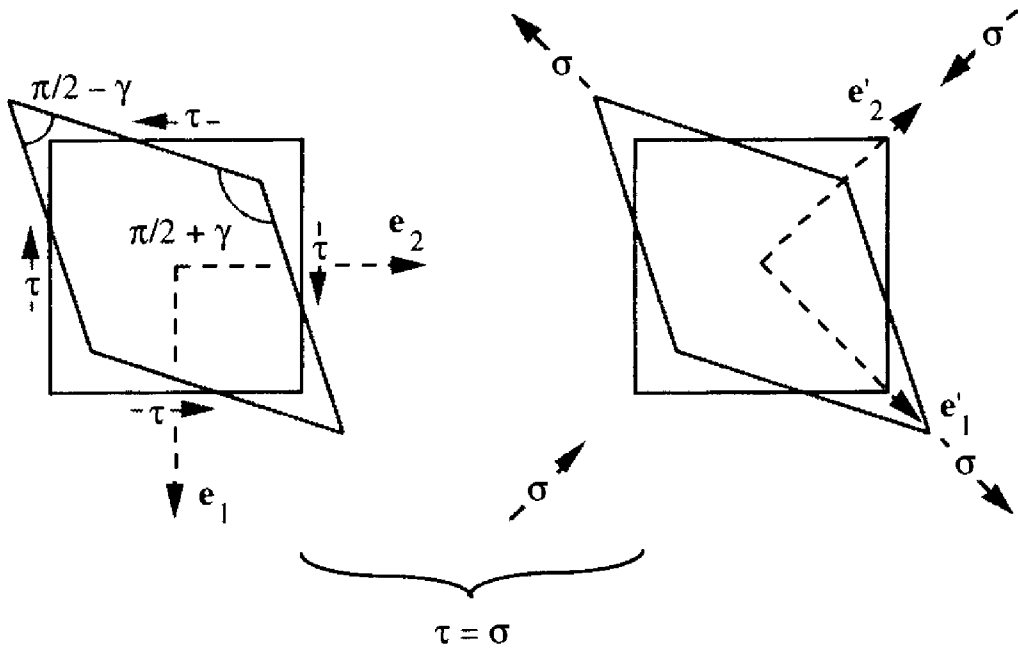


Fig. 4.13. A change in coordinate system $(\mathbf{e}_1, \mathbf{e}_2) \rightarrow (\mathbf{e}'_1, \mathbf{e}'_2)$ transforms the transverse stresses $\tau = \sigma_{12} = \sigma_{21}$ into longitudinal stresses $\sigma = \sigma'_{11} = -\sigma'_{22}$

characterizes the relation between the stresses $\boldsymbol{\sigma}$ and the deformations $\boldsymbol{\varepsilon}$, both of which are tensors of rank 2:

$$\left. \begin{aligned} \varepsilon_{mn} &= \sum_p \sum_q S_{mnpq} \sigma_{pq} \\ \sigma_{mn} &= \sum_p \sum_q C_{mnpq} \varepsilon_{pq} \end{aligned} \right\} \quad (4.55)$$

with

S_{mnpq} : tensor of the elastic constants ('compliance');

C_{mnpq} : tensor of the elastic moduli ('stiffness').

The tensors $\boldsymbol{\sigma}$ and $\boldsymbol{\varepsilon}$ are symmetric, $\varepsilon_{mn} = \varepsilon_{nm}$, $\sigma_{mn} = \sigma_{nm}$, hence

$$S_{mnpq} = S_{nmpq} = S_{mnqp} = S_{nmqp}. \quad (4.56)$$

These conditions allow us to use the Voigt notation, (equations (4.41) and (4.42)):

$$\varepsilon_i = \sum_j S_{ij} \sigma_j; \quad \sigma_i = \sum_j C_{ij} \varepsilon_j. \quad (4.57)$$

Remembering that $\varepsilon_j = 2\varepsilon_{mn}$ for $m \neq n$ from equation (4.42), and that $S_{mnpq} \sigma_{pq} + S_{mnqp} \sigma_{qp} = 2S_{mnpq} \sigma_{pq}$ according to equation (4.56), the coefficients of

equation (4.57) become:

$$S_{ij} = \left\{ \begin{array}{ll} S_{mnpq} & (i \text{ and } j \text{ are } 1,2,3) \\ 2S_{mnpq} & (i \text{ or } j \text{ are } 4,5,6) \\ 4S_{mnpq} & (i \text{ and } j \text{ are } 4,5,6) \end{array} \right\}; \tag{4.58}$$

$$C_{mnpq} = C_{ij}.$$

The S_{ij} and C_{ij} form 6×6 matrices, $\mathbf{C} = \mathbf{S}^{-1}$ (for more detailed information, see Section 4.4.6). In order to derive the transformation properties, however, it is necessary to use the four indices.

By analogy with the tensors of rank 2, \mathbf{C} and \mathbf{S} can be considered to be the sum of a symmetric tensor and an antisymmetric tensor (4.20):

$$\begin{array}{ll} \text{symmetric:} & \frac{1}{2}(S_{ij} + S_{ji}); \frac{1}{2}(C_{ij} + C_{ji}); \\ \text{antisymmetric:} & \frac{1}{2}(S_{ij} - S_{ji}); \frac{1}{2}(C_{ij} - C_{ji}). \end{array}$$

The *longitudinal effect* ϵ_L is the expansion of the crystal in the direction of a uniaxial stress. Following from equation (4.33), the stress σ parallel to \mathbf{l} is represented by a tensor whose elements are $\sigma l_m l_n$. The resulting deformation is

$$\epsilon_{mn} = \sigma \sum_p \sum_q S_{mnpq} l_p l_q.$$

The longitudinal effect is thus

$$\epsilon_L = \sum_m \sum_n \epsilon_{mn} l_m l_n = \sigma \sum_{mnpq} S_{mnpq} l_m l_n l_p l_q = \sigma S_L. \tag{4.59}$$

The product $l_m l_n l_p l_q$ is invariant with respect to all permutations of the indices. The result of this is that S_L only represents the totally symmetric part of \mathbf{S} with respect to the indices. In particular, any possible antisymmetric component of \mathbf{S} will only add a pure *transverse effect* to the transverse effects inherent to the symmetric part.

The surface of rank 4

$$\sum_{mnpq} S_{mnpq} x_m x_n x_p x_q = 1$$

represents the part of \mathbf{S} that is totally symmetric with respect to the indices. The length of a vector from the origin to a point $(x_1, x_2, x_3) = r(l_1, l_2, l_3)$ on the surface is $r = S_L^{-1/4}$. For the surface

$$\frac{1}{r^5} \sum_{mnpq} S_{mnpq} x_m x_n x_p x_q = 1 \text{ with } r^2 = x_1^2 + x_2^2 + x_3^2,$$

the length of r is equal to S_L . The surface represented by $1/S_L$ is called the elasticity surface because $1/S_L$ can be compared to an anisotropic Young's modulus.

The strain energy of a solid is equal to the scalar product of the applied force and the resulting elongation. The energy per unit volume is thus equal to the product of a stress σ and a corresponding strain ϵ ; more precisely, we calculate the products of the stresses σ_{mn} and the strains ϵ_{mn} which are parallel to them,

$$w = \int_0^\sigma \sum_m^3 \sum_n^3 \epsilon_{mn} d\sigma_{mn} = \int_0^\sigma \sum_m^3 \sum_n^3 \sum_p^3 \sum_q^3 S_{mnpq} \sigma_{pq} d\sigma_{mn}. \tag{4.60}$$

Equation (4.60) is a curvilinear integral. We can arrive at the final stress σ in different ways: for example, we can first apply σ_{11} ($\sigma_{22} = \sigma_{33} = \sigma_{12} = \sigma_{13} = \sigma_{23} = 0$), then σ_{22} (σ_{11} constant, $\sigma_{33} = \sigma_{12} = \sigma_{13} = \sigma_{23} = 0$), and so on to σ_{23} . Any other order in the application of the σ_{mn} leads to the same final state of stress and hence results in the same value of w . This argument implies that the matrix \mathbf{S} of dimension $[6 \times 6]$ is symmetric,

$$\left. \begin{aligned} S_{mnpq} &= S_{pqmn}; & S_{ij} &= S_{ji} \\ C_{mnpq} &= C_{pqmn}; & C_{ij} &= C_{ji} \end{aligned} \right\} \tag{4.61}$$

By analogy with the electric polarization (4.47), the antisymmetric part of the tensor \mathbf{S} does not contribute to the energy because it represents a pure transverse effect. There is no energetic reason for this effect to appear and the antisymmetric part of \mathbf{S} is considered to be zero. The deformation energy becomes

$$w = \frac{1}{2} \sum_m^3 \sum_n^3 \sum_p^3 \sum_q^3 S_{mnpq} \sigma_{mn} \sigma_{pq} = \frac{1}{2} \sum_m^3 \sum_n^3 \epsilon_{mn} \sigma_{mn} = \frac{1}{2} \sum_i^6 \epsilon_i \sigma_i. \tag{4.62}$$

From equations (4.56) and (4.61), it follows that the terms of \mathbf{S} and \mathbf{C} are equal for the following permutation of indices:

$$mnpq = mnqp = nmpq = nmqp = pqmn = qpmn = pqnm = qpnm.$$

However, as $S_{mnpq} \neq S_{mpnq}$, the tensor is not totally symmetric. The elastic behavior of a triclinic crystal is thus characterized by 21 elastic constants or moduli whose indices are:

tensor notation						Voigt notation					
1111	1122	1133	1123	1113	1112	11	12	13	14	15	16
	2222	2233	2223	2213	2212		22	23	24	25	26
		3333	3323	3313	3312			33	34	35	36
			2323	2313	2312				44	45	46
				1313	1312					55	56
					1212						66

groups 1, $\bar{1}$ (4.63)

The elasticity tensor transforms according to equation (4.7), i.e. like the product of four coordinates. An inversion center transforms the coordinates (x_1, x_2, x_3) into $(x'_1, x'_2, x'_3) = (-x_1, -x_2, -x_3)$, hence $S'_{mnpq} = (-1)^4 S_{mnpq} = S_{mnpq}$. Thus the tensor is invariant with respect to inversion.

A tensor of even rank (2, 4, 6, ...) is invariant with respect to a center of inversion. A center of symmetry $\bar{1}$ is an intrinsic symmetry element of the tensor.

A study of the 11 Laue classes is hence sufficient to characterize tensors of even rank.

A mirror plane perpendicular to e_3 transforms (x_1, x_2, x_3) into $(x'_1, x'_2, x'_3) = (x_1, x_2, -x_3)$, hence $S'_{mnpq} = (-1)^j S_{mnpq}$ where j is the number of indices with the value 3. If the tensor is invariant with respect to the reflection, $S'_{mnpq} = S_{mnpq}$. In the Voigt notation, it has the following form:

11	12	13	0	0	16
	22	23	0	0	26
		33	0	0	36
			44	45	0
				55	0
					66

groups 11m, 112, 112/m (4.64)

The reader is invited to derive the form of the tensor for the other Laue classes or is referred to the literature (e.g. J. F. Nye, *Physical Properties of Crystals*). The cubic classes merit an additional comment: they cannot be distinguished with respect to elasticity:

S_{11}	S_{12}	—	S_{12}	0	0	0
S_{12}	S_{11}		S_{12}	0	0	0
S_{12}	—	S_{12}	S_{11}	0	0	0
0	0		0	S_{44}	0	0
0	0		0	0	S_{44}	0
0	0		0	0	0	S_{44}

cubic classes, 3 terms; the matrix **C** has the same form. (4.65)

We have seen that isotropic bodies have two independent elastic moduli. Thus, cubic crystals are not isotropic with respect to their elasticity. For an isotropic

body, the *condition supplementary* to the cubic conditions is

$$S_{44} = 2(S_{11} - S_{12}); C_{44} = \frac{1}{2}(C_{11} - C_{12}); \text{isotropic} \quad (4.66)$$

We thus obtain that:

$$\varepsilon_1 = S_{11}\sigma_1 + S_{12}\sigma_2 + S_{12}\sigma_3 = \{\sigma_1 - m(\sigma_2 + \sigma_3)\}/E, \text{ in accordance with equations (4.49) and (4.51);}$$

$$\varepsilon_4 = 2(S_{11} - S_{12})\sigma_4 = \sigma_4/G, \text{ in accordance with equation (4.50);}$$

hence

$$S_{11} = 1/E; S_{12} = -m/E; 2(S_{11} - S_{12}) = 1/G. \quad (4.67)$$

From this, relations (4.53) and (4.54) are easy to deduce. The relations for the moduli C_{ij} are more complex:

$$C_{11} = \frac{S_{11} + S_{12}}{(S_{11} - S_{12})(S_{11} + 2S_{12})}; \quad C_{12} = \frac{-S_{12}}{(S_{11} - S_{12})(S_{11} + 2S_{12})};$$

$$C_{44} = \frac{1}{2(S_{11} - S_{12})} = \frac{1}{2}(C_{11} - C_{12}). \quad (4.68)$$

The elastic constants obey certain other supplementary conditions. Thus, the deformation energy is positive,

$$2w = \sum_{i=1}^6 \varepsilon_i \sigma_i > 0.$$

From this, for a cubic crystal, we deduce that

$$S_{11}(\sigma_1^2 + \sigma_2^2 + \sigma_3^2) + 2S_{12}(\sigma_1\sigma_2 + \sigma_1\sigma_3 + \sigma_2\sigma_3) + S_{44}(\sigma_4^2 + \sigma_5^2 + \sigma_6^2) > 0;$$

by setting $\sigma_2 = \sigma_3 = \sigma_4 = \sigma_5 = \sigma_6 = 0$: $S_{11} > 0$;

by setting $\sigma_1 = \sigma_2, \sigma_3 = \sigma_4 = \sigma_5 = \sigma_6 = 0$: $S_{11} + S_{12} > 0$;

by setting $\sigma_1 = \sigma_2 = \sigma_3, \sigma_4 = \sigma_5 = \sigma_6 = 0$: $S_{11} + 2S_{12} > 0$;

by setting $\sigma_1 = \sigma_2 = \sigma_3 = 0$: $S_{44} > 0$.

Hence $S_{11} > 0, S_{11} > 2|S_{12}|, S_{44} > 0$.

In the isotropic case, we obtain:

$$E > 0, G > 0, m < \frac{1}{2}.$$

The effect of a hydrostatic pressure applied to a crystal is described by

$$\varepsilon_{mn} = -h_{mn}\sigma, \quad h_{mn} = \sum_p^3 S_{mnp p}. \quad (4.69)$$

With the help of equation (4.40), the compressibility of the crystal becomes:

$$\begin{aligned} \kappa &= \frac{V - V'}{V\sigma} = \frac{-\epsilon_{11} - \epsilon_{22} - \epsilon_{33}}{\sigma} = \sum_m^3 \sum_p^3 S_{mmp} \\ &= (S_{11} + S_{22} + S_{33}) + 2(S_{12} + S_{13} + S_{23}). \end{aligned} \tag{4.70}$$

For an isotropic solid: $\kappa = \frac{3}{E}(1 - 2m)$.

EXAMPLE

Right handed quartz, SiO₂, symmetry 32, e₁ parallel to 2, e₄ parallel to 3. This symmetry imposes on the tensor S the following form:

S_{11}	S_{12}	S_{13}	S_{14}	0	0
	S_{11}	S_{13}	$-S_{14}$	0	0
		S_{33}	0	0	0
			S_{44}	0	0
				S_{44}	$2S_{14}$
					$2(S_{11} - S_{12})$

The tensor C has the same form with the difference that $C_{56} = C_{14}$, $C_{66} = \frac{1}{2}(C_{11} - C_{12})$. The elastic constants (in the absence of an electric field, Section 4.4.6) are in units of $10^{-12} \text{ Pa}^{-1} = 10^{-4} \text{ kbar}^{-1}$:

$$S_{11} = 17.294; \quad S_{33} = 12.021; \quad S_{12} = -2.825; \quad S_{13} = -1.615; \quad S_{14} = -5.756; \\ S_{44} = 26.457.$$

The elastic moduli are in units of $10^{11} \text{ Pa} = 10^3 \text{ kbar}$:

$$C_{11} = 0.8674; \quad C_{33} = 1.072; \quad C_{12} = 0.0699; \quad C_{13} = 0.1191; \quad C_{14} = -0.1791; \\ C_{44} = 0.5794.$$

A uniaxial stress of $1 \text{ kbar} = 10^8 \text{ Pa}$ parallel to e₁ (twofold axis) produces the following deformations in units of 10^{-3} :

$$\epsilon_1 = 1.73; \quad \epsilon_2 = -0.28; \quad \epsilon_3 = -0.16; \quad \epsilon_4 = 2\epsilon_{23} = 0.58; \quad \epsilon_5 = \epsilon_6 = 0,$$

i.e. a lengthening along the twofold axis and an anisotropic shortening accompanied by shear in the plane perpendicular to the twofold axis. The longitudinal effect is $\epsilon_L = 1.73 \times 10^{-3}$.

4.4.3 ELASTIC WAVES IN A CRYSTAL

Figure 4.14 shows a volume element $dx_1 dx_2 dx_3$ centered at (x_1, x_2, x_3) . During the passage of an elastic wave, a force **f** acts on this volume element. **f** may be

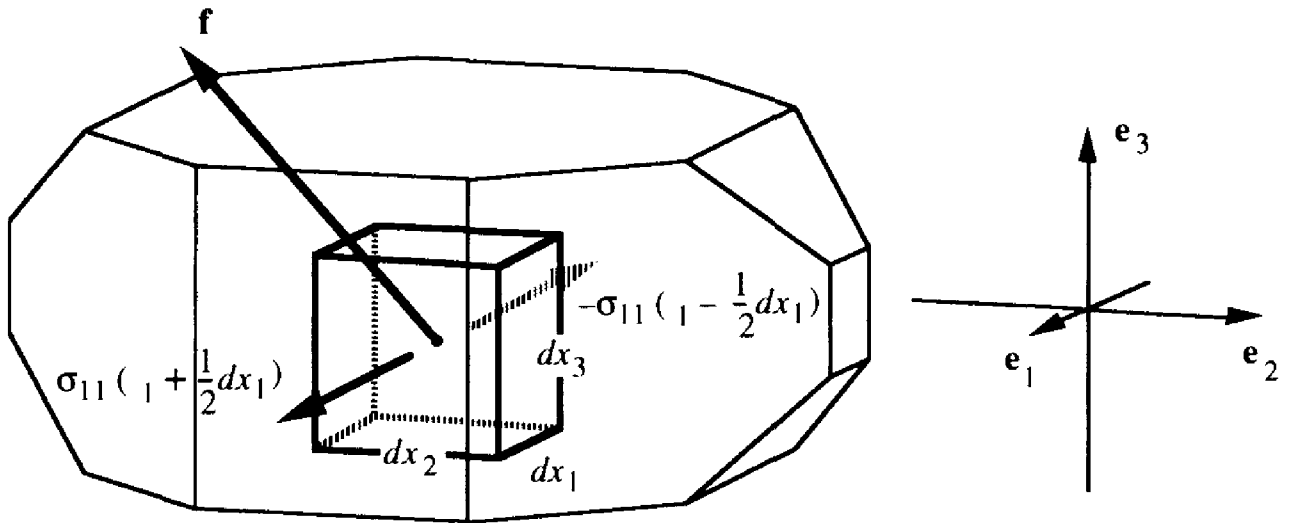


Fig. 4.14. Forces acting on a volume element during the passage of an elastic wave

calculated by means of the stress tensor $\sigma(x_1, x_2, x_3)$ which, in this case, is a function of x_1, x_2, x_3 .

Let us consider the component f_1 of the force \mathbf{f} parallel to \mathbf{e}_1 . The contribution of σ_{11} acting on the two faces of the volume element perpendicular to \mathbf{e}_1 is

$$\text{for the front face: } \sigma_{11}(x_1 + \frac{1}{2}dx_1, x_2, x_3)dx_2dx_3;$$

$$\text{for the rear face: } -\sigma_{11}(x_1 - \frac{1}{2}dx_1, x_2, x_3)dx_2dx_3.$$

In a similar manner, we can obtain the contributions of σ_{12} and σ_{13} acting on the faces perpendicular to \mathbf{e}_2 and \mathbf{e}_3 respectively. The components of \mathbf{f} are thus

$$f_1 = \left(\frac{\partial \sigma_{11}}{\partial x_1} + \frac{\partial \sigma_{12}}{\partial x_2} + \frac{\partial \sigma_{13}}{\partial x_3} \right) dx_1 dx_2 dx_3,$$

$$f_2 = \left(\frac{\partial \sigma_{12}}{\partial x_1} + \frac{\partial \sigma_{22}}{\partial x_2} + \frac{\partial \sigma_{23}}{\partial x_3} \right) dx_1 dx_2 dx_3,$$

$$f_3 = \left(\frac{\partial \sigma_{13}}{\partial x_1} + \frac{\partial \sigma_{23}}{\partial x_2} + \frac{\partial \sigma_{33}}{\partial x_3} \right) dx_1 dx_2 dx_3.$$

The stress $\sigma(x_1, x_2, x_3)$ generates an inhomogeneous deformation in the crystal,

$$\sigma_{mn}(x_1, x_2, x_3) = \sum_p \sum_q C_{mnpq} \varepsilon_{pq}(x_1, x_2, x_3).$$

According to equation (4.36), the strain is the derivative of the displacement \mathbf{u} of the volume element with respect to the undeformed crystal,

$$\varepsilon_{pq}(x_1, x_2, x_3) = \frac{\partial u_p(x_1, x_2, x_3)}{\partial x_q} = \frac{\partial u_q(x_1, x_2, x_3)}{\partial x_p}.$$

The force acting on the volume element is thus related to the second derivatives of the elastic displacements,

$$f_m = dx_1 dx_2 dx_3 \sum_{n=1}^3 \frac{\partial \sigma_{mn}}{\partial x_n} = dx_1 dx_2 dx_3 \sum_n \sum_p \sum_q C_{mnpq} \frac{\partial^2 u_p}{\partial x_n \partial x_q}.$$

It is equally given by the acceleration of the volume element,

$$f_m = dx_1 dx_2 dx_3 \rho \frac{\partial^2 u_m}{\partial t^2},$$

where ρ is the density of the crystal and t the time. From this we obtain the differential wave equation

$$\rho \frac{\partial^2 u_m}{\partial t^2} = \sum_n \sum_p \sum_q C_{mnpq} \frac{\partial^2 u_p}{\partial x_n \partial x_q}. \tag{4.71}$$

The general solution of equation (4.71) for an isotropic solid shows the existence of waves that are purely longitudinal (compressive) and purely transverse (shear). In the more difficult case of an anisotropic solid, we consider the existence of a plane wave represented by

$$\mathbf{u} = A \mathbf{p} \exp[2\pi i(\mathbf{n} \cdot \mathbf{x} - vt)/\lambda],$$

where A is the amplitude, \mathbf{p} the polarization vector ($\|\mathbf{p}\| = 1$), $\mathbf{n} = (n_1, n_2, n_3)^T$ the wave vector normal to the plane of the wave ($\|\mathbf{n}\| = 1$), v the speed of propagation and λ the wavelength. We can then easily calculate the quantities in equation (4.71),

$$\frac{\partial^2 u_p}{\partial x_n \partial x_q} = -\frac{4\pi^2}{\lambda^2} n_n n_q u_p; \quad \frac{\partial^2 u_m}{\partial t^2} = -4\pi^2 v^2 u_m;$$

$$\rho v^2 p_m = \sum_n \sum_p \sum_q C_{mnpq} n_n n_q p_p.$$

This is an equation of eigenvalues and eigenvectors,

$$\rho v^2 \mathbf{p} = \mathbf{B} \mathbf{p}; \quad B_{mn} = \sum_r \sum_s C_{mrns} n_r n_s. \tag{4.72}$$

We can deduce from equation (4.72) that:

- for each wave vector \mathbf{n} , there are in general three elastic waves which propagate at different rates v_i , the eigenvalues of \mathbf{B} being ρv_i^2 ;
- the three waves are polarized along the eigenvectors of \mathbf{B} ; the vectors \mathbf{p}_i are mutually perpendicular, but are, in general, neither parallel nor perpendicular to \mathbf{n} ;
- if two eigenvalues are equal, $v_i^2 = v_j^2$, any linear combination $\mathbf{p} = a \mathbf{p}_i + b \mathbf{p}_j$ is also a solution for equation (4.72); all of the corresponding waves can exist in the crystal.

By employing equation (4.58), we obtain explicitly for **B**:

$$B_{11} = C_{11}n_1^2 + C_{66}n_2^2 + C_{55}n_3^2 + 2C_{16}n_1n_2 + 2C_{15}n_1n_3 + 2C_{56}n_2n_3$$

$$B_{22} = C_{66}n_1^2 + C_{22}n_2^2 + C_{44}n_3^2 + 2C_{26}n_1n_2 + 2C_{46}n_1n_3 + 2C_{24}n_2n_3$$

$$B_{33} = C_{55}n_1^2 + C_{44}n_2^2 + C_{33}n_3^2 + 2C_{45}n_1n_2 + 2C_{35}n_1n_3 + 2C_{34}n_2n_3$$

$$B_{12} = C_{16}n_1^2 + C_{26}n_2^2 + C_{45}n_3^2 + (C_{12} + C_{66})n_1n_2 + (C_{14} + C_{56})n_1n_3 \\ + (C_{46} + C_{25})n_2n_3$$

$$B_{13} = C_{15}n_1^2 + C_{46}n_2^2 + C_{35}n_3^2 + (C_{14} + C_{56})n_1n_2 + (C_{13} + C_{55})n_1n_3 \\ + (C_{36} + C_{45})n_2n_3$$

$$B_{23} = C_{56}n_1^2 + C_{24}n_2^2 + C_{34}n_3^2 + (C_{46} + C_{25})n_1n_2 + (C_{36} + C_{45})n_1n_3 \\ + (C_{23} + C_{44})n_2n_3$$

In an isotropic medium, by using equations (4.65), (4.66), (4.67) and (4.68), we obtain:

$$\mathbf{B} = \begin{pmatrix} \frac{1}{2}(C_{11} + C_{12})n_1^2 + \frac{1}{2}(C_{11} - C_{12}) & \frac{1}{2}(C_{11} + C_{12})n_1n_2 & \frac{1}{2}(C_{11} + C_{12})n_1n_3 \\ \frac{1}{2}(C_{11} + C_{12})n_1n_2 & \frac{1}{2}(C_{11} + C_{12})n_2^2 + \frac{1}{2}(C_{11} - C_{12}) & \frac{1}{2}(C_{11} + C_{12})n_2n_3 \\ \frac{1}{2}(C_{11} + C_{12})n_1n_3 & \frac{1}{2}(C_{11} + C_{12})n_2n_3 & \frac{1}{2}(C_{11} + C_{12})n_3^2 + \frac{1}{2}(C_{11} - C_{12}) \end{pmatrix}$$

The magnitudes $\frac{1}{2}(C_{11} + C_{12})$ and $\frac{1}{2}(C_{11} - C_{12})$ are the *Lamé moduli*. The eigenvalues and eigenvectors of **B** are

- $\rho v_1^2 = C_{11} = E \frac{1 - m}{(1 + m)(1 - 2m)}$; $\mathbf{p}_1 = \mathbf{n}$, longitudinal wave;

- $\rho v_2^2 = \rho v_3^2 = \frac{1}{2}(C_{11} - C_{12}) = E \frac{1}{2(1 + m)} = G/E$; \mathbf{p}_2 and \mathbf{p}_3 are perpendicular to \mathbf{n} ; transverse waves.

E is Young's modulus, G the shear modulus and m Poisson's number. The ratio of the rates in an isotropic medium is;

$$\frac{v_1}{v_{2,3}} = \left(\frac{2(1 - m)}{1 - 2m} \right)^{1/2}; \quad \frac{v_1}{v_{2,3}} > \sqrt{2}.$$

4.4.4 PYROELECTRICITY: TENSOR OF RANK 1

When subjected to a temperature change, certain crystals become electrically polarized. Tourmaline, a silicate of boron and aluminum, symmetry $3m$, is the best-known example. On heating, such a crystal becomes negatively charged on one side and positively charged on the other. Pyroelectricity is a tensor of rank 1 (vector),

$$\mathbf{P} = \mathbf{p}\Delta T, \quad (4.73)$$

where \mathbf{P} is the electric polarization or the dipole moment per unit volume, and ΔT the temperature change.

A change in coordinate system transforms the polar vector \mathbf{p} according to equation (4.5). It is easy to show that the pyroelectric effect can only appear in *directions which are polar and unique*, and hence only in the following groups:

- 1 (\mathbf{p} can point in any direction);
- m (\mathbf{p} is parallel to the mirror plane);
- 2, 3, 4, 6, $mm2$, $3m$, $4mm$, $6mm$ (\mathbf{p} is parallel to the unique axis).

The pyroelectric effect is due, above all, to the piezoelectric effect (Section 4.4.5). During heating the crystal deforms because of the thermal expansion,

$$\varepsilon_{mn} = e_{mn} \Delta T, \quad \text{thermal expansion} \tag{4.74}$$

This strain carries with it a piezoelectric effect,

$$\begin{aligned} \sigma_{mn} &= \sum_p \sum_q C_{mnpq} \varepsilon_{pq} = \sum_p \sum_q C_{mnpq} e_{pq} \Delta T, \quad \text{elasticity (Section 4.4.2)} \\ P_i &= \sum_m \sum_n d_{imn} \sigma_{mn}, \quad \text{piezoelectricity (Section 4.4.5)} \\ p_i &= \sum_m \sum_n \sum_p \sum_q d_{imn} C_{mnpq} e_{pq}. \end{aligned} \tag{4.75}$$

The primary pyroelectric effect (i.e. at constant volume) is extremely small.

EXAMPLE. Tourmaline, crystal class $3m$.

$p_1 = p_2 = 0$; $p_3 = 4 \times 10^{-6}$ Coulomb $m^{-2} \text{ deg}^{-1}$. The dielectric constant down the threefold axis is $\varepsilon_{33} = 7.1$. The corresponding electric susceptibility is thus $\chi_{33} = 6.1$. The electrostatic field E_3 necessary to create the same polarization as a rise in temperature of 1°C is calculated by setting $P_3 = \varepsilon_0 \chi_{33} E_3 = p_3$, thus $E_3 = 740$ volt/cm.

4.4.5 PIEZOELECTRICITY: TENSOR OF RANK 3

In certain crystals we observe an electric polarization \mathbf{P} (i.e. a dipole moment per unit volume) on the application of a stress σ , due to the rearrangement of the charges in the unit cell (Fig. 4.15). This is known as the piezoelectric effect, characterized by a tensor of rank 3,

$$P_i = \sum_m \sum_n d_{imn} \sigma_{mn}. \tag{4.76}$$

The inverse piezoelectric effect is the strain ε of a crystal due to the application of

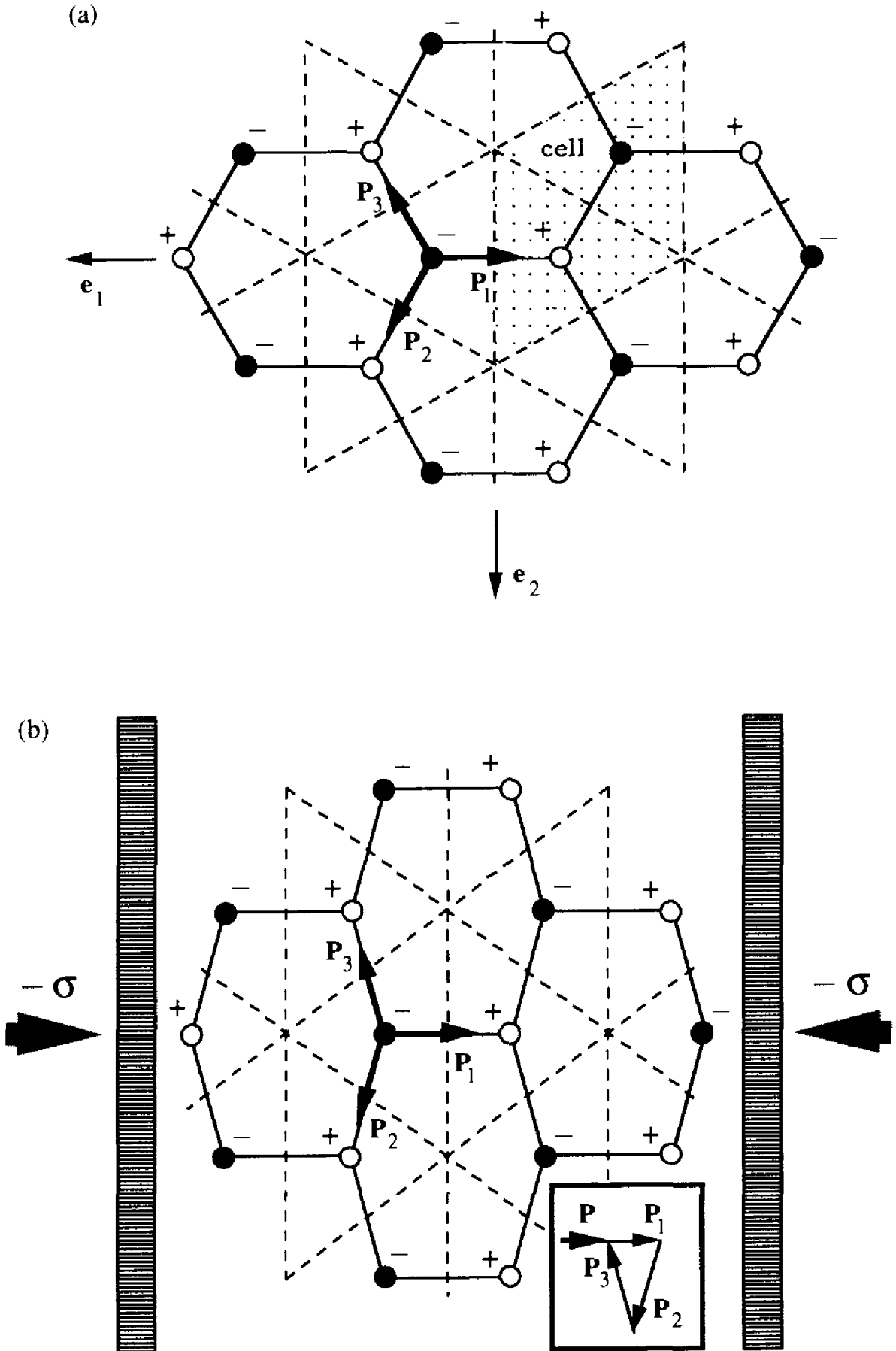


Fig. 4.15. Piezoelectric property of a two-dimensional structure: undeformed structure A^+B^- of symmetry $p31m$; the resultant of the dipole moments is zero (a); the stress $-\sigma$ (compression) creates an imbalance of charges; the resulting dipole moment per unit cell is \mathbf{P} (b)

an electric field \mathbf{E} ,

$$\epsilon_{mn} = \sum_i^3 d_{imn}^* E_i. \tag{4.77}$$

We will show in Section 4.4.6 that

$$d_{imn}^* = d_{imn}. \tag{4.78}$$

COMMENT. The inverse effect does not correspond to an inverse tensor where \mathbf{P} would be the cause and $\boldsymbol{\sigma}$ the effect! For the computation of such a tensor, see below.

$\boldsymbol{\sigma}$ and $\boldsymbol{\epsilon}$ are symmetric tensors. Therefore d_{imn} is symmetric with respect to the indices m and n :

$$d_{imn} = d_{inm}; \quad \text{but } d_{imn} \neq d_{min}. \tag{4.79}$$

By using the Voigt notation (Section 4.3.3), \mathbf{d} can be represented by a 3×6 matrix. Thus, by using equation (4.78), equations (4.76) and (4.77) become:

$$P_i = \sum_j^6 d_{ij} \sigma_j; \quad \epsilon_j = \sum_i^3 d_{ij} E_i. \tag{4.80}$$

$$d_{ij} = \begin{cases} d_{imn} & (j = 1, 2, 3) \\ 2d_{imn} & (j = 4, 5, 6) \end{cases}$$

The effect resulting from a uniaxial stress σ parallel to \mathbf{l} (4.33) is expressed by:

$$P_i = \sigma \sum_m^3 \sum_n^3 d_{imn} l_m l_n,$$

and the longitudinal effect P_L is thus:

$$P_L = \sum_i^3 P_i l_i = \sigma \sum_i^3 \sum_m^3 \sum_n^3 d_{imn} l_i l_m l_n = d_L \sigma. \tag{4.81}$$

We can represent d_L in an analogous manner to equation (4.59). However, such a figure represents only the totally symmetric part of the tensor.

If the coordinate system is transformed by the matrix \mathbf{U} , \mathbf{d} is transformed according to equation (4.7):

$$d'_{mnp} = \sum_r^3 \sum_s^3 \sum_t^3 u_{mr} u_{ns} u_{pt} d_{rst}.$$

Hence, the totally symmetric part of the tensor transforms like the product of three coordinates. An inversion (center of symmetry $\bar{1}$) transforms (x_1, x_2, x_3) into $(x'_1, x'_2, x'_3) = (-x_1, -x_2, -x_3)$, thus $d'_{imn} = (-1)^3 d_{imn} = -d_{imn}$. If the tensor is invariant with respect to $\bar{1}$, $d'_{imn} = d_{imn} = 0$. Consequently, piezoelectricity can only appear in non-centrosymmetric crystals.

A tensor of odd rank becomes zero in the presence of a center of symmetry $\bar{1}$. In contrast, a tensor of even rank is invariant with respect to an inversion center. A center of symmetry is an intrinsic symmetry element of such a tensor (Section 4.4.2).

A twofold axis parallel to \mathbf{e}_2 transforms (x_1, x_2, x_3) into $(x'_1, x'_2, x'_3) = (-x_1, x_2, -x_3)$. In this case, $d'_{imn} = (-1)^j d_{imn}$ where j is the number of indices with values 1 and 3. For a tensor which is invariant with respect to such an axis, $d'_{imn} = d_{imn}$; thus $d_{imn} = 0$ for j odd. The tensor is hence of the form

tensor notation	Voigt notation																																				
<table style="width: 100%; border-collapse: collapse;"> <tr><td style="padding: 2px 10px;">0</td><td style="padding: 2px 10px;">0</td><td style="padding: 2px 10px;">0</td><td style="padding: 2px 10px;">123</td><td style="padding: 2px 10px;">0</td><td style="padding: 2px 10px;">112</td></tr> <tr><td style="padding: 2px 10px;">211</td><td style="padding: 2px 10px;">222</td><td style="padding: 2px 10px;">233</td><td style="padding: 2px 10px;">0</td><td style="padding: 2px 10px;">213</td><td style="padding: 2px 10px;">0</td></tr> <tr><td style="padding: 2px 10px;">0</td><td style="padding: 2px 10px;">0</td><td style="padding: 2px 10px;">0</td><td style="padding: 2px 10px;">323</td><td style="padding: 2px 10px;">0</td><td style="padding: 2px 10px;">312</td></tr> </table>	0	0	0	123	0	112	211	222	233	0	213	0	0	0	0	323	0	312	<table style="width: 100%; border-collapse: collapse;"> <tr><td style="padding: 2px 10px;">0</td><td style="padding: 2px 10px;">0</td><td style="padding: 2px 10px;">0</td><td style="padding: 2px 10px;">14</td><td style="padding: 2px 10px;">0</td><td style="padding: 2px 10px;">16</td></tr> <tr><td style="padding: 2px 10px;">21</td><td style="padding: 2px 10px;">22</td><td style="padding: 2px 10px;">23</td><td style="padding: 2px 10px;">0</td><td style="padding: 2px 10px;">25</td><td style="padding: 2px 10px;">0</td></tr> <tr><td style="padding: 2px 10px;">0</td><td style="padding: 2px 10px;">0</td><td style="padding: 2px 10px;">0</td><td style="padding: 2px 10px;">34</td><td style="padding: 2px 10px;">0</td><td style="padding: 2px 10px;">36</td></tr> </table>	0	0	0	14	0	16	21	22	23	0	25	0	0	0	0	34	0	36
0	0	0	123	0	112																																
211	222	233	0	213	0																																
0	0	0	323	0	312																																
0	0	0	14	0	16																																
21	22	23	0	25	0																																
0	0	0	34	0	36																																
group 121,	unique axis \mathbf{e}_2 (4.82)																																				

A mirror plane \mathbf{m} normal to \mathbf{e}_2 gives a complementary result:

tensor notation	Voigt notation																																				
<table style="width: 100%; border-collapse: collapse;"> <tr><td style="padding: 2px 10px;">111</td><td style="padding: 2px 10px;">122</td><td style="padding: 2px 10px;">133</td><td style="padding: 2px 10px;">0</td><td style="padding: 2px 10px;">113</td><td style="padding: 2px 10px;">0</td></tr> <tr><td style="padding: 2px 10px;">0</td><td style="padding: 2px 10px;">0</td><td style="padding: 2px 10px;">0</td><td style="padding: 2px 10px;">223</td><td style="padding: 2px 10px;">0</td><td style="padding: 2px 10px;">212</td></tr> <tr><td style="padding: 2px 10px;">311</td><td style="padding: 2px 10px;">322</td><td style="padding: 2px 10px;">333</td><td style="padding: 2px 10px;">0</td><td style="padding: 2px 10px;">313</td><td style="padding: 2px 10px;">0</td></tr> </table>	111	122	133	0	113	0	0	0	0	223	0	212	311	322	333	0	313	0	<table style="width: 100%; border-collapse: collapse;"> <tr><td style="padding: 2px 10px;">11</td><td style="padding: 2px 10px;">12</td><td style="padding: 2px 10px;">13</td><td style="padding: 2px 10px;">0</td><td style="padding: 2px 10px;">15</td><td style="padding: 2px 10px;">0</td></tr> <tr><td style="padding: 2px 10px;">0</td><td style="padding: 2px 10px;">0</td><td style="padding: 2px 10px;">0</td><td style="padding: 2px 10px;">24</td><td style="padding: 2px 10px;">0</td><td style="padding: 2px 10px;">26</td></tr> <tr><td style="padding: 2px 10px;">31</td><td style="padding: 2px 10px;">32</td><td style="padding: 2px 10px;">33</td><td style="padding: 2px 10px;">0</td><td style="padding: 2px 10px;">35</td><td style="padding: 2px 10px;">0</td></tr> </table>	11	12	13	0	15	0	0	0	0	24	0	26	31	32	33	0	35	0
111	122	133	0	113	0																																
0	0	0	223	0	212																																
311	322	333	0	313	0																																
11	12	13	0	15	0																																
0	0	0	24	0	26																																
31	32	33	0	35	0																																
group 1m1,	unique axis \mathbf{e}_2 (4.83)																																				

The reader is invited to derive the form of the tensor for the other non-centrosymmetric groups and/or to refer to the literature (for example, J. F. Nye, *Physical Properties of Crystals*). Piezoelectricity can exist in all these groups except the group 432 where the tensor cancels out. This fact may be understood on the basis of a useful theorem that we present without proof (C. Hermann, *Z. Kristallogr.* 89, 32–48, 1934):

A tensor of rank R has cylindrical symmetry with respect to a rotation axis of order superior or equal to $R + 1$.

Thus, a symmetric tensor of rank 2 is characterized by an ellipsoid of revolution for threefold, fourfold and sixfold symmetries. With respect to piezoelectricity, the hexagonal groups impose the same conditions on the tensor as the corresponding tetragonal groups (422 \leftrightarrow 622, 4mm \leftrightarrow 6mm, etc.). Because a piezoelectric polarization can only develop along a polar direction, the effect is zero in any direction perpendicular to a fourfold or sixfold axis. Consequently,

the effect cannot exist in the group 432. In the case of the elasticity tensor, hexagonal groups generate the cylindrical symmetry ∞/mmm .

In the literature we find not only the piezoelectric constants discussed above but also the inverse tensors, less directly related to experiment, which characterize the stresses resulting from an electrostatic field, as well as the polarization resulting from a strain:

$$\sigma_{mn} = \sum_i^3 e_{imn} E_i; \quad P_i = \sum_m^3 \sum_n^3 e_{imn} \epsilon_{mn}. \tag{4.84}$$

The relation between \mathbf{e} and \mathbf{d} may be calculated by using the elasticity tensor which expresses ϵ as a function of σ :

$$\begin{aligned} d_{ipq} &= \sum_m^3 \sum_n^3 e_{imn} S_{mnpq}; & d_{ik} &= \sum_j^6 e_{ij} S_{jk}; \\ e_{ipq} &= \sum_m^3 \sum_n^3 d_{imn} C_{mnpq}; & e_{ik} &= \sum_j^6 d_{ij} C_{jk}. \end{aligned} \tag{4.85}$$

EXAMPLES

The tensor d_{imn} ($i, m, n = 1$ and 2) characteristic of the two-dimensional structure of symmetry $p31m$ represented in Fig. 4.15 is:

tensor notation			Voigt notation		
d_{111}	$-d_{111}$	0	d_{11}	$-d_{11}$	0
0	0	$-d_{111}$	0	0	$-2d_{11}$

where \mathbf{e}_1 is parallel to the mirror plane m and to the bond $B \rightarrow A$, and \mathbf{e}_2 is perpendicular to m and to $B \rightarrow A$. The polarization resulting from a stress becomes:

$$P_1 = d_{111}(\sigma_{11} - \sigma_{22}) = d_{11}(\sigma_1 - \sigma_2); \quad P_2 = -d_{111}\sigma_{12} = -2d_{11}\sigma_6. \tag{4.86}$$

The interpretation of the result for P_1 is clear (Fig. 4.15(b)): a compression along the bond produces the same effect as an expansion perpendicular to the bond. A uniaxial stress σ parallel to $\mathbf{l} = (l_1, l_2)$, $\|\mathbf{l}\| = 1$ gives:

$$\begin{aligned} P_1 &= d_{11}\sigma(l_1^2 - l_2^2); & P_2 &= -2d_{11}\sigma l_1 l_2; \\ \|\mathbf{P}\|^2 &= \sigma^2 d_{11}^2, \text{ independent of the direction of } \mathbf{l}. \end{aligned}$$

The angle between \mathbf{P} and \mathbf{l} is

$$\cos(\mathbf{P}/\mathbf{l}) = (4l_1^2 - 3)l_1.$$

From this we deduce that the effect is purely longitudinal for $l_1 = 1$ or $-\frac{1}{2}$, i.e. for a stress parallel to the bond $B \rightarrow A$. For $l_1 = 0$ or $\pm\sqrt{3}/2$, the effect is purely transverse: the stress is then perpendicular and the polarization parallel to the bond $B \rightarrow A$. This result is easily explained with the help of Fig. 4.15(b). If the stress is diagonal with respect to \mathbf{e}_1 and \mathbf{e}_2 , $l_1 = l_2 = 1/\sqrt{2}$, we obtain a polarization perpendicular to the bond.

This example corresponds exactly to the properties of quartz (SiO_2) cut perpendicular to the threefold axis. Quartz is the most important piezoelectric crystal for technical applications:

Right-handed quartz, crystal class **32** (example from Sections 4.4.1 and 4.4.2). The tensor \mathbf{d} has the form (Voigt notation):

d_{11}	$-d_{11}$	0	d_{14}	0	0
0	0	0	0	$-d_{14}$	$-2d_{11}$
0	0	0	0	0	0

$d_{11} = 2.30 \times 10^{-12}$ C/N, $d_{14} = -0.67 \times 10^{-12}$ C/N; 1 Coulomb/Newton = 1 meter/Volt = 10^8 C m $^{-2}$ kbar $^{-1}$. A stress perpendicular to the threefold axis, $(\sigma_1 \ \sigma_2 \ 0 \ 0 \ 0 \ \sigma_6)$, gives the polarization $P_1 = d_{11}(\sigma_1 - \sigma_2)$, $P_2 = -2d_{11}\sigma_6$. We obtain equation (4.86) by eliminating the coordinate along \mathbf{e}_3 . A uniaxial stress of 1 bar (10^5 Pa, 1 atmosphere) gives a polarization of 2.30×10^{-7} C/m 2 . The electric susceptibility χ_{11} is 3.5 (Section 4.4.1). Thus the polarization corresponds to an electric field of 74 V/cm.

NOTE. A stress σ_1 of 1 bar with no electric field ($\mathbf{E} = 0$), or an electric field E_1 of 74 V/cm with no mechanical stress ($\boldsymbol{\sigma} = 0$) gives the same polarization, but the strain of the crystal is not the same in the two cases. For the case of the stress σ_1 at $\mathbf{E} = 0$, see Section 4.4.2. E_1 at $\boldsymbol{\sigma} = 0$ gives $\varepsilon_1 = d_{11}E_1$, $\varepsilon_2 = -d_{11}E_1$, $\varepsilon_4 = 2\varepsilon_{23} = d_{14}E_1$. For $E_1 = 100$ V/cm = 10^4 V/m, $\varepsilon_1 = -\varepsilon_2 = 2.3 \times 10^{-8}$, $\varepsilon_4 = -0.67 \times 10^{-8}$. The principal effect ε_1 and ε_2 is represented in Fig. 4.16.

The vibration induced by $\pm \mathbf{E}$ allows the frequency of an electric resonant circuit (used, for example, in a quartz watch) to be stabilized. Quartz is also used in the manufacture of acoustic generators. The theory which accounts for this dynamic effect comprises the calculation of the elastic vibrations of the crystal (Section 4.4.3) induced by an alternating electric field $E_1 \cos \omega t$ parallel to \mathbf{e}_1 in the absence of external stresses. The importance of quartz is due to the fact that it is chemically inert and very stable, and, even if the elastic and piezoelectric constants vary with temperature, it is possible to cut crystal plates with orientations such that their natural frequencies are constant over a large temperature

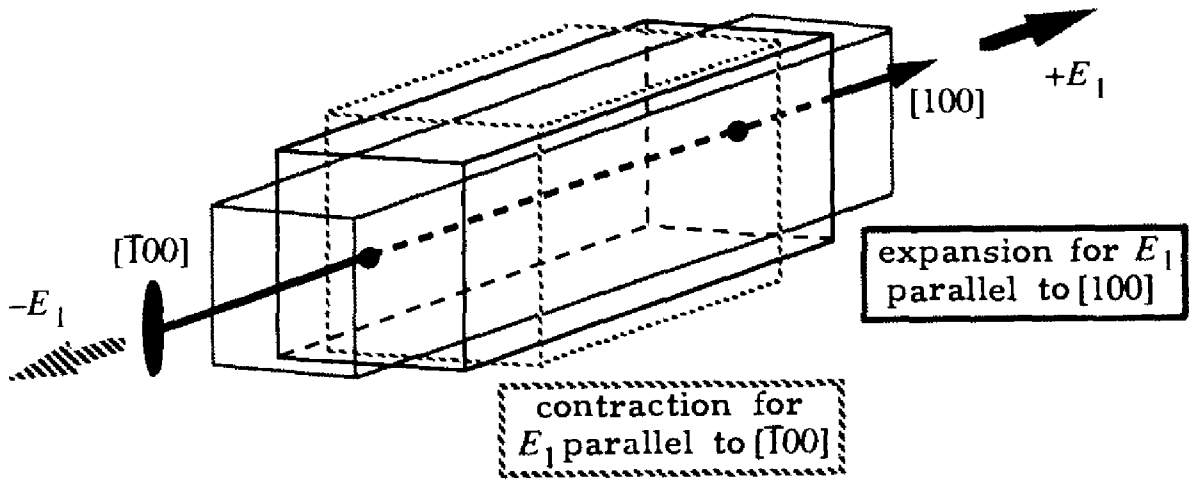


Fig. 4.16. Strain of a quartz rod induced by an electric field $\pm E_1$ down the twofold axis

range. The piezoelectric effect of ceramics with the perovskite structure is exploited in gas lighters.

4.4.6 GENERAL DESCRIPTION OF EQUILIBRIUM PROPERTIES

The anisotropic properties described in Sections 4.4.1 to 4.4.5 are not all independent. The strain ϵ is not only a function of the mechanical stresses σ to which the crystal is submitted, it is equally a function of the electric field E (inverse piezoelectric effect) and of the temperature ΔT (thermal expansion):

$$\epsilon_{mn} = \epsilon_{mn}(\sigma_{pq}, E_p, \Delta T), \quad (p, q \text{ from } 1 \text{ to } 3). \tag{4.87}$$

The electric polarization \mathbf{P} and the entropy \mathbf{S} of the crystal depend on the same quantities $\sigma_{pq}, E_p, \Delta T$. A reversible temperature change ΔT implies an entropy change per unit volume of:

$$\Delta S = (C/T)\Delta T,$$

C being the specific heat and T the absolute temperature. The corresponding thermal energy per unit volume is:

$$\Delta Q = T\Delta S = C\Delta T. \tag{4.88}$$

Following equation (4.3) we can see that σ, E and ΔT are the causes of the effects ϵ, \mathbf{P} and ΔS . By developing the terms (4.87) into a Taylor series about the points

$\varepsilon = 0$, $\mathbf{E} = 0$, $\Delta\mathbf{S} = 0$, on keeping only the linear terms, we obtain:

$$\begin{aligned}\varepsilon_{mn} &= \sum_p \sum_q S_{mnpq}^{E,T} \sigma_{pq} + \sum_p d_{pmn}^{*\sigma,T} E_p + e_{mn}^{\sigma,E} \Delta T, \\ P_m &= \sum_p \sum_q d_{mpq}^{E,T} \sigma_{pq} + \varepsilon_0 \sum_p \chi_{mp}^{\sigma,T} E_p + p_m^{\sigma,E} \Delta T, \\ \Delta\mathbf{S} &= \sum_p \sum_q e_{pq}^{*E,T} \sigma_{pq} + \sum_q p_q^{*\sigma,T} E_q + (\mathbf{C}^{\sigma,E}/T) \Delta T.\end{aligned}\quad (4.89)$$

The exponents (E, T) , (σ, T) and (σ, E) signify (at constant electric field and constant temperature), (at constant stress and constant temperature), and (at constant stress and constant electric field) respectively. The individual terms are:

$$\begin{aligned}S_{mnpq}^{E,T} &= \left(\frac{\partial \varepsilon_{mn}}{\partial \sigma_{pq}} \right)_{E,T} && : \text{elastic constants (Section 4.4.2);} \\ d_{pmn}^{*\sigma,T} &= \left(\frac{\partial \varepsilon_{mn}}{\partial E_p} \right)_{\sigma,T} && : \text{inverse piezoelectricity (Section 4.4.5);} \\ e_{mn}^{\sigma,E} &= \left(\frac{\partial \varepsilon_{mn}}{\partial T} \right)_{\sigma,E} && : \text{thermal expansion (Section 4.4.4);} \\ d_{mpq}^{E,T} &= \left(\frac{\partial P_m}{\partial \sigma_{pq}} \right)_{E,T} && : \text{piezoelectricity (Section 4.4.5);} \\ \chi_{mp}^{\sigma,T} &= \frac{1}{\varepsilon_0} \left(\frac{\partial P_m}{\partial E_p} \right)_{\sigma,T} && : \text{electric susceptibility (Section 4.4.1);} \\ p_m^{\sigma,E} &= \left(\frac{\partial P_m}{\partial T} \right)_{\sigma,E} && : \text{pyroelectricity (Section 4.4.4);} \\ e_{pq}^{*E,T} &= \left(\frac{\partial \mathbf{S}}{\partial \sigma_{pq}} \right)_{E,T} && : \text{piezocaloric effect;} \\ p_q^{*\sigma,T} &= \left(\frac{\partial \mathbf{S}}{\partial E_q} \right)_{\sigma,T} && : \text{electrocaloric effect;} \\ \mathbf{C}^{\sigma,E}/T &= \left(\frac{\partial \mathbf{S}}{\partial T} \right)_{\sigma,E} && : \text{specific heat; } \mathbf{C}^{\sigma,E} = \mathbf{C}_p \text{ (at constant pressure).}\end{aligned}$$

By using the Voigt notation, we represent equation (4.89) by a 10×10 symmetric matrix. Figure 4.17 shows this matrix and its inverse. The energy change per unit volume of a crystal subjected to $\boldsymbol{\sigma}$, \mathbf{E} and ΔT in a *reversible* manner is equal to the sum of the strain energy (4.62), the electric polarization

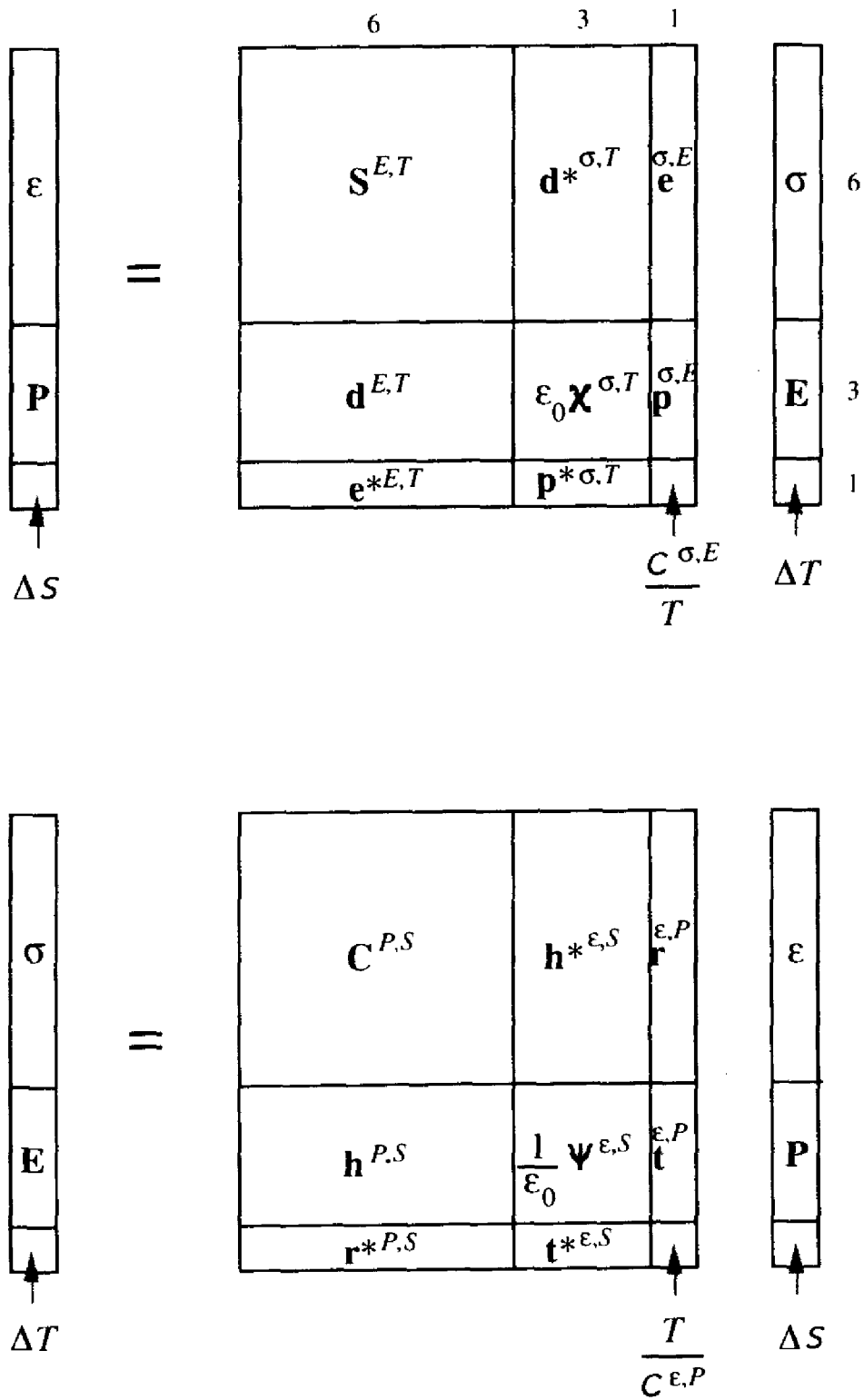


Fig. 4.17. The 10 × 10 matrix and its inverse

energy (4.47) and the thermal energy (4.88):

$$w = \int_0^{\sigma, E, T} \left\{ \sum_m^3 \sum_n^3 \varepsilon_{mn} d\sigma_{mn} + \varepsilon_0 \sum_m^3 P_m dE_m + C dT \right\} \quad (4.90)$$

Unlike equation (4.47), integral (4.90) contains the polarization energy without the energy of the electric field $\varepsilon_0 \|\mathbf{E}\|^2/2$. By analogy with equation (4.60), integral (4.90) is curvilinear. The same final state $\boldsymbol{\sigma}$, \mathbf{E} and T , and hence the same energy w , may be attained by subjecting the crystal consecutively to the components of stress, electric field and temperature in any order. It follows from this argument that the 10×10 matrices in Fig. 4.17 are symmetric. The inverse and direct piezoelectric tensors are thus numerically identical (4.78):

$$d_{pmn}^{*\sigma, T} = d_{pmn}^{E, T} \quad (4.91)$$

In the same way we can recognize the correspondence between:

- thermal expansion and the piezocaloric effect, $e_{mn}^{\sigma, E} = e_{mn}^{*E, T}$, (4.92)
- pyroelectricity and the electrocaloric effect, $p_m^{\sigma, E} = p_m^{*\sigma, T}$. (4.93)

We see that the sub-matrix $\mathbf{C}^{P, S}$ is not the inverse of the sub-matrix $\mathbf{S}^{E, T}$, hence $\mathbf{C}^{E, T} \neq \mathbf{C}^{P, S}$: the elastic moduli at constant electric field and constant temperature are different from the moduli at constant electric polarization and constant entropy. The specific heat $\mathbf{C}^{\varepsilon, P}$ (at constant strain and polarization) is commonly called C_v (specific heat at constant volume), whereas $\mathbf{C}^{\sigma, E} = \mathbf{C}_p$ (specific heat at constant pressure).

4.5 CRYSTAL OPTICS

4.5.1 BIREFRINGENCE

Among the anisotropic properties of crystals, one of the most spectacular is birefringence. There are numerous scientific and technical applications. The best-known birefringent crystal is calcite, CaCO_3 , symmetry $\bar{3}m$ (Erasmus Bartholin, 1669): the image of an object viewed through a calcite crystal appears doubled except when looking down the threefold axis. A light ray which penetrates into the crystal divides into two rays with perpendicular polarizations. One ray, called *extraordinary*, does not obey Snell's law of refraction. The other, the *ordinary* ray, does obey Snell's law; its polarization direction is perpendicular to the threefold axis (Fig. 4.18). In general, in crystals of low symmetry (triclinic, monoclinic, orthorhombic), neither of the two rays obeys Snell's law and are thus both extraordinary rays.

The most important application of crystal optics is the identification of crystals and single-crystal domains in polycrystalline aggregates. The polarizing micro-

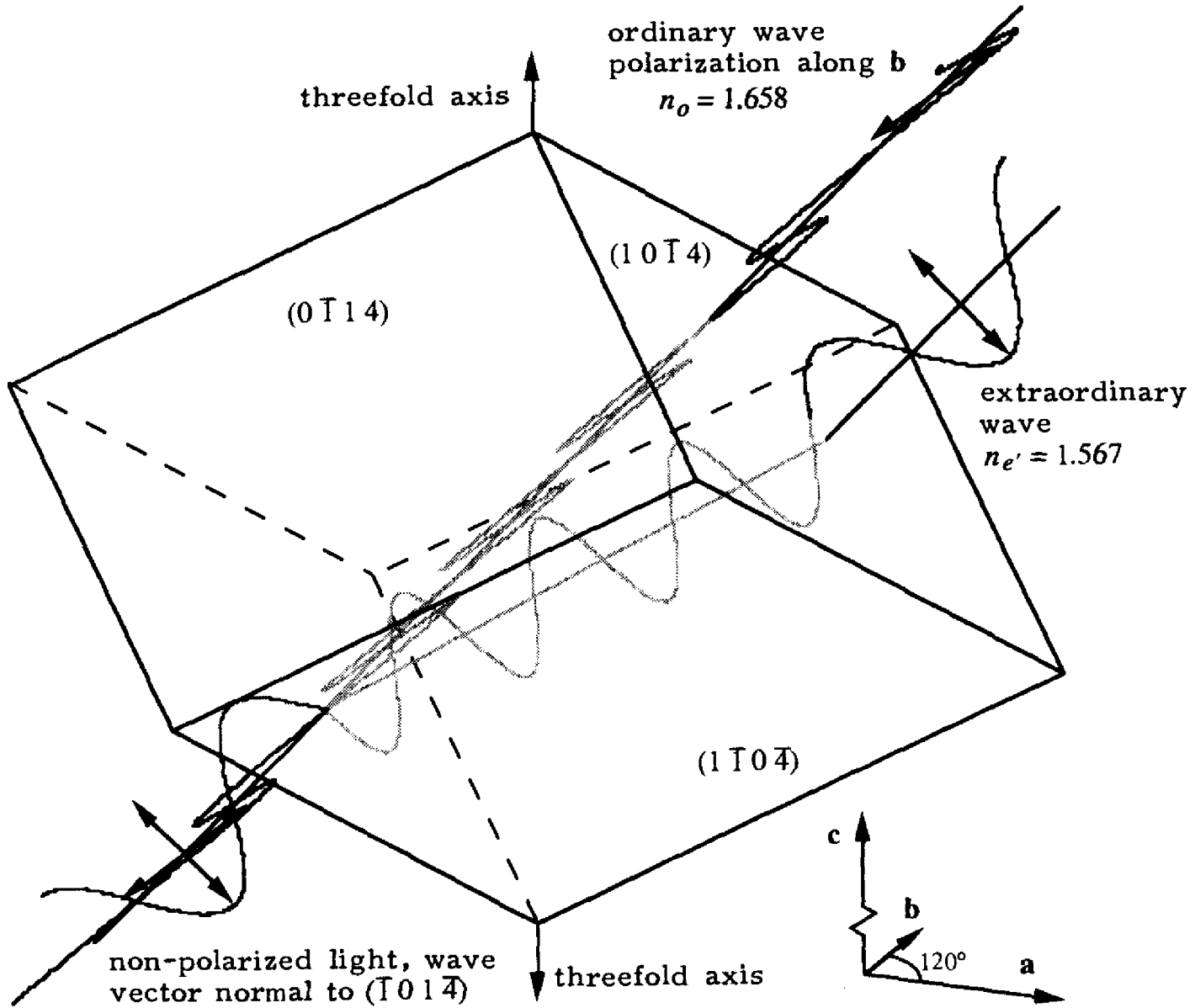


Fig. 4.18. Ordinary and extraordinary rays in calcite

scope (Section 4.5.6) is an indispensable tool of the mineralogist. The reader interested by this technique should consult the specialist literature.

4.5.2 WAVE NORMAL AND LIGHT RAY

Maxwell's equations allow us to explain birefringence if we take into account the crystal anisotropy:

$$\text{curl } \mathbf{H} = \frac{\partial \mathbf{D}}{\partial t}, \quad \text{insulating crystals, hence no electric current:}$$

$$\text{curl } \mathbf{E} = -\frac{\partial \mathbf{B}}{\partial t};$$

$\mathbf{D} = \varepsilon_0 \boldsymbol{\varepsilon} \mathbf{E}$ $\boldsymbol{\varepsilon}$ is a tensor of rank 2 (Section 4.46);

$\mathbf{B} = \mu_0 \boldsymbol{\mu} \mathbf{H}$ $\boldsymbol{\mu}$ is the relative magnetic permeability tensor.

μ_0 is the permeability of free space. The relation between the magnetic induction \mathbf{B} and the magnetic field \mathbf{H} is exactly analogous to that which relates the electric displacement \mathbf{D} and the electric field \mathbf{E} (Section 4.4.1). With the exception of ferromagnetic crystals (which are only rarely transparent), the eigenvalues of $\boldsymbol{\mu}$ are close to 1:

$$\mu \approx 1 \pm 10^{-5}; \quad + \text{paramagnetic, } - \text{diamagnetic.}$$

Hence, there is no risk in neglecting the tensor nature of $\boldsymbol{\mu}$ and supposing that $\mathbf{B} \approx \mu_0 \boldsymbol{\mu} \mathbf{H} \approx \mu_0 \mathbf{H}$. In contrast, the eigenvalues of $\boldsymbol{\varepsilon}$ are very different from 1 (between 4 and 5 for quartz, Section 4.4.1) and the tensor nature of $\boldsymbol{\varepsilon}$ has important consequences. The terms of this tensor also vary with the frequency of light.

Consider the existence of a plane wave in the interior of the crystal:

$$\mathbf{E} = \mathbf{E}_0 e^{i(\omega t - \mathbf{k} \cdot \mathbf{r})} = \mathbf{E}_0 \psi, \quad \omega = 2\pi\nu, \quad \|\mathbf{k}\| = \frac{2\pi}{\lambda}, \quad (\text{equation (3.6)}),$$

where ν is the frequency and λ the wavelength. Following the rules of vector algebra we obtain:

$$\text{curl } \mathbf{E} = \text{curl}(\mathbf{E}_0 \psi) = \psi \text{curl } \mathbf{E}_0 + \text{grad } \psi \times \mathbf{E}_0 = \text{grad } \psi \times \mathbf{E}_0,$$

$$\text{curl } \mathbf{E} = -i[\mathbf{k} \times \mathbf{E}_0] e^{i(\omega t - \mathbf{k} \cdot \mathbf{r})} = -\frac{\partial \mathbf{B}}{\partial t},$$

$$\mathbf{B} = \frac{1}{\omega} [\mathbf{k} \times \mathbf{E}_0] e^{i(\omega t - \mathbf{k} \cdot \mathbf{r})} = \mu_0 \boldsymbol{\mu} \mathbf{H}. \quad (4.94)$$

In a similar manner, for \mathbf{D} we obtain:

$$\mathbf{D} = \frac{1}{\mu \mu_0 \omega^2} \{ [\mathbf{k} \times \mathbf{E}_0] \times \mathbf{k} \} e^{i(\omega t - \mathbf{k} \cdot \mathbf{r})} = \varepsilon_0 \boldsymbol{\varepsilon} \mathbf{E}. \quad (4.95)$$

Remember that $\{ [\mathbf{k} \times \mathbf{E}_0] \times \mathbf{k} \} = \|\mathbf{k}\|^2 \mathbf{E}_0 - \mathbf{k}(\mathbf{E}_0 \cdot \mathbf{k})$.

We note that $\mathbf{B} \cdot \mathbf{E} = \mathbf{B} \cdot \mathbf{k} = \mathbf{B} \cdot \mathbf{D} = \mathbf{D} \cdot \mathbf{k} = 0$, but in general, $\mathbf{E} \cdot \mathbf{k} \neq 0$. The energy flux carried by the wave is given by the Poynting vector:

$$\mathbf{S} = [\mathbf{E} \times \mathbf{H}], \text{ light ray.} \quad (4.96)$$

Indeed, we can easily show that

$$\begin{aligned} \text{div } \mathbf{S} &= \text{div}[\mathbf{E} \times \mathbf{H}] = \mathbf{H} \cdot \text{curl } \mathbf{E} - \mathbf{E} \cdot \text{curl } \mathbf{H} = -\mathbf{H} \cdot \frac{\partial \mathbf{B}}{\partial t} - \mathbf{E} \cdot \frac{\partial \mathbf{D}}{\partial t}, \\ \mathbf{E} \cdot \frac{\partial \mathbf{D}}{\partial t} &= \varepsilon_0 \sum_m^3 \sum_n^3 \varepsilon_{mn} E_m \frac{\partial E_n}{\partial t} = \frac{1}{2} \varepsilon_0 \frac{\partial}{\partial t} \sum_m^3 \sum_n^3 \varepsilon_{mn} E_m E_n. \end{aligned}$$

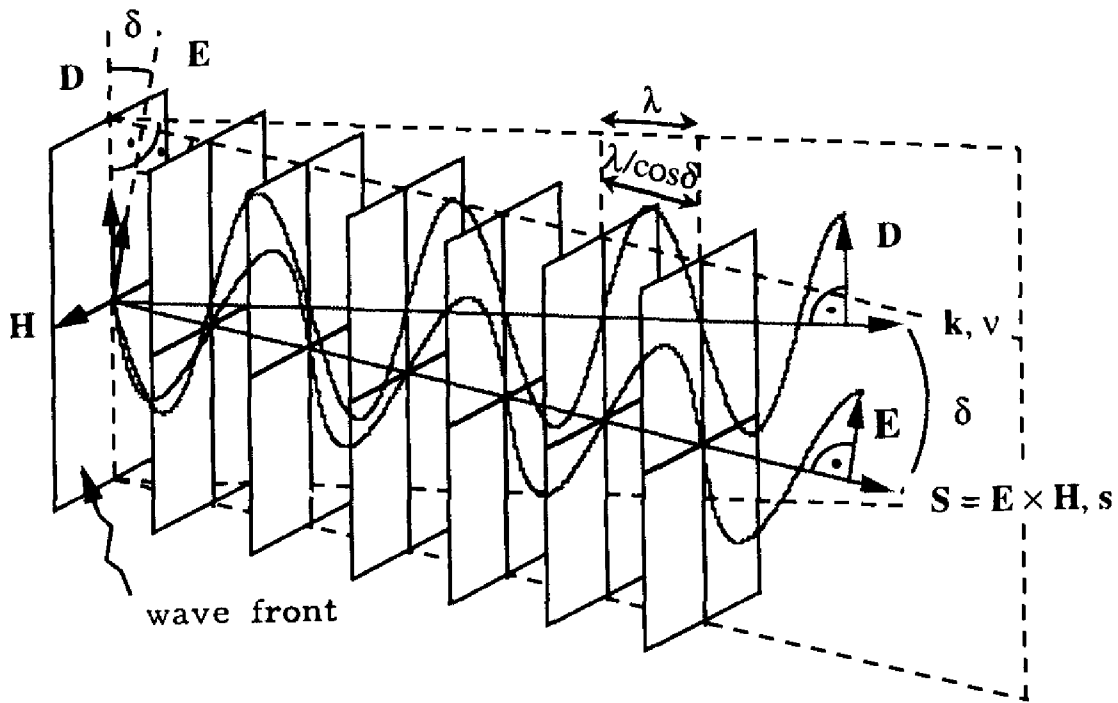


Fig. 4.19. Representation of the vectors \mathbf{H} , \mathbf{E} , \mathbf{D} , \mathbf{v} , \mathbf{s}

Using relation (4.47), for the electric energy density w_{el} we obtain:

$$\mathbf{E} \cdot \frac{\partial \mathbf{D}}{\partial t} = \frac{\partial w_{el}}{\partial t},$$

and in an analogous manner for the magnetic energy density:

$$\mathbf{H} \cdot \frac{\partial \mathbf{B}}{\partial t} = \frac{1}{2} \mu_0 \frac{\partial}{\partial t} \sum_m^3 \sum_n^3 \mu_{mn} H_m H_n = \frac{\partial w_{mag}}{\partial t}.$$

The energy density of the wave is $w_{el} + w_{mag} = w_{tot}$:

$$\text{div } \mathbf{S} = - \frac{\partial w_{tot}}{\partial t}. \tag{4.97}$$

\mathbf{S} is indeed the energy flux per unit area.

We define the unit vectors \mathbf{v} and \mathbf{s} , $\|\mathbf{v}\|^2 = \|\mathbf{s}\|^2 = 1$, as follows:

$$\begin{aligned} \mathbf{k} &= \|\mathbf{k}\| \mathbf{v}, & \mathbf{v} &= \text{normal to the plane wave;} \\ \mathbf{S} &= \|\mathbf{S}\| \mathbf{s}, & \mathbf{s} &= \text{direction of the light ray.} \end{aligned}$$

The wave normal \mathbf{v} is perpendicular to the plane of the wave (locus of constant phase) $\mathbf{k} \cdot \mathbf{r} = (2\pi/\lambda) \mathbf{v} \cdot \mathbf{r} = \text{constant}$. The rate of propagation in the direction of \mathbf{v} is $v_n = \omega / \|\mathbf{k}\|$. In the direction of \mathbf{s} (Fig. 4.19), the rate of propagation is $v_s = v_n / \cos \delta$, where δ is the angle between \mathbf{D} and \mathbf{E} . With the help of equations

(4.94), (4.95) and (4.96), for \mathbf{H} , \mathbf{E} , \mathbf{D} , \mathbf{v} and \mathbf{s} , we obtain:

$$\mathbf{H} = \frac{1}{\mu\mu_0 v_n} [\mathbf{v} \times \mathbf{E}] = v_n [\mathbf{v} \times \mathbf{D}] = \frac{1}{\mu\mu_0 v_s} [\mathbf{s} \times \mathbf{E}] = v_s [\mathbf{s} \times \mathbf{D}],$$

$$\mathbf{D} = \frac{1}{v_n} [\mathbf{H} \times \mathbf{v}] = \frac{1}{\mu\mu_0 v_n^2} \{\mathbf{E} - \mathbf{v}(\mathbf{v} \cdot \mathbf{E})\}, \quad (4.98)$$

$$\mathbf{E} = \mu\mu_0 v_s [\mathbf{H} \times \mathbf{s}] = \mu\mu_0 v_s^2 \{\mathbf{D} - \mathbf{s}(\mathbf{s} \cdot \mathbf{D})\}. \quad (4.99)$$

Figure 4.19 illustrates these relationships. It is important to distinguish between the *wave normal* \mathbf{v} and the *light ray* \mathbf{s} . The plane of the wave is always perpendicular to \mathbf{v} . It contains \mathbf{D} but not \mathbf{E} . The plane wave is transverse with respect to \mathbf{v} , but it is not purely transverse with respect to \mathbf{s} . An analogous effect is observed for elastic waves in a crystal (Section 4.4.3), which are neither purely transverse or purely longitudinal in general. In addition, we note that

$$\text{div } \mathbf{D} = -ik \cdot \mathbf{D} = 0, \text{ but } \text{div } \mathbf{E} = -ik \cdot \mathbf{E} = -ikE \sin \delta \neq 0.$$

4.5.3 SNELL'S LAW

In order to simplify the discussion, let us choose a coordinate system based on the eigenvectors of the tensor ϵ : $D_i = \epsilon_0 \epsilon_i E_i (i = 1, 2, 3)$. First, let us calculate the waves which can propagate in the direction of a given wave normal $\mathbf{v} = (v_1, v_2, v_3)$.

With equation (4.98) we obtain:

$$D_i \left\{ v_n^2 \mu_0 \mu - \frac{1}{\epsilon_0 \epsilon_i} \right\} + v_i (\mathbf{v} \cdot \mathbf{E}) = 0,$$

$$D_i = \frac{v_i (\mathbf{v} \cdot \mathbf{E}) \epsilon_0 \epsilon_i}{1 - \epsilon_0 \epsilon_i \mu_0 \mu v_n^2}; \quad \sum_i^3 D_i v_i = 0,$$

$$\sum_i^3 \frac{\epsilon_i v_i^2}{1 - v_n^2 \mu_0 \mu \epsilon_0 \epsilon_i} = 0, \quad (4.100)$$

$$\sum_i^3 \epsilon_i v_i^2 (1 - v_n^2 \mu_0 \mu \epsilon_0 \epsilon_j) (1 - v_n^2 \mu_0 \mu \epsilon_0 \epsilon_k) = 0. \quad (i \neq j \neq k) \quad (4.101)$$

Equation (4.101) is a quadratic function of v_n^2 . For each direction \mathbf{v} , there are two solutions, $v_n'^2$ and $v_n''^2$. For example, for $\mathbf{v} = (1, 0, 0)$, we obtain:

$$v_n' = v_2 = \frac{1}{\sqrt{\mu_0 \mu \epsilon_0 \epsilon_2}}; \quad v_n'' = v_3 = \frac{1}{\sqrt{\mu_0 \mu \epsilon_0 \epsilon_3}}.$$

Using these relations, equation (4.100) becomes:

$$\frac{v_1^2}{v_1^2 - v_n^2} + \frac{v_2^2}{v_2^2 - v_n^2} + \frac{v_3^2}{v_3^2 - v_n^2} = 0, \tag{4.102}$$

$$D_1 : D_2 : D_3 = \frac{v_1}{v_1^2 - v_n^2} : \frac{v_2}{v_2^2 - v_n^2} : \frac{v_3}{v_3^2 - v_n^2} \tag{4.103}$$

$$v_i = \frac{1}{\sqrt{\mu_0 \mu \epsilon_0 \epsilon_i}}. \tag{4.104}$$

The two vectors \mathbf{D}' and \mathbf{D}'' correspond to the two solutions, $v_n'^2$ and $v_n''^2$ from equation (4.102). The scalar product $\mathbf{D}' \cdot \mathbf{D}''$ is obtained from equation (4.103) by use of the formula

$$\frac{1}{ab} = -\frac{1}{a-b} \left(\frac{1}{a} - \frac{1}{b} \right)$$

from which we can deduce that $\mathbf{D}' \cdot \mathbf{D}'' = 0$. \mathbf{D}' is thus perpendicular to \mathbf{D}'' .

In a given direction \mathbf{v} of a wave normal, two waves can propagate with different speeds v_n' and v_n'' . The polarizations of the corresponding electric displacements are perpendicular: $\mathbf{D}' \cdot \mathbf{D}'' = \mathbf{H}' \cdot \mathbf{H}'' = 0$. In contrast, the vectors \mathbf{E}' and \mathbf{E}'' are not perpendicular, and the light rays \mathbf{s}' and \mathbf{s}'' are not coincident.

For the waves propagating in a given direction $\mathbf{s} = (s_1, s_2, s_3)$ of the light ray, from equation (4.99) we can carry out an analogous calculation:

$$\frac{s_1^2}{v_1^{-2} - v_s^{-2}} + \frac{s_2^2}{v_2^{-2} - v_s^{-2}} + \frac{s_3^2}{v_3^{-2} - v_s^{-2}} = 0, \tag{4.105}$$

$$E_1 : E_2 : E_3 = \frac{s_1}{v_1^{-2} - v_s^{-2}} : \frac{s_2}{v_2^{-2} - v_s^{-2}} : \frac{s_3}{v_3^{-2} - v_s^{-2}}, \tag{4.106}$$

$$v_i = \frac{1}{\sqrt{\mu_0 \mu \epsilon_0 \epsilon_i}}.$$

Two vectors \mathbf{E}' and \mathbf{E}'' correspond to the two solutions $v_s'^2$ and $v_s''^2$ from equation (4.105). From equation (4.106) we obtain the scalar product $\mathbf{E}' \cdot \mathbf{E}'' = 0$.

In a given direction \mathbf{s} of a light ray, two waves can propagate with different speeds v_s' and v_s'' . The polarizations of the corresponding electric fields are perpendicular: $\mathbf{E}' \cdot \mathbf{E}'' = \mathbf{H}' \cdot \mathbf{H}'' = 0$. In contrast, the vectors \mathbf{D}' and \mathbf{D}'' are not perpendicular, and the wave normals \mathbf{v}' and \mathbf{v}'' are not coincident.

Thus, there are two types of birefringence, one with respect to the light rays and the other with respect to the wave normals. The relative importance of the two types depends on the laws of refraction.

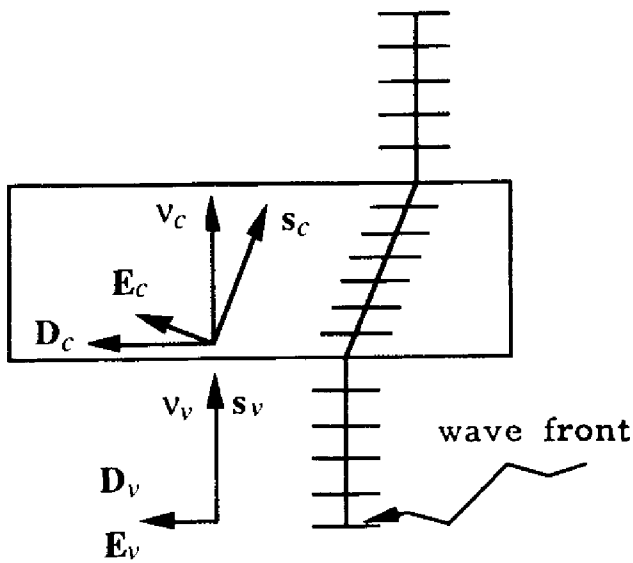


Fig. 4.20. Incident ray of polarized light normal to a crystal face

Figure 4.20 shows an incident ray of polarized light perpendicular to the face of a crystal. According to the continuity conditions (Section 4.4.1), the electric displacement in the crystal D_c is parallel to that in the vacuum D_v , whereas the electric fields E_v and E_c are not necessarily parallel. It follows that the light ray s undergoes refraction and does not obey Snell's law, in contrast to the wave normal v . Using similar arguments for the general case of oblique incidence at the vacuum/crystal interface, it can be shown that

the normal to the wave obeys Snell's law; the light ray does not obey Snell's law.

Figure 4.20 shows that waves can be created in any direction v in a crystal. It is sufficient that the incident light be perpendicular to a crystal plate cut in a chosen direction. For a non-polarized incident ray, the crystal produces two light rays of mutually perpendicular polarizations D' and D'' . If one of the two rays is suppressed, the crystal emits a ray that is perfectly polarized. This is the principle of the Nicol prism. In contrast, the creation of a wave in a selected direction s is not so simple.

4.5.4 FLETCHER INDICATRIX

The reference ellipsoid of the tensor $\phi = \epsilon^{-1}$ characterizes the birefringence of the normal to the wave. Still in the coordinate system of the eigenvectors of ϵ , by introducing $D = D(d_1, d_2, d_3)$ and $d_1^2 + d_2^2 + d_3^2 = 1$ into equation (4.98), we obtain:

$$v_n^2 = \frac{E \cdot D}{D^2 \mu_0 \mu} = \frac{1}{\mu_0 \mu \epsilon_0} \left\{ \frac{d_1^2}{\epsilon_1} + \frac{d_2^2}{\epsilon_2} + \frac{d_3^2}{\epsilon_3} \right\}, \text{ and with equation (4.104)}$$

$$v_n^2 = v_1^2 d_1^2 + v_2^2 d_2^2 + v_3^2 d_3^2.$$

The index of refraction n is the ratio between the speed of propagation in a vacuum and in the crystal. It concerns the rate v_n because the light ray does not obey Snell's law:

$$n = \frac{v_0}{v_n} = \frac{\lambda_0}{\lambda}$$

$$\frac{1}{n^2} = \frac{d_1^2}{n_1^2} + \frac{d_2^2}{n_2^2} + \frac{d_3^2}{n_3^2} \tag{4.107}$$

Equation (4.107) gives the indices of refraction for a wave polarized in the direction $\mathbf{D} = D(d_1, d_2, d_3)$. The ellipsoid

$$\frac{x_1^2}{n_1^2} + \frac{x_2^2}{n_2^2} + \frac{x_3^2}{n_3^2} = 1 \tag{4.108}$$

is called the *Fletcher (1892) indicatrix* or the *ellipsoid of the indices*. The length r of a ray from the center of the ellipsoid to the surface and parallel to \mathbf{D} equals n :

$$x_i = rd_i \rightarrow r = n.$$

This result is hardly surprising. In an isotropic medium, the speed of light is $v = (\mu_0 \mu \epsilon_0 \epsilon)^{-1/2}$, from which we can deduce that the refractive index $n = (\mu \epsilon)^{1/2} \approx \sqrt{\epsilon}$ because $\mu \approx 1$. In an anisotropic medium, we must consider the longitudinal dielectric effect $\mathbf{E}_L = (\epsilon_{L,D})^{-1} \mathbf{D}$ parallel to \mathbf{D} and not $\mathbf{D}_L = \epsilon_{L,E} \mathbf{E}$ parallel to \mathbf{E} because the fact that $v < v_0$ is due to the displacement of charges under the influence of an electric field. This longitudinal effect is represented by the tensor ellipsoid $\phi = \epsilon^{-1}$. In an arbitrary coordinate system, from equation (4.46) we obtain:

$$E_m \frac{1}{\epsilon_0} \sum_n \phi_{mn} D_n = \frac{D}{\epsilon_0} \sum_n \phi_{mn} d_n,$$

$$\sum_m \sum_n \phi_{mn} d_m d_n = \phi_L = \frac{1}{\epsilon_{L,D}} = \text{longitudinal effect parallel to } \mathbf{D}.$$

The Fletcher indicatrix

$$\sum_m \sum_n \phi_{mn} x_m x_n = 1$$

is the ellipsoid which has the property that the length of the ray in the direction of \mathbf{D} is $r = 1/\sqrt{\phi_L} = \sqrt{\epsilon_{L,D}} = n$ in agreement with equation (4.23).

The normal to the tangent plane of this ellipsoid determines the direction of \mathbf{E} (equation (4.25), Fig. 4.3). It is evident that the normal \mathbf{v} of a wave \mathbf{D} polarized along a principal axis of the ellipsoid is coincident with the corresponding light ray \mathbf{s} . This is the reason the principal rates v_1, v_2 and v_3 are the same in

equation (4.103) and (4.106). The corresponding values n_i in equation (4.108) are the *principal refractive indices*.

The Fletcher indicatrix was deduced from equation (4.98). In an analogous manner, we can obtain from equation (4.99) an ellipsoid which represents the tensor ε and hence the rates v_s :

$$\frac{1}{v_s^2} = \frac{e_1^2}{v_1^2} + \frac{e_2^2}{v_2^2} + \frac{e_3^2}{v_3^2}; \quad \mathbf{E} = E(e_1, e_2, e_3); \quad e_1^2 + e_2^2 + e_3^2 = 1.$$

The ellipsoid $n_1^2 x_1^2 + n_2^2 x_2^2 + n_3^2 x_3^2 = 1$, called the *rate ellipsoid*, has the property that the length of the ray parallel to \mathbf{E} is $r = v_s/v_0$.

The Fletcher indicatrix allows the determination of the polarizations and refractive indices of the waves which propagate in a crystal along the normal \mathbf{v} . The intersection of the ellipsoid and the plane perpendicular to \mathbf{v} which passes through the center is an ellipse. The vector \mathbf{D} normal to \mathbf{v} lies in this plane.

Remembering that the indicatrix represents the tensor ε^{-1} , for a given direction of \mathbf{D} , \mathbf{E} is thus the normal to the tangent plane (Fig. 4.3). In addition, \mathbf{D} , \mathbf{E} and \mathbf{v} are coplanar (Fig. 4.19). Figure 4.21 shows that these conditions determine the polarizations of the two waves associated with \mathbf{v} ; \mathbf{D}' and \mathbf{D}'' are parallel to the two principal axes of the ellipse.

Construction permitting the derivation of the two waves associated with a normal \mathbf{v} by means of the Fletcher indicatrix (Fig. 4.22):

The plane perpendicular to \mathbf{v} which passes through the center of the indicatrix is constructed. The intersection of the plane and the ellipsoid is an ellipse. The polarizations \mathbf{D}' and \mathbf{D}'' are parallel to the principal axis of the

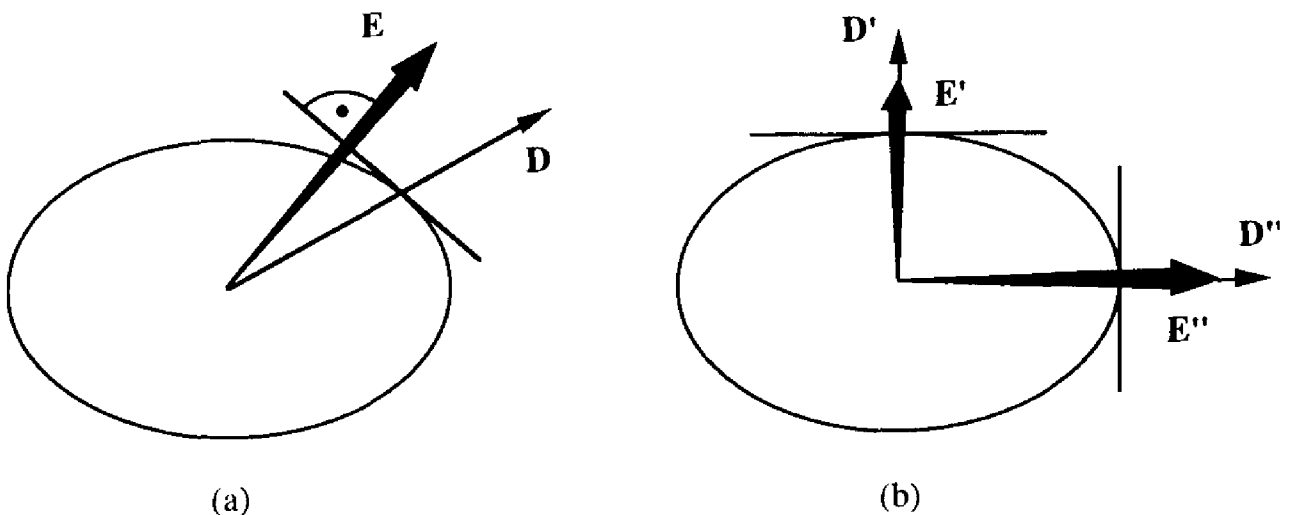


Fig. 4.21. Ellipse from the intersection of the indicatrix and of the plane perpendicular to \mathbf{v} . \mathbf{E} is constructed for a given direction of \mathbf{D} according to Fig. 4.3. The tangent plane is not perpendicular to the plane of the page and, hence, \mathbf{E} is not perpendicular to \mathbf{v} . Only in (b) are the vectors \mathbf{v} , \mathbf{D} and \mathbf{E} coplanar

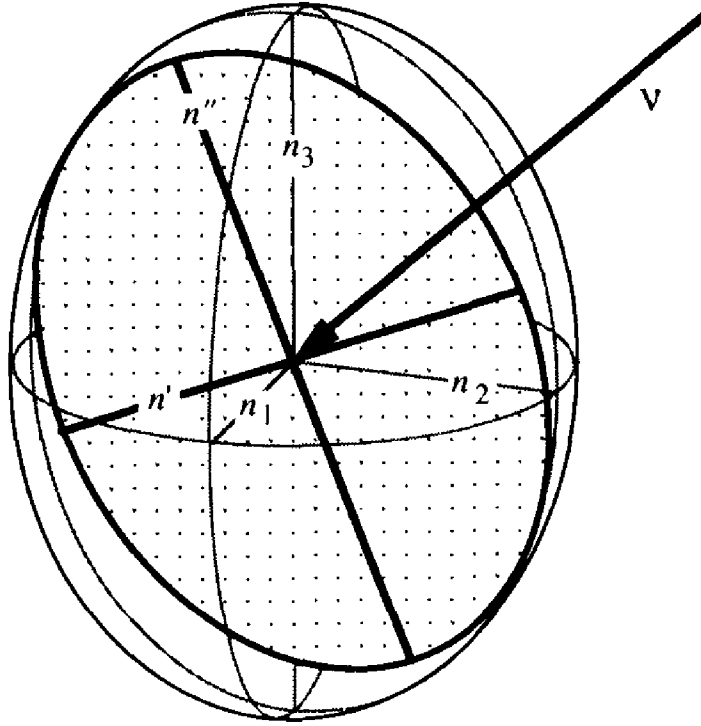


Fig. 4.22. Construction allowing the determination of the indices of refraction and the polarizations of two waves associated with a normal v

ellipse, whereas the refractive indices n' and n'' are equal to half the lengths of these axes. We find that $n_1 \leq n' \leq n_2 \leq n'' \leq n_3$ where n_1, n_2 and n_3 are the principal indices of refraction.

4.5.5 OPTICAL AXES

For an arbitrary ellipsoid $n_1 \neq n_2 \neq n_3$, there are two planes for which the intersections are circles of radius n_2 . The directions perpendicular to these planes are the *optical axes (or binormals)*; they lie in the plane n_1/n_3 . The waves with normal v parallel to an optical axis propagate with a random polarization D . The optical axes are, however, not directions of isotropy. Each polarization corresponds to one direction s of the light ray which only coincides with v for D parallel to n_2 . Internal conical refraction is an effect that is due to this anisotropy (Fig. 4.23(a)). The light rays whose normals propagate down a binormal form a cone in the interior of the crystal. After leaving the crystal, the directions of propagation of the light rays are parallel.

The indicatrix of the rates v_s is of no practical importance. It also has optical axes (*biradials*) which are not coincident with the binormals. Waves whose light ray s is parallel to a biradial can propagate with any polarization E . However, there is a different wave normal v for each polarization. The angle of refraction of

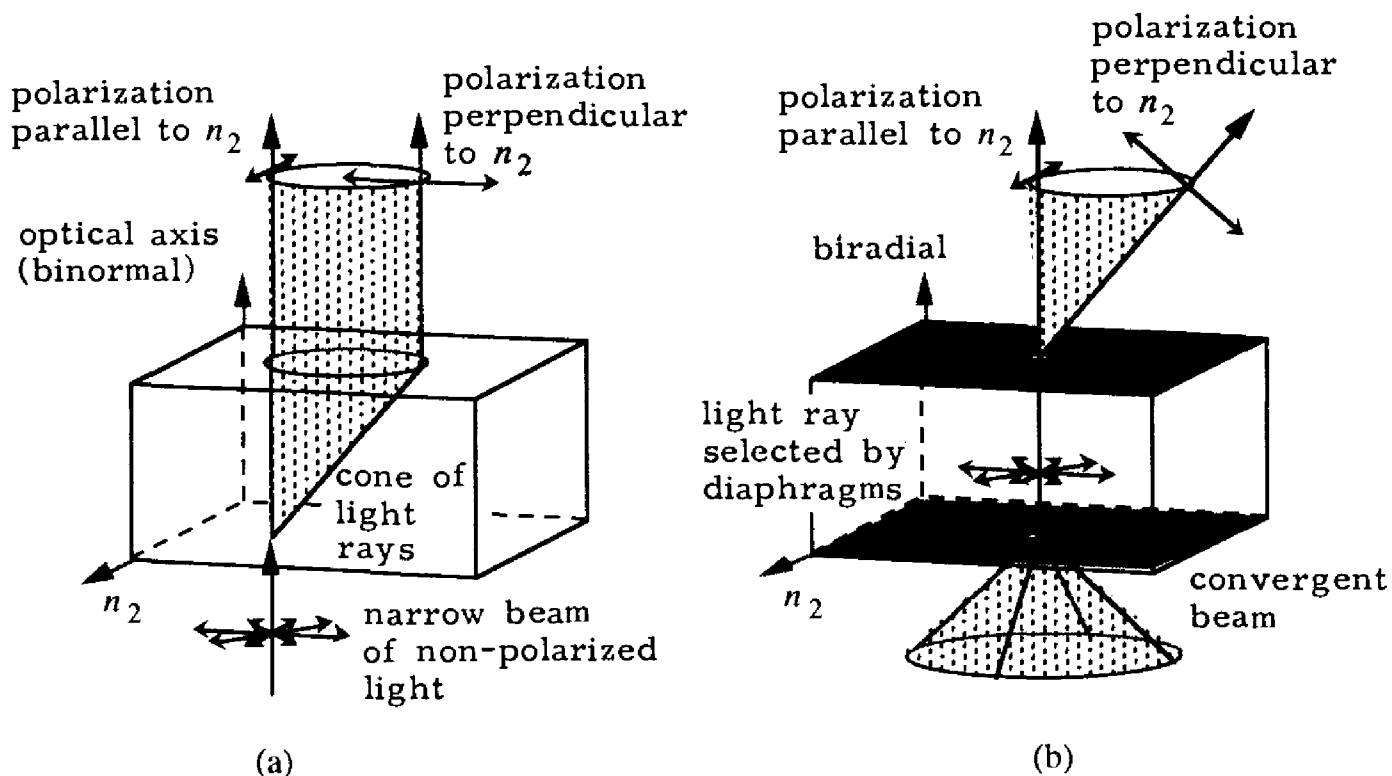


Fig. 4.23. Internal conical refraction (binormal) (a); external conical refraction (biradial) (b); the arrows indicate the light rays and their polarizations

a wave whose light ray propagates along a biradial depends on the polarization. This effect leads to external conical refraction (Fig. 4.23(b)).

The directions n_1 and n_3 are the *bisectors* of the angles between the optical axes; n_2 is the *optical normal*. The *optical sign of the crystal* is defined as follows (Fig. 4.24):

positive + n_3 acute bisector, n_1 obtuse bisector;
negative - n_1 acute bisector, n_3 obtuse bisector.

For $n_1 \neq n_2 \neq n_3$ there are *two* optical axes, hence the crystal is *biaxial*. If the indicatrix is an ellipsoid of revolution, there is only one optical axis, the rotation axis, and the crystal is *uniaxial*. The optical axis of a uniaxial crystal is a direction of isotropy. For any direction \mathbf{v} , there is a wave whose polarization is *perpendicular* to the optical axis, and for which \mathbf{s} is therefore parallel to \mathbf{v} , and \mathbf{E} parallel to \mathbf{D} (Fig. 4.25). This wave is the *ordinary wave* and it behaves like a wave in an isotropic medium. Its refractive index is symbolized by n_o . For the *extraordinary wave*, \mathbf{s} and \mathbf{v} are not coincident (Fig. 4.18). The corresponding refractive index n_e takes a value intermediate between n_o and the length of the principal axis n_e . The *optical sign* is defined as follows:

positive + $n_1 = n_2 = n_o, n_3 = n_e, n_e > n_o$, oblong ellipsoid;
negative - $n_2 = n_3 = n_o, n_1 = n_e, n_e > n_o$, oblate ellipsoid.

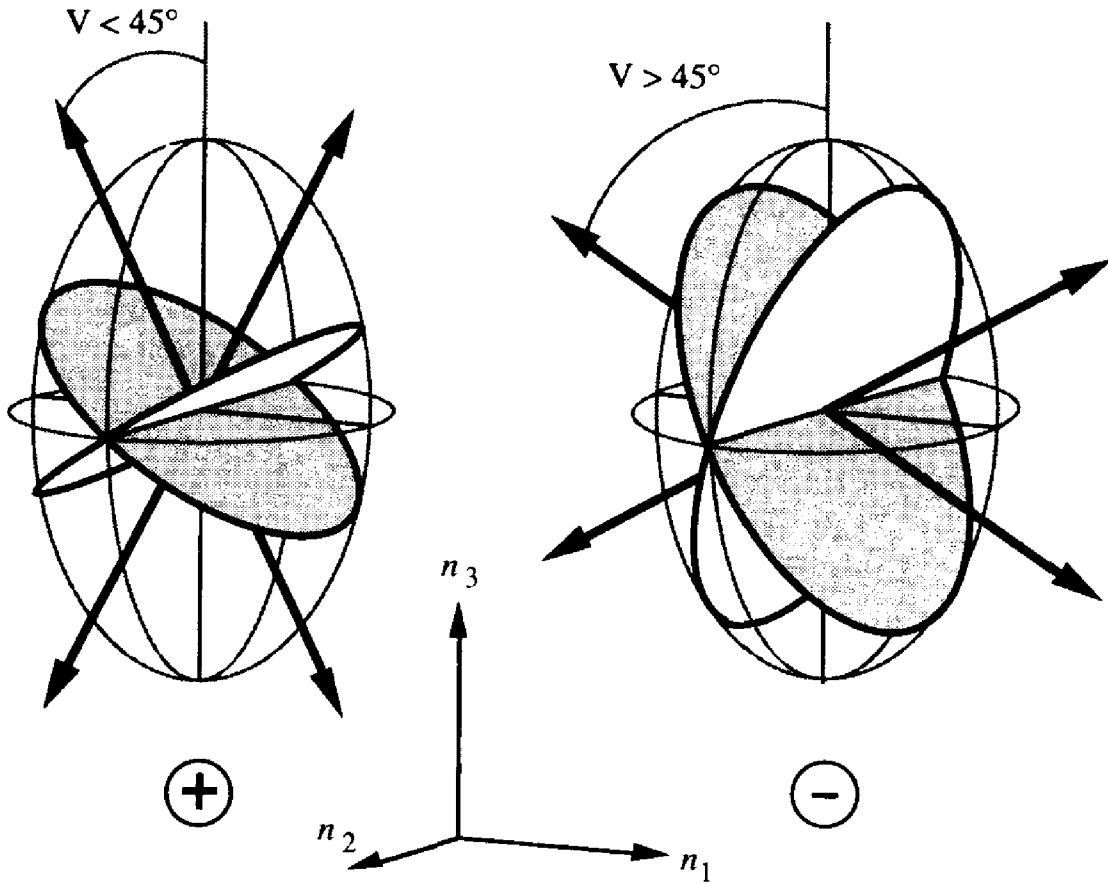


Fig. 4.24. Optical sign of a biaxial crystal

Triclinic, monoclinic and orthorhombic crystals are biaxial; trigonal, tetragonal and hexagonal crystals are uniaxial; whereas cubic crystals are isotropic (Section 4.2.5).

Let us cite the optical properties of two important minerals as examples: the optical sign of quartz (SiO_2) is positive (+), $n_o = 1.5442$, $n_e = 1.5533$; that of calcite (CaCO_3) is negative (-), $n_o = 1.6584$, $n_e = 1.4865$.

The light from a point source in the interior of a crystal does not generally propagate as a spherical wave. The surface of the wave is represented by the set of points (x_1, x_2, x_3) whose distance from the source in the direction $\mathbf{s} = (s_1, s_2, s_3)$ is equal to v_s :

$$x_i = r s_i, \quad r^2 = x_1^2 + x_2^2 + x_3^2 = v_s^2.$$

From equation (4.105) we obtain:

$$x_1^2 v_1^2 (r^2 - v_2^2 - v_3^2) + x_2^2 v_2^2 (r^2 - v_1^2 - v_3^2) + x_3^2 v_3^2 (r^2 - v_1^2 - v_2^2) + v_1^2 v_2^2 v_3^2 = 0.$$

This fourth-order equation represents two distinct surfaces which intersect in the biradials. For a negative uniaxial crystal $v_2^2 = v_3^2$, these surfaces are a sphere and

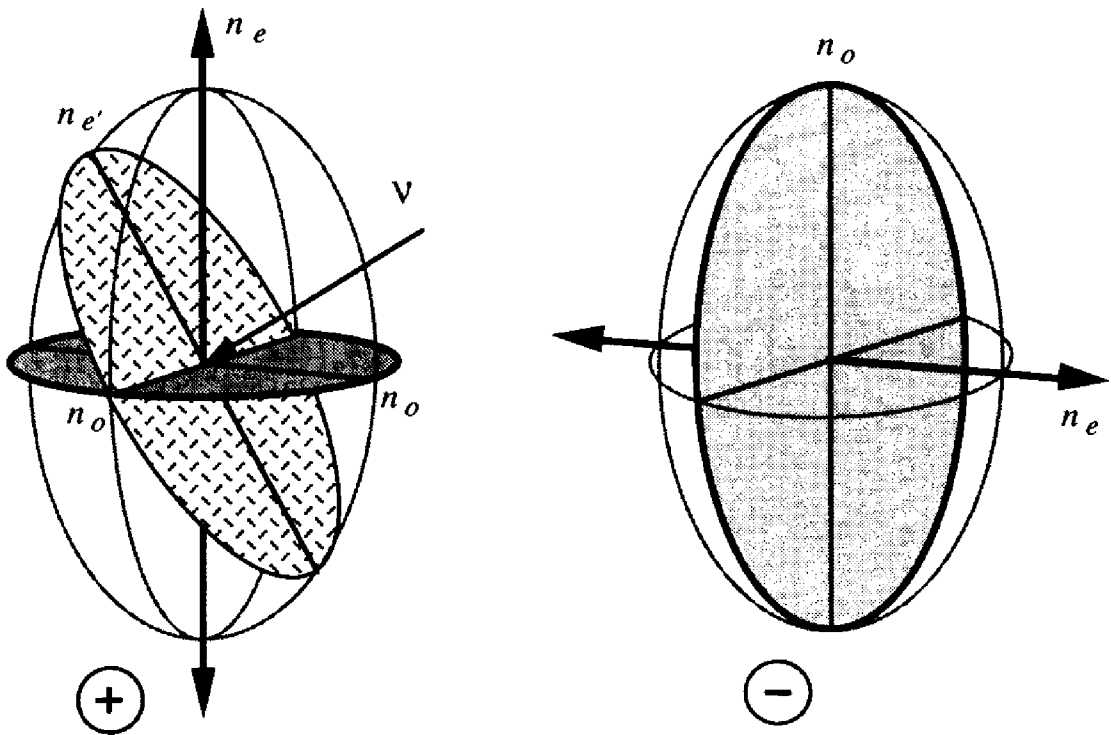


Fig. 4.25. Positive and negative uniaxial indicatrices

an ellipsoid of revolution:

$$r^2 = v_2^2; \quad \frac{x_1^2}{v_2^2} + \frac{y^2 + z^2}{v_1^2} = 1.$$

They allow us to illustrate the refraction of light using Huygens' principle (Fig. 4.26).

4.5.6 POLARIZING MICROSCOPE

Birefringent crystals may be studied either with parallel light (*orthoscopy*) or with convergent light (*conoscopy*). In order to make the majority of minerals transparent, thin sections are prepared whose thickness is of the order of 0.02 to 0.04 mm. The crystal is placed between two polarizers whose orientations are perpendicular to each other. Figure 4.27 shows the orthoscopic set-up. The intensity of the polarized light incident on the crystal is I_p . After the second polarizer (the analyzer), the intensity is I_A . These intensities may be calculated with the aid of Fig. 4.28.

The components s and t along n'' and n' of the amplitude D_p transmitted by the first polarizer are:

$$s = D_p \cos \psi; \quad t = D_p \sin \psi.$$

The components a_1 and a_2 of s and t parallel to the amplitude D_A transmitted by the analyzer are:

$$a_1 = -a_2 = \frac{1}{2} D_p \sin 2\psi.$$

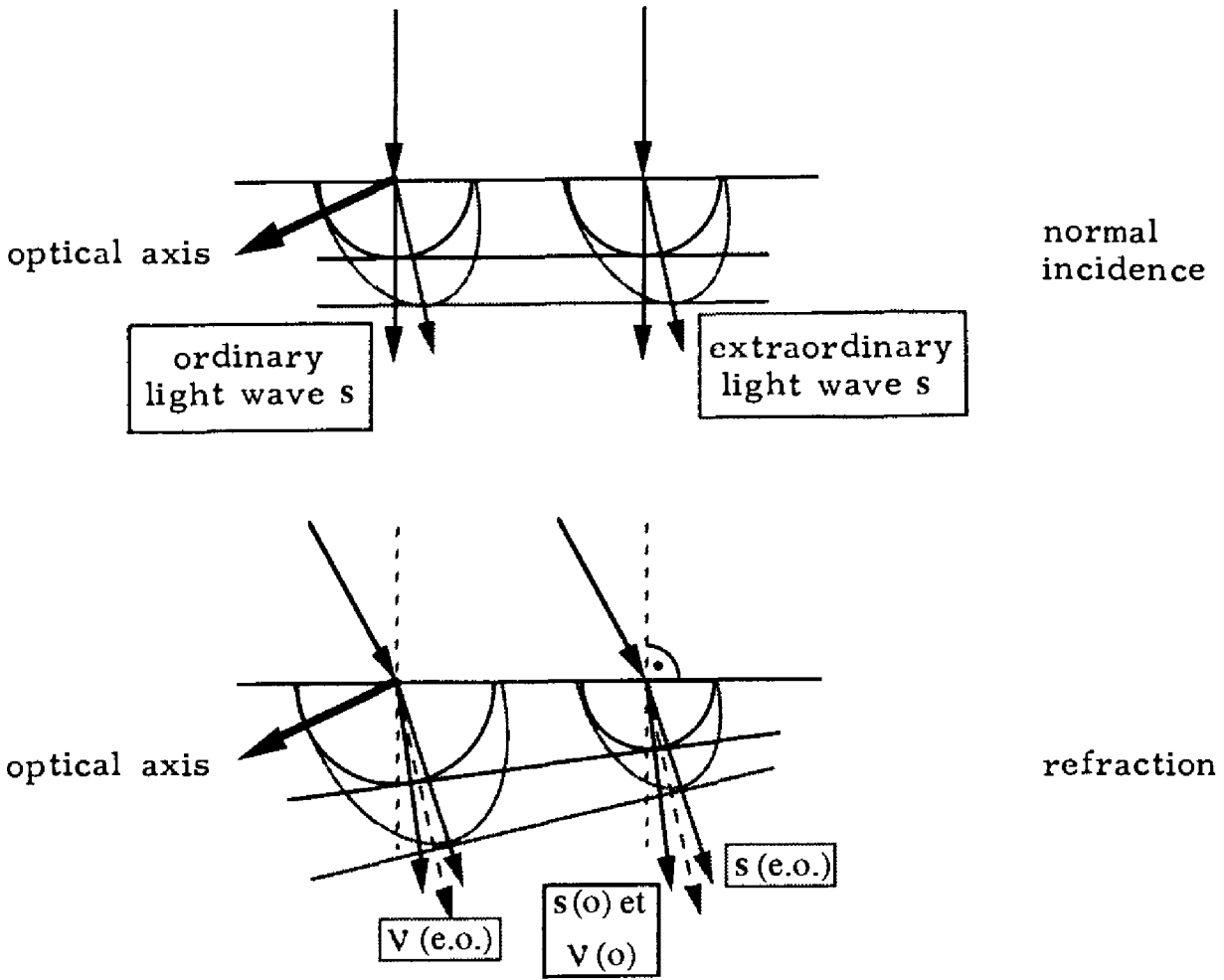


Fig. 4.26. Refraction according to Huygens' principle; the wave fronts and the light rays in a uniaxial crystal

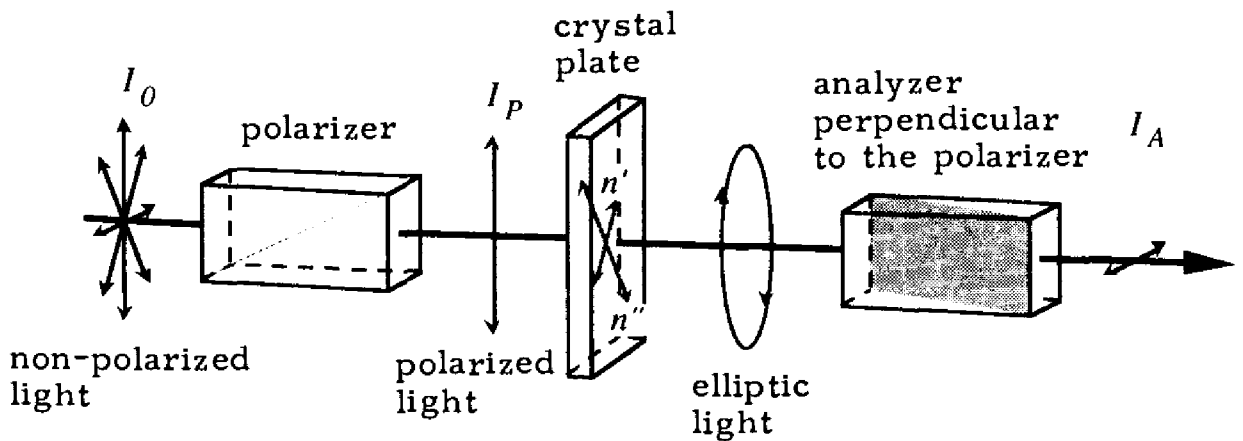


Fig. 4.27. Orthoscopic arrangement

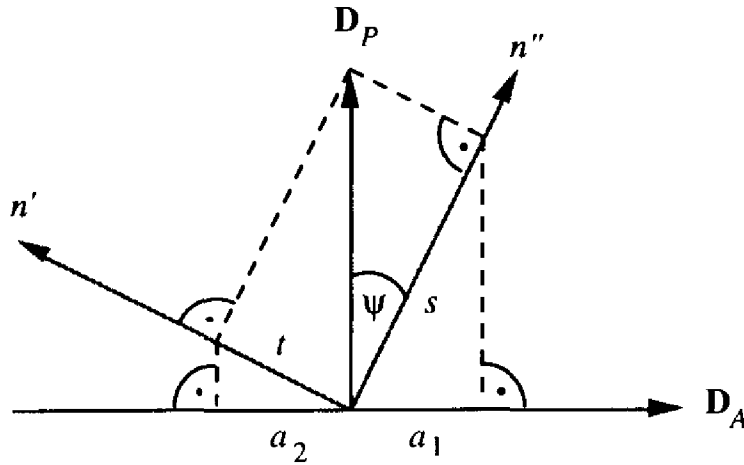


Fig. 4.28. D_P , D_A are the polarization vectors of the polarizer and analyzer; n' and n'' are the refractive indices and polarization directions of the waves traversing the crystal

Let d be the thickness of the crystal, n' one of the two indices of refraction, λ_0 and λ' the wavelengths in the vacuum and in the crystal, and v_0 , $v_{n'}$ the corresponding rates. The thickness of the crystal can be expressed in units of wavelength:

$$n' = \frac{v_0}{v_{n'}} = \frac{\lambda_0}{\lambda'}, \quad \frac{d}{\lambda'} = \frac{d}{\lambda_0} n'.$$

The wave n'' moves more slowly in the crystal than the wave n' . This results in a phase difference δ between the two waves:

$$\delta = \frac{2\pi d}{\lambda_0} (n'' - n').$$

The waves a_1 and a_2 transmitted by the analyzer interfere and the resultant wave D_A becomes:

$$D_A = a_1 + a_2 e^{i\delta} = \frac{1}{2} D_P \sin 2\psi (1 - e^{i\delta}).$$

The intensities I being proportional to $|D|^2$, we obtain the Fresnel (1821) equation:

$$I_A = I_P \sin^2 2\psi \sin^2 \left[\frac{\pi}{\lambda_0} d (n'' - n') \right]. \quad (4.109)$$

I_A goes to zero under the following conditions:

- $\psi = m\pi/2$; n'' and n' are parallel to the analyzer and polarizer. We can thus determine the directions of n'' and n' .
- $d(n'' - n') = m\lambda_0$; the path difference is an integral multiple of λ_0 . With polychromatic light we observe colors. $d(n'' - n')$ is called the *birefringence* of the thin section.

The identification of n'' and n' in a crystal of unknown orientation may be obtained with the help of a crystal plate of known orientation and birefringence (Fig. 4.29). The polarizing microscope is equipped with a gypsum plate with birefringence $d(n'' - n') = 551 \text{ nm}$ (red in the first order). Colors of *addition* and *subtraction* are obtained according to the orientation of the unknown crystal with respect to the plate.

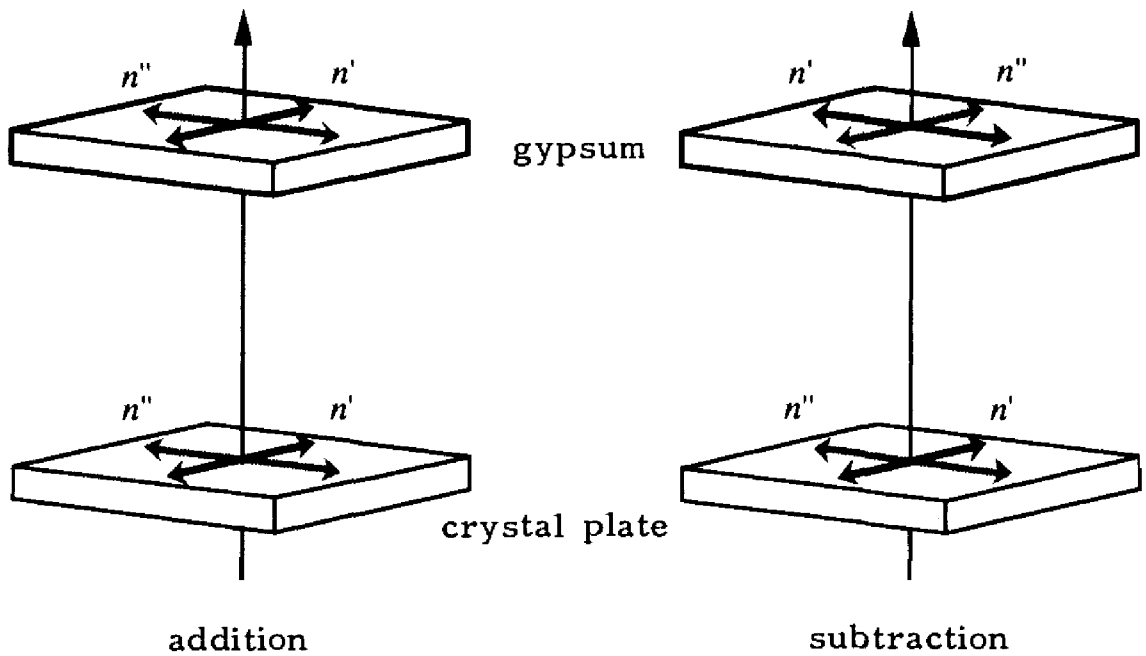


Fig. 4.29. Addition and subtraction

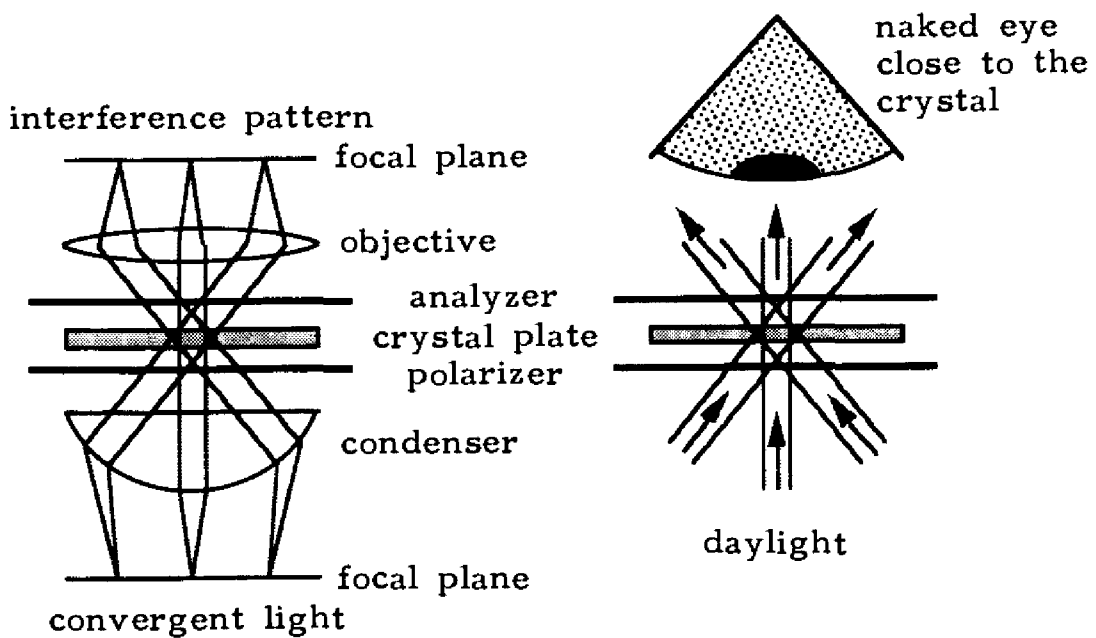


Fig. 4.30. Conoscopic method with the help of a microscope and with the naked eye

The conoscopic set-up is illustrated in Fig. 4.30. The light incident on the crystal is convergent. The light rays traverse the crystal in different directions which each have a characteristic birefringence $d(n'' - n')$. The birefringence varies above all because of the anisotropy of the crystal. A small supplementary variation is due to the different pathlengths of the light through the crystal and to the refraction of rays inclined with respect to the surface.

We do not observe an image of the crystal in the focal plane of the objective of the microscope, but an interference pattern. Each point in this plane corresponds to the direction of a wave normal characterized by a birefringence, and hence, by an interference color or light intensity. The intensity goes to zero for all waves polarized according to the polarizer and the analyzer. The interference figures are characteristic of the crystal symmetry, the optical sign and the orientation of the indicatrix.

CHAPTER 5

Exercises

5.1 EXERCISES RELATING TO CHAPTER 1

5.1.1

Determine the Miller indices of the 12 faces that form a rhombododecahedron (Fig. 5.1). The coordinate system is defined by $a_1 = a_2 = a_3$, $\alpha_1 = \alpha_2 = \alpha_3 = 90^\circ$. Each face is parallel to one of the axes of the coordinate system. Calculate the angles between the faces of the rhombododecahedron which have a common edge.

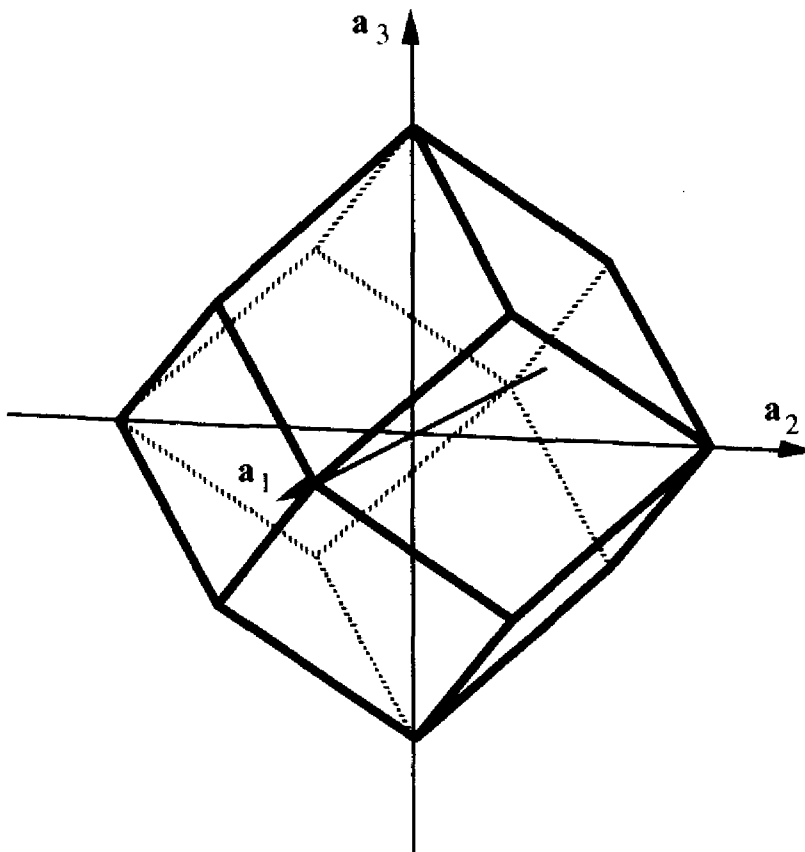


Figure 5.1. Rhombododecahedron

SOLUTION:

The indices are shown in Fig. 5.2. Parallel to a face (hkl) there is another face $(\bar{h}\bar{k}\bar{l})$. The angle ρ between two faces $(h_1k_1l_1)$ and $(h_2k_2l_2)$ is given by:

$$\cos \rho = \frac{\mathbf{r}_1^* \cdot \mathbf{r}_2^*}{r_1^* r_2^*}, \quad \text{where } \mathbf{r}_i^* = h_i \mathbf{a}^* + k_i \mathbf{b}^* + l_i \mathbf{c}^*; \quad r_i^* = \|\mathbf{r}_i^*\|.$$

The reciprocal coordinate system is $a_1^* = a_2^* = a_3^* = 1/a$, $\alpha_1^* = \alpha_2^* = \alpha_3^* = 90^\circ$. $\mathbf{r}_1^* \cdot \mathbf{r}_2^* = a^{-2}(h_1 h_2 + k_1 k_2 + l_1 l_2)$, $r_i^* = a^{-1}(h_i^2 + k_i^2 + l_i^2)^{1/2}$; $\cos(110; 101) = \cos(101; 011) = \cos(011; 110) = 1/2$. The angles are 60° .

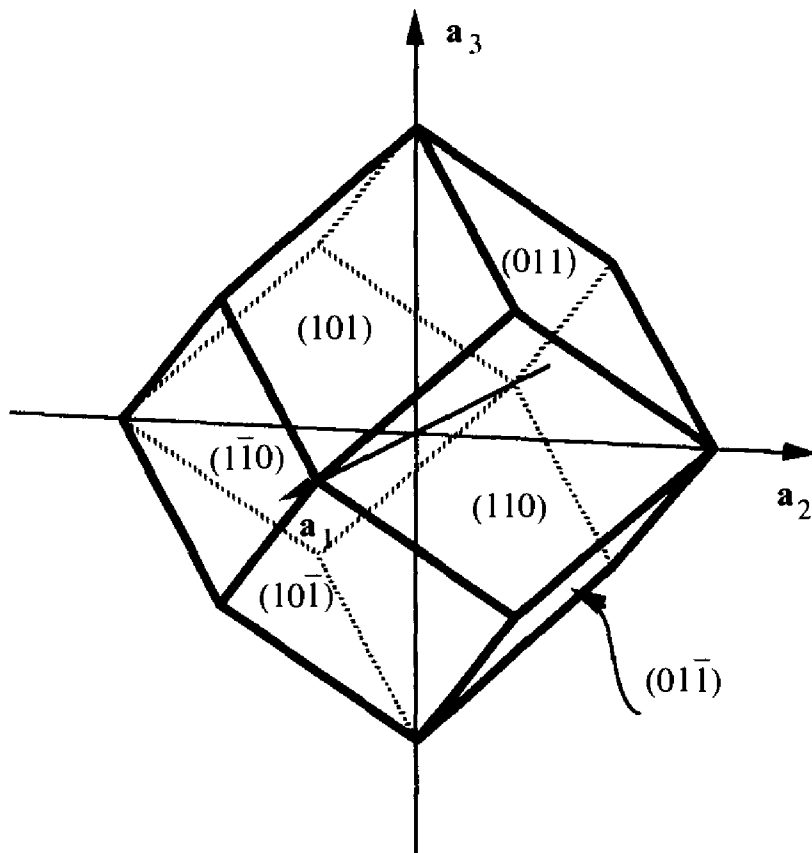


Figure 5.2. Indices of the faces of a rhombododecahedron

5.1.2

An *orthorhombic* coordinate system is characterized by $a \neq b \neq c$, $\alpha = \beta = \gamma = 90^\circ$. Let the ratios $a:b:c = 1:2:3$. Calculate the angle between the normal to the face (112) and the direction $[112]$. Also calculate the angles between the directions (121) and $[121]$, as well as between (211) and $[211]$.

SOLUTION:

The angle ψ_{112} between the vectors $\mathbf{R}^* = \mathbf{a}^* + \mathbf{b}^* + 2\mathbf{c}^*$, perpendicular to the face (112) , and $\mathbf{R} = \mathbf{a} + \mathbf{b} + 2\mathbf{c}$ is $\cos \psi_{112} = (\mathbf{R} \cdot \mathbf{R}^*) / (R R^*)$. The reciprocal coordinate system is orthogonal as is the coordinate system \mathbf{a} , \mathbf{b} , \mathbf{c} ; $a^* = \|\mathbf{b} \times \mathbf{c}\| / (\mathbf{a} \cdot \mathbf{b} \cdot \mathbf{c}) = 6a^2 / 6a^3 = 1/a$, $b^* = 1/(2a)$, $c^* = 1/(3a)$. $\mathbf{R} \cdot \mathbf{R}^* = 6$, $R^2 = a^2 + b^2 + 4c^2 = 41a^2$, $R^{*2} = a^{*2} + b^{*2} + 4c^{*2} =$

$61/36a^2$. Hence $\cos \psi_{112} = 0.7199$; $\psi_{112} = 43.96^\circ$. In an analogous way we obtain $\psi_{121} = 35.92^\circ$ and $\psi_{211} = 45.83^\circ$.

5.1.3

A hexagonal coordinate system is characterized by $a = b \neq c$, $\alpha = \beta = 90^\circ$, $\gamma = 120^\circ$. Sketch the $(\bar{2}10)$ face. Determine the angles between $(\bar{2}10)$ and the **a** and **b** axes. Determine the indices of the faces of the two prisms in Fig. 5.3.

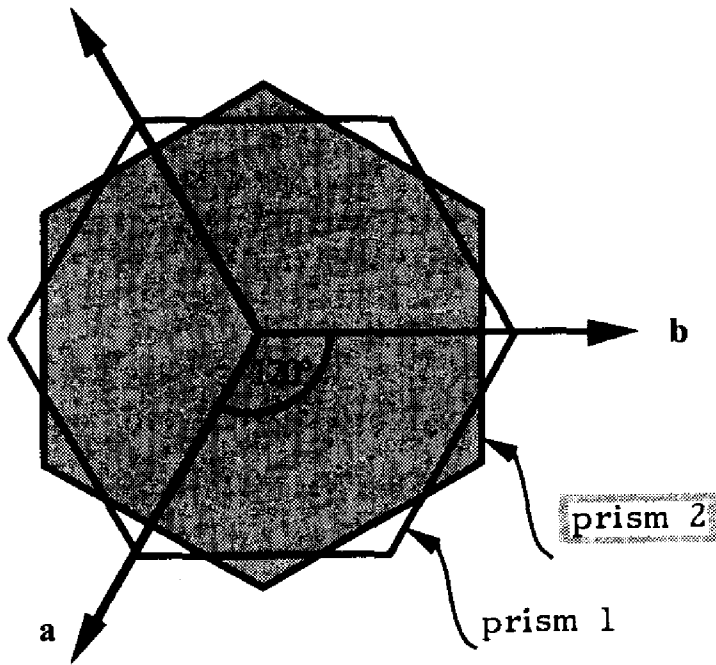


Figure 5.3. Hexagonal prisms

SOLUTION:

The face $(\bar{2}10)$ is perpendicular to **a**. The indices of the faces of the two prisms are given in Fig. 5.4.

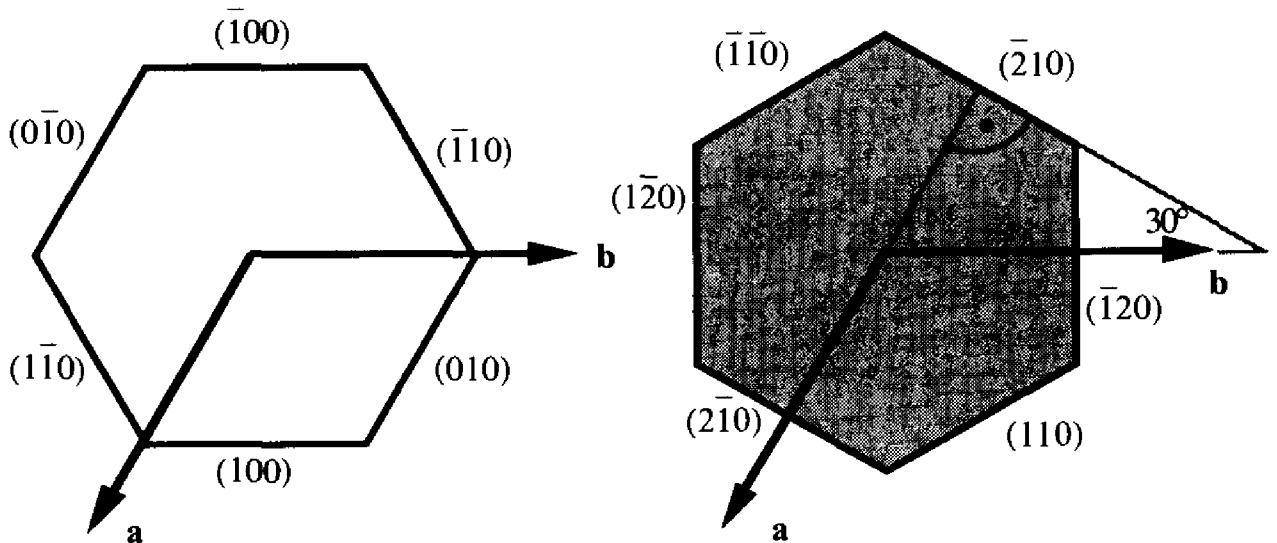


Figure 5.4. Indices of the faces of two hexagonal prisms

5.1.4

Let ϕ_1, ϕ_2 and ϕ_3 be the angles between the normal to the (111) face and the $\mathbf{a}_1, \mathbf{a}_2$ and \mathbf{a}_3 axes of some non-unitary coordinate system. Show that the ratios of the norms of the vectors $\mathbf{a}_1, \mathbf{a}_2$ and \mathbf{a}_3 are given by $a_1:a_2:a_3 = 1/\cos \phi_1:1/\cos \phi_2:1/\cos \phi_3$. Let ψ_1, ψ_2 and ψ_3 be the angles between the normal to the (123) face and the $\mathbf{a}_1, \mathbf{a}_2$ and \mathbf{a}_3 axes. Determine the ratios $a_1:a_2:a_3$ as a function of these angles.

SOLUTION:

$$\begin{aligned}\cos \phi_1 &= (\mathbf{r}_{111}^* \cdot \mathbf{a}_1) / (r_{111}^* a_1) = 1 / (r_{111}^* a_1); \quad \mathbf{r}_{111}^* = \mathbf{a}_1^* + \mathbf{a}_2^* + \mathbf{a}_3^* \\ \cos \phi_2 &= (\mathbf{r}_{111}^* \cdot \mathbf{a}_2) / (r_{111}^* a_2) = 1 / (r_{111}^* a_2) \\ \cos \phi_3 &= (\mathbf{r}_{111}^* \cdot \mathbf{a}_3) / (r_{111}^* a_3) = 1 / (r_{111}^* a_3)\end{aligned}$$

from which

$$\cos \phi_1 : \cos \phi_2 : \cos \phi_3 = 1/a_1 : 1/a_2 : 1/a_3. \quad \text{q.e.d.}$$

In an analogous manner we obtain

$$\begin{aligned}\cos \psi_1 &= (\mathbf{r}_{123}^* \cdot \mathbf{a}_1) / (r_{123}^* a_1) = 1 / (r_{123}^* a_1) \\ \cos \psi_2 &= 2 / (r_{123}^* a_2) \\ \cos \psi_3 &= 3 / (r_{123}^* a_3) \\ a_1 : a_2 : a_3 &= 1/\cos \psi_1 : 2/\cos \psi_2 : 3/\cos \psi_3.\end{aligned}$$

5.1.5

Find the necessary condition such that three faces with the Miller indices $(h_1 k_1 l_1)$, $(h_2 k_2 l_2)$ and $(h_3 k_3 l_3)$ belong to the same zone, i.e. that they be parallel to the same direction.

SOLUTION:

The three vectors $\mathbf{r}_i^* = h_i \mathbf{a}^* + k_i \mathbf{b}^* + l_i \mathbf{c}^*$ are coplanar if $(\mathbf{r}_1^* \times \mathbf{r}_2^*) \cdot \mathbf{r}_3^* = 0$. It then follows that the determinant formed from the coordinates h_i, k_i, l_i cancels:

$$D = \begin{vmatrix} h_1 & k_1 & l_1 \\ h_2 & k_2 & l_2 \\ h_3 & k_3 & l_3 \end{vmatrix} = 0.$$

5.1.6

Figure 5.5 shows a crystal of anorthite, $\text{CaAl}_2\text{Si}_2\text{O}_8$, a member of the feldspar group. The crystal is centrosymmetric. For each face (hkl) there is a parallel face

$(\bar{h}\bar{k}\bar{l})$. Each pair of parallel faces is identified by a letter. The edges are numbered, parallel edges being characterized by the same number.

Choose four faces which allow the definition of a coordinate system, **a**, **b**, **c**. Determine the Miller indices for as many faces and edges as possible.

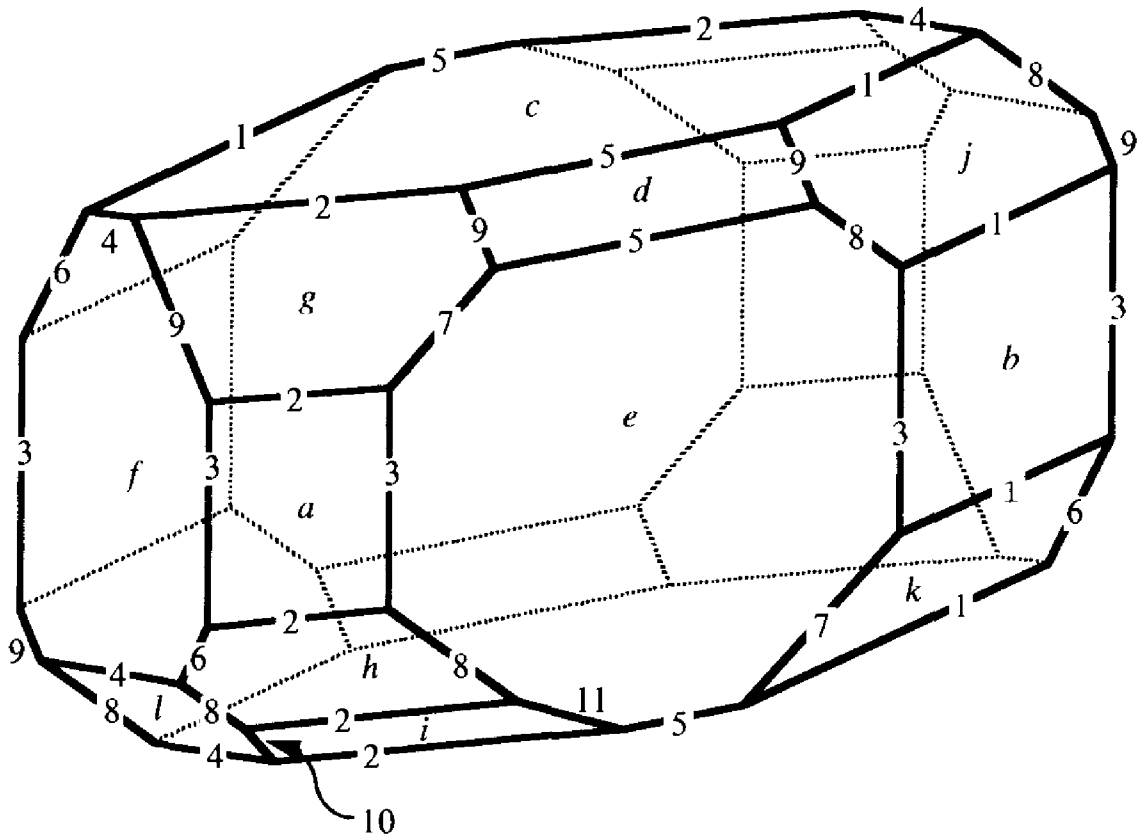


Figure 5.5. Anorthite crystal

SOLUTION:

Knowing that the most conspicuous edges correspond to important lattice lines, the coordinate system is defined starting from the faces *a*, *b* and *c*: $a = (100)$, $b = (010)$, $c = (001)$. The base vectors $\mathbf{a} = [100]$, $\mathbf{b} = [010]$ and $\mathbf{c} = [001]$ are thus parallel to the edges 1, 2 and 3. We assign the indices (111) to the face *d*, in order to fix the ratio of the norms of **a**, **b** and **c**. Clearly it is possible to imagine other choices of coordinate system, e.g. the faces *f*, *e*, *c* and *g*.

The faces which are parallel to the same edge belong to a zone. Their normals \mathbf{r}_{hkl}^* lie in the plane perpendicular to the edge. From the indices (hkl) of two faces, using the relation (1.20), the indices $[uvw]$ of the edge common to the two faces may be calculated. From the indices $[uvw]$ of two edges, the indices (hkl) of the two faces defined by these edges may be calculated. First we calculate the indices for edges 1, 2, 3 and 5, the intersections of the four faces (100), (010), (001) and (111). Starting from the indices of these edges, the indices of other faces may be calculated, which, in their turn, may be used to calculate the indices of other edges.

It is possible to deduce the indices of the faces without explicitly calculating the indices of the zones. Because the normals to three faces \mathbf{r}_1^* , \mathbf{r}_2^* , \mathbf{r}_3^* belonging to the same zone lie in the same plane, $\mathbf{r}_3^* = s\mathbf{r}_1^* + t\mathbf{r}_2^*$ where *s* and *t* are real numbers. The indices of the faces *a*, *b*, *c* and *d* are known. Because the face *e* belongs both to the zone {*a*, *b*} and to the zone {*c*, *d*},

we find:

$$(h_e, k_e, l_e) = s_3(h_a, k_a, l_a) + t_3(h_b, k_b, l_b) = s_5(h_c, k_c, l_c) + t_5(h_d, k_d, l_d) \\ = s_3(1, 0, 0) + t_3(0, 1, 0) = s_5(0, 0, 1) + t_5(1, 1, 1)$$

from which $s_3 = t_5, t_3 = t_5$ and $s_5 + t_5 = 0$ which allows the solution $s_3 = t_3 = t_5 = -s_5 = 1$. Finally, $(h_e, k_e, l_e) = (1, 1, 0)$.

We see that all the faces of zone 1 have indices of the type $(0mn)$, those of zone 2 indices of the type $(m0n)$, and those of zone 3 indices of the type $(mn0)$. Thus, let us assign to f the indices $(m\bar{n}0)$ with $m, n > 0$. The indices of all the other faces (except i) can be derived as a function of m and n (or multiple thereof):

- zones 1 and 9 → j : $(0, m + n, m)$
- zones 2 and 9 → g : $(m + n, 0, n)$
- zones 1 and 7 → k : $(0, m + n, \bar{n})$
- zones 2 and 8 → h : $(m + n, 0, \bar{m})$
- zones 4 and 8 → l : (m, \bar{n}, \bar{m})
- zones 4 and 6 → f : $(m, \bar{n}, n - m)$ or $(m, \bar{n}, 0)$.

From the two expressions giving the indices for the face f , we can deduce that $m = n$. On setting $m = 1$ we obtain:

- a : (100) 1: $[100]$
- b : (010) 2: $[010]$
- c : (001) 3: $[001]$
- d : (111) 4: $[110]$
- e : (110) 5: $[\bar{1}10]$
- f : $(1\bar{1}0)$ 6: $[112]$
- g : (201) 7: $[\bar{1}12]$
- h : $(20\bar{1})$ 8: $[1\bar{1}2]$
- i : $(p0\bar{q})$ 9: $[\bar{1}\bar{1}2]$
- j : (021) 10: $[q, -p + q, p]$
- k : $(02\bar{1})$ 11: $[q, \bar{q}, p]$
- l : $(1\bar{1}\bar{1})$

The information thus set out does not allow us to find the indices of face i because the edges 10 and 11 only belong to two faces and not to three. By considering the angles between the faces it can be shown that $p = q$.

5.2 EXERCISES RELATING TO CHAPTER 2

5.2.1

- a) List the set of symmetry operations which leave invariant a regular triangular pyramid (crystal class $3m$, Figs. 2.17 and 2.20).
- b) Establish the multiplication table for the corresponding group.
- c) Is the group Abelian? What are the characteristics of the multiplication table for an Abelian group?
- d) Find two operations which generate the complete set of operations of the group.

- e) Find all of the sub-groups, i.e. all the subsets of operations forming a group.
- f) Find all equivalence classes of the group. By definition, the equivalence class of operation A contains the operations B such that $B = XAX^{-1}$, X covering all the operations of the group.
- g) Represent the operations of the group by 2×2 matrices using a unitary coordinate system, on the one hand, and an oblique coordinate system adapted to the threefold symmetry, on the other.
- h) Let M_u and M_o be the representations of the same group operation in the unitary coordinate system and in the oblique coordinate system respectively. Find the matrix T such that $T^{-1}M_uT = M_o$.

SOLUTION:

- a) The threefold axis and the three mirror planes of the group $3m$ correspond to the symmetry operations $\{E, A_3, A_3^2, I'_2, I''_2, I'''_2\}$.

b) **Table 5.1** Multiplication table for the group $3m$. The order of multiplication is M_2M_1 , i.e. M_1 is executed before M_2

	M_2	E	A_3	A_3^2	I'_2	I''_2	I'''_2
M_1							
E		E	A_3	A_3^2	I'_2	I''_2	I'''_2
A_3		A_3	A_3^2	E	I''_2	I'''_2	I'_2
A_3^2		A_3^2	E	A_3	I'''_2	I'_2	I''_2
I'_2		I'_2	I'''_2	I''_2	E	A_3^2	A_3
I''_2		I''_2	I'_2	I'''_2	A_3	E	A_3^2
I'''_2		I'''_2	I''_2	I'_2	A_3^2	A_3	E

- c) The group is non-Abelian. The multiplication table of an Abelian group is symmetric with respect to the principal diagonal.
- d) The group $3m$ may be generated from a rotation and a reflection, e.g. from A_3 and I'_2 .
- e) $\{E, A_3, A_3^2\}$, $\{E, I'_2\}$, $\{E, I''_2\}$, $\{E, I'''_2\}$.

- f) E class: $\{XEX^{-1}\} = \{E\}$
 A_3 class: $\{XA_3X^{-1}\} = \{A_3, A_3^2\}$
 I'_2 class: $\{XI'_2X^{-1}\} = \{I'_2, I''_2, I'''_2\}$

- g) Let the base vectors of a unitary coordinate system be e_1 parallel to the mirror plane m_1 and e_2 perpendicular to m_1 :

$$E = \begin{pmatrix} 1 & 0 \\ 0 & 1 \end{pmatrix}, \quad A_3 = \begin{pmatrix} \cos \phi & -\sin \phi \\ \sin \phi & \cos \phi \end{pmatrix}, \quad A_3^2 = \begin{pmatrix} \cos \phi & \sin \phi \\ -\sin \phi & \cos \phi \end{pmatrix},$$

$$I'_2 = \begin{pmatrix} 1 & 0 \\ 0 & -1 \end{pmatrix}, \quad I''_2 = \begin{pmatrix} \cos \phi & -\sin \phi \\ -\sin \phi & -\cos \phi \end{pmatrix}, \quad I'''_2 = \begin{pmatrix} \cos \phi & \sin \phi \\ \sin \phi & -\cos \phi \end{pmatrix}, \quad \phi = 2\pi/3.$$

The base vectors of the oblique coordinate system a_1 and a_2 are chosen parallel to the

edges of the triangle such that $a_1 = a_2$, $\gamma = 2\pi/3$:

$$\begin{aligned} E &= \begin{pmatrix} 1 & 0 \\ 0 & 1 \end{pmatrix}, & A_3 &= \begin{pmatrix} 1 & -1 \\ 1 & -1 \end{pmatrix}, & A_3^2 &= \begin{pmatrix} -1 & 1 \\ -1 & 0 \end{pmatrix}, \\ l'_2 &= \begin{pmatrix} 1 & -1 \\ 0 & -1 \end{pmatrix}, & l''_2 &= \begin{pmatrix} -1 & 0 \\ -1 & 1 \end{pmatrix}, & l'''_2 &= \begin{pmatrix} 0 & 1 \\ 1 & 0 \end{pmatrix}. \end{aligned}$$

h) The matrix T is the transformation matrix from the oblique coordinate system to the unitary system,

$$\begin{aligned} \begin{pmatrix} e_1 \\ e_2 \end{pmatrix} &= (T^{-1})^T \begin{pmatrix} a_1 \\ a_2 \end{pmatrix}, & \begin{pmatrix} x_{\text{unitary}} \\ y_{\text{unitary}} \end{pmatrix} &= T \begin{pmatrix} x_{\text{oblique}} \\ y_{\text{oblique}} \end{pmatrix}, \\ T &= \begin{pmatrix} 1 & -1/2 \\ 0 & \sqrt{3}/2 \end{pmatrix}, & T^{-1} &= \begin{pmatrix} 1 & 1/\sqrt{3} \\ 0 & 2/\sqrt{3} \end{pmatrix}. \end{aligned}$$

5.2.2

Figure 5.6 shows some cubes whose faces have been decorated. Identify the corresponding point groups with the aid of Fig. 2.17. Create other symmetries using a wooden or cardboard cube by decorating the faces in an appropriate manner.

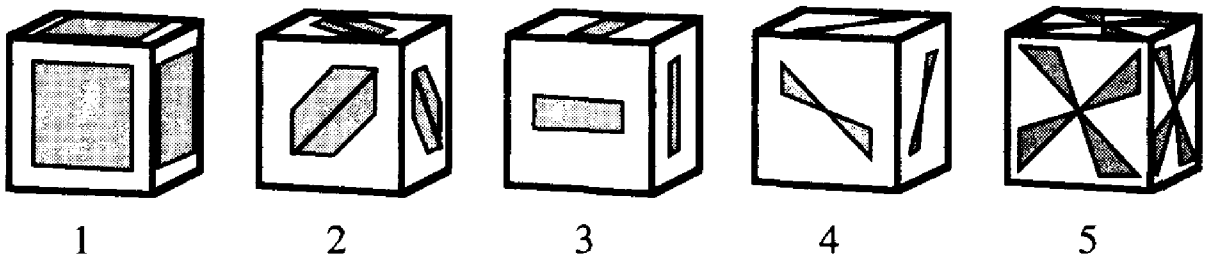


Figure 5.6. Symmetries of decorated cubes

SOLUTION:

(1) $m\bar{3}m$, (2) $\bar{4}3m$, (3) $m\bar{3}$, (4) 23 , (5) 432

5.2.3

Find the symmetry elements and the unit cells for the two-dimensional structures in Fig. 5.7. Compare your results with Fig. 2.29

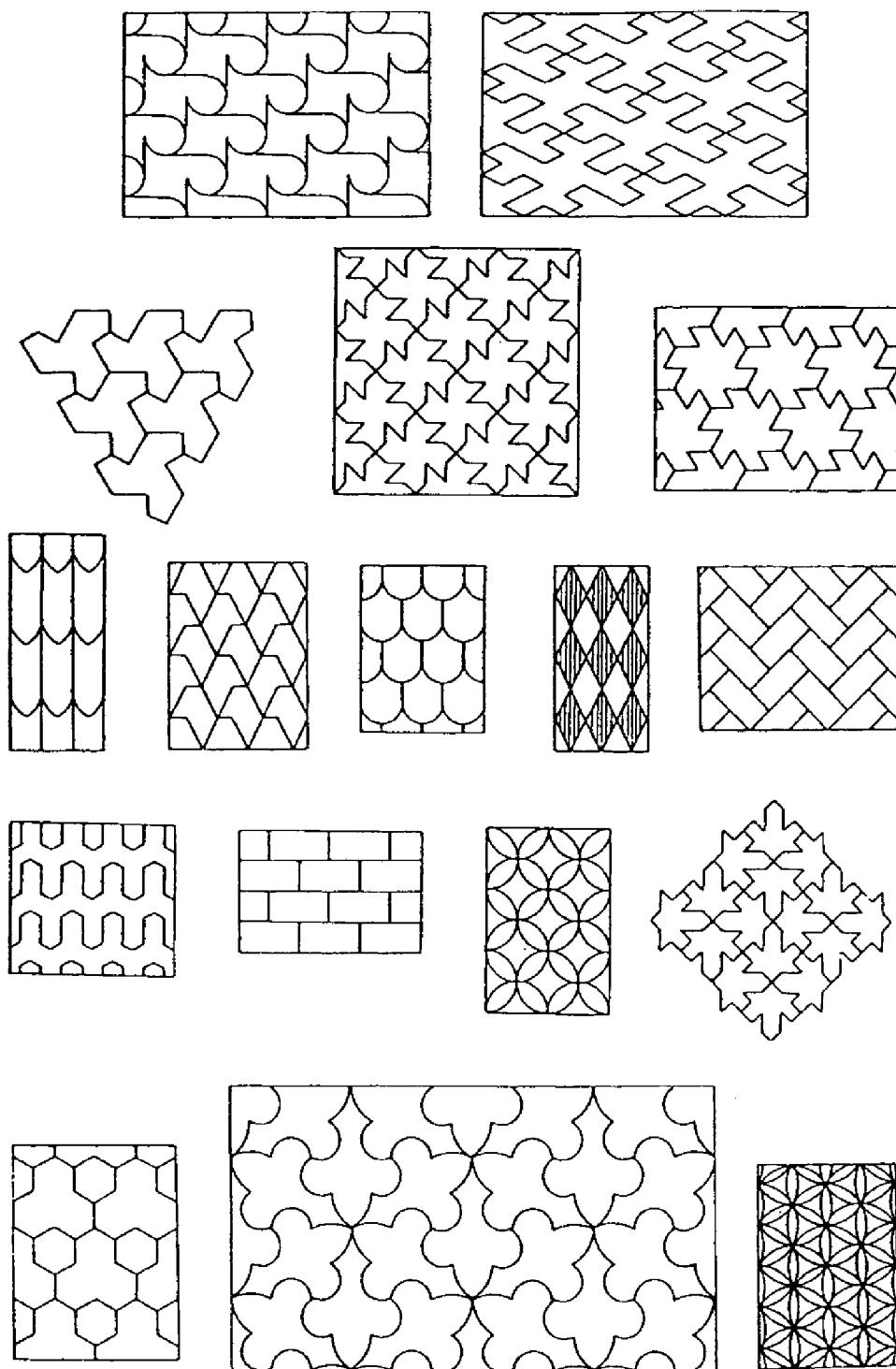


Figure 5.7. 17 plane groups illustrated by G. Polya (*Z. Kristallogr.* 60, 278–282, 1924)

5.2.4

Determine the general and special positions (orbits) along with the symmetry elements for the plane group $p4gm$.

METHOD. The group is generated by a glide line g parallel to an edge and a mirror line m parallel to a diagonal of a square. Draw several square unit cells

on squared paper as well as the two generating elements. Mark with a point a general position in one cell. Avoid choosing special coordinates like $1/2$ or $1/4$. Generate the other equivalent points by using the lines m and g , and the translations. After determining the complete orbit, mark all of the symmetry elements on the diagram and compare the result with Fig. 2.29. Move the origin of the coordinate system onto a fourfold rotation point and calculate the coordinates of the orbit with respect to this origin. Determine the coordinates of all the special orbits and the symmetries corresponding to these points.

SOLUTION:

The coordinates of a general orbit are (Fig. 5.8):

$$x, y; \mathbf{g} \rightarrow \frac{1}{2} + x, \bar{y}; \mathbf{m} \rightarrow \bar{y}, \frac{1}{2} + x; \mathbf{g} \rightarrow \frac{1}{2} - y, \frac{1}{2} - x; \mathbf{m} \rightarrow \frac{1}{2} - x, \frac{1}{2} - y; \mathbf{g} \rightarrow \bar{x}, \frac{1}{2} + y; \\ \mathbf{m} \rightarrow \frac{1}{2} + y, \bar{x}; \mathbf{g} \rightarrow y, x; \mathbf{m} \rightarrow x, y.$$

If the origin is moved to the fourfold symmetry point with coordinates $(-\frac{1}{4}, \frac{1}{4})$, the general orbit becomes: $x, y; \bar{y}, x; \bar{x}, \bar{y}; y, \bar{x}; \frac{1}{2} + y; \frac{1}{2} + x; \frac{1}{2} - x, \frac{1}{2} + y; \frac{1}{2} - y, \frac{1}{2} - x; \frac{1}{2} + x, \frac{1}{2} - y$. The special orbits with their corresponding symmetries are:

symmetry m :	$x, \frac{1}{2} + x; \frac{1}{2} - x, x; \bar{x}, \frac{1}{2} - x; \frac{1}{2} + x, \bar{x}$.
symmetry $2mm$:	$\frac{1}{2}, 0; 0, \frac{1}{2}$.
symmetry 4 :	$0, 0; \frac{1}{2}, \frac{1}{2}$.

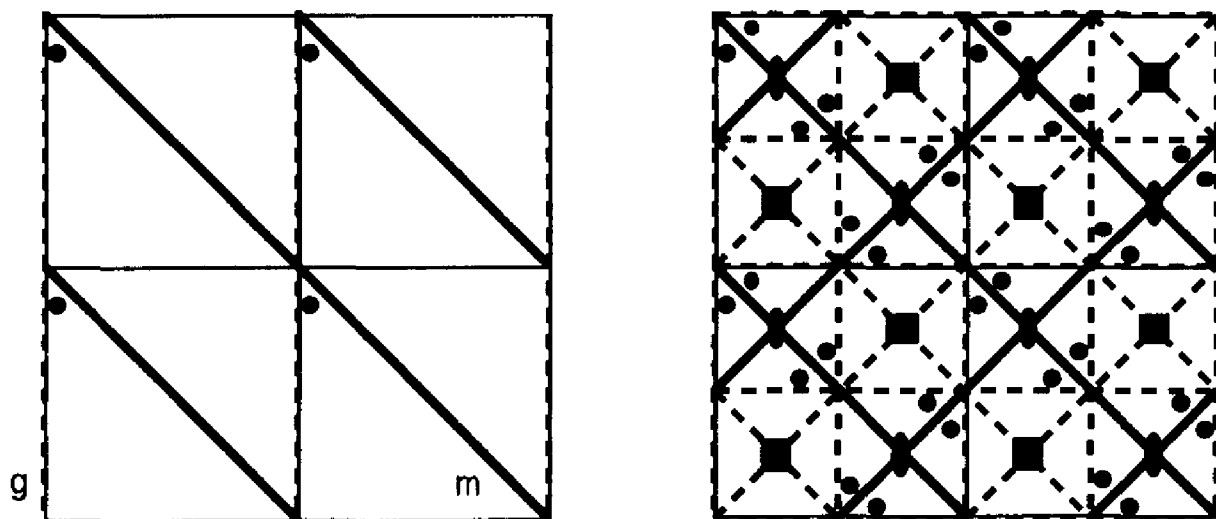


Figure 5.8. Construction of an orbit starting from the generator symmetry elements

5.2.5

Determine the general and special positions along with the symmetry elements for the space groups $Pnma$, $P\bar{4}2_1c$ and $R\bar{3}c$ by analogy with Exercise 5.2.4.

The generators 2_1 and c can be chosen for $P\bar{4}2_1c$, and 2 and c for $R\bar{3}c$, because these symmetry elements intersect (Section 2.5.2). Verify your results with the extracts from the *International Tables* given in Section 2.7.4.

5.2.6

The structural parameters for calcite are given in Section 2.8. Sketch the projections of the structure down the $[100]$ and $[210]$ directions. Calculate the shortest C–O and Ca–O distances along with the O–Ca–O angles. Determine the coordination number (with respect to oxygen) of calcium.

SOLUTION:

The C–O distance is $ax = 1.28 \text{ \AA}$. The Ca atom located at the origin $(0, 0, 0)$ is surrounded by six oxygen atoms located at the points $\pm(\frac{2}{3} - x, \frac{1}{3}, \frac{1}{12})$; $\pm(-\frac{1}{3}, \frac{1}{3} - x, \frac{1}{12})$; $\pm(-\frac{1}{3} + x, x - \frac{2}{3}, \frac{1}{12})$; these coordinates define an octahedron slightly elongated along c . Taking into account the metric of the unit cell (1.16), the distance Ca–O becomes $[(x^2 - x + \frac{1}{3})a^2 + (\frac{1}{12}c)^2]^{1/2} = 2.356 \text{ \AA}$. The three angles O–Ca–O have values of 87.58° , 92.42° and 180° .

5.3 EXERCISES RELATING TO CHAPTER 3

5.3.1

Given a crystal lattice with dimensions $a = 5 \text{ \AA}$, $b = 10 \text{ \AA}$, $c = 15 \text{ \AA}$, $\alpha = \beta = 90^\circ$, $\gamma = 120^\circ$ and radiation with a wavelength $\lambda = 1.5418 \text{ \AA}$ (CuK α radiation):

- Determine the parameters of the reciprocal lattice a^* , b^* , c^* , α^* , β^* , γ^* and the volumes of the direct and reciprocal unit cells.
- Calculate the d spacing and the diffraction angle θ for the series of lattice planes (321) .
- Let the incident beam be perpendicular to the c axis. Determine graphically, using the Ewald construction, the crystal orientation required to observe the reflection (320) . This orientation can be defined by the angles between the incident beam s_0 and the vectors \mathbf{a}^* and \mathbf{b}^* . Calculate these angles.
- Determine the maximum number of Bragg reflections that could be observed with CuK α radiation.
- Give the maximum values of the indices of the observable reflections h_{\max} , k_{\max} , l_{\max} .

SOLUTION:

a) According to equations (1.6) to (1.15), $V = abc \sin \gamma = (\sqrt{3}/2)abc = 649.52 \text{ \AA}^3$;

$$\alpha^* = \beta^* = 90^\circ, \gamma^* = 60^\circ;$$

$$a^* = 1/(a \sin \gamma) = 0.23094 \text{ \AA}^{-1};$$

$$b^* = 1/(b \sin \gamma) = 0.11547 \text{ \AA}^{-1};$$

$$c^* = 1/c = 0.06667 \text{ \AA}^{-1}.$$

The volume of the reciprocal unit cell is $V^* = 1/V = 0.0015396 \text{ \AA}^{-3}$.

b) $d_{321} = \|\mathbf{3a}^* + \mathbf{2b}^* + \mathbf{c}^*\|^{-1} = (9a^{*2} + 4b^{*2} + c^{*2} + 12a^*b^*\cos\gamma^*)^{-1/2} = 1.197 \text{ \AA}$; $\sin\theta = \lambda/(2d_{321}) = 0.6440$; $\theta_{321} = 40.09^\circ$.

c) The graphical construction (Fig. 5.9) gives two solutions for the orientation of the crystal. The angle $(\mathbf{s}_0; \mathbf{a}^*)$ is the sum of the angles $(\mathbf{s}_0; \mathbf{r}_{320}^*)$ and $(\mathbf{a}^*; \mathbf{r}_{320}^*)$; the other angles are calculated in an analogous manner:

$$(\mathbf{s}_0; \mathbf{a}^*) = 143.83^\circ; (\mathbf{s}_0; \mathbf{b}^*) = 83.83^\circ; (\mathbf{s}; \mathbf{a}^*) = 63.96^\circ; (\mathbf{s}; \mathbf{b}^*) = 3.96^\circ;$$

$$(\mathbf{s}'_0; \mathbf{a}^*) = 116.04^\circ; (\mathbf{s}'_0; \mathbf{b}^*) = 176.04^\circ; (\mathbf{s}'_0; \mathbf{a}^*) = 36.17^\circ; (\mathbf{s}'_0; \mathbf{b}^*) = 96.17^\circ.$$

It is clear that the $\mathbf{s}'_0 = -\mathbf{s}$, $\mathbf{s} = -\mathbf{s}_0$.

d) The reciprocal lattice points which can cut the Ewald sphere are located in a sphere of radius $2/\lambda$ centered on the origin of the reciprocal lattice (Fig. 5.9). The number of lattice points N contained in the limiting sphere is given by the ratio of the volume of this sphere to that of the reciprocal unit cell,

$$N = V_{\text{sphere}}/V^* = V_{\text{sphere}}V = \frac{4\pi}{3}\left(\frac{2}{\lambda}\right)^3 (abc \sin \gamma) = 5939.$$

e) The maximum values of the indices are given by the ratios of the radius of the limiting sphere $2/\lambda$ to the lattice lengths $a^* \sin \gamma^* = 1/a$, $b^* \sin \gamma^* = 1/b$ and $c^* = 1/c$ (Fig. 3.20).

$$h_{\text{max}} = 2a/\lambda = 6.49 \approx 6, k_{\text{max}} = 13, l_{\text{max}} = 19.$$

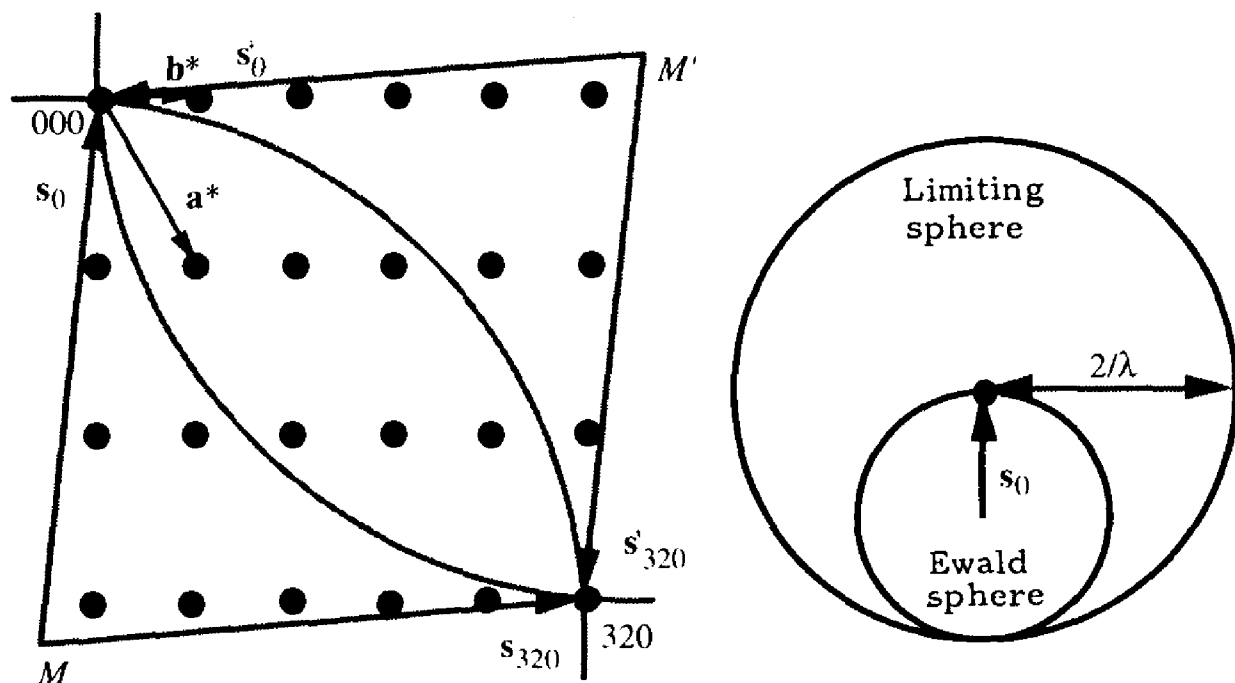


Figure 5.9. Reflection by the 320 planes (left) and the limiting sphere (right)

5.3.2

Table 5.2 contains the results of measurements made on the powder diffractograms of four cubic substances obtained with $\text{CuK}\alpha$ radiation of wavelength $\lambda = 1.5418 \text{ \AA}$. The Bragg angles θ were measured with a precision of 0.01° ; the intensities I are normalized such that $I = 100$ for the strongest line. Find the indices hkl of the reflections and the lattice constants (Section 3.5.3). For each compound, identify the systematic absences and deduce the Bravais lattice (Table 3.2).

SOLUTION:

Several lattice planes are characterized by the same value of $s = h^2 + k^2 + l^2$ (Section 3.5.3). The indices hkl given in Table 5.3 represent one of them with all positive indices. If the Laue class is $m\bar{3}m$, these planes are symmetry equivalent. Clearly, the diffractograms do not allow the five cubic crystal classes or the two cubic Laue classes to be distinguished. The lattice constants may be calculated by using equation (3.47), $(\lambda/2a)^2 = \sum \sin^2 \theta / \sum s$.

NaCl: $a = 5.6404 \text{ \AA}$. The indices hkl all have the same parity, hence the Bravais lattice is F centered. Line No. 10 is a superposition of two lines which are not symmetry equivalent.

CuZn: $a = 2.948 \text{ \AA}$. There are no systematic absences, hence the lattice is P.

W: $a = 3.165 \text{ \AA}$. The hkl satisfy the condition $h + k + l = 2n$, hence the lattice is I. Note that $s = 1$ cannot be assigned to the first line because the value for the seventh line would then become 7 which is impossible (Section 3.5.3).

Si: $a = 5.431 \text{ \AA}$. The lattice is F as is the case for NaCl. However, we can see that there are supplementary absences for $h + k + l \neq 4n + 2$, in particular, the line 222 is absent. For this reason, when a crystal of Si is used as monochromator (reflection 111) the monochromatic radiation is not contaminated by radiation with wavelength $\lambda/2$.

$$\left(\frac{1.5418}{2a}\right)^2 =$$

Table 5.2 Bragg angles θ for four cubic substances

Line No.	NaCl		CuZn		W		Si	
	$\theta [^\circ]$	I	$\theta [^\circ]$	I	$\theta [^\circ]$	I	$\theta [^\circ]$	I
1	13.68	13	15.15	6	20.15	100	14.23	100
2	15.86	100	21.75	100	29.16	15	23.67	55
3	22.74	55	26.93	1	36.63	23	28.08	30
4	26.95	2	31.53	15	43.55	8	34.60	6
5	28.26	15	35.76	2	50.38	11	38.22	11
6	33.14	6	39.85	29	57.53	4	44.06	12
7	36.57	1	47.72	5	65.69	18	47.52	6
8	37.69	11	51.65	1	76.99	2	53.42	3
9	42.03	7	55.81	8			57.11	7
10	45.25	1	60.13	1			63.86	8

Table 5.3 Indexing of the powder diffractograms for four cubic substances
($s = h^2 + k^2 + l^2$)

Line No.	NaCl		CuZn		W		Si	
	s	h, k, l	s	h, k, l	s	h, k, l	s	h, k, l
1	3	111	1	100	2	110	3	111
2	4	200	2	110	4	200	8	220
3	8	220	3	111	6	211	11	311
4	11	311	4	200	8	220	16	400
5	12	222	5	210	10	310	19	331
6	16	400	6	211	12	222	24	422
7	19	331	8	220	14	321	27	511/333
8	20	420	9	300/221	16	400	32	440
9	24	422	10	310			35	531
10	27	511/333	11	311			40	620

5.3.3

a) Compare the intensities in Table 5.2 to the values calculated on the basis of a spherical atom model. In order to compare the intensities of neighboring lines it is necessary to take into account the multiplicity m . (Section 3.5.3) and the structure factor $F(hkl)$ (Section 3.7.1). The calculation may be simplified by neglecting the Lorentz (3.60) and polarization (3.19) factors, as well as the decrease in the form factors and the Debye–Waller factor as a function of $\sin \theta/\lambda$ (Sections 3.3.3 and 3.3.4). The atomic coordinates are:

NaCl: Space group $Fm\bar{3}m$.

$(0, 0, 0) +; (1/2, 1/2, 0) +; (1/2, 0, 1/2) +; (0, 1/2, 1/2) +.$

4 Cl at $0, 0, 0$; 4 Na at $1/2, 1/2, 1/2$.

CuZn: Space group $Pm\bar{3}m$.

Cu at $0, 0, 0$; Zn at $1/2, 1/2, 1/2$.

Zn occupies the center of the unit cell. Why is the lattice not I centered?

W: Space group $Im\bar{3}m$.

$(0, 0, 0) +; (1/2, 1/2, 1/2) +.$

2 W at $0, 0, 0$.

Si: Space group $Fd\bar{3}m$.

$(0, 0, 0) +; (1/2, 1/2, 0) +; (1/2, 0, 1/2) +; (0, 1/2, 1/2) +.$

8 Si at $0, 0, 0$; $1/4, 1/4, 1/4$.

b) Derive the systematic absences. Explain the alternating strong and weak lines.

SOLUTION:

NaCl: $|F(hkl)|^2 = 16\{[f_{Cl}]_r + (-1)^{h+k+l}[f_{Na}]_r\}^2$ if h, k and l have the same parity, otherwise 0; $m = 8, 6, 12, 24, 8, 6, 24, 24, 24, 24 + 8$.

- CuZn: $|F(hkl)|^2 = \{ [f_{\text{Cu}}]_t + (-1)^{h+k+l} [f_{\text{Zn}}]_t \}^2$; $m = 6, 12, 8, 6, 24, 24, 12, 6 + 24, 24, 24$. For $h + k + l = 2n + 1$, Cu and Zn scatter out of phase and the intensity is weak. The lattice is not I centered because $(\mathbf{a}_1 + \mathbf{a}_2 + \mathbf{a}_3)/2$ is not a translation.
- W: $|F(hkl)|^2 = 4[f_{\text{W}}]_t^2$ if $h + k + l = 2n$, otherwise 0; $m = 12, 6, 24, 12, 24, 8, 48, 6$. For $h + k + l = 2n + 1$ the atoms in the unit cell scatter out of phase and the intensities cancel. Due to the multiplicity factor, strong and weak lines alternate.
- Si: $|F(hkl)|^2 = 64[f_{\text{Si}}]_t^2$ if h, k and l are even and $h + k + l \neq 4n + 2$, $32[f_{\text{Si}}]_t^2$ if h, k and l are odd, otherwise 0; $m = 8, 12, 24, 6, 24, 24, 24 + 8, 12, 48, 24$. It is interesting to note that the absence of the reflection 222 is not due to the space group, but to the special arrangement of the atoms in the unit cell. In fact, $F(222) = 0$ only if the electron density of the silicon atom is spherical (Section 3.3.3). Precise measurements carried out on a single crystal show that this intensity is very weak, but not zero. This is due to the Si-Si chemical bond and to anharmonic thermal vibrations.

5.3.4

Determine the space groups characterized by the following reflection conditions:

- orthorhombic; hkl : $k + l = 2n$; $0kl$: $k = 2n$; $h0l$: $h = 2n$.
- tetragonal; hkl : no absences; $00l$: $l = 4n$; $h00$: $h = 2n$.
- tetragonal; hkl : no absences; $0kl$: $l = 2n$; hhl : $l = 2n$.
- tetragonal; hkl : no absences; $hk0$: $h + k = 2n$; $0kl$: $l = 2n$; hhl : $l = 2n$.
- trigonal, Laue class $\bar{3}m$; hkl : $-h + k + l = 3n$.
- trigonal, Laue class $\bar{3}m1$; hkl : no absences; $00l$: $l = 3n$.
- hexagonal; hkl : no absences; hhl : $l = 2n$.
- cubic; hkl : $k + l, h + l, h + k = 2n$; $h00$: $h = 4n$.
- cubic, Laue class $m\bar{3}m$; hkl : $k + l, h + l, h + k = 2n$.

SOLUTION:

- Aba2** or **Abam**. In the *International Tables*, **Abam** is given in another orientation with the symbol **Cmca**.
- P4₁2₁2** or **P4₃2₁2**. These groups are enantiomorphs. They cannot be distinguished if the structure factors obey Friedel's law (Section 3.7.2). The tetragonal symmetry implies the reflection condition $0k0$: $k = 2n$.
- P4cc** or **P4/mcc**. The tetragonal symmetry implies the reflection conditions $h0l$: $l = 2n$; $h\bar{h}l$: $l = 2n$.
- P4/ncc**. The tetragonal symmetry implies the reflection conditions $h0l$: $l = 2n$; $h\bar{h}l$: $l = 2n$.
- R3m** or **R32** or **R $\bar{3}m$** .
- P3₁21** or **P3₂21**. These groups are enantiomorphs. The mirror planes of $\bar{3}m1$ are perpendicular to the shortest translations of the triangular lattice plane.
- P6₃mc** or **P6₃/mmc**. The hexagonal symmetry implies the reflection conditions $2h\bar{h}l$: $l = 2n$; $\bar{h}2hl$: $l = 2n$.
- F4₁32**. The cubic symmetry implies the reflection conditions $0k0$: $k = 4n$; $00l$: $l = 4n$.
- F432** or **F43m** or **Fm $\bar{3}m$** .

5.3.5

Is there any advantage in choosing the Laue method to determine the space group of a crystal?

SOLUTION:

No, because it is difficult to observe the systematic absences. In general, a diffracted ray contains several orders of a reflection HKL . For example, all the reflections $00l$ are superimposed.

5.3.6

At temperatures above 120°C , the structure of BaTiO_3 is cubic, space group $\text{Pm}\bar{3}\text{m}$, $a \approx 4 \text{ \AA}$. At 120° there is a phase change and the crystal becomes ferroelectric. Between 0 and 120° the structure is tetragonal, space group $\text{P}4\text{mm}$, $a = 3.99 \text{ \AA}$, $c = 4.03 \text{ \AA}$ (at room temperature). We may observe this transition by using the powder method (Section 3.5.3) because certain lines in the powder pattern split when the structure changes from cubic to tetragonal. Which ones?

SOLUTION:

For a tetragonal structure, equation (3.46) becomes:

$$\left(\frac{2 \sin \theta}{\lambda}\right)^2 = \frac{(h^2 + k^2)}{a^2} + \frac{l^2}{c^2}$$

If $h \neq k \neq l \neq h$, the line from the cubic pattern splits into three lines; if two indices are equal, it doubles; if $h = k = l$, it is unchanged.

5.4 EXERCISES RELATING TO CHAPTER 4

5.4.1

Show that a sphere cut from an anisotropic crystal subjected to hydrostatic pressure deforms into an ellipsoid and determine the orientation of its principal axes.

SOLUTION:

Equation (4.69) gives the strain ϵ as a function of hydrostatic pressure σ . The undeformed sphere is represented by the equation $x_1^2 + x_2^2 + x_3^2 = r^2$. After deformation we obtain:

$$x'_m = \sum_n^3 (\delta_{mn} - \sigma h_{mn}) x_n.$$

In the coordinate system of the eigenvectors of \mathbf{h} and $\boldsymbol{\varepsilon}$, the equation of the deformed sphere becomes:

$$\frac{(x'_1)^2}{(1 - \sigma h_{11})^2} + \frac{(x'_2)^2}{(1 - \sigma h_{22})^2} + \frac{(x'_3)^2}{(1 - \sigma h_{33})^2} = r^2$$

which is the equation of an ellipsoid.

5.4.2

The mineral calcite, CaCO_3 , is trigonal (Section 2.8). In order to determine the thermal expansion tensor \mathbf{e} (4.74), the Bragg angles for the lines 330 and 00,18 were measured from powder patterns obtained at two different temperatures:

$$\begin{aligned} T = 40^\circ\text{C}: \quad 2\theta_{330} &= 136.27^\circ & 2\theta_{00,18} &= 108.82^\circ \\ T = 140^\circ\text{C}: \quad 2\theta_{330} &= 136.43^\circ & 2\theta_{00,18} &= 108.42^\circ. \end{aligned}$$

The wavelength of the radiation used was $\lambda = 1.54051 \text{ \AA}$ ($\text{CuK}\alpha_1$). Calculate the components of the tensor \mathbf{e} . In which direction is the thermal expansion zero?

SOLUTION:

Using the metric of the trigonal system, equation (3.46) becomes:

$$\left(\frac{2 \sin \theta}{\lambda}\right)^2 = d_{hki}^{-2} = (h^2 + k^2 + hk)a^{*2} + l^2c^{*2}; \quad a^* = \frac{2}{\sqrt{3}a}, \quad c^* = \frac{1}{c}.$$

$$a = 6d_{330}; \quad c = 18d_{00,18}.$$

Thus we can calculate a and c at 40°C and at 140°C . The strain tensor $\boldsymbol{\varepsilon}$ and the thermal expansion tensor \mathbf{e} have the form of equation (4.13). The strains after heating are $\varepsilon_{11} = [a_{140} - a_{40}]/a_{40}$ and $\varepsilon_{33} = [c_{140} - c_{40}]/c_{40}$, thus $e_{11} = -6 \times 10^{-6}$ and $e_{33} = 25 \times 10^{-6}$ per $^\circ\text{C}$. The thermal expansion down the unit vector $\mathbf{l} = (l_1, l_2, l_3)$ is:

$$e_L(\mathbf{l}) = (1 - l_3^2)e_{11} + l_3^2e_{33}.$$

This value goes to zero for $\Theta = 64^\circ$, where $\Theta = \arccos(l_3)$, the angle between the vector \mathbf{l} and the threefold axis.

5.4.3

The structure of copper is cubic, crystal class $m\bar{3}m$. The elastic moduli are $C_{11} = 1.76$; $C_{12} = 1.29$, $C_{44} = 0.75 \times 10^{11} \text{ Pa}$. The density is $d = 8.92 \text{ g cm}^{-3}$. Calculate the rate of propagation v and the direction of polarization of the plane waves with wave normals parallel to $[100]$, $[111]$, $[110]$, $[210]$, $[211]$. Calculate the angles between the wave normals and the polarization directions.

SOLUTION:

For each wave normal \mathbf{n} , the matrix \mathbf{B} (4.72) is obtained by using the tensor for the elastic moduli with cubic symmetry (4.65). The eigenvectors and eigenvalues of \mathbf{B} may then be calculated. By taking into account the symmetry of the crystal, this information may be obtained without calculating the characteristic polynomial for \mathbf{B} .

In the propagation directions $[100]$ and $[111]$, any transverse polarization is possible. The polarization direction of the transverse waves propagating parallel to $[110]$ are $[\bar{1}10]$ and $[001]$, i.e. the directions perpendicular to the mirror planes. If \mathbf{n} is parallel to $[210]$ and $[211]$, the polarization direction of one of the waves is perpendicular to a mirror plane; the two other waves are neither transverse nor longitudinal. Table 5.4 summarizes these results.

Table 5.4 Elastic plane waves in copper: rate of propagation v in km/s and angles between the directions of propagation and polarization

\mathbf{n}	longitudinal		transverse		transverse	
	v	angle	v	angle	v	angle
$[100]$	4.44	0.00	2.90	90.00	2.90	90.00
$[111]$	5.24	0.00	2.14	90.00	2.14	90.00
$[110]$	5.05	0.00	1.62	90.00	2.90	90.00
$[210]$	4.88	8.25	2.08	98.25	2.90	90.00
$[211]$	5.08	7.28	2.05	97.28	2.55	90.00

5.4.4

KH_2PO_4 (Section 3.9.2, Fig. 3.41) has a piezoelectric modulus that is particularly large at low temperature. The crystal class is $\bar{4}2m$. At 122 K, $d_{36} = 2 \times 10^{-8}$ C/N; at room temperature, d_{36} falls by a factor of about a thousand to 1.7×10^{-11} C/N. The other moduli are negligible.

Determine the independent terms of the piezoelectric tensor, the vectors \mathbf{e}_1 and \mathbf{e}_2 of the coordinate system should be chosen parallel to the twofold axes and \mathbf{e}_3 parallel to the $\bar{4}$ axis. If a square crystal plate of KH_2PO_4 is cut in such a way that the sides are parallel to the twofold axes and an electric field of 3000 V/cm is applied to \mathbf{e}_3 , i.e. perpendicular to the plate, determine the deformation of the plate.

SOLUTION:

The independent moduli of the tensor are d_{14} , $d_{25} = d_{14}$ and d_{36} . The inverse piezoelectric effect (4.77) results in a deformation $\varepsilon_6 = 2\varepsilon_{12} = d_{36}E_3$, where d_{36} is given in C/N = m/V. A square plate of side a deforms to give a diamond,

$$\mathbf{a}'_1 = a[1 + \varepsilon_{11}, \varepsilon_{12}, \varepsilon_{13}], \quad \mathbf{a}'_2 = a[\varepsilon_{12}, 1 + \varepsilon_{22}, \varepsilon_{23}].$$

The angle in the diamond $\gamma = \pi/2 - \varepsilon_6$. At 122 K, we obtain $\gamma = 89.66^\circ$.

5.4.5

The important birefringence of the mineral calcite CaCO_3 is well known. The structural parameters are given in Section 2.8. The refractive indices are $n_o = 1.6584$ and $n_e = 1.4865$. Crystals are frequently found in the form of $\{104\}$ rhombohedra composed of six equivalent faces $(104), (0\bar{1}4), (\bar{1}14), (\bar{1}0\bar{4}), (01\bar{4}), (1\bar{1}\bar{4})$.

Imagine an incident electromagnetic wave, non-polarized, normal to the face $(\bar{1}0\bar{4})$. Determine the vectors characterizing the waves which propagate in the crystal—electric displacements \mathbf{D} , electric fields \mathbf{E} , light rays \mathbf{s} . Calculate the distance separating the images of an object observed through a crystal with a thickness of 3 cm.

SOLUTION:

The axes of the unitary coordinate system are chosen in the following manner: \mathbf{e}_1 parallel to \mathbf{a}^* , \mathbf{e}_2 parallel to \mathbf{b} , \mathbf{e}_3 parallel to \mathbf{c} . The reciprocal vectors are given in Exercise 5.4.2. The reciprocal vector $\mathbf{a}^* + 4\mathbf{c}^* = a^*\mathbf{e}_1 + 4c^*\mathbf{e}_3$ is coincident with the normal to the wave ν . The angle η between ν and \mathbf{e}_3 are calculated thus:

$$\cos^2 \eta = \frac{12}{12 + (c/a)^2}; \quad \nu^T = (\sin \eta, 0, \cos \eta); \quad \eta = 44.53^\circ.$$

The electric displacement of the ordinary wave \mathbf{D}_o is perpendicular to ν and to \mathbf{e}_3 . The electric displacement of the extraordinary wave \mathbf{D}_e , lies in the plane $(\nu; \mathbf{e}_3)$. The directions of \mathbf{D}_o and \mathbf{D}_e are represented by vectors of norm 1,

$$\mathbf{D}_o^T = (0, 1, 0); \quad \mathbf{D}_e^T = (-\cos \eta, 0, \sin \eta).$$

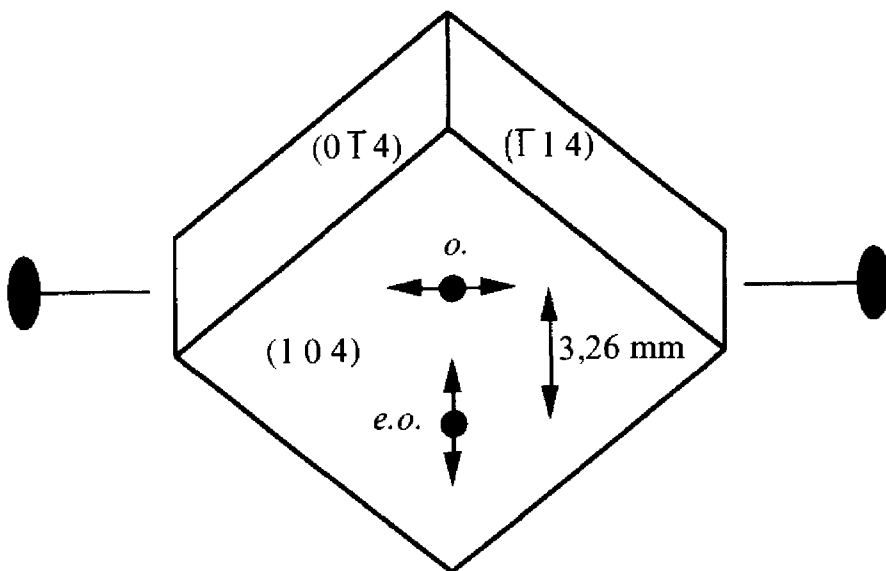


Figure 5.10. Ordinary (o.) and extraordinary (e.o.) waves in calcite

The refractive indices are calculated by using equation (4.107): $n_o = 1.6584$ and $n_e = 1.5668$. By multiplying \mathbf{D} with the inverse dielectric tensor $\boldsymbol{\epsilon}^{-1}$, we obtain the direction of \mathbf{E} ,

$$\mathbf{E} = \text{parallel to } \begin{pmatrix} n_o^{-2} & 0 & 0 \\ 0 & n_o^{-2} & 0 \\ 0 & 0 & n_e^{-2} \end{pmatrix} \mathbf{D}.$$

The electric fields \mathbf{E}_o and $\mathbf{E}_{e'}$ of norm 1 are

$$\mathbf{E}_{e'}^T = \frac{1}{\sqrt{n_e^4 + (n_o^4 - n_e^4) \sin^2 \eta}} (-n_e^2 \cos \eta, 0, n_o^2 \sin \eta), \quad \mathbf{E}_o^T = (0, 1, 0).$$

The light rays \mathbf{s}_o and $\mathbf{s}_{e'}$ lie in the planes $(\mathbf{D}_o; \mathbf{E}_o)$ and $(\mathbf{D}_{e'}; \mathbf{E}_{e'})$. The angle δ between \mathbf{s}_o and $\mathbf{s}_{e'}$ may be calculated thus:

$$\mathbf{s}_o = \mathbf{v}, \quad \mathbf{s}_{e'}^T = \frac{1}{\sqrt{n_e^4 + (n_o^4 - n_e^4) \sin^2 \eta}} (\eta_o^2 \sin \eta, 0, n_e^2 \cos \eta).$$

$$\cos \delta = \frac{n_e^2 + (n_o^2 - n_e^2) \sin^2 \eta}{\sqrt{n_e^4 + (n_o^4 - n_e^4) \sin^4 \eta}} = \frac{n_o n_e}{n_{e'} \sqrt{n_o^2 + n_e^2 - n_{e'}^2}}, \quad \delta = 6.23^\circ$$

The distance separating the two images is equal to $30 \sin \delta = 3.26$ mm (Fig. 5.10).

Index

- absence(s)
 - integral, 143
 - serial, 143
 - systematic, 143
 - zonal, 143
- absorption edge, 132, 133
- absorption of X-rays, 133
- affine transformation, 24
- amplitude
 - structure, 138, 150
- anisotropy, 1, 157
- anomalous dispersion, 102, 142
- aperiodic structure, 18
- atomic scattering factor, 106
- axis
 - optical, 209
 - rotation, 30
 - screw, 35
- β filter, 134
- Bernhardi principle, 7
- biaxial crystal, 210
- binormal, 209
- biradial, 209
- birefringence, 200
- Bragg's law, 114
- Bravais lattice, 62, 80
- Bravais' law, 16, 29
- calcite, 86, 200, 211, 226, 232, 234
- camera
 - Debye–Scherrer, 128
- canonical base, 56
- cell(s)
 - centered, 14
 - multiple, 14
 - primitive, 14
 - simple, 14
 - unit, 12
 - Wigner–Seitz, 15
- center of inversion, 301, 185, 194
- center of symmetry, 30, 142, 147, 185, 193
- characteristic spectrum, 130
- chemical disorder, 20
- chirality, 27, 44
- class(es), 42
 - Bravais, 62
 - crystal, 42, 46, 75, 76, 80
 - equivalence, 42
 - Laue, 50, 80, 124, 142
- classical electron, 102
- composite structure, 19
- compositional disorder, 20
- compressibility, 187
- condenser, 177
- conductivity
 - electrical, 180
 - thermal, 180
- conoscopy, 211
- constant dihedral angles
 - law of, 7
- constant(s)
 - dielectric, 177
 - elastic, 182, 198
- construction
 - Ewald, 116, 121
- continuous spectrum, 130
- contravariance, 6
- convolution, 108, 151
- convolution product, 108
- coordinate system
 - non-unitary, 2, 8, 12
 - reciprocal, 2
 - rhombohedral, 58

- unitary, 2, 6, 26
- covariance, 6
- crystal, 1, 18
 - biaxial, 210
 - incommensurate, 18
 - liquid, 21
 - one-dimensional, 118
 - two-dimensional, 118
 - uniaxial, 210
- crystal family, 67
- crystal monochromator, 134
- crystal optics, 200

- Debye–Scherrer camera, 128
- Debye–Waller factor, 109
- defect
 - structural, 20
- dielectric constant, 177
- diffraction, 91, 95
- disorder, 20
 - chemical, 20
 - compositional, 20
- displacement factor, 109
- dual polyhedra, 49

- edge, 15
- effect
 - electrocaloric, 198
 - longitudinal, 165
 - piezocaloric, 198
 - transverse, 165
- elastic constants, 182, 198
- elastic moduli, 182
- elastic wave, 187
- electric displacement, 176
- electric susceptibility, 177, 198
- electrocaloric effect, 198
- electron density, 102
- ellipsoid
 - rate, 207
- enantiomorph, 44
- equations
 - Laue, 111, 112
- Ewald construction, 116, 121
- Ewald sphere, 116
- expansion
 - thermal, 180, 191, 198
- extinction, 104

- face, 15
- factor(s)
 - atomic scattering, 106
 - Debye–Waller, 109
 - displacement, 109
 - form, 106
 - Lorentz, 141
 - multiplicity, 129
 - polarization, 101
 - structure, 111, 138
 - temperature, 109
- family
 - crystal, 80
- fixed point, 29
- Fletcher indicatrix, 206
- form factor, 106
- Fourier series, 149
- Fourier transform, 103
- Friedel's law, 141
- function
 - interference, 94
 - Patterson, 151

- generator, 42
- glide plane, 35
- group(s), 25, 31
 - Abelian, 26
 - abstract, 61
 - cyclic, 26
 - factor, 41
 - icosahedral, 49
 - non-crystallographic, 49
 - octahedral, 49
 - plane, 40, 68
 - point, 28, 40
 - space, 40, 73, 76
 - tetrahedral, 49

- habit, 7
- hemihedry, 68
- Hermann–Mauguin system, 28, 46, 58
- holohedry, 68
- Hooke's law, 180
- hydrostatic pressure, 172, 186

- improper rotation, 27
- incommensurate crystal, 18
- index (of refraction), 206
- indicatrix
 - Fletcher, 206
- indices
 - Miller, 9
 - Miller–Bravais, 86

- rational, 8
- integrated intensity, 137, 139, 141
- interference function, 94
- international system, 28, 46, 58
- inverse piezoelectricity, 198
- inversion, 28
- inversion center, 185, 194
- isotropy, 1, 157

- Lamé moduli, 190
- lattice
 - Bravais, 62, 80
 - reciprocal, 17, 112
 - translational, 11, 12
- lattice base, 12, 56
- lattice line, 15
- lattice plane, 15
- lattice points, 12
- Laue class, 50, 124, 142
- Laue equations, 111, 112
- Laue method, 120
- law
 - Bragg's, 114
 - Bravais', 16, 29
 - Friedel's, 141
 - Hooke's, 180
- law of constant dihedral angles, 7
- light ray, 202
- line
 - lattice, 15
- liquid crystal, 21
- Lorentz factor, 141

- magnetic susceptibility, 180
- matrix
 - idempotent, 32
 - orthogonal, 26
- merohedry, 67
- method
 - Laue, 120
 - powder, 127
 - rotating crystal, 125
- metric, 39, 57
- metric tensor, 5
- Miller indices, 9
- mirror, 28
- mirror plane, 30
- moduli
 - elastic, 182
 - Lamé, 190
- modulus
 - shear, 180
 - Young's, 180
- monochromatization, 133
- monochromator, 134
- motif, 1, 11, 12
- multiplicity, 71, 129

- net
 - Wulff, 10
- Neumann principle, 162
- neutrons, 89
- non-unitary coordinate system, 2, 8, 12
- normal (to a plane wave), 203
- number
 - Poisson's, 181, 190

- ogdohedry, 68
- operation
 - symmetry, 12
- optical axis, 210
- optical grating, 93
- optical sign, 209
- orbit, 71
- order, 20, 24
- orthoscopy, 212

- Patterson function, 151
- periodicity, 1, 12
- phase problem, 91, 99, 104, 150
- piezocaloric effect, 198
- piezoelectricity, 191, 198
 - inverse, 198
- plane
 - glide, 35
 - lattice, 15
- Platonic solids, 46, 48
- point group, 28, 40
- points
 - lattice, 12
- Poisson's number, 181, 190
- polarization factor, 101
- position
 - general, 71
 - special, 71
- powder method, 127
- pressure
 - hydrostatic, 172, 186
- principle
 - Bernhardi, 7
 - Neumann, 162
- product

- scalar, 6
- vector, 6
- projection
 - stereographic, 10
- pyroelectricity, 190, 198
- quartz, 180, 187, 196, 210
- quasi-crystal, 18
- quasi-periodic structure, 18
- radiation
 - white, 130
- rank (of a tensor), 159
- rate ellipsoid, 207
- reciprocal coordinate system, 2
- reciprocal lattice, 17, 112
- reciprocal metric tensor, 6
- reference ellipsoid, 166
- reference hyperboloid, 167
- reflection, 28
- representation of a group, 26
- representation of an operation, 24, 27
- rotating crystal method, 125
- rotation, 27
- rotoinversion, 27, 28
- rotoreflexion, 27
- rutile, 180
- scattering, 99, 102
- scattering factor(s)
 - atomic, 106
- scattering length, 100
- Schoenflies system, 28, 46, 60
- screw axis, 35
- series
 - Fourier, 149
- shear modulus, 180
- sign
 - optical, 209
- space group, 76
- specific heat, 197, 198
- spectrum
 - characteristic, 130
 - continuous, 130
- sphere
 - Ewald, 116
- squared structure, 150
- stereographic projection, 10
- strain tensor, 174
- stress, 170
 - uniaxial, 172
- stress tensor, 170
- structural defect, 20
- structure, 11
 - aperiodic, 18
 - composite, 19
 - quasi-periodic, 18
 - squared, 150
- structure amplitude, 138, 150
- structure factor, 111, 138
- susceptibility
 - electric, 177, 198
 - magnetic, 180
- symmetry, 24
 - center of, 30, 142, 147, 185, 193
 - site, 71
- symmetry element, 30, 31
- symmetry operation, 12
 - geometrical, 24
- synchrotron, 124, 136
- system
 - Bravais, 67, 80
 - crystal, 56, 67, 80
 - Hermann–Mauguin, 28, 46, 58
 - international, 28, 46, 58
 - Schoenflies, 28, 46, 60
- systematic absences, 143
- temperature factor, 109
- tensor, 159, 161
 - metric, 5
 - reciprocal metric, 6
 - strain, 174
 - stress, 170
- tensor (of even rank), 185
- tensor (of odd rank), 194
- tetartohedry, 68
- thermal expansion, 180, 191, 198
- thermal motion, 20
- tourmaline, 191
- transform
 - Fourier, 103
- translation, 29, 38
- translational lattice, 11, 12
- tube
 - X-ray, 129
- twin, 67
- uniaxial crystal, 210
- unit cell, 12
- unitary coordinate system, 2, 6, 26

vector

axial, 164

polar, 164

Voigt notation, 176

wave

elastic, 187

white radiation, 130

Wigner–Seitz cell, 15

Wulff net, 10

Wyckoff symbol, 71

X-ray tube, 129

X-rays, 89

Young's modulus, 180

zone, 10, 122

CRYSTALLOGRAPHY

Dieter Schwarzenbach

*Director of the Institute of Crystallography,
University of Lausanne, Switzerland*

Translated from the French by **A. Alan Pinkerton**,
University of Toledo, USA

Due to its interdisciplinary nature, crystallography is of major importance to a wide range of scientific disciplines including physics, chemistry, molecular biology, materials science and mineralogy. However, information is currently divided amongst traditional physics, chemistry and materials science books. This book collates previously disparate literature into one comprehensive and practical source, providing a thorough understanding of the information contained in crystallographic data files and the application of x-ray diffraction methods. The book has been written for final year and postgraduate students.

ISBN 0-471-95598-1



9 780471 955986

JOHN WILEY & SONS

Chichester · New York · Brisbane · Toronto · Singapore

